2024

A large-sample X-ray absorption line analysis in search of the missing baryons in the hot WHIM

David Spence

A LARGE-SAMPLE X-RAY ABSORPTION LINE ANALYSIS IN SEARCH OF THE MISSING BARYONS IN THE HOT WHIM

David Spence

A DISSERTATION

Submitted in partial fulfillment of the requirements
for the degree of Doctor of Philosophy
in
The Department of Physics & Astronomy
to
The Graduate School
of
The University of Alabama in Huntsville

August 2024

Approved by:

Dr. Massimiliano Bonamente, Research Advisor/Committee Chair
Dr. Stephen Walker, Committee Member
Dr. Ming Sun, Committee Member
Dr. Richard Lieu, Committee Member
Dr. James Miller, Committee Member
Dr. James Miller, Department Chair
Dr. Rainer Steinwandt, College Dean
Dr. Jon Hakkila, Graduate Dean

Abstract

A LARGE-SAMPLE X-RAY ABSORPTION LINE ANALYSIS IN SEARCH OF THE MISSING BARYONS IN THE HOT WHIM

David Spence

A dissertation submitted in partial fulfillment of the requirements for the degree of Doctor of Philosophy

Physics & Astronomy

The University of Alabama in Huntsville

August 2024

A well known problem in astrophysics that has seen a significant amount of investigation in recent years is the "missing baryons problem", in which up to 40% of baryons have been reported missing at low redshifts [62]. Predictions show that these remaining baryons are likely residing within the Warm-Hot Intergalactic Medium (WHIM). The process of finding these baryons involves searching for absorption line systems in the WHIM and using column densities of those absorbing ions to calculate the cosmological density of the medium. Several wide scale FUV studies (*e.g.,* [21]) have been completed to work towards solving this problem, but there has yet to be a study of such scope in the X-ray band of wavelengths. Using a sample of 51 X-ray sources from *FUSE* and *HST*, this project seeks to be the conclusive work on the presence of WHIM absorption in X-ray quasars. Using the spectral analysis software `SPEX`, the sample of 51 X-ray sources was searched for O VII and O VIII absorption lines at redshifts from prior O VI and H I detections, as well as at $z = 0$ in search for galactic oxygen. In total, we report 8 possible absorption line systems of O VII and O VIII. Upper limits of the resultant column densities found from both the entire

sample's absorption line search and the possible detections reported were used to put constraints on the cosmological density of baryons in the universe due to the WHIM, Ω_{WHIM}. These results were then compared to the baryonic density expected to be contributed by the WHIM. Being the first and only large scale X-ray search for WHIM absorption of its kind, this work gives the most comprehensive and definitive look at WHIM oxygen absorption in X-ray quasars and an answer to the missing baryons problem.

Acknowledgements

I would like to express my thanks and gratitude to everyone who supported me throughout my college and graduate school studies. Without their effort and support, I would not have made it to where I am today.

Thank you to Dr. Max Bonamente, for guiding me through my studies and research, supporting me throughout this project, and serving as my graduate advisor. You have been a kind, understanding, and helpful force during my journey through graduate school. Thank you to Dr. Stephen Walker, Dr. Ming Sun, Dr. Richard Lieu, and Dr. James Miller for serving on my PhD committee. Thank you to the UAH Department of Physics and Astronomy for funding my studies and research during this project.

Thank you to my family, my parents, grandparents, and brothers, for believing in me every step of the way and supporting me in numerous ways. Your support through my life, college studies, and graduate school was instrumental into getting me to the person that I am. Thank you for your encouragement of my love for science and my interests throughout my life. Without them, none of this would have been possible. Thank you to Nora, to all of your love and support, and inspiring me to never give up.

Thank you to my friends, Ian, Cory, Phillip, and others, for being there for me and spending time together when I needed it most. Our fun together gave me the energy to continue my progression towards my goals and aspirations.

Thank you to Corvid Technologies, for your support in providing funding for the final duration of this project.

Table of Contents

List of Figures

List of Tables

Chapter 1. Introduction

1.1 Background

1.1.1 The Missing Baryons Problem

According to current estimates, the cosmological density of the universe due to baryons (Ω_b) is only about 5% of the total budget, while dark matter and dark energy represent around 70% and 25% respectively [1]. The makeup of the universe's baryons are mostly found in the Intergalactic Medium (IGM), with fewer than expected being reported in typical matter such as galaxies at about 10% [62]. In the IGM, measurements of baryons can be separated into the categories of high and low redshift detections. In the high redshift sector, most of the baryons have been accounted for in the "Lyman-α forest". In the low redshift sectors, the makeup of baryons is not so clearly accounted for. An estimated amount of up to 40% of baryons have been reported missing in the low redshift region [62]. This 30-40% amount of missing baryons is a well known open question, known as "the missing baryons problem" most commonly. Simulations predict the solution to this problem is that the Warm Hot Intergalactic Medium (WHIM) contains these unaccounted for baryons [22, 67]. The WHIM is the large scale structural medium between galaxies that has been formed into a sort

of "cosmic web" [15]. Throughout the WHIM, a series of processes including star formation and AGN (Active Galactic Nuclei) activity produce gas shocks. These shocks ultimately result in ion and election heating and the ability to observe the ionization of oxygen ions [15]. These oxygen ions (particularly O VII and O VIII) and the detection of their absorption lines are the primary focus of this project, primarily because of their ionization curves peeking in the higher temperatures of focus in comparison to other ions (see Section 3.3.1). Through the detection of these absorption lines found in the spectra of AGNs, a column density of the associated oxygen ion and ultimately an estimate of the cosmological density of baryons due to the WHIM can be calculated. An illustration of this observation process is shown in Figure 1.1.

Breaking down the WHIM into regions of varying temperatures, a significant amount of work is already completed on analyzing the low temperature regions. Most absorption lines from ions at low temperature fall in the FUV spectrum, and have found quite a bit of success in finding absorption lines in observations from *FUSE* (Far Ultraviolet Spectroscopic Explorer) and *HST*/*COS* (Hubble Space Telescope/Cosmic Origins Spectrograph). The relatively high range of temperatures are the focus of current work, and this project. These temperatures, $\log T(K) \geq 6$, include prominent absorption lines that fall into the X-ray range of observations. Figure 1.2 shows a pie chart of the current estimates of low redshift data for baryons, created from data pulled from [62] and [21]. The pie chart shows that around 40% of baryons are unaccounted for.

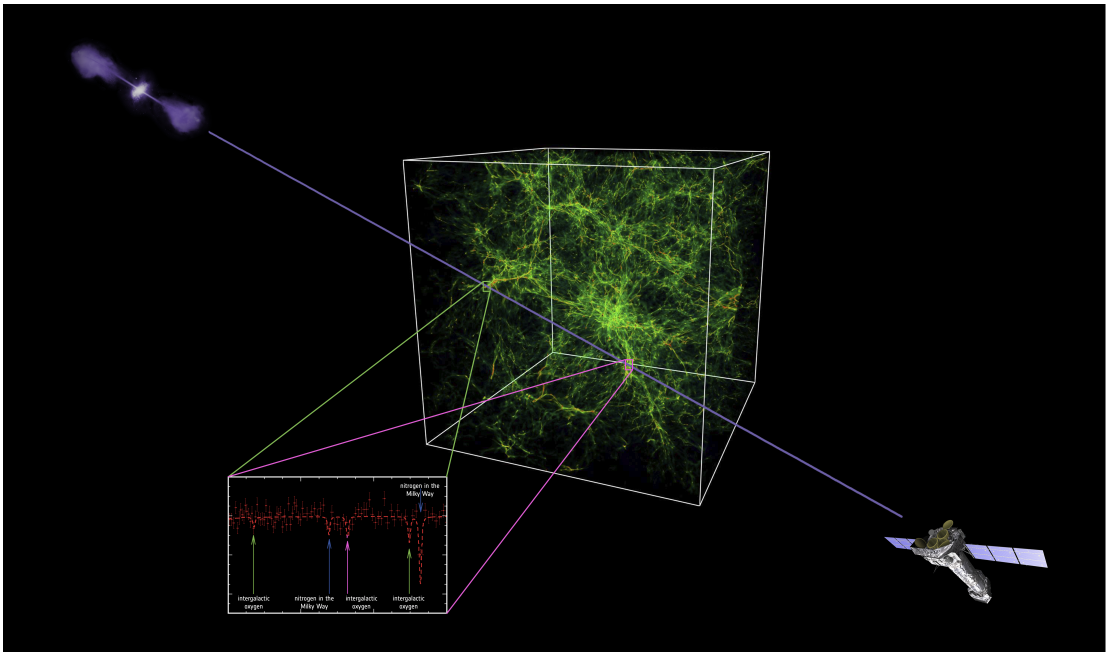

Figure 1.1: An artist's impression of the method of observing the WHIM using the *XMM-Newton* telescope, shown with a simulation of the WHIM completed by Princeton University. Absorption lines are measured in spectras along sightlines through the WHIM towards bright active galactic nuclei (AGN). The absorption lines displayed in the figure are from [54].

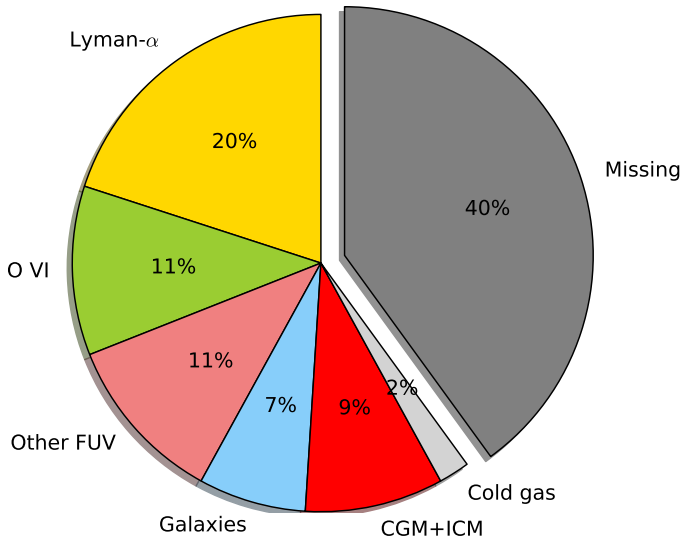

Figure 1.2: The low-redshift baryon budget, adapted from [21] and [62]. An estimated 40% of the budget is missing, and suspected to reside within the Warm-Hot Intergalactic Medium.

1.1.2 Current Literature

Despite the challenges associated with the flux of available background sources and the resolutions and sensitivity of the X–ray spectrometers, a few detections of absorption lines from the WHIM have been reported, including two in the spectrum of the quasar 1ES 1553+113 [54, 53], which is the subject of Section 2.2. Other detections of the WHIM through X–ray absorption include PKS 2155-304 [27, 25], although the detection was not confirmed by others [75, 17, 50]; Mrk 421 by [56], which was however followed by reports of non–detections by [58] and [74]; H 2356-309 by [24] and [13]; Mrk 501 by [59], Ton S180 [2] and in 3C 273 [3], and finally in PG 1116+215 by [8]. Finally, a tentative detection in

H 1821+643 was reported by [46] using stacking of signals at different redshifts, using a method that is similar to the one used and explained in Section 2.2.

The study of `EAGLE` hydrodynamical simulations by [70] suggests that there is significant correlation between O VI and H I BLA FUV absorption lines and prominent X–ray ions such as O VII and O VIII. This correlation motivates our search for X–ray counterparts to FUV absorption lines in the data sample used in this project, with FUV detections reported by the *HST* and *FUSE* surveys of [65] and [21] (Section 3.1). Although a significant amount of work has already been completed in analyzing the WHIM for X-ray absorption, most if not all of these papers have only analyzed a single or very few sources in their analysis. This project seeks to add to the pool of current literature by becoming the most comprehensive analysis of X-ray absorption in the WHIM.

1.2 Goals of Project

The goals behind this project were multi-faceted. The main objective was to put constraints onto the cosmological density of baryons due to the WHIM, and to compare that result to the expected 40% missing value of the current budget's estimate (see Figure 1.2). The aim is to create these constraints through the usage of our calculation of upper limits on the column density of the respective ions, and by extension their contributions to the cosmological density. In conjunction with this analysis, another goal was to report any possible absorption line detections in the sample for O VII and O VIII ions. These absorption lines were reported for both galactic oxygen, as well as absorption at redshifted wavelengths used from

prior O VI and H I detections. In order to provide a improved estimate of the baryonic density due to the WHIM, these possible detections at O VI and H I priors were further analyzed for their individual estimates of the baryonic density. Combined, this project's goal is to study the nature of oxygen ion absorption in a large number of sources, and to become the largest and most comprehensive search for O VII and O VIII ion absorption in the WHIM of its kind. This ultimately leads into the goal to have the results of this project provide a significant amount of work towards solving the missing baryons problem.

1.3 Instruments, Software, and Data

As this project is a search for X-ray absorption lines in the WHIM, X-ray data from online archives were used from two primary telescopes; *XMM-Newton* and *Chandra*. As mentioned previously, these observations were from the *FUSE* and *HST/COS* missions. According to [12, 23] and the *XMM-Newton* website[1], *XMM-Newton* is an X-ray telescope launched in 1999 that has been used to make a plethora of observations that are all easily obtainable on an online archive. The Reflection Grating Spectrometer (RGS) onboard the telescope is an array of reflection gratings that defract the observed X-rays to what are known as CCD detectors (dedicated charge coupled devices) (pictured in Figure 1.3). There are two of these spectrometers onboard, known as "RGS1" and "RGS2". The result for our use is a spectrum over a range of 5-35Å with an estimated resolution of about 10mÅ per bin (later re-binned to 20mÅ).

[1] `https://www.cosmos.esa.int/web/xmm-newton/technical-details-rgs`

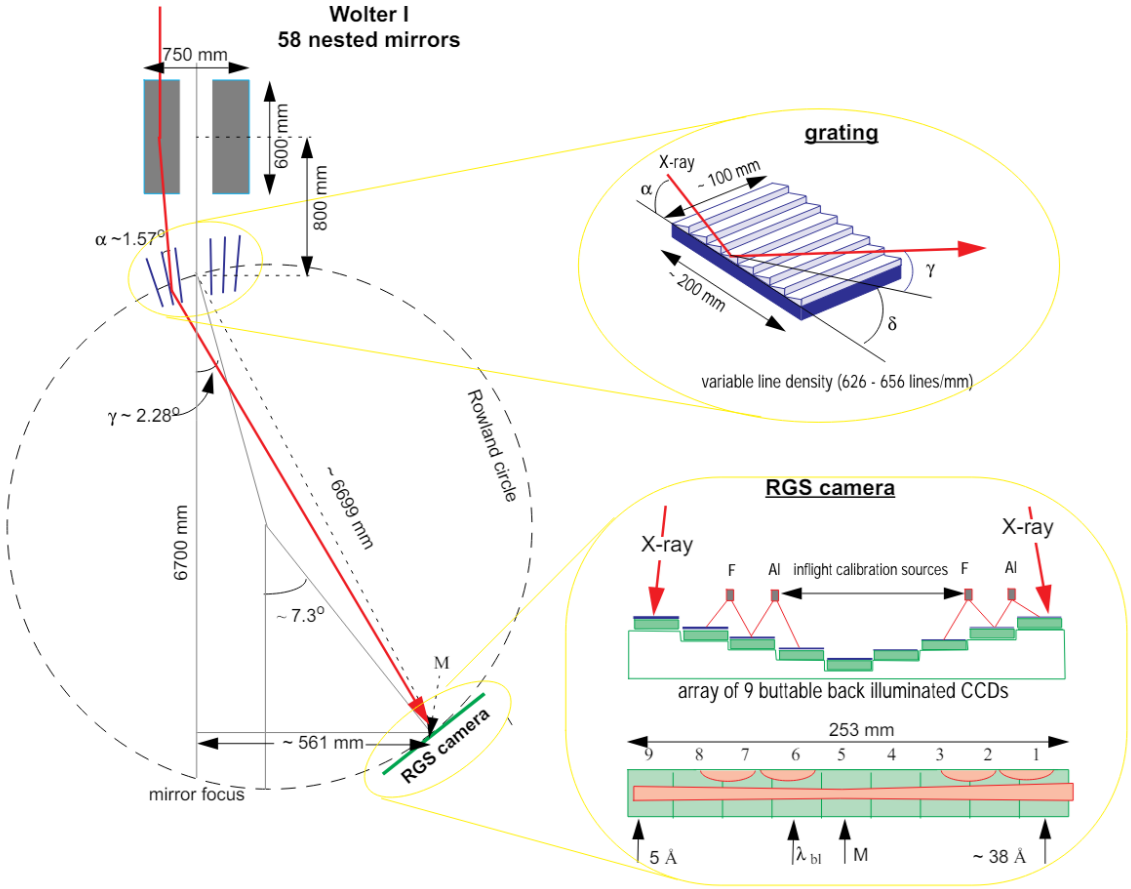

Figure 1.3: The schematic layout of the RGS instrument on-board *XMM-Newton*, from [12].

Similarly to *XMM-Newton*, the *Chandra* X-ray Observatory was launched in 1999 with the purpose of observing X-rays in hot regions of the universe. *Chandra* has several detectors on board, including the ACIS (Advanced CCD Imaging Spectrometer), and two high resolution spectrometers known as LETGS (Low Energy Transmission Grating Spectrometer) and HETGS (High Energy Transmission Grating Spectrometer). All *Chandra* observations from this project were completed using the HRC (High Resolution Camera) instrument on board *Chandra*, and the LETG spectrometer.

The data for this project were acquired from the online archives of both *XMM-Newton* and *Chandra*[2]. This was completed through the use of an automated script that queried the archives with a list of sources and downloaded the corresponding observations for each. Fortunately, both of the archives have the ability to download sources remotely through commands and external tools, so this process was straightforward to accomplish. A more thorough explanation of the data acquisiton process and further data reduction and conversion into usable file formats is in Section 3.2.

The primary software used for the spectral analysis of this project was `SPEX`[3]. `SPEX` is a software package developed at the Space Research Organization of the Netherlands (SRON) for the usage of modeling hot plasmas in X-ray spectra [42, 43]. `SPEX` is specifically suited to analyze spectra from telescopes such as *XMM-Newton* and *Chandra*, making the software an ideal candidate for our

[2]The archives for *XMM-Newton* and *Chandra* can be visited at `https://nxsa.esac.esa.int/nxsa-web/#home` and `https://cxc.harvard.edu/cda/` respectively.

[3]`https://www.sron.nl/astrophysics-spex/`

analysis. Typically, SPEX is used as a command line software, where fit and parameter commands are input individually to yield fit statistics and information to the terminal. In an analysis of small magnitudes, this workflow is not an issue. A project with the scope of this one could not physically be done by hand through the command line, even with the use of SPEX command files. Luckily, SPEX has an additional package that allows for the usage of SPEX through the Python framework, called Pyspextools, or PYSPEX. With the usage of Python, the analysis can be automated to significantly reduce the time needed to analyze hundreds of different fits. In addition to this, the PYSPEX package includes the ability to record any parameter value of the fits as variables in Python, a process not easily completed with the usual SPEX package. Thus, with the usage of Python and PYSPEX, a large pipeline was created to process the sample, fit the massive amounts of sources, save and manipulate fit values and plots, and ultimately create readable outputs of the results of the analysis in a timely manner.

Secondary software and languages used for this project included:

- Bash and C-shell scripts for manipulating aspects of the data reduction and large scale file management.
- CIAO (Chandra Interactive Analysis of Observations) for the data reduction of the *Chandra* data sample.
- SAS (Scientific Analysis System) and Trafo for their ability to reduce *XMM-Newton* data, and further convert them into a usable SPEX file format.

1.4 Project Structure

The main goal of this project is to constrain Ω_b, the cosmological density of baryons, using X-ray sources from the *XMM-Newton* and *Chandra* telescopes. Numerous papers ([54],[53], etc.) have already published similar analyses on single X-ray sources with calculations of Ω_b. Analyses completed on single sources only account for small sectors of the observable universe and by extension the WHIM. This project seeks to expand that search to an analysis of 51 X-ray observations, which will ultimately provide a more significant idea of the entire makeup of the WHIM's baryonic matter. As a result, this was the largest multi-spectra study done on X-ray spectra in the WHIM in search for absorption lines and multi-wavelength measurements of the physical properties of the WHIM.

As such a large sample of sources was used, the structure of this project was multi-part. An initial paper was written over the modelling methods and fit statistic used for this project (Section 2.1). Then, an initial analysis was completed for a single source, which served as a case study and testing of the analysis methods that would be extended to the remaining sample (Section 2.2). After this was completed, the full analysis of the sample was split into several parts: sample downloading and processing (Section 3.2), automation of the analysis completed in the case study, and the main analysis and calculations (Section 3.3). A discussion over the statistical methods, analysis, and simulations used for the process of the data analysis and overall project are discussed in Section 4. The primary analysis and calculation of upper limits required the majority of the time and

work for the project, and the results are listed in (Section 5.1). Along the way, a search for galactic O VII and O VIII at $z = 0$ was completed as well (Section 5.3). Following the main and sub-analyses, the remaining part of the project included comparing our results to previous results at select observations (Section 5.2), and a more thorough study of possible detections made from the main analysis (Section 5.4). Following all of these studies and results, a final calculation of the baryonic density due to the WHIM was made and related to the known baryonic density of the universe and expected value of 40% (Section 5.5).

Chapter 2. Previously Published Papers in Support of Current Work

2.1 Paper "A semi–analytical solution to the maximum–likelihood fit of Poisson data to a linear model using the Cash statistic" [11]

2.1.1 Background

Throughout the analyses of this project and of the case study on 1ES1553+113, the statistic known as the "C-statistic" was used when fitting data. This stat is commonly used for the analysis of low–count Poisson data, and is especially attractive in its usage on data with null counts and data that cannot be combined or re-binned without loss of resolution. This statistic and its applications on linear models was studied further in a paper I co-authored that provides a method of its use in measuring best-fit parameters of Poisson data. [11]. Specifically, this paper presented a new maximum-likelihood solution for the best-fit parameters of a linear model using the C-statistic.

The solution found in the paper provided a new and simple method to measure the best-fit parameters of a linear model for any Poisson-based data, including data that have null counts. This new method also works with the requirement that the best-fit linear model is non-negative. The method allows

for the user to skip over the use of the χ^2 statistic entirely in favor of a simple algorithm that fits Poisson data of any size and count rate with a linear model.

2.1.2 Overview

The primary focus of this paper was over the best-fit parameters of a linear model, commonly shown as the relationship between y and x: $f(x) = a + bx$. In the paper, a convenient and equivalent parameterization was used, defined by:

$$f(x) = \lambda(1 + a(x - x_A)), \tag{2.1}$$

where λ and a are the adjustable parameters, and x_A is the fiducial value of the x variable. A visual representation of this model can be seen in Figure 2.1. Through the minimization of the C statistic of Equation 2.1, we also found that

$$\lambda(a) = \frac{M}{R(1 + a\frac{R}{2})}, \tag{2.2}$$

where $R = x_B - x_A$ is the range of the x variable and M is the total number of counts.

Ultimately, the problem of finding the solutions for the parameter a reduce to the problem of finding the zeros of the function $F(a)$,

$$F(a) \equiv 1 + \frac{R}{2}(a - \frac{M}{g(a)}), \tag{2.3}$$

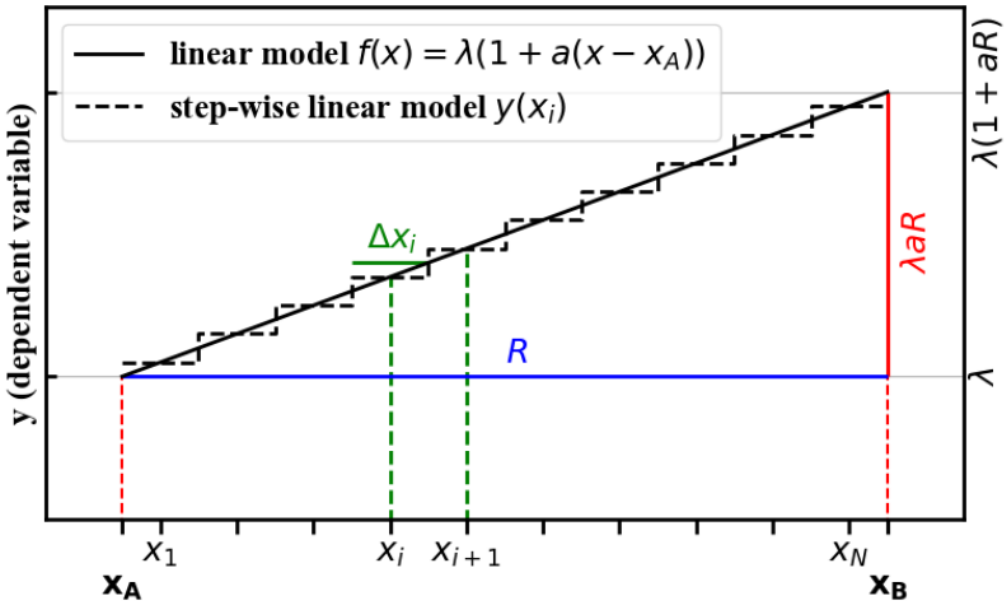

Figure 2.1: Linear model according to Equation 2.1. In this illustration, the functions $f(x)$, in units of counts per unit x, and $y(x_i)$, in units of total counts in the bin, follow one another closely because a bin size value of $\Delta x = 1$ was used.

where $g(a)$ is:

$$g(a) \equiv \sum_{i=1}^{N} y_i \frac{x_i - x_A}{1 + a(x_i - x_A)}. \tag{2.4}$$

One of the key properties of this function is that the zeros of $g(a)$ are points of singularity for $F(a)$, which can be seen in Figure 2.2. To find the maximum-likelihood estimators a and λ of the linear model in Equation 2.1, the solution of $F(a) = 0$ must be found. In order to do this, the cases of M for Equation 2.3 were studied and expanded upon in the paper. Ultimately, this resulted in the conclusion that:

- for $M = 0$ counts, the dataset will have no positive measurements in the range of the independent variable, and is therefore uninteresting.
- $M = 1$ count results in an $F(a) = 0$ that has no solutions, meaning the maximum-likelihood solution cannot be found.
- $M \geq 2$ allows for the maximum-likelihood solution to be solved for certain cases. Of which, it is possible to find certain properties that lead to criteria that solve $F(a) = 0$. An example of an $F(a)$ with no solution, and $g(a)$ with $M = 2$ for 100 data points is in Figure 2.2.

Upon studying the possible solutions for the maximum-likelihood parameters of Equation 2.1, we found that for data with M total counts, distributed over $n \leq M$ of the N available bins, there are $n - 1$ possible values of a that are a solution for $F(a) = 0$ (given that λ follows Equation 2.2). Next, the additional requirement that the model was non-negative in all bins was addressed. This is

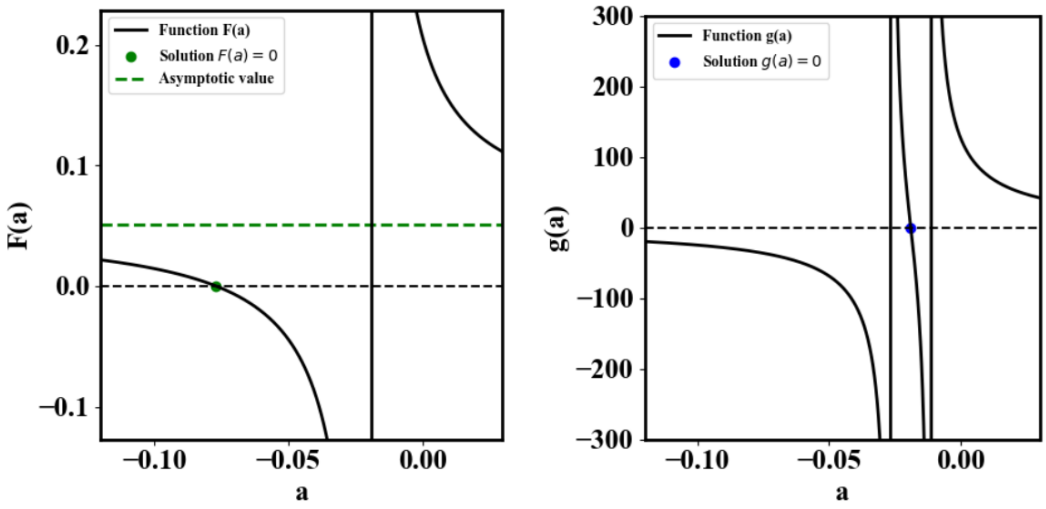

Figure 2.2: (Left:) Function $F(a)$ for a representative data set $M = 2$, with 100 data points $x_i = i - 0.5$, $i = 1, ..., 100$, and $y_{38} = y_{89} = 1$. (Right:) Function $g(a)$ for the same data set. Note that the zeros of $g(a)$ are points of singularity for $F(a)$.

important, as it allows for the Poisson statistics to apply and for the C statistic to be calculated. In order to satisfy the need to have a linear model that is applicable to any situation, a model that is defined as follows was proposed:

1. The model of Equation 2.1 is used if it has an acceptable solution.

2. If the model does not have an acceptable solution, the model is parameterized as one of the following three functions:

   (a) A one-parameter linear model pivoted to zero at the initial point x_A:

$$f_A(x) = \lambda_A(x - x_A) \tag{2.5}$$

   for which $y_A(x_A) = 0$, and with $\lambda_A \geq 0$.

(b) A one-parameter linear model pivoted to zero at the final point x_B:

$$f_B(x) = \lambda_B(1 - \frac{x - x_A}{R}) \tag{2.6}$$

for which $y_B(x_B) = 0$, and with $\lambda_B \geq 0$.

(c) A one-parameter constant model:

$$f_C(x) = \lambda_C. \tag{2.7}$$

With the choice of these three parameterizations and the initial linear model, it was then shown that there exists a simple analytical solution for the maximum-likelihood best-fit parameters for any dataset. These analytical solutions are as follows:

1.
$$\lambda_A = \frac{2M}{R^2} > 0 \tag{2.8}$$

2.
$$\lambda_B = \frac{2M}{R} > 0 \tag{2.9}$$

3.
$$\lambda_C = \frac{M}{R}, \tag{2.10}$$

where λ_A, λ_B, and λ_C are the analytical solutions to the models in Equations 2.5, 2.6, and 2.7, respectively. With these results, a new method to find the

best fit parameters of a linear model for the fit to integer valued counting data was shown. This extends to any dataset, including those with gaps, which were studied further (along with the modifications required to solve these cases) in the paper. An example of the various models defined on the case of a dataset with gaps is shown in Figure 2.3. This model guarantees a unique and straightforward non-negative solution for any Poisson data set. This leads to uniqueness of the best fit model when the solution shown is available.

In relation to the project as a whole, this study of finding a solution to the maximum-likelihood fit of Poisson data formed the base of work and knowledge around the C statistic and Poisson data used for the analysis. Although this particular method was not used specifically in the analysis of the entire sample later on (Section 3.3), familiarizing myself with similar datasets and the primary analysis statistic used in the full analysis was quite useful. This is particularly relevant in the case of the data sample in regards to *XMM-Newton*, as a significant amount of this data had a low amount of counts (see Section 6.1), where the χ^2 and C statistics differ significantly.

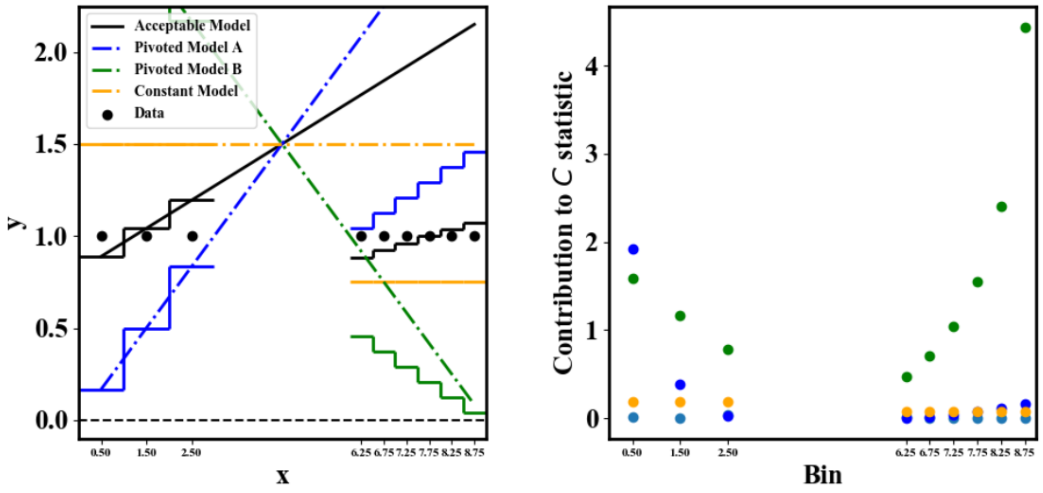

Figure 2.3: Best-fit linear models for data with non-uniform bins and with a gap in the data. The dot-dashed curve are the density functions and the solid step-wise curves are the models $y(x_i)$ for the integer data.

2.2 Paper "A search for the missing baryons with X–ray absorption lines towards the blazar 1ES 1553+113" [64]

2.2.1 Overview

Because of the large amount of sources needed for this project's census of X-ray WHIM absorption lines, a preliminary case study was needed for a single source. This case study was completed on a quasar known as 1ES 1553+113. Because of the source's extreme brightness as a blazar (see Figure 2.4) and easily defined continuum, a significant amount of prior work had already been completed in studying this source (eg. [21] and [54]). This made 1ES 1553+113 a prime candidate for testing the methods of analysis that would be expanded further to the entire sample.

This case study of 1ES 1553+113 featured a search for O VII, O VIII, and Ne IX absorption lines at eight fixed redshifts that had prior O VI or H I broad Lyman-α absorption line detections from *HST* data. Two primary methods of analysis were used in this paper; the `SPEX spline` and `slab` model, and a method of stacking sections of the spectra's expected wavelength ranges of the prior redshift detections on top of each other.

The `slab` model method involved fitting the data with a thin slab absorption model (`slab` in `SPEX`). This model allows for the calculation of the transmission of a slab of material, specifically where every ion's column density is displayed separately. In conjunction with this, a base cubic spline model (`spline` in `SPEX`) was implemented. Given that a power law model did not provide a satisfactory

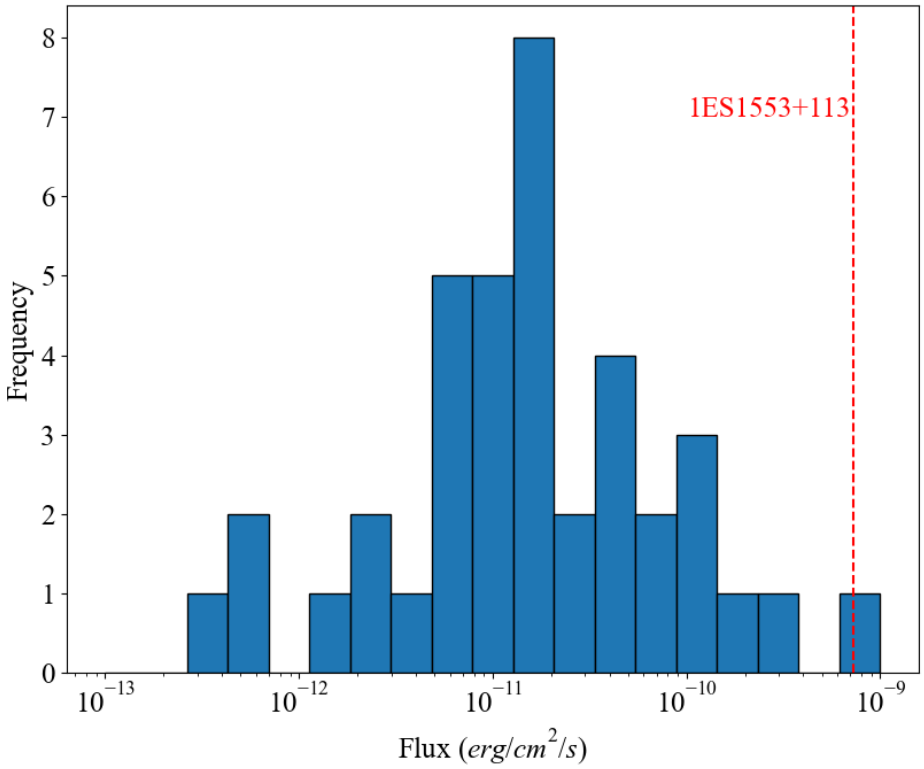

Figure 2.4: Histogram of the 41 available X-ray Fluxes (acquired from the NASA/IPAC Extragalactic Database) of the data sample's sources (Section 3.1). Among the entire sample, 1ES 1553+113 is extremely bright at a flux of $10^{-9.13} erg/cm^2/s$ indicated by the red dashed line in the plot.

Table 2.1: Results of the spectral fits to the 1ES1553+113 *XMM-Newton* data with the `SPEX` `spline` and `slab` models.

	z		C stat.		O VII		O VIII		Ne IX		ΔC (dof)
#	Value	Fixed/Free	Value	d.o.f.	$\log N(\mathrm{cm}^{-2})$	$\Delta\ C$	$\log N(\mathrm{cm}^{-2})$	$\Delta\ C$	$\log N(\mathrm{cm}^{-2})$	$\Delta\ C$	
Redshift priors from FUV											
1	0.1876	Fixed	1861.8	1478	$15.13^{+0.19}_{-0.31}$	4.2	$15.3^{+0.3}_{-8.3}$	0.8	$15.26^{+0.26}_{-0.62}$	1.8	6.8 (3)
2	0.1878	Fixed					—				
3	0.1898	Fixed	1865.8	1478	$9.3^{+5.3}_{-2.3}$	0.0	$15.50^{+0.24}_{-0.49}$	2.3	$15.26^{+0.26}_{-0.66}$	1.7	4.0 (3)
4	0.3950	Fixed	1869.6	1478	$14.7^{+0.4}_{-7.7}$	0.3	$14.0^{+1.1}_{-7.0}$	0.0	$8.0^{+6.3}_{-1.0}$	0.0	0 (3)
5	0.0347	Fixed	1869.7	1478	$14.5^{+0.6}_{-7.5}$	0.1	$13.6^{+1.5}_{-6.6}$	0.1	$7.0^{+8.0}_{-0.0}$	0.1	0.1 (3)
6	0.0427	Fixed	1869.0	1478	$14.9^{+0.4}_{-7.9}$	0.5	$15.0^{+0.4}_{-8.0}$	0.8	$7.0^{+7.4}_{-0.0}$	0.7	0.6 (3)
7	0.0636	Fixed	1869.1	1479	—		$9.4^{+5.7}_{-2.4}$	0.0	$15.1^{+0.4}_{-8.1}$	0.7	0.7 (2)
8	0.2186	Fixed	1867.9	1480	$14.97^{+0.24}_{-0.57}$	2.0	—		—		—
Redshifts from [54]											
9	$0.4336^{+0.0005}_{-0.0003}$	Free	1835.6	1477	15.74±0.11	30.9	$14.2^{+0.9}_{-7.2}$	0.0	$15.30^{+0.25}_{-0.38}$	2.6	34.1 (4)
10	$0.3557^{+0.0006}_{-0.0006}$	Free	1864.3	1477	15.29±0.22	4.8	$9.9^{+5.7}_{-2.9}$	0.0	$14.0\ ^{+0.3}_{-7.0}$	0.7	5.5 (4)

fit over the range of interest due to the large count rate of the source, the cubic spline model was chosen for its flexibility. For each of the 8 redshift priors used, a separate `spline` and `slab` model was used. This entire process was automated through the use of Python, which allowed for multiple fits to be completed automatically given the input redshifts. This automatic analysis would later go on to form the basis of the automatic analysis method used for the entire sample, detailed in Section 3.3. The results of these eight fits, plus an additional two fits at redshifts claimed for positive detections in [54] are shown in Table 2.1.

The redshift stacking method was based on a process completed in [46], in which regions of the spectrum were shifted such that all lines were centered around the unredshifted wavelength of the ion. This was completed by first introducing several power law models in `SPEX`, and connecting those to a number of `line` models equal to the number of FUV prior detection redshifts of 1ES 1553+113. All regions and data outside of a 1.0Å band around any absorption lines were

removed, and the models were fit to the data accordingly. These fits and data were then brought into Python and shifted to be centered around 21.6Å or 18.96Å (the expected rest wavelength of O VII and O VIII respectively). The data and models were summed, and the corresponding ratio of the stacked and summed data to the model were plotted. These plots can be seen in Figure 2.5.

Additionally, more fits were completed on several of the redshifts of significant interest. These fits used a power-law and `line` model in a very similar fashion to the stacked spectra's analysis. Importantly, these fits would go on later to form the basis of the method and model used for the analysis of the entire sample (explained more thoroughly in Section 3.3.4). The results of these fits can be seen in Table 2.2. Although the *XMM-Newton* archive data were the primary focus of this paper, as a matter of comparison and supplementary information, these `line` fits were extended to the 1ES 1553+113 *Chandra* data that were previously collected. These fits and their comparisons to the *XMM-Newton* fits in regards to the model parameters and ΔC values are listed in table 2.3.

2.2.2 Results

The analysis on 1ES 1553+113 for the eight fixed redshifts yielded one possible detection of O VII at a redshift $z \simeq 0.1877$ with an O VI prior, with a statistical significance that was equivalent to a 2.6–σ confidence level. The analysis of the two detections reported by F. Nicastro [54] resulted in the confirmation of the detection of O VII Kα at $z = 0.4339$, and a lack of statistical significant

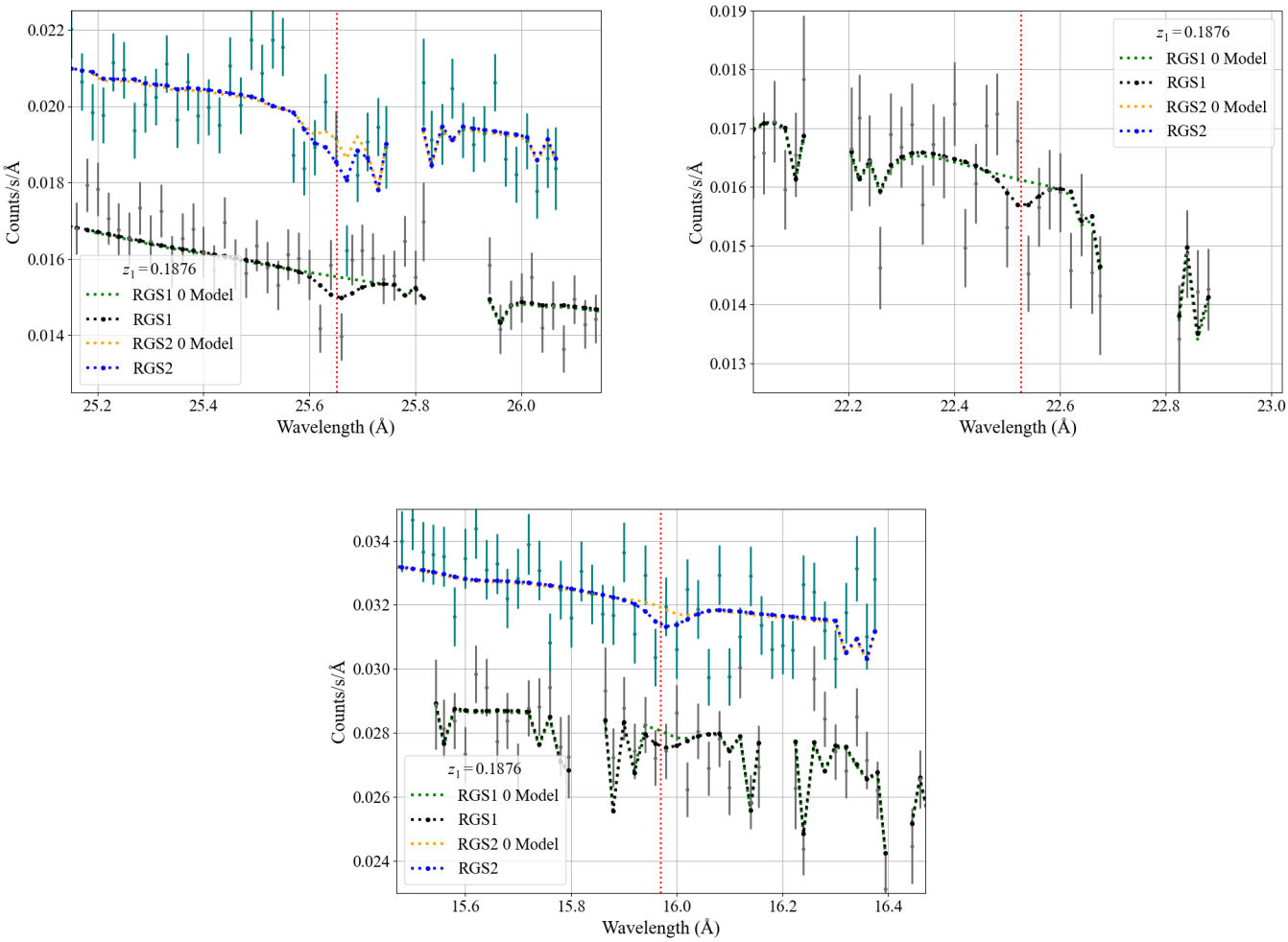

Figure 2.5: Portions of the *XMM-Newton* spectra of 1ES 1553+113 centered around expected O VII (top left), O VIII (top right), and Ne IX (bottom) ions at a redshift of $z = 0.1876$. The blue data (RGS2) were shifted by a factor 1.2 for clarity. The vertical red dotted line denotes the expected absorption line wavelength.

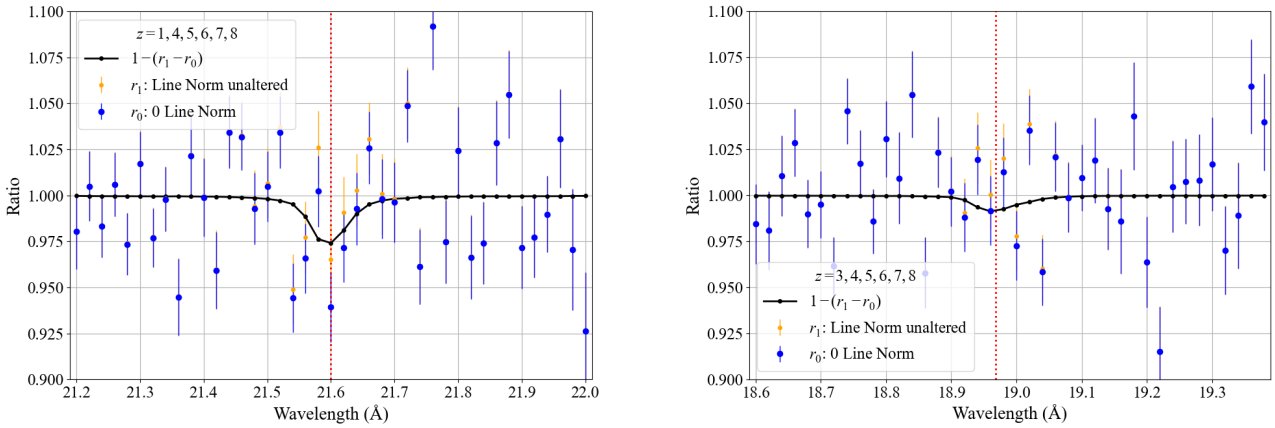

Figure 2.6: (Left) Stacked spectrum for all 1ES 1553+113 O VII lines with FUV priors. The orange data points are the ratio of the stacked data to the model, and the blue data points are the ratio when the O VII line model is zeroed out, to highlight any deficit of counts near the expected line wavelength. In black is the difference between these two ratios. (Right) Same spectrum, but for O VIII lines with FUV priors. The vertical lines mark the rest wavelength of the lines.

Table 2.2: Additional fits using a power–law continuum model and a `line` model. For each regression, a band of 1 Å around the expected line center was used in the fit. For the lines with FUV priors, the line center was fixed. For the other lines from [54], the line center was left free to vary, and the index of the power-law was fixed at a fiducial value. The last two columns report the redshift–trial–corrected P–values, according to the binomial distribution method, and using a simulation following the [44] method. For the `line` model, the implied column densities are estimated from the measured equivalent widths, assuming optically thin lines (*i.e.*, Eq. 2 of [8]).

Target line	$C_{\rm min}$	power–law component		line component			ΔC	p–value	Corrected p–value	
	(d.o.f.)	norm.	index	λ (Å)	τ_0	$\log N(\mathrm{cm}^{-2})$	(d.o.f.)		$P_{\rm binom}$	$P_{\rm sim}$
O VII $z=0.1876$ (# 1)	103.5(87)	$1968\pm^{685}_{481}$	$0.886\pm^{0.385}_{0.412}$	25.6545	$0.57\pm^{0.27}_{0.25}$	$15.26\pm^{.14}_{.21}$	6.6(1)	1.0×10^{-2}	—	—
		$1909\pm^{661}_{463}$								
O VIII $z=0.1898$ (#3)	38.4(28)	$760.9\pm^{8.0}_{6.7}$	2.0	22.569	$0.41\pm^{0.45}_{0.31}$	$15.53\pm^{.23}_{.33}$	1.6(1)	0.21	—	—
O VII $z=0.4339$ (free)	119.7(87)	$486.0\pm^{5.2}_{5.4}$	2.5	$30.975\pm^{0.009}_{0.007}$	$3.33\pm^{1.45}_{1.10}$	$15.73\pm^{.13}_{.05}$	29.9(2)	3.2×10^{-7}	4×10^{-5}	¡0.001
		$476.0\pm^{4.5}_{4.6}$								
O VII $z=0.3551$ (free)	117.6(90)	$814.6\pm^{8.6}_{7.2}$	2.0	$29.283\pm^{0.020}_{0.008}$	$0.92\pm^{0.63}_{0.35}$	$15.38\pm^{.22}_{.13}$	8.2(2)	1.7×10^{-2}	0.88	0.46
		$780\pm^{7.5}_{5.5}$								

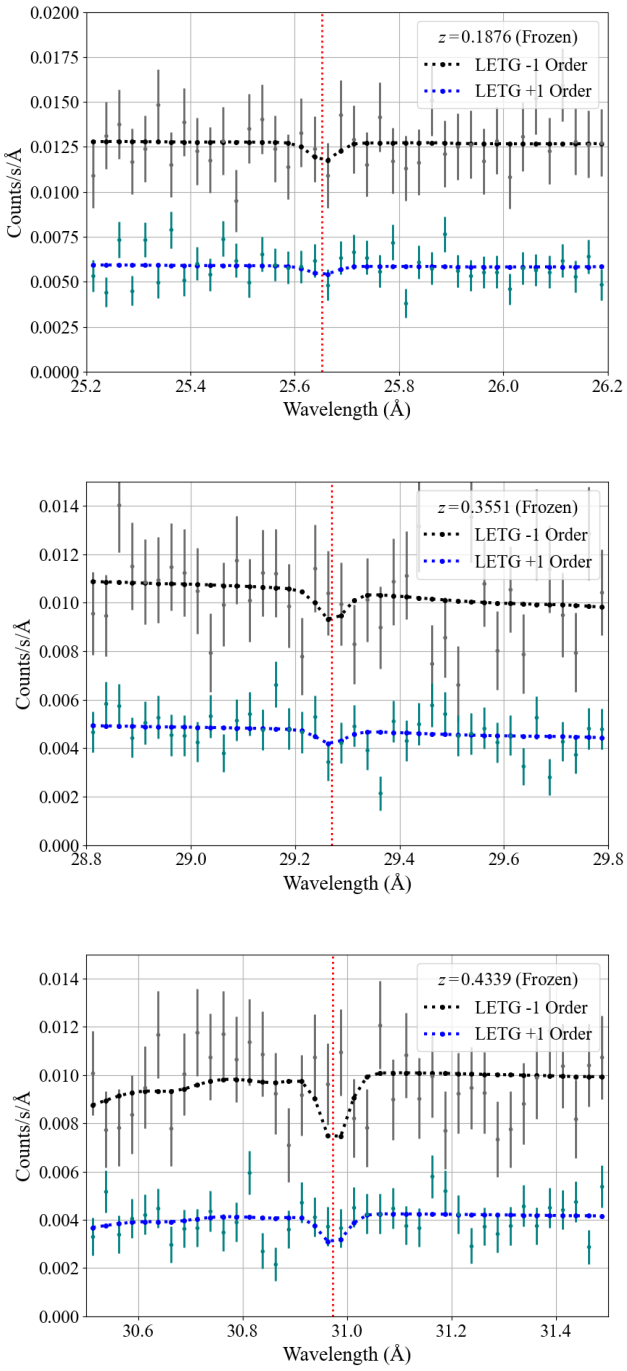

Figure 2.7: *Chandra* HRC LETG spectra in 1 Å intervals around the three wavelengths of interest. The -1 order spectra were rescaled by a factor of two, for clarity.

Table 2.3: Results of the power–law plus `line` model for the *Chandra* LETG data. The ΔC statistic refers to zeroing out the nested `line` component. The rightmost column reports the ΔC statistic corresponding to the comparison between the best–fit model, and a model where the `line` component was fixed at the *XMM-Newton* RGS best–fit values from Table 2.2, instead of the best–fit from *Chandra* data (this table).

Target line	$C_{\rm min}$	power–law component		line component				RGS best-fit	
	(d.o.f.)	norm.	index	λ (Å)	τ_0	$\log N(\mathrm{cm}^{-2})$	ΔC	ΔC	d.o.f.
O VII $z = 0.1876$ (# 1)	80.66(77)	$1510\pm^{31}_{31}$	2.0	25.6545	$0.32\pm^{0.60}_{0.46}$	$15.03\pm^{0.34}$	0.44	0.2	1
O VIII $z = 0.1898$ (#3)	28.82(30)	$1369\pm^{35}_{35}$	2.0	22.5693	$1.37\pm^{2.2}_{1.0}$	$15.87\pm^{0.22}_{0.45}$	2.09	—	—
O VII $z = 0.4339$ (free)	92.45(76)	$876\pm^{21}_{20}$	2.5	31.0138	$0.51\pm^{0.7}_{1.0}$	$15.23\pm^{0.31}$	0.77	10.9	2
O VII $z = 0.3551$ (free)	97.26(76)	$1426\pm^{33}_{32}$	2.0	29.3492	$2.06\pm^{1.1}_{1.1}$	$15.70\pm^{0.11}_{0.24}$	6.58	5.3	2

evidence for the other detection. The stacked spectra analysis did not reveal any evidence for the presence of additional X–ray absorbing WHIM.

Using the O VII upper limit of $15.13\pm^{0.19}_{0.31}$ cm^{-2} given from the slab model analysis provided a $\Omega_{OVII} = (22 \pm 11) \times 10^{-6}$ and a corresponding cosmological density of $\Omega_{WHIM,X} = 0.021 \pm 0.011(\frac{A}{0.1Solar})^{-1}(\frac{f_{ion}}{1.0})^{-1}$. Finally, using this cosmological density and the standard expectation of $\Omega_b \simeq 0.048$, we obtained a $\frac{\Omega_{WHIM,X}}{\Omega_b} = 0.44 \pm 0.22$. This 44% ratio of baryons detected to the total baryonic budget aligns very closely with the suspected amount 40% of missing baryons in the hot WHIM.

Although the $\frac{\Omega_{WHIM,X}}{\Omega_b}$ value corresponded to a significant fraction of the cosmological density of the present-day baryons, the limited statistical significance of 2.6-σ caused for a determination of the absorption line detection to be tentative. If this line is interpreted as a detection however, it would indicate significant evidence towards the WHIM containing the missing baryons. Given this

information, the conclusion that a large sample of X-ray sources was required to make an accurate determination of the cosmological density of the WHIM was made, as the results of our analysis on 1ES 1553+113 proved quite promising in the way of calculating the baryonic budget contributed by the hot WHIM.

2.2.3 Extension To Main Analysis

In addition to the promising results of the analysis, the feasibility study on the ability to extended this analysis to a large sample of sources was a success. Throughout the process of analysing 1ES 1553+113, various elements required for a larger analysis were developed. First, the pipeline for data reduction of a source with multiple observations into a single spectral file was created in the form of several scripts. This allowed for the entire sample acquisition and reduction process to be nearly completely automated. For a sample of over 50 sources, this saved a significant amount of time for the analysis.

Next, the implimentation of `SPEX` and the corresponding analyses into Python using `PYSPEX` was learned and developed. Although this process was used for the purpose of only completing several fits for 1ES 1553+113, its usage in automating the >1000 fits in the main analysis proved to be invaluable. Included in this process was the ability to manipulate and create large amounts of `SPEX` command files at once, and output the plots of every fit completed, including different variations (such as zeroed plots). Manipulating model and fit parameters for hundreds of fits at a time became intuitive and simple through the usage of these scripts and pipeline. In addition to this, the co-moving distances, column

density expectations, final cosmological density Ω_{WHIM}, and other associated values calculated in this paper were extended to the main analysis as well (see Section 3.3.4).

Finally, the usage of several different `SPEX` models in the analysis in this paper allowed for the experimentation of what methods would be used for the main analysis. Not only was a familiarity with the `line` model and its parameters developed, but the decision of its usage and implementation was decided based on the results of the analysis completed on 1ES 1553+113.

Chapter 3. Data and Data Analysis

3.1 The Sample

Although a number of analyses have been completed on the WHIM through X-ray sources (including the case study described in Section 2.2), a larger sample size is needed for an accurate representation of the local universe and WHIM. This sample requires a large number of sources with both previously analyzed FUV systems and X-ray observations that are readily available. The sample chosen for this project is a combination of both [65] and [21], for a total of 51 sources from the FUSE and HST/COS missions. These sources have both FUV priors detections and X-ray data, making them prime candidates for analysis. This sample is shown in Table 3.1, with information about each source's FUV O VI and H I BLA systems as well as information on the *XMM-Newton* and *Chandra* data available.

After the main sample was chosen, the process of sorting and creating a list of redshifts to search for in the analysis was needed. Tables of all redshift priors of both O VI and H I were collected from [21] and [65], which contained information on the FUV systems. Among this information was the O VI and H I prior detection redshifts and column densities. Because of significant overlap between the two compiled papers, as well as the format of O VI information being

contained in doublets for [21], further reduction of these redshifts was required. This was completed by filtering out all duplicate redshifts of the same source between the papers, with a resolution of the filter of $z = 0.00015$. Following this initial filter, sources in doublet format were either combined together through a weighting process of 2 to 1 in favor of 1032, or the values were reported alone if the doublet did not have a pair. The compiled results of these prior detections are in Tables 3.2 and 3.3. Ultimately, these prior detection redshifts would go on to be the redshifts used in the main analysis of this project.

Table 3.1: List of X-ray sources with O VI and/or H I BLA priors. "FUV systems" is the number of O VI and H I BLA priors. The number of pointed observations per source and the total exposure time in ks is also reported under "Number of obs. and time (ks)" for both *XMM-Newton* and *Chandra* data. This sample forms the list of all 51 sources used for the primary analysis of this project.

	Source	z	FUV systems		Number of obs. and time (ks)				
			OVI	HI BLA	XMM		Chandra		
1	1ES1028+511	0.3604	4	3	5	312	1	149	•
2	1ES1553+113	0.4140	7	4	22	1998	3	496	•
3	3C249	0.3115	4	2	1	37	0	0	•
4	3C273	0.1583	10	4	35	1282	2	70	•
5	3C66A	0.3347	2	1	2	27	0	0	•
6	H1821+643	0.2968	15	7	15	130	4	470	•
7	H2356-309	0.1651	2	4	9	704	11	587	•
8	HE0056-3622	0.1641	2	0	4	186	0	0	•
9	HE0226-4110	0.4934	61	3	1	33	0	0	•
10	IRASF22456-5125	0.1000	8	2	4	108	0	0	•
11	MR2251-178	0.0640	1	7	10	610	1	78	•
12	Mrk421	0.0300	1	0	102	2876	38	639	•
13	Mrk478	0.0791	0	3	5	252	1	80	•
14	Mrk876	0.1290	6	6	2	21	0	0	•
15	NGC7469	0.0163	3	1	11	857	0	0	•
16	PG0157+001	0.1631	1	0	1	15	0	0	•
17	PG0003+158	0.4509	17	5	1	26	0	0	•
18	PG0804+761	0.1000	4	3	3	103	0	0	•
19	PG0832+251	0.3298	5	8	1	23	0	0	•
20	PG0838+770	0.1310	0	3	1	24	0	0	•
21	PG0953+414	0.2341	11	2	1	16	0	0	•
22	PG1048+342	0.1671	0	2	1	33	0	0	•
23	PG1115+407	0.1546	5	3	1	21	0	0	•
24	PG1116+215	0.1763	9	9	6	395	11	356	•
25	PG1211+143	0.0809	4	2	12	883	3	134	•
26	PG1216+069	0.3313	8	8	1	17	0	0	•
27	PG1229+204	0.0630	0	1	1	26	0	0	•
28	PG1259+593	0.4778	14	10	1	34	0	0	•

	Source	z	FUV systems			X–ray data			
29	PG1307+085	0.1550	2	1	1	14	0	0	•
30	PG1309+355	0.1829	11	5	1	30	0	0	•
31	PG1444+407	0.2673	6	1	1	22	0	0	•
32	PG1626+554	0.1330	1	1	1	11	0	0	•
33	PHL1811	0.1920	13	6	2	92	0	0	•
34	PKS0312-770	0.2230	2	1	4	153	0	0	•
35	PKS0405-123	0.5740	26	13	2	170	4	376	•
36	PKS0558-504	0.1372	0	1	20	1096	0	0	•
37	PKS1302-102	0.2784	11	8	1	16	0	0	•
38	PKS2005-489	0.0710	1	0	3	62	4	282	•
39	PKS2155-304	0.1165	2	4	36	2191	15	319	•
40	PMNJ1103-2329	0.1860	5	0	2	27	0	0	•
41	PMNJ2345-1555	0.6210	12	5	1	32	0	0	•
42	Q1230+0115	0.1170	15	13	1	71	0	0	•
43	QSO0045+3926	0.1340	2	2	1	17	0	0	•
44	RBS1892	0.2000	3	6	1	22	0	0	•
45	RBS542	0.1040	2	2	11	369	0	0	•
46	RXJ0439.6-5311	0.2430	7	2	2	162	0	0	•
47	S50716+714	0.2315	1	4	5	180	0	0	•
48	TonS210	0.1160	0	2	1	9	0	0	•
49	Ton28	0.3297	7	1	3	108	0	0	•
50	Ton580	0.2902	2	0	2	48	0	0	•
51	TonS180	0.0620	3	1	4	223	1	77	•

3.2 Data Processing

3.2.1 Acquisition and Reduction

Processing the data from the sample followed a three step process. First, using a list of the names of sources needed, a search was done on the *XMM-Newton* and *Chandra* data archives using an automated script. This script found the observations from their respective databases, and downloaded every observation made on each of the sources into an organized folder structure. Following this download, another series of shell and Python scripts were used to reduce the data and combine multiple observations in each source into one spectral file. The respective software for both *XMM-Newton* and *Chandra* were used in this process. For the *XMM-Newton* files, *XMM-Newton* SAS (Science Analysis Software) was used to combine multiple observations in each source, rebin the data,

Table 3.2: List of O VI absorption line systems from the T12/D16 samples. A '^{M}' indicates that there was an OVI 1032 and 1038 doublet present. These 1032 and 1038 doublet values were averaged into one value on a weighted system of 2:1 respectively. A '*' indicates a duplicate redshift in both Danforth and Tilton. The corresponding Tilton duplicates are omitted from the table. A complete list is available in Table A.1.

#	Name	Redshift	$\log N$ (cm^{-2})	b (km s^{-1})	Source
1	1es1028	0.12314	14.3±0.1	41.37±5.57	Danforth^M
2	1es1028	0.13706	13.6±0.1	14.50±6.30	Danforth^{1032}
3	1es1028	0.33735	13.9±0.1	72.87±15.73	Danforth^M
4	1es1553	0.18759	13.8±0.1	12.10±3.00	Danforth^M
5	1es1553	0.18775	13.9±0.1	23.40±4.50	Danforth^M
6	1es1553	0.18984	13.4±1.5	23.37±6.57	Danforth^M
7	1es1553	0.21631	13.3±0.1	19.80±5.80	Danforth^{1032}
8	1es1553	0.31130	13.4±0.1	31.90±7.50	Danforth^{1032}
9	1es1553	0.37868	12.9±0.2	17.30±3.70	Danforth^{1032}
10	1es1553	0.39497	13.9±0.1	44.07±3.33	Danforth^M
..					

Table 3.3: List of H I BLA absorption line systems from the T12/D16 samples. A '*' indicates a duplicate redshift in both Danforth and Tilton. The corresponding Tilton duplicates are omitted from the table. A complete list is available in Table A.2.

#	Name	Redshift	$\log N$ (cm^{-2})	b (km s^{-1})	Source
1	1es1028	0.13714	13.3±0.1	91.60±24.00	Danforth
2	1es1028	0.20383	13.2±0.1	63.60±14.20	Danforth
3	1es1028	0.22121	13.4±0.8	68.60±71.40	Danforth
4	1es1553	0.03466	13.1±0.0	72.00±9.40	Danforth
5	1es1553	0.04273	13.4±0.0	63.00±4.50	Danforth
6	1es1553	0.06364	13.0±0.2	76.30±19.90	Danforth
7	1es1553	0.21869	12.7±0.1	62.60±21.80	Danforth
.					

separate the RGS1 and RGS2 detectors in the spectrum file, and to create the background spectrum. *Chandra*'s software, CIAO (Chandra Interactive Analysis of Observations), followed a similar process to *XMM-Newton*'s SAS. CIAO was used to reprocess the *Chandra* data into .pha files, and to further combine the observations of each source. Finally, with all of the source files processed and combined into singular spectra, these spectra were converted into a format usable in `SPEX` using a software called "Trafo". Trafo allows for the conversion of file formats such as ".FIT" (*XMM-Newton*) or ".pha" (*Chandra*) into `SPEX` spectrum ".spo" and response ".res" files. This was completed again with the aid of automated scripts created to go through each source individually and run Trafo on their respective spectral files.

3.2.2 Data Exclusions and CCD Gaps

In addition to processing the data into a usable format for `SPEX` and the analysis, each spectrum were studied for regions that needed to be excluded from the analysis. The LETG (*Chandra*) and RGS (*XMM-Newton*) spectrometers onboard the telescopes used for this project contain numerous regions of measurement errors and "bad pixels". These regions typically contain data points that are skewed significantly from the spectrum and interfere with the models used to fit to the data described in section 3.3. Another example of the regions that needed to be removed were areas of the spectrum with absorption of ions other than O VII and O VIII. Ions such as O I, O II, etc. were occasionally observed through galactic absorption, which resulted in a similar issue with fitting as the

bad pixels had. To deal with this, a series of exclusion zones were recorded. All initial fits that resulted in a reduced C statistic of 1.5 or higher were inspected for these zones, and the removal of these poor data points continued until every fit had a sufficient reduced C statistic. In conjunction with poor data point removal, a plethora of these poor fits were improved simply my allowing the index parameter to become a free variable with the model. In these cases, the index values in Tables B.1-C.8 are listed as values other than 1.0 (the value set for the fixed index). Many of the spectrums contained evidence of intrinsic O VII absorption lines within the range of their redshifted O VII or O VIII searches as well, which severely skews the model away from the continuum. As a result, a base exclusion of 21.5-21.7 was used for all regions in both *XMM-Newton* and *Chandra* spectra. Additionally, *XMM-Newton* features a significant amount of inefficiencies around this region, so *XMM-Newton*'s exclusion of this range was extended to be 21.5-21.9Å.

Early on in the *XMM-Newton* mission, electronics problems caused two of the CCD assemblies to fail (one in both RGS1 and RGS2 respectively). This resulted in data being completely absent from 11-14Å for RGS1, and 20-24Å for RGS2 [1]. Typically this would not be an issue for the data processing as these regions would not have any data for their respective regions. However, a number of the sources used in this project have observations in the *XMM-Newton* archive dating back to before this CCD hardware failure. Because of this, the reduction and merging process of the observations of those sources created unsatisfactory

[1]From *XMM-Newton* Calibration Note XMM-SOC-CAL-TN-0030 issue 7.11: `https://xmmweb.esac.esa.int/docs/documents/CAL-TN-0030.pdf`

data in those regions. As the merging process essentially "averages" all of the observations of their source, the average of both empty data and proper data resulted in large errors and faulty data. Because of this and the majority of the project's *XMM-Newton* observations containing no data in these regions, an additional exclusion of 20-24Å for RGS2 was made for all *XMM-Newton* sources. The 11-14Å exclusion was not needed as the wavelengths searched were always higher than this range.

3.2.3 Poor C_{min} Fits

During the process of excluding data points from poor fits, a number of fits were found that simply could not have their C statistic reduced further, or otherwise could not achieve a proper fit. This occurred for a variety of reasons, including:

- A significant amount of data inefficiencies (specifically for the RGS spectrometers on *XMM-Newton*) or inherent gaps in the data that lie directly on the suspected wavelength of possible absorption lines. This results in a poor fit as the model is unable to fit properly to this inefficiency, and the inefficiency cannot be removed as it is on the wavelength of focus.

- The data reduction process resulted in a continuum that is difficult to model. As described above, some sources that are old enough to have differing observations in the archive from modern observations created spectra that resulted in poor fits.

- The quality of the data and low count rates of many sources. As many of the *XMM-Newton* spectra are of particularly low quality and low count rates, the model can have a difficult time fitting these spectra occasionally.

Although a significant amount of work went into making sure every fit was sufficiently satifactory (below a value of 1.5 reduced $C_{\rm min}$), these issues still resulted in a number of these higher reduced C statistic fits being reported. These fits are indicated by a "*" next to their fit statistic in the full analysis results Tables B.1-C.8, and the abbreviated results in Tables 5.1-5.16.

3.3 Data Analysis

3.3.1 Atomic Properties and Absorption

As previously stated, the ions of focus for this project are O VII and O VIII. Besides the predictions of `EAGLE` simulations showing that O VII and O VIII have a high correlation to O VI and H I FUV priors, O VII and O VIII also have ionization curves that peak in the temperatures of interest in this study. Specifically, at 10^6 K, O VII and O VIII are the oxygen ions with the highest ionization fraction. A plot of these ionization fractions is shown in Figure 3.1. Ne IX is another ion of interest in this temperature region, but ultimately the decision was made to forgo the analysis of this ion. This is described more in the later section on limitations of the project, Section 6.1. Although the absorption line analysis in this project is conducted on O VII and O VIII primarily, the discussion over other oxygen ions and galactic lines is quite important. In the

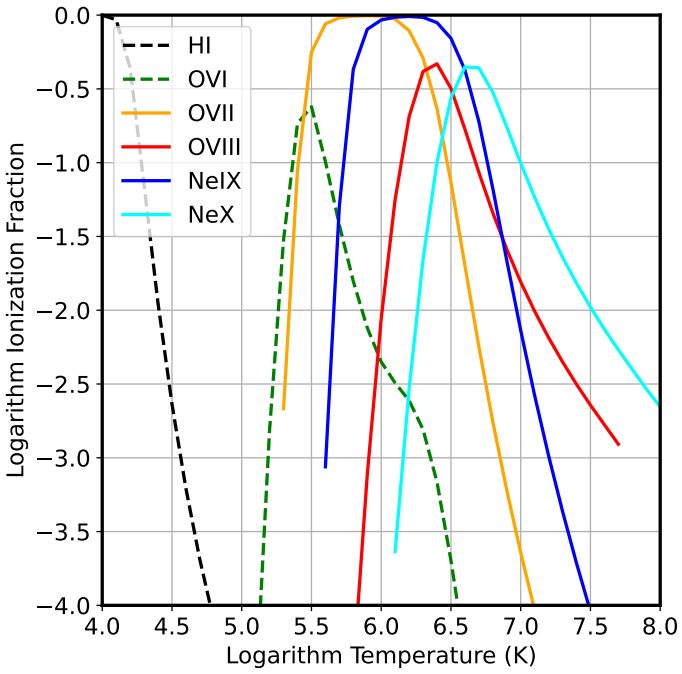

Figure 3.1: Ionization curves of key ions from [48]. Note that the oxygen ions of interest fall in the expected temperature range of the WHIM, $10^5 - 10^7$K.

Table 3.4: Wavelengths and atomic properties of key WHIM lines, and of inner–shell oxygen Galactic lines that may cause confusion in the identification of redshifted oxygen WHIM lines. References for atomic data: [68] (V96); [38] (G05); [33] (G15); [35] and [53] (G11). See also Table 1 of [51] for other lines of relevance to the WHIM, and [31] for other $K\alpha$ atomic data for oxygen.

Ion	Line	Wavelength (Å)	Osc. strength	Reference
		WHIM lines		
O VII	$1s^2 - 1s2p$ (Heα)	21.602	0.696	V96
O VII	$1s^2 - 1s3p$(Heβ)	18.629	0.146	V96
O VIII	$1s - 2p$ (Lyα)	18.969 (18.973,18.967)	0.416	V96
O VIII	$1s - 3p$ (Lyβ)	16.006 (16.007,16.006)	0.079	V96
Ne IX	$1s^2 - 1s2p$ (Heα)	13.447	0.724	V96
Ne X	$1s - 2p$ (Lyα)	12.134 (12.138,12.132)	0.416	V96
		Galactic lines		
O I	$2p^4 - [1s]2p^5$	23.506	—	G15
O I	$2p^4 - [1s]2p^4 3p$	22.889	—	G15
O II	$2p^3 - [1s]2p^4$	23.346	—	G15
O II	$2p^3 - [1s]2p^3 3p$	22.287	—	G15
O III	$2p^2 - [1s]2p^3$	23.110, 23.057	—	G15
O IV	$1s^2 2s^2 2p - 1s2s^2 2p^2$	22.741	0.46	G05
O V	$1s^2 2s^2 - 1s2s^2 2p$	22.363	0.55	G05
O VI	$2s^2 - [1s]2s2p$	22.024	—	G15
N II	$1s^2 2s^2 2p^2 - 1s2s^2 2p^3$	29.99-31.16	—	G11

analyzed spectra, absorption from these other ions is observed often, and in a near identical visual fashion to O VII and O VIII. Because of the sheer size of the sample and amount of redshifts searched in the analysis, galactic lines (oxygen mainly) are observed in many of the expected wavelength ranges of the ions of focus. These occurrences are generally indistinguishable from real detections, and as such a large amount of overlapping wavelengths were discounted as oxygen galactic lines.

The galactic lines and WHIM absorption line wavelengths are listed in Table 3.4.

3.3.2 Automation of Analysis

Using the methodology from our paper studying 1ES1553+113, that analysis (namely the line model analysis) was extended to the entire sample in several parts. To begin, a list of all O VI and H I priors for the sample was created, similar to the eight priors used in the 1ES1553+113 case study. The list of O VI and H I prior detections provided a master reference for all of the redshifts and corresponding O VI and H I column densities for analysis. A script was created to automate the creation of the separate `SPEX` command files for each redshift prior in the sample. These files included not only the model parameters and fit commands for the `line` and power law models used in the analysis, but also the exclusion regions and plot commands as well. More information on the `line` model and its parameters is in Section 3.3.3. Coupled with this, an automated Python script using `PYSPEX` and the aforementioned command files was made.

This Python script executed each command file on their respective spectral files, and output all of the resultant parameters into a table for the respective data instrument (*XMM-Newton* or *Chandra*), ion (O VII or O VIII), and FUV prior (O VI or H I). After the first round of the analysis was done, a pass was made over every fit recorded in search for a reduced C statistic higher than 1.5. These fits were then input into respective tables and analyzed individually to create a master "ignore" command file for the fits to use. This was done by searching for regions in the spectra with poor data quality or "bad" pixels, and removing those regions using the `SPEX ignore` command (Section 3.2.2).

After the automated scripts were complete and all the resultant fits had a satisfactory reduced C statistic, the calculation of the WHIM's contribution to the baryonic density of the universe ($\Omega_{WHIM,X}/\Omega_b$) could begin.

3.3.3 The Line Model

After the preliminary analysis using `SPEX` was completed on 1ES1553+113 (Section 2.2), the decision of what model to use was up for debate. In the case study, both the spline/slab and line model method were used in the analysis. The primary decider in the decision came down to the implimentation of absorption line modeling in both models. The `slab` model in `SPEX` only allows for absorption, whereas the `line` allows for both absorption and emission lines through the τ_0 parameter. This feature of the `line` model satisfies the critera for hypothesis testing with a χ^2 distribution for the resulting ΔC statistics. Although this model does not have the convenient features of the `slab` model (*i.e.*, the atomic

physics needed to interpret a fluctuation as an ion column density), this additional regression is more readily capable of answering the question of whether there is a line–like fluctuation in correspondence of the expected X–ray lines. For this reason, the `line` model was used in the final analysis of the entire data sample. As per the `SPEX` manual[2], the line model calculates the transmission $T(E)$ for a single spectral emission or absorption model. The line profile is the convolution between a Gaussian and a Lorentzian profile known as the Voigt profile:

$$T(E) = e^{-\tau(E)}, \tag{3.1}$$

where $\tau(E)$ is the optical depth defined by:

$$\tau(E) = \tau_0 K(x, y) \tag{3.2}$$

with $K(x, y)$ as the Voigt profile given by:

$$K(x, y) = \frac{y}{\pi} \int_{-\infty}^{\infty} \frac{e^{-t^2}}{y^2 + (x - t)^2}\, dt, \tag{3.3}$$

where x and y are:

$$x = \frac{2\sqrt{\ln 2}}{F_g}(E - E_0) \tag{3.4}$$

$$y = \sqrt{\ln 2}\frac{F_l}{F_d}, \tag{3.5}$$

where F_g is the full width at half maximum of the Gaussian component, F_l is the full width at half maximum of the Lorentzian component, and E_0 is the line

[2] `SPEX` manual link here

Table 3.5: `SPEX` line model parameter values for analysis. $\lambda_{O_{ion}}$ indicates the expected wavelength of the given oxygen ion at zero redshift, or the galactic line. $(1+z)$ is the shift factor that redshifts (of redshift value z) the wavelength to the value of the expected absorption line.

Parameter	SPEX name	value	status
τ_0	tau0	2.0	free
type	type	1	–
F_g (Å)	awhg	0.01	fixed
F_l (Å)	awhl	0.0	–
E_0 (Å)	wl	$\lambda_{O_{ion}}(1+z)$	fixed

centroid. Importantly, the `line` model also calculates the equivalent width of the absorption line, which is explored further in its use for calculating the column density in Section 3.3.4.

As the process of analysis is automated, the usage of the `line` model in `SPEX` was completed entirely using command files for each redshift searched. Every command file assigned values and statuses to each parameter in the `line` model before the initial fit and value collection in the scripts. These parameter manipulations are listed in Table 3.5.

After assigning these values, *XMM-Newton* data were given special care as they contain two regions (RGS1 and RGS2) in comparison to *Chandra*'s one. This was done by copying the entire first sector of the model, and coupling the region 2 parameters to their region 1 counterparts. Coupling links the RGS2 parameters to the RGS1 parameters, giving them the same value. This means that a change in the RGS1 parameters also adjusts the RGS2 parameter accordingly. Following

this coupling, the data are fit once again and plotted to an image file for later inspection.

3.3.4 Calculations and Analysis

In order to use the results of the analysis in the calculations for the baryonic density of the WHIM, the column density and subsequent upper limits of those column densities are needed. Because the line model in `SPEX` contains an equivalent width parameter connected to its τ_0 value, the column density N (in units of cm^{-2}) of each fit can easily be calculated using Equation 2 from [8]:

$$N = 1.13 \times 10^{20} \frac{W_\lambda}{\lambda^2 f} \ \mathrm{cm}^{-2}, \tag{3.6}$$

where f is the oscillator strength for O VII or O VIII (depending on the current analysis, see Table 3.4), W_λ is the equivalent width in Å given by the line model in `SPEX`, and λ is the wavelength of O VII or O VIII at zero redshift. And of course in order to calculate $\log N$, the base 10 logarithm of N is taken. According to this equation, the equivalent width W_λ and column density N follow a linear relationship. However, we have observed that at higher values of W_λ or τ_0, this relationship does not hold properly. To account for this, typically the effects of the "curve of growth" are taken into consideration. The curve of growth calculates how a line strength (equivalent width) increases in correspondence to the optical depth of that line's increase. An example of this curve of growth for O VII from [49] is shown in Figure 3.2. An associated parameter with this curve of growth is the b (velocity dispersion) parameter of the plasma, which is a function of

temperature. Because the exact temperature of the plasma is unknown for this project, the b parameter is an unknown parameter that could not be measured for our analysis. As a result of this, we came to the decision to exclude the effects of the curve of growth in the calculation of the column density with the equivalent width. The result of this is that $\log N$ is systematically underestimated when the τ_0 (and by extension W_λ) are very large.

Although the exact temperature was not calculated for this analysis, a possible method for calculating the temperature of the plasma of study is discussed in [3] or [2]. This method involves relating the O VIII and O VII line ratios to estimate the temperature of the medium along the sightlines of focus. Specifically, constraints can be put onto the temperature through the ratio of the equivalent widths of various ions to the ions of focus. In [2] for example, the equivalent width of Ne IX, Fe XVII, O VII, and N VII were all compared to O VIII in order to constrain the CIE temperature. This method is similar to that of comparing iron (Fe) K and L-shell line ratios as well, described in papers such as [16].

Using Equation 3.6, the upper limit of the column density of oxygen in each fit can be calculated using the upper limits of τ_0. This is done by calculating the upper and lower error of the τ_0 using the "error" command in `SPEX`, and then setting that τ_0 parameter to the average of the absolute value of those upper and lower errors:

$$\tau_0{}^{+} = \frac{|\tau_{0+err}| + |\tau_{0-err}|}{2}. \tag{3.7}$$

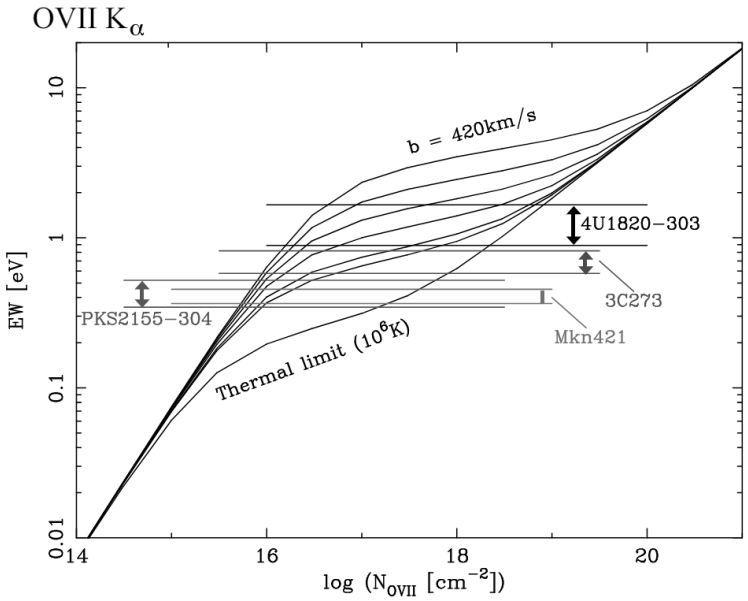

Figure 3.2: An example of the curve of growth for O VII $K\alpha$ from [49]. The different curves correspond to different values of b, which is an unknown quantity for our analysis. The horizontal lines are equivalent widths associated with different observations.

Using this method for calculating the upper limit of τ_0 ensures that the value of ${\tau_0}^+$ is positive, as setting the τ_0 parameter to a negative value in `SPEX` results in a negative equivalent width. This results in a negative column density (using Equation 3.6), which is unusable in the analysis and further equations to calculate Ω values.

In `SPEX` the τ_0 parameter's value is then set to ${\tau_0}^+$, and the fit is recalculated using the "calc" command to yield the corresponding equivalent width value. Using Equation 3.6, this "${W_\lambda}^+$" is used to calculate an upper limit on the column density, N^+ for each fit. All of the N^+ were then paired with their matching O VI or H I prior column densities stored in text files, and read into a Python script to calculate the values corresponding to the analysis in [64]. First, the expectation of undetectable $N_{ion,j}$ is calculated using the prior column densities and the N^+ for each fit:

$$E[N^+_{ion,j}] = \frac{\int_0^{N^+_{ion,j}} N_{\rm ion} P(N_{\rm ion}) dN_{\rm ion}}{\int_0^{N^+_{ion,j}} P(N_{\rm ion}) dN_{\rm ion}}, \tag{3.8}$$

$$E[N^+_{ion,j}] = \sum_{j=1}^{N_i} E[N^+_{ion,j}] \tag{3.9}$$

and the density of the ion, ρ_{ion} was calculated using:

$$\rho_{ion} = m_{ion} \frac{E[N^+_{ion}]}{\sum D_i}, \tag{3.10}$$

where m_{ion} is the atomic mass of the ion (16u for oxygen), $E[N^{+}_{ion}]$ is the expectation of the ion's upper limits, and $\sum D_i$ is the sum of the effective distances D_i for the given detector and prior type:

$$D_i = (\frac{3}{4}\frac{A}{\pi}(V_c(z_{max}) - V_c(z_{min})))^{1/3}, \tag{3.11}$$

where A is the solar abundance determined by the ion, z_{max} is the actual estimated redshift of the source, $z_{min} = 0$, and V_c is the comoving volume. Finally, given the calculation of ρ_{ion}, the cosmological density $\Omega_{WHIM,ion}$ can be calculated using the mass density of an ion, Ω_{ion}:

$$\Omega_{ion} = \frac{\rho_{ion}}{\rho_c}, \tag{3.12}$$

where ρ_c is the critical density of baryons at the present epoch. Corresponding to this,

$$\Omega_{WHIM,ion} = \Omega_{ion}\frac{\mu\ m_H}{m_{ion}}\frac{1}{A \cdot f_{ion}(T)}, \tag{3.13}$$

where f_{ion} is the previously mentioned oscillator strength of the ion, and $\frac{\mu\ m_H}{m_{ion}}$ is the mass ratio of hydrogen to the ion in atomic mass units. Ultimately, this cosmological density of the WHIM is compared to the entire baryon budget $\Omega_b \simeq 0.048$:

$$\frac{\Omega_{WHIM,ion}}{\Omega_b} = Ratio_{WHIM,ion}, \tag{3.14}$$

which is the ratio of the cosmological density of the WHIM's baryons to the cosmological density of the baryons in the universe. This describes the estimated baryon amount contributed to the baryonic budget by the WHIM. This of course is the final desired value, as the missing baryon problem described in Section 1 is about the discrepancy of censuses for sources of baryons contributing to the overall cosmological density of the universe's baryons versus the expected value of those censuses results being Ω_b. The overall goal of these calculations is to see if the calculated cosmological density of the WHIM corresponds to that 40% value expected if the WHIM was the contribution missing from the total baryonic budget. If these values align to a sufficiently close margin, the results of this analysis would imply that the missing baryons were contained within the WHIM. As the analysis on the main sample focuses primarily on upper limits, the upper constrains put on this ratio could also show that current hypotheses are not disproven given the upper constraints are higher than the expected amount of missing baryons.

Chapter 4. Statistics and Statistical Analysis

As this project's main objective is to search for absorption lines in the hot WHIM, a number of considerations and statistics involving the search of these lines is warranted. Our main interface with these absorption lines is through spectral analysis, and seeing a deviation of data (and their corresponding line model) at expected absorption line wavelengths. These deviations occur as a result of the absorption of specific wavelengths of light by a gas, in our case expected O VII and O VIII ions in the WHIM.

4.1 Absorption Line Statistics

4.1.1 EAGLE Simulations

The purpose of using the spectral models provided by `SPEX` is to determine the presence of X-ray absorbing material along the sightline at a fixed redshift. This is done through the search and analysis of X-ray absorption lines in the spectra. As described in Section 3.1, the presence of FUV absorption line prior detections may act as sign-posts for the higher-temperature ions. This is important as searching prior known redshifts is significantly more efficient than performing a blind search at all redshifts for a source. Completing this search of absorption lines assumes that the WHIM is multi-phase, and that lower-temperature ions

provide a prior for the redshift that increases the statistical significance and the overall credibility of any associated X-ray detection. This assumption is consistent with the positive detections made using 3C 273, Ton S180, and PG 1116+215 [3, 2, 8]. The use of FUV ions as indicators for O VII and O VIII is also suggested by the analysis of `EAGLE` (Evolution and Assembly of GaLaxies and their Environments) simulations by [70], who finds significant correlation between both O VI and H I absorption with both O VII and O VIII. Figure 4.1, reproduced from [70], illustrates the `EAGLE` predictions for these distributions of the column densities of O VI and O VII ions in a 100^3 Mpc^3 simulation of the universe at low redshift, and for the distribution of H I and O VII. These joint distributions are the basis for the prediction of the amount of O VII present along the sightline. The same analysis could be repeated for O VIII, or other X–ray ions. For these ions, there is no information on line widths that was used for their selection, and therefore they represent the entire ionic budget in the `EAGLE` simulations. The distributions of temperature and abundances of the gas used for Figure 4.1 are described in detail in [70]. At $\log N_{\rm OVII}({\rm cm}^{-2}) > 15$, the temperature of the gas is primarily in the range $\log T({\rm K}) = 5.5 - 6.5$, while at $\log N_{\rm OVII}({\rm cm}^{-2}) > 16$ the temperatures are typically $\log T({\rm K}) = 6.0 - 6.5$. The metallicity of the absorbers is almost entirely in the range $\log A = -1$ to -0.5 Solar.

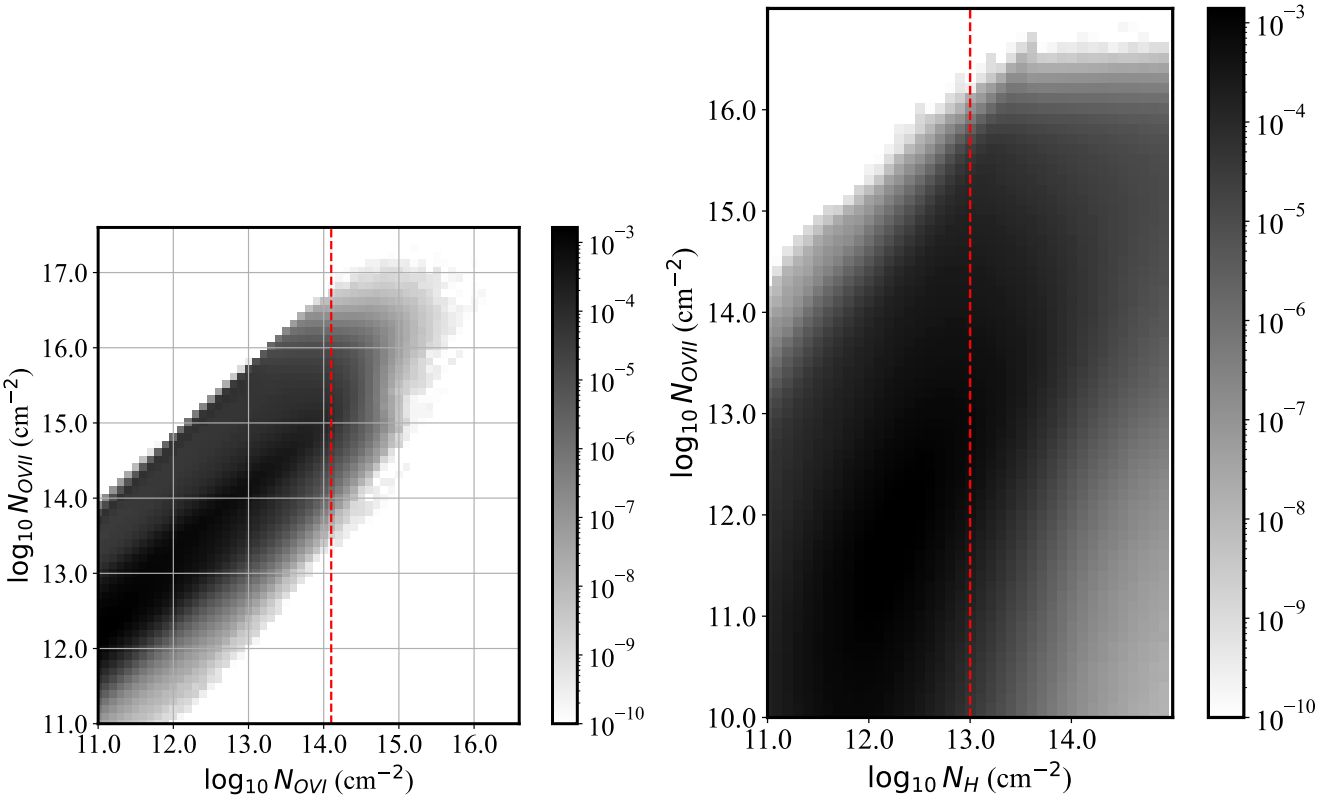

Figure 4.1: Joint probability distribution of (a) O VII and O VI, and (b) O VII and H I, from the `EAGLE` simulations of [70]. The red lines represent respectively the value of the combined O VI column density detected for an absorber corresponding to a O VI column density of $\log N(\text{O VI}) = 14.1$, which feature a possible *XMM-Newton* detection of O VII, and the value of a characteristic H I BLA detection for 4 separate systems. The distribution represents the number of sightlines in `EAGLE` with those column density values, and therefore they are not normalized.

We start by defining the probability p_j that a sightline with a detected O VI column density $N_{\rm OVI}$ at a specific redshift z_j has an amount of O VII larger than the upper limit,

$$p_j = P(N_{\rm OVII} > N^{+}_{\rm OVII} | N_{\rm OVI}). \tag{4.1}$$

Such probability distribution is illustrated in Figure 4.2, which is obtained from a vertical slice of Fig. 4.1 at a given value of the O VI column density. The same considerations apply to H I, whereby the probability in Equation 4.1 is obtained by conditioning on the column density $N_{\rm HI}$ instead of $N_{\rm OVI}$. Equation 4.1 reads as the probability that the column density exceeds the upper limit, given the value of the detected O VI column density. Given that the systems under consideration are those with a known value of the O VI and H I column density, the conditional probabilities of Equation 4.1 illustrated in Figure 4.3 can be immediately used to evaluate the probability p_j by evaluating the integrated probability above the upper limit. This probability quantifies what $p_j < 1$ fraction of O VII absorbers, by number, is observable because of the limits in sensitivity of the X–ray data. Usually this value is small, indicating that the data can only detect a small fraction of possible `EAGLE`–predicted O VII absorbers.

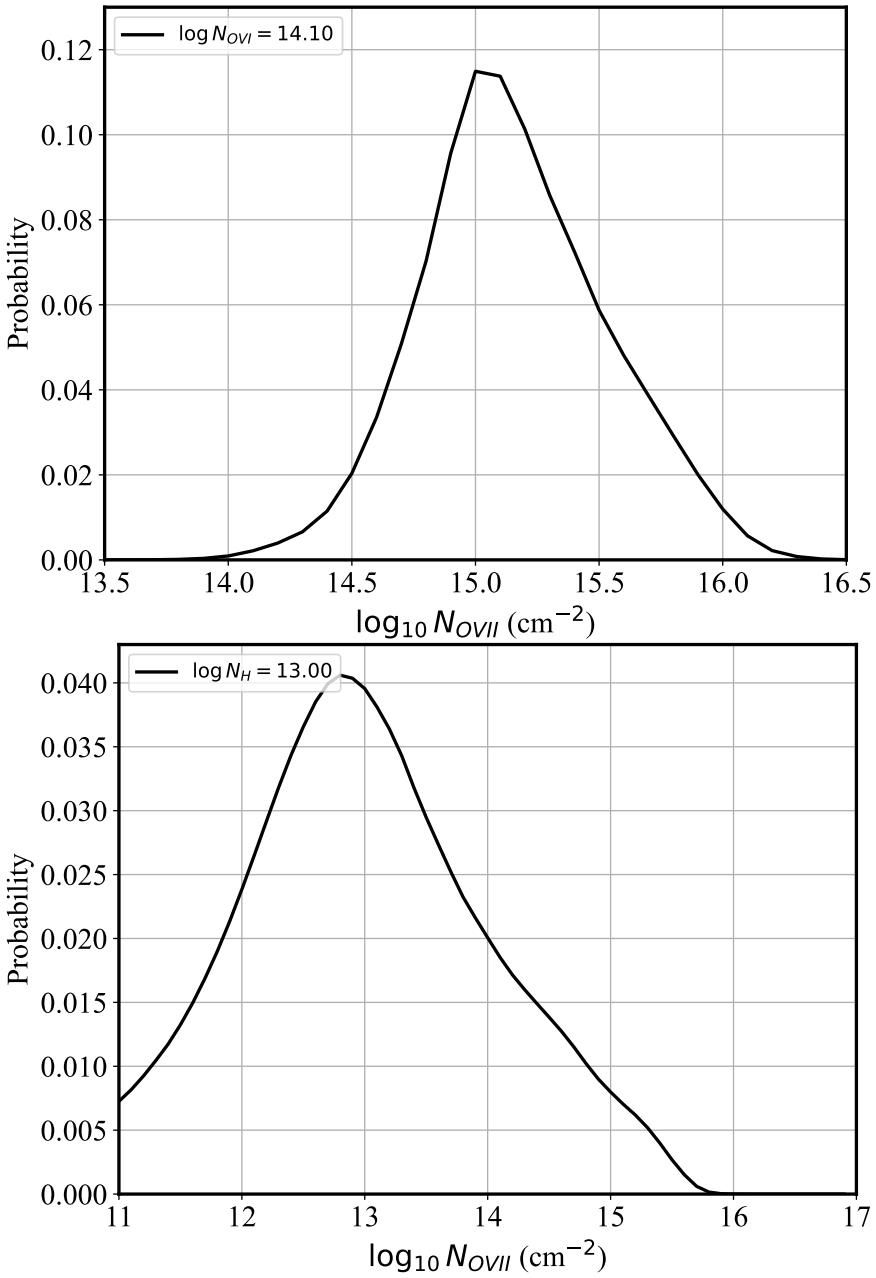

Figure 4.2: Conditional probability distribution of (a) O VII given a range of O VI, and (b) O VII given H I, from [70]. The distributions correspond to the solid red lines in Fig. 4.1, and have been normalized to a total probability of one.

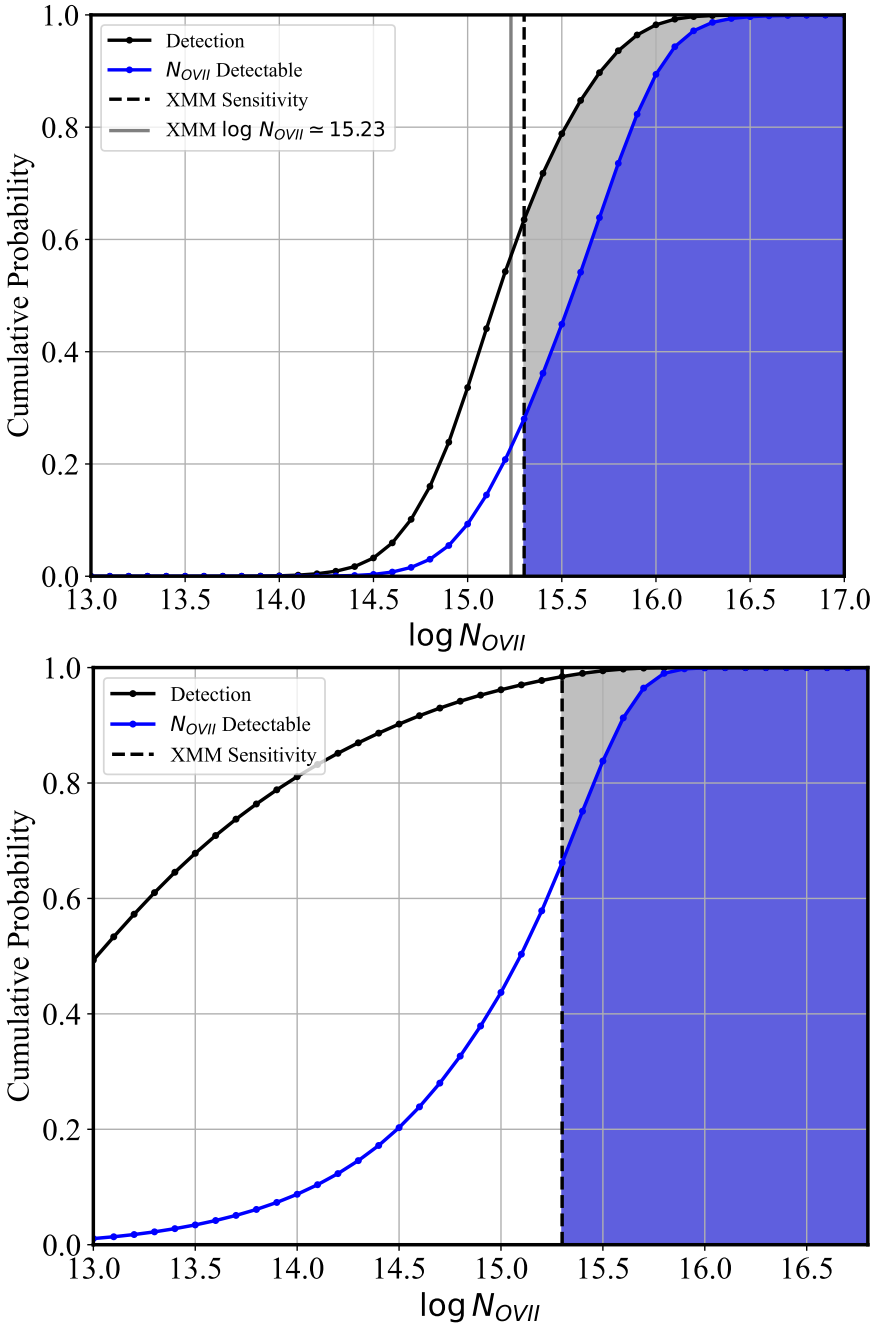

Figure 4.3: (a) Cumulative distributions for O VII with an O VI prior, and (b) for O VII with H I priors. In both panels, black is the cumulative probability distributions for the possible detection of an O VII line, for a fixed value of O VI as in Figure 4.2. In blue, for the same distributions, is the cumulative fraction P_j of the column density of O VII above a given threshold, according to Equation 4.2. On the left panel, for a sensitivity of approximately $\log N = 15.3$ (15.1) for O VII, `EAGLE` predicts that a sightline with $\log N_{\rm OVI} = 14.1$ is expected to have a probability $p = 0.36$ (0.56) to intercept a sightline with $\log N_{\rm OVII} \geq 15.3$ (15.1), and it is is sensitive to a fraction $P_j \simeq 0.72$ (0.86) of O VII.

Since the only detectable absorbers (in the CGM and in filaments alike) are the ones with the highest column density, it is necessary to evaluate another probability that describes the *fraction of the O VII column density* detectable above the upper limit. This probability is defined as:

$$P_j = \frac{\int_{N^+_{\rm OVII}}^{\infty} P(N_{\rm OVII}/N_{\rm OVI}) dN_{\rm OVII}}{\int_0^{\infty} P(N_{\rm OVII}/N_{\rm OVI}) dN_{\rm OVII}}, \tag{4.2}$$

where $P(N_{\rm OVII}/N_{\rm OVI})$ is the same conditional probability distribution used in Equation 4.1, and it is weighed by the ion column density $dN_{\rm OVII}$. This probability describes the cumulative fraction of O VII column density that is detectable, and it is a larger number than p_j because the larger column densities are the observable ones. The evaluation of P_j is illustrated in Figure 4.3, where the solid black curve is the cumulative distribution of the marginal probability distribution in Figure 4.2, and the blue curve represents the fraction of O VII column density present *below* that value of $\log N_{\rm OVII}$, *i.e.*, its cumulative distribution function. For example, for $\log N^+_{\rm OVII} = 15.3$, the curve in the left panel shows $p_j \simeq 0.36$, corresponding to a fraction $P_j \simeq 0.72$ of O VII *above* that limit. For the same source, these probabilities P_j will in general vary with the redshift of the O VI priors, although variations are not expected to be large if the X–ray data have a similar S/N throughout their redshift coverage, as is the case for most of our data.

In summary, the correction provided by P_j according to Equation 4.2 probability follows the assumption that O VII absorbers are associated with O VI (or H I), and therefore we use the measured O VI (or H I) column density to esti-

mate the fraction of column density that is missed because of the limited X–ray resolution. A similar analysis can be performed using different simulations, in order to address the dependence of the results on the assumed distribution of the absorbing gas. While an in–depth comparison of these distributions among various simulations goes beyond the scope of this project, I will point out that the `CAMELS` cosmological simulations in [14] feature a similar distribution of O VII vs. H I column densities (see their Figure 4) to the one from `EAGLE` used in this project. In general, however, the distribution of column densities of ions are quite sensitive to the choice of simulation methods.

4.1.2 The Blind Search Method and ΔC Fit Statistic

To aid in the measurement of the absorbers of focus, the ΔC statistic is used. The ΔC statistic is a likelihood–ratio statistic, as described by S.S. Wilks [71, 72] and is widely used for astronomical statistics (*e.g.,* [18]; [57]). As described in [19], a likelihood-ratio statistic such as ΔC (and other statistics such as the $\Delta\chi^2$ and F statistics) are asymptotically distributed like the χ^2 statistic given a sufficiently large amount of counts for the source [40, 11]. As described in Section 2.2 and 3.3.3, the usage of the `slab` model does not meet these requirements for testing the null hypothesis, so a power law model supplemented by a `line` model was used. As this combination of models allows for positive and negative fluxes around the expected absorption line center, the criteria for testing the null hypothesis with a χ^2 statistic are satisfied. A more thorough explanation of the line model and the decision to use it in the entire analysis is in Section 3.3.3.

When Studying the absorption lines present in the analysis, the statistical significance of a possible detection comes into question. In order to evaluate the statistical significance of the detection of a serendipitous line, *i.e.*, of a line that did not have a predetermined wavelength, it is necessary to account for the number of 'redshift trials', or independent opportunities to detect such feature, as originally proposed by [44]. A serendipitous or blind search is such that there are multiple opportunities to interpret the deepest fluctuation in the data as a possible absorption line. A general method to evaluate the probability of occurrence of such fluctuations in a blind search is that of performing a numerical simulation that includes all the relevant parameters of the search, such as the wavelength range spanned, the shape of the line–spread function (LSF), and the resolution of the instrument. Accordingly, we completed a simulation that uses the *XMM-Newton* LSF model as parameterized by [44], with a line center that can vary between $\lambda_1 = 23.5$ Å and $\lambda_2 = 32$ Å, in Figure 4.4.

To emulate the blind search method in our numerical simulation, we stepped the possible absorption line LSF model by a wavelength interval that is smaller than the 20 mÅ data bin (*i.e.*, by 10 mÅ), and identified the distribution of the ΔC statistic associated with the *strongest negative fluctuation* during this search, by comparing two fits obtained, respectively, with and without the line component. Since our data are generally in the large–count limit in each bin, with at least 400 counts per bin, the ΔC statistic was approximated by the corresponding $\Delta\chi^2$ statistic, assuming a Gaussian distribution for the counts in each bin. It is important to point out that, as also suggested by [44], the details of the contin-

uum model are not important, since the fit can be performed on the standardized deviations from such best–fit model, where each bin follows a standard Gaussian distribution, under the hypothesis that the data follow the model. The distribution of this maximum $\Delta\chi^2$ of the search, which approximates the sought–after distribution of the maximum ΔC, is reported in Figure 4.4.

Importantly, the distribution in Figure 4.4 can be immediately used to identify critical values of the ΔC statistic, and thus determine whether the measured statistics for a given line are significant or not.

4.1.3 Absorption Line Detection Sensitivity

In order to understand the sensitivity required to make a positive absorption line detection, an investigation of the constraints set by statistical and systematic uncertainties was completed. The RGS1 and RGS2 1st order effective area calibration uncertainties have been estimated as ∼2% in the 10–30 Å band, except for certain regions (such as near the oxygen edge) where 3-5% uncertainties may occur [41]. The uncertainties in the calibration of the effective area for the LETG/HRC instruments have been estimated at $\leq 10\%$ across the entire band.[1]

In order to evaluate the effect of possible effective area calibration inaccuracy on our results, we approximated the effect as a 2% dip in the predicted continuum flux within a bin of 60 mÅ size, *i.e.* the RGS resolution element, relative to the surrounding continuum. This is intended as a means to model a typical scenario in which a mis–calibrated effective area leads to a spurious absorption

[1] See https://cxc.cfa.harvard.edu/cal/Letg/LetgHrcEA/

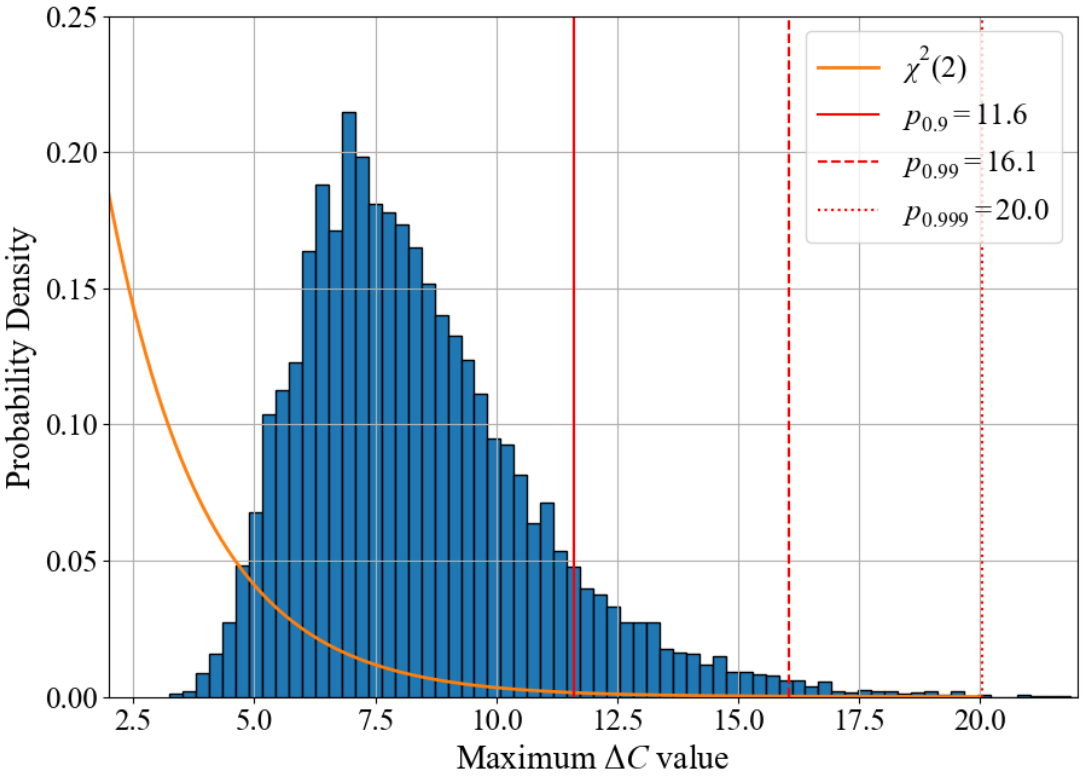

Figure 4.4: Monte Carlo simulation of the sampling distribution of the ΔC statistic for the blind search of absorption lines, under the hypothesis that there are no absorption lines (following the method of [44]). For comparison it is also plotted against the $\chi^2(2)$ distribution, which applies to the detection of an absorption model with two free parameters, but without accounting for redshift trials. The vertical red lines indicate the probabilities 0.9, 0.99, and 0.999 and the corresponding ΔC of those probabilites.

line–like feature. We then modelled this feature with a Gaussian line model (`line` in `SPEX`) with a broadening of 100 km/s at a nominal wavelength of 20 Å, and found that this feature requires a value of the optical depth parameter $\tau_0 = 0.37$, producing an absorption line with equivalent width of $\mathrm{EW_{sys}} = 2.7$ mÅ. This corresponds to $\log N_{\mathrm{ion}}$ ($\mathrm{cm^{-2}}$) $\simeq 15.0$, using a `slab` model for an He–α O VII absorption line. This is an indication that typical systematic uncertainties do not permit the detection of O VII column densities less that approximately $\log N_{\mathrm{OVII}}$ ($\mathrm{cm^{-2}}$) = 15.0. For the *Chandra* HRC data, a 10% uncertainty in the effective area in a resolution element of ∼60 mÅ corresponds to a value of $\tau_0 = 1.1$, and it results in the inability to detect absorption lines with below $\mathrm{EW_{sys}} = 14$ mÅ. In turn, this corresponds to an O VII column density of $\log N_{\mathrm{ion}}$ ($\mathrm{cm^{-2}}$) $\simeq 15.7$, following the same analysis as for the *XMM-Newton* data.

We then calculated the relative statistical uncertainties of the RGS and HRC spectra, using the background-subtracted count rate and its statistical uncertainty within each resolution element across the full waveband of the data. We then converted the relative statistical uncertainties into the equivalent width of a spurious line allowed by the statistical uncertainties scaling linearly (2% relative error corresponding to 2.7 mÅ as above), see Figure 4.5. This calculation provides two useful results. First, the number of photons is so high that the level of the statistical uncertainties of the data are comparable to that of the systematic uncertainties. Second, the *Chandra* HRC/LETG data are significantly less sensitive than the RGS data, primarily due to their lower exposure time.

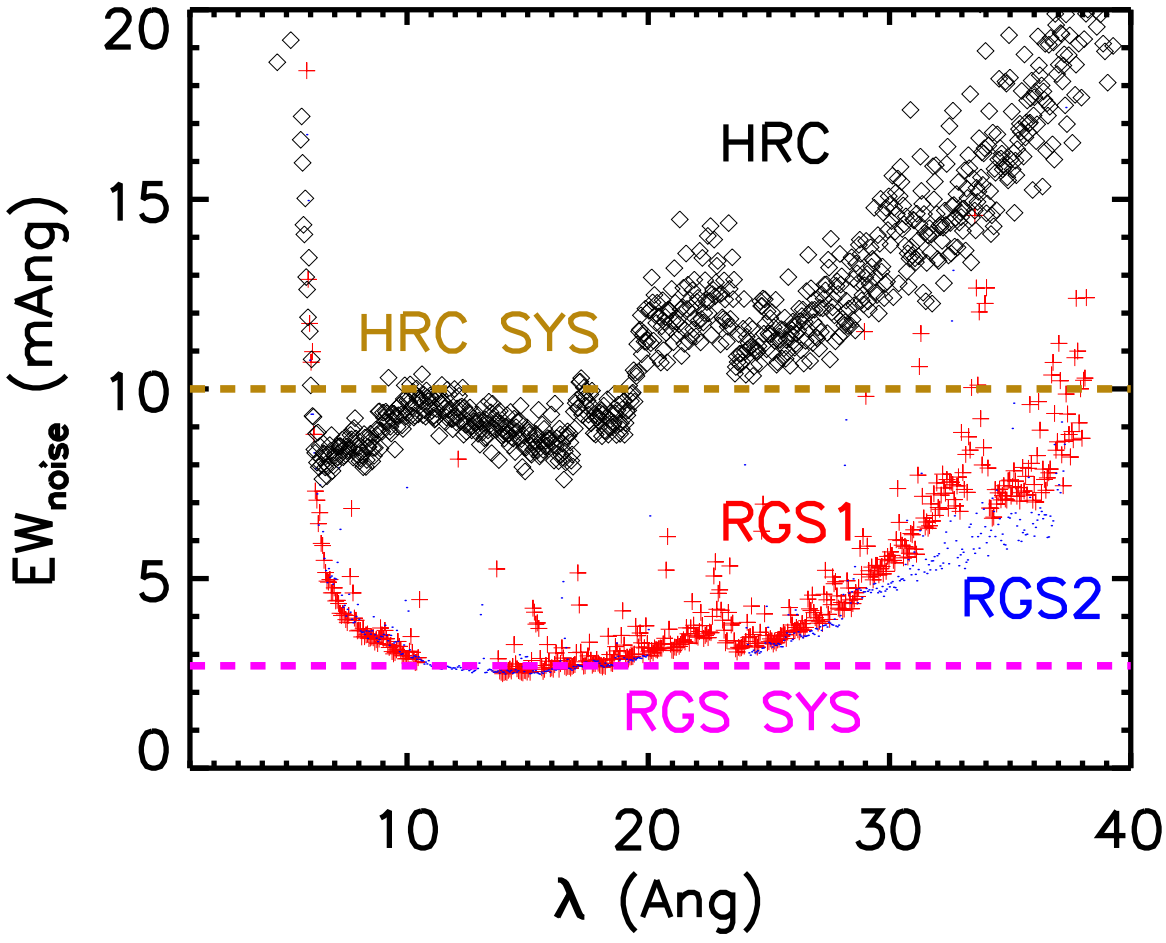

Figure 4.5: The noise level in terms of the equivalent width of an absorption line for RGS1 (red), RGS2 (blue) and HRC (black). The limits set by the effective area systematics for RGS and HRC are indicated with purple and brown dashed lines, respectively.

4.2 Statistical Methods for Model Parameters

The base model used in the analysis of the sample in this project was the simple power law model. This model was chosen for both its simplicity and easily manipulated parameters, as well as the model's ability to fit well to X-ray data. A simple power law being the relationship between two quantities that scales based on an exponential power. Known as `pow` in `SPEX`, The model is implemented as a simple power law model with the possibility of a break, where the spectrum is given by:

$$F(E) = AE^{-\Gamma}e^{\eta(E)}, \tag{4.3}$$

where E is the photon energy measured in keV, F is the photon flux with units of 10^{44} ph s^{-1} keV^{-1}, Γ is the photon index, and $\eta(E)$ is:

$$\eta(E) = \frac{r\xi + \sqrt{r^2\xi^2 + b^2(1-r^2)}}{1-r^2}, \tag{4.4}$$

where $\xi = \ln E/E_0$, and the break energy E_0 and smoothness of the break b are model parameters set in `SPEX`. These conditions lead to two extremes; for high energy situations, ξ approaches ∞ (or at least a sufficiently high value) such that $\lim_{\xi\to\infty}\eta(E) = \frac{2r\xi}{1-r^2}$. For low energy situations where ξ approaches $-\infty$, $\lim_{\xi\to-\infty}\eta(E) = 0$. Thus, the break in the spectrum is at $\Delta\Gamma = \frac{2r\xi}{1-r^2}$. Finally, solving for r gives:

$$r = \frac{\sqrt{1+(\Delta\Gamma)^2}-1}{|\Delta\Gamma|}. \tag{4.5}$$

During the fitting process in the analysis, typically the Γ ("gamm") parameter was fixed at a value of 1. If this proved to be insufficient for a proper fit, the parameter was allowed to be free and change as determined by `SPEX` in order to achieve the best fit. This, along with the normalization of each power law can be seen in the main analysis results, Tables B.1-C.8.

As described in Section 3.3.3, using the power law alone would be insufficient as it contains no way to model for absorption lines, just a simple continuum. Because of this, the `line` model was introduced in conjunction with the power law model. Together, they allowed for the modeling of the spectra's base continuum, and the implementation of absorption line detection and modeling at the expected absorption line wavelengths.

The absorption line model used in the data analysis in this project is known as the line model in `SPEX` (see section 3.3). This line model has a number of parameters, but most notably it contains a parameter known as "tau0" or "τ_0". τ_0 is the optical depth at the absorption line center, where positive and negative values correspond to absorption and emission respectively. This property is essential to the line model's usage in the analysis. As the `slab` model used and described in Section 2.2 does not satisfy the requirements for testing the null hypothesis with a likelihood–ratio test. The τ_0 parameter's ability to have a negative or positive flux satisfies the criteria for hypothesis testing with a χ^2 distribution for the resulting ΔC statistics. To measure the desirable ΔC statistic, the τ_0 parameter was fixed to a value of 0.0 (corresponding to no absorption present) and refit to the model. This allowed for the comparison between the

observed line model and that same model as if no absorption were present, which essentially displays the strength of the absorption line. Using this new C statistic value, a ΔC was calculated and reported in Tables B.1-C.8.

4.3 Upper Limit Methods

4.3.1 Confidence Intervals On Model Parameters

The task of estimating one or more model parameters θ, in this case the single parameter τ_0 for the line component, is a central problem in modern statistics. The point estimate is obtained via the method of maximum-likelihood, which was pioneered by R. A. Fisher (*e.g.,* [29]), and it is the method that we follow via the minimization of the $C_{\rm min}$ statistic. The determination of confidence intervals on model parameters in essence consists of devising a suitable method to 'invert' probabilities, *i.e.*, converting a probability of the observed quantity given an unknown parameter, to a probability statement regarding the true model parameters. All the considerations provided in the following apply to the general case of a confidence interval with both lower and upper limit, although they are illustrated here for an upper limit, given the case at hand.

Let x be one of the i observations of the unknown parameter $\theta = \tau_0$, *i.e.*, one of the entries in Tables B.1-C.8. In general, the observations could be of a different *statistic* x that is related to the true parameter θ, although in this case it is a measurement of the parameter itself, via the parametric spectral fits described in Section 3.3. The (true) parameter θ is not only unknown, but

it is also *fixed*; this is a standard tenet of the classical statistical approach to parameter estimation (for example, see Section 12.4 of [73] or [52]). The statistic or measurement x, on the other hand, is a *random variable* that is assumed to have a known distribution, and for which it is therefore meaningful to calculate probabilities of occurrence of any set of values. In the case at hand, for example,

$$\mathrm{P}(x \leq x^u|\theta) = 1 - \alpha \tag{4.6}$$

with α a small number, say $\alpha = 0.05$ (*e.g.,* [69] but other choices are also reasonable), the number x^u would be an upper limit with confidence $1-\alpha$, say 95%. This means that, given the distribution of the statistic, 95% of the observations should yield a value lower than x^u. The notation used for the probability means that one has to assume a value for the true parameter θ, which is of course unknown. Often the distribution of a measured statistic is normal, and this is the assumption we make in this case. The same considerations apply for other distributions.

A *confidence interval* on a parameter, on the other hand, can be defined as

$$\mathrm{P}(\theta \leq \theta^u|\theta) = 1 - \alpha, \tag{4.7}$$

which is misleadingly similar in form to Equation 4.6. In fact, what is random here is the data range $(0, \theta^u)$, and not θ. [2] Therefore, the interpretation of Equation

[2] In general, when the parameter θ is a function of different statistic x, the data range or set X^u (*i.e.*, for $x \in X^u$) corresponds to a random range $\overline{\theta}(X^u)$ for the parameter such that:

$$\mathrm{P}(\theta \leq \overline{\theta}(X^u)|\theta) = 1 - \alpha \tag{4.8}$$

see *e.g.,* [73]. This notation could be extended also to more than one parameter θ.

4.7 is that the data measured range includes the true value θ in a $1-\alpha$ fraction of cases when such experiment is repeated. A clear and concise textbook explanation of this method is provided in Chapter 11 of [60], and a more theoretical discussion in Chapter 12 of [73], which summarizes the original [52] method for confidence interval estimation.

4.3.2 Feldman-Cousins Method

For applications in the physical sciences, often an additional complication arises that is concerned with certain parameter values being 'unphysical', for a given application. Consider as an example one of the measurements from the results Table B.1, say $\tau_0 = -3.86^{+0.55}_{-0.40}$ in line 17 of the table. A negative best–fit value means that there is evidence for an *emission line* feature at that wavelength. This feature is likely caused by a random fluctuation of the Poisson spectrum at that wavelength, or the presence of an unrelated emission phenomenon, or perhaps a combination of both. Either way, a formal confidence interval on the measured parameter τ_0 would remain negative, which would make it impossible to answer the question at hand.

The seminal contribution by [28] addresses this exact issue that is present in our data, whereas our question requires that the true parameter is non–negative. Their idea is to consider confidence intervals on the unknown parameter of the absorption line process, which we indicate as θ to distinguish it from the

measurement itself, based on the ratio of two probabilities or likelihoods,

$$R = \frac{P(\tau_0|\theta)}{P(\tau_0|\theta_{\rm best})} \tag{4.9}$$

with $\theta_{\rm best} = \max(0, \tau_0)$. Possible values of the unknown parameter θ are then chosen among those with the largest value of R, subject to the constraint $\theta \geq 0$, while the measurement τ_0 can in fact be negative. This method, hereafter referred to as the FC method, requires the specification of the conditional distributions in Equation 4.9, which in this case we assume to be Gaussian, and it returns a range $(\theta_{min}, \theta_{max})$ as a confidence interval at a given level of confidence.[3]

To implement the FC confidence interval method, we start with the assumption that the probability distribution $P(\tau_0|\theta)$ is normal. This assumption is somewhat at odds with the asymmetric errors provided by the $\Delta C = 1$ method for several sources, which indicate a more complex probability model than the Gaussian. In fact, a normal distribution for the parameter τ_0 would result in a parabolic log–likelihood function, and therefore symmetric ΔC intervals (see, *e.g.,* Section 2.3 of [39]). Nonetheless, we proceed with the Gaussian assumption as an approximation, and set the standard deviation of the distribution equal to the average of the two errors (*e.g.,* we assume $\sigma = 0.47$ for the measurement $\tau_0 = -3.86^{+0.55}_{-0.40}$) and is thereafter considered as a fixed parameter. Our crude method to average the positive and negative error bars is simply one of convenience, given the size of the sample. We expect that the errors introduced by this

[3]The method is explained in detail in Sec. IV B of [28]. For Python, this method is implemented in the `gammapy` software version ≤ 0.7, or from the `FCpy` software [37].

method for a given upper limit would average down when inferences are made for the entire sample.

Moreover, we also adjust the best–fit value to the midpoint of the range (*e.g.*, $\tau_{0,\mathrm{adj}} = -3.79$); we will compare results with and without this adjustment to test the effects on our results. Upon division by the assumed σ parameter, all scaled measurements $x = \tau_0/\sigma$ are therefore assumed to be distributed like a Gaussian with unit variance, $x \sim N(\theta, 1)$, and to these scaled values we can then apply the same FC method.

The situation is illustrated in Figure 4.6, which reproduces closely the example provided by Figure 10 of [28] that applies to a Gaussian with unit variance. The band is constructed horizontally for a given value of the mean $\mu = \theta$, by requiring

$$\int_{x_L}^{x^U} P(x|\theta)dx = 1 - \alpha$$

with the choice of $\alpha = 0.1$, so that a horizontal range contains 90% of probability. The FC requires that the limits x_L and x^U are chosen in such a way that they bracket the maximum of R according to Equation 4.9, which contains the assumption that the parent mean must be non–negative. For a given standardized measurement $x_i = \tau_{0,i}/\sigma_i$, the upper limit is the intersection of the vertical line at $x = x_i$ with the red upper limit curve (see Figure 4.6). Even in those cases with a sufficiently large value of x_i, we only consider an upper limit θ_i^U, and ignore the lower limit, as a further conservative measure. The FC method therefore yields an upper limit to the line parameter $\tau_{0,i}^U = \theta_i^U \, \sigma_i$, which is then immediately translated into N_i^+.

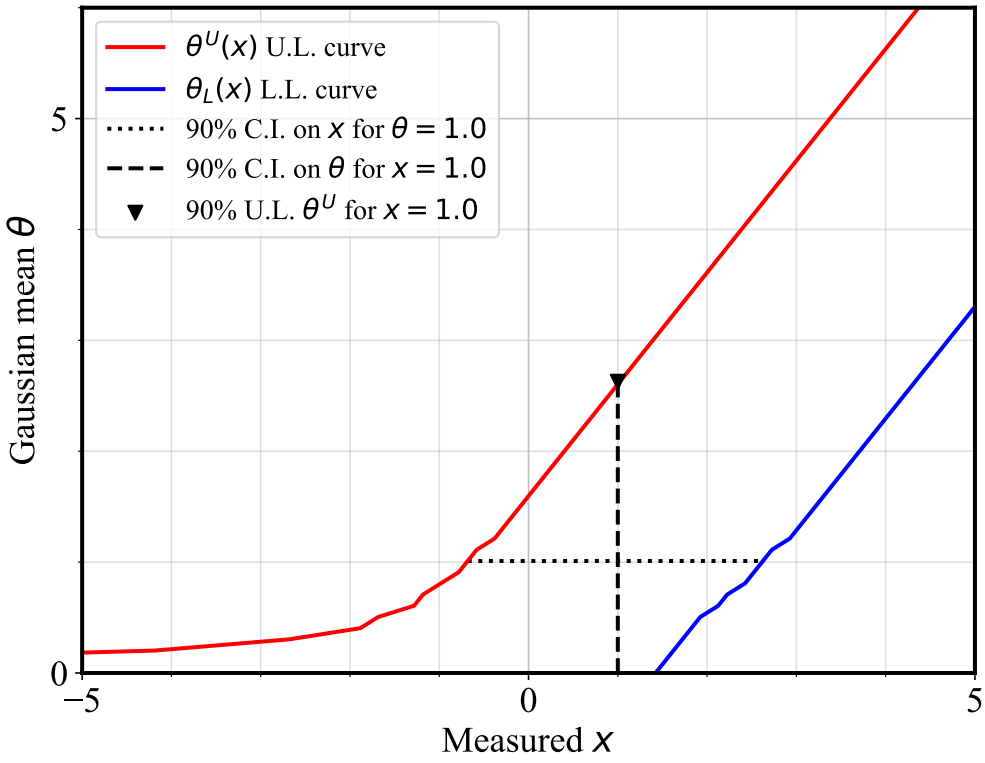

Figure 4.6: The Feldman–Cousins 90% confidence band for Gaussian measurements x, with unit variance ($\sigma^2 = 1$) and mean μ. A horizontal line between the two curves at a given value of μ is a 90% confidence interval on possible measurements drawn from that distribution. A vertical interval between the two curves at the value of a possible measurement x is a 90% confidence interval on the possible parent mean μ.

Notice how the FC method avoids the *empty interval* problem, which would appear for substantially negative measurements such as the one already considered. *If* we were to choose the measured value of $\tau_0 = -3.86$ as the best–fit estimate for the true Gaussian mean, then a 90% confidence interval would remain negative. This problem is solved by the use of the likelihood ratio, and was one of the main motivations behind the method developed by [28].

4.3.3 Sensitivity Method

An alternative method to use the measured τ_0 parameters to set upper limits on its parent value θ is also considered. The method is based on the following considerations. First, the best–fit value itself (*i.e.*, $\tau_0 = -3.86$ for the sample entry) is not interesting, since a best–fit value that is positive or negative simply means that the center of the possible line falls at a position with a number of detected counts that is (randomly) either lower or greater than the neighboring points, respectively. Second, the most useful part of the regression is the measurement of the parameter's uncertainty, which reflects the ability of a given set of data to constrain the model, or its 'sensitivity'. In fact, a similar fit to a `line` model in a neighboring portion of the spectrum would necessarily have a different best–fit parameter τ_0, but a similar uncertainty, since the data have similar number of counts, and the null model (*i.e.*, the power–law) is smooth over the ± 1 Å range under consideration.

The interest is in setting an upper limit to θ, as a means to find the largest value for the unknown parameter that is allowed by the data, at a given

confidence level. This is akin to what is usually done in source detection with Poisson statistics (*e.g.,* [47]). In this case, however, we assume that the sampling distribution of the parameter $\tau_{0,i}$ for a specific regression is a Gaussian with unknown mean $\theta \geq 0$, and a variance given by the measured variance σ_i^2, same as in the previous method. This means that a measurement is $x_i = \tau_{0,i} \sim N(\theta, \sigma_i^2)$.

According to this assumption, the one–sided confidence range on θ with significance α is set by the condition

$$P(x > 0|\theta) \geq 1 - \alpha \quad \text{or} \quad P(x \leq 0|\theta) \leq \alpha \tag{4.10}$$

with α the usual small probability, say $\alpha = 0.1$ for a 90% confidence level. Equation 4.10 means that one allows (at most) a small residual probability α to measure a negative value for the parameter, when the true parameter is θ. In other words, 90% of the times a measurement is made from a distribution with such value of θ, the measurement will be positive. It is immediate to see that, given the normal sampling distribution, Equation 4.10 is satisfied by:

$$\theta \geq 1.65\sigma, \tag{4.11}$$

which can be interpreted as the 90% C.I. on θ. [4]

[4] An equivalent method is used to set upper limits to the Poisson mean, see *e.g.,* Ch. 7 of [9] and [34].

Looking at this confidence interval in a different way, Equation 4.10 also implies, for the choice of $\alpha = 0.1$,

$$P\left(\frac{x-\theta}{\sigma} \leq -1.65\right) = P(\theta \geq x + 1.65\,\sigma)P(\theta \geq \theta^u) \leq \alpha, \tag{4.12}$$

with all θ values satisfying Equation 4.12 being the values in this confidence interval for the parameter θ, and for a given measurement $x \geq 0$. This is the type of 'classical' confidence intervals discussed in Sec. 4.3.1 in the introduction of this Appendix. [5] The one–sided confidence interval with confidence $\geq 1 - \alpha$ is

$$S(x) = (x + 1.65\,\sigma, \infty), \tag{4.13}$$

and it is also referred to as a *fiducial* confidence interval [*e.g.,* 30, 73]. The 'fiducial' qualifier is introduced because it relates to a statement on a fixed parameter, and not on a traditional random variable (such as the measurement x). [6] The fiducial confidence interval $S(x)$ necessarily depends on the measurement x (see, *e.g.,* textbook examples in [60, 9]).

If we take the smallest value allowed, $x = 0$, as speculated at the beginning of the section, then (4.11) and (4.13) coincide, as one would expect. In general, using z_α as the one–sided z–score associated with a residual probability α, $P(z \geq$

[5] It is clear that θ is and remains fixed, so the last inequality should be read right–to–left, *i.e.*, the random interval $(x + 1.65\,\sigma, \infty)$ contains the unknown value of θ a fraction α of times that the measurement of x is made. This consideration is mostly interesting for theoretical purposes, and in practice the data analyst needs not worry about it.

[6] Further to the interpretation of fiducial confidence intervals, [30] attempted to introduce the concept of *fiducial probability distribution* on the parameter θ, leveraging the formal similarity between (4.10) and (4.12) [see also discussion in Sec. 12.4 of 73]. Such concept has not gained general acceptance, also given certain difficulties with multi–variable problems [see, *e.g.,* 66].

$z_\alpha) = \alpha$ (*e.g.,* for $\alpha = 0.1, 0.01, 0.001$, $z_\alpha = 1.65, 2.58, 3.29$), we can generalize these argument and set the $1-\alpha$ sensitivity upper limit to the Gaussian parameter θ as

$$\theta \leq z_\alpha \, \sigma. \tag{4.14}$$

It is useful to notice that the classical confidence interval (Equation 4.13) associated with a given measurement x could be used instead, given that all such measurements are available in the tables. However, as pointed out by [28], a measurement $x \leq z_\alpha \, \sigma$, such as the sample entry considered before, would yield a formal confidence interval that remains negative. Given that only positive values of the $\theta = \tau_0$ parameter are physically meaningful, certain measurements give rise to the *empty interval* problem, when the interval is intersected with the physically allowed range. This is in fact one of the reasons for the [28] method, which was presented in Section 4.3.2. The 'sensitivity' method can therefore be viewed as a simplified FC method, where the actual measurement is ignored and replaced by the null–hypothesis value of zero, and without the enforcement of the likelihood–ratio ordering of likelihoods.

Chapter 5. Results of Data Analysis

5.1 Primary Analysis and Upper Limits

The primary analysis completed for this project was that of the automated SPEX-driven fits of both the *XMM-Newton* and *Chandra* data. In all, there were 8 cases studied for the sample; for both *XMM-Newton* and *Chandra*, O VII with both O VI and H I prior detections, and O VIII with both O VI and H I prior detections. A truncated form of these 8 tables along with the corresponding upper limit tables for each are shown in Tables 5.1 - 5.16. The tables in their entirety are shown in Appendix Tables B.1 - C.8. Overall, there were over 1000 unique fits completed, with a corresponding upper limit calculated according to Equation 3.7 for each of these fits. The distribution of the corresponding ΔC statistics and amounts of positive τ_0 parameters (model indicated absorption) compared to the expected distribution function of a $\chi^2(1)$ variable (representing the null hypothesis that there are no emission or absorption lines in the sample) are shown in Figures 5.1 and 5.2.

Table 5.1: An abbreviated version of the O VII measurements with *XMM-Newton* data, at the prior redshift from the O VI lines from Table A.1. Column "%" reports the percent background level, $B/S+B$, where B is the background count rate, and S the source count rate. Entries with an asterisk sign indicate poor fits; entries that have a '$---$' sign indicate lines that fall in a region of reduced efficiency, and therefore they could not be constrained (see Sec. 3.2.2). The full version of this data is in Table B.1.

Target line		cmin	RGS1		RGS2		power–law		line component			ΔC
Name	z	(d.o.f.)	avg exp (s)	%	avg exp (s)	%	norm.	index	λ (Å)	τ_0	log N(cm^{-2})	(d.o.f.)
1es1028	0.12314 (#1)	95.40(79)	144787	10	147275	7	$1102\pm^{30}_{30}$	1.00	24.2598	$0.55\pm^{1.74}_{0.88}$	$15.24\pm^{0.44}_{nan}$	0.40
1es1028	0.13706 (#2)	92.82(90)	143804	9	146370	7	$1121\pm^{33}_{32}$	1.00	24.5605	$-0.31\pm^{0.85}_{0.56}$	$nan\pm^{nan}_{nan}$	0.22
1es1028	0.33735 (#3)	86.46(91)	145450	17	146420	22	$1324\pm^{48}_{46}$	1.00	28.8868	$-0.78\pm^{0.84}_{0.57}$	$nan\pm^{nan}_{nan}$	1.08
1es1553	0.18759 (#4)	102.10(88)	1793737	7	1757303	7	$1796\pm^{13}_{12}$	1.00	25.6519	$0.60\pm^{0.32}_{0.26}$	$15.27\pm^{0.15}_{0.21}$	7.82
1es1553	0.18775 (#5)	102.34(88)	1793737	7	1757303	7	$1796\pm^{13}_{12}$	1.00	25.6554	$0.57\pm^{0.30}_{0.25}$	$15.26\pm^{0.15}_{0.22}$	7.53
1es1553	0.18984 (#6)	105.72(86)	1794800	7	1753128	7	$1778\pm^{12}_{12}$	1.00	25.7005	$-0.05\pm^{0.17}_{0.23}$	$nan\pm^{nan}_{nan}$	0.16
1es1553	0.21631 (#7)	84.95(81)	1756247	7	1757203	8	$1778\pm^{14}_{14}$	1.00	26.2723	$0.19\pm^{0.25}_{0.22}$	$14.83\pm^{0.33}_{nan}$	0.95
1es1553	0.31130 (#8)	113.79(90)	1740303	11	1677696	14	$1807\pm^{15}_{15}$	1.00	28.3241	$-0.15\pm^{0.26}_{0.23}$	$nan\pm^{nan}_{nan}$	0.45
1es1553	0.37868 (#9)	119.25(98)	1809416	21	1817188	12	$1834\pm^{17}_{17}$	1.00	29.7795	$0.00\pm^{0.09}_{0.80}$	$13.08\pm^{1.43}_{nan}$	-0.04
1es1553	0.39497 (#10)	90.13(98)	1751580	21	1813451	12	$1810\pm^{18}_{18}$	1.00	30.1314	$0.02\pm^{0.38}_{0.24}$	$13.80\pm^{1.32}_{nan}$	0.02
3c249	0.24676 (#11)	78.14(93)	2639	31	2524	34	$282\pm^{141}_{104}$	1.00	26.9300	$-1.24\pm^{1.07E+12}_{28.76}$	$nan\pm^{nan}_{nan}$	0.03
3c249	0.30788 (#12)	81.25(88)	2639	20	2535	85	$697\pm^{234}_{175}$	1.00	28.2502	$9.81E04\pm^{1.00E+20}_{9.82E+04}$	$16.21\pm^{0.25}_{nan}$	0.35
3c249	0.30809 (#13)	81.15(88)	2639	20	2535	85	$701\pm^{236}_{177}$	1.00	28.2547	$1.45E+07\pm^{1.00E+20}_{1.45E+07}$	$16.29\pm^{0.17}_{nan}$	0.47
3c249	0.31364 (#14)	78.36(88)	2639	20	2538	62	$758\pm^{250}_{193}$	1.00	28.3746	$9.44E+12\pm^{1.00E+20}_{9.44E+12}$	$16.41\pm^{0.05}_{inf}$	1.72
3c273	0.00337 (#15)	–	–	–	–	–	–	–	21.6728	–	–	–
.....												

Table 5.2: An abbreviated version of the O VII upper limit measurements with *XMM-Newton* data, at the prior redshift from the O VI lines from Table A.1. The τ_0 in this table is calculated through the previous table's τ_0 errors, given by Equation 3.7. The corresponding column density was calculated using this value. The full version of this data is in Table B.2.

Target line		cmin	RGS1	RGS2	power–law		line component			ΔC
Name	z	(d.o.f.)	avg exp (s)	avg exp (s)	norm.	index	λ (Å)	τ_0	$\log N + (\mathrm{cm}^{-2})$	(d.o.f.)
1es1028	0.12314 (#1)	95.40(79)	144787	147275	$1102\pm^{30}_{30}$	1.00	24.2598	1.31	15.53	0.40
1es1028	0.13706 (#2)	92.82(90)	143804	146370	$1121\pm^{33}_{32}$	1.00	24.5605	0.71	15.33	0.22
1es1028	0.33735 (#3)	86.46(91)	145450	146420	$1324\pm^{48}_{46}$	1.00	28.8868	0.70	15.33	1.08
1es1553	0.18759 (#4)	102.10(88)	1793737	1757303	$1796\pm^{13}_{12}$	1.00	25.6519	0.29	14.99	7.82
1es1553	0.18775 (#5)	102.34(88)	1793737	1757303	$1796\pm^{13}_{12}$	1.00	25.6554	0.27	14.97	7.53
1es1553	0.18984 (#6)	105.72(86)	1794800	1753128	$1778\pm^{12}_{12}$	1.00	25.7005	0.20	14.85	0.16
1es1553	0.21631 (#7)	84.95(81)	1756247	1757203	$1778\pm^{14}_{14}$	1.00	26.2723	0.24	14.91	0.95
1es1553	0.31130 (#8)	113.79(90)	1740303	1677696	$1807\pm^{15}_{15}$	1.00	28.3241	0.24	14.92	0.45
1es1553	0.37868 (#9)	119.25(98)	1809416	1817188	$1834\pm^{17}_{17}$	1.00	29.7795	0.44	15.16	-0.04
1es1553	0.39497 (#10)	90.13(98)	1751580	1813451	$1810\pm^{18}_{18}$	1.00	30.1314	0.31	15.02	0.02
3c249	0.24676 (#11)	78.14(93)	2639	2524	$282\pm^{141}_{104}$	1.00	26.9300	5.33E+11	16.40	0.03
3c249	0.30788 (#12)	81.25(88)	2639	2535	$697\pm^{234}_{175}$	1.00	28.2502	5.00E+19	16.46	0.35
3c249	0.30809 (#13)	81.15(88)	2639	2535	$701\pm^{236}_{177}$	1.00	28.2547	5.00E+19	16.46	0.47
3c249	0.31364 (#14)	78.36(88)	2639	2538	$758\pm^{250}_{193}$	1.00	28.3746	5.00E+19	16.46	1.72
3c273	0.00337 (#15)	–	–	–	–	–	21.6728	–	–	–
.....										

Table 5.3: An abbreviated version of the O VII measurements with *XMM-Newton* data, at the prior redshift from the H I lines from Table A.2. The full version of this data is in Table B.3.

Target line		cmin	RGS1		RGS2		power–law		line component			ΔC
Name	z	(d.o.f.)	avg exp (s)	%	avg exp (s)	%	norm.	index	λ (Å)	τ_0	$\log N(\mathrm{cm}^{-2})$	(d.o.f.)
1es1028	0.13714 (#1)	92.78(90)	143804	9	146370	7	$1121\pm^{32}_{32}$	1.00	24.5622	$-0.33\pm^{0.82}_{0.55}$	$nan\pm^{nan}_{nan}$	0.27
1es1028	0.20383 (#2)	114.22(94)	146421	9	145107	9	$1207\pm^{32}_{35}$	1.00	26.0027	$0.03\pm^{0.97}_{0.83}$	$14.01\pm^{1.43}_{nan}$	-0.01
1es1028	0.22121 (#3)	101.58(92)	144278	9	146704	9	$1198\pm^{35}_{35}$	1.00	26.3781	$-0.70\pm^{0.67}_{0.48}$	$nan\pm^{nan}_{nan}$	1.33
1es1553	0.03466 (#4)	38.25(27)	1791095	9	nan	nan	$747\pm^{397}_{326}$	1.97	22.3487	$-0.18\pm^{0.33}_{0.25}$	$nan\pm^{nan}_{nan}$	0.53
1es1553	0.04273 (#5)	30.79(21)	1784759	9	nan	nan	$489\pm^{628}_{294}$	2.72	22.5230	$0.51\pm^{0.64}_{0.44}$	$15.21\pm^{0.28}_{0.85}$	2.85
1es1553	0.06364 (#6*)	64.48(28)	1661330	9	nan	nan	$27\pm^{12}_{9}$	7.49	22.9746	$0.53\pm^{0.63}_{0.44}$	$15.22\pm^{0.27}_{0.73}$	1.84
1es1553	0.21869 (#7)	108.81(87)	1691684	7	1788288	8	$1010\pm^{415}_{304}$	1.74	26.3237	$-0.01\pm^{0.65}_{0.08}$	$nan\pm^{nan}_{nan}$	-0.07
3c249	0.13470 (#8)	67.71(86)	2642	7	2524	10	$336\pm^{146}_{105}$	1.00	24.5095	$9.67E+04\pm^{1.00E+20}_{9.68E+04}$	$16.21\pm^{0.25}_{nan}$	0.52
3c249	0.26664 (#9)	79.78(93)	2639	31	2524	59	$306\pm^{146}_{111}$	1.00	27.3594	$0.17\pm^{1.00E+20}_{30.17}$	$14.78\pm^{1.68}_{nan}$	-0.00
3c273	0.00758 (#10)	–	–	–	–	–	–	–	21.7637	–	–	–
3c273	0.06707 (#11*)	35.22(22)	897879	5	nan	nan	$4641\pm^{37}_{41}$	1.00	23.0487	$0.24\pm^{0.31}_{0.30}$	$14.91\pm^{0.32}_{nan}$	0.86
3c273	0.07359 (#12*)	45.49(29)	930374	5	nan	nan	$4656\pm^{32}_{34}$	1.00	23.1895	$-0.10\pm^{0.21}_{0.19}$	$nan\pm^{nan}_{nan}$	0.39
3c273	0.13960 (#13)	68.74(61)	892303	4	1027847	3	$5246\pm^{31}_{31}$	1.00	24.6154	$-0.39\pm^{0.12}_{0.11}$	$nan\pm^{nan}_{nan}$	12.82
h1821	0.00944 (#14)	–	–	–	–	–	–	–	21.8039	–	–	–
h1821	0.06779 (#15)	48.43(43)	28966	55	nan	nan	$1081\pm^{99}_{91}$	1.00	23.0643	$8.21E+04\pm^{1.00E+20}_{5.68E+04}$	$16.18\pm^{0.28}_{0.02}$	1.16
.....												

Table 5.4: An abbreviated version of the O VII upper limit measurements with *XMM-Newton* data, at the prior redshift from the H I lines from Table A.2. The full version of this data is in Table B.4.

Target line		cmin	RGS1	RGS2	power–law		line component			ΔC
Name	z	(d.o.f.)	avg exp (s)	avg exp (s)	norm.	index	λ (Å)	τ_0	$\log N + (\mathrm{cm}^{-2})$	(d.o.f.)
1es1028	0.13714 (#1)	92.78(90)	143804	146370	$1121\pm^{32}_{32}$	1.00	24.5622	0.68	15.31	0.27
1es1028	0.20383 (#2)	114.22(94)	146421	145107	$1207\pm^{32}_{35}$	1.00	26.0027	0.90	15.41	-0.01
1es1028	0.22121 (#3)	101.58(92)	144278	146704	$1198\pm^{35}_{35}$	1.00	26.3781	0.58	15.26	1.33
1es1553	0.03466 (#4)	38.25(27)	1791095	nan	$747\pm^{397}_{326}$	1.97	22.3487	0.29	14.99	0.53
1es1553	0.04273 (#5)	30.79(21)	1784759	nan	$489\pm^{628}_{294}$	2.72	22.5230	0.54	15.23	2.85
1es1553	0.06364 (#6*)	64.48(28)	1661330	nan	$27\pm^{12}_{9}$	7.49	22.9746	0.53	15.23	1.84
1es1553	0.21869 (#7)	108.81(87)	1691684	1788288	$1010\pm^{415}_{304}$	1.74	26.3237	0.36	15.08	-0.07
3c249	0.13470 (#8)	67.71(86)	2642	2524	$336\pm^{146}_{105}$	1.00	24.5095	5.00E+19	16.46	0.52
3c249	0.26664 (#9)	79.78(93)	2639	2524	$306\pm^{146}_{111}$	1.00	27.3594	5.00E+19	16.46	-0.00
3c273	0.00758 (#10)	–	–	–	–	–	21.7637	–	–	–
3c273	0.06707 (#11*)	35.22(22)	897879	nan	$4641\pm^{37}_{41}$	1.00	23.0487	0.30	15.01	0.86
3c273	0.07359 (#12*)	45.49(29)	930374	nan	$4656\pm^{32}_{34}$	1.00	23.1895	0.20	14.84	0.39
3c273	0.13960 (#13)	68.74(61)	892303	1027847	$5246\pm^{31}_{31}$	1.00	24.6154	0.12	14.62	12.82
h1821	0.00944 (#14)	–	–	–	–	–	21.8039	–	–	–
h1821	0.06779 (#15)	48.43(43)	28966	nan	$1081\pm^{99}_{91}$	1.00	23.0643	5.00E+19	16.46	1.16
.....										

Table 5.5: An abbreviated version of the O VIII measurements with *XMM-Newton* data, at the prior redshift from the O VI lines from Table A.1. The full version of this data is in Table B.5.

Target line		cmin	RGS1		RGS2		power–law		line component			ΔC
Name	z	(d.o.f.)	avg exp (s)	%	avg exp (s)	%	norm.	index	λ (Å)	τ_0	$\log N(\mathrm{cm}^{-2})$	(d.o.f.)
1es1028	0.12314 (#1)	33.31(31)	146792	8	nan	nan	$963\pm^{40}_{26}$	1.00	21.2947	$0.02\pm^{3.99}_{0.61}$	$14.13\pm^{2.00}_{nan}$	0.01
1es1028	0.13706 (#2)	–	–	–	–	–	–	–	21.5587	–	–	–
1es1028	0.33735 (#3)	92.62(96)	147900	8	144798	8	$1196\pm^{31}_{31}$	1.00	25.3562	$5.01\pm^{15.34}_{3.36}$	$16.16\pm^{0.15}_{0.24}$	6.58
1es1553	0.18759 (#4)	29.26(27)	1729540	9	nan	nan	$540\pm^{318}_{194}$	2.55	22.5167	$0.37\pm^{0.44}_{0.33}$	$15.43\pm^{0.29}_{0.90}$	1.81
1es1553	0.18775 (#5)	28.91(27)	1729540	9	nan	nan	$550\pm^{295}_{211}$	2.52	22.5197	$0.39\pm^{0.49}_{0.31}$	$15.45\pm^{0.29}_{0.62}$	2.20
1es1553	0.18984 (#6)	25.62(27)	1729542	9	nan	nan	$406\pm^{219}_{140}$	3.05	22.5594	$0.98\pm^{0.60}_{0.48}$	$15.77\pm^{0.14}_{0.23}$	8.20
1es1553	0.21631 (#7)	33.20(25)	1723969	9	nan	nan	$60\pm^{36}_{21}$	6.19	23.0612	$-0.08\pm^{0.43}_{0.30}$	$nan\pm^{nan}_{nan}$	0.03
1es1553	0.31130 (#8)	113.12(91)	1744157	7	1748313	7	$2268\pm^{757}_{440}$	0.67	24.8622	$1.01\pm^{0.37}_{0.33}$	$15.80\pm^{0.10}_{0.14}$	17.08
1es1553	0.37868 (#9)	113.07(88)	1784762	7	1713272	8	$1213\pm^{467}_{336}$	1.52	26.1398	$1.03\pm^{0.44}_{0.35}$	$15.79\pm^{0.11}_{0.14}$	15.34
1es1553	0.39497 (#10)	118.64(92)	1704141	7	1756581	9	$481\pm^{192}_{138}$	2.74	26.4486	$-0.20\pm^{0.19}_{0.18}$	$nan\pm^{nan}_{nan}$	1.31
3c249	0.24676 (#11)	41.19(50)	2644	37	2524	inf	$373\pm^{135}_{107}$	1.00	23.6386	$43.49\pm^{1.00E+20}_{73.49}$	$16.33\pm^{0.47}_{nan}$	0.10
3c249	0.30788 (#12)	70.28(91)	2641	15	2524	8	$269\pm^{119}_{90}$	1.00	24.7974	$-1.35\pm^{1.00E+20}_{2.77}$	$nan\pm^{nan}_{nan}$	0.05
3c249	0.30809 (#13)	70.31(91)	2641	15	2524	8	$271\pm^{119}_{91}$	1.00	24.8014	$-0.85\pm^{3.10E+14}_{29.15}$	$nan\pm^{nan}_{nan}$	0.02
3c249	0.31364 (#14)	73.37(90)	2640	17	2524	5	$377\pm^{139}_{111}$	1.00	24.9066	$4.71E+06\pm^{1.00E+20}_{4.71E+06}$	$16.62\pm^{0.18}_{nan}$	1.07
3c273	0.00337 (#15)	122.62(82)	1002935	3	1016589	3	$2162\pm^{179}_{168}$	2.23	19.0239	$-0.01\pm^{0.61}_{0.03}$	$nan\pm^{nan}_{nan}$	-0.27
.....												

Table 5.6: An abbreviated version of the O VIII upper limit measurements with *XMM-Newton* data, at the prior redshift from the O VI lines from Table A.1. The full version of this data is in Table B.6.

Target line		cmin	RGS1	RGS2	power–law		line component			ΔC
Name	z	(d.o.f.)	avg exp (s)	avg exp (s)	norm.	index	λ (Å)	τ_0	$\log N + (\mathrm{cm}^{-2})$	(d.o.f.)
1es1028	0.12314 (#1)	33.31(31)	146792	nan	$963\pm^{40}_{26}$	1.00	21.2947	2.30	16.01	0.01
1es1028	0.13706 (#2)	–	–	–	–	–	21.5587	–	–	–
1es1028	0.33735 (#3)	92.62(96)	147900	144798	$1196\pm^{31}_{31}$	1.00	25.3562	9.35	16.25	6.58
1es1553	0.18759 (#4)	29.26(27)	1729540	nan	$540\pm^{318}_{194}$	2.55	22.5167	0.39	15.45	1.81
1es1553	0.18775 (#5)	28.91(27)	1729540	nan	$550\pm^{295}_{211}$	2.52	22.5197	0.40	15.46	2.20
1es1553	0.18984 (#6)	25.62(27)	1729542	nan	$406\pm^{219}_{140}$	3.05	22.5594	0.54	15.56	8.20
1es1553	0.21631 (#7)	33.20(25)	1723969	nan	$60\pm^{36}_{21}$	6.19	23.0612	0.36	15.42	0.03
1es1553	0.31130 (#8)	113.12(91)	1744157	1748313	$2268\pm^{757}_{440}$	0.67	24.8622	0.35	15.41	17.08
1es1553	0.37868 (#9)	113.07(88)	1784762	1713272	$1213\pm^{467}_{336}$	1.52	26.1398	0.40	15.45	15.34
1es1553	0.39497 (#10)	118.64(92)	1704141	1756581	$481\pm^{192}_{138}$	2.74	26.4486	0.19	15.15	1.31
3c249	0.24676 (#11)	41.19(50)	2644	2524	$373\pm^{135}_{107}$	1.00	23.6386	5.00E+19	16.80	0.10
3c249	0.30788 (#12)	70.28(91)	2641	2524	$269\pm^{119}_{90}$	1.00	24.7974	5.00E+19	16.75	0.05
3c249	0.30809 (#13)	70.31(91)	2641	2524	$271\pm^{119}_{91}$	1.00	24.8014	1.55E+14	16.78	0.02
3c249	0.31364 (#14)	73.37(90)	2640	2524	$377\pm^{139}_{111}$	1.00	24.9066	5.00E+19	16.80	1.07
3c273	0.00337 (#15)	122.62(82)	1002935	1016589	$2162\pm^{179}_{168}$	2.23	19.0239	0.32	15.37	-0.27
.....										

Table 5.7: An abbreviated version of the O VIII measurements with *XMM-Newton* data, at the prior redshift from the H I lines from Table A.2. The full version of this data is in Table B.7.

Target line		cmin	RGS1		RGS2		power–law		line component			ΔC
Name	z	(d.o.f.)	avg exp (s)	%	avg exp (s)	%	norm.	index	λ (Å)	τ_0	$\log N(\mathrm{cm}^{-2})$	(d.o.f.)
1es1028	0.13714 (#1)	–	–	–	–	–	–	–	21.5602	–	–	–
1es1028	0.20383 (#2)	62.35(44)	146640	9	nan	nan	$1006\pm^{29}_{29}$	1.00	22.8246	$0.05\pm^{2.21}_{0.94}$	$14.58\pm^{1.44}_{nan}$	0.01
1es1028	0.22121 (#3)	57.62(42)	144940	9	nan	nan	$1031\pm^{32}_{31}$	1.00	23.1541	$-1.47\pm^{0.70}_{0.53}$	$nan\pm^{nan}_{nan}$	3.89
1es1553	0.03466 (#4)	90.75(81)	1722815	7	1780022	7	$752\pm^{116}_{96}$	2.09	19.6172	$-0.03\pm^{0.65}_{0.06}$	$nan\pm^{nan}_{nan}$	-0.41
1es1553	0.04273 (#5)	89.06(72)	1720386	8	1774803	7	$776\pm^{127}_{108}$	2.01	19.7702	$0.08\pm^{0.18}_{0.21}$	$14.82\pm^{0.47}_{nan}$	0.14
1es1553	0.06364 (#6)	46.18(56)	1785421	8	1740261	7	$1161\pm^{253}_{220}$	1.18	20.1666	$0.07\pm^{0.22}_{0.32}$	$14.72\pm^{0.61}_{nan}$	-0.04
1es1553	0.21869 (#7)	36.89(28)	1666450	9	nan	nan	$36\pm^{20}_{13}$	7.01	23.1064	$-0.43\pm^{0.30}_{0.26}$	$nan\pm^{nan}_{nan}$	2.52
3c249	0.13470 (#8)	–	–	–	–	–	–	–	21.5139	–	–	–
3c249	0.26664 (#9)	53.79(69)	2644	23	2524	18	$320\pm^{120}_{95}$	1.00	24.0155	$1.16E+13\pm^{1.00E+20}_{1.16E+13}$	$16.75\pm^{0.05}_{inf}$	1.35
3c273	0.00758 (#10)	83.67(67)	1048814	3	1012144	3	$3696\pm^{17}_{17}$	1.00	19.1037	$0.04\pm^{0.42}_{0.05}$	$14.45\pm^{1.06}_{nan}$	0.77
3c273	0.06707 (#11)	77.60(60)	1015660	4	1019511	4	$3919\pm^{16}_{16}$	1.00	20.2316	$-0.04\pm^{0.44}_{0.08}$	$nan\pm^{nan}_{nan}$	-0.35
3c273	0.07359 (#12)	63.12(54)	922775	4	1018570	4	$3920\pm^{17}_{16}$	1.00	20.3553	$-0.03\pm^{0.41}_{0.09}$	$nan\pm^{nan}_{nan}$	-0.21
3c273	0.13960 (#13)	–	–	–	–	–	–	–	21.6068	–	–	–
h1821	0.00944 (#14)	120.55(98)	30556	35	43312	33	$1002\pm^{55}_{53}$	1.00	19.1390	$-0.92\pm^{1.21}_{0.70}$	$nan\pm^{nan}_{nan}$	0.86
h1821	0.06779 (#15)	81.53(61)	31940	36	43282	34	$1055\pm^{61}_{60}$	1.00	20.2453	$-0.65\pm^{3.61}_{1.09}$	$nan\pm^{nan}_{nan}$	0.15
.....												

Table 5.8: An abbreviated version of the O VIII upper limit measurements with *XMM-Newton* data, at the prior redshift from the H I lines from Table A.2. The full version of this data is in Table B.8.

Target line		cmin	RGS1	RGS2	power–law		line component			ΔC
Name	z	(d.o.f.)	avg exp (s)	avg exp (s)	norm.	index	λ (Å)	τ_0	$\log N + (\mathrm{cm}^{-2})$	(d.o.f.)
1es1028	0.13714 (#1)	–	–	–	–	–	21.5602	–	–	–
1es1028	0.20383 (#2)	62.35(44)	146640	nan	$1006\pm^{29}_{29}$	1.00	22.8246	1.57	15.92	0.01
1es1028	0.22121 (#3)	57.62(42)	144940	nan	$1031\pm^{32}_{31}$	1.00	23.1541	0.62	15.62	3.89
1es1553	0.03466 (#4)	90.75(81)	1722815	1780022	$752\pm^{116}_{96}$	2.09	19.6172	0.35	15.41	-0.41
1es1553	0.04273 (#5)	89.06(72)	1720386	1774803	$776\pm^{127}_{108}$	2.01	19.7702	0.19	15.17	0.14
1es1553	0.06364 (#6)	46.18(56)	1785421	1740261	$1161\pm^{253}_{220}$	1.18	20.1666	0.27	15.31	-0.04
1es1553	0.21869 (#7)	36.89(28)	1666450	nan	$36\pm^{20}_{13}$	7.01	23.1064	0.28	15.32	2.52
3c249	0.13470 (#8)	–	–	–	–	–	21.5139	–	–	–
3c249	0.26664 (#9)	53.79(69)	2644	2524	$320\pm^{120}_{95}$	1.00	24.0155	5.00E+19	16.80	1.35
3c273	0.00758 (#10)	83.67(67)	1048814	1012144	$3696\pm^{17}_{17}$	1.00	19.1037	0.23	15.24	0.77
3c273	0.06707 (#11)	77.60(60)	1015660	1019511	$3919\pm^{16}_{16}$	1.00	20.2316	0.26	15.29	-0.35
3c273	0.07359 (#12)	63.12(54)	922775	1018570	$3920\pm^{17}_{16}$	1.00	20.3553	0.25	15.27	-0.21
3c273	0.13960 (#13)	–	–	–	–	–	21.6068	–	–	–
h1821	0.00944 (#14)	120.55(98)	30556	43312	$1002\pm^{55}_{53}$	1.00	19.1390	0.95	15.77	0.86
h1821	0.06779 (#15)	81.53(61)	31940	43282	$1055\pm^{61}_{60}$	1.00	20.2453	2.35	16.02	0.15
.....										

Table 5.9: An abbreviated version of the O VII measurements with *Chandra* data, at the prior redshift from the O VI lines from Table A.1. The full version of this data is in Table C.1.

Target line		cmin	LETG		power–law		line component			ΔC
Name	z	(d.o.f.)	avg exp (s)	%	norm.	index	λ (Å)	τ_0	$\log N(\mathrm{cm}^{-2})$	(d.o.f.)
1es1028	0.12314 (#1)	32.34(39)	148933	24	$1757\pm^{63}_{62}$	1	24.2598	$-0.56\pm^{0.97}_{0.68}$	$nan\pm^{nan}_{nan}$	0.44
1es1028	0.13706 (#2)	35.52(39)	148933	24	$1830\pm^{64}_{63}$	1	24.5605	$1.29\pm^{3.09}_{1.34}$	$15.56\pm^{0.30}_{nan}$	0.99
1es1028	0.33735 (#3)	37.26(39)	148933	25	$2138\pm^{81}_{79}$	1	28.8868	$-0.66\pm^{0.98}_{0.74}$	$nan\pm^{nan}_{nan}$	0.56
1es1553	0.18759 (#4)	44.14(38)	495645	22	$3135\pm^{48}_{48}$	1	25.6519	$0.34\pm^{0.57}_{0.46}$	$15.06\pm^{0.37}_{nan}$	0.58
1es1553	0.18775 (#5)	44.13(38)	495645	22	$3135\pm^{48}_{48}$	1	25.6554	$0.35\pm^{0.62}_{0.47}$	$15.07\pm^{0.37}_{nan}$	0.58
1es1553	0.18984 (#6)	42.53(38)	495645	22	$3106\pm^{48}_{48}$	1	25.7005	$-0.38\pm^{0.40}_{0.36}$	$nan\pm^{nan}_{nan}$	1.00
1es1553	0.21631 (#7)	51.98(38)	495645	23	$3137\pm^{49}_{49}$	1	26.2723	$0.29\pm^{0.58}_{0.46}$	$15.00\pm^{0.42}_{nan}$	0.42
1es1553	0.31130 (#8)	36.35(38)	495645	25	$3202\pm^{53}_{54}$	1	28.3241	$-0.04\pm^{0.53}_{0.44}$	$nan\pm^{nan}_{nan}$	0.01
1es1553	0.37868 (#9)	48.60(38)	495645	28	$3322\pm^{62}_{61}$	1	29.7795	$-0.69\pm^{0.39}_{0.33}$	$nan\pm^{nan}_{nan}$	2.89
1es1553	0.39497 (#10)	39.90(38)	495645	28	$3374\pm^{65}_{64}$	1	30.1314	$-0.48\pm^{0.47}_{0.37}$	$nan\pm^{nan}_{nan}$	1.16
h1821	0.02438 (#11)	44.15(32)	470152	2	$888\pm^{22}_{21}$	1	22.1266	$0.33\pm^{0.73}_{0.58}$	$15.05\pm^{0.44}_{nan}$	0.32
h1821	0.10817 (#12)	50.75(39)	470152	1	$1103\pm^{21}_{21}$	1	23.9365	$-1.08\pm^{0.34}_{0.31}$	$nan\pm^{nan}_{nan}$	8.78
h1821	0.12133 (#13)	46.33(38)	470152	1	$1202\pm^{22}_{22}$	1	24.2207	$0.22\pm^{0.59}_{0.46}$	$14.89\pm^{0.49}_{nan}$	0.22
h1821	0.12147 (#14)	46.13(38)	470152	1	$1203\pm^{22}_{22}$	1	24.2238	$0.32\pm^{0.57}_{0.49}$	$15.04\pm^{0.39}_{nan}$	0.44
h1821	0.16992 (#15)	37.35(38)	470152	1	$1107\pm^{23}_{23}$	1	25.2703	$-0.07\pm^{0.57}_{0.45}$	$nan\pm^{nan}_{nan}$	0.02
.....										

Table 5.10: An abbreviated version of the O VII upper limit measurements with *Chandra* data, at the prior redshift from the O VI lines from Table A.1. The full version of this data is in Table C.2.

Target line		cmin	RGS1	power–law		line component			ΔC
Name	z	(d.o.f.)	avg exp (s)	norm.	index	λ (Å)	τ_0	$\log N^+(\mathrm{cm}^{-2})$	(d.o.f.)
1es1028	0.12314 (#1)	32.34(39)	148933	$1757\pm^{63}_{62}$	1	24.2598	0.83	15.40	0.44
1es1028	0.13706 (#2)	35.52(39)	148933	$1830\pm^{64}_{63}$	1	24.5605	2.22	15.71	0.99
1es1028	0.33735 (#3)	37.26(39)	148933	$2138\pm^{81}_{79}$	1	28.8868	0.86	15.43	0.56
1es1553	0.18759 (#4)	44.14(38)	495645	$3135\pm^{48}_{48}$	1	25.6519	0.51	15.23	0.58
1es1553	0.18775 (#5)	44.13(38)	495645	$3135\pm^{48}_{48}$	1	25.6554	0.55	15.24	0.58
1es1553	0.18984 (#6)	42.53(38)	495645	$3106\pm^{48}_{48}$	1	25.7005	0.38	15.11	1.00
1es1553	0.21631 (#7)	51.98(38)	495645	$3137\pm^{49}_{49}$	1	26.2723	0.52	15.23	0.42
1es1553	0.31130 (#8)	36.35(38)	495645	$3202\pm^{53}_{54}$	1	28.3241	0.48	15.21	0.01
1es1553	0.37868 (#9)	48.60(38)	495645	$3322\pm^{62}_{61}$	1	29.7795	0.36	15.08	2.89
1es1553	0.39497 (#10)	39.90(38)	495645	$3374\pm^{65}_{64}$	1	30.1314	0.42	15.13	1.16
h1821	0.02438 (#11)	44.15(32)	470152	$888\pm^{22}_{21}$	1	22.1266	0.66	15.32	0.32
h1821	0.10817 (#12)	50.75(39)	470152	$1103\pm^{21}_{21}$	1	23.9365	0.33	15.05	8.78
h1821	0.12133 (#13)	46.33(38)	470152	$1202\pm^{22}_{22}$	1	24.2207	0.53	15.23	0.22
h1821	0.12147 (#14)	46.13(38)	470152	$1203\pm^{22}_{22}$	1	24.2238	0.53	15.24	0.44
h1821	0.16992 (#15)	37.35(38)	470152	$1107\pm^{23}_{23}$	1	25.2703	0.51	15.21	0.02
.....									

Table 5.11: An abbreviated version of the O VII measurements with *Chandra* data, at the prior redshift from the H I lines from Table A.2. The full version of this data is in Table C.3.

Target line		cmin	RGS1		power–law		line component			ΔC
Name	z	(d.o.f.)	avg exp (s)	%	norm.	index	λ (Å)	τ_0	$\log N(\mathrm{cm}^{-2})$	(d.o.f.)
1es1028	0.13714 (#1)	35.38(39)	148933	24	$1831\pm^{64}_{63}$	1	24.5622	$1.34\pm^{2.73}_{1.32}$	$15.58\pm^{0.28}_{1.74}$	1.14
1es1028	0.20383 (#2)	38.65(38)	148933	24	$1963\pm^{69}_{68}$	1	26.0027	$1.18\pm^{2.92}_{1.29}$	$15.52\pm^{0.31}_{nan}$	0.87
1es1028	0.22121 (#3)	35.87(38)	148933	23	$2058\pm^{71}_{70}$	1	26.3781	$0.80\pm^{2.27}_{1.13}$	$15.39\pm^{0.38}_{nan}$	0.48
1es1553	0.03466 (#4)	38.20(38)	495645	25	$2408\pm^{40}_{39}$	1	22.3487	$-0.03\pm^{0.50}_{0.43}$	$nan\pm^{nan}_{nan}$	0.00
1es1553	0.04273 (#5)	54.53(38)	495645	25	$2461\pm^{41}_{41}$	1	22.5230	$0.31\pm^{0.61}_{0.49}$	$15.03\pm^{0.41}_{nan}$	0.42
1es1553	0.06364 (#6)	48.63(38)	495645	24	$2557\pm^{43}_{42}$	1	22.9746	$-1.05\pm^{0.36}_{0.32}$	$nan\pm^{nan}_{nan}$	7.56
1es1553	0.21869 (#7)	44.59(38)	495645	23	$3121\pm^{49}_{48}$	1	26.3237	$-0.47\pm^{0.39}_{0.35}$	$nan\pm^{nan}_{nan}$	1.52
3c273	0.00758 (#8)	31.25(31)	69608	8	$5771\pm^{159}_{155}$	1	21.7637	$0.01\pm^{0.82}_{0.62}$	$13.58\pm^{1.83}_{nan}$	0.00
3c273	0.06707 (#9)	47.38(38)	69608	9	$6182\pm^{155}_{152}$	1	23.0487	$-0.98\pm^{0.55}_{0.47}$	$nan\pm^{nan}_{nan}$	3.03
3c273	0.07359 (#10)	46.82(39)	69608	8	$6324\pm^{156}_{154}$	1	23.1895	$2.44\pm^{3.08}_{1.40}$	$15.74\pm^{0.15}_{0.25}$	5.26
3c273	0.13960 (#11)	35.63(39)	69608	7	$7537\pm^{171}_{168}$	1	24.6154	$0.62\pm^{1.06}_{0.73}$	$15.29\pm^{0.33}_{nan}$	0.77
h1821	0.00944 (#12)	21.13(18)	470152	2	$900\pm^{29}_{28}$	1	21.8039	$-0.36\pm^{0.52}_{0.42}$	$nan\pm^{nan}_{nan}$	0.63
h1821	0.06779 (#13)	35.37(36)	470152	2	$970\pm^{23}_{22}$	1	23.0643	$-0.12\pm^{0.68}_{0.56}$	$nan\pm^{nan}_{nan}$	0.04
h1821	0.08483 (#14)	41.18(32)	470152	2	$1048\pm^{24}_{23}$	1	23.4323	$-0.01\pm^{0.53}_{0.42}$	$nan\pm^{nan}_{nan}$	0.00
h1821	0.12147 (#15)	46.13(38)	470152	1	$1203\pm^{22}_{22}$	1	24.2238	$0.32\pm^{0.57}_{0.49}$	$15.04\pm^{0.39}_{nan}$	0.44
.....										

Table 5.12: An abbreviated version of the O VII upper limit measurements with *Chandra* data, at the prior redshift from the H I lines from Table A.2. The full version of this data is in Table C.4.

Target line		cmin	RGS1	power–law		line component			ΔC
Name	z	(d.o.f.)	avg exp (s)	norm.	index	λ (Å)	τ_0	$\log N^{+}(\mathrm{cm}^{-2})$	(d.o.f.)
1es1028	0.13714 (#1)	35.38(39)	148933	$1831\pm^{64}_{63}$	1	24.5622	2.02	15.70	1.14
1es1028	0.20383 (#2)	38.65(38)	148933	$1963\pm^{69}_{68}$	1	26.0027	2.11	15.69	0.87
1es1028	0.22121 (#3)	35.87(38)	148933	$2058\pm^{71}_{70}$	1	26.3781	1.70	15.62	0.48
1es1553	0.03466 (#4)	38.20(38)	495645	$2408\pm^{40}_{39}$	1	22.3487	0.47	15.19	0.00
1es1553	0.04273 (#5)	54.53(38)	495645	$2461\pm^{41}_{41}$	1	22.5230	0.55	15.25	0.42
1es1553	0.06364 (#6)	48.63(38)	495645	$2557\pm^{43}_{42}$	1	22.9746	0.34	15.07	7.56
1es1553	0.21869 (#7)	44.59(38)	495645	$3121\pm^{49}_{48}$	1	26.3237	0.37	15.10	1.52
3c273	0.00758 (#8)	31.25(31)	69608	$5771\pm^{159}_{155}$	1	21.7637	0.72	15.36	0.00
3c273	0.06707 (#9)	47.38(38)	69608	$6182\pm^{155}_{152}$	1	23.0487	0.51	15.23	3.03
3c273	0.07359 (#10)	46.82(39)	69608	$6324\pm^{156}_{154}$	1	23.1895	2.24	15.72	5.26
3c273	0.13960 (#11)	35.63(39)	69608	$7537\pm^{171}_{168}$	1	24.6154	0.89	15.43	0.77
h1821	0.00944 (#12)	21.13(18)	470152	$900\pm^{29}_{28}$	1	21.8039	0.47	15.18	0.63
h1821	0.06779 (#13)	35.37(36)	470152	$970\pm^{23}_{22}$	1	23.0643	0.62	15.30	0.04
h1821	0.08483 (#14)	41.18(32)	470152	$1048\pm^{24}_{23}$	1	23.4323	0.48	15.18	0.00
h1821	0.12147 (#15)	46.13(38)	470152	$1203\pm^{22}_{22}$	1	24.2238	0.53	15.24	0.44
.....									

Table 5.13: An abbreviated version of the O VIII measurements with *Chandra* data, at the prior redshift from the O VI lines from Table A.1. The full version of this data is in Table C.5.

Target line		cmin	RGS1		power–law		line component			ΔC
Name	z	(d.o.f.)	avg exp (s)	%	norm.	index	λ (Å)	τ_0	$\log N(\mathrm{cm}^{-2})$	(d.o.f.)
1es1028	0.12314 (#1)	35.82(30)	148933	23	$1585\pm^{62}_{61}$	1	21.2947	$-0.79\pm^{0.77}_{0.55}$	$nan\pm^{nan}_{nan}$	1.19
1es1028	0.13706 (#2)	–	–	–	–	–	21.5587	–	–	–
1es1028	0.33735 (#3)	34.59(38)	148933	24	$1851\pm^{66}_{65}$	1	25.3562	$-0.24\pm^{1.24}_{0.72}$	$nan\pm^{nan}_{nan}$	0.07
1es1553	0.18759 (#4)	43.76(33)	495645	25	$2462\pm^{44}_{44}$	1	22.5167	$0.23\pm^{0.63}_{0.47}$	$15.23\pm^{0.50}_{nan}$	0.23
1es1553	0.18775 (#5)	43.78(32)	495645	25	$2464\pm^{44}_{44}$	1	22.5197	$0.24\pm^{0.63}_{0.48}$	$15.25\pm^{0.48}_{nan}$	0.23
1es1553	0.18984 (#6)	40.55(33)	495645	25	$2490\pm^{43}_{43}$	1	22.5594	$0.20\pm^{1.23}_{0.76}$	$15.18\pm^{0.73}_{nan}$	0.06
1es1553	0.21631 (#7)	30.16(26)	495645	24	$2584\pm^{53}_{52}$	1	23.0612	$-0.45\pm^{0.44}_{0.38}$	$nan\pm^{nan}_{nan}$	1.20
1es1553	0.31130 (#8)	50.56(39)	495645	22	$2998\pm^{46}_{44}$	1	24.8622	$-0.05\pm^{0.58}_{0.33}$	$nan\pm^{nan}_{nan}$	-0.03
1es1553	0.37868 (#9)	48.06(39)	495645	23	$3124\pm^{49}_{48}$	1	26.1398	$-0.37\pm^{0.41}_{0.35}$	$nan\pm^{nan}_{nan}$	0.89
1es1553	0.39497 (#10)	41.84(38)	495645	23	$3095\pm^{49}_{49}$	1	26.4486	$-0.63\pm^{0.38}_{0.33}$	$nan\pm^{nan}_{nan}$	2.79
h1821	0.02438 (#11)	37.76(38)	470152	2	$858\pm^{15}_{14}$	1	19.4222	$0.63\pm^{0.63}_{0.50}$	$15.63\pm^{0.24}_{0.63}$	1.80
h1821	0.10817 (#12)	44.34(38)	470152	2	$854\pm^{17}_{17}$	1	21.0109	$-0.90\pm^{0.39}_{0.34}$	$nan\pm^{nan}_{nan}$	4.97
h1821	0.12133 (#13)	42.59(31)	470152	2	$879\pm^{20}_{20}$	1	21.2604	$-0.16\pm^{0.53}_{0.45}$	$nan\pm^{nan}_{nan}$	0.12
h1821	0.12147 (#14)	42.69(31)	470152	2	$880\pm^{20}_{20}$	1	21.2631	$-0.03\pm^{0.54}_{0.47}$	$nan\pm^{nan}_{nan}$	0.00
h1821	0.16992 (#15)	54.02(38)	470152	2	$895\pm^{20}_{20}$	1	22.1817	$0.27\pm^{0.78}_{0.56}$	$15.29\pm^{0.50}_{nan}$	0.20
.....										

Table 5.14: An abbreviated version of the O VIII upper limit measurements with *Chandra* data, at the prior redshift from the O VI lines from Table A.1. The full version of this data is in Table C.6.

Target line		cmin	RGS1	power–law		line component			ΔC
Name	z	(d.o.f.)	avg exp (s)	norm.	index	λ (Å)	τ_0	$\log N^+(\mathrm{cm}^{-2})$	(d.o.f.)
1es1028	0.12314 (#1)	35.82(30)	148933	$1585\pm^{62}_{61}$	1	21.2947	0.66	15.64	1.19
1es1028	0.13706 (#2)	–	–	–	–	21.5587	–	–	–
1es1028	0.33735 (#3)	34.59(38)	148933	$1851\pm^{66}_{65}$	1	25.3562	0.98	15.77	0.07
1es1553	0.18759 (#4)	43.76(33)	495645	$2462\pm^{44}_{44}$	1	22.5167	0.55	15.58	0.23
1es1553	0.18775 (#5)	43.78(32)	495645	$2464\pm^{44}_{44}$	1	22.5197	0.56	15.58	0.23
1es1553	0.18984 (#6)	40.55(33)	495645	$2490\pm^{43}_{43}$	1	22.5594	0.99	15.80	0.06
1es1553	0.21631 (#7)	30.16(26)	495645	$2584\pm^{53}_{52}$	1	23.0612	0.41	15.48	1.20
1es1553	0.31130 (#8)	50.56(39)	495645	$2998\pm^{46}_{44}$	1	24.8622	0.45	15.52	-0.03
1es1553	0.37868 (#9)	48.06(39)	495645	$3124\pm^{49}_{48}$	1	26.1398	0.38	15.45	0.89
1es1553	0.39497 (#10)	41.84(38)	495645	$3095\pm^{49}_{49}$	1	26.4486	0.35	15.42	2.79
h1821	0.02438 (#11)	37.76(38)	470152	$858\pm^{15}_{14}$	1	19.4222	0.56	15.59	1.80
h1821	0.10817 (#12)	44.34(38)	470152	$854\pm^{17}_{17}$	1	21.0109	0.37	15.43	4.97
h1821	0.12133 (#13)	42.59(31)	470152	$879\pm^{20}_{20}$	1	21.2604	0.49	15.55	0.12
h1821	0.12147 (#14)	42.69(31)	470152	$880\pm^{20}_{20}$	1	21.2631	0.51	15.56	0.00
h1821	0.16992 (#15)	54.02(38)	470152	$895\pm^{20}_{20}$	1	22.1817	0.67	15.65	0.20
.....									

Table 5.15: An abbreviated version of the O VIII measurements with *Chandra* data, at the prior redshift from the H I lines from Table A.2. The full version of this data is in Table C.7.

Target line		cmin	RGS1		power–law		line component			ΔC
Name	z	(d.o.f.)	avg exp (s)	%	norm.	index	λ (Å)	τ_0	$\log N(\mathrm{cm}^{-2})$	(d.o.f.)
1es1028	0.13714 (#1)	–	–	–	–	–	21.5602	–	–	–
1es1028	0.20383 (#2)	24.47(38)	148933	25	$1653\pm^{61}_{59}$	1	22.8246	$-1.22\pm^{0.69}_{0.52}$	$nan\pm^{nan}_{nan}$	2.76
1es1028	0.22121 (#3)	26.80(38)	148933	25	$1757\pm^{63}_{61}$	1	23.1541	$3.82\pm^{13.01}_{2.75}$	$16.13\pm^{0.19}_{0.32}$	3.68
1es1553	0.03466 (#4)	51.93(39)	495645	21	$2174\pm^{31}_{31}$	1	19.6172	$0.21\pm^{0.53}_{0.42}$	$15.19\pm^{0.49}_{nan}$	0.23
1es1553	0.04273 (#5)	42.22(38)	495645	22	$2213\pm^{32}_{32}$	1	19.7702	$0.00\pm^{0.58}_{0.35}$	$13.57\pm^{2.03}_{nan}$	0.00
1es1553	0.06364 (#6)	42.31(39)	495645	23	$2255\pm^{35}_{35}$	1	20.1666	$0.86\pm^{0.85}_{0.59}$	$15.74\pm^{0.21}_{0.44}$	2.66
1es1553	0.21869 (#7)	36.69(30)	495645	24	$2585\pm^{49}_{48}$	1	23.1064	$-0.35\pm^{0.43}_{0.35}$	$nan\pm^{nan}_{nan}$	0.78
3c273	0.00758 (#8)	49.20(38)	69608	6	$5103\pm^{101}_{99}$	1	19.1037	$1.21\pm^{1.27}_{0.81}$	$15.85\pm^{0.19}_{0.39}$	3.07
3c273	0.06707 (#9)	46.91(39)	69608	8	$5560\pm^{124}_{134}$	1	20.2316	$0.02\pm^{0.67}_{0.65}$	$14.14\pm^{1.51}_{nan}$	-0.01
3c273	0.07359 (#10)	43.29(38)	69608	8	$5652\pm^{130}_{128}$	1	20.3553	$1.00\pm^{1.61}_{0.87}$	$15.78\pm^{0.25}_{0.79}$	1.54
3c273	0.13960 (#11)	–	–	–	–	–	21.6068	–	–	–
h1821	0.00944 (#12)	38.66(39)	470152	2	$824\pm^{14}_{14}$	1	19.1390	$-0.32\pm^{0.39}_{0.35}$	$nan\pm^{nan}_{nan}$	0.75
h1821	0.06779 (#13)	39.35(38)	470152	2	$852\pm^{16}_{15}$	1	20.2453	$2.02\pm^{1.67}_{0.98}$	$15.98\pm^{0.13}_{0.19}$	7.79
h1821	0.08483 (#14)	44.68(39)	470152	2	$843\pm^{16}_{16}$	1	20.5684	$-0.26\pm^{0.45}_{0.37}$	$nan\pm^{nan}_{nan}$	0.39
h1821	0.12147 (#15)	42.69(31)	470152	2	$880\pm^{20}_{20}$	1	21.2631	$-0.03\pm^{0.54}_{0.47}$	$nan\pm^{nan}_{nan}$	0.00
.....										

Table 5.16: An abbreviated version of the O VIII upper limit measurements with *Chandra* data, at the prior redshift from the H I lines from Table A.2. The full version of this data is in Table C.8.

Target line		cmin	RGS1	power–law		line component			ΔC
Name	z	(d.o.f.)	avg exp (s)	norm.	index	λ (Å)	τ_0	$\log N^+(\mathrm{cm}^{-2})$	(d.o.f.)
1es1028	0.13714 (#1)	–	–	–	–	21.5602	–	–	–
1es1028	0.20383 (#2)	24.47(38)	148933	$1653\pm^{61}_{59}$	1	22.8246	0.61	15.63	2.76
1es1028	0.22121 (#3)	26.80(38)	148933	$1757\pm^{63}_{61}$	1	23.1541	7.88	16.23	3.68
1es1553	0.03466 (#4)	51.93(39)	495645	$2174\pm^{31}_{31}$	1	19.6172	0.48	15.52	0.23
1es1553	0.04273 (#5)	42.22(38)	495645	$2213\pm^{32}_{32}$	1	19.7702	0.46	15.51	0.00
1es1553	0.06364 (#6)	42.31(39)	495645	$2255\pm^{35}_{35}$	1	20.1666	0.72	15.68	2.66
1es1553	0.21869 (#7)	36.69(30)	495645	$2585\pm^{49}_{48}$	1	23.1064	0.39	15.44	0.78
3c273	0.00758 (#8)	49.20(38)	69608	$5103\pm^{101}_{99}$	1	19.1037	1.04	15.81	3.07
3c273	0.06707 (#9)	46.91(39)	69608	$5560\pm^{124}_{134}$	1	20.2316	0.66	15.64	-0.01
3c273	0.07359 (#10)	43.29(38)	69608	$5652\pm^{130}_{128}$	1	20.3553	1.24	15.85	1.54
3c273	0.13960 (#11)	–	–	–	–	21.6068	–	–	–
h1821	0.00944 (#12)	38.66(39)	470152	$824\pm^{14}_{14}$	1	19.1390	0.37	15.44	0.75
h1821	0.06779 (#13)	39.35(38)	470152	$852\pm^{16}_{15}$	1	20.2453	1.33	15.87	7.79
h1821	0.08483 (#14)	44.68(39)	470152	$843\pm^{16}_{16}$	1	20.5684	0.41	15.46	0.39
h1821	0.12147 (#15)	42.69(31)	470152	$880\pm^{20}_{20}$	1	21.2631	0.51	15.56	0.00
.....									

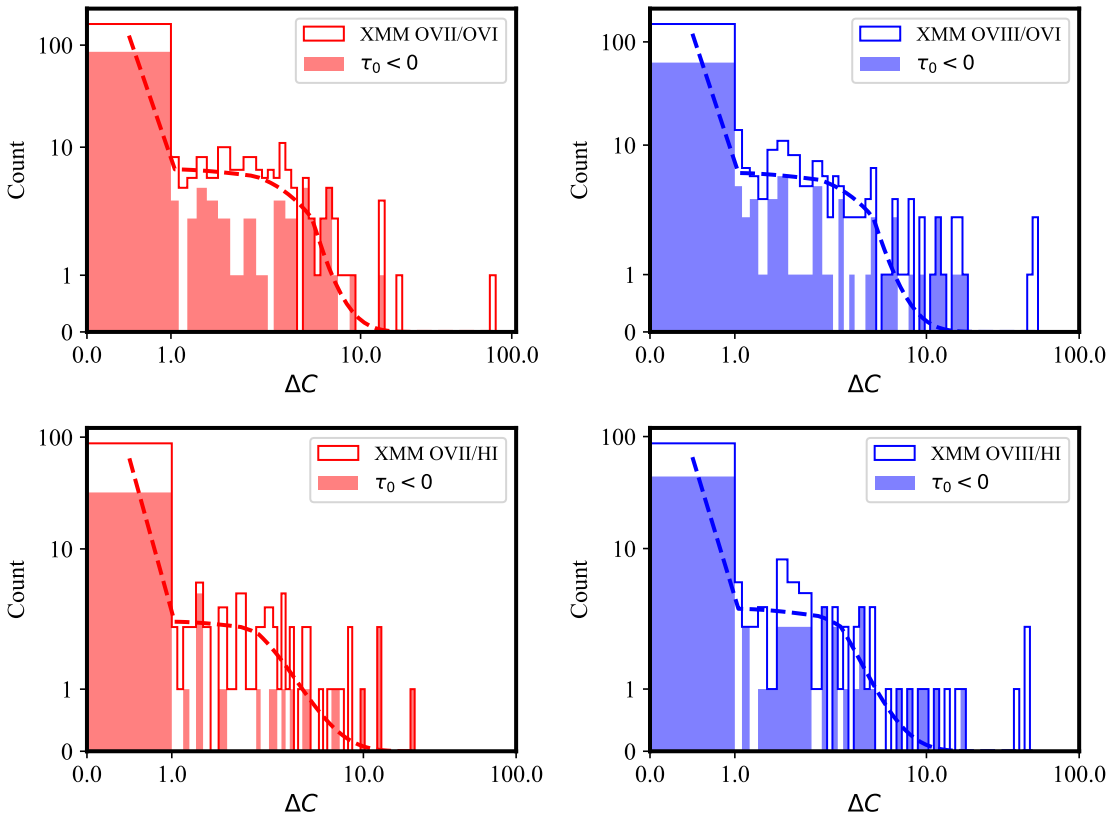

Figure 5.1: Distribution of ΔC statistics for the detection of possible absorption lines for the *XMM-Newton* fits. The dashed line represents the expected cumulative distribution function (CDF) of a $\chi^2(1)$ variable, representing the null hypothesis that there are no emission or absorption lines in the sample. Note that the `symlog` scale and the logarithmic binning contribute to the shape of the CDF. For this figure, we only report statistics for fits with $C_{min}/d.o.f. \leq 3$. To further aid in the identification of possible absorption line detection, the sub–set of fits with negative best–fit parameter τ_0, and therefore with *positive* excess flux above the continuum, were highlighted with a solid histogram plot. Possible absorption line detections are therefore for large values of the ΔC statistic, and with an open histogram.

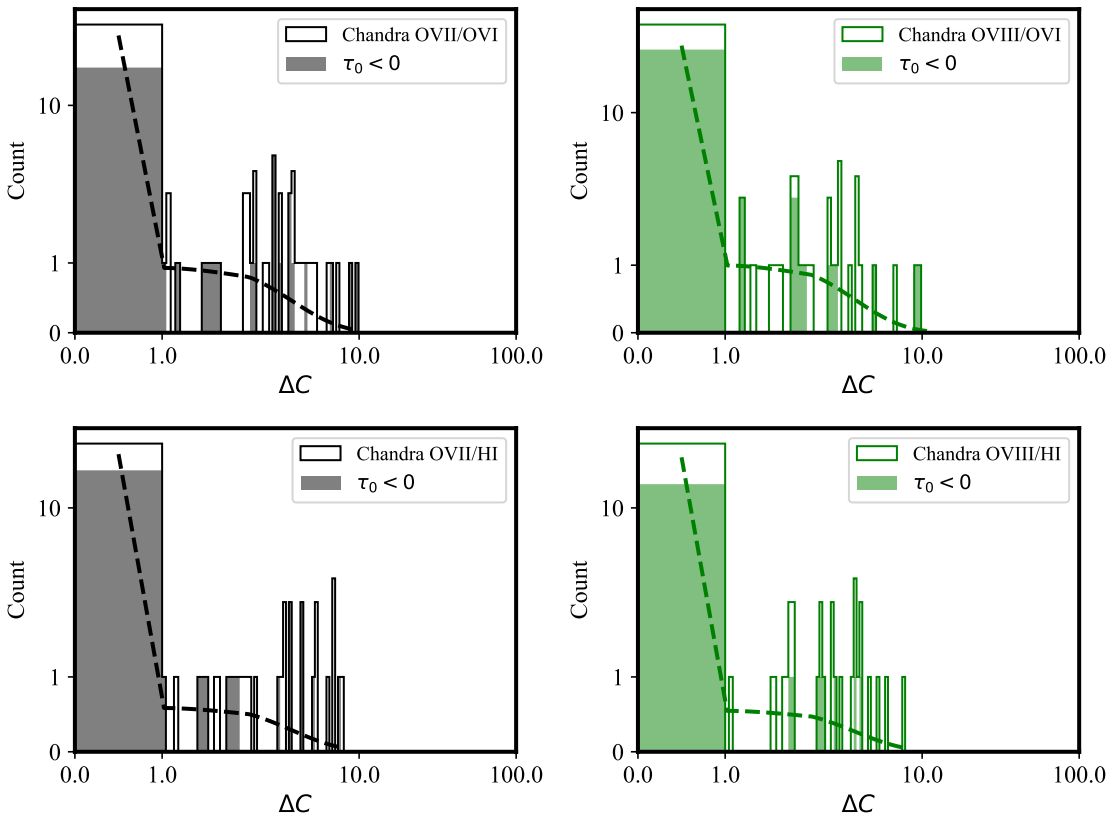

Figure 5.2: Distribution of *Chandra* ΔC statistics for the detection of possible absorption lines. See Figure 5.1 for more information.

5.2 Observations and Redshifts With Previously Reported Detections

As the data sample for this project is so comprehensive (the largest of its kind), there is overlap in our analysis and that of several other papers and previous analyses. Specifically, a number of previously reported detections in other works were analyzed in this project. These prior detections are listed in Table 5.17, and individually explained below:

- 1ES 1553+113: The [64] analysis is virtually identical to that provided in this work, and the putative O VII corresponding to an O VI absorber at $z \simeq 0.188$ is found with similar significance as the earlier publication. Given the limited S/N, this should not be regarded as a conclusive detection.

- 3C 273: The putative O VIII detected by [3] at $z = 0.090$ is not conclusively detected in these obseravtions. Note that the [3] results were based on a modelling of all WHIM species via a `slab` model, which included the putative detection of Ne IX, which we do not investigate in this project.

- Mrk 421: The putative O VII absorption line at $z = 0.011$ tentatively detected by [56] falls close to a known RGS detector artifact near 21.8 Å that was excluded in our analysis. This is consistent with the non–detections reported by [58] and [74].

- PG 1116+215: The current *Chandra* analysis is based on all available observations, whereas the original report of a detection by [8] was based only on the earlier observation. The later observations, reported in [10], had sig-

nificantly higher background, which could not detect the line. The *XMM-Newton* observations have an RGS gap near the putative line, and do not provide useful data.

- PKS 2155-304: [27, 26, 25] reported a possible $z = 0.0543$ O VIII line, which would fall between the two O VI priors investigated in this project (at $z = 0.054$ and 0.057), which were investigated by [50]. [75, 17] did not confirm those results on the O VIII line. [50] did not find evidence of any O VII lines at the FUV prior redshifts, and found marginal evidence of a possible O VIII line at one of the two redshifts, but with inconsistent results among the instruments used. Our analysis do not detect O VIII absorption at either of the two FUV priors that were investigated.

  Moreover, at those redshifts, any O VII absorption would fall near an inefficiency in the detectors at 22.7-22.8 Å that makes the assessment very uncertain. Specifically, system 266 ($z = 0.054$, $\lambda = 22.7675$ Å) has a very poor fit if the data in the inefficiency are included, and that fit should not be considered useful. And system 267 ($z = 0.057$, $\lambda = 22.8327$ Å), with the 22.7-22.8 Å data removed from the fit, does not feature significant absorption. This spectrum can be seen in Figure 5.3.

- Ton S180: The tentative *XMM-Newton* detection of O VII corresponding to an O VI prior by [2] is confirmed by this re–analysis (see system 308).

Table 5.17: Analysis of selected sources with prior reported detection of possible WHIM X–ray absorption lines.

Source	Species	Redshift	FUV Prior		References	Notes
			ID	ΔC (XMM; Chandra)		
1ES 1553+113	O VII	0.4335, 0.3551		—	[54]	No FUV priors were used in the search
	O VII	0.1878	#4,5(OVI)	(7.82, 7.53; 0.58,0.58)	[64]	This was reported as a marginal detection.
3C 273	O VIII	0.090	#21(OVI)	(1.16; 6.58)	[3]	(Redshifted O VII coincides with Galactic O I).
H 1821+643	O VII	(Stacked)		—	[46]	Several FUV priors were stacked
H 2356-309	O VII	0.03		—	[24, 13]	No FUV priors were used in the search
Mrk 421	O VII	0.011	#231	$(---;9.92^{(*)})$	[56, 58, 74]	#231 uses O VI prior at 0.0100, not used in search. XMM redshifted O VII was unavailable (21.5-21.9Å ignored)
	O VII	0.027		—		
PG 1116+215	O VIII	0.093	#76,77(HI)	(0.19, 0.212; 0.5,0.61)	[8, 10]	XMM has nearby detector gap.
PKS 0558-123	O VII	0.117		—	[55]	#213 is O VI prior at z=0.1047, nearby
PKS 2155-304	O VIII	0.0543			[26, 25, 27, 75, 17]	No FUV priors used in the search; detection is contested.
PKS 2155-304	O VIII	0.054	#266(OVI)	(0; 0.73)	[50]	Disagreement among instruments in N19.
		0.057	#267(OVI), #129(HI)	(0, 0; 0.1, 0.1)		
Ton S180	O VII	0.04579	#308(OVI)	$(14.4; 2.08^{(*)})$	[2]	XMM detection confirmed, Chandra had low S/N, as originally noted.

Notes: $(*)$ Model has emission line feature with negative τ_0.

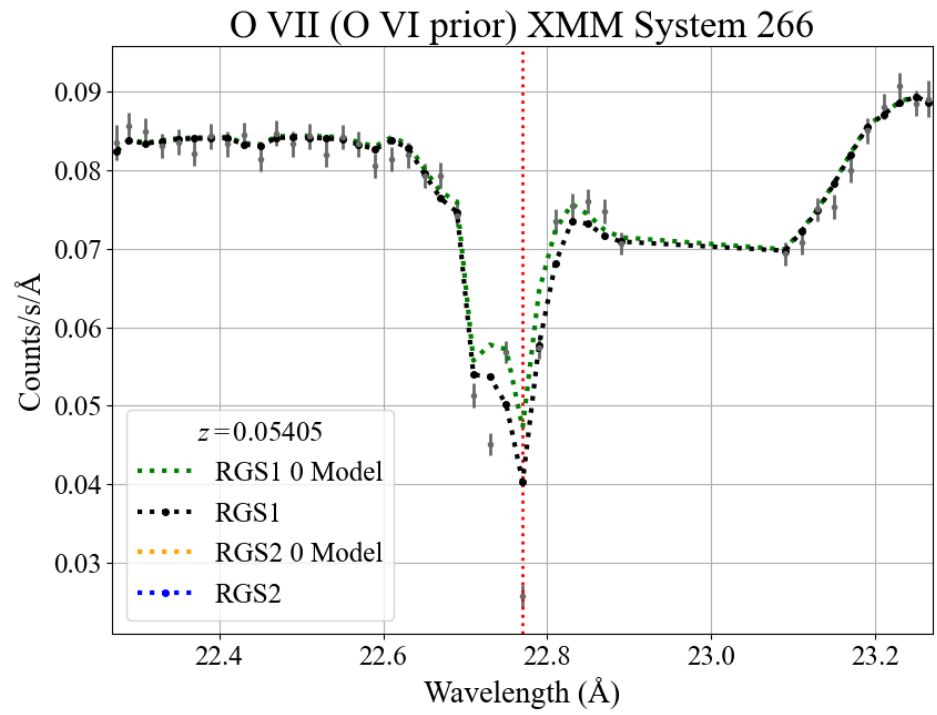

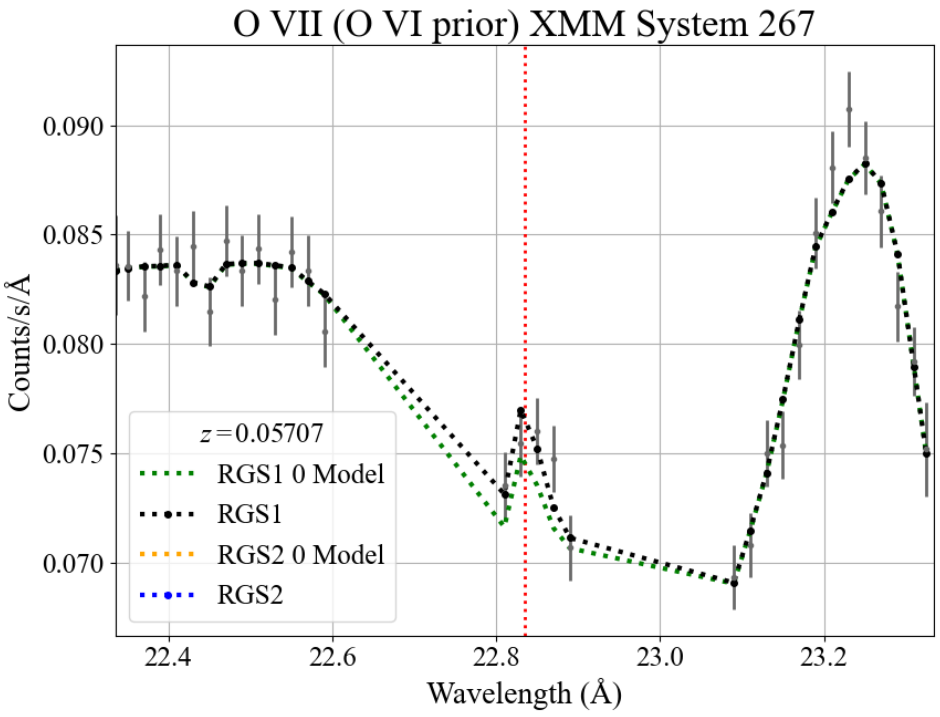

Figure 5.3: PKS 2155 *XMM-Newton* data system 266 and 267, O VII with O VI priors. "0 Model" indicates the model with the τ_0 value frozen and set to 0, mimicking the scenario in which no absorption or emission is present. Note the significant inefficiency around ∼22.78Å that remains similar between the model and 0 model in system 266, and significant data removal required for system 267.

Overall, the results of our analysis on previously detected absorption lines was mixed but insightful. Several of the observations were seemingly reconfirmed by our analysis (1ES 1553+113 $z = 0.1878$, Ton S180 $z = 0.04579$), which in and of its self is a positive result. Because of both the quality of the *XMM-Newton* data and the exclusion of 21.5-21.9Å in our analysis, a majority of the prior detections for O VII and O VIII were deemed inconclusive or provided evidence of non-detections. High background amounts and significant amounts of inefficiencies in the *XMM-Newton* spectra created a large amount of difficulties around the expected wavelengths being analyzed. This limitation is discussed more in Section 6.1.

5.3 Galactic Oxygen at $z = 0$

Another aspect of the analysis in this project was the ability to search for galactic oxygen O VII and O VIII at every source. This process was completed simply by repeating the main analysis of searching for possible detections at prior detections, but by instead using the rest wavelength of the resonance lines of O VII and O VIII at $\lambda = 21.602$Å and 18.797Å respectively. The details and results of this search are shown in Table 5.18.

If these results are interpreted with a cutoff of $\Delta C \geq 6.6$ indicating possible detection, a total of 7 possible detections for both galatic O VII (1ES 1553+113, 3C 273, Mrk421, NGC7469, PKS2005-489, and PKS2155-304) and O VIII (3C 273, H2356-309, MR2251-178, Mrk421, PG1211+143, and PKS2155-304) were made through this analysis.

Table 5.18: Results of the search for galactic O VII and O VIII for every source available in the sample. The ΔC values denote the difference in the C statistic between the model fit at the rest wavelengths for their respective ions, and the statistic after the τ_0 parameter was set to 0. "LARGE" indicates a ΔC value significantly larger than 1000. In practice, this indicates a range of data with large inefficiencies around the expected galactic line's wavelength.

		XMM o7		Chandra o7		XMM o8		Chandra o8	
#	Source	DOF	ΔC	DOF	ΔC	DOF	ΔC	DOF	ΔC
1	1ES1028+511	46	0.47	38	2.35	94	2.62	38	0.56
2	1ES1553+113	48	28.49	38	0.91	97	-0.04	38	1.46
3	3C249.1	45	0.12	–	–	91	0.27	–	–
4	3C273	47	249.47	38	15.05	98	26.86	38	5.22
5	E1821+643	48	3.45	38	0.08	98	5.65	38	0.01
6	H2356-309	48	1.92	38	2.66	97	7.52	38	0.17
7	Q0056-363	47	2.89	–	–	97	0.30	–	–
8	RXJ0228-40	46	0.94	–	–	94	0.03	–	–
9	REJ2248-511	47	1.62	–	–	97	1.62	–	–
10	MR2251-178	47	2.76	38	2.46	98	8.19	38	1.15
11	Mrk421	47	657.27	38	285.93	99	2.38	38	44.76
12	MARK876	47	1.85	–	–	97	0.87	–	–
13	NGC7469	48	15.50	–	–	98	1.83	–	–
14	1ES1101-232	45	5.59	–	–	94	1.62	–	–
15	PG0003+158	46	0.04	–	–	94	0.45	–	–
16	Mrk1014	46	0.02	–	–	93	0.07	–	–
17	PG0804+761	48	0.29	–	–	99	5.66	–	–
18	FBQSJ083535.8+24594	46	0.07	–	–	93	LARGE	–	–
19	PG0953+414	45	3.23	–	–	91	0.01	–	–
20	PG1115+407	46	2.52	–	–	91	0.01	–	–
21	PG1116+215	47	1.51	38	1.23	95	1.28	38	1.87
22	PG1211+143	47	4.57	38	4.77	97	10.00	38	0.02
23	PG1216+069	46	1.16	–	–	94	0.02	–	–
24	PG1259+593	46	0.18	–	–	94	0.04	–	–
25	PG1307+085	46	0.36	–	–	92	1.32	–	–
26	PG1309+355	45	2.77	–	–	91	1.09	–	–
27	PG1444+407	46	0.75	–	–	92	1.03	–	–
28	PG1626+554	46	0.01	–	–	94	0.24	–	–
29	PHL1811	46	LARGE	–	–	95	LARGE	–	–
30	PKS0312-770	46	0.32	–	–	93	0.88	–	–
31	PKS0405-1219	46	0.36	38	0.07	94	0.46	38	0.14
32	PKS2005-489	46	19.79	–	–	95	0.10	–	–
33	PKS2155-304	47	230.59	38	37.37	98	88.58	38	13.73
34	M31Halo28	45	LARGE	–	–	94	LARGE	–	–
35	RXJ1230.8+0115	46	1.45	–	–	93	LARGE	–	–
36	RBS1892	46	0.27	–	–	94	-0.00	–	–
37	1H0419-577	48	3.90	–	–	97	2.24	–	–
38	RXJ0439.6-5311	46	6.17	–	–	95	0.01	–	–
39	S50716+714	46	0.37	–	–	95	1.46	–	–
40	Ton28	46	1.29	–	–	95	0.66	–	–
41	TonS180	46	0.07	38	0.63	97	4.40	38	2.77

5.4 Possible Detections

A number of the completed fits during the analysis resulted in characteristics indicative of a positive absorption line detection. These characteristics usually corresponded to a high ΔC value of the fit, a significant positive τ_0 value, and a significantly absorption line observation upon visual inspection of the fit's plot. The cutoff for these fits was decided to be at $\Delta C = 6.6$, corresponding to $\sim 98.9\%$ on a $\chi^2(1)$ distribution. These fits are as follows, generally with a preference for higher ΔC values first;

- 3C 273, O VII at O VI prior, system 21 ($z = 0.09018$) in Table B.1, $\underline{\Delta C = 78.3}$, $C_{\rm min}$/d.o.f.=100.60/47. The line, which is the strongest detection in the sample, appears at wavelengths $\lambda = 23.5479$, which is similar to galactic O I ($\lambda = 23.506$). [3] has already discussed the difficulties in disentangling the galactic O I absorption from possible redshifted O VII absorption, and we do not further attempt to determine its galactic versus WHIM origin. We simply note that [3] reported possible detection of O VIII at the redshift of system 21, so it is also possible that part of the O VII absorption is in fact due to the WHIM. The line is not highly significant in the *Chandra* data (system 77, $\Delta C = 3.9$).

  WHIM detection status: ..... uncertain.

- 3C 273, O VII at O VI priors, system 23, $z = 0.1466$, $\underline{\Delta C = 17.9}$, $C_{\rm min}$/d.o.f.=91.01/79. The redshift of the source is $z = 0.158$, so if this is an intrinsic line it would imply a line–of–sight velocity towards the observer of $v = -3,300$ km s^{-1},

which appears quite large to be intrinsic to the source. This redshift was not examined by [3], because the O VI absorption did not have a reported b parameter. The line is not present in the *Chandra* data (system 79, best–fit $\tau_0 < 0$). The spectrum is shown in Figure 5.6

WHIM detection status: ..... possible detection.

- Ton S180, O VII at O VI prior, system 308 in Table B.1, $z = 0.0456$, $\underline{\Delta C = 14.4}$, $C_{\rm min}$/d.o.f.=39.89/45. This is a confirmation of the previous detection of this line by [2]. The *Chandra* data do not have a significant detection because of the lower S/N of the spectrum, as previously noted also by [2]. The spectrum is shown in Figure 5.4

  WHIM detection status: ..... possible detection.

- PG 1211, O VII at O VI prior, system 180 in Table B.1, $z = 0.05117$, $\underline{\Delta C = 13.5}$, $C_{\rm min}$/d.o.f.=45.23/34. The line is located at $\lambda = 22.705$, which is near the Galactic O IV line at $\lambda = 22.74$ Å. Moreover, the line falls on a region of reduced efficiency, which might not be perfectly calibrated, casting doubts on its reality. The *Chandra* data do not show any absorption.

  WHIM detection status: ..... uncertain.

- 1ES 1553+113, O VII at O VI prior, systems 4 and 5 in Table B.1, $z = 0.18759, 0.18775$, $\underline{\Delta C = 7.8, 7.5}$, $C_{\rm min}$/d.o.f.= 102.1/88, 102.3/88. The two systems are indistinguishable at the resolution of the *XMM-Newton* data. This is the same system that was tentatively identified by [64], and therefore

this re–analysis finds similar results. The spectra are show in Figure 5.5

WHIM detection status: ..... possible detection.

- PKS 0405-123, O VII at O VI prior, system 45 Table C.1 (*Chandra*), $z = 0.16566$, $\underline{\Delta C = 7.2}$, $C_{\rm min}$/d.o.f.= 45.81/38. The corresponding *XMM-Newton* spectrum does not show significant absorption, although it has shorter exposure than the *Chandra* data.

  WHIM detection status: ..... uncertain.

- NGC 7469, O VIII at O VI priors, systems 121 through 123 ($z = 0.0962 - 0.0115$) in Table B.5, $\underline{\Delta C = 45.8, 53.8, 53.4}$, $C_{\rm min}$/d.o.f.=84.33/74, 94.79/74, 85.80 74. Also, H I BLA prior, system 46 ($z = 0.00981$), $\Delta C = 51.6$.

  NGC 7469 is a well–known Seyfert 1 galaxy at $z = 0.0164$, and the redshifted O VIII Ly α line falls near $\lambda = 19.2$Å. The *XMM-Newton* X–ray spectra have been previously analyzed by several groups [*e.g.,* 7, 61, 6, 36]. The earlier analyses identified a putative O VIII Ly α emission line intrinsic to the galaxy at an observed wavelength $\lambda \simeq 19.3$Å. Moreover, the same analyses already detected at high significance the possible O VIII Ly α absorption line we also detect, which they attributed to an unidentified warm absorber associated with the galaxy at a peculiar velocity of $\sim -1,000$ km s^{-1} towards the observer.

  The photoionization modelling of the warm absorber by [36] does not take into account the O VI and the H I BLA priors we have used for our search. It is therefore possible to speculate that the O VIII absorption line is in

fact associated with a genuine line–of–sight WHIM absorber, rather than an intrinsic absorber, although the intrinsic origin with peculiar velocity along the sightline cannot be discarded.

WHIM detection status: ..... uncertain.

- 1ES 1553, O VIII at O VI prior, system 8, $z = 0.31130$, $\underline{\Delta C = 17.08}$, $C_{\rm min}$/d.o.f.=113.12/91. This redshift was not searched by [64], because it only had the λ=1032 Å O VI absorption line detected. The Chandra data do not show any absorption at this redshift (system 8). There is no associated O VII at this redshift. The spectrum is shown in Figure 5.7

  WHIM detection status: ..... possible detection.

- 1ES 1553, O VIII at O VI prior, system 9, $z = 0.37868$, $\underline{\Delta C = 15.34}$, $C_{\rm min}$/d.o.f.=113.07/88. There is no O VII at this redshift. It was not observed by [64], because it only had the λ=1032 Å O VI absorption line detected. The spectrum is shown in Figure 5.7

  WHIM detection status: ..... possible detection.

- 1ES 1553, O VIII at O VI prior, system 9, $z = 0.1898$, $\underline{\Delta C = 8.2}$, $C_{\rm min}$/d.o.f.=25.62/27. This line is at $\lambda = 22.5594$Å, with two galactic O V and O IV lines approximately 0.1Å away on either side. In [64], this line had a smaller significance of $\Delta C = 2.3$, and it was not reported as significant.

  WHIM detection status: ..... uncertain.

- Mkn 421, O VIII at O VI prior, system 114, $z = 0.010$, $\underline{\Delta C = 9.7}$, $C_{\rm min}$/d.o.f.=95.39/57. The corresponding *Chandra* data, system 81, could not be fit to the usual

1 Å band around the line, because the continuum has an unusual shape, likely because the spectrum is the result of averaging different states of the source. The *Chandra* data does not indicate presence of absorption.

WHIM detection status: ..... uncertain.

- PKS 0405-123, O VIII at O VI prior, system 259, $z = 0.36329$, $\underline{\Delta C = 8.0}$, $C_{\rm min}$/d.o.f.=110.13/94. The *Chandra* data do not have an absorption feature at this redshift.

  WHIM detection status: ..... uncertain.

- PG 0804+761, O VII at H I prior, system 52, $z = 0.0502$, $\underline{\Delta C = 7.4}$, $C_{\rm min}$/d.o.f.=46.31/37. This is a short *XMM-Newton* exposure, and there are no *Chandra* data.

  WHIM detection status: ..... uncertain.

- PG 1116+215, O VII at H I prior, system, $z = 0.0838$, $\underline{\Delta C = 8.2}$, $C_{\rm min}$/d.o.f.=46.62/32. The *Chandra* data, which were used in [8], do not have absorption at this redshift.

  WHIM detection status: ..... uncertain.

- S50716+714, O VII at H I prior, system 159, $z = 0.0883$, $\underline{\Delta C = 8.0}$, $C_{\rm min}$/d.o.f.=48.91/39. There are no available *Chandra* data for this source.

  WHIM detection status: ..... uncertain.

- H1821+643, O VII at H I prior, system 16 (*Chandra*), $z = 0.19817$, $\underline{\Delta C = 6.9}$, $C_{\rm min}$/d.o.f.=30.74/38. The substantially shorter *XMM-Newton* data do not

have absorption at this redshift.

WHIM detection status: ..... uncertain.

- MR 2251-178, O VII at H I prior, systems 28 and 29 (*Chandra*), $z = 0.0633, 0.0638$, $\underline{\Delta C = 6.8, 8.0}$, $C_{\rm min}$/d.o.f.=50.52/39, 48.05/38. The redshift of the source is $z = 0.064$, so this is probably intrinsic absorption.

  WHIM detection status: ..... uncertain.

- PG 1116+215, O VII at H I prior, system 38 (*Chandra*), $z = 0.13373$, $\underline{\Delta C = 7.0}$, $C_{\rm min}$/d.o.f.=41.71/34. The *Chandra* analysis of [8] showed a marginal absorption feature from the longer observation available for this source. The *XMM-Newton* data have marginal absorption at that redshift (system 79, $\Delta C = 5.4$). The spectrum is shown in Figure 5.9.

  WHIM detection status: ..... possible detection.

- MR 2251-178, O VIII at H I prior, systems 33 through 36 ($z = 0.0619 - 0.0638$) of Table B.7, $\underline{\Delta C = 16.53, 38.9, 45.7, 45.5}$, $C_{\rm min}$/d.o.f.=62.95/47, 50.87/49, 44.88/49, 45.72/49. MR 2251-178 is a quasar at $z = 0.064$ whose X–ray emission with *ROSAT* and *RXTE* was previously studied respectively by [45] and [4]. Interestingly, the low–resolution *ROSAT* data analyzed by [45] did indicate the presence of intrinsic O VII and O VIII absorption. At a nominal difference of just $\Delta z \leq 0.002$, it is reasonable to speculate that the detected absorption is intrinsic to the source, implying peculiar sight–line negative velocities of $v \geq -600$ km s^{-1}, which are common for quasars and

AGNs.

WHIM detection status: ..... uncertain.

- PKS 0405, O VIII at H I prior, system 121, $z = 0.19456$, $\underline{\Delta C = 13.4}$, $C_{\rm min}$/d.o.f.=47.40/42. The source is at $z = 0.574$, and the line is at $\lambda = 22.6489$ Å, with the nearest galactic line being O IV at $\lambda = 22.74$ Å. There is no O VII absorption line detected. The spectrum is shown in Figure 5.8.

  WHIM detection status: ..... possible detection.

- H1821+643, O VIII at H I prior, system 13 (*Chandra*), $z = 0.0678$, $\underline{\Delta C = 7.8}$, $C_{\rm min}$/d.o.f.=39.35/38. The substantially shorter *XMM-Newton* data do not have absorption at this redshift.

  WHIM detection status: ..... uncertain.

In all, 7 possible detections (for a total of 8 systems) were reported in our full analysis of the sample, those being:

1. 3C 273, O VII at O VI prior, system 23 $z = 0.1466$.
2. Ton S180, O VII at O VI prior, system 308 $z = 0.0456$.
3. 1ES 1553+113, O VII at O VI prior, systems 4-5 $z = 0.18759, 0.1877$.
4. 1ES 1553+113, O VIII at O VI prior, system 8 $z = 0.31130$.
5. 1ES 1553+113, O VIII at O VI prior, system 9 $z = 0.37868$.
6. PG 1116+21, O VII at H I prior, system 38 (*Chandra*) $z = 0.13373$.
7. PKS 0405, O VIII at H I prior, system 121 $z = 0.19456$

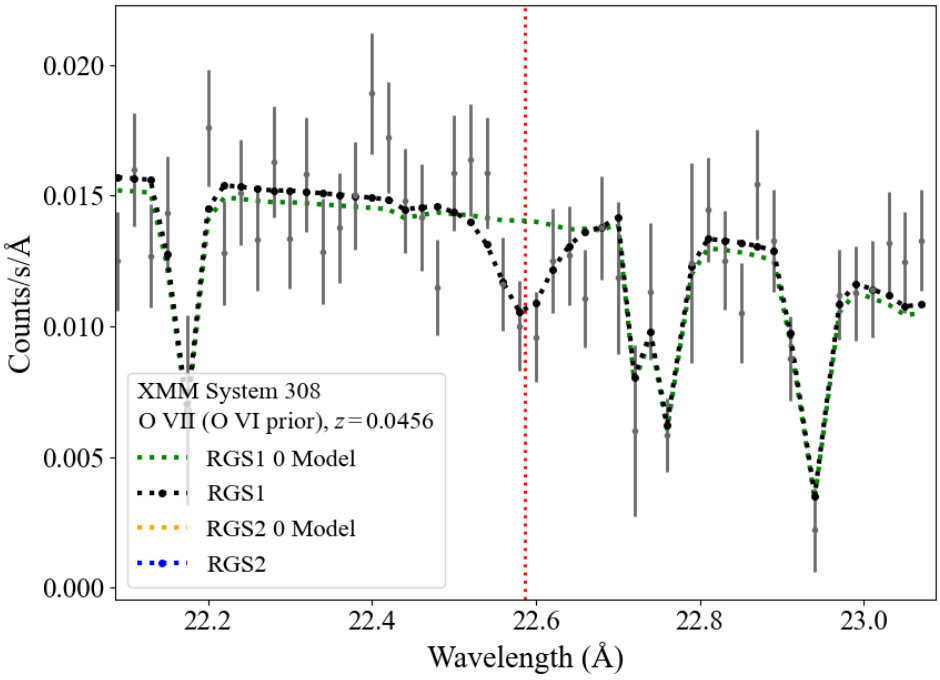

Figure 5.4: Ton S180 *XMM-Newton* data system 308, O VII with O VI priors.

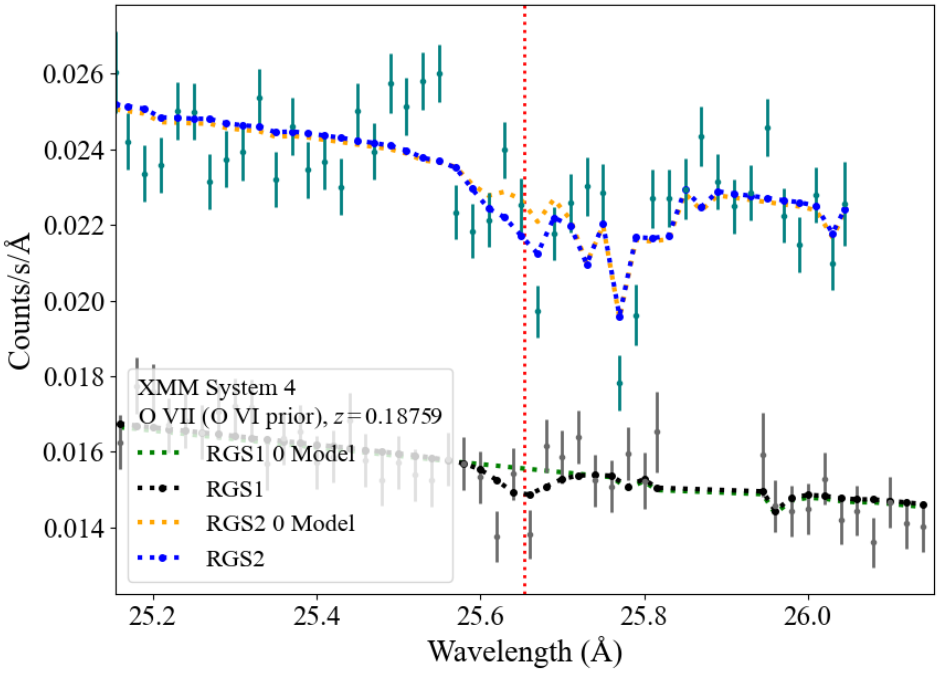

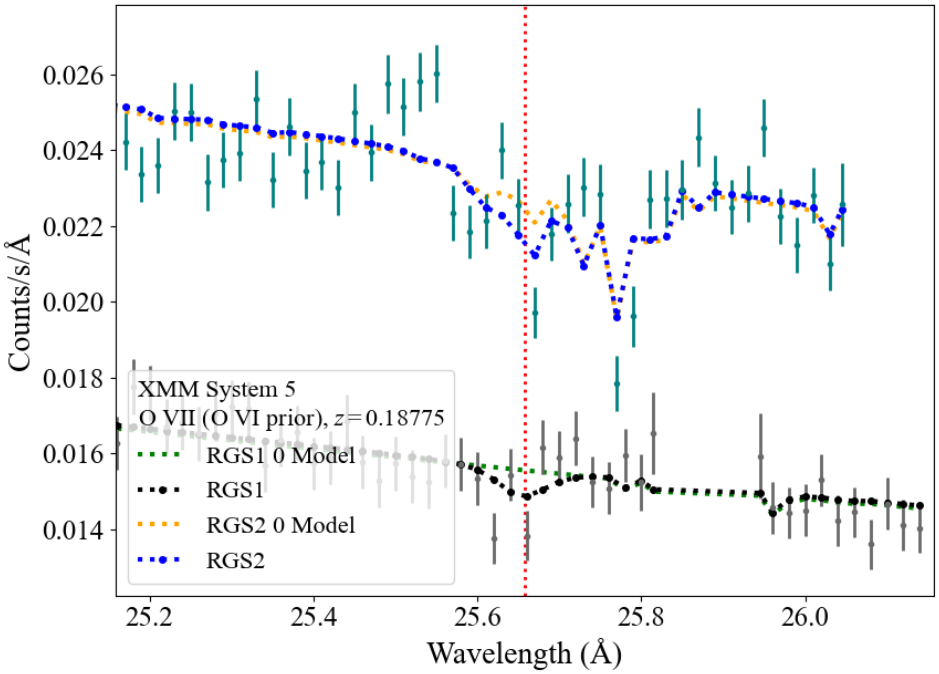

Figure 5.5: 1ES 1553+113 *XMM-Newton* data system 4-5, O VII with O VI priors.

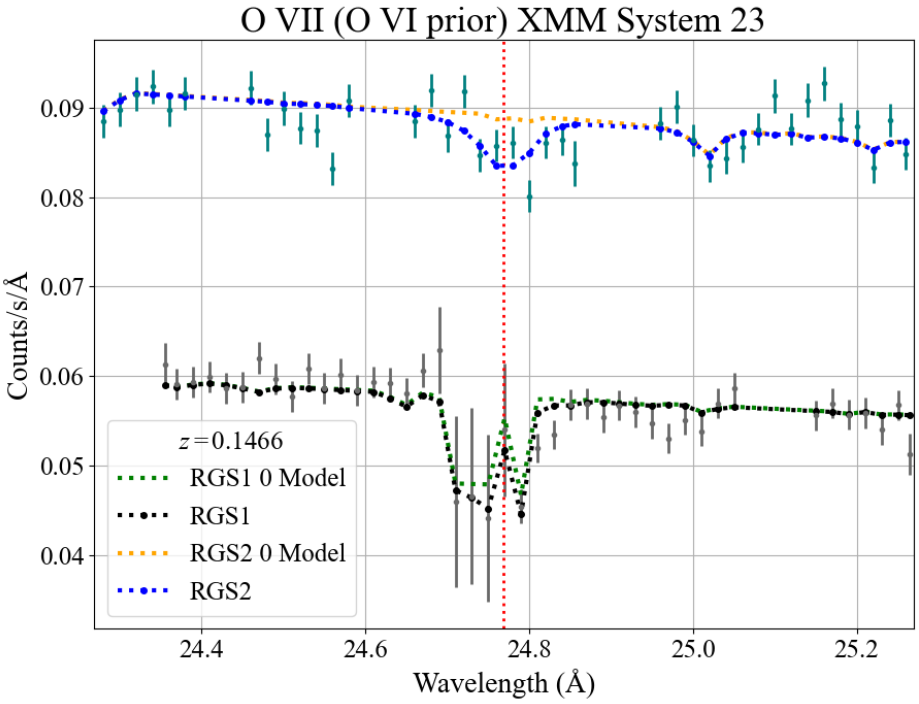

Figure 5.6: 3C 273 *XMM-Newton* data system 23, O VII with O VI priors.

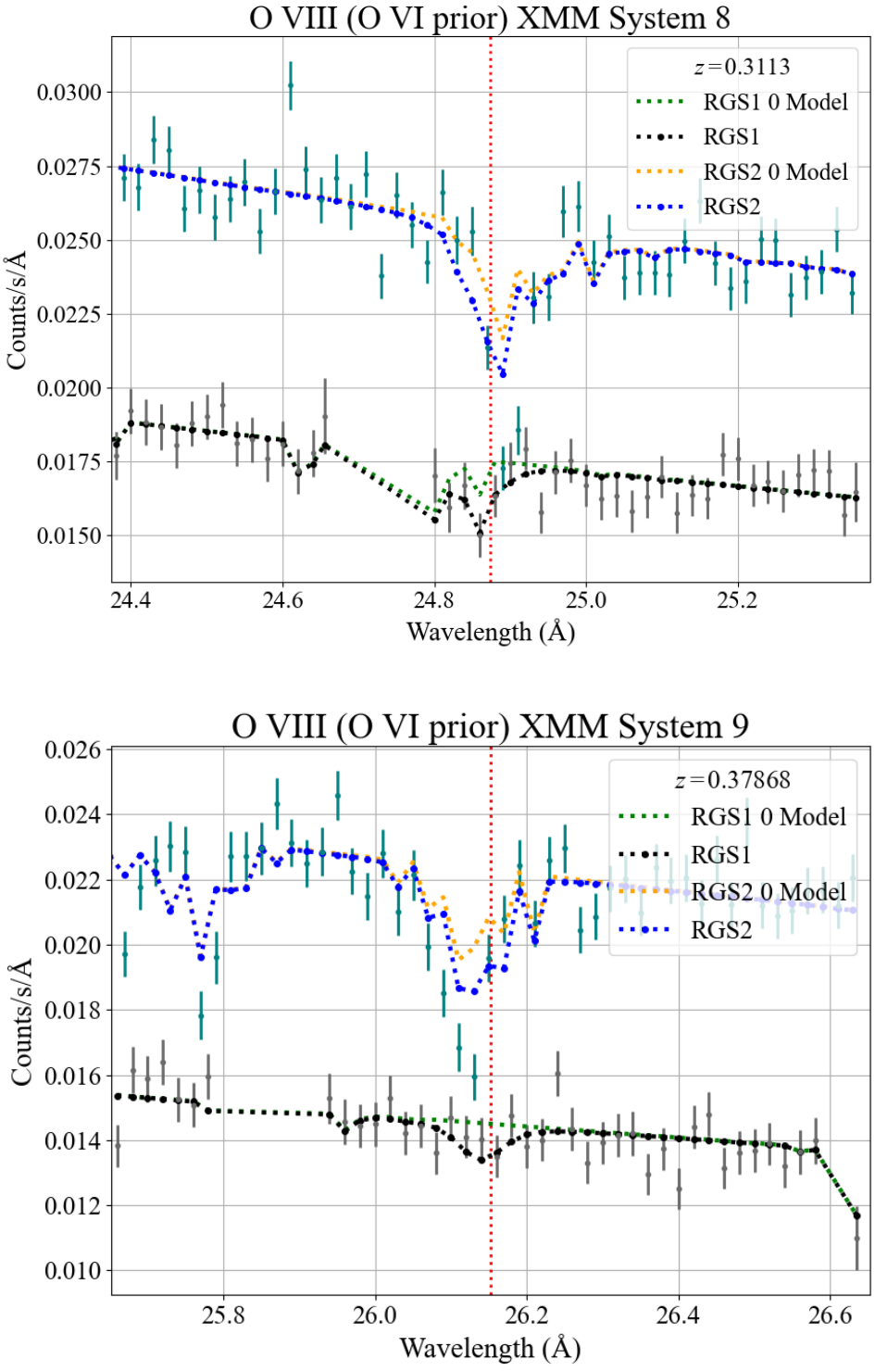

Figure 5.7: 1ES 1553+113 *XMM-Newton* data system 8-9, O VIII with O VI priors.

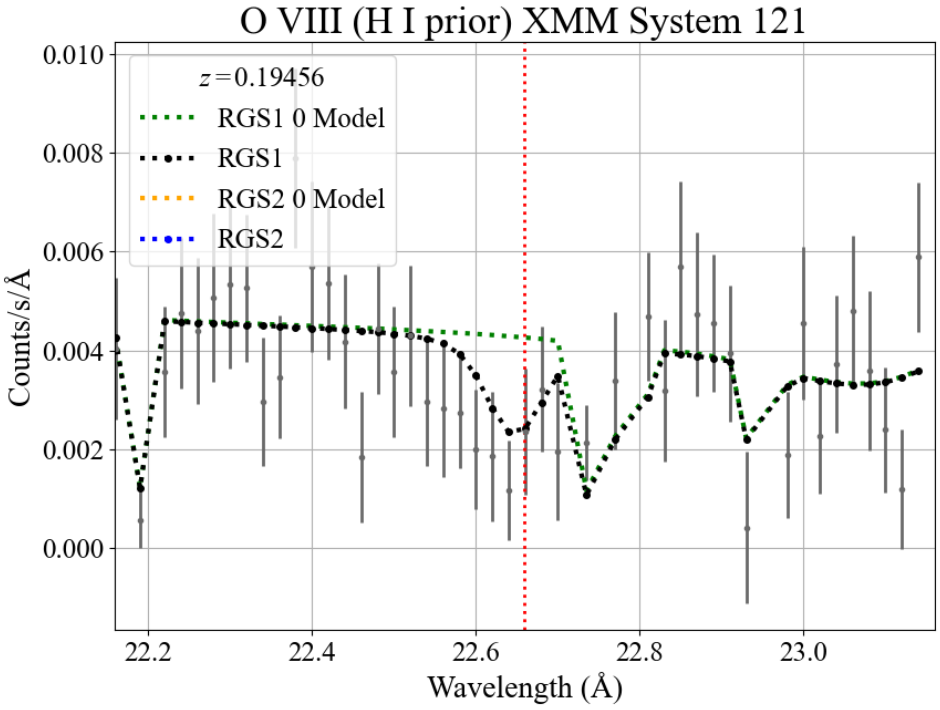

Figure 5.8: PKS0405 *XMM-Newton* data system 121, O VIII with H I priors.

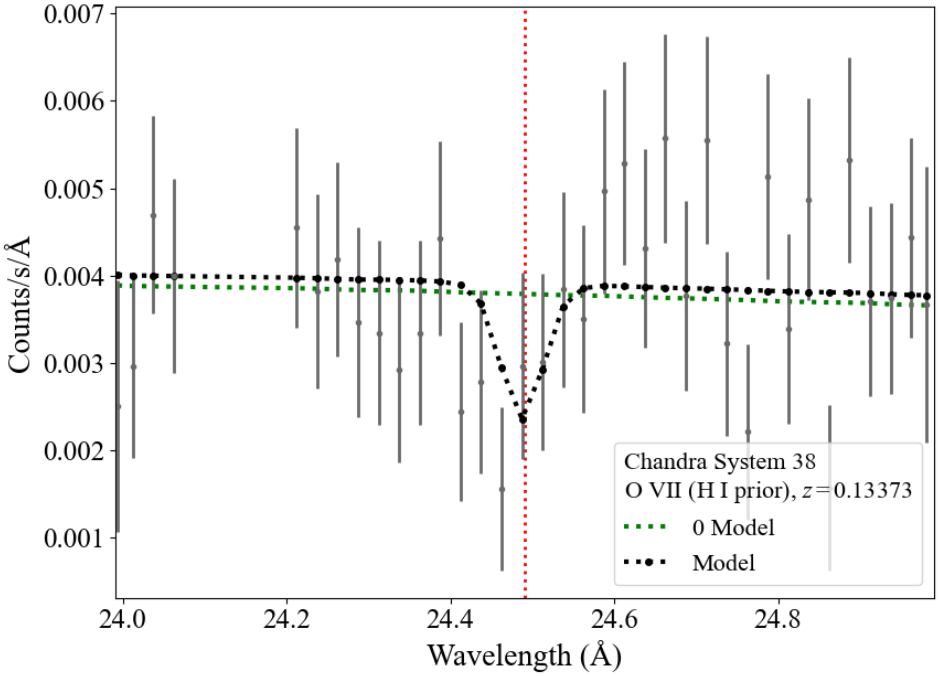

Figure 5.9: PG 1116+21 *Chandra* data system 38, O VII with H I priors.

5.5 Estimation of Baryonic Density

Using the results of the analysis and a Python script which adapts the equations described in Section 3.3.4, an estimation of the baryonic density of the universe due to the WHIM was easily calculated. First, all of the column density upper limits were imported into a Python script. Alongside this, the sample table information including redshifts, source names, and O VI prior detection column densities were all imported and matched to their corresponding upper limits. As described in Section 4.3, the upper limits were then split into two different values according to the sensitivity and F.C. method, which are reported separately in the results of this section. Following this, the expectation of each upper limit is calculated according to Equation 3.8 and stored. A plot of these expectation results can be seen in Figures 5.10 and 5.11 for the *XMM-Newton* and *Chandra* data respectively. After this is completed, the summation of those expectations is completed according to Equation 3.9. A corresponding distance summation was computed corresponding to Equation 3.11, in the form of

$$D_{sum} = \sum_{i=1}^{n} D_i, \tag{5.1}$$

where n is the total number of sources used, and D_i is the effective distance of each of those sources. Following this, ρ_{ion} was calculated using Equation 3.10, Ω_{ion} using Equation 3.12, and finally the cosmological density of the WHIM due to the ion, $\Omega_{WHIM,ion}$, using Equation 3.13. This $\Omega_{WHIM,ion}$ was then used for the final comparison with Ω_b to yield the ratio of the cosmological density of baryons

due to the WHIM to the universe's cosmological density of baryons. The results of these calculations for each individual sample are in Tables 5.19-5.26, and the compiled results of all analyses is in Table 5.27.

Because of the limitations described later in Section 6.1, the overall analysis results only provide conservative upper limits on these estimates of the cosmological density of baryons. To supplement these results, we completed the same analysis done on the upper limits for the individual sample systems that yielded possible detections detailed in Section 5.4. These results were compiled according to their respective ion (O VII and O VIII), and provide a more accurate estimate of the baryonic density based on possible detections rather than broad constraints set by upper limits. These results are detailed in Table 5.28. Note that for this analysis, only 3 of the 5 possible O VII, and 2 of the possible 3 O VIII detections were used. This is because of their high τ_0 and column density values. This indicates a lack of quality data for those fits, which resulted in the decision to omit them from these calculations of the cosmological density.

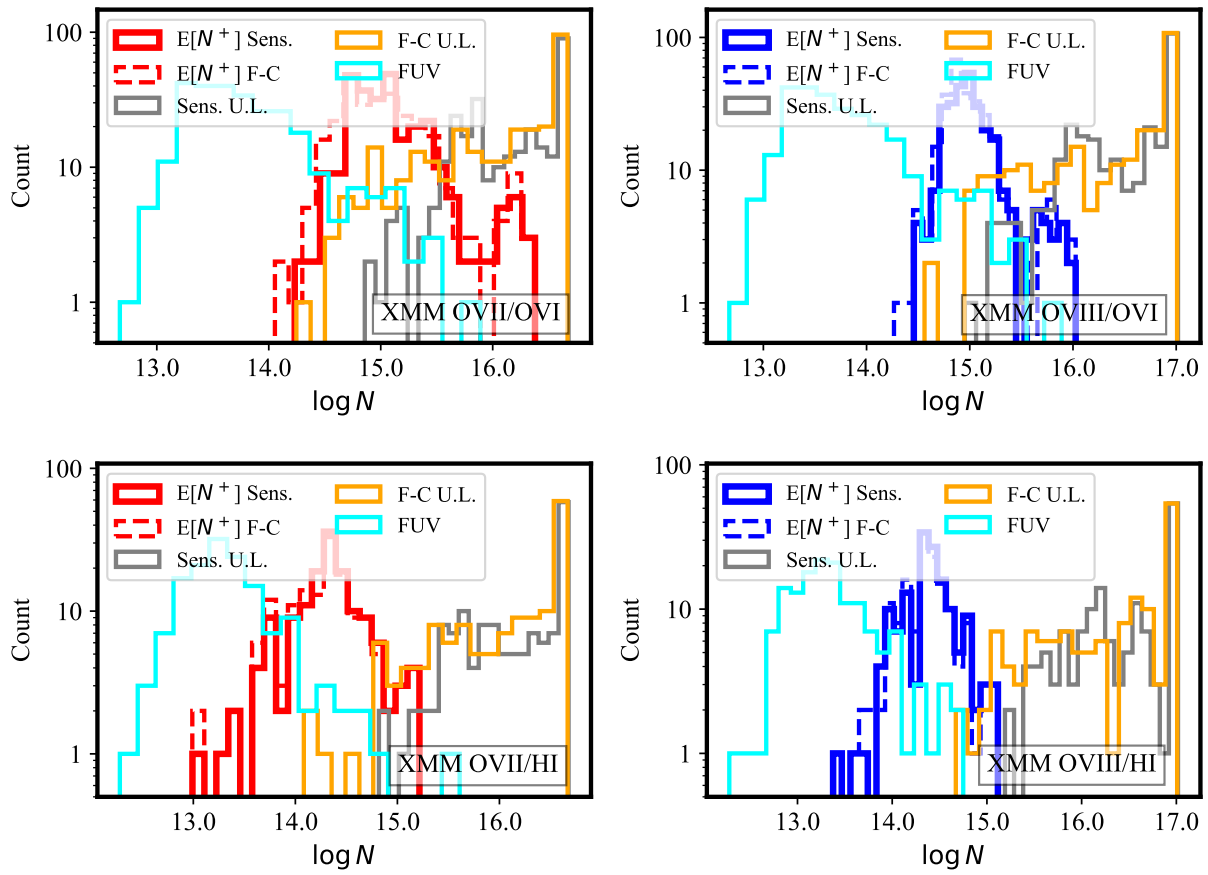

Figure 5.10: Distribution of E[N^+] for all absorption line systems that are summed in Equation (3.9), calculated using the "sensitivity" and the Feldman–Cousins methods, for the *XMM-Newton* data. Also shown are the upper limits to the measurable column densities for the two methods, which are used to calculate the expectations E[N^+]. The two methods generally yield comparable results.

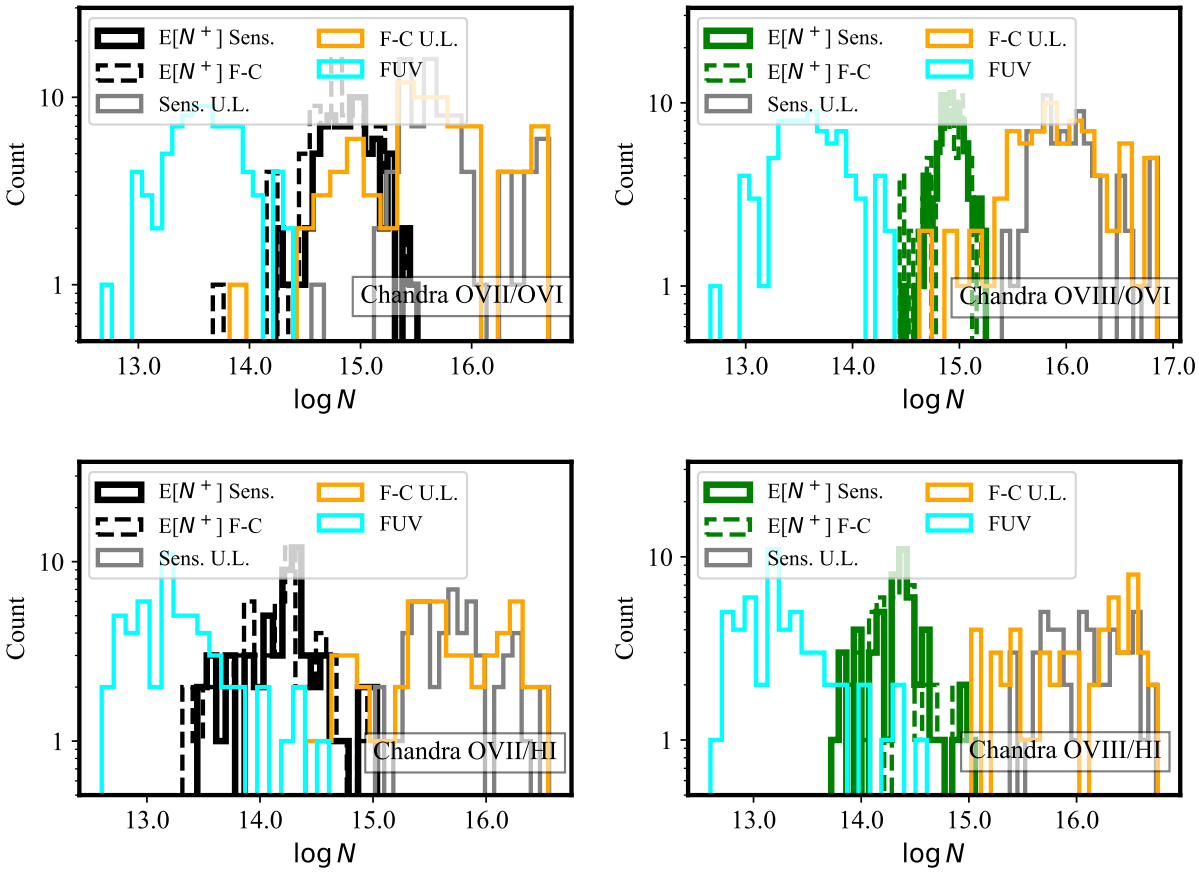

Figure 5.11: Same as Fig. 5.10, for the *Chandra* data.

Table 5.19: *XMM-Newton* O VII with O VI priors Ω calculation results. D indicates the distance as calculated by Equation 3.11, $\frac{\Omega_X}{\Omega_b}$ is the ratio between the cosmological density of baryons due to the WHIM and the cosmological density of baryons in the universe, and N is the column density for each source. Non sub-scripted entries use the sensitivity upper limit method (Section 4.3.3), and "FC" sub-scripted results are using the FC upper limit method (Section 4.3.2).

Sample			ΣD	ΣN_{O_x}	$< \frac{\Omega_X}{\Omega_b}$	$\Sigma N_{O_x,FC}$	$< \frac{\Omega_{X,FC}}{\Omega_b}$
XMM OVII/OVI			32264.7	$6.18e+17$	7.940	$5.92e+17$	7.605
Source-by-source breakdown							
#	name	#Obs	D	ΣN_{O_x}	$< \frac{\Omega_X}{\Omega_b}$	$\Sigma N_{O_x,FC}$	$< \frac{\Omega_{X,FC}}{\Omega_b}$
1	tons180	3	203.1	$2.59e+15$	5.280	$2.63e+15$	5.372
2	pks2005	1	240.6	$7.58e+14$	1.306	$5.77e+14$	0.994
3	pg0804	3	360.3	$4.28e+15$	4.921	$3.84e+15$	4.414
4	i22456	8	367.3	$2.79e+16$	31.510	$2.54e+16$	28.704
5	rbs542	2	376.7	$6.06e+15$	6.674	$6.52e+15$	7.181
6	pks2155	1	427.7	$4.02e+14$	0.390	$1.13e+14$	0.110
7	q1230	15	429.7	$1.44e+17$	138.520	$1.43e+17$	137.960
8	mrk876	5	478.3	$9.66e+15$	8.374	$9.66e+15$	8.374
9	pg1626	1	494.5	$4.86e+14$	0.408	$2.47e+14$	0.207
10	pg1115	5	581.1	$1.12e+16$	8.001	$1.06e+16$	7.536
11	pg1307	2	582.7	$2.93e+15$	2.088	$2.93e+15$	2.088
12	3c273	6	595.8	$2.59e+15$	1.805	$3.20e+15$	2.228
13	pg0157	1	614.9	$7.19e+14$	0.485	$7.19e+14$	0.485
14	he0056	2	618.9	$1.08e+15$	0.722	$1.03e+15$	0.692
15	h2356	2	622.8	$1.97e+15$	1.311	$2.26e+15$	1.504
16	pg1116	9	667.1	$8.30e+15$	5.160	$8.61e+15$	5.350
17	pg1309	11	693.1	$1.39e+17$	83.218	$1.39e+17$	83.218
18	p1103	5	705.3	$6.34e+15$	3.727	$5.34e+15$	3.139
19	phl1811	4	728.8	$9.49e+15$	5.398	$9.49e+15$	5.398
20	rbs1892	3	760.0	$4.91e+15$	2.679	$4.55e+15$	2.482
21	pg1211	3	856.7	$4.74e+15$	2.294	$3.95e+15$	1.913
22	pks0312	2	858.6	$1.17e+16$	5.633	$1.17e+16$	5.633
23	s50716	1	881.6	$1.18e+15$	0.556	$1.10e+15$	0.517
24	pg0953	10	891.6	$1.11e+16$	5.177	$7.89e+15$	3.669
25	rxj0439	6	925.5	$1.39e+16$	6.242	$1.39e+16$	6.243
26	pg1444	6	1019.7	$5.70e+15$	2.319	$3.34e+15$	1.359
27	h1821	15	1127.3	$1.58e+16$	5.815	$1.32e+16$	4.861
28	3c249	4	1179.5	$8.06e+15$	2.834	$8.06e+15$	2.834
29	ton28	9	1245.5	$1.13e+16$	3.776	$1.05e+16$	3.505
30	pg0832	5	1248.1	$7.45e+15$	2.474	$7.18e+15$	2.387
31	pg1216	8	1253.5	$1.31e+16$	4.331	$1.29e+16$	4.279
32	1es1028	3	1358.1	$3.86e+15$	1.178	$3.64e+15$	1.110
33	1es1553	7	1546.3	$3.54e+15$	0.951	$4.14e+15$	1.110
34	pg0003	16	1672.4	$2.89e+16$	7.174	$2.49e+16$	6.168
35	pg1259	12	1762.7	$1.30e+16$	3.066	$1.30e+16$	3.066
36	he0226	61	1814.4	$5.18e+16$	11.834	$4.70e+16$	10.749
37	pks0405	25	2074.1	$2.82e+16$	5.638	$2.54e+16$	5.088

Table 5.20: *XMM-Newton* O VIII with O VI priors Ω calculation results.

Sample			ΣD	ΣN_{O_x}	$< \frac{\Omega_X}{\Omega_b}$	$\Sigma N_{O_x,FC}$	$< \frac{\Omega_{X,FC}}{\Omega_b}$
XMM OVIII/OVI			31856.7	$3.84e+17$	49.945	$3.61e+17$	46.938
Source-by-source breakdown							
#	name	#Obs	D	ΣN_{O_x}	$\frac{\Omega_X}{\Omega_b}$	$\Sigma N_{O_x,FC}$	$\frac{\Omega_{X,FC}}{\Omega_b}$
1	ngc7469	3	69.4	$4.44e+15$	265.160	$4.66e+15$	278.632
2	mrk421	1	127.6	$3.12e+14$	10.140	$3.66e+14$	11.884
3	tons180	3	261.7	$2.47e+15$	39.214	$2.46e+15$	38.911
4	mr2251	1	270.1	$5.28e+14$	8.109	$2.62e+14$	4.023
5	pks2005	1	299.1	$8.67e+14$	12.016	$6.02e+14$	8.341
6	pg0804	4	418.5	$4.20e+15$	41.608	$4.02e+15$	39.858
7	i22456	8	425.4	$2.61e+16$	254.779	$2.61e+16$	254.779
8	rbs542	2	434.8	$5.87e+15$	55.944	$3.46e+15$	32.996
9	pks2155	2	485.6	$1.15e+15$	9.860	$1.30e+15$	11.091
10	q1230	15	487.6	$6.33e+16$	537.918	$5.31e+16$	451.865
11	mrk876	6	536.1	$7.35e+15$	56.896	$7.16e+15$	55.387
12	pg1626	1	552.1	$6.68e+14$	5.019	$4.39e+14$	3.300
13	pg1115	3	573.1	$3.26e+15$	23.617	$3.26e+15$	23.617
14	3c273	9	587.9	$4.53e+15$	31.929	$4.43e+15$	31.254
15	he0056	2	610.9	$1.28e+15$	8.711	$1.28e+15$	8.711
16	h2356	2	614.9	$2.22e+15$	14.956	$2.22e+15$	14.956
17	pg1116	8	659.2	$7.06e+15$	44.388	$6.99e+15$	43.996
18	pg1309	11	685.2	$5.81e+16$	351.409	$5.81e+16$	351.409
19	p1103	1	697.4	$1.39e+15$	8.263	$1.39e+15$	8.263
20	phl1811	3	720.9	$2.55e+15$	14.671	$2.55e+15$	14.684
21	rbs1892	3	752.1	$3.62e+15$	19.943	$3.62e+15$	19.943
22	pg1211	4	848.9	$4.65e+15$	22.700	$4.29e+15$	20.969
23	pks0312	2	850.8	$5.65e+15$	27.554	$5.65e+15$	27.554
24	s50716	1	873.8	$1.08e+15$	5.133	$1.08e+15$	5.133
25	pg0953	7	883.8	$7.21e+15$	33.847	$6.99e+15$	32.806
26	rxj0439	6	917.8	$9.13e+15$	41.253	$8.14e+15$	36.776
27	pg1444	6	1011.9	$5.74e+15$	23.504	$5.21e+15$	21.368
28	h1821	15	1119.6	$1.46e+16$	54.110	$1.34e+16$	49.448
29	3c249	4	1171.9	$5.28e+15$	18.694	$5.28e+15$	18.694
30	ton28	6	1237.9	$5.05e+15$	16.908	$4.67e+15$	15.657
31	pg0832	4	1240.5	$4.57e+15$	15.282	$4.57e+15$	15.282
32	pg1216	7	1245.9	$8.46e+15$	28.150	$8.46e+15$	28.150
33	1es1028	2	1350.6	$2.81e+15$	8.638	$2.81e+15$	8.638
34	1es1553	7	1538.8	$5.12e+15$	13.790	$5.20e+15$	14.008
35	pg0003	16	1665.1	$2.04e+16$	50.909	$1.96e+16$	48.932
36	pg1259	14	1755.4	$1.27e+16$	30.066	$1.18e+16$	27.840
37	he0226	59	1807.1	$4.70e+16$	107.871	$4.46e+16$	102.312
38	pks0405	24	2067.0	$2.29e+16$	46.002	$2.10e+16$	42.199

Table 5.21: *XMM-Newton* O VII with H I priors Ω calculation results.

Sample			ΣD	ΣN_{O_x}	$< \frac{\Omega_X}{\Omega_b}$	$\Sigma N_{O_x,FC}$	$< \frac{\Omega_{X,FC}}{\Omega_b}$
XMM OVII/HI			33330.8	$4.22e+16$	0.525	$3.98e+16$	0.495
Source-by-source breakdown							
#	name	#Obs	D	ΣN_{O_x}	$< \frac{\Omega_X}{\Omega_b}$	$\Sigma N_{O_x,FC}$	$< \frac{\Omega_{X,FC}}{\Omega_b}$
1	tons180	1	203.1	$3.54e+14$	0.724	$3.17e+14$	0.647
2	pg1229	1	207.3	$8.62e+13$	0.172	$8.62e+13$	0.172
3	mr2251	6	211.5	$3.15e+15$	6.176	$3.19e+15$	6.249
4	mrk478	3	274.2	$5.78e+14$	0.874	$5.83e+14$	0.882
5	pg0804	3	360.3	$1.38e+14$	0.159	$1.38e+14$	0.159
6	i22456	1	367.3	$1.30e+15$	1.470	$1.30e+15$	1.470
7	rbs542	2	376.7	$1.44e+14$	0.159	$1.44e+14$	0.159
8	tons210	2	425.7	$2.39e+14$	0.233	$2.39e+14$	0.233
9	pks2155	2	427.7	$3.02e+14$	0.293	$1.85e+14$	0.179
10	q1230	13	429.7	$4.51e+15$	4.349	$4.35e+15$	4.199
11	mrk876	5	478.3	$7.03e+14$	0.609	$7.03e+14$	0.609
12	pg0838	3	486.4	$5.57e+14$	0.475	$5.57e+14$	0.475
13	pg1626	1	494.5	$2.42e+14$	0.203	$4.87e+13$	0.041
14	q0045	1	498.5	$2.02e+14$	0.168	$2.02e+14$	0.168
15	pks0558	1	511.4	$1.01e+14$	0.082	$1.01e+14$	0.082
16	pg1115	3	581.1	$5.23e+14$	0.373	$5.23e+14$	0.373
17	pg1307	1	582.7	$2.47e+14$	0.176	$1.19e+14$	0.085
18	3c273	3	595.8	$9.85e+13$	0.069	$7.72e+13$	0.054
19	h2356	4	622.8	$8.44e+14$	0.562	$8.37e+14$	0.557
20	pg1048	1	630.8	$2.02e+14$	0.132	$2.02e+14$	0.132
21	pg1116	7	667.1	$1.25e+15$	0.774	$1.19e+15$	0.738
22	pg1309	5	693.1	$3.69e+15$	2.211	$3.69e+15$	2.211
23	phl1811	1	728.8	$1.20e+14$	0.068	$1.20e+14$	0.068
24	rbs1892	6	760.0	$1.62e+15$	0.884	$1.50e+15$	0.819
25	pg1211	2	856.7	$4.25e+14$	0.206	$4.10e+14$	0.198
26	pks0312	1	858.6	$6.44e+14$	0.311	$6.44e+14$	0.311
27	s50716	3	881.6	$4.06e+14$	0.191	$4.00e+14$	0.188
28	pg0953	2	891.6	$3.56e+14$	0.165	$3.56e+14$	0.165
29	rxj0439	1	925.5	$2.97e+14$	0.133	$3.01e+14$	0.135
30	pg1444	1	1019.7	$2.77e+14$	0.113	$1.91e+14$	0.078
31	h1821	6	1127.3	$1.26e+15$	0.464	$1.22e+15$	0.450
32	3c249	2	1179.5	$3.97e+14$	0.139	$3.97e+14$	0.139
33	ton28	1	1245.5	$2.67e+14$	0.089	$2.67e+14$	0.089
34	pg0832	8	1248.1	$3.94e+15$	1.310	$3.74e+15$	1.244
35	pg1216	7	1253.5	$4.29e+15$	1.418	$4.20e+15$	1.390
36	1es1028	3	1358.1	$5.37e+14$	0.164	$4.45e+14$	0.136
37	1es1553	4	1546.3	$4.14e+14$	0.111	$4.43e+14$	0.119
38	pg0003	5	1672.4	$1.24e+15$	0.308	$1.07e+15$	0.266
39	pg1259	10	1762.7	$2.90e+15$	0.683	$2.90e+15$	0.682
40	he0226	3	1814.4	$6.41e+14$	0.147	$6.41e+14$	0.146
41	pks0405	12	2074.1	$2.69e+15$	0.538	$1.77e+15$	0.354

Table 5.22: *XMM-Newton* O VIII with H I priors Ω calculation results.

Sample			ΣD	ΣN_{O_x}	$< \frac{\Omega_X}{\Omega_b}$	$\Sigma N_{O_x,FC}$	$< \frac{\Omega_{X,FC}}{\Omega_b}$
XMM OVIII/HI			33514.4	$4.48e+16$	5.549	$4.25e+16$	5.257
Source-by-source breakdown							
#	name	#Obs	D	ΣN_{O_x}	$< \frac{\Omega_X}{\Omega_b}$	$\Sigma N_{O_x,FC}$	$< \frac{\Omega_{X,FC}}{\Omega_b}$
1	ngc7469	1	69.4	$3.00e+14$	17.941	$3.03e+14$	18.095
2	tons180	1	261.7	$4.08e+14$	6.472	$4.08e+14$	6.472
3	pg1229	1	265.9	$1.22e+14$	1.909	$1.22e+14$	1.909
4	mr2251	7	270.1	$3.73e+15$	57.226	$3.31e+15$	50.832
5	mrk478	3	332.6	$6.63e+14$	8.265	$6.63e+14$	8.265
6	pg0804	3	418.5	$2.25e+14$	2.232	$2.25e+14$	2.232
7	i22456	2	425.4	$1.24e+15$	12.045	$1.20e+15$	11.706
8	rbs542	2	434.8	$2.15e+14$	2.051	$2.14e+14$	2.046
9	tons210	2	483.6	$3.14e+14$	2.694	$3.13e+14$	2.686
10	pks2155	3	485.6	$8.21e+14$	7.008	$7.81e+14$	6.673
11	q1230	12	487.6	$4.14e+15$	35.172	$4.11e+15$	34.991
12	mrk876	6	536.1	$1.04e+15$	8.029	$9.02e+14$	6.977
13	pg0838	3	544.1	$6.46e+14$	4.926	$6.46e+14$	4.926
14	pg1626	1	552.1	$3.38e+14$	2.537	$3.38e+14$	2.537
15	pks0558	1	569.0	$1.30e+14$	0.947	$5.85e+13$	0.426
16	pg1115	3	573.1	$6.19e+14$	4.478	$6.19e+14$	4.478
17	pg1307	1	574.7	$2.75e+14$	1.985	$2.73e+14$	1.969
18	3c273	3	587.9	$2.84e+14$	2.002	$2.84e+14$	2.000
19	h2356	4	614.9	$1.04e+15$	7.009	$8.88e+14$	5.992
20	pg1048	2	622.8	$8.18e+14$	5.447	$8.18e+14$	5.447
21	pg1116	6	659.2	$1.17e+15$	7.356	$1.08e+15$	6.819
22	pg1309	5	685.2	$3.31e+15$	20.054	$3.31e+15$	20.054
23	phl1811	4	720.9	$1.39e+15$	7.978	$1.39e+15$	7.978
24	rbs1892	6	752.1	$1.71e+15$	9.401	$1.52e+15$	8.353
25	pg1211	2	848.9	$4.47e+14$	2.184	$3.04e+14$	1.487
26	pks0312	1	850.8	$5.87e+14$	2.862	$5.87e+14$	2.862
27	s50716	3	873.8	$5.90e+14$	2.801	$5.24e+14$	2.487
28	pg0953	2	883.8	$4.10e+14$	1.923	$4.06e+14$	1.907
29	rxj0439	2	917.8	$6.87e+14$	3.103	$6.87e+14$	3.103
30	pg1444	1	1011.9	$3.00e+14$	1.231	$1.65e+14$	0.675
31	h1821	7	1119.6	$1.52e+15$	5.616	$1.51e+15$	5.590
32	3c249	1	1171.9	$2.53e+14$	0.894	$2.53e+14$	0.894
33	ton28	1	1237.9	$2.75e+14$	0.921	$2.73e+14$	0.914
34	pg0832	5	1240.5	$1.71e+15$	5.726	$1.59e+15$	5.323
35	pg1216	8	1245.9	$4.19e+15$	13.947	$4.13e+15$	13.736
36	1es1028	2	1350.6	$4.89e+14$	1.501	$3.80e+14$	1.168
37	1es1553	4	1538.8	$5.82e+14$	1.569	$5.92e+14$	1.595
38	pg0003	5	1665.1	$1.34e+15$	3.333	$1.25e+15$	3.115
39	pg1259	9	1755.4	$2.71e+15$	6.392	$2.71e+15$	6.392
40	he0226	2	1807.1	$5.90e+14$	1.355	$5.73e+14$	1.315
41	pks0405	12	2067.0	$3.24e+15$	6.505	$2.77e+15$	5.560

Table 5.23: *Chandra* O VII with O VI priors Ω calculation results.

Sample			ΣD	ΣN_{O_x}	$< \frac{\Omega_X}{\Omega_b}$	$\Sigma N_{O_x,FC}$	$< \frac{\Omega_{X,FC}}{\Omega_b}$
Chandra OVII/OVI			9999.7	$7.49e+16$	3.107	$6.90e+16$	2.860
Source-by-source breakdown							
#	name	#Obs	D	ΣN_{O_x}	$< \frac{\Omega_X}{\Omega_b}$	$\Sigma N_{O_x,FC}$	$< \frac{\Omega_{X,FC}}{\Omega_b}$
1	mrk421	1	68.5	$1.84e+14$	1.112	$4.68e+13$	0.283
2	tons180	3	203.1	$2.15e+15$	4.400	$1.58e+15$	3.218
3	mr2251	1	211.5	$6.16e+14$	1.207	$6.16e+14$	1.207
4	pks2005	1	240.6	$7.58e+14$	1.306	$6.31e+14$	1.088
5	pks2155	2	427.7	$9.67e+14$	0.938	$1.26e+15$	1.224
6	3c273	9	595.8	$4.80e+15$	3.339	$4.18e+15$	2.909
7	h2356	2	622.8	$2.24e+15$	1.491	$2.83e+15$	1.886
8	pg1116	9	667.1	$7.76e+15$	4.824	$6.62e+15$	4.113
9	pg1211	4	856.7	$6.17e+15$	2.986	$6.35e+15$	3.071
10	h1821	15	1127.3	$1.21e+16$	4.456	$1.08e+16$	3.976
11	1es1028	3	1358.1	$3.89e+15$	1.186	$3.33e+15$	1.018
12	1es1553	7	1546.3	$4.37e+15$	1.172	$4.22e+15$	1.132
13	pks0405	25	2074.1	$2.89e+16$	5.781	$2.65e+16$	5.297

Table 5.24: *Chandra* O VIII with O VI priors Ω calculation results.

Sample			ΣD	ΣN_{O_x}	$< \frac{\Omega_X}{\Omega_b}$	$\Sigma N_{O_x,FC}$	$< \frac{\Omega_{X,FC}}{\Omega_b}$
Chandra OVIII/OVI			10103.5	$7.19e+16$	29.498	$6.65e+16$	27.310
Source-by-source breakdown							
#	name	#Obs	D	ΣN_{O_x}	$< \frac{\Omega_X}{\Omega_b}$	$\Sigma N_{O_x,FC}$	$< \frac{\Omega_{X,FC}}{\Omega_b}$
1	tons180	3	261.7	$2.39e+15$	37.871	$2.20e+15$	34.798
2	mr2251	1	270.1	$7.39e+14$	11.345	$7.42e+14$	11.395
3	pks2005	1	299.1	$8.33e+14$	11.541	$6.99e+14$	9.692
4	pks2155	2	485.6	$1.30e+15$	11.113	$1.45e+15$	12.340
5	3c273	10	587.9	$6.92e+15$	48.825	$6.06e+15$	42.781
6	h2356	2	614.9	$2.14e+15$	14.408	$2.14e+15$	14.408
7	pg1116	8	659.2	$7.05e+15$	44.354	$6.72e+15$	42.282
8	pg1211	4	848.9	$4.96e+15$	24.233	$4.73e+15$	23.130
9	h1821	15	1119.6	$1.32e+16$	48.834	$1.07e+16$	39.502
10	1es1028	2	1350.6	$2.75e+15$	8.435	$2.41e+15$	7.390
11	1es1553	7	1538.8	$5.47e+15$	14.734	$4.98e+15$	13.434
12	pks0405	25	2067.0	$2.41e+16$	48.424	$2.37e+16$	47.628

Table 5.25: *Chandra* O VII with H I priors Ω calculation results.

Sample			ΣD	ΣN_{O_x}	$< \frac{\Omega_X}{\Omega_b}$	$\Sigma N_{O_x,FC}$	$< \frac{\Omega_{X,FC}}{\Omega_b}$
Chandra OVII/HI			9964.8	$1.32e+16$	0.549	$1.20e+16$	0.501
Source-by-source breakdown							
#	name	#Obs	D	ΣN_{O_x}	$< \frac{\Omega_X}{\Omega_b}$	$\Sigma N_{O_x,FC}$	$< \frac{\Omega_{X,FC}}{\Omega_b}$
1	tons180	1	203.1	$3.90e+14$	0.796	$3.54e+14$	0.724
2	mr2251	7	211.5	$4.23e+15$	8.294	$4.21e+15$	8.257
3	mrk478	3	274.2	$5.40e+14$	0.816	$4.15e+14$	0.628
4	pks2155	3	427.7	$4.72e+14$	0.457	$5.80e+14$	0.562
5	3c273	4	595.8	$2.31e+14$	0.160	$2.25e+14$	0.157
6	h2356	4	622.8	$7.10e+14$	0.473	$6.02e+14$	0.401
7	pg1116	7	667.1	$1.17e+15$	0.726	$1.04e+15$	0.643
8	pg1211	2	856.7	$4.16e+14$	0.201	$2.80e+14$	0.136
9	h1821	7	1127.3	$1.04e+15$	0.381	$9.53e+14$	0.351
10	1es1028	3	1358.1	$6.77e+14$	0.207	$6.93e+14$	0.212
11	1es1553	4	1546.3	$4.44e+14$	0.119	$4.02e+14$	0.108
12	pks0405	12	2074.1	$2.89e+15$	0.578	$2.29e+15$	0.457

Table 5.26: *Chandra* O VIII with H I priors Ω calculation results.

Sample			ΣD	ΣN_{O_x}	$< \frac{\Omega_X}{\Omega_b}$	$\Sigma N_{O_x,FC}$	$< \frac{\Omega_{X,FC}}{\Omega_b}$
Chandra OVIII/HI			10136.9	$1.49e+16$	6.115	$1.42e+16$	5.825
Source-by-source breakdown							
#	name	#Obs	D	ΣN_{O_x}	$< \frac{\Omega_X}{\Omega_b}$	$\Sigma N_{O_x,FC}$	$< \frac{\Omega_{X,FC}}{\Omega_b}$
1	tons180	1	261.7	$4.08e+14$	6.472	$3.02e+14$	4.786
2	mr2251	7	270.1	$4.25e+15$	65.249	$4.21e+15$	64.614
3	mrk478	3	332.6	$6.54e+14$	8.147	$5.54e+14$	6.912
4	pks2155	3	485.6	$7.25e+14$	6.194	$7.59e+14$	6.482
5	3c273	3	587.9	$3.02e+14$	2.133	$3.02e+14$	2.133
6	h2356	4	614.9	$1.01e+15$	6.809	$8.35e+14$	5.632
7	pg1116	6	659.2	$1.18e+15$	7.415	$1.17e+15$	7.371
8	pg1211	2	848.9	$5.24e+14$	2.560	$4.53e+14$	2.213
9	h1821	7	1119.6	$1.46e+15$	5.390	$1.35e+15$	4.994
10	1es1028	2	1350.6	$4.96e+14$	1.524	$4.11e+14$	1.262
11	1es1553	4	1538.8	$6.57e+14$	1.771	$6.61e+14$	1.782
12	pks0405	12	2067.0	$3.29e+15$	6.595	$3.23e+15$	6.485

Table 5.27: Compiled Ω results for all analysis sets for *XMM-Newton* and *Chandra* data, O VII and O VIII, with O VI and H I prior detections.

Sample	ΣD	ΣN_{O_x}	$< \frac{\Omega_X}{\Omega_b}$	$\Sigma N_{O_x,FC}$	$< \frac{\Omega_{X,FC}}{\Omega_b}$
XMM OVII/OVI	$3.23e+04$	$6.18e+17$	7.940	$5.92e+17$	7.605
Chandra OVII/OVI	$1.00e+04$	$7.49e+16$	3.107	$6.90e+16$	2.860
XMM OVIII/OVI	$3.19e+04$	$3.84e+17$	49.945	$3.61e+17$	46.938
Chandra OVIII/OVI	$1.01e+04$	$7.19e+16$	29.498	$6.65e+16$	27.310
XMM OVII/HI	$3.33e+04$	$4.22e+16$	0.525	$3.98e+16$	0.495
Chandra OVII/HI	$9.96e+03$	$1.32e+16$	0.549	$1.20e+16$	0.501
XMM OVIII/HI	$3.35e+04$	$4.48e+16$	5.549	$4.25e+16$	5.257
Chandra OVIII/HI	$1.01e+04$	$1.49e+16$	6.115	$1.42e+16$	5.825

Table 5.28: Compiled Ω results for all of the possible detections reported in Section 5.4 with quality data for *XMM-Newton* and *Chandra* data. Included are 3 O VII systems with possible detections, and 2 possible O VIII detections results. D is in units of Mpc and N_{O_x} is in units of cm^{-2}.

Ion	# Detections	ΣD	$\Sigma \log N_{O_x}$	$\frac{\Omega_{O_x}}{\Omega_b}$
O VII	3	65595.566	$7.289e+15 \pm 1.781e+15$	0.046 ± 0.011
O VIII	2	65371.114	$1.690e+16 \pm 4.442e+15$	0.536 ± 0.141

The result of these analyses show that for the entire sample, the upper limits set on $\frac{\Omega_X}{\Omega_b}$ were generally rather conservative in nature (Table 5.27). Nearly all values from the entire sample's analysis (columns "$< \frac{\Omega_X}{\Omega_b}$" and "$< \frac{\Omega_{X,FC}}{\Omega_b}$" in Table 5.27) were around an order of magnitude higher than the suspected amount ($\frac{\Omega_X}{\Omega_b} \approx 0.40$) of baryons in the hot WHIM. Despite this, all of the upper constrains on this ratio were above the expected amount of baryons to be in the WHIM. These results are discussed further in Section 6.2, in addition to the limitations of the analysis in Section 6.1.

In regards to the calculations completed on just the possible detections from Section 5.4 (Table 5.28), these ratios were significantly closer to what we would expect. Specifically, the ratio calculated using the O VIII detections was directly in-line with the amount of missing baryons predicted to be in the WHIM ($53.6\% \pm 14.1\%$ in comparison to the expected 40%). If these results are true, this calculation provides substantial evidence towards the solution of the missing baryons being the baryons existing in the hot WHIM. These results should be regarded as tentative though, as there were too many limitations to consider them highly accurate. Primarily, the lack of an exact measurement of the medium's properties along the sightlines analyzed such as temperature restrict the confidence in this calculation. Without an exact temperature or ionization fraction for example, these values could shift significantly. Just as the full sample's result's implications are discussed more, these possible detection $< \frac{\Omega_X}{\Omega_b}$ calculations are further explored in Sections 6.1 and 6.2.

Chapter 6. Discussion and Conclusions

6.1 Constraints and Limitations

This project compiled an enormous amount of spectral data, calculations, and analyses of *XMM-Newton* and *Chandra* observations in order to study the WHIM. Because of the length of analysis, and the scope of the project, a number of constraints and limitations were encountered during the process. Several additional analyses not present in the project were discussed but ultimately never came to fruition due to time constraints as well.

As the scope of O VI and H I priors from [21] and [65] was so large, the primary analysis of the project was restricted to a search of just O VII and O VIII. As with the paper we wrote over 1ES 1553+113 (Section 2.2), a study of Ne IX was considered but ultimately forgone due to time constraints. `EAGLE` simulations (see Section 4.1.1) demonstrate the high correlation between O VII and O VI or H I prior detections (*e.g.,* Figure 4.1), so the search for oxygen ions became the main focus of the project. In addition to this, several of the scripts written for calculating the final values of the cosmological densities were already written for the usage of oxygen ions.

Another aspect of the 1ES 1553+113 analysis that did not make it into the final project and analysis was the process of stacking multiple redshifts from

each source on top of each other. The primary reason for the omission of this were time constraints, and the volume of work required to do this. The current implementation of the analysis scripts allows for the automation of most of the work, as the results are output individually for each redshift in a list. To stack the data, several additional aspects would need to be taken into consideration and developed. The process of stacking involves creating separate regions for each section of a source's spectrum that have redshift priors sufficiently close to each other. As each source is unique and the associated redshifts are as well, the number of regions used in `SPEX` would have to be hand picked for each source to our discretion. Doing this for just 1ES 1553+113 was simple, but the extension of this to 50 more sources would require a significant amount of care. In addition to the `SPEX` regions issue, another Python pipeline would need to be written to plot all of the different redshifted fits into combined plots such as Figure 2.6. This would also include the need for a pipeline of extracting the fit data from the analysis in `PYSPEX` of each stacked fit, which was never developed.

Overall, the data used in the project, particularly from *XMM-Newton* was lackluster in many regards. A significant amount of the sources and observations used in the analysis had very small count rates, and in many cases had background data higher than the overall count rate of the spectrum. This of course introduces a large amount of uncertainty in these ranges, and reduces the trust in these source's results and ability to detect absorption lines in them. In the cases where data used were not in the significantly low counts, the sensitivity was still not high. Currently, the best X-ray data are only sensitive to O VII column density

well in excess of 10^{15} cm^{-2}, while the FUV data are able to detect column densities of order 10^{13} cm^{-2}.

In regards to the process of data acquisition and reduction, there were a few considerations and slight issues present. First, because of the size of the sample used, several of the sources have been observed for quite some time. When compiling the different observations present for each source and reducing them into usable spectra, these older and newer observations are all combined together. As mentioned in Section 3.2.2, *XMM-Newton* has had several detector problems and malfunctions throughout its lifespan. These issues have resulted in poor data at these points after the malfunctions, which were then combined with the observations before the malfunction as well. Another example would be efficiencies made, or calibrations completed during different time frames of the instrument's lifespan, resulting in a slightly different spectrum for a source in different years. All of this comes together to influence certain areas of well known older discovered spectra to have poor data. Another limitation of this project in the same style as this, is that because of the length of time required to complete the analysis and project as a whole, undoubtedly new observations have been made on a number of the sources in the sample. After a certain point, new data being recorded onto the *XMM-Newton* and *Chandra* archives were not downloaded and reduced. As a result, any observations made after around $\sim$2022 were not included in this analysis.

Another limitation partially introduced by the poor *XMM-Newton* data was the exclusion of the use of the curve of growth relationship between the

equivalent width of a line and the column density (Section 3.3.4, Figure 3.2). Although this does not inherently come as a result of the poor *XMM-Newton* data (as the lack of a measurable b parameter is the reason for its exclusion), the data quality brings about the effects of the exclusion. This is because the result of not using the curve of growth relationship is that the linear relationship currently used in accordance to Equation 3.6 does not hold in the case of high τ_0 (and by extension equivalent width) values. These extremely high τ_0 and τ_0 errors are closely correlated with the quality of the fits, which was an issue with *XMM-Newton* data at times. Continuing to use the linear relationship instead of calculating the curve of growth resulted in systematically underestimated column densities in circumstances in which τ_0 was very large. Related to the lack of a measurable b parameter of the data, the inability to measure the exact temperature and by extension calculate the abundance to use was a limitation on the calculations of the cosmological densities. As these values had to be estimated, the final values should be regarded as an estimate with the abundances used as assumptions.

Galactic O VII around 21.6Å and *XMM-Newton*'s poor data around the 21.7-21.9Å band limited the usage of a significant amount of prior redshifts for certain sources, especially those at lower redshifts and observed by *XMM-Newton*. Because of these bands, a large number of sources had to be partially or completely excluded from the analysis. Any possible line with an expected wavelength inside this band yielded either poor fits, or a false detection at 21.6Å. These exclusions

ultimately limited the analysis on several sources with prior detected absorption lines (Section 5.2), so their comparison to our analysis was not possible.

In conjunction with the limitation of the 21.5-21.7/21.9Å band, galactic absorption of other oxygen ions were detected throughout the analysis. Originally, there was a plan to document and report these cases of galactic oxygen, but time constraints and the tremendous amount of work that would be required resulted in the omission of that analysis from the project. Instead, an analysis of only galactic O VII and O VIII was completed. Any bands with detected galactic oxygen ions that interfered with the fits of the expected lines were excluded.

`PYSPEX` and `SPEX` had slight deviations in results in some circumstances. Perhaps because of the nature of the `PYSPEX` software being unfinished and the complexity of spectral fits, there were small differences between fit statistics and values in comparisons between `PYSPEX` and `SPEX`. In rare circumstances, fits were individually manipulated because fit results yielded by `PYSPEX` were incorrect. The usual culprit of this was the fit statistic or model parameters becoming "stuck" and needing to be changed slightly and refit to return to their correct values. These issues were dealt with however, and the remaining fits should be taken as accurate. Despite the differences between the two, the significance of the deviations was not large enough to cause any major changes in the results of the analysis. The more significant limitation this imposed was the time it took to care for each of these improper fits by `PYSPEX` individually.

6.2 Discussion of Results

This project served as the most comprehensive and large scale search for oxygen X-ray absorption lines in the WHIM ever, with the goal of drawing inferences and putting constraints on the cosmological density of the WHIM, $\Omega_{WHIM,X}$, and to find a solution to the missing baryons problem in this search of the WHIM. The primary method of analysis used was based on the search of X-ray absorption lines at fixed reshifts where prior FUV observations have identified possible absorption from the lower-temperature WHIM, and the use of joint distribution functions of FUV and X-ray ions based on cosmological simulations.

Within the framework of this methodology, we searched 51 *XMM-Newton* and *Chandra* spectra for prominent resonant absorption lines from the intervening WHIM. Through the usage of the spectral analysis software `SPEX` and its Python package `PYSPEX`, we were able to automate the analysis of over 1000 different fits across the search of O VII and O VIII with O VI or H I prior detections. Through this analysis, a column density and corresponding upper limit was calculated for every fit using both the Feldman-Cousins and sensitivity methods (See section 4.3). Using these column density upper limits and the respective FUV prior for each, the cosmological density of the WHIM was computed for every fit, and compiled for the entire analysis (Table 5.27). Similar to the 1ES 1553+113 paper results discussion (Section 2.2.2) and the explanation of the goals of the project in Section 1.2, these cosmological densities of the WHIM were directly compared to the known cosmological density of baryons, Ω_b ($\frac{\Omega_X}{\Omega_b}$ in Tables 5.19-5.27).

Overall, the result of the comparisons $\frac{\Omega_X}{\Omega_b}$ were mixed among the sample searches. Ideally, a value of the ratio marginally higher than 0.4 was expected, but the majority of the results yielded values several orders of magnitude higher than this. This would indicate that the values of the upper limits and the corresponding summation of their expectations (Equation 3.9) for each source and sample is significantly larger than expected than the amount needed to account for the missing baryons. The reasoning for these high expectations and overall high Ω ratio is multi-faceted. Several sources of this and possible explanations are:

1. Higher O VI prior sample ratio values relative to H I priors could be because `EAGLE` predicts less O VII and O VIII for H I priors than O VI. This is responsible for around an order of magnitude difference between the two.

2. O VIII values are significantly larger than O VII because of the choice of f_{ion} for each (Equation 3.13). O VII and O VIII were assigned f_{ion} values of 1.0 and 0.1 respectively, which corresponds to an order of magnitude shift in results. This is around the exact amount the results between O VI and O VIII are shifted by.

3. Unknown exact values of the temperature of the gas in the WHIM being analyzed and estimated abundance values introduce unknown amounts of error to the results. This was discussed in Section 6.1.

4. Poor overall data of the sample, specifically *XMM-Newton*, caused many fit statistics and parameters to be larger and regarded as more significant than they likely actually are. A large amount of these poor fits or data with low

count rates could have resulted in column densities being too high and the respective ratios of the cosmological densities to increase.

Despite these large values however, these results were generally expected. As the calculated upper limits of the column densities were rather conservative (much larger than needed, due to numerous assumptions made), the results of the $\frac{\Omega_X}{\Omega_b}$ ratios were as well. These results ultimately show that our analysis of the *XMM-Newton* and *Chandra* X-ray data do not disprove the proposed solution to the missing baryons problem that the WHIM contains the unaccounted for percentage of Ω_b. The expected results for this solution to be true would align with ours, as the $\sim 40\%$ value is below all of our upper constraints on the ratio of the cosmological densities.

Another exciting result of the work completed in this project is the various possible absorption line detections (Section 5.4), including those that reconfirmed a few previously detected lines (Section 5.2). In total, 8 different redshifts (1ES 1553+113 O VII at $z = 0.18759, 0.18775$ and O VIII at $z = 0.3113, 0.37868$, 3C 273 O VII at $z = 0.1466$, PG 1116+215 O VII at $z = 0.13373$, Ton S180 O VII at $z = 0.04579$, and PKS 0405 O VIII at $z = 0.19456$) yielded tentative detections, 2 of which being previous detections being further confirmed. Although these detections need further inspection and to be studied individually, the result of 8 possible detections is promising at the very least. If a majority of these detections are true, they would be a substantial addition to the body of work studying X-ray absorption in the WHIM.

After the compiled results of the $\frac{\Omega_X}{\Omega_b}$ ratios for the entire sample were finished, more $\frac{\Omega_X}{\Omega_b}$ ratios were calculated for several of the possible detections in Section 5.4 (several possible detections were omitted because of their poor data). These values are perhaps even more significant than the ratios calculated from the upper limits. This is because they provide a cosmological density of the WHIM from a possible detection directly. Instead of an upper limit of the column densities, the exact calculated column density from the analysis was used. This yields a value of $\frac{\Omega_X}{\Omega_b}$ that can be taken at face value; an actual estimate of the specific amount of baryons contributed by the WHIM according to that source. This is the method used in the original 1ES 1553+113 paper that motivated the analysis of the entire sample, which yielded promising values that aligned closely to the expected missing Ω_b (Section 2.2.2). Detailed in Table 5.28, the results of these calculations were compiled into summations by O VII and O VIII. For O VII, an Ω ratio value of 0.046 ± 0.011 was found, and a value of 0.536 ± 0.141 for O VIII. As mentioned previously (Section 5.5), these results are significantly more in line with what was expected from the search for baryons in the WHIM. If these values are accurate, they indicate with a large amount of certainty that there is evidence towards O VII and O VIII being present in the WHIM in significant amounts. O VIII specifically shows promising results, as the ratio calculated for the 2 detections used aligns extremely closely (and within range) to the expected amount of missing baryons in the WHIM.

Finally, another supplementary result proposed by this project is the possible detection of numerous galactic O VII and O VIII lines. These results are

listed in Section 5.3, displaying a total of 14 (7 O VII and 7 O VIII) possible detections in our sample. Although this result does not have any direct implications on the search for the missing baryons in the WHIM, it still could be useful for future analyses on the subject. Future searches and research could use this information to disregard possible detections made around these wavelengths for specific sources.

Regardless of the conservative nature of several of the results from this project (especially in regards to the analysis of the full sample's upper limits), the objective to contribute more towards solving the missing baryons problem and to become the most comprehensive analysis of WHIM X-ray absorption was generally a success. All results correlated directly with the results that would be expected from the missing baryons being contained within the hot WHIM. The upper constraints put on the ratio of the cosmological density due to the WHIM to the overall cosmological density were above the expected values. Several of the cosmological densities calculated for possible detections aligned relatively closely to these values as well. In conjunction with this, the project provided further evidence for several source's proposed prior oxygen detections. Finally, a number of possible galactic O VII and O VIII detections were found, contributing even more information regarding the nature and spectra of various AGNs. These results all come together to form undoubtedly the largest and most detailed search and analysis of its kind over the WHIM using X-ray spectra.

6.3 Future Work

In the short term, the plans for this project and the work contained within it are to present the results for publication, similar to that of the paper over 1ES 1553+113. As the scope of the project has become quite large over time, there have been discussions on the possibility of splitting the work in this project into two papers. The first paper would contain the overall results, analysis, and general work towards reducing and analyzing the entire sample. This would contain a list of the possible new detections described in Section 5.4, the confirmation of prior detections from Section 5.2, and the calculation of the upper limits for the main analysis as well. Following this, a second work would be published regarding the cosmological implications of our results and work towards compiling the results of the first paper in a more sophisticated manner that explores the assumptions required more. Included in this paper would be a more mindful calculation of various parameters and methods in the current analysis. We believe that by corresponding with simulation experts, we could develop an improved method for compiling the Ω ratio results. Other inclusions to the paper would include the introduction of the curve of growth relationship for calculating the column densities (see Section 3.3.4 and 6.1), and a more in depth look into each possible detection result. The plan is to submit these papers for publication in the late summer or fall of 2024. After this, however, my inclusion in this work will be completed and transferred over to the collaborators and my advisor. With this,

all of the scripts and pipelines developed for the analyses and data reduction will continue to be used in future work.

As described in Section 6.1, there were a number of limitations and aspects of the analysis that had to be omitted or forgone due to time constraints. Of this, a future search for Ne IX using the data analysis pipeline and process used in this project is certainly possible. This would provide an even more comprehensive look at absorption lines and the composition of the WHIM, and their correlation to the cosmological density of baryons within it. In combination with this, another analysis of these sources in the form of a stacked redshift analysis is possible. There would be a significant amount of work required to complete this, but the compiled results could give a bigger picture of the absorption lines of interest over the current analysis using just the column density upper limits.

As discussed in Section 6.1, a large scale and more comprehensive search of galactic oxygen in the WHIM is another piece of work that could easily be extended from this project. Although a search was conducted for O VII and O VIII at $z = 0$, the search was slightly rudimentary, and the analysis was nowhere near the detail to that of the search for oxygen at FUV priors in this project. Doing a more complete analysis of all oxygen ions described in Table 3.4 could contribute even more information regarding the sample of sources to future researchers.

As the quality of the data, specifically from *XMM-Newton* was a significant limitation in this study of the WHIM (Section 6.1), possible future searches for the X-ray absorbing WHIM could use instruments from future missions such

as *Athena* [*e.g.,* 5], *Arcus* [63], *Lynx* [32] or *HUBS* [20]. Hypothetically, these new instruments would be significantly more sensitive than *XMM-Newton* and *Chandra*, allowing for the detection of absorption lines to be easier. A similar project to this one completed using newer instruments could provide even more accurate results without the limitation of the poor data and low counts that our instruments had.

References

[1] N. Aghanim, Y. Akrami, M. Ashdown, J. Aumont, C. Baccigalupi, M. Ballardini, A. J. Banday, R. B. Barreiro, N. Bartolo, S. Basak, R. Battye, K. Benabed, J.-P. Bernard, M. Bersanelli, P. Bielewicz, J. J. Bock, J. R. Bond, J. Borrill, F. R. Bouchet, F. Boulanger, M. Bucher, C. Burigana, R. C. Butler, E. Calabrese, J.-F. Cardoso, J. Carron, A. Challinor, H. C. Chiang, J. Chluba, L. P. L. Colombo, C. Combet, D. Contreras, B. P. Crill, F. Cuttaia, P. de Bernardis, G. de Zotti, J. Delabrouille, J.-M. Delouis, E. Di Valentino, J. M. Diego, O. Doré, M. Douspis, A. Ducout, X. Dupac, S. Dusini, G. Efstathiou, F. Elsner, T. A. Enßlin, H. K. Eriksen, Y. Fantaye, M. Farhang, J. Fergusson, R. Fernandez-Cobos, F. Finelli, F. Forastieri, M. Frailis, A. A. Fraisse, E. Franceschi, A. Frolov, S. Galeotta, S. Galli, K. Ganga, R. T. Génova-Santos, M. Gerbino, T. Ghosh, J. González-Nuevo, K. M. Górski, S. Gratton, A. Gruppuso, J. E. Gudmundsson, J. Hamann, W. Handley, F. K. Hansen, D. Herranz, S. R. Hildebrandt, E. Hivon, Z. Huang, A. H. Jaffe, W. C. Jones, A. Karakci, E. Keihänen, R. Keskitalo, K. Kiiveri, J. Kim, T. S. Kisner, L. Knox, N. Krachmalnicoff, M. Kunz, H. Kurki-Suonio, G. Lagache, J.-M. Lamarre, A. Lasenby, M. Lattanzi, C. R. Lawrence, M. Le Jeune, P. Lemos, J. Lesgourgues, F. Levrier, A. Lewis, M. Liguori, P. B. Lilje, M. Lilley, V. Lindholm, M. López-Caniego, P. M. Lubin, Y.-Z. Ma, J. F. Macías-Pérez, G. Maggio, D. Maino, N. Mandolesi, A. Mangilli, A. Marcos-Caballero, M. Maris, P. G. Martin, M. Martinelli, E. Martínez-González, S. Matarrese, N. Mauri, J. D. McEwen, P. R. Meinhold, A. Melchiorri, A. Mennella, M. Migliaccio, M. Millea, S. Mitra, M.-A. Miville-Deschênes, D. Molinari, L. Montier, G. Morgante, A. Moss, P. Natoli, H. U. Nørgaard-Nielsen, L. Pagano, D. Paoletti, B. Partridge, G. Patanchon, H. V. Peiris, F. Perrotta, V. Pettorino, F. Piacentini, L. Polastri, G. Polenta, J.-L. Puget, J. P. Rachen, M. Reinecke, M. Remazeilles, A. Renzi, G. Rocha, C. Rosset, G. Roudier, J. A. Rubiño-Martín, B. Ruiz-Granados, L. Salvati, M. Sandri, M. Savelainen, D. Scott, E. P. S. Shellard, C. Sirignano, G. Sirri, L. D. Spencer, R. Sunyaev, A.-S. Suur-Uski, J. A. Tauber, D. Tavagnacco, M. Tenti, L. Toffolatti, M. Tomasi, T. Trombetti, L. Valenziano, J. Valiviita, B. Van Tent, L. Vibert, P. Vielva, F. Villa, N. Vittorio, B. D. Wandelt, I. K. Wehus, M. White, S. D. M. White, A. Zacchei, and A. Zonca. Planck2018 results: Vi. cosmological parameters. *Astronomy & Astrophysics*, 641:A6, September 2020.

[2] J. Ahoranta, A. Finoguenov, M. Bonamente, E. Tilton, N. Wijers, S. Muzahid, and J. Schaye. Discovery of a multiphase OVI and OVII absorber in the circumgalactic/intergalactic transition region. *arXiv e-prints*, page arXiv:2109.12146, September 2021.

[3] Ahoranta, Jussi, Nevalainen, Jukka, Wijers, Nastasha, Finoguenov, Alexis, Bonamente, Massimiliano, Tempel, Elmo, Tilton, Evan, Schaye, Joop, Kaastra, Jelle, and Gozaliasl, Ghassem. Hot whim counterparts of fuv ovi absorbers: Evidence in the line-of-sight towards quasar 3c 273. *Astronomy & Astrophysics*, 634:A106, 2020.

[4] P. Arévalo, P. Uttley, S. Kaspi, E. Breedt, P. Lira, and I. M. McHardy. Correlated X-ray/optical variability in the quasar MR2251-178. *Monthly Notices of the Royal Astronomical Society*, 389(3):1479–1488, September 2008.

[5] Didier Barret, Anne Decourchelle, Andy Fabian, Matteo Guainazzi, Kirpal Nandra, Randall Smith, and Jan-Willem den Herder. The Athena space X-ray observatory and the astrophysics of hot plasma. *Astronomische Nachrichten*, 341(2):224–235, February 2020.

[6] Ehud Behar, Uria Peretz, Gerard A. Kriss, Jelle Kaastra, Nahum Arav, Stefano Bianchi, Graziella Branduardi-Raymont, Massimo Cappi, Elisa Costantini, Barbara De Marco, Laura Di Gesu, Jacobo Ebrero, Shai Kaspi, Missagh Mehdipour, Stéphane Paltani, Pierre-Olivier Petrucci, Gabriele Ponti, and Francesco Ursini. Multi-wavelength campaign on NGC 7469. I. The rich 640 ks RGS spectrum. *Astronomy & Astrophysics*, 601:A17, May 2017.

[7] A. J. Blustin, G. Branduardi-Raymont, E. Behar, J. S. Kaastra, G. A. Kriss, M. J. Page, S. M. Kahn, M. Sako, and K. C. Steenbrugge. Multiwavelength studies of the Seyfert 1 galaxy NGC 7469 II. X-ray and UV observations with XMM-Newton. *Astronomy & Astrophysics*, 403:481–492, May 2003.

[8] M. Bonamente, J. Nevalainen, E. Tilton, J. Liivamägi, E. Tempel, P. Heinämäki, and T. Fang. A possiblechandraandhubble space telescopedetection of extragalactic whim towards pg 1116+215. *Monthly Notices of the Royal Astronomical Society*, 457(4):4236–4247, Feb 2016.

[9] Massimiliano Bonamente. Systematic errors in the maximum-likelihood regression of Poisson count data: introducing the overdispersed χ^2 distribution.

Monthly Notices of the Royal Astronomical Society, 522(2):1987–2001, June 2023.

[10] Massimiliano Bonamente, Jussi Ahoranta, Jukka Nevalainen, and Patrick Holt. New chandra observations of PG 1116+215 to investigate an extragalactic o viii WHIM absorption line. *Research Notes of the AAS*, 3(5):75, may 2019.

[11] Massimiliano Bonamente and David Spence. A semi-analytical solution to the maximum-likelihood fit of poisson data to a linear model using the cash statistic. *Journal of Applied Statistics*, pages 1–31, 09 2020.

[12] A. Brinkman, H. Aarts, A. den Boggende, T. Bootsma, L. Dubbeldam, J. den Herder, J. Kaastra, P. de Korte, B. van Leeuwen, R. Mewe, F. Paerels, C. de Vries, J. Cottam, T. Decker, S. Kahn, A. Rasmussen, J. Spodek, G. Branduardi-Raymont, P. Guttridge, K. Thomsen, A. Zehnder, and M. Guedel. The Reflection Grating Spectrometer onboard XMM. In *Science with XMM*, page 2, January 1998.

[13] D. A. Buote, L. Zappacosta, T. Fang, P. J. Humphrey, F. Gastaldello, and G. Tagliaferri. X-Ray Absorption by WHIM in the Sculptor Wall. *The Astrophysical Journal*, 695:1351–1356, April 2009.

[14] Amanda Butler Contreras, Erwin T. Lau, Benjamin D. Oppenheimer, Ákos Bogdán, Megan Tillman, Daisuke Nagai, Orsolya E. Kovács, and Blakesley Burkhart. X-ray absorption lines in the warm-hot intergalactic medium: probing Chandra observations with the CAMEL simulations. *Monthly Notices of the Royal Astronomical Society*, 519(2):2251–2261, February 2023.

[15] A. M. Bykov, F. B. S. Paerels, and V. Petrosian. Equilibration processes in the warm-hot intergalactic medium. *Space Science Reviews*, 134(1–4):141–153, February 2008.

[16] H. Böhringer, E. Belsole, J. Kennea, K. Matsushita, S. Molendi, D. M. Worrall, R. F. Mushotzky, M. Ehle, M. Guainazzi, I. Sakelliou, G. Stewart, W. T. Vestrand, and S. Dos Santos. Xmm-newton observations of m 87 and its x-ray halo. *Astronomy & Astrophysics*, 365(1):L181–L187, January 2001.

[17] I. Cagnoni, F. Nicastro, L. Maraschi, A. Treves, and F. Tavecchio. A View of PKS 2155-304 with XMM-Newton Reflection Grating Spectrometers. *The Astrophysical Journal*, 603:449–455, March 2004.

[18] W. Cash. Parameter estimation in astronomy through application of the likelihood ratio. *The Astrophysical Journal*, 228:939, March 1979.

[19] H. Cramer. *Mathematical Methods of Statistics*. Princeton University Press, Princeton, 1946.

[20] W. Cui, LB. Chen, B. Gao, and et al. Hubs: Hot universe baryon surveyor. *J. Low Temp Phys.*, page 502–509, 2020.

[21] Charles W. Danforth, Brian A. Keeney, Evan M. Tilton, J. Michael Shull, John T. Stocke, Matthew Stevans, Matthew M. Pieri, Blair D. Savage, Kevin France, David Syphers, and et al. Anhst/cos survey of the low-redshift intergalactic medium. i. survey, methodology, and overall results. *The Astrophysical Journal*, 817(2):111, Jan 2016.

[22] Romeel Dave, Renyue Cen, Jeremiah P. Ostriker, Greg L. Bryan, Lars Hernquist, Neal Katz, David H. Weinberg, Michael L. Norman, and Brian O'Shea. Baryons in the warm-hot intergalactic medium. *The Astrophysical Journal*, 552(2):473–483, May 2001.

[23] den Herder, J. W., Brinkman, A. C., Kahn, S. M., Branduardi-Raymont, G., Thomsen, K., Aarts, H., Audard, M., Bixler, J. V., den Boggende, A. J., Cottam, J., Decker, T., Dubbeldam, L., Erd, C., Goulooze, H., Güdel, M., Guttridge, P., Hailey, C. J., Al Janabi, K., Kaastra, J. S., de Korte, P. A. J., van Leeuwen, B. J., Mauche, C., McCalden, A. J., Mewe, R., Naber, A., Paerels, F. B., Peterson, J. R., Rasmussen, A. P., Rees, K., Sakelliou, I., Sako, M., Spodek, J., Stern, M., Tamura, T., Tandy, J., de Vries, C. P., Welch, S., and Zehnder, A. The reflection grating spectrometer on board xmm-newton. *Astronomy & Astrophysics*, 365(1):L7–L17, 2001.

[24] T. Fang, D. A. Buote, P. J. Humphrey, C. R. Canizares, L. Zappacosta, R. Maiolino, G. Tagliaferri, and F. Gastaldello. Confirmation of X-ray Absorption by Warm-Hot Intergalactic Medium in the Sculptor Wall. *The Astrophysical Journal*, 714:1715–1724, May 2010.

[25] T. Fang, C. R. Canizares, and Y. Yao. Confirming the Detection of an Intergalactic X-Ray Absorber toward PKS 2155-304. *The Astrophysical Journal*, 670:992–999, December 2007.

[26] T. Fang, R. A. C. Croft, W. T. Sanders, J. Houck, R. Davé, N. Katz, D. H. Weinberg, and L. Hernquist. Simulation of Soft X-Ray Emission Lines from the Missing Baryons. *The Astrophysical Journal*, 623:612–626, April 2005.

[27] T. Fang, H. L. Marshall, J. C. Lee, D. S. Davis, and C. R. Canizares. Chandra Detection of O VIII Lyα Absorption from an Overdense Region in the Intergalactic Medium. *The Astrophysical Journal*, 572:L127–L130, June 2002.

[28] Gary J. Feldman and Robert D. Cousins. A unified approach to the classical statistical analysis of small signals. *Physical Review D*, 57:3873–3889, 1997.

[29] R.A. Fisher. *Statistical Methods for Research Workers*. Oliver and Boyd, Edinburgh, 1925.

[30] R.A. Fisher. The fuducial argument in statistical inference. *Annals of Eugenics*, 6(4):391–398, 1935.

[31] J. García, C. Mendoza, M. A. Bautista, T. W. Gorczyca, T. R. Kallman, and P. Palmeri. K-Shell Photoabsorption of Oxygen Ions. *The Astrophysical Journal Supplement Series*, 158(1):68–79, May 2005.

[32] Jessica A. Gaskin, Douglas A. Swartz, Alexey Vikhlinin, Feryal Özel, Karen E. Gelmis, Jonathan W. Arenberg, Simon R. Bandler, Mark W. Bautz, Marta M. Civitani, Alexandra Dominguez, Megan E. Eckart, Abraham D. Falcone, Enectali Figueroa-Feliciano, Mark D. Freeman, Hans M. Günther, Keith A. Havey, Ralf K. Heilmann, Kiranmayee Kilaru, Ralph P. Kraft, Kevin S. McCarley, Randall L. McEntaffer, Giovanni Pareschi, William Purcell, Paul B. Reid, Mark L. Schattenburg, Daniel A. Schwartz, Eric D. Schwartz, Harvey D. Tananbaum, Grant R. Tremblay, William W. Zhang, and John A. Zuhone. Lynx X-Ray Observatory: an overview. *Journal of Astronomical Telescopes, Instruments, and Systems*, 5:021001, April 2019.

[33] E. Gatuzz, J. García, T. R. Kallman, C. Mendoza, and T. W. Gorczyca. ISMabs: A Comprehensive X-Ray Absorption Model for the Interstellar Medium. *The Astrophysical Journal*, 800:29, February 2015.

[34] N. Gehrels. Confidence limits for small numbers of events in astrophysical data. *The Astrophysical Journal*, 303:336–346, April 1986.

[35] M F Gharaibeh, J M Bizau, D Cubaynes, S Guilbaud, N El Hassan, M M Al Shorman, C Miron, C Nicolas, E Robert, C Blancard, and B M McLaughlin. K-shell photoionization of singly ionized atomic nitrogen: experiment and theory. *Journal of Physics B: Atomic, Molecular and Optical Physics*, 44(17):175208, aug 2011.

[36] S. Grafton-Waters, G. Branduardi-Raymont, M. Mehdipour, M. J. Page, E. Behar, J. Kaastra, N. Arav, S. Bianchi, E. Costantini, J. Ebrero, L. Di Gesu, S. Kaspi, G. A. Kriss, B. De Marco, J. Mao, R. Middei, U. Peretz, P. O. Petrucci, and G. Ponti. Multi-wavelength campaign on NGC 7469. VI. Photoionisation modelling of the emission line regions and the warm absorber. *Astronomy & Astrophysics*, 633:A62, January 2020.

[37] E. Groopman. FCpy Computer Software, 2023.

[38] Ming Feng Gu, Mike Schmidt, Peter Beiersdorfer, Hui Chen, Daniel B. Thorn, Elmar Trabert, Ehud Behar, and Steven M. Kahn. Laboratory measurement and theoretical modeling of k-shell x-ray lines from inner-shell excited and ionized ions of oxygen. *The Astrophysical Journal*, 627(2):1066–1071, Jul 2005.

[39] M. James. *Statistical Methods in Experimental Physics, Second Ed.* World Scientific, 2006.

[40] J. S. Kaastra. On the use of c-stat in testing models for x-ray spectra. *Astronomy Astrophysics*, 605:A51, Sep 2017.

[41] J. S. Kaastra, C. de Vries, and J.W. den Herder. Effective Area Calibration of the RGS. 2018.

[42] J. S. Kaastra, R. Mewe, and H. Nieuwenhuijzen. SPEX: a new code for spectral analysis of X UV spectra. In K. Yamashita and T. Watanabe, editors, *UV and X-ray Spectroscopy of Astrophysical and Laboratory Plasmas*, pages 411–414, 1996.

[43] J. S. Kaastra, A. J. J. Raassen, J. de Plaa, and Liyi Gu. Spex x-ray spectral fitting package, 2023.

[44] J. S. Kaastra, N. Werner, J. W. A. den Herder, F. B. S. Paerels, J. de Plaa, A. P. Rasmussen, and C. P. de Vries. The O VII X-Ray Forest toward Markarian 421: Consistency between XMM-Newton and Chandra. *The Astrophysical Journal*, 652(1):189–197, November 2006.

[45] S. Komossa, M. Gliozzi, and I. Papadakis. The warm absorber of the quasar MR2251-178. *Astronomical and Astrophysical Transactions*, 20(2):329–331, August 2001.

[46] Orsolya E. Kovács, Ákos Bogdán, Randall K. Smith, Ralph P. Kraft, and William R. Forman. Detection of the missing baryons toward the sightline of h1821+643. *The Astrophysical Journal*, 872(1):83, February 2019.

[47] T. P. Li and Y. Q. Ma. Analysis methods for results in gamma-ray astronomy. *The Astrophysical Journal*, 272:317–324, September 1983.

[48] P. Mazzotta, G. Mazzitelli, S. Colafrancesco, and N. Vittorio. Ionization balance for optically thin plasmas: Rate coefficients for all atoms and ions of the elements h to ni. *Astronomy and Astrophysics Supplement Series*, 133(3):403–409, Dec 1998.

[49] Kazuhisa Mitsuda. Observational signatures of the warm-hot intergalactic medium and x-ray absorption lines by the halo of our galaxy. *Chinese Journal of Astronomy and Astrophysics*, 3(S1):169, dec 2003.

[50] J. Nevalainen, E. Tempel, J. Ahoranta, L. J. Liivamägi, M. Bonamente, E. Tilton, J. Kaastra, T. Fang, P. Heinämäki, E. Saar, and A. Finoguenov. To be or not to be: the case of the hot WHIM absorption in the blazar PKS 2155-304 sight line. *Astronomy & Astrophysics*, 621:A88, January 2019.

[51] J. Nevalainen, B. Wakker, J. Kaastra, M. Bonamente, S. Snowden, F. Paerels, and C. de Vries. Discovery of Galactic O iv and O v X-ray absorption due to transition temperature gas in the PKS 2155-304 spectrum. *Astronomy & Astrophysics*, 605:A47, September 2017.

[52] J. Neyman. Outline of a theory of statistical estimation based on the classical theory of probability. *Philosophical Transactions of the Royal Society of London. Series A, Mathematical and Physical Sciences*, 236(767):333–380, 1937.

[53] F. Nicastro. Confirming the Detection of two WHIM Systems along the Line of Sight to 1ES 1553+113. *arXiv e-prints*, November 2018.

[54] F. Nicastro, J. Kaastra, Y. Krongold, S. Borgani, E. Branchini, R. Cen, M. Dadina, C. W. Danforth, M. Elvis, F. Fiore, and et al. Observations of the missing baryons in the warm–hot intergalactic medium. *Nature*, 558(7710):406–409, Jun 2018.

[55] F. Nicastro, Y. Krongold, D. Fields, M. L. Conciatore, L. Zappacosta, M. Elvis, S. Mathur, and I. Papadakis. Xmm-newton and fuse tentative evidence for a whim filament along the line of sight to pks 0558-504. *The Astrophysical Journal*, 715(2):854, may 2010.

[56] F. Nicastro, S. Mathur, M. Elvis, J. Drake, F. Fiore, T. Fang, A. Fruscione, Y. Krongold, H. Marshall, and R. Williams. Chandra Detection of the First X-Ray Forest along the Line of Sight To Markarian 421. *The Astrophysical Journal*, 629:700–718, August 2005.

[57] Rostislav Protassov, David A. van Dyk, Alanna Connors, Vinay L. Kashyap, and Aneta Siemiginowska. Statistics, Handle with Care: Detecting Multiple Model Components with the Likelihood Ratio Test. *The Astrophysical Journal*, 571(1):545–559, May 2002.

[58] A. P. Rasmussen, S. M. Kahn, F. Paerels, J. W. d. Herder, J. Kaastra, and C. de Vries. On the Putative Detection of z 0 X-Ray Absorption Features in the Spectrum of Mrk 421. *The Astrophysical Journal*, 656:129–138, February 2007.

[59] B. Ren, T. Fang, and D. A. Buote. X-Ray Absorption by the Warm-hot Intergalactic Medium in the Hercules Supercluster. *The Astrophysical Journal*, 782:L6, February 2014.

[60] V.K. Rohatgi. *An introduction to probability theory and mathematical statistics*. Wiley, New York, 1976.

[61] Jennifer E. Scott, Gerard A. Kriss, Julia C. Lee, Jessica Kim Quijano, Michael Brotherton, Claude R. Canizares, Richard F. Green, John Hutchings, Mary Elizabeth Kaiser, Herman Marshall, William Oegerle, Patrick Ogle, and Wei Zheng. Intrinsic Absorption in the Spectrum of NGC 7469:

Simultaneous Chandra, FUSE, and STIS Observations. *The Astrophysical Journal*, 634(1):193–209, November 2005.

[62] J. Michael Shull, Britton D. Smith, and Charles W. Danforth. The baryon census in a multiphase intergalactic medium: 30% of the baryons may still be missing. *The Astrophysical Journal*, 759(1):23, Oct 2012.

[63] Randall K. Smith, Margaret Abraham, Grace Baird, Marshall Bautz, Jay Bookbinder, Joel Bregman, Laura Brenneman, Nancy Brickhouse, David Burrows, Vadim Burwitz, Joseph Bushman, Claude Canizares, Deepto Chakrabarty, Peter Cheimets, Elisa Costantini, Simon Dawson, Casey DeRoo, Abraham Falcone, Adam Foster, Luigi Gallo, Catherine E. Grant, H. Moritz Günther, Ralf K. Heilmann, Butler Hine, David Huenemoerder, Steve Jara, Jelle Kaastra, Ingo Kreykenbohm, Kristin Madsen, Michael McDonald, Michael McEachen, Randall McEntaffer, Herman Marshall, Eric Miller, Jon Miller, Elisabeth Morse, Richard Mushotzky, Kirpal Nandra, Michael A. Nowak, Frits Paerels, Robert Petre, Katja Poppenhaeger, Andrew Ptak, Paul Reid, Karolyn Ronzano, Jeremy Sanders, Mark Schattenburg, Jonathan Schonfeld, Norbert Schulz, Alan Smale, Pasquale Temi, Lynne Valencic, Stephen Walker, Richard Willingale, Joern Wilms, and Scott Wolk. Arcus: the soft x-ray grating explorer. In *UV, X-Ray, and Gamma-Ray Space Instrumentation for Astronomy XXI*, volume 11118 of *Society of Photo-Optical Instrumentation Engineers (SPIE) Conference Series*, page 111180W, September 2019.

[64] David Spence, Massimiliano Bonamente, Jukka Nevalainen, Toni Tuominen, Jussi Ahoranta, Jelle de Plaa, Wenhao Liu, and Nastasha Wijers. A search for the missing baryons with X-ray absorption lines towards the blazar 1ES 1553+113. *Monthly Notices of the Royal Astronomical Society*, 523(2):2329–2350, August 2023.

[65] Evan M. Tilton, Charles W. Danforth, J. Michael Shull, and Teresa L. Ross. The low-redshift intergalactic medium as seen in archival legacyhst/stis andfusedata. *The Astrophysical Journal*, 759(2):112, Oct 2012.

[66] John W. Tukey. Some Examples with Fiducial Relevance. *The Annals of Mathematical Statistics*, 28(3):687 – 695, 1957.

[67] T. Tuominen, J. Nevalainen, E. Tempel, T. Kuutma, N. Wijers, J. Schaye, P. Heinämäki, M. Bonamente, and P. Ganeshaiah Veena. An EAGLE view of the missing baryons. *Astronomy & Astrophysics*, 646:A156, February 2021.

[68] D.A. Verner, E.M. Verner, and G.J. Ferland. Atomic data for permitted resonance lines of atoms and ions from h to si, and s, ar, ca, and fe. *Atomic Data and Nuclear Data Tables*, 64(1):1–180, Sep 1996.

[69] Ronald L. Wasserstein and Nicole A. Lazar. The ASA's statement on p-values: Context, process, and purpose. *The American Statistician*, 70(2):129–133, 2016.

[70] Nastasha A. Wijers, Joop Schaye, Benjamin D. Oppenheimer, Robert A. Crain, and Fabrizio Nicastro. The abundance and physical properties of O VII and O VIII X-ray absorption systems in the EAGLE simulations. *arXiv e-prints*, page arXiv:1904.01057, Apr 2019.

[71] S. S. Wilks. The large-sample distribution of the likelihood ratio for testing composite hypotheses. *Ann. Math. Statist.*, 9(1):60–62, 03 1938.

[72] S.S. Wilks. *Mathematical Statistics*. Princeton University Press, Princeton, 1943.

[73] S.S. Wilks. *Mathematical Statistics, Sec. Ed.* J. Wiley and Sons, 1962.

[74] Y. Yao, J. M. Shull, Q. D. Wang, and W. Cash. Detecting the Warm-Hot Intergalactic Medium through X-Ray Absorption Lines. *The Astrophysical Journal*, 746:166, February 2012.

[75] Y. Yao, T. M. Tripp, Q. D. Wang, C. W. Danforth, C. R. Canizares, J. M. Shull, H. L. Marshall, and L. Song. X-raying the Intergalactic O VI Absorbers. *The Astrophysical Journal*, 697:1784–1792, June 2009.

Appendix A. O VI and H I BLA Priors Table

Table A.1: O VI FUV prior detections table, adapted from the results of [21] ("Danforth") and [65] ("Tilton"). A '^{M}' indicates that there was an OVI 1032 and 1038 doublet present. These 1032 and 1038 doublet values were averaged into one value on a weighted system of 2:1 respectively. A '*' indicates a duplicate redshift in both Danforth and Tilton. The corresponding Tilton duplicates are omitted from the table.

#	Name	Redshift	$\log N$ (cm^{-2})	b (km s^{-1})	Source
1	1es1028	0.12314	14.3±0.1	41.37±5.57	Danforth^M
2	1es1028	0.13706	13.6±0.1	14.50±6.30	Danforth^{1032}
3	1es1028	0.33735	13.9±0.1	72.87±15.73	Danforth^M
4	1es1553	0.18759	13.8±0.1	12.10±3.00	Danforth^M
5	1es1553	0.18775	13.9±0.1	23.40±4.50	Danforth^M
6	1es1553	0.18984	13.4±1.5	23.37±6.57	Danforth^M
7	1es1553	0.21631	13.3±0.1	19.80±5.80	Danforth^{1032}
8	1es1553	0.31130	13.4±0.1	31.90±7.50	Danforth^{1032}
9	1es1553	0.37868	12.9±0.2	17.30±3.70	Danforth^{1032}
10	1es1553	0.39497	13.9±0.1	44.07±3.33	Danforth^M
11	1sj1032	0.17007	14.3±0.0	42.00±3.80	Danforth^{1032}
12	3c249	0.24676	13.8±0.1	24.70±2.50	Tilton
13	3c249	0.30788	13.9±0.2	23.30±6.10	Tilton
14	3c249	0.30809	14.5±0.0	20.00±1.00	Tilton
15	3c249	0.31364	13.8±0.1	13.30±1.00	Tilton
16	3c263	0.11388	13.7±0.1	33.10±8.20	Danforth^{1032}
17	3c263	0.14078	13.7±0.1	45.10±6.97	Danforth^M
18	3c263	0.29204	13.0±0.2	21.40±9.60	Danforth^{1032}
19	3c263	0.32566	14.0±0.0	32.57±2.47	Danforth^M
20	3c263	0.44677	13.9±0.1	64.10±10.70	Danforth^{1038}
21	3c263	0.52690	13.9±0.1	38.47±7.00	Danforth^M
22	3c263	0.52801	13.5±0.1	48.00±14.40	Danforth^{1032}
23	3c273	0.00337	13.4±0.1	28.00±1.00	Tilton
24	3c273	0.00533	13.0±0.0	0.00±0.00	Tilton
25	3c273	0.00764	13.1±0.2	25.00±9.00	Tilton
26	3c273	0.02947	13.4±0.0	0.00±0.00	Tilton
27	3c273	0.04898	14.0±0.0	0.00±0.00	Tilton

28	3c273	0.06655	13.4±0.0	0.00±0.00	Tilton
29	3c273	0.09018	13.3±0.1	22.20±10.80	Tilton
30	3c273	0.12007	13.4±0.1	20.03±3.23	Danforth^{M,*}
31	3c273	0.14660	13.5±0.0	0.00±0.00	Tilton
32	3c273	0.15784	13.1±0.1	30.30±4.90	Danforth^{1032*}
33	3c351	0.21789	14.0±0.0	74.40±8.60	Tilton
34	3c351	0.22093	14.3±0.0	48.50±3.50	Tilton
35	3c351	0.31635	13.7±0.1	22.70±3.30	Tilton
36	3c351	0.31657	14.0±0.1	23.40±2.40	Tilton
37	3c351	0.31687	14.0±0.1	31.80±2.90	Tilton
38	3c351	0.32086	12.9±0.2	30.00±0.00	Tilton
39	3c57	0.17002	13.6±0.1	43.50±12.40	Danforth^{1032}
40	3c57	0.24987	13.6±0.1	10.40±3.80	Danforth^{1032}
41	3c57	0.25022	13.8±0.1	60.00±12.20	Danforth^{1032}
42	3c57	0.27821	13.8±0.1	28.40±5.37	Danforth^{M}
43	3c57	0.28669	13.6±0.2	40.30±8.80	Danforth^{1032}
44	3c57	0.29238	14.3±0.0	41.53±2.50	Danforth^{M}
45	3c57	0.32010	13.8±0.1	26.60±9.30	Danforth^{1038}
46	3c57	0.32301	13.4±0.1	19.63±7.43	Danforth^{M}
47	3c57	0.32368	13.7±0.2	34.90±16.90	Danforth^{1038}
48	3c57	0.32405	14.1±0.1	74.33±25.17	Danforth^{M}
49	3c57	0.32460	14.1±0.1	39.93±6.17	Danforth^{M}
50	3c57	0.32780	13.7±0.1	40.80±15.13	Danforth^{M}
51	3c57	0.32820	14.5±0.0	38.83±2.00	Danforth^{M}
52	3c57	0.32902	13.9±0.0	29.03±3.97	Danforth^{M}
53	3c57	0.33332	13.7±0.1	29.97±7.40	Danforth^{M}
54	3c57	0.38342	14.0±0.0	23.03±2.43	Danforth^{M}
55	3c57	0.40187	13.2±0.1	5.20±5.20	Danforth^{1032}
56	3c57	0.40211	13.5±0.1	26.83±8.40	Danforth^{M}
57	3c57	0.43164	14.0±0.1	56.40±7.00	Danforth^{1032}
58	3c57	0.53325	13.9±0.1	12.33±2.67	Danforth^{M}
59	3c57	0.57997	14.1±0.1	21.53±4.27	Danforth^{M}
60	3c57	0.66914	13.9±0.1	13.23±3.87	Danforth^{M}
61	3c57	0.66948	13.9±0.1	14.97±4.53	Danforth^{M}
62	3c57	0.66976	14.2±0.1	15.80±2.63	Danforth^{M}
63	3c66a	0.24258	14.2±0.0	25.63±2.10	Danforth^{M}
64	3c66a	0.32824	13.4±0.1	35.30±12.70	Danforth^{1032}
65	b0117	0.14191	13.3±0.1	13.60±8.60	Danforth^{1032}

66	b0117	0.19073	13.6±0.1	15.10±2.70	Danforth^{M}
67	b0117	0.34848	13.9±0.1	47.80±8.23	Danforth^{M}
68	b0117	0.34861	13.8±0.1	17.63±3.83	Danforth^{M}
69	f1010	0.11326	14.0±0.2	52.10±15.90	Danforth^{1032}
70	f1010	0.19113	13.3±0.2	19.30±12.10	Danforth^{1032}
71	f1010	0.19319	13.7±0.1	9.07±2.33	Danforth^{M}
72	f1010	0.25473	18.0±0.3	30.10±0.50	Danforth^{1032}
73	h1821	0.02438	13.4±0.1	21.00±7.50	Tilton
74	h1821	0.10817	13.2±0.1	10.00±0.00	Tilton
75	h1821	0.12133	14.0±0.0	76.00±12.00	Tilton
76	h1821	0.12147	13.7±0.1	50.30±8.60	Danforth^{1032}
77	h1821	0.16992	13.8±0.0	100.00±0.00	Danforth^{1032}
78	h1821	0.17043	13.6±0.0	57.60±7.50	Danforth^{1032}
79	h1821	0.21326	13.6±0.0	23.77±2.83	Danforth^{M,*}
80	h1821	0.22497	14.3±0.0	45.17±1.43	Danforth^{M,*}
81	h1821	0.22522	13.1±0.1	5.00±0.00	Danforth^{M,*}
82	h1821	0.22639	13.5±0.0	17.43±2.37	Danforth^{M,*}
83	h1821	0.24531	13.7±0.0	26.90±2.43	Danforth^{M,*}
84	h1821	0.26657	13.7±0.1	33.00±4.47	Danforth^{M,*}
85	h1821	0.28800	13.4±0.1	29.87±4.40	Danforth^{M}
86	h1821	0.29658	13.9±0.0	19.03±1.57	Danforth^{M,*}
87	h1821	0.29680	14.0±0.0	36.40±2.47	Danforth^{M,*}
88	h2356	0.11461	14.1±0.3	100.00±0.00	Danforth^{1032}
89	h2356	0.16512	13.6±0.1	16.00±7.10	Danforth^{1032}
90	he0056	0.16392	13.4±0.1	23.20±7.40	Danforth^{1032}
91	he0056	0.16492	13.1±0.2	20.30±11.10	Danforth^{1032}
92	he0153	0.13221	13.2±0.2	12.93±11.03	Danforth^{M}
93	he0153	0.14844	13.9±0.1	54.10±9.43	Danforth^{M}
94	he0153	0.14886	14.1±0.0	29.00±3.10	Danforth^{1032}
95	he0153	0.17089	13.8±0.1	23.30±3.20	Danforth^{1032}
96	he0153	0.19885	13.7±0.1	77.50±3.63	Danforth^{M}
97	he0153	0.22202	13.6±0.1	18.60±7.80	Danforth^{1038}
98	he0153	0.22600	14.2±0.0	33.00±2.33	Danforth^{M}
99	he0153	0.29091	13.7±0.1	25.00±8.87	Danforth^{M}
100	he0153	0.29115	13.9±0.1	21.77±4.43	Danforth^{M}
101	he0153	0.39774	13.1±0.2	28.50±10.80	Danforth^{1032}
102	he0153	0.40027	14.3±0.0	34.90±2.43	Danforth^{M}
103	he0153	0.40058	13.4±0.2	20.93±8.87	Danforth^{M}

104	he0226	0.01746	13.7±0.1	13.00±9.00	Tilton
105	he0226	0.02679	13.3±0.0	0.00±0.00	Tilton
106	he0226	0.04121	13.5±0.0	0.00±0.00	Tilton
107	he0226	0.04535	13.3±0.0	0.00±0.00	Tilton
108	he0226	0.04609	13.4±0.0	0.00±0.00	Tilton
109	he0226	0.06015	13.3±0.0	0.00±0.00	Tilton
110	he0226	0.06083	13.3±0.0	0.00±0.00	Tilton
111	he0226	0.07023	13.2±0.0	0.00±0.00	Tilton
112	he0226	0.08375	13.3±0.0	0.00±0.00	Tilton
113	he0226	0.08901	13.3±0.0	0.00±0.00	Tilton
114	he0226	0.08938	13.1±0.0	0.00±0.00	Tilton
115	he0226	0.08950	13.2±0.0	0.00±0.00	Tilton
116	he0226	0.09220	13.3±0.0	0.00±0.00	Tilton
117	he0226	0.10668	13.5±0.0	0.00±0.00	Tilton
118	he0226	0.11514	13.2±0.0	0.00±0.00	Tilton
119	he0226	0.11680	13.4±0.0	0.00±0.00	Tilton
120	he0226	0.11733	13.2±0.0	0.00±0.00	Tilton
121	he0226	0.12589	13.2±0.0	0.00±0.00	Tilton
122	he0226	0.13832	13.3±0.0	0.00±0.00	Tilton
123	he0226	0.15175	13.7±0.0	0.00±0.00	Tilton
124	he0226	0.15549	13.6±0.0	0.00±0.00	Tilton
125	he0226	0.16237	13.7±0.0	0.00±0.00	Tilton
126	he0226	0.16339	13.6±0.0	0.00±0.00	Tilton
127	he0226	0.16971	14.2±0.0	0.00±0.00	Tilton
128	he0226	0.18619	13.5±0.0	0.00±0.00	Tilton
129	he0226	0.18811	13.3±0.0	0.00±0.00	Tilton
130	he0226	0.18891	13.2±0.0	0.00±0.00	Tilton
131	he0226	0.19374	13.4±0.0	0.00±0.00	Tilton
132	he0226	0.19453	13.3±0.0	0.00±0.00	Tilton
133	he0226	0.19860	13.7±0.0	0.00±0.00	Tilton
134	he0226	0.20055	13.4±0.0	0.00±0.00	Tilton
135	he0226	0.20703	14.4±0.0	35.23±1.27	Danforth^{M,*}
136	he0226	0.22009	13.0±0.1	11.20±6.80	Danforth^{1032*}
137	he0226	0.22099	13.3±0.0	0.00±0.00	Tilton
138	he0226	0.23009	13.3±0.0	0.00±0.00	Tilton
139	he0226	0.23964	13.3±0.0	0.00±0.00	Tilton
140	he0226	0.24522	13.1±0.2	16.00±10.40	Danforth^{1032*}
141	he0226	0.25099	13.2±0.0	0.00±0.00	Tilton

142	he0226	0.27155	13.2±0.0	0.00±0.00	Tilton
143	he0226	0.27956	13.2±0.0	0.00±0.00	Tilton
144	he0226	0.28041	13.2±0.0	0.00±0.00	Tilton
145	he0226	0.29134	13.3±0.0	0.00±0.00	Tilton
146	he0226	0.29213	13.4±0.0	0.00±0.00	Tilton
147	he0226	0.30939	13.4±0.1	45.90±12.00	Danforth^{1032*}
148	he0226	0.31833	13.0±0.2	6.00±3.00	Tilton
149	he0226	0.33965	13.2±0.1	12.70±5.10	Danforth^{1032}
150	he0226	0.34036	13.9±0.0	25.87±2.23	Danforth^{M,*}
151	he0226	0.35493	12.9±0.3	13.00±9.00	Tilton
152	he0226	0.35528	13.7±0.1	34.80±4.47	Danforth^{M,*}
153	he0226	0.37281	13.3±0.0	0.00±0.00	Tilton
154	he0226	0.38420	13.3±0.0	0.00±0.00	Tilton
155	he0226	0.38636	13.4±0.0	0.00±0.00	Tilton
156	he0226	0.39642	13.5±0.1	51.70±7.70	Danforth^{1032*}
157	he0226	0.39692	13.3±0.1	21.80±4.50	Danforth^{1032}
158	he0226	0.39890	13.5±0.0	0.00±0.00	Tilton
159	he0226	0.40034	13.4±0.0	0.00±0.00	Tilton
160	he0226	0.40274	13.3±0.0	0.00±0.00	Tilton
161	he0226	0.49225	14.4±0.1	34.93±3.37	Danforth^{M,*}
162	he0226	0.49254	14.5±0.0	22.13±1.90	Danforth^{M,*}
163	he0226	0.49280	14.0±0.2	27.90±22.60	Danforth^{M,*}
164	he0226	0.49309	14.0±0.2	41.50±5.60	Danforth^{M,*}
165	he0238	0.27918	13.3±0.2	30.20±11.20	Danforth^{1032}
166	he0238	0.31404	13.4±0.1	24.10±2.80	Danforth^{M}
167	he0238	0.40107	13.5±0.2	18.43±6.47	Danforth^{M}
168	he0238	0.42387	14.4±0.0	52.03±3.33	Danforth^{M}
169	he0238	0.42431	14.1±0.0	22.83±2.47	Danforth^{M}
170	he0238	0.47203	14.1±0.0	20.47±2.27	Danforth^{M}
171	he0238	0.47230	13.7±0.1	12.40±3.33	Danforth^{M}
172	he0238	0.60294	14.2±0.1	66.80±13.10	Danforth^{1038}
173	he0238	0.60334	14.1±0.0	80.80±9.90	Danforth^{1032}
174	he0238	0.60364	13.7±0.3	33.40±18.50	Danforth^{1038}
175	he0238	0.60431	14.5±0.2	87.40±28.37	Danforth^{M}
176	he0238	0.60493	14.1±0.4	65.60±25.90	Danforth^{M}
177	he0238	0.60912	14.5±0.1	89.80±7.20	Danforth^{1032}
178	he0238	0.60938	14.7±0.0	100.00±0.00	Danforth^{1038}
179	he0238	0.61015	14.3±0.1	79.00±9.90	Danforth^{1032}

180	he0238	0.61091	13.8±0.1	29.33±6.20	Danforth^{M}
181	he0435	0.24490	13.9±0.2	33.73±13.93	Danforth^{M}
182	he0435	0.29849	13.8±0.2	37.40±9.40	Danforth^{1032}
183	he0435	0.31319	14.0±0.1	10.97±3.67	Danforth^{M}
184	he0435	0.39225	14.1±0.1	46.67±9.80	Danforth^{M}
185	he0435	0.39266	14.0±0.1	33.97±7.67	Danforth^{M}
186	he0435	0.40921	14.1±0.1	80.33±9.80	Danforth^{M}
187	he0435	0.40997	14.5±0.0	58.83±4.13	Danforth^{M}
188	hs0624	0.06342	14.2±0.2	57.10±21.60	Tilton
189	hs0624	0.07573	13.9±0.0	0.00±0.00	Tilton
190	hs0624	0.20482	13.4±0.2	28.00±12.00	Tilton
191	hs0624	0.20531	13.1±0.2	20.00±0.00	Tilton
192	hs0624	0.21134	13.1±0.2	20.00±0.00	Tilton
193	hs0624	0.22329	13.0±0.4	11.00±0.00	Tilton
194	hs0624	0.25230	13.2±0.1	27.00±8.80	Tilton
195	hs0624	0.29984	13.1±0.0	0.00±0.00	Tilton
196	hs0624	0.31794	13.7±0.1	29.00±1.60	Tilton
197	hs0624	0.33980	13.5±0.1	37.30±5.30	Tilton
198	hs0624	0.34863	13.1±0.0	0.00±0.00	Tilton
199	hs0624	0.37034	12.8±0.2	8.00±3.70	Tilton
200	hs0624	0.37058	13.6±0.0	19.90±2.40	Tilton
201	hs0624	0.37095	13.6±0.0	24.40±1.90	Tilton
202	hs1102	0.20136	13.2±0.2	22.10±6.40	Danforth^{1032}
203	hs1102	0.20653	14.2±0.0	33.33±3.60	Danforth^{M}
204	hs1102	0.23882	14.8±0.0	34.53±1.97	Danforth^{M}
205	hs1102	0.26162	14.0±0.3	34.10±12.40	Danforth^{1038}
206	hs1102	0.28902	13.8±0.1	56.10±13.20	Danforth^{1032}
207	hs1102	0.28924	13.6±0.2	34.20±10.70	Danforth^{1032}
208	hs1102	0.28974	14.2±0.1	38.27±5.27	Danforth^{M}
209	hs1102	0.31046	14.3±0.0	28.27±2.40	Danforth^{M}
210	hs1102	0.33619	13.5±0.3	43.20±19.60	Danforth^{1032}
211	hs1102	0.38188	13.9±0.1	30.13±3.73	Danforth^{M}
212	hs1102	0.40794	13.8±0.1	33.83±7.57	Danforth^{M}
213	hs1102	0.40978	14.1±0.0	73.60±4.67	Danforth^{M}
214	hs1102	0.43768	13.8±0.1	18.33±4.63	Danforth^{M}
215	hs1102	0.43807	14.1±0.0	32.73±4.77	Danforth^{M}
216	hs1102	0.48393	14.3±0.1	51.90±7.10	Danforth^{M}
217	hs1102	0.48432	14.3±0.1	44.13±8.17	Danforth^{M}

218	hs1102	0.48495	14.4±0.1	96.90±22.80	Danforth^{1032}
219	hs1102	0.48525	14.3±0.0	100.00±0.00	Danforth^{1038}
220	hs1102	0.48637	14.5±0.0	77.80±6.10	Danforth^{1038}
221	hs1102	0.50606	13.8±0.1	61.60±8.90	Danforth^{1032}
222	i22456	0.09858	14.7±0.0	48.70±2.10	Danforth^{M}
223	i22456	0.09895	14.4±0.1	33.80±5.00	Danforth^{1032}
224	i22456	0.09931	14.9±0.0	70.37±3.90	Danforth^{M}
225	i22456	0.09959	14.0±0.0	9.60±2.30	Danforth^{1038}
226	i22456	0.09989	14.8±0.0	34.57±1.37	Danforth^{M}
227	i22456	0.10034	14.7±0.0	50.57±1.80	Danforth^{M}
228	i22456	0.10101	15.4±0.0	55.57±1.30	Danforth^{M}
229	i22456	0.10146	14.0±0.0	23.20±3.90	Danforth^{1032}
230	mr2251	0.01070	13.4±0.2	14.00±0.00	Tilton
231	mrk421	0.01009	13.2±0.0	0.00±0.00	Tilton
232	mrk876	0.00311	13.6±0.1	25.00±6.00	Tilton
233	mrk876	0.06248	13.6±0.1	35.00±2.00	Tilton
234	mrk876	0.08579	14.1±0.1	51.00±5.20	Tilton
235	mrk876	0.11488	14.4±0.0	45.47±1.90	Danforth^{M,*}
236	mrk876	0.11517	13.7±0.1	52.93±9.30	Danforth^{M}
237	mrk876	0.11588	14.2±0.0	28.67±1.47	Danforth^{M,*}
238	ngc7469	0.00962	14.1±0.1	28.60±6.00	Tilton
239	ngc7469	0.00994	14.7±0.0	41.60±3.00	Tilton
240	ngc7469	0.01153	13.4±0.2	19.00±10.00	Tilton
241	p1103	0.13556	13.8±0.2	83.50±26.10	Danforth^{1032}
242	p1103	0.13937	13.7±0.2	20.60±11.00	Danforth^{M}
243	p1103	0.14099	13.6±0.2	11.97±10.70	Danforth^{M}
244	p1103	0.14126	14.2±0.1	55.50±13.50	Danforth^{M}
245	p1103	0.17277	14.1±0.0	28.30±0.50	Danforth^{1032}
246	pg0003	0.16521	13.8±0.2	61.03±13.67	Danforth^{M}
247	pg0003	0.20907	13.7±0.1	34.10±5.70	Danforth^{1032}
248	pg0003	0.29021	14.2±0.0	37.30±4.67	Danforth^{M}
249	pg0003	0.30551	13.2±0.2	22.40±16.30	Danforth^{1032}
250	pg0003	0.30569	13.3±0.2	19.00±13.73	Danforth^{M}
251	pg0003	0.34757	14.3±0.0	29.47±2.60	Danforth^{M}
252	pg0003	0.34788	13.9±0.1	15.47±2.70	Danforth^{M}
253	pg0003	0.36452	14.3±0.0	40.43±2.30	Danforth^{M}
254	pg0003	0.36508	14.5±0.0	27.60±1.40	Danforth^{1032}
255	pg0003	0.36572	14.1±0.1	36.17±5.43	Danforth^{M}

256	pg0003	0.36621	14.1±0.0	30.53±2.53	Danforth^{M}
257	pg0003	0.37029	13.6±0.1	61.60±11.50	Danforth^{1032}
258	pg0003	0.38608	13.8±0.1	23.83±4.10	Danforth^{M}
259	pg0003	0.38639	13.9±0.1	36.77±5.90	Danforth^{M}
260	pg0003	0.40138	14.3±0.0	32.80±1.87	Danforth^{M}
261	pg0003	0.42192	14.3±0.0	27.67±1.97	Danforth^{M}
262	pg0157	0.14621	13.4±0.2	13.10±9.40	Danforth^{1032}
263	pg0804	0.00382	13.5±0.2	17.00±0.00	Tilton
264	pg0804	0.01851	13.2±0.0	0.00±0.00	Tilton
265	pg0804	0.10216	14.2±0.0	50.03±3.87	Danforth^{M}
266	pg0804	0.10230	14.0±0.1	34.30±3.10	Tilton
267	pg0832	0.10772	13.5±0.0	17.80±1.00	Danforth^{1038}
268	pg0832	0.13230	14.0±0.2	100.00±0.00	Danforth^{1032}
269	pg0832	0.15276	13.8±0.2	52.20±20.10	Danforth^{1032}
270	pg0832	0.23308	13.8±0.2	54.30±14.80	Danforth^{1032}
271	pg0832	0.32567	14.1±0.1	60.83±7.80	Danforth^{M}
272	pg0953	0.01560	13.7±0.2	11.00±0.00	Tilton
273	pg0953	0.05891	13.9±0.1	26.00±8.00	Tilton
274	pg0953	0.06807	14.3±0.1	13.50±1.80	Tilton
275	pg0953	0.11827	13.3±0.2	12.00±0.00	Tilton
276	pg0953	0.14236	14.0±0.0	20.63±2.37	Danforth^{M,*}
277	pg0953	0.14263	13.6±0.1	27.17±5.87	Danforth^{M}
278	pg0953	0.14307	13.3±0.1	36.43±4.63	Danforth^{M}
279	pg0953	0.22967	13.9±0.0	33.97±2.37	Danforth^{M,*}
280	pg0953	0.23251	13.4±0.1	19.20±2.80	Danforth^{1032}
281	pg0953	0.23351	13.5±0.1	10.53±2.40	Danforth^{M,*}
282	pg1001	0.13773	14.1±0.1	47.30±5.93	Danforth^{M}
283	pg1001	0.21259	13.4±0.1	24.70±6.70	Danforth^{1032}
284	pg1001	0.27333	13.3±0.2	20.07±10.07	Danforth^{M}
285	pg1001	0.33018	14.2±0.1	10.67±1.20	Danforth^{M}
286	pg1049	0.19406	13.7±0.2	27.60±11.37	Danforth^{M}
287	pg1049	0.32490	13.7±0.3	51.80±15.80	Danforth^{M}
288	pg1049	0.32545	13.7±0.1	54.40±20.30	Danforth^{1032}
289	pg1049	0.32569	14.4±0.1	82.60±20.60	Danforth^{1038}
290	pg1049	0.33481	14.4±0.1	90.00±13.50	Danforth^{1032}
291	pg1049	0.33531	14.5±0.0	100.00±0.00	Danforth^{1032}
292	pg1049	0.33904	14.1±0.1	51.63±8.57	Danforth^{M}
293	pg1049	0.34006	15.1±0.0	80.77±4.07	Danforth^{M}

294	pg1049	0.34096	14.9±0.0	80.10±7.43	Danforth^{M}
295	pg1049	0.34181	15.1±0.0	68.97±4.83	Danforth^{M}
296	pg1049	0.34260	14.6±0.0	76.90±10.43	Danforth^{M}
297	pg1115	0.12285	13.6±0.2	28.67±12.13	Danforth^{M}
298	pg1115	0.12313	13.8±0.1	29.87±11.33	Danforth^{M}
299	pg1115	0.13104	14.0±0.1	39.40±6.13	Danforth^{M}
300	pg1115	0.15456	14.3±0.1	27.37±3.57	Danforth^{M}
301	pg1115	0.15467	14.7±0.0	26.50±2.00	Danforth^{1032}
302	pg1116	0.05900	13.5±0.2	20.00±4.00	Tilton
303	pg1116	0.05927	13.5±0.2	12.30±5.70	Tilton
304	pg1116	0.11895	13.6±0.2	78.90±17.40	Danforth^{1032}
305	pg1116	0.13852	13.8±0.1	33.87±4.00	Danforth^{M,*}
306	pg1116	0.16539	13.7±0.3	35.07±16.97	Danforth^{M}
307	pg1116	0.16554	13.9±0.1	20.70±3.20	Danforth^{M,*}
308	pg1116	0.16610	13.6±0.0	0.00±0.00	Tilton
309	pg1116	0.16686	13.5±0.0	0.00±0.00	Tilton
310	pg1116	0.17343	13.3±0.1	40.90±8.80	Danforth^{1032*}
311	pg1121	0.19245	13.4±0.1	17.10±7.70	Danforth^{1032}
312	pg1121	0.21986	14.3±0.0	43.00±2.60	Danforth^{M}
313	pg1211	0.00711	13.8±0.1	41.00±7.00	Tilton
314	pg1211	0.05117	14.3±0.1	53.00±9.50	Tilton
315	pg1211	0.06449	14.1±0.0	47.20±5.40	Tilton
316	pg1211	0.06491	13.7±0.1	26.60±5.10	Tilton
317	pg1216	0.12362	14.2±0.1	32.10±7.27	Danforth^{M,*}
318	pg1216	0.12389	14.1±0.1	32.43±8.73	Danforth^{M,*}
319	pg1216	0.12463	13.8±0.5	6.00±41.00	Tilton
320	pg1216	0.12485	14.2±0.1	60.00±9.03	Danforth^{M,*}
321	pg1216	0.13499	13.8±0.1	100.00±0.00	Danforth^{1032}
322	pg1216	0.26768	13.7±0.6	19.00±2.00	Tilton
323	pg1216	0.28199	13.8±0.2	47.17±11.20	Danforth^{M}
324	pg1216	0.28237	13.6±0.1	14.43±5.40	Danforth^{M}
325	pg1222	0.16715	13.5±0.2	5.00±0.00	Danforth^{M}
326	pg1222	0.22263	13.9±0.1	30.47±5.77	Danforth^{M}
327	pg1222	0.24184	14.2±0.2	30.10±7.80	Danforth^{M}
328	pg1222	0.24454	14.1±0.1	25.13±4.17	Danforth^{M}
329	pg1222	0.34686	13.6±0.2	30.17±10.03	Danforth^{M}
330	pg1222	0.34941	13.8±0.1	42.37±6.20	Danforth^{M}
331	pg1222	0.36375	13.6±0.1	32.13±6.67	Danforth^{M}

332	pg1222	0.37616	13.5±0.1	31.60±5.70	Danforth^{1032}
333	pg1222	0.37706	13.8±0.1	28.53±4.93	Danforth^{M}
334	pg1222	0.37730	13.5±0.1	29.83±8.23	Danforth^{M}
335	pg1222	0.37842	14.1±0.0	38.97±3.43	Danforth^{M}
336	pg1222	0.37869	13.4±0.1	19.37±6.13	Danforth^{M}
337	pg1222	0.39726	13.1±0.2	34.50±6.40	Danforth^{1032}
338	pg1222	0.40828	13.1±0.2	30.50±12.70	Danforth^{1032}
339	pg1222	0.42130	13.9±0.1	32.20±3.97	Danforth^{M}
340	pg1222	0.42308	14.0±0.0	18.77±1.97	Danforth^{M}
341	pg1259	0.00220	13.6±0.1	75.00±0.00	Tilton
342	pg1259	0.00762	13.3±0.1	24.00±16.00	Tilton
343	pg1259	0.02217	13.4±0.2	34.00±15.00	Tilton
344	pg1259	0.04606	13.9±0.1	39.00±12.00	Tilton
345	pg1259	0.04650	13.8±0.1	24.00±4.00	Tilton
346	pg1259	0.19576	13.7±0.1	21.90±3.57	Danforth^{M}
347	pg1259	0.21940	14.1±0.0	38.30±2.60	Danforth^{M,*}
348	pg1259	0.21953	13.6±0.1	14.20±2.00	Tilton
349	pg1259	0.22313	13.6±0.1	50.50±17.50	Tilton
350	pg1259	0.23284	13.5±0.1	17.00±8.00	Tilton
351	pg1259	0.23956	13.4±0.1	24.00±7.20	Danforth^{1032}
352	pg1259	0.25973	13.8±0.1	52.70±7.60	Danforth^{1032*}
353	pg1259	0.31979	13.3±0.1	17.67±6.13	Danforth^{M,*}
354	pg1259	0.32472	13.3±0.1	14.00±8.00	Tilton
355	pg1307	0.14187	13.9±0.1	42.03±12.67	Danforth^{M}
356	pg1307	0.14214	13.8±0.1	15.90±5.07	Danforth^{M}
357	pg1309	0.17586	14.4±0.1	30.50±2.27	Danforth^{M}
358	pg1309	0.17745	15.2±0.0	100.00±0.00	Danforth^{1038}
359	pg1309	0.17866	15.9±0.0	100.00±0.00	Danforth^{1038}
360	pg1309	0.17930	15.5±0.0	99.60±8.20	Danforth^{1038}
361	pg1309	0.17979	15.2±0.0	73.60±7.20	Danforth^{1038}
362	pg1309	0.18069	15.2±0.0	74.20±3.50	Danforth^{1038}
363	pg1309	0.18117	15.1±0.0	100.00±0.00	Danforth^{1032}
364	pg1309	0.18139	14.9±0.0	60.00±5.30	Danforth^{1038}
365	pg1309	0.18145	14.8±0.0	100.00±0.00	Danforth^{1038}
366	pg1309	0.18192	14.3±0.0	69.60±5.60	Danforth^{1032}
367	pg1309	0.18698	14.0±2.5	28.00±9.90	Danforth^{1038}
368	pg1424	0.12120	14.0±0.2	41.30±23.90	Danforth^{1032}
369	pg1424	0.12152	14.4±0.1	32.17±4.43	Danforth^{M}

370	pg1424	0.14689	13.9±0.2	48.13±19.27	Danforth^{M}
371	pg1424	0.14712	13.7±0.2	16.20±9.30	Danforth^{1032}
372	pg1424	0.33947	13.5±0.1	18.20±8.27	Danforth^{M}
373	pg1424	0.33988	13.6±0.1	13.77±4.37	Danforth^{M}
374	pg1424	0.38633	13.8±0.1	33.53±10.60	Danforth^{M}
375	pg1424	0.38662	14.1±0.0	24.13±1.90	Danforth^{M}
376	pg1424	0.42884	13.1±0.1	7.10±9.80	Danforth^{1032}
377	pg1424	0.60369	13.4±0.1	10.10±5.60	Danforth^{1032}
378	pg1444	0.22031	13.9±0.1	49.00±2.00	Tilton
379	pg1444	0.22676	13.3±0.1	27.00±5.00	Tilton
380	pg1444	0.26690	13.8±0.0	11.50±1.00	Tilton
381	pg1444	0.26728	13.5±0.1	14.90±3.80	Tilton
382	pg1444	0.26738	13.9±0.1	8.40±1.30	Tilton
383	pg1444	0.26747	13.5±0.1	11.90±2.90	Tilton
384	pg1626	0.13075	13.3±0.2	31.40±11.10	Danforth^{1032}
385	phl1811	0.07344	13.0±0.0	0.00±0.00	Tilton
386	phl1811	0.07768	13.6±0.1	31.00±16.00	Tilton
387	phl1811	0.08131	13.9±0.2	7.90±5.20	Tilton
388	phl1811	0.13239	13.9±0.1	59.27±10.23	Danforth^{M,*}
389	phl1811	0.13282	13.6±0.1	21.07±5.73	Danforth^{M,*}
390	phl1811	0.13318	13.7±0.1	37.63±5.97	Danforth^{M,*}
391	phl1811	0.13545	13.5±0.2	32.80±11.30	Danforth^{1038}
392	phl1811	0.15752	13.5±0.1	37.03±10.37	Danforth^{M}
393	phl1811	0.15786	13.6±0.1	29.03±5.83	Danforth^{M,*}
394	phl1811	0.17652	14.1±0.0	18.10±2.20	Danforth^{1038*}
395	phl1811	0.19157	13.5±0.1	23.37±5.17	Danforth^{M,*}
396	phl1811	0.19194	14.7±0.0	34.87±1.70	Danforth^{M,*}
397	phl1811	0.19220	13.6±0.2	30.30±17.47	Danforth^{M,*}
398	phl2525	0.20154	14.1±0.0	19.40±2.13	Danforth^{M}
399	phl2525	0.20207	13.6±0.1	19.13±4.60	Danforth^{M}
400	phl2525	0.20605	14.0±0.1	39.73±6.70	Danforth^{M}
401	pks0312	0.20188	13.8±0.1	40.00±0.00	Tilton
402	pks0312	0.20275	14.9±0.1	65.40±1.30	Tilton
403	pks0405	0.09192	13.8±0.0	25.00±10.00	Tilton
404	pks0405	0.09647	13.7±0.3	31.30±7.60	Danforth^{1038*}
405	pks0405	0.14808	13.7±0.0	85.07±1.67	Danforth^{M}
406	pks0405	0.16566	13.0±0.2	7.90±8.10	Danforth^{1038}
407	pks0405	0.16606	14.1±0.0	74.20±3.20	Danforth^{1032*}

408	pks0405	0.16659	13.9±0.1	31.20±4.70	Danforth^{M}
409	pks0405	0.16688	14.2±0.1	40.33±8.93	Danforth^{M}
410	pks0405	0.16712	14.4±0.1	36.90±3.03	Danforth^{M,*}
411	pks0405	0.18257	13.7±2.0	34.70±4.97	Danforth^{M,*}
412	pks0405	0.18289	13.8±0.6	18.53±1.47	Danforth^{M,*}
413	pks0405	0.24052	13.5±0.1	33.60±4.30	Danforth^{M}
414	pks0405	0.24094	13.0±0.1	26.00±7.80	Danforth^{1032}
415	pks0405	0.24547	12.7±0.2	8.40±7.70	Danforth^{1032}
416	pks0405	0.29762	13.6±0.1	66.87±6.50	Danforth^{M}
417	pks0405	0.34188	13.5±0.0	37.30±3.50	Danforth^{1032}
418	pks0405	0.34225	13.3±0.0	24.00±3.40	Danforth^{1032}
419	pks0405	0.35092	13.3±0.2	35.00±7.00	Tilton
420	pks0405	0.36075	13.2±0.0	29.60±4.30	Danforth^{1032*}
421	pks0405	0.36151	13.9±0.0	32.17±1.43	Danforth^{M,*}
422	pks0405	0.36329	13.5±0.0	17.97±1.67	Danforth^{M,*}
423	pks0405	0.40570	13.6±0.0	0.00±0.00	Tilton
424	pks0405	0.40890	13.2±0.1	36.93±6.70	Danforth^{M}
425	pks0405	0.49505	14.3±0.0	32.50±2.53	Danforth^{M,*}
426	pks0405	0.49530	13.8±0.1	15.97±2.63	Danforth^{M,*}
427	pks0405	0.55506	14.0±0.1	27.90±3.13	Danforth^{M}
428	pks0552	0.11067	13.9±0.1	33.60±12.30	Danforth^{1038}
429	pks0552	0.14861	13.6±0.1	13.50±5.50	Danforth^{1032}
430	pks0552	0.14893	13.8±0.1	45.80±11.50	Danforth^{1032}
431	pks0552	0.18726	13.7±0.1	31.40±9.30	Danforth^{1032}
432	pks0552	0.25380	13.5±1.6	25.17±7.50	Danforth^{M}
433	pks0552	0.27850	13.7±0.1	100.00±0.00	Danforth^{1032}
434	pks0552	0.28570	13.8±0.1	28.40±4.63	Danforth^{M}
435	pks0552	0.34489	13.1±0.2	27.30±8.10	Danforth^{1032}
436	pks0552	0.37621	13.6±0.1	43.90±10.17	Danforth^{M}
437	pks0552	0.37655	13.6±0.1	25.20±4.93	Danforth^{M}
438	pks0552	0.37974	13.1±0.1	24.50±8.30	Danforth^{1032}
439	pks0552	0.39346	13.3±0.1	21.30±6.50	Danforth^{1032}
440	pks0552	0.42511	13.2±0.2	25.40±12.60	Danforth^{1032}
441	pks0552	0.44610	13.6±0.1	24.83±6.53	Danforth^{M}
442	pks0552	0.59449	13.4±0.1	10.20±4.60	Danforth^{1032}
443	pks0552	0.63163	13.8±0.1	8.83±3.73	Danforth^{M}
444	pks0552	0.63186	13.9±0.1	14.10±3.10	Danforth^{M}
445	pks0637	0.12291	14.1±0.1	43.87±5.67	Danforth^{M}

446	pks0637	0.14420	13.8±0.1	29.30±10.30	Danforth^{1038}
447	pks0637	0.16107	14.1±0.1	52.77±7.50	Danforth^{M}
448	pks0637	0.20475	13.6±0.2	48.57±15.07	Danforth^{M}
449	pks0637	0.24873	14.0±0.1	62.50±13.40	Danforth^{1038}
450	pks0637	0.30079	13.8±0.1	25.77±7.70	Danforth^{M}
451	pks0637	0.30107	14.0±0.0	26.20±2.80	Danforth^{1032}
452	pks0637	0.38642	13.8±0.1	28.77±3.97	Danforth^{M}
453	pks0637	0.40897	13.8±0.1	60.60±18.20	Danforth^{1038}
454	pks0637	0.41753	14.2±0.0	45.33±4.60	Danforth^{M}
455	pks0637	0.45294	13.7±0.1	36.10±11.60	Danforth^{M}
456	pks0637	0.46848	13.9±0.1	55.10±11.30	Danforth^{M}
457	pks1302	0.04225	14.4±0.1	54.00±3.00	Tilton
458	pks1302	0.06474	13.7±0.2	42.00±0.00	Tilton
459	pks1302	0.09486	13.9±0.2	61.60±17.80	Tilton
460	pks1302	0.09891	14.0±0.1	54.00±4.00	Tilton
461	pks1302	0.14518	13.8±0.1	31.67±6.33	Danforth^{M,*}
462	pks1302	0.14552	13.4±0.1	23.10±8.80	Danforth^{1032*}
463	pks1302	0.20438	13.6±0.1	38.00±3.80	Tilton
464	pks1302	0.22563	13.9±0.1	33.13±4.67	Danforth^{M,*}
465	pks1302	0.22743	13.5±0.1	10.37±3.50	Danforth^{M,*}
466	pks1302	0.25288	12.9±0.2	8.00±3.00	Tilton
467	pks1302	0.25299	13.4±0.3	30.90±10.80	Danforth^{1032}
468	pks2005	0.06490	13.6±0.1	30.70±0.00	Tilton
469	pks2155	0.05405	13.6±0.1	14.00±6.00	Tilton
470	pks2155	0.05707	13.6±0.1	24.00±7.00	Tilton
471	pmn2345	0.19957	14.4±0.1	53.00±6.90	Danforth^{1038}
472	pmn2345	0.37816	13.5±0.2	57.80±16.20	Danforth^{1032}
473	pmn2345	0.39704	13.7±0.2	48.10±9.10	Danforth^{1032}
474	pmn2345	0.42744	14.0±0.1	16.27±3.57	Danforth^{M}
475	pmn2345	0.43053	13.8±0.1	23.73±6.77	Danforth^{M}
476	pmn2345	0.43755	13.7±0.2	33.37±9.23	Danforth^{M}
477	pmn2345	0.51360	14.0±0.1	22.90±5.37	Danforth^{M}
478	pmn2345	0.53517	13.5±0.2	11.20±7.80	Danforth^{1032}
479	pmn2345	0.59970	14.0±0.2	42.00±7.90	Danforth^{1032}
480	pmn2345	0.61135	13.5±0.1	10.00±6.90	Danforth^{1032}
481	pmn2345	0.61155	13.8±0.2	20.00±6.30	Danforth^{1038}
482	pmn2345	0.61196	14.4±0.1	47.70±5.53	Danforth^{M}
483	q0045	0.11052	13.8±0.2	45.47±9.40	Danforth^{M}

484	q0045	0.13521	15.0±0.0	32.67±0.93	Danforth^{M}
485	q1230	0.09518	14.5±0.0	100.00±0.00	Danforth^{1038}
486	q1230	0.10318	13.4±0.2	100.00±0.00	Danforth^{1032}
487	q1230	0.10445	13.4±0.1	15.30±5.50	Danforth^{1032}
488	q1230	0.10530	15.1±0.0	89.83±2.30	Danforth^{M,*}
489	q1230	0.10596	15.1±0.0	100.00±0.00	Danforth^{M,*}
490	q1230	0.10666	15.0±0.0	76.87±2.30	Danforth^{M,*}
491	q1230	0.10809	14.1±0.1	34.93±3.93	Danforth^{M}
492	q1230	0.10820	14.6±0.1	78.10±10.90	Danforth^{1032}
493	q1230	0.10861	14.6±0.0	100.00±0.00	Danforth^{M}
494	q1230	0.10906	15.0±0.0	100.00±0.00	Danforth^{1032}
495	q1230	0.10935	15.5±0.0	100.00±0.00	Danforth^{1038}
496	q1230	0.10956	15.1±0.0	100.00±0.00	Danforth^{1032}
497	q1230	0.11707	15.2±0.0	48.67±1.20	Danforth^{M}
498	q1230	0.11743	14.8±0.0	22.70±1.37	Danforth^{M}
499	q1230	0.11781	15.0±0.0	41.10±0.93	Danforth^{M}
500	rbs1892	0.15752	14.3±0.0	46.13±4.50	Danforth^{M}
501	rbs1892	0.17133	13.7±0.1	41.00±10.20	Danforth^{1032}
502	rbs1892	0.19874	13.7±0.1	9.07±2.80	Danforth^{M}
503	rbs542	0.10323	15.5±0.0	62.60±0.87	Danforth^{M}
504	rbs542	0.10379	14.7±0.0	29.17±0.57	Danforth^{M}
505	rxj0439	0.11547	14.1±0.1	35.87±8.73	Danforth^{M}
506	rxj0439	0.21833	13.5±0.1	11.80±5.70	Danforth^{1032}
507	rxj0439	0.24235	14.3±0.1	26.13±6.03	Danforth^{M}
508	rxj0439	0.24258	14.3±0.1	15.23±3.70	Danforth^{M}
509	rxj0439	0.24313	14.7±0.0	43.03±3.53	Danforth^{M}
510	rxj0439	0.24387	13.9±0.1	40.00±8.93	Danforth^{M}
511	rxj2154	0.15689	13.8±0.1	33.53±6.00	Danforth^{M}
512	rxj2154	0.15862	13.6±0.1	33.13±10.50	Danforth^{M}
513	rxj2154	0.15889	13.7±0.1	9.23±3.93	Danforth^{M}
514	s080908	0.12865	14.1±0.1	90.60±8.87	Danforth^{M}
515	s080908	0.30757	14.5±0.0	32.77±2.60	Danforth^{M}
516	s080908	0.32236	14.3±0.5	7.30±3.30	Danforth^{1032}
517	s080908	0.37184	13.9±0.1	23.27±4.77	Danforth^{M}
518	s080908	0.40733	13.7±0.1	17.87±9.63	Danforth^{M}
519	s080908	0.40764	14.0±0.1	30.40±9.97	Danforth^{M}
520	s080908	0.41759	14.1±0.1	49.23±7.50	Danforth^{M}
521	s080908	0.51541	13.8±0.1	48.00±18.40	Danforth^{1032}

522	s080908	0.60328	13.8±0.2	18.80±5.07	Danforth^{M}
523	s080908	0.61912	14.9±0.0	43.30±3.30	Danforth^{1038}
524	s080908	0.65652	16.5±0.3	28.83±3.17	Danforth^{M}
525	s080908	0.65727	14.4±0.2	13.30±3.10	Danforth^{1032}
526	s080908	0.65745	14.2±0.1	23.90±6.10	Danforth^{1038}
527	s080908	0.65761	16.4±9.6	6.50±13.70	Danforth^{1038}
528	s09255b	0.29645	14.5±0.0	34.17±2.73	Danforth^{M}
529	s09255b	0.30927	13.7±0.2	29.53±11.47	Danforth^{M}
530	s092909	0.14489	13.9±0.1	100.00±0.00	Danforth^{1032}
531	s092909	0.16671	14.2±0.1	49.83±7.47	Danforth^{M}
532	s094952	0.16442	13.6±0.1	26.60±12.20	Danforth^{1032}
533	s094952	0.35167	14.0±0.1	40.20±8.47	Danforth^{M}
534	s094952	0.36551	14.3±0.1	41.07±6.13	Danforth^{M}
535	s094952	0.36580	14.0±0.1	43.60±11.40	Danforth^{M}
536	s135712	0.09753	14.5±0.1	61.20±13.50	Danforth^{1038}
537	s135712	0.14701	14.5±0.0	65.90±3.60	Danforth^{1032}
538	s50716	0.23145	13.8±0.0	14.00±2.03	Danforth^{M}
539	sbs1108	0.16559	14.2±0.0	23.20±1.40	Danforth^{1032}
540	sbs1108	0.32014	13.7±0.1	12.60±4.30	Danforth^{1032}
541	sbs1108	0.33424	13.7±0.1	100.00±0.00	Danforth^{1032}
542	sbs1108	0.33522	13.9±0.1	49.00±9.47	Danforth^{M}
543	sbs1108	0.34523	13.8±0.1	23.97±4.70	Danforth^{M}
544	sbs1108	0.43579	13.8±0.1	17.00±4.63	Danforth^{M}
545	sbs1108	0.46320	13.8±0.2	45.80±13.80	Danforth^{M}
546	sbs1108	0.46846	13.8±0.1	22.93±6.17	Danforth^{M}
547	sbs1108	0.48712	13.8±0.1	27.17±4.63	Danforth^{M}
548	sbs1108	0.61764	13.7±0.1	22.80±8.20	Danforth^{1032}
549	sbs1122	0.15545	14.1±0.1	44.30±7.17	Danforth^{M}
550	sbs1122	0.19439	13.9±0.1	27.40±7.17	Danforth^{M}
551	sbs1122	0.21209	14.0±0.1	29.80±8.00	Danforth^{1032}
552	sbs1122	0.25712	14.5±0.0	29.10±2.70	Danforth^{1032}
553	sbs1122	0.31236	14.4±0.0	32.87±4.33	Danforth^{M}
554	sbs1122	0.31274	14.0±0.1	25.33±6.07	Danforth^{M}
555	sbs1122	0.42009	13.9±0.1	28.70±4.70	Danforth^{1032}
556	sbs1122	0.57049	13.9±0.1	24.40±6.50	Danforth^{M}
557	ton236	0.19452	14.1±0.1	69.13±4.07	Danforth^{M}
558	ton236	0.21887	13.9±0.1	67.30±12.70	Danforth^{1032}
559	ton236	0.21919	13.8±0.3	38.90±14.20	Danforth^{1038}

560	ton236	0.25876	13.7±0.1	5.00±0.00	Danforth^{1032}
561	ton236	0.25896	13.6±0.1	7.30±5.50	Danforth^{1032}
562	ton236	0.39942	13.8±0.1	100.00±0.00	Danforth^{1032}
563	ton236	0.43738	14.3±0.0	33.13±2.40	Danforth^{M}
564	ton236	0.44804	13.2±0.1	16.60±7.80	Danforth^{1032}
565	ton28	0.13746	14.2±0.3	18.20±7.90	Tilton
566	ton28	0.13781	13.8±0.2	13.60±7.50	Tilton
567	ton28	0.17251	13.7±0.1	26.00±8.00	Tilton
568	ton28	0.24292	13.2±0.2	11.00±5.00	Tilton
569	ton28	0.24859	13.1±0.2	13.00±5.00	Tilton
570	ton28	0.27338	13.3±0.1	20.00±3.70	Tilton
571	ton28	0.33021	14.2±0.0	9.90±0.70	Tilton
572	ton580	0.20258	13.4±0.1	20.90±8.30	Danforth^{1032}
573	ton580	0.29171	13.2±0.1	12.00±6.40	Danforth^{1032}
574	tons180	0.02340	13.5±0.1	30.00±0.00	Tilton
575	tons180	0.04360	13.4±0.0	40.00±0.00	Tilton
576	tons180	0.04560	13.7±0.1	33.30±0.00	Tilton

Table A.2: H I BLA FUV prior detections table, adapted from the results of [21] ("Danforth") and [65] ("Tilton"). A '*' indicates a duplicate redshift in both Danforth and Tilton. The corresponding Tilton duplicates are omitted from the table.

#	Name	Redshift	$\log N$ (cm^{-2})	b (km s^{-1})	Source
1	1es1028	0.13714	13.3±0.1	91.60±24.00	Danforth
2	1es1028	0.20383	13.2±0.1	63.60±14.20	Danforth
3	1es1028	0.22121	13.4±0.8	68.60±71.40	Danforth
4	1es1553	0.03466	13.1±0.0	72.00±9.40	Danforth
5	1es1553	0.04273	13.4±0.0	63.00±4.50	Danforth
6	1es1553	0.06364	13.0±0.2	76.30±19.90	Danforth
7	1es1553	0.21869	12.7±0.1	62.60±21.80	Danforth
8	3c249	0.13470	13.1±0.1	65.00±2.00	Tilton
9	3c249	0.26664	13.3±0.1	67.00±19.00	Tilton
10	3c263	0.06003	13.0±0.1	71.30±21.70	Danforth
11	3c263	0.14073	13.5±0.1	83.70±11.70	Danforth
12	3c263	0.26322	12.9±0.1	61.00±17.40	Danforth
13	3c263	0.31025	13.1±0.1	81.90±19.80	Danforth
14	3c263	0.37740	13.4±0.1	85.80±11.30	Danforth
15	3c273	0.00758	13.0±0.0	74.40±8.60	Danforth

16	3c273	0.06707	12.6±0.1	73.60±27.60	Danforth
17	3c273	0.07359	12.8±0.1	99.70±18.00	Danforth
18	3c273	0.13960	12.6±0.1	64.90±8.70	Danforth
19	3c351	0.06008	13.2±0.1	67.00±8.00	Tilton
20	3c351	0.06592	13.9±0.0	118.20±5.60	Tilton
21	3c351	0.18191	13.4±0.1	106.00±4.00	Tilton
22	3c57	0.19558	13.2±0.1	71.30±12.00	Danforth
23	3c57	0.25994	13.3±0.1	150.00±0.00	Danforth
24	3c57	0.37357	13.7±0.0	62.00±6.70	Danforth
25	3c57	0.44937	13.6±0.1	64.90±13.90	Danforth
26	3c66a	0.08850	13.4±0.1	100.00±0.00	Danforth
27	b0117	0.14156	13.7±0.0	69.10±5.40	Danforth
28	b0117	0.16029	13.0±0.1	95.60±29.50	Danforth
29	f1010	0.01614	13.2±0.1	88.30±31.00	Danforth
30	h1821	0.00944	13.0±0.0	61.20±6.90	Danforth
31	h1821	0.06779	12.7±0.1	87.50±20.80	Danforth
32	h1821	0.08483	12.9±0.1	80.60±17.30	Danforth
33	h1821	0.12147	13.8±0.1	77.00±5.00	Tilton
34	h1821	0.19817	12.9±0.1	71.50±11.60	Danforth
35	h1821	0.21321	13.6±0.1	100.00±0.00	Danforth
36	h1821	0.24531	13.2±0.1	72.00±22.50	Danforth
37	h2356	0.03830	13.3±0.1	92.40±20.00	Danforth
38	h2356	0.07881	13.4±0.2	99.80±34.30	Danforth
39	h2356	0.10467	13.5±0.1	71.90±10.80	Danforth
40	h2356	0.15613	13.6±0.1	61.00±15.40	Danforth
41	he0153	0.11318	13.7±0.0	69.60±3.70	Danforth
42	he0153	0.17060	13.7±0.0	100.00±0.00	Danforth
43	he0226	0.14274	12.8±0.1	63.50±13.20	Danforth
44	he0226	0.39890	13.6±0.1	84.00±27.00	Tilton
45	he0226	0.41024	13.3±0.1	69.40±12.10	Danforth
46	he0238	0.10641	13.3±0.1	60.50±6.20	Danforth
47	he0238	0.14922	13.1±0.1	75.20±22.00	Danforth
48	he0238	0.18747	13.1±0.0	62.60±7.90	Danforth
49	he0238	0.27913	13.4±0.0	62.10±7.30	Danforth
50	he0238	0.33435	13.7±0.0	61.30±4.20	Danforth
51	he0435	0.00549	14.0±0.1	67.50±15.90	Danforth
52	he0435	0.09037	13.4±0.2	98.20±21.50	Danforth
53	he0435	0.15328	13.3±0.1	71.50±18.50	Danforth

54	he0435	0.16107	13.5±0.1	66.10±9.50	Danforth
55	he0435	0.39044	13.9±0.1	62.70±7.90	Danforth
56	he0435	0.40988	13.6±0.1	100.00±0.00	Danforth
57	he0435	0.42218	13.7±0.0	71.80±6.70	Danforth
58	hs0624	0.05515	13.7±0.2	84.00±30.70	Tilton
59	hs0624	0.09005	13.5±0.0	122.00±3.00	Tilton
60	hs0624	0.31045	13.4±0.3	62.00±40.30	Tilton
61	hs1102	0.09533	13.2±0.1	76.50±23.20	Danforth
62	hs1102	0.18746	13.0±0.2	67.70±29.20	Danforth
63	hs1102	0.21101	13.6±0.1	130.80±28.00	Danforth
64	hs1102	0.21762	13.7±0.0	114.80±9.40	Danforth
65	hs1102	0.25125	13.6±0.1	108.40±23.40	Danforth
66	hs1102	0.25365	13.4±0.1	100.00±0.00	Danforth
67	hs1102	0.25794	13.5±0.1	150.00±0.00	Danforth
68	hs1102	0.25867	13.8±0.2	84.10±27.20	Danforth
69	hs1102	0.28713	13.2±0.1	63.00±17.30	Danforth
70	hs1102	0.40856	13.5±0.1	100.00±0.00	Danforth
71	hs1102	0.40970	13.7±0.2	100.00±0.00	Danforth
72	hs1102	0.41874	13.7±0.7	130.60±54.40	Danforth
73	hs1102	0.42280	14.2±0.0	65.90±4.00	Danforth
74	hs1102	0.46827	13.8±0.0	81.10±2.00	Danforth
75	i06229	0.01218	13.1±0.1	100.00±0.00	Danforth
76	i06229	0.05260	13.3±0.1	76.00±17.50	Danforth
77	i22456	0.00443	12.8±0.1	75.70±15.40	Danforth
78	i22456	0.09941	14.6±0.0	62.80±0.60	Danforth
79	mr2251	0.01068	14.6±0.7	69.00±4.00	Tilton
80	mr2251	0.01449	12.9±0.1	78.90±18.20	Danforth
81	mr2251	0.06131	13.2±0.0	64.50±2.90	Danforth
82	mr2251	0.06190	14.0±0.0	79.20±0.90	Danforth
83	mr2251	0.06276	14.3±0.0	100.00±0.00	Danforth
84	mr2251	0.06327	14.2±0.0	98.90±3.40	Danforth
85	mr2251	0.06381	13.8±0.0	69.70±2.20	Danforth
86	mrk106	0.06330	13.0±0.1	64.70±18.70	Danforth
87	mrk106	0.07672	13.2±0.1	72.50±19.80	Danforth
88	mrk478	0.06166	13.2±0.1	97.00±19.70	Danforth
89	mrk478	0.06578	13.0±0.1	64.20±22.30	Danforth
90	mrk478	0.07213	13.3±0.0	100.00±0.00	Danforth
91	mrk876	0.01159	13.2±0.1	84.90±10.10	Danforth

92	mrk876	0.05598	12.8±0.1	79.60±18.90	Danforth
93	mrk876	0.08709	12.3±0.2	68.20±35.10	Danforth
94	mrk876	0.08858	13.6±0.0	70.30±2.70	Danforth
95	mrk876	0.08917	12.9±0.1	100.00±0.00	Danforth
96	mrk876	0.11487	13.2±0.1	74.00±6.00	Tilton
97	ngc7469	0.00981	13.5±0.1	132.70±27.60	Tilton
98	pg0003	0.08299	13.8±0.0	64.40±6.40	Danforth
99	pg0003	0.17139	12.9±0.1	102.90±29.10	Danforth
100	pg0003	0.22541	13.1±0.1	92.80±18.60	Danforth
101	pg0003	0.38633	13.5±0.2	86.70±32.30	Danforth
102	pg0003	0.42051	13.4±0.1	63.90±9.30	Danforth
103	pg0804	0.05015	12.8±0.1	69.80±14.60	Danforth
104	pg0804	0.05576	12.8±10.0	64.20±99.90	Danforth
105	pg0804	0.36379	12.5±0.3	63.20±8.20	Danforth
106	pg0832	0.01753	15.6±0.2	87.30±5.40	Danforth
107	pg0832	0.02793	13.6±0.2	65.90±18.50	Danforth
108	pg0832	0.08748	13.4±0.1	116.70±31.70	Danforth
109	pg0832	0.10171	13.9±0.1	60.90±8.00	Danforth
110	pg0832	0.18391	13.3±0.1	130.50±38.30	Danforth
111	pg0832	0.27503	13.6±0.1	60.60±12.50	Danforth
112	pg0832	0.27694	13.6±0.1	150.00±0.00	Danforth
113	pg0832	0.32572	13.3±0.1	60.20±11.10	Danforth
114	pg0838	0.06583	13.3±0.1	81.20±14.30	Danforth
115	pg0838	0.08628	13.1±0.2	148.80±42.90	Danforth
116	pg0838	0.12676	13.1±0.1	91.90±13.20	Danforth
117	pg0953	0.16319	13.0±0.1	74.90±10.00	Danforth
118	pg0953	0.19221	13.3±0.1	63.80±14.60	Tilton
119	pg1001	0.00165	13.9±1.3	60.60±51.80	Danforth
120	pg1001	0.21343	13.9±0.0	100.00±0.00	Danforth
121	pg1048	0.00642	14.0±0.1	86.90±8.90	Danforth
122	pg1048	0.02414	13.2±0.1	66.70±13.00	Danforth
123	pg1049	0.03015	13.4±0.1	100.00±0.00	Danforth
124	pg1049	0.06313	13.6±0.1	86.30±13.20	Danforth
125	pg1049	0.12706	13.6±0.1	63.30±9.70	Danforth
126	pg1049	0.14980	13.3±0.1	72.00±10.50	Danforth
127	pg1049	0.16322	13.2±0.2	100.00±0.00	Danforth
128	pg1049	0.32523	13.3±0.1	105.90±32.00	Danforth
129	pg1049	0.34016	13.5±0.1	100.00±0.00	Danforth

130	pg1049	0.34187	14.1±0.0	64.30±4.00	Danforth
131	pg1115	0.09511	13.2±0.1	68.30±12.50	Danforth
132	pg1115	0.12059	13.0±0.1	73.50±20.20	Danforth
133	pg1115	0.12741	13.2±0.1	100.00±0.00	Danforth
134	pg1116	0.04114	13.2±0.0	69.50±8.40	Danforth*
135	pg1116	0.06251	13.1±0.0	71.20±5.70	Tilton
136	pg1116	0.08382	13.2±0.1	63.80±13.80	Danforth
137	pg1116	0.09210	12.8±0.1	68.80±22.30	Danforth
138	pg1116	0.09281	13.1±0.1	77.40±11.90	Danforth*
139	pg1116	0.13373	13.2±0.0	81.30±6.00	Tilton
140	pg1116	0.13851	13.5±0.2	80.80±16.20	Danforth
141	pg1121	0.00791	13.3±0.1	99.00±25.00	Danforth
142	pg1121	0.07727	13.5±0.1	60.90±13.30	Danforth
143	pg1121	0.18078	13.5±0.1	150.00±0.00	Danforth
144	pg1121	0.18869	13.1±0.1	70.40±20.40	Danforth
145	pg1121	0.21814	12.9±0.1	69.50±22.70	Danforth
146	pg1121	0.21992	13.9±0.0	80.70±2.20	Danforth
147	pg1211	0.02586	13.5±0.0	70.00±2.00	Tilton
148	pg1211	0.05443	13.2±0.0	98.00±1.00	Tilton
149	pg1216	0.00842	13.4±0.1	100.00±0.00	Danforth
150	pg1216	0.07969	13.2±0.1	66.80±14.50	Danforth
151	pg1216	0.12372	14.8±0.1	70.80±3.40	Tilton
152	pg1216	0.12473	14.7±0.1	73.60±3.50	Tilton
153	pg1216	0.17950	13.2±0.1	64.80±11.10	Danforth
154	pg1216	0.20014	13.6±0.0	60.60±6.90	Danforth
155	pg1216	0.21258	13.0±0.1	60.50±19.80	Danforth
156	pg1216	0.28204	13.9±1.2	78.60±22.50	Danforth
157	pg1222	0.15554	13.9±0.0	64.70±3.00	Danforth
158	pg1222	0.24198	13.6±0.1	91.40±12.50	Danforth
159	pg1222	0.26075	12.9±0.1	60.20±17.70	Danforth
160	pg1222	0.32786	13.2±0.1	84.70±28.00	Danforth
161	pg1222	0.36749	13.7±0.0	96.20±10.60	Danforth
162	pg1222	0.37471	13.8±0.1	100.00±0.00	Danforth
163	pg1222	0.37721	13.6±0.1	72.80±17.20	Danforth
164	pg1222	0.37840	13.5±1.4	61.40±67.10	Danforth
165	pg1229	0.05018	12.9±0.1	61.90±19.80	Danforth
166	pg1259	0.05563	13.4±0.0	70.70±5.90	Danforth
167	pg1259	0.15136	13.3±0.1	62.20±3.70	Tilton

168	pg1259	0.16647	13.3±0.1	93.30±8.90	Tilton
169	pg1259	0.17893	13.1±0.1	83.70±11.90	Tilton
170	pg1259	0.22376	13.0±0.1	76.50±17.90	Danforth
171	pg1259	0.24126	13.4±0.1	89.10±6.90	Tilton
172	pg1259	0.31974	14.0±0.0	70.30±3.10	Tilton
173	pg1259	0.36212	13.4±0.1	100.00±0.00	Danforth
174	pg1259	0.38254	13.5±0.0	82.20±8.90	Danforth
175	pg1259	0.38266	13.7±0.1	137.00±19.00	Tilton
176	pg1307	0.08345	13.4±0.1	84.60±7.10	Danforth
177	pg1309	0.03861	13.4±0.1	62.70±12.10	Danforth
178	pg1309	0.17740	13.9±0.0	65.10±5.30	Danforth
179	pg1309	0.17852	14.5±0.1	150.00±0.00	Danforth
180	pg1309	0.17918	14.4±0.0	128.90±8.10	Danforth
181	pg1309	0.18143	13.9±0.0	94.90±9.90	Danforth
182	pg1424	0.01908	13.5±0.1	96.00±14.30	Danforth
183	pg1424	0.25044	13.0±0.1	74.40±22.10	Danforth
184	pg1424	0.36260	13.2±0.1	82.40±23.40	Danforth
185	pg1444	0.22031	13.5±0.0	76.00±7.60	Tilton
186	pg1626	0.06137	13.6±0.0	60.50±6.60	Danforth
187	phl1811	0.05143	13.7±0.0	72.80±5.10	Danforth
188	phl1811	0.05813	13.2±0.1	89.50±16.80	Danforth
189	phl1811	0.08085	13.9±0.1	91.80±11.60	Danforth
190	phl1811	0.08163	13.2±0.0	100.00±0.00	Danforth
191	phl1811	0.12003	13.0±0.1	77.40±16.90	Danforth
192	phl1811	0.15787	13.2±0.1	70.40±9.90	Danforth
193	phl2525	0.06548	13.2±0.1	100.00±0.00	Danforth
194	phl2525	0.06682	13.4±0.1	64.80±14.20	Danforth
195	phl2525	0.08351	13.4±0.1	66.70±16.90	Danforth
196	phl2525	0.14869	13.1±0.1	65.20±16.20	Danforth
197	phl2525	0.17002	13.3±0.1	116.00±42.10	Danforth
198	pks0312	0.11454	14.0±0.0	79.00±4.00	Tilton
199	pks0405	0.02510	13.2±0.1	144.30±26.50	Danforth
200	pks0405	0.05902	13.3±0.1	62.30±11.10	Tilton
201	pks0405	0.09719	13.6±0.0	100.00±0.00	Danforth
202	pks0405	0.10152	13.2±0.1	67.90±11.30	Tilton
203	pks0405	0.10298	13.4±0.1	73.70±12.00	Tilton
204	pks0405	0.19456	12.8±0.1	63.60±8.10	Danforth*
205	pks0405	0.21976	12.7±0.1	70.20±18.80	Danforth

206	pks0405	0.24564	13.1±0.1	77.40±14.80	Danforth
207	pks0405	0.29748	13.2±0.1	66.00±11.70	Danforth
208	pks0405	0.31016	12.9±0.1	76.70±20.20	Danforth
209	pks0405	0.32502	13.7±0.0	85.50±6.10	Tilton
210	pks0405	0.49508	14.3±0.0	64.90±7.70	Tilton
211	pks0552	0.26916	13.2±0.1	68.40±13.10	Danforth
212	pks0552	0.35661	13.3±0.1	64.70±9.50	Danforth
213	pks0558	0.10472	13.0±0.1	79.50±35.00	Danforth
214	pks0637	0.14272	13.1±0.1	77.90±13.80	Danforth
215	pks0637	0.16082	13.4±0.1	100.00±0.00	Danforth
216	pks0637	0.17428	13.0±0.1	72.20±16.30	Danforth
217	pks0637	0.36408	13.5±0.1	86.70±13.00	Danforth
218	pks0637	0.41784	13.7±0.1	100.00±0.00	Danforth
219	pks1302	0.01956	13.3±0.1	66.20±9.50	Danforth
220	pks1302	0.03281	13.1±0.1	62.80±14.60	Danforth
221	pks1302	0.14531	15.4±0.1	61.80±3.90	Tilton
222	pks1302	0.19281	13.6±0.1	68.90±14.10	Tilton
223	pks1302	0.23679	13.4±0.0	69.70±6.90	Danforth
224	pks1302	0.23752	13.0±0.1	74.70±26.90	Danforth
225	pks1302	0.24885	13.4±0.1	77.00±19.00	Tilton
226	pks1302	0.25120	13.7±0.0	71.40±4.10	Danforth
227	pks2155	0.05708	14.1±0.0	67.90±1.70	Danforth*
228	pks2155	0.06236	12.8±0.1	69.10±22.20	Danforth
229	pks2155	0.10586	13.5±0.0	66.00±4.00	Tilton
230	pmn2345	0.28405	13.5±0.1	81.80±13.80	Danforth
231	pmn2345	0.31540	13.7±0.0	60.10±7.30	Danforth
232	pmn2345	0.37828	14.3±0.0	65.70±2.90	Danforth
233	pmn2345	0.43000	13.5±0.1	63.00±18.10	Danforth
234	pmn2345	0.47074	13.6±0.0	87.10±3.10	Danforth
235	q0045	0.05590	13.2±0.1	66.80±12.80	Danforth
236	q0045	0.06377	13.0±0.1	70.60±23.20	Danforth
237	q1230	0.08344	13.3±0.0	65.00±6.00	Tilton
238	q1230	0.08540	12.8±0.1	94.60±26.80	Danforth
239	q1230	0.09444	13.0±0.1	69.70±10.10	Danforth
240	q1230	0.10000	13.2±0.1	61.00±8.00	Tilton
241	q1230	0.10525	14.0±0.1	75.00±4.00	Tilton
242	q1230	0.10549	14.1±0.0	87.30±3.30	Danforth
243	q1230	0.10566	14.0±0.1	121.70±28.60	Tilton

244	q1230	0.10612	13.4±0.1	76.40±15.40	Danforth
245	q1230	0.10639	13.8±0.0	64.30±3.40	Tilton
246	q1230	0.10660	13.5±0.1	61.90±4.00	Danforth
247	q1230	0.10853	12.8±0.1	92.60±21.50	Danforth
248	q1230	0.10940	13.8±0.0	100.00±0.00	Danforth
249	q1230	0.12103	13.5±0.0	69.40±3.60	Tilton
250	rbs144	0.04528	13.1±0.1	62.30±12.70	Danforth
251	rbs1892	0.15567	13.3±0.1	150.00±0.00	Danforth
252	rbs1892	0.15633	13.4±0.0	150.00±0.00	Danforth
253	rbs1892	0.16343	13.8±0.0	67.60±2.70	Danforth
254	rbs1892	0.17001	13.2±0.1	100.00±0.00	Danforth
255	rbs1892	0.17155	13.4±0.1	100.00±0.00	Danforth
256	rbs1892	0.17185	13.2±0.1	84.70±14.20	Danforth
257	rbs542	0.04455	12.9±0.0	70.80±7.80	Danforth
258	rbs542	0.04992	12.8±0.1	62.10±13.30	Danforth
259	rxj0439	0.00550	13.7±0.2	67.90±15.90	Danforth
260	rxj0439	0.17680	13.5±0.1	100.00±0.00	Danforth
261	rxj0956	0.03471	13.8±0.0	64.80±5.90	Danforth
262	rxj0956	0.06924	13.2±0.1	67.30±18.50	Danforth
263	rxj0956	0.10858	13.3±0.1	74.30±21.00	Danforth
264	rxj0956	0.12796	13.6±0.1	89.60±11.00	Danforth
265	rxj0956	0.14704	13.2±0.1	88.40±25.40	Danforth
266	rxj0956	0.15101	13.0±0.1	81.80±22.40	Danforth
267	rxj2154	0.23009	13.1±0.1	68.20±17.40	Danforth
268	s080908	0.05775	13.5±0.1	150.00±0.00	Danforth
269	s080908	0.06391	13.6±0.2	149.00±46.10	Danforth
270	s080908	0.14214	13.4±0.1	94.80±15.00	Danforth
271	s080908	0.16001	13.4±0.1	76.00±9.70	Danforth
272	s080908	0.38700	13.4±0.2	100.00±0.00	Danforth
273	s09255b	0.13118	13.4±0.1	86.70±12.00	Danforth
274	s092909	0.16491	13.8±0.0	63.60±5.70	Danforth
275	s092909	0.23508	13.5±0.0	83.10±8.20	Danforth
276	s094952	0.06581	13.4±0.1	90.00±28.60	Danforth
277	s094952	0.16442	13.4±1.0	63.40±55.70	Danforth
278	s135712	0.14702	14.0±0.0	79.90±1.90	Danforth
279	s50716	0.00989	13.1±0.1	61.90±12.90	Danforth
280	s50716	0.01766	13.1±0.1	89.50±13.60	Danforth
281	s50716	0.08834	13.1±0.1	150.00±0.00	Danforth

282	s50716	0.14936	12.9±0.1	150.00±0.00	Danforth
283	sbs1108	0.02497	13.8±0.0	79.40±3.10	Danforth
284	sbs1108	0.25715	13.7±0.0	61.40±6.50	Danforth
285	sbs1108	0.41402	13.6±0.1	81.20±18.30	Danforth
286	sbs1122	0.04709	13.3±0.1	62.00±13.00	Danforth
287	sbs1122	0.13699	13.3±0.2	77.60±32.70	Danforth
288	sbs1122	0.13812	13.6±0.1	100.00±0.00	Danforth
289	sbs1122	0.13865	13.8±0.1	150.00±0.00	Danforth
290	sbs1122	0.15271	13.5±0.2	74.50±23.30	Danforth
291	sbs1122	0.36707	13.7±0.1	82.90±13.80	Danforth
292	ton1187	0.01504	13.7±0.1	96.20±14.60	Danforth
293	ton1187	0.05216	13.5±0.2	61.20±9.80	Danforth
294	ton1187	0.07687	13.1±0.1	83.70±20.30	Danforth
295	ton28	0.03357	13.4±0.1	75.00±7.00	Tilton
296	tons180	0.04304	13.8±0.4	81.00±15.00	Tilton
297	tons210	0.06763	13.0±0.1	61.10±21.80	Danforth
298	tons210	0.08558	13.1±0.1	73.00±12.60	Danforth

Appendix B. Analysis Tables, *XMM-Newton*

Table B.1: O VII measurements with *XMM-Newton* data, at the prior redshift from the O VI lines from Table A.1. Column "%" reports the percent background level, $B/S+B$, where B is the background count rate, and S the source count rate. Entries with an asterisk sign indicate poor fits; entries that have a '$---$' sign indicate lines that fall in a region of reduced efficiency, and therefore they could not be constrained (see Sec. 3.2.2).

Target line		cmin	RGS1		RGS2		power–law		line component			ΔC
Name	z	(d.o.f.)	avg exp (s)	%	avg exp (s)	%	norm.	index	λ (Å)	τ_0	$\log N(\mathrm{cm}^{-2})$	(d.o.f.)
1es1028	0.12314 (#1)	95.40(79)	144787	10	147275	7	$1102\pm^{30}_{30}$	1.00	24.2598	$0.55\pm^{1.74}_{0.88}$	$15.24\pm^{0.44}_{nan}$	0.40
1es1028	0.13706 (#2)	92.82(90)	143804	9	146370	7	$1121\pm^{33}_{32}$	1.00	24.5605	$-0.31\pm^{0.85}_{0.56}$	$nan\pm^{nan}_{nan}$	0.22
1es1028	0.33735 (#3)	86.46(91)	145450	17	146420	22	$1324\pm^{48}_{46}$	1.00	28.8868	$-0.78\pm^{0.84}_{0.57}$	$nan\pm^{nan}_{nan}$	1.08
1es1553	0.18759 (#4)	102.10(88)	1793737	7	1757303	7	$1796\pm^{13}_{12}$	1.00	25.6519	$0.60\pm^{0.32}_{0.26}$	$15.27\pm^{0.15}_{0.21}$	7.82
1es1553	0.18775 (#5)	102.34(88)	1793737	7	1757303	7	$1796\pm^{13}_{12}$	1.00	25.6554	$0.57\pm^{0.30}_{0.25}$	$15.26\pm^{0.15}_{0.22}$	7.53
1es1553	0.18984 (#6)	105.72(86)	1794800	7	1753128	7	$1778\pm^{12}_{12}$	1.00	25.7005	$-0.05\pm^{0.17}_{0.23}$	$nan\pm^{nan}_{nan}$	0.16
1es1553	0.21631 (#7)	84.95(81)	1756247	7	1757203	8	$1778\pm^{14}_{14}$	1.00	26.2723	$0.19\pm^{0.25}_{0.22}$	$14.83\pm^{0.33}_{nan}$	0.95
1es1553	0.31130 (#8)	113.79(90)	1740303	11	1677696	14	$1807\pm^{15}_{15}$	1.00	28.3241	$-0.15\pm^{0.26}_{0.23}$	$nan\pm^{nan}_{nan}$	0.45
1es1553	0.37868 (#9)	119.25(98)	1809416	21	1817188	12	$1834\pm^{17}_{17}$	1.00	29.7795	$0.00\pm^{0.09}_{0.80}$	$13.08\pm^{1.43}_{nan}$	-0.04
1es1553	0.39497 (#10)	90.13(98)	1751580	21	1813451	12	$1810\pm^{18}_{18}$	1.00	30.1314	$0.02\pm^{0.38}_{0.24}$	$13.80\pm^{1.32}_{nan}$	0.02
3c249	0.24676 (#11)	78.14(93)	2639	31	2524	34	$282\pm^{141}_{104}$	1.00	26.9300	$-1.24\pm^{1.07E+12}_{28.76}$	$nan\pm^{nan}_{nan}$	0.03
3c249	0.30788 (#12)	81.25(88)	2639	20	2535	85	$697\pm^{234}_{175}$	1.00	28.2502	$9.81E+04\pm^{1.00E+20}_{9.82E+04}$	$16.21\pm^{0.25}_{nan}$	0.35
3c249	0.30809 (#13)	81.15(88)	2639	20	2535	85	$701\pm^{236}_{177}$	1.00	28.2547	$1.45E+07\pm^{1.00E+20}_{1.45E+07}$	$16.29\pm^{0.17}_{nan}$	0.47
3c249	0.31364 (#14)	78.36(88)	2639	20	2538	62	$758\pm^{250}_{193}$	1.00	28.3746	$9.44E+12\pm^{1.00E+20}_{9.44E+12}$	$16.41\pm^{0.05}_{inf}$	1.72
3c273	0.00337 (#15)	–	–	–	–	–	–	–	21.6728	–	–	–
3c273	0.00533 (#16)	–	–	–	–	–	–	–	21.7151	–	–	–
3c273	0.00764 (#17)	–	–	–	–	–	–	–	21.7650	–	–	–
3c273	0.02947 (#18*)	61.61(38)	995937	4	nan	nan	$4600\pm^{1762}_{886}$	0.84	22.2366	$-0.05\pm^{0.26}_{0.16}$	$nan\pm^{nan}_{nan}$	-0.00
3c273	0.04898 (#19)	63.63(45)	936604	4	nan	nan	$1268\pm^{345}_{291}$	3.02	22.6580	$0.14\pm^{0.30}_{0.17}$	$14.69\pm^{0.47}_{nan}$	0.84
3c273	0.06655 (#20*)	153.93(46)	912160	5	nan	nan	$1021\pm^{260}_{212}$	3.36	23.0375	$-0.60\pm^{0.18}_{0.17}$	$nan\pm^{nan}_{nan}$	10.40
3c273	0.09018 (#21*)	100.60(47)	996642	4	nan	nan	$931\pm^{250}_{186}$	3.57	23.5479	$2.95\pm^{0.87}_{0.66}$	$15.73\pm^{0.05}_{0.06}$	78.29
3c273	0.12007 (#22)	53.39(62)	1024121	4	1027398	3	$1102\pm^{252}_{235}$	3.32	24.1935	$0.23\pm^{0.14}_{0.18}$	$14.90\pm^{0.19}_{0.59}$	2.79
3c273	0.14660 (#23)	91.01(79)	921050	4	1030884	3	$2069\pm^{402}_{386}$	2.37	24.7666	$0.81\pm^{0.31}_{0.24}$	$15.38\pm^{0.10}_{0.13}$	17.90
3c273	0.15784 (#24)	115.64(86)	931929	3	1033805	3	$1143\pm^{230}_{202}$	3.21	25.0093	$0.17\pm^{0.12}_{0.18}$	$14.77\pm^{0.22}_{nan}$	1.10
h1821	0.02438 (#25)	–	–	–	–	–	–	–	22.1266	–	–	–
h1821	0.10817 (#26)	95.28(70)	31345	52	42458	43	$1133\pm^{91}_{88}$	1.00	23.9365	$1.53\pm^{793.68}_{2.95}$	$15.57\pm^{0.53}_{nan}$	0.11
h1821	0.12133 (#27)	100.65(84)	29451	50	43368	41	$1293\pm^{89}_{87}$	1.00	24.2207	$8.45\pm^{2.57E+03}_{8.13}$	$15.90\pm^{0.27}_{0.88}$	1.69
h1821	0.12147 (#28)	100.41(84)	29451	50	43368	41	$1292\pm^{89}_{85}$	1.00	24.2238	$10.15\pm^{2.65E+04}_{9.34}$	$15.88\pm^{0.29}_{0.50}$	1.90
h1821	0.16992 (#29)	141.11(98)	32964	48	42688	43	$1380\pm^{94}_{90}$	1.00	25.2703	$-1.12\pm^{1.44}_{0.78}$	$nan\pm^{nan}_{nan}$	0.88

h1821	0.17043 (#30)	142.88(98)	32977	48	42408	42	$1382\pm^{93}_{90}$	1.00	25.2813	$-1.34\pm^{1.11}_{0.64}$	$nan\pm^{nan}_{nan}$	1.58
h1821	0.21326 (#31)	109.00(98)	31699	49	41854	43	$1642\pm^{109}_{108}$	1.00	26.2064	$707.25\pm^{3.46E+07}_{694.75}$	$16.11\pm^{0.18}_{0.19}$	2.96
h1821	0.22497 (#32)	122.07(98)	32383	49	43022	44	$1546\pm^{108}_{106}$	1.00	26.4594	$-0.26\pm^{3.67}_{1.19}$	$nan\pm^{nan}_{nan}$	0.03
h1821	0.22522 (#33)	122.01(98)	32383	49	43022	44	$1543\pm^{109}_{106}$	1.00	26.4648	$-0.46\pm^{2.70}_{1.05}$	$nan\pm^{nan}_{nan}$	0.10
h1821	0.22639 (#34)	119.71(98)	32358	49	43044	44	$1535\pm^{108}_{104}$	1.00	26.4900	$-1.12\pm^{1.36}_{0.72}$	$nan\pm^{nan}_{nan}$	0.95
h1821	0.24531 (#35)	119.80(98)	31065	49	44448	47	$1591\pm^{120}_{113}$	1.00	26.8987	$0.44\pm^{17.76}_{1.60}$	$15.15\pm^{0.78}_{nan}$	0.06
h1821	0.26657 (#36)	111.36(98)	30604	55	44448	47	$1501\pm^{135}_{123}$	1.00	27.3579	$707.89\pm^{2.35E+07}_{715.63}$	$16.08\pm^{0.21}_{nan}$	3.28
h1821	0.28800 (#37)	134.30(98)	30054	55	39392	45	$1661\pm^{136}_{133}$	1.00	27.8208	$22.47\pm^{2.85E+05}_{22.44}$	$15.96\pm^{0.25}_{1.97}$	1.58
h1821	0.29658 (#38)	134.83(98)	31075	56	39131	45	$1569\pm^{132}_{127}$	1.00	28.0061	$-2.37\pm^{0.69}_{0.52}$	$nan\pm^{nan}_{nan}$	6.80
h1821	0.29680 (#39)	135.23(98)	31075	56	39131	45	$1574\pm^{131}_{127}$	1.00	28.0109	$-2.21\pm^{0.66}_{0.48}$	$nan\pm^{nan}_{nan}$	6.28
h2356	0.11461 (#40)	85.19(77)	491451	7	516214	6	$1312\pm^{17}_{17}$	1.00	24.0756	$0.55\pm^{0.70}_{0.51}$	$15.24\pm^{0.28}_{1.07}$	1.54
h2356	0.16512 (#41)	111.39(97)	497056	6	504552	6	$1325\pm^{18}_{18}$	1.00	25.1666	$0.04\pm^{0.66}_{0.29}$	$14.13\pm^{1.20}_{nan}$	0.06
he0056	0.16392 (#42)	96.42(92)	162630	15	161955	14	$479\pm^{20}_{19}$	1.00	25.1407	$0.03\pm^{1.70}_{0.98}$	$14.08\pm^{1.54}_{nan}$	-0.00
he0056	0.16492 (#43)	99.30(92)	162629	15	161955	14	$478\pm^{20}_{19}$	1.00	25.1623	$-0.18\pm^{1.66}_{0.79}$	$nan\pm^{nan}_{nan}$	0.02
he0226	0.01746 (#44)	23.70(19)	31712	30	nan	nan	$123\pm^{40}_{35}$	1.00	21.9771	$-2.31\pm^{5.19}_{1.35}$	$nan\pm^{nan}_{nan}$	0.85
he0226	0.02679 (#45)	39.57(27)	31712	41	nan	nan	$114\pm^{31}_{27}$	1.00	22.1787	$-3.11\pm^{2.38E+04}_{1.79}$	$nan\pm^{nan}_{nan}$	0.51
he0226	0.04121 (#46)	45.84(33)	31712	36	nan	nan	$158\pm^{38}_{27}$	1.00	22.4901	$168.50\pm^{1.00E+20}_{198.50}$	$16.09\pm^{0.32}_{nan}$	0.70
he0226	0.04535 (#47)	43.77(36)	31712	36	nan	nan	$177\pm^{31}_{29}$	1.00	22.5796	$1.29E+09\pm^{1.00E+20}_{1.29E+09}$	$16.35\pm^{0.11}_{inf}$	3.25
he0226	0.04609 (#48)	44.36(37)	31712	35	nan	nan	$176\pm^{42}_{29}$	1.00	22.5955	$2.47E+09\pm^{1.00E+20}_{2.47E+09}$	$16.35\pm^{0.11}_{inf}$	3.70
he0226	0.06015 (#49)	53.36(41)	31712	44	nan	nan	$149\pm^{30}_{27}$	1.00	22.8992	$-2.25\pm^{244.16}_{1.55}$	$nan\pm^{nan}_{nan}$	0.40
he0226	0.06083 (#50)	51.97(41)	31712	45	nan	nan	$141\pm^{29}_{26}$	1.00	22.9139	$-3.28\pm^{2.88}_{1.36}$	$nan\pm^{nan}_{nan}$	1.36
he0226	0.07023 (#51)	37.36(40)	31713	38	nan	nan	$187\pm^{31}_{30}$	1.00	23.1170	$32.55\pm^{1.00E+20}_{62.55}$	$15.97\pm^{0.44}_{nan}$	0.11
he0226	0.08375 (#52)	44.35(43)	31713	37	nan	nan	$188\pm^{31}_{29}$	1.00	23.4090	$-2.59\pm^{301.77}_{1.31}$	$nan\pm^{nan}_{nan}$	0.56
he0226	0.08901 (#53)	43.41(45)	31713	43	nan	nan	$177\pm^{31}_{27}$	1.00	23.5226	$8.73\pm^{1.02E+17}_{38.73}$	$15.87\pm^{0.59}_{nan}$	0.17
he0226	0.08938 (#54)	43.45(45)	31713	44	nan	nan	$177\pm^{28}_{26}$	1.00	23.5306	$1.19E+03\pm^{1.00E+20}_{1.22E+03}$	$16.12\pm^{0.34}_{nan}$	0.44
he0226	0.08950 (#55)	43.43(45)	31713	44	nan	nan	$177\pm^{30}_{25}$	1.00	23.5332	$630.24\pm^{1.00E+20}_{660.24}$	$16.11\pm^{0.30}_{nan}$	0.45
he0226	0.09220 (#56)	50.37(48)	31713	46	31705	38	$158\pm^{28}_{27}$	1.00	23.5915	$0.55\pm^{3.02E+14}_{30.55}$	$15.24\pm^{1.18}_{nan}$	0.00
he0226	0.10668 (#57)	72.04(63)	31713	37	31705	20	$193\pm^{37}_{27}$	1.00	23.9043	$6.36E+10\pm^{1.00E+20}_{6.36E+10}$	$16.36\pm^{0.10}_{inf}$	2.49
he0226	0.11514 (#58)	76.88(72)	31713	32	31705	20	$222\pm^{39}_{30}$	1.00	24.0870	$1.55E+06\pm^{1.00E+20}_{1.55E+06}$	$16.28\pm^{0.12}_{nan}$	2.99
he0226	0.11680 (#59)	80.69(74)	31713	30	31705	22	$229\pm^{34}_{28}$	1.00	24.1229	$119.13\pm^{1.00E+20}_{149.13}$	$16.07\pm^{0.34}_{nan}$	0.56
he0226	0.11733 (#60)	85.55(74)	31713	29	31705	23	$230\pm^{32}_{28}$	1.00	24.1343	$19.10\pm^{1.00E+20}_{49.10}$	$15.93\pm^{0.48}_{nan}$	0.27
he0226	0.12589 (#61)	80.14(78)	31713	27	31705	22	$242\pm^{34}_{31}$	1.00	24.3192	$-1.16\pm^{58.93}_{1.64}$	$nan\pm^{nan}_{nan}$	0.16
he0226	0.13832 (#62)	83.89(87)	31710	20	31705	24	$263\pm^{36}_{33}$	1.00	24.5877	$-1.75\pm^{3.60}_{1.11}$	$nan\pm^{nan}_{nan}$	0.65
he0226	0.15175 (#63)	89.30(91)	31708	21	31705	27	$251\pm^{34}_{31}$	1.00	24.8778	$0.23\pm^{1.12E+04}_{2.27}$	$14.89\pm^{1.28}_{nan}$	0.00
he0226	0.15549 (#64)	93.36(91)	31708	24	31705	27	$240\pm^{34}_{31}$	1.00	24.9586	$3.72\pm^{5.71E+07}_{33.72}$	$15.77\pm^{0.56}_{nan}$	0.18
he0226	0.16237 (#65)	100.56(90)	31707	25	31705	26	$223\pm^{34}_{30}$	1.00	25.1072	$5.77\pm^{3.14E+08}_{35.77}$	$15.85\pm^{0.50}_{nan}$	0.28
he0226	0.16339 (#66)	99.03(90)	31706	25	31705	25	$228\pm^{34}_{29}$	1.00	25.1292	$612.65\pm^{1.00E+20}_{642.65}$	$16.11\pm^{0.30}_{nan}$	1.02

he0226	0.16971 (#67)	101.88(94)	31706	22	31705	30	$234\pm^{33}_{30}$	1.00	25.2657	$-1.03\pm^{61.71}_{1.53}$	$nan\pm^{nan}_{nan}$	0.13
he0226	0.18619 (#68)	124.06(95)	31706	22	31705	21	$245\pm^{33}_{30}$	1.00	25.6217	$-1.65\pm^{3.25}_{1.07}$	$nan\pm^{nan}_{nan}$	0.65
he0226	0.18811 (#69)	120.64(94)	31706	21	31704	21	$254\pm^{34}_{31}$	1.00	25.6632	$-1.84\pm^{3.24}_{1.22}$	$nan\pm^{nan}_{nan}$	0.71
he0226	0.18891 (#70)	118.10(94)	31706	22	31704	20	$247\pm^{33}_{31}$	1.00	25.6805	$-2.01\pm^{2.34}_{1.01}$	$nan\pm^{nan}_{nan}$	1.08
he0226	0.19374 (#71)	104.01(94)	31706	23	31704	18	$234\pm^{33}_{31}$	1.00	25.7848	$-3.59\pm^{1.12}_{0.82}$	$nan\pm^{nan}_{nan}$	5.57
he0226	0.19453 (#72)	106.55(94)	31706	23	31704	20	$233\pm^{33}_{31}$	1.00	25.8018	$-3.53\pm^{1.02}_{0.75}$	$nan\pm^{nan}_{nan}$	6.18
he0226	0.19860 (#73)	120.02(93)	31706	23	31704	24	$266\pm^{35}_{32}$	1.00	25.8898	$-1.54\pm^{7.29}_{1.22}$	$nan\pm^{nan}_{nan}$	0.39
he0226	0.20055 (#74)	120.40(93)	31706	21	31704	25	$280\pm^{35}_{33}$	1.00	25.9319	$4.37\pm^{2.13E+05}_{34.37}$	$15.80\pm^{0.46}_{nan}$	0.23
he0226	0.20703 (#75)	112.17(93)	31706	18	31704	26	$314\pm^{36}_{34}$	1.00	26.0718	$765.45\pm^{4.05E+15}_{795.45}$	$16.11\pm^{0.31}_{nan}$	1.31
he0226	0.22009 (#76)	120.76(87)	31706	24	31704	26	$255\pm^{37}_{34}$	1.00	26.3539	$-1.10\pm^{13.00}_{1.41}$	$nan\pm^{nan}_{nan}$	0.19
he0226	0.22099 (#77)	119.34(87)	31706	25	31704	26	$260\pm^{36}_{34}$	1.00	26.3734	$4.64\pm^{2.98E+05}_{34.64}$	$15.81\pm^{0.43}_{nan}$	0.27
he0226	0.23009 (#78)	123.04(89)	31707	24	31704	29	$282\pm^{39}_{35}$	1.00	26.5699	$0.13\pm^{2.30E+04}_{2.35}$	$14.66\pm^{1.50}_{nan}$	0.00
he0226	0.23964 (#79)	122.92(92)	31707	22	31704	37	$314\pm^{41}_{38}$	1.00	26.7762	$1.90E+03\pm^{2.14E+13}_{1.93E+03}$	$16.15\pm^{0.23}_{nan}$	1.38
he0226	0.24522 (#80)	115.07(90)	31708	23	31704	33	$293\pm^{42}_{39}$	1.00	26.8968	$-0.17\pm^{1.60E+03}_{2.00}$	$nan\pm^{nan}_{nan}$	0.00
he0226	0.25099 (#81)	119.85(90)	31708	28	31704	34	$270\pm^{40}_{37}$	1.00	27.0214	$-1.36\pm^{5.58}_{1.41}$	$nan\pm^{nan}_{nan}$	0.34
he0226	0.27155 (#82)	120.66(94)	31709	34	31704	39	$262\pm^{40}_{37}$	1.00	27.4655	$888.46\pm^{5.79E+09}_{918.46}$	$16.11\pm^{0.24}_{nan}$	1.18
he0226	0.27956 (#83)	118.26(89)	31709	31	31704	43	$292\pm^{43}_{39}$	1.00	27.6385	$1.19E+06\pm^{1.00E+20}_{1.19E+06}$	$16.28\pm^{0.13}_{nan}$	2.01
he0226	0.28041 (#84)	121.45(88)	31709	34	31704	43	$281\pm^{46}_{39}$	1.00	27.6569	$170.80\pm^{1.00E+20}_{200.80}$	$16.10\pm^{0.31}_{nan}$	0.86
he0226	0.29134 (#85)	114.15(85)	31709	29	31707	48	$303\pm^{45}_{41}$	1.00	27.8929	$-0.65\pm^{752.83}_{1.62}$	$nan\pm^{nan}_{nan}$	0.04
he0226	0.29213 (#86)	114.62(85)	31709	28	31707	51	$318\pm^{47}_{42}$	1.00	27.9100	$1.25\pm^{4.71E+06}_{31.25}$	$15.51\pm^{0.73}_{nan}$	0.06
he0226	0.30939 (#87)	100.48(87)	31709	28	31713	53	$363\pm^{48}_{46}$	1.00	28.2828	$-0.03\pm^{4.28E+05}_{2.50}$	$nan\pm^{nan}_{nan}$	0.00
he0226	0.31833 (#88)	104.18(83)	31709	30	31716	69	$375\pm^{58}_{51}$	1.00	28.4759	$1.78\pm^{2.86E+11}_{31.78}$	$15.62\pm^{0.74}_{nan}$	0.06
he0226	0.33965 (#89)	125.18(89)	31713	43	31717	52	$336\pm^{56}_{52}$	1.00	28.9364	$5.62E+04\pm^{1.00E+20}_{5.62E+04}$	$16.21\pm^{0.25}_{nan}$	2.50
he0226	0.34036 (#90)	130.69(90)	31713	45	31717	51	$335\pm^{56}_{52}$	1.00	28.9518	$1.66E+03\pm^{1.00E+20}_{1.69E+03}$	$16.13\pm^{0.33}_{nan}$	1.44
he0226	0.35493 (#91)	120.67(92)	31716	48	31717	58	$281\pm^{58}_{52}$	1.00	29.2665	$-2.95\pm^{1.31}_{0.76}$	$nan\pm^{nan}_{nan}$	3.03
he0226	0.35528 (#92)	120.85(92)	31716	48	31717	58	$282\pm^{58}_{53}$	1.00	29.2740	$-3.10\pm^{1.52}_{0.87}$	$nan\pm^{nan}_{nan}$	2.77
he0226	0.37281 (#93)	111.76(99)	31717	47	31717	48	$352\pm^{79}_{56}$	1.00	29.6527	$1.30E+06\pm^{1.00E+20}_{1.30E+06}$	$16.24\pm^{0.22}_{nan}$	2.58
he0226	0.38420 (#94)	114.74(94)	31717	46	31717	61	$360\pm^{63}_{58}$	1.00	29.8987	$0.97\pm^{7.80E+09}_{30.97}$	$15.45\pm^{0.88}_{nan}$	0.03
he0226	0.38636 (#95)	107.14(90)	31717	47	31717	64	$355\pm^{72}_{57}$	1.00	29.9454	$879.88\pm^{1.00E+20}_{909.88}$	$16.11\pm^{0.30}_{nan}$	0.74
he0226	0.39642 (#96)	117.89(86)	31717	52	31717	71	$283\pm^{60}_{53}$	1.00	30.1627	$-1.85\pm^{10.21}_{1.29}$	$nan\pm^{nan}_{nan}$	0.48
he0226	0.39692 (#97)	121.57(86)	31717	54	31717	69	$282\pm^{62}_{55}$	1.00	30.1735	$-0.90\pm^{1.84E+04}_{2.15}$	$nan\pm^{nan}_{nan}$	0.04
he0226	0.39890 (#98)	118.58(86)	31717	53	31717	70	$289\pm^{62}_{55}$	1.00	30.2162	$-1.49\pm^{3.14E+03}_{1.63}$	$nan\pm^{nan}_{nan}$	0.18
he0226	0.40034 (#99)	117.15(85)	31717	51	31717	70	$273\pm^{59}_{53}$	1.00	30.2473	$-2.89\pm^{1.59}_{0.93}$	$nan\pm^{nan}_{nan}$	2.43
he0226	0.40274 (#100)	121.91(83)	31717	49	31717	70	$307\pm^{63}_{57}$	1.00	30.2992	$-0.82\pm^{4.88E+06}_{2.14}$	$nan\pm^{nan}_{nan}$	0.03
he0226	0.49225 (#101)	130.27(93)	31722	61	31717	60	$423\pm^{80}_{73}$	1.00	32.2326	$-2.37\pm^{2.87}_{1.13}$	$nan\pm^{nan}_{nan}$	1.03
he0226	0.49254 (#102)	123.54(92)	31722	60	31717	59	$434\pm^{80}_{74}$	1.00	32.2389	$-2.05\pm^{3.73}_{1.06}$	$nan\pm^{nan}_{nan}$	0.77
he0226	0.49280 (#103)	123.59(92)	31722	60	31717	59	$435\pm^{81}_{74}$	1.00	32.2445	$-2.07\pm^{4.37}_{1.19}$	$nan\pm^{nan}_{nan}$	0.70

he0226	0.49309 (#104)	129.01(93)	31722	62	31717	59	$423\pm^{79}_{73}$	1.00	32.2507	$-2.25\pm^{4.38}_{1.34}$	$nan\pm^{nan}_{nan}$	0.71
i22456	0.09858 (#105)	68.71(60)	79883	52	72481	44	$656\pm^{39}_{37}$	1.00	23.7293	$0.29\pm^{30.11}_{1.67}$	$15.00\pm^{0.98}_{nan}$	0.02
i22456	0.09895 (#106)	68.38(60)	79752	52	73453	44	$659\pm^{38}_{37}$	1.00	23.7373	$0.26\pm^{27.35}_{1.70}$	$14.95\pm^{1.00}_{nan}$	0.01
i22456	0.09931 (#107)	68.39(60)	79752	52	73453	44	$657\pm^{37}_{37}$	1.00	23.7451	$-0.10\pm^{14.31}_{1.52}$	$nan\pm^{nan}_{nan}$	0.00
i22456	0.09959 (#108)	74.98(61)	79883	51	73453	44	$669\pm^{37}_{37}$	1.00	23.7511	$-0.12\pm^{7.55}_{1.34}$	$nan\pm^{nan}_{nan}$	0.00
i22456	0.09989 (#109)	68.68(61)	79752	51	74286	44	$651\pm^{38}_{37}$	1.00	23.7576	$-0.71\pm^{3.30}_{1.08}$	$nan\pm^{nan}_{nan}$	0.18
i22456	0.10034 (#110)	69.76(62)	79883	51	74286	44	$656\pm^{37}_{37}$	1.00	23.7673	$-0.82\pm^{2.55}_{1.00}$	$nan\pm^{nan}_{nan}$	0.30
i22456	0.10101 (#111)	73.32(62)	79121	51	75007	45	$657\pm^{38}_{37}$	1.00	23.7818	$-0.83\pm^{2.69}_{1.11}$	$nan\pm^{nan}_{nan}$	0.26
i22456	0.10146 (#112)	75.43(63)	77663	55	75007	45	$665\pm^{36}_{42}$	1.00	23.7915	$-0.07\pm^{4.28}_{1.75}$	$nan\pm^{nan}_{nan}$	0.02
mr2251	0.01070 (#113)	–	–	–	–	–	–	–	21.8311	–	–	–
mrk421	0.01009 (#114)	–	–	–	–	–	–	–	21.8179	–	–	–
mrk876	0.00311 (#115)	–	–	–	–	–	–	–	21.6672	–	–	–
mrk876	0.06248 (#116)	41.89(45)	2651	13	nan	nan	$495\pm^{152}_{120}$	1.00	22.9496	$1.62E+13\pm^{1.00E+20}_{1.62E+13}$	$16.41\pm^{0.05}_{inf}$	0.83
mrk876	0.08579 (#117)	36.44(46)	2765	11	nan	nan	$357\pm^{118}_{97}$	1.00	23.4531	$2.06E+16\pm^{1.00E+20}_{2.06E+16}$	$16.46\pm^{0.00}_{inf}$	1.63
mrk876	0.11488 (#118)	73.35(75)	2743	19	2633	28	$529\pm^{144}_{121}$	1.00	24.0814	$0.21\pm^{1.00E+20}_{30.21}$	$14.86\pm^{1.60}_{nan}$	0.00
mrk876	0.11517 (#119)	75.24(76)	2746	18	2633	25	$567\pm^{149}_{126}$	1.00	24.0877	$4.09\pm^{1.00E+20}_{34.09}$	$15.79\pm^{0.62}_{nan}$	0.05
mrk876	0.11588 (#120)	76.60(76)	2743	17	2636	25	$603\pm^{153}_{130}$	1.00	24.1030	$44.70\pm^{1.00E+20}_{74.70}$	$16.00\pm^{0.46}_{nan}$	0.14
ngc7469	0.00962 (#121)	–	–	–	–	–	–	–	21.8078	–	–	–
ngc7469	0.00994 (#122)	–	–	–	–	–	–	–	21.8147	–	–	–
ngc7469	0.01153 (#123)	–	–	–	–	–	–	–	21.8490	–	–	–
p1103	0.13556 (#124)	87.53(87)	15673	4	15681	4	$3494\pm^{169}_{164}$	1.00	24.5281	$-0.67\pm^{1.25}_{0.75}$	$nan\pm^{nan}_{nan}$	0.47
p1103	0.13937 (#125)	91.46(88)	15673	4	15681	4	$3603\pm^{170}_{165}$	1.00	24.6104	$1.92\pm^{16.76}_{2.07}$	$15.64\pm^{0.31}_{nan}$	0.98
p1103	0.14099 (#126)	96.68(88)	15673	4	15681	4	$3562\pm^{166}_{161}$	1.00	24.6454	$-0.49\pm^{1.42}_{0.75}$	$nan\pm^{nan}_{nan}$	0.24
p1103	0.14126 (#127)	97.21(89)	15673	4	15681	4	$3537\pm^{166}_{160}$	1.00	24.6512	$-0.76\pm^{1.17}_{0.73}$	$nan\pm^{nan}_{nan}$	0.62
p1103	0.17277 (#128)	83.97(94)	15671	3	15681	5	$3424\pm^{156}_{152}$	1.00	25.3318	$-0.78\pm^{1.21}_{0.77}$	$nan\pm^{nan}_{nan}$	0.61
pg0003	0.16521 (#129)	110.21(91)	13034	29	12941	15	$284\pm^{60}_{53}$	1.00	25.1685	$-1.83\pm^{9.33}_{1.39}$	$nan\pm^{nan}_{nan}$	0.44
pg0003	0.20907 (#130)	119.20(94)	13033	23	12875	32	$302\pm^{63}_{55}$	1.00	26.1159	$-1.58\pm^{413.20}_{1.88}$	$nan\pm^{nan}_{nan}$	0.18
pg0003	0.29021 (#131)	124.39(88)	13035	43	12849	33	$347\pm^{85}_{74}$	1.00	27.8685	$-0.71\pm^{4.65E+04}_{2.41}$	$nan\pm^{nan}_{nan}$	0.03
pg0003	0.30551 (#132*)	138.04(89)	13035	53	12885	39	$291\pm^{75}_{64}$	1.00	28.1990	$-3.06\pm^{2.40}_{1.08}$	$nan\pm^{nan}_{nan}$	1.53
pg0003	0.30569 (#133*)	137.89(89)	13035	53	12885	39	$292\pm^{74}_{64}$	1.00	28.2029	$-3.27\pm^{2.34}_{1.18}$	$nan\pm^{nan}_{nan}$	1.68
pg0003	0.34757 (#134)	105.38(90)	13039	75	12932	59	$231\pm^{86}_{68}$	1.00	29.1075	$-4.17\pm^{1.46}_{0.98}$	$nan\pm^{nan}_{nan}$	4.27
pg0003	0.34788 (#135)	105.00(90)	13039	75	12932	59	$229\pm^{84}_{68}$	1.00	29.1142	$-4.49\pm^{1.50}_{1.07}$	$nan\pm^{nan}_{nan}$	4.76
pg0003	0.36452 (#136)	126.87(94)	13041	78	12932	54	$361\pm^{143}_{107}$	1.00	29.4736	$4.88E+06\pm^{1.00E+20}_{4.88E+06}$	$16.28\pm^{0.12}_{nan}$	2.32
pg0003	0.36508 (#137)	128.24(95)	13041	80	12932	54	$358\pm^{99}_{86}$	1.00	29.4857	$4.18E+12\pm^{1.00E+20}_{4.18E+12}$	$16.41\pm^{0.05}_{inf}$	3.18
pg0003	0.36572 (#138)	128.74(97)	13041	80	12932	54	$356\pm^{99}_{85}$	1.00	29.4996	$2.12E+16\pm^{1.00E+20}_{2.12E+16}$	$16.46\pm^{0.00}_{inf}$	3.55
pg0003	0.36621 (#139)	130.11(96)	13041	80	12932	53	$349\pm^{116}_{93}$	1.00	29.5101	$2.61E+12\pm^{1.00E+20}_{2.61E+12}$	$16.41\pm^{0.05}_{inf}$	3.05
pg0003	0.37029 (#140)	139.10(98)	13041	87	12932	56	$313\pm^{91}_{78}$	1.00	29.5983	$2.06E+03\pm^{1.00E+20}_{2.09E+03}$	$16.15\pm^{0.31}_{nan}$	0.44

pg0003	0.38608 (#141)	106.39(88)	13041	125	12920	51	$115\pm^{65}_{46}$	1.00	29.9393	$-4.99\pm^{0.89}_{0.78}$	$nan\pm^{nan}_{nan}$	13.26
pg0003	0.38639 (#142)	114.18(87)	13041	119	12920	57	$151\pm^{74}_{56}$	1.00	29.9460	$-5.40\pm^{1.28}_{1.06}$	$nan\pm^{nan}_{nan}$	8.98
pg0003	0.40138 (#143)	124.56(86)	13041	79	12886	53	$432\pm^{127}_{117}$	1.00	30.2698	$2.71E+12\pm^{1.00E+20}_{2.71E+12}$	$16.41\pm^{0.05}_{inf}$	2.95
pg0003	0.42192 (#144)	120.23(94)	13041	89	12843	41	$378\pm^{116}_{97}$	1.00	30.7135	$-2.22\pm^{2.71E+06}_{1.75}$	$nan\pm^{nan}_{nan}$	0.26
pg0157	0.14621 (#145)	89.37(90)	3707	30	3516	41	$333\pm^{101}_{84}$	1.00	24.7581	$1.21E+03\pm^{1.00E+20}_{1.24E+03}$	$16.12\pm^{0.34}_{nan}$	0.32
pg0804	0.00382 (#146)	–	–	–	–	–	–	–	21.6825	–	–	–
pg0804	0.01851 (#147)	16.80(23)	29128	12	nan	nan	$945\pm^{97}_{92}$	1.00	21.9998	$-1.81\pm^{1.53}_{0.87}$	$nan\pm^{nan}_{nan}$	1.89
pg0804	0.10216 (#148)	79.20(62)	28053	6	28091	3	$1727\pm^{87}_{84}$	1.00	23.8067	$-0.51\pm^{2.91}_{1.02}$	$nan\pm^{nan}_{nan}$	0.11
pg0804	0.10230 (#149)	79.21(62)	28053	6	28091	3	$1728\pm^{87}_{84}$	1.00	23.8097	$-0.47\pm^{2.82}_{1.16}$	$nan\pm^{nan}_{nan}$	0.10
pg0832	0.10772 (#150)	80.67(64)	20655	63	20637	75	$76\pm^{24}_{21}$	1.00	23.9268	$-3.20\pm^{2.96}_{1.25}$	$nan\pm^{nan}_{nan}$	1.33
pg0832	0.13230 (#151)	108.67(84)	20655	92	20637	151	$61\pm^{24}_{19}$	1.00	24.4577	$-0.85\pm^{1.00E+20}_{29.15}$	$nan\pm^{nan}_{nan}$	0.01
pg0832	0.15276 (#152)	120.88(91)	20654	102	20637	191	$47\pm^{21}_{16}$	1.00	24.8996	$2.53E+05\pm^{1.00E+20}_{2.53E+05}$	$16.25\pm^{0.16}_{nan}$	0.35
pg0832	0.23308 (#153)	129.97(95)	20655	89	20637	102	$82\pm^{28}_{23}$	1.00	26.6345	$-3.17\pm^{1.00E+04}_{1.79}$	$nan\pm^{nan}_{nan}$	0.58
pg0832	0.32567 (#154)	75.57(61)	20656	168	20645	75	$67\pm^{36}_{26}$	1.00	28.6345	$-1.01\pm^{1.00E+20}_{28.99}$	$nan\pm^{nan}_{nan}$	0.03
pg0953	0.01560 (#155)	28.56(26)	12792	15	nan	nan	$420\pm^{81}_{73}$	1.00	21.9370	$-2.59\pm^{2.65}_{1.33}$	$nan\pm^{nan}_{nan}$	1.29
pg0953	0.05891 (#156)	62.59(44)	12792	17	nan	nan	$452\pm^{68}_{62}$	1.00	22.8725	$-1.64\pm^{201.57}_{1.47}$	$nan\pm^{nan}_{nan}$	0.26
pg0953	0.06807 (#157)	48.31(41)	12792	16	nan	nan	$546\pm^{89}_{74}$	1.00	23.0703	$3.07E+12\pm^{1.00E+20}_{3.07E+12}$	$16.41\pm^{0.05}_{inf}$	3.12
pg0953	0.11827 (#158)	75.73(75)	12792	18	12309	9	$500\pm^{67}_{61}$	1.00	24.1546	$-0.43\pm^{90.04}_{1.66}$	$nan\pm^{nan}_{nan}$	0.02
pg0953	0.14236 (#159)	105.46(88)	12786	21	12309	8	$548\pm^{75}_{68}$	1.00	24.6750	$-3.03\pm^{0.91}_{0.63}$	$nan\pm^{nan}_{nan}$	5.66
pg0953	0.14263 (#160)	109.34(89)	12785	22	12309	8	$547\pm^{74}_{69}$	1.00	24.6808	$-2.96\pm^{0.83}_{0.58}$	$nan\pm^{nan}_{nan}$	5.97
pg0953	0.14307 (#161)	107.64(88)	12785	22	12309	8	$540\pm^{74}_{68}$	1.00	24.6903	$-3.05\pm^{0.81}_{0.57}$	$nan\pm^{nan}_{nan}$	6.36
pg0953	0.22967 (#162)	126.93(87)	12777	8	12309	16	$692\pm^{88}_{81}$	1.00	26.5609	$-2.57\pm^{1.33}_{0.84}$	$nan\pm^{nan}_{nan}$	2.87
pg0953	0.23251 (#163)	116.37(87)	12777	9	12309	16	$645\pm^{85}_{78}$	1.00	26.6222	$-2.98\pm^{1.09}_{0.74}$	$nan\pm^{nan}_{nan}$	4.37
pg0953	0.23351 (#164)	118.01(88)	12777	9	12309	15	$650\pm^{85}_{78}$	1.00	26.6438	$-2.92\pm^{1.42}_{0.87}$	$nan\pm^{nan}_{nan}$	2.94
pg1115	0.12285 (#165)	111.34(78)	17510	36	16953	10	$307\pm^{48}_{44}$	1.00	24.2536	$2.73E+06\pm^{1.00E+20}_{2.73E+06}$	$16.28\pm^{0.12}_{nan}$	3.46
pg1115	0.12313 (#166)	110.77(77)	17510	37	16953	10	$298\pm^{64}_{43}$	1.00	24.2596	$154.01\pm^{1.00E+20}_{184.01}$	$16.04\pm^{0.42}_{nan}$	1.57
pg1115	0.13104 (#167*)	126.82(83)	17517	38	16953	13	$303\pm^{52}_{47}$	1.00	24.4305	$2.10\pm^{7.83E+05}_{32.10}$	$15.66\pm^{0.57}_{nan}$	0.14
pg1115	0.15456 (#168*)	137.20(89)	17538	26	16953	15	$351\pm^{52}_{48}$	1.00	24.9385	$-1.25\pm^{14.84}_{1.36}$	$nan\pm^{nan}_{nan}$	0.22
pg1115	0.15467 (#169*)	137.21(89)	17538	26	16953	15	$351\pm^{53}_{48}$	1.00	24.9409	$-1.19\pm^{13.28}_{1.32}$	$nan\pm^{nan}_{nan}$	0.21
pg1116	0.05900 (#170)	49.53(36)	281330	15	nan	nan	$597\pm^{19}_{19}$	1.00	22.8744	$3.08\pm^{18.52}_{2.71}$	$15.74\pm^{0.24}_{0.65}$	2.02
pg1116	0.05927 (#171)	43.85(35)	280940	15	nan	nan	$590\pm^{19}_{19}$	1.00	22.8802	$2.47\pm^{24.40}_{2.27}$	$15.70\pm^{0.26}_{0.85}$	1.62
pg1116	0.11895 (#172)	95.95(79)	285653	15	287248	12	$652\pm^{16}_{16}$	1.00	24.1693	$-0.41\pm^{0.72}_{0.52}$	$nan\pm^{nan}_{nan}$	0.50
pg1116	0.13852 (#173)	94.61(91)	277702	15	291047	12	$693\pm^{19}_{19}$	1.00	24.5920	$1.53\pm^{2.90}_{1.20}$	$15.58\pm^{0.23}_{0.53}$	2.43
pg1116	0.16539 (#174)	104.05(93)	289660	12	291047	10	$750\pm^{19}_{19}$	1.00	25.1724	$1.15\pm^{2.07}_{1.03}$	$15.49\pm^{0.26}_{0.86}$	1.66
pg1116	0.16554 (#175)	100.41(92)	289658	12	290943	10	$751\pm^{19}_{19}$	1.00	25.1757	$1.29\pm^{2.32}_{1.05}$	$15.54\pm^{0.24}_{0.62}$	2.12
pg1116	0.16610 (#176)	106.71(93)	289658	11	291047	10	$760\pm^{19}_{19}$	1.00	25.1878	$1.79\pm^{3.14}_{1.32}$	$15.62\pm^{0.21}_{0.44}$	3.04
pg1116	0.16686 (#177)	105.29(92)	291239	11	290943	10	$756\pm^{19}_{19}$	1.00	25.2042	$1.73\pm^{3.60}_{1.25}$	$15.62\pm^{0.21}_{0.43}$	3.07

pg1116	0.17343 (#178)	112.47(96)	296094	11	285607	10	$756\pm^{18}_{18}$	1.00	25.3461	$0.82\pm^{1.68}_{0.89}$	$15.38\pm^{0.32}_{nan}$	0.98
pg1211	0.00711 (#179)	–	–	–	–	–	–	–	21.7536	–	–	–
pg1211	0.05117 (#180)	45.23(34)	736547	13	nan	nan	$672\pm^{13}_{13}$	1.00	22.7053	$201.73\pm^{3.78E+05}_{184.38}$	$16.06\pm^{0.16}_{0.12}$	13.49
pg1211	0.06449 (#181)	–	–	–	–	–	–	–	22.9930	–	–	–
pg1211	0.06491 (#182)	–	–	–	–	–	–	–	23.0021	–	–	–
pg1216	0.12362 (#183)	106.86(78)	11245	36	11258	15	$185\pm^{46}_{40}$	1.00	24.2702	$1.23E+12\pm^{1.00E+20}_{1.23E+12}$	$16.41\pm^{0.00}_{inf}$	4.18
pg1216	0.12389 (#184)	105.56(77)	11245	36	11258	15	$183\pm^{66}_{49}$	1.00	24.2760	$1.71E+04\pm^{1.00E+20}_{1.72E+04}$	$16.21\pm^{0.26}_{nan}$	2.64
pg1216	0.12463 (#185)	107.31(78)	11245	36	11258	15	$187\pm^{46}_{40}$	1.00	24.2920	$1.14E+07\pm^{1.00E+20}_{1.14E+07}$	$16.29\pm^{0.18}_{nan}$	2.41
pg1216	0.12485 (#186)	106.17(77)	11245	36	11258	15	$186\pm^{46}_{40}$	1.00	24.2968	$7.83E+04\pm^{1.00E+20}_{7.83E+04}$	$16.21\pm^{0.25}_{nan}$	1.71
pg1216	0.13499 (#187)	116.72(86)	11248	35	11258	16	$192\pm^{50}_{43}$	1.00	24.5158	$2.34\pm^{1.06E+13}_{32.34}$	$15.68\pm^{0.69}_{nan}$	0.06
pg1216	0.26768 (#188)	113.01(93)	11258	41	11258	73	$223\pm^{67}_{53}$	1.00	27.3819	$14.94\pm^{1.00E+20}_{44.94}$	$15.91\pm^{0.55}_{nan}$	0.14
pg1216	0.28199 (#189)	112.68(89)	11258	41	11258	68	$237\pm^{66}_{56}$	1.00	27.6910	$-2.60\pm^{4.73}_{1.22}$	$nan\pm^{nan}_{nan}$	0.87
pg1216	0.28237 (#190)	112.03(88)	11258	41	11258	68	$245\pm^{68}_{57}$	1.00	27.6992	$-2.15\pm^{330.94}_{1.38}$	$nan\pm^{nan}_{nan}$	0.43
pg1259	0.00220 (#191)	–	–	–	–	–	–	–	21.6475	–	–	–
pg1259	0.00762 (#192)	–	–	–	–	–	–	–	21.7646	–	–	–
pg1259	0.02217 (#193)	31.57(30)	11484	31	nan	nan	$172\pm^{52}_{46}$	1.00	22.0789	$37.76\pm^{1.00E+20}_{67.76}$	$15.99\pm^{0.47}_{nan}$	0.12
pg1259	0.04606 (#194)	45.32(42)	11485	41	nan	nan	$178\pm^{51}_{39}$	1.00	22.5949	$4.41E+09\pm^{1.00E+20}_{4.41E+09}$	$16.35\pm^{0.11}_{inf}$	1.04
pg1259	0.04650 (#195)	43.77(42)	11485	37	nan	nan	$188\pm^{53}_{41}$	1.00	22.6044	$4.23E+09\pm^{1.00E+20}_{4.23E+09}$	$16.35\pm^{0.11}_{inf}$	1.02
pg1259	0.19576 (#196)	107.87(92)	11483	28	11479	32	$236\pm^{54}_{46}$	1.00	25.8284	$-2.09\pm^{25.68}_{1.50}$	$nan\pm^{nan}_{nan}$	0.42
pg1259	0.21940 (#197)	110.09(92)	11483	38	11479	41	$267\pm^{65}_{56}$	1.00	26.3390	$-1.52\pm^{3.11E+05}_{2.22}$	$nan\pm^{nan}_{nan}$	0.10
pg1259	0.21953 (#198)	110.10(92)	11483	38	11479	41	$267\pm^{65}_{56}$	1.00	26.3418	$-1.36\pm^{8.12E+06}_{1.90}$	$nan\pm^{nan}_{nan}$	0.09
pg1259	0.22313 (#199)	105.90(93)	11483	32	11479	49	$275\pm^{64}_{56}$	1.00	26.4196	$-0.23\pm^{6.24E+09}_{2.86}$	$nan\pm^{nan}_{nan}$	0.00
pg1259	0.23284 (#200)	120.10(95)	11483	44	11479	68	$235\pm^{60}_{51}$	1.00	26.6293	$6.49E+07\pm^{1.00E+20}_{6.49E+07}$	$16.32\pm^{0.14}_{-0.14}$	1.29
pg1259	0.23956 (#201)	123.67(95)	11483	62	11479	61	$179\pm^{54}_{45}$	1.00	26.7745	$0.89\pm^{2.33E+14}_{30.89}$	$15.41\pm^{1.01}_{nan}$	0.01
pg1259	0.25973 (#202)	111.65(93)	11483	81	11479	66	$126\pm^{49}_{39}$	1.00	27.2102	$2.29E+04\pm^{1.00E+20}_{2.29E+04}$	$16.21\pm^{0.26}_{nan}$	0.83
pg1259	0.31979 (#203)	80.12(82)	11483	42	11480	55	$296\pm^{92}_{70}$	1.00	28.5075	$1.46E+05\pm^{1.00E+20}_{1.46E+05}$	$16.22\pm^{0.24}_{nan}$	0.67
pg1259	0.32472 (#204)	90.97(82)	11484	43	11480	66	$337\pm^{109}_{77}$	1.00	28.6140	$5.09E+09\pm^{1.00E+20}_{5.09E+09}$	$16.35\pm^{0.11}_{inf}$	2.56
pg1307	0.14187 (#205)	117.92(89)	9837	52	9504	88	$210\pm^{60}_{45}$	1.00	24.6644	$2.26E+04\pm^{1.00E+20}_{2.26E+04}$	$16.21\pm^{0.26}_{nan}$	0.58
pg1307	0.14214 (#206)	117.74(88)	9837	52	9504	88	$211\pm^{60}_{46}$	1.00	24.6702	$5.01E+06\pm^{1.00E+20}_{5.01E+06}$	$16.28\pm^{0.18}_{nan}$	0.69
pg1309	0.17586 (#207)	112.33(93)	27265	31	26163	75	$153\pm^{28}_{25}$	1.00	25.3986	$3.69E+12\pm^{1.00E+20}_{3.69E+12}$	$16.41\pm^{0.05}_{inf}$	3.00
pg1309	0.17745 (#208)	117.17(95)	27265	32	26163	73	$150\pm^{36}_{25}$	1.00	25.4329	$2.70E+06\pm^{1.00E+20}_{2.70E+06}$	$16.28\pm^{0.12}_{nan}$	1.76
pg1309	0.17866 (#209)	121.37(94)	27265	33	26163	75	$155\pm^{35}_{25}$	1.00	25.4591	$5.56E+09\pm^{1.00E+20}_{5.56E+09}$	$16.35\pm^{0.11}_{inf}$	2.13
pg1309	0.17930 (#210)	120.67(95)	27265	33	26163	75	$156\pm^{33}_{26}$	1.00	25.4729	$4.80E+09\pm^{1.00E+20}_{4.80E+09}$	$16.35\pm^{0.11}_{inf}$	1.89
pg1309	0.17979 (#211)	121.42(94)	27265	31	26163	75	$157\pm^{29}_{25}$	1.00	25.4835	$4.66E+07\pm^{1.00E+20}_{4.66E+07}$	$16.31\pm^{0.16}_{nan}$	1.65
pg1309	0.18069 (#212)	121.63(94)	27265	33	26163	73	$147\pm^{27}_{25}$	1.00	25.5029	$4.34E+03\pm^{1.00E+20}_{4.37E+03}$	$16.19\pm^{0.27}_{nan}$	0.54
pg1309	0.18117 (#213)	119.61(95)	27265	33	26163	75	$144\pm^{29}_{25}$	1.00	25.5133	$36.84\pm^{1.00E+20}_{66.84}$	$15.99\pm^{0.47}_{nan}$	0.17

pg1309	0.18139 (#214)	116.87(93)	27265	33	26163	75	$141\pm^{28}_{24}$	1.00	25.5180	$7.15\pm^{1.00E+20}_{37.15}$	$15.85\pm^{0.56}_{nan}$	0.10
pg1309	0.18145 (#215)	116.88(93)	27265	33	26163	75	$141\pm^{29}_{25}$	1.00	25.5193	$6.05\pm^{1.00E+20}_{36.05}$	$15.85\pm^{0.61}_{nan}$	0.09
pg1309	0.18192 (#216)	114.96(94)	27265	33	26163	78	$145\pm^{29}_{25}$	1.00	25.5295	$3.81\pm^{1.00E+20}_{33.81}$	$15.78\pm^{0.68}_{nan}$	0.06
pg1309	0.18698 (#217)	107.23(91)	27265	35	26163	78	$158\pm^{35}_{26}$	1.00	25.6388	$9.01E+09\pm^{1.00E+20}_{9.01E+09}$	$16.35\pm^{0.11}_{inf}$	1.76
pg1444	0.22031 (#218)	113.67(93)	17674	27	17137	35	$183\pm^{40}_{35}$	1.00	26.3587	$-2.51\pm^{2.34}_{1.07}$	$nan\pm^{nan}_{nan}$	1.34
pg1444	0.22676 (#219)	127.72(94)	17674	34	17137	39	$179\pm^{40}_{35}$	1.00	26.4980	$1.03\pm^{9.66E+12}_{31.03}$	$15.45\pm^{0.95}_{nan}$	0.03
pg1444	0.26690 (#220)	132.30(93)	17674	56	17137	57	$145\pm^{39}_{33}$	1.00	27.3650	$-3.50\pm^{1.38}_{0.84}$	$nan\pm^{nan}_{nan}$	3.41
pg1444	0.26728 (#221)	132.11(94)	17674	56	17137	57	$146\pm^{40}_{34}$	1.00	27.3732	$-3.72\pm^{1.42}_{0.90}$	$nan\pm^{nan}_{nan}$	3.67
pg1444	0.26738 (#222)	132.08(94)	17674	56	17137	57	$146\pm^{40}_{34}$	1.00	27.3754	$-3.39\pm^{1.24}_{0.78}$	$nan\pm^{nan}_{nan}$	3.70
pg1444	0.26747 (#223)	127.49(93)	17674	58	17137	61	$143\pm^{39}_{33}$	1.00	27.3774	$-3.71\pm^{1.15}_{0.78}$	$nan\pm^{nan}_{nan}$	4.74
pg1626	0.13075 (#224)	124.04(83)	69157	66	68865	77	$386\pm^{48}_{46}$	1.00	24.4242	$-2.57\pm^{0.92}_{0.60}$	$nan\pm^{nan}_{nan}$	4.32
phl1811	0.07344 (#225)	–	–	–	–	–	–	–	23.1863	–	–	–
phl1811	0.07768 (#226)	–	–	–	–	–	–	–	23.2779	–	–	–
phl1811	0.08131 (#227)	–	–	–	–	–	–	–	23.3563	–	–	–
phl1811	0.13239 (#228)	–	–	–	–	–	–	–	24.4596	–	–	–
phl1811	0.13282 (#229)	–	–	–	–	–	–	–	24.4689	–	–	–
phl1811	0.13318 (#230)	–	–	–	–	–	–	–	24.4767	–	–	–
phl1811	0.13545 (#231)	–	–	–	–	–	–	–	24.5257	–	–	–
phl1811	0.15752 (#232)	–	–	–	–	–	–	–	25.0024	–	–	–
phl1811	0.15786 (#233)	–	–	–	–	–	–	–	25.0098	–	–	–
phl1811	0.17652 (#234)	118.26(84)	79254	89	77556	75	$35\pm^{12}_{11}$	1.00	25.4128	$7.11E+04\pm^{1.00E+20}_{7.11E+04}$	$16.21\pm^{0.25}_{nan}$	1.08
phl1811	0.19157 (#235*)	164.17(89)	79254	101	76738	99	$35\pm^{13}_{11}$	1.00	25.7379	$141.21\pm^{1.00E+20}_{171.21}$	$16.09\pm^{0.32}_{nan}$	0.13
phl1811	0.19194 (#236*)	167.21(88)	79254	103	76682	100	$34\pm^{13}_{11}$	1.00	25.7459	$46.75\pm^{1.00E+20}_{76.75}$	$16.00\pm^{0.46}_{nan}$	0.06
phl1811	0.19220 (#237*)	167.23(88)	79254	103	76682	100	$34\pm^{12}_{11}$	1.00	25.7515	$8.42\pm^{1.00E+20}_{38.42}$	$15.90\pm^{0.56}_{nan}$	0.03
pks0312	0.20188 (#238)	93.47(64)	23858	44	22982	36	$161\pm^{40}_{35}$	1.00	25.9606	$3.90E+06\pm^{1.00E+20}_{3.90E+06}$	$16.28\pm^{0.12}_{nan}$	1.94
pks0312	0.20275 (#239*)	99.01(66)	23858	48	22982	37	$154\pm^{39}_{33}$	1.00	25.9794	$4.48E+06\pm^{1.00E+20}_{4.48E+06}$	$16.28\pm^{0.12}_{nan}$	1.41
pks0405	0.09192 (#240)	67.08(46)	137245	21	nan	nan	$358\pm^{19}_{18}$	1.00	23.5855	$-0.55\pm^{2.90}_{1.06}$	$nan\pm^{nan}_{nan}$	0.13
pks0405	0.09647 (#241)	69.21(48)	135771	21	138649	18	$361\pm^{19}_{19}$	1.00	23.6838	$-1.25\pm^{1.51}_{0.79}$	$nan\pm^{nan}_{nan}$	0.98
pks0405	0.14808 (#242)	88.65(90)	136323	20	137234	20	$373\pm^{19}_{19}$	1.00	24.7985	$-0.66\pm^{2.09}_{0.99}$	$nan\pm^{nan}_{nan}$	0.23
pks0405	0.16566 (#243)	79.70(91)	137140	18	137234	21	$394\pm^{21}_{20}$	1.00	25.1783	$4.27\pm^{309.84}_{4.00}$	$15.80\pm^{0.27}_{0.83}$	1.67
pks0405	0.16606 (#244)	79.75(92)	136407	17	137234	21	$395\pm^{21}_{20}$	1.00	25.1869	$4.75\pm^{228.47}_{4.41}$	$15.81\pm^{0.25}_{0.75}$	1.78
pks0405	0.16659 (#245)	78.27(91)	137924	18	137234	22	$394\pm^{21}_{20}$	1.00	25.1983	$5.60\pm^{767.40}_{5.11}$	$15.84\pm^{0.24}_{0.65}$	2.01
pks0405	0.16688 (#246)	78.15(91)	137924	18	137234	22	$395\pm^{21}_{20}$	1.00	25.2046	$8.37\pm^{265.42}_{7.69}$	$15.87\pm^{0.23}_{0.54}$	2.16
pks0405	0.16712 (#247)	83.54(92)	137941	18	137234	22	$391\pm^{21}_{20}$	1.00	25.2098	$6.94\pm^{643.47}_{6.36}$	$15.86\pm^{0.24}_{0.60}$	2.15
pks0405	0.18257 (#248)	113.72(95)	137986	22	136490	21	$365\pm^{20}_{19}$	1.00	25.5435	$-0.51\pm^{1.96}_{0.97}$	$nan\pm^{nan}_{nan}$	0.17
pks0405	0.18289 (#249)	114.40(96)	138000	21	136490	21	$365\pm^{20}_{19}$	1.00	25.5504	$-0.29\pm^{2.50}_{1.00}$	$nan\pm^{nan}_{nan}$	0.05
pks0405	0.24052 (#250)	109.18(95)	137976	21	138647	29	$413\pm^{23}_{22}$	1.00	26.7952	$3.89\pm^{1.05E+03}_{3.98}$	$15.78\pm^{0.31}_{nan}$	1.03

pks0405	0.24094 (#251)	104.97(95)	137961	21	138647	30	$410\pm^{23}_{22}$	1.00	26.8043	$5.51\pm^{1.53E+03}_{5.63}$	$15.82\pm^{0.31}_{nan}$	1.15
pks0405	0.24547 (#252)	98.26(94)	136439	23	138647	30	$386\pm^{23}_{23}$	1.00	26.9022	$-0.96\pm^{1.43}_{0.82}$	$nan\pm^{nan}_{nan}$	0.69
pks0405	0.29762 (#253)	98.20(89)	135766	33	137130	34	$382\pm^{27}_{26}$	1.00	28.0286	$-0.21\pm^{3.56}_{1.16}$	$nan\pm^{nan}_{nan}$	0.02
pks0405	0.34188 (#254)	98.93(90)	136321	40	138714	46	$379\pm^{29}_{28}$	1.00	28.9846	$-1.69\pm^{2.22}_{1.03}$	$nan\pm^{nan}_{nan}$	0.90
pks0405	0.34225 (#255)	98.19(90)	136322	40	138714	47	$381\pm^{29}_{28}$	1.00	28.9926	$-1.80\pm^{1.83}_{0.88}$	$nan\pm^{nan}_{nan}$	1.22
pks0405	0.35092 (#256)	86.77(91)	136325	43	138714	47	$392\pm^{32}_{31}$	1.00	29.1799	$118.44\pm^{1.95E+09}_{117.08}$	$16.08\pm^{0.22}_{0.52}$	2.55
pks0405	0.36075 (#257)	90.38(93)	137923	45	138714	45	$385\pm^{33}_{32}$	1.00	29.3922	$93.75\pm^{1.18E+09}_{90.97}$	$16.06\pm^{0.24}_{0.33}$	2.11
pks0405	0.36151 (#258)	92.10(93)	137923	46	138714	46	$376\pm^{32}_{32}$	1.00	29.4086	$23.36\pm^{1.43E+05}_{24.12}$	$15.95\pm^{0.27}_{nan}$	1.10
pks0405	0.36329 (#259)	96.83(94)	138708	47	138714	45	$363\pm^{32}_{31}$	1.00	29.4471	$-0.68\pm^{3.27}_{1.20}$	$nan\pm^{nan}_{nan}$	0.16
pks0405	0.40570 (#260)	120.73(84)	137132	41	133905	45	$452\pm^{35}_{34}$	1.00	30.3631	$39.93\pm^{2.27E+06}_{41.65}$	$15.99\pm^{0.26}_{nan}$	0.79
pks0405	0.40890 (#261)	110.16(86)	137167	39	134014	47	$491\pm^{42}_{35}$	1.00	30.4322	$1.00E+07\pm^{1.00E+20}_{9.95E+06}$	$16.29\pm^{0.18}_{0.08}$	6.95
pks0405	0.49505 (#262)	112.27(94)	138729	51	137202	58	$536\pm^{45}_{43}$	1.00	32.2931	$-2.10\pm^{0.90}_{0.58}$	$nan\pm^{nan}_{nan}$	3.45
pks0405	0.49530 (#263)	108.35(92)	138729	51	137169	58	$528\pm^{45}_{43}$	1.00	32.2985	$-2.48\pm^{0.99}_{0.69}$	$nan\pm^{nan}_{nan}$	4.18
pks0405	0.55506 (#264)	104.58(82)	132269	59	134976	41	$444\pm^{57}_{54}$	1.00	33.5893	$2.18E+05\pm^{1.00E+20}_{2.12E+05}$	$16.26\pm^{0.15}_{0.14}$	2.35
pks2005	0.06490 (#265)	59.89(42)	53473	5	nan	nan	$2202\pm^{73}_{71}$	1.00	23.0018	$-0.87\pm^{1.18}_{0.68}$	$nan\pm^{nan}_{nan}$	0.74
pks2155	0.05405 (#266)	–	–	–	–	–	–	–	22.7675	–	–	–
pks2155	0.05707 (#267)	20.80(28)	1697089	3	nan	nan	$679\pm^{108}_{82}$	4.85	22.8327	$-0.26\pm^{0.11}_{0.13}$	$nan\pm^{nan}_{nan}$	5.24
q0045	0.11052 (#268)	–	–	–	–	–	–	–	23.9872	–	–	–
q0045	0.13521 (#269)	–	–	–	–	–	–	–	24.5205	–	–	–
q1230	0.09518 (#270)	63.84(48)	39335	57	39139	83	$112\pm^{23}_{20}$	1.00	23.6559	$1.24E+03\pm^{1.00E+20}_{1.27E+03}$	$16.12\pm^{0.34}_{nan}$	0.60
q1230	0.10318 (#271)	59.80(44)	39335	55	39139	69	$93\pm^{26}_{23}$	1.00	23.8287	$-3.93\pm^{2.04}_{1.33}$	$nan\pm^{nan}_{nan}$	2.91
q1230	0.10445 (#272)	62.04(47)	39335	57	39139	64	$100\pm^{26}_{23}$	1.00	23.8561	$-3.24\pm^{3.05}_{1.49}$	$nan\pm^{nan}_{nan}$	1.45
q1230	0.10530 (#273)	62.81(47)	39335	57	39139	59	$106\pm^{27}_{24}$	1.00	23.8745	$-2.31\pm^{1.93E+04}_{2.00}$	$nan\pm^{nan}_{nan}$	0.34
q1230	0.10596 (#274)	63.04(47)	39335	57	39139	59	$111\pm^{27}_{24}$	1.00	23.8887	$-0.71\pm^{2.31E+08}_{2.48}$	$nan\pm^{nan}_{nan}$	0.01
q1230	0.10666 (#275)	63.05(47)	39335	57	39139	59	$113\pm^{26}_{24}$	1.00	23.9039	$0.65\pm^{3.29E+16}_{30.65}$	$15.30\pm^{1.16}_{nan}$	0.00
q1230	0.10809 (#276)	59.85(45)	39335	59	39139	59	$103\pm^{26}_{23}$	1.00	23.9347	$-1.44\pm^{1.00E+20}_{2.10}$	$nan\pm^{nan}_{nan}$	0.06
q1230	0.10820 (#277)	62.54(45)	39335	60	39139	59	$103\pm^{26}_{23}$	1.00	23.9371	$-1.59\pm^{1.00E+20}_{2.24}$	$nan\pm^{nan}_{nan}$	0.08
q1230	0.10861 (#278)	59.64(45)	39335	58	39139	55	$105\pm^{26}_{23}$	1.00	23.9460	$-1.69\pm^{1.00E+20}_{2.08}$	$nan\pm^{nan}_{nan}$	0.10
q1230	0.10906 (#279)	61.31(47)	39335	59	39139	55	$101\pm^{26}_{23}$	1.00	23.9557	$-2.14\pm^{2.35E+16}_{1.90}$	$nan\pm^{nan}_{nan}$	0.20
q1230	0.10935 (#280)	61.34(47)	39335	59	39139	55	$102\pm^{26}_{23}$	1.00	23.9620	$-1.88\pm^{1.00E+20}_{1.72}$	$nan\pm^{nan}_{nan}$	0.16
q1230	0.10956 (#281)	61.25(46)	39335	58	39139	55	$107\pm^{27}_{24}$	1.00	23.9665	$-1.54\pm^{1.00E+20}_{2.51}$	$nan\pm^{nan}_{nan}$	0.07
q1230	0.11707 (#282)	70.22(56)	39335	56	39139	61	$120\pm^{31}_{23}$	1.00	24.1287	$1.72E+04\pm^{1.00E+20}_{1.72E+04}$	$16.21\pm^{0.26}_{nan}$	1.38
q1230	0.11743 (#283)	71.60(58)	39335	55	39139	59	$121\pm^{30}_{24}$	1.00	24.1365	$1.61E+04\pm^{1.00E+20}_{1.61E+04}$	$16.20\pm^{0.23}_{nan}$	1.25
q1230	0.11781 (#284)	71.89(58)	39335	55	39139	59	$120\pm^{26}_{23}$	1.00	24.1447	$1.50E+03\pm^{1.00E+20}_{1.53E+03}$	$16.12\pm^{0.34}_{nan}$	0.91
rbs1892	0.15752 (#285)	86.45(91)	4935	52	4865	20	$220\pm^{84}_{67}$	1.00	25.0024	$-2.48\pm^{7.21}_{1.42}$	$nan\pm^{nan}_{nan}$	0.66
rbs1892	0.17133 (#286)	86.80(94)	4937	48	4865	27	$309\pm^{139}_{95}$	1.00	25.3007	$7.28E+08\pm^{1.00E+20}_{7.28E+08}$	$16.35\pm^{0.11}_{inf}$	2.67
rbs1892	0.19874 (#287)	104.23(94)	4937	29	4849	49	$500\pm^{129}_{110}$	1.00	25.8928	$-1.31\pm^{1.34E+11}_{2.25}$	$nan\pm^{nan}_{nan}$	0.06

rbs542	0.10323 (#288)	86.68(64)	192553	9	181905	6	$1543\pm^{32}_{31}$	1.00	23.8298	$0.31\pm^{1.26}_{0.76}$	$15.02\pm^{0.57}_{nan}$	0.16
rbs542	0.10379 (#289)	87.77(65)	192488	8	181905	6	$1551\pm^{32}_{32}$	1.00	23.8419	$0.63\pm^{1.69}_{0.90}$	$15.29\pm^{0.39}_{nan}$	0.52
rxj0439	0.11547 (#290)	95.23(74)	148931	18	151265	13	$506\pm^{20}_{20}$	1.00	24.0942	$-0.07\pm^{2.68}_{1.03}$	$nan\pm^{nan}_{nan}$	-0.00
rxj0439	0.21833 (#291)	118.05(95)	147527	14	149811	17	$588\pm^{27}_{26}$	1.00	26.3159	$2.54\pm^{18.65}_{2.52}$	$15.70\pm^{0.27}_{1.77}$	1.26
rxj0439	0.24235 (#292)	94.71(94)	148524	17	152414	20	$592\pm^{28}_{27}$	1.00	26.8348	$2.06\pm^{42.43}_{2.31}$	$15.66\pm^{0.33}_{nan}$	0.81
rxj0439	0.24258 (#293)	103.01(95)	147411	16	152414	20	$590\pm^{28}_{27}$	1.00	26.8397	$2.33\pm^{27.65}_{2.51}$	$15.68\pm^{0.31}_{nan}$	0.92
rxj0439	0.24313 (#294)	94.82(94)	147411	16	152414	19	$592\pm^{28}_{27}$	1.00	26.8516	$1.25\pm^{10.07}_{1.71}$	$15.52\pm^{0.40}_{nan}$	0.50
rxj0439	0.24387 (#295)	93.90(94)	147412	16	152414	20	$593\pm^{29}_{27}$	1.00	26.8676	$0.20\pm^{3.28}_{1.06}$	$14.84\pm^{0.92}_{nan}$	0.04
s50716	0.23145 (#296)	93.47(94)	75297	11	76133	14	$887\pm^{42}_{41}$	1.00	26.5993	$-0.22\pm^{2.24}_{0.98}$	$nan\pm^{nan}_{nan}$	0.03
ton28	0.13746 (#297)	111.07(90)	83595	34	86028	35	$225\pm^{23}_{21}$	1.00	24.5691	$1.60\pm^{3.50E+03}_{2.97}$	$15.59\pm^{0.55}_{nan}$	0.16
ton28	0.13773 (#298)	110.95(90)	83595	34	86028	35	$227\pm^{22}_{22}$	1.00	24.5750	$3.14\pm^{3.83E+04}_{4.38}$	$15.75\pm^{0.42}_{nan}$	0.30
ton28	0.13781 (#299)	111.91(90)	83595	34	86028	34	$227\pm^{23}_{22}$	1.00	24.5767	$3.47\pm^{7.02E+04}_{4.65}$	$15.77\pm^{0.43}_{nan}$	0.35
ton28	0.17251 (#300)	98.29(95)	86114	26	85104	36	$203\pm^{19}_{18}$	1.00	25.3262	$-2.07\pm^{1.13}_{0.69}$	$nan\pm^{nan}_{nan}$	2.67
ton28	0.21259 (#301)	116.22(89)	84885	36	83740	41	$193\pm^{24}_{22}$	1.00	26.1919	$0.89\pm^{699.95}_{2.51}$	$15.42\pm^{0.69}_{nan}$	0.06
ton28	0.24292 (#302)	105.70(82)	83762	37	86136	41	$178\pm^{26}_{24}$	1.00	26.8471	$-2.01\pm^{1.89}_{0.96}$	$nan\pm^{nan}_{nan}$	1.35
ton28	0.24859 (#303*)	126.01(83)	83842	34	86136	36	$232\pm^{28}_{26}$	1.00	26.9695	$-1.05\pm^{3.86}_{1.10}$	$nan\pm^{nan}_{nan}$	0.31
ton28	0.27338 (#304)	112.36(81)	83758	31	86136	36	$267\pm^{32}_{30}$	1.00	27.5050	$-1.96\pm^{1.29}_{0.72}$	$nan\pm^{nan}_{nan}$	2.14
ton28	0.33021 (#305)	117.99(85)	83660	49	84983	57	$277\pm^{37}_{34}$	1.00	28.7325	$-0.78\pm^{170.49}_{1.47}$	$nan\pm^{nan}_{nan}$	0.08
tons180	0.02340 (#306)	40.94(32)	193565	8	nan	nan	$1151\pm^{32}_{30}$	1.00	22.1054	$0.86\pm^{2.71}_{1.07}$	$15.40\pm^{0.37}_{nan}$	0.73
tons180	0.04360 (#307)	48.00(45)	180786	8	nan	nan	$1149\pm^{28}_{27}$	1.00	22.5418	$0.29\pm^{1.61}_{0.84}$	$14.99\pm^{0.64}_{nan}$	0.10
tons180	0.04560 (#308)	39.89(45)	180786	8	nan	nan	$1198\pm^{28}_{27}$	1.00	22.5850	$69.38\pm^{4.72E+03}_{56.06}$	$16.02\pm^{0.11}_{0.11}$	14.42

Table B.2: O VII upper limit measurements with *XMM-Newton* data, at the prior redshift from the O VI lines from Table A.1. The τ_0 in this table is calculated through the previous table's τ_0 errors, given by Equation 3.7. The corresponding column density was calculated using this value.

Target line		cmin	RGS1	RGS2	power–law		line component			ΔC
Name	z	(d.o.f.)	avg exp (s)	avg exp (s)	norm.	index	λ (Å)	τ_0	$\log N + (\mathrm{cm}^{-2})$	(d.o.f.)
1es1028	0.12314 (#1)	95.40(79)	144787	147275	$1102\pm^{30}_{30}$	1.00	24.2598	1.31	15.53	0.40
1es1028	0.13706 (#2)	92.82(90)	143804	146370	$1121\pm^{33}_{32}$	1.00	24.5605	0.71	15.33	0.22
1es1028	0.33735 (#3)	86.46(91)	145450	146420	$1324\pm^{48}_{46}$	1.00	28.8868	0.70	15.33	1.08
1es1553	0.18759 (#4)	102.10(88)	1793737	1757303	$1796\pm^{13}_{12}$	1.00	25.6519	0.29	14.99	7.82
1es1553	0.18775 (#5)	102.34(88)	1793737	1757303	$1796\pm^{13}_{12}$	1.00	25.6554	0.27	14.97	7.53
1es1553	0.18984 (#6)	105.72(86)	1794800	1753128	$1778\pm^{12}_{12}$	1.00	25.7005	0.20	14.85	0.16
1es1553	0.21631 (#7)	84.95(81)	1756247	1757203	$1778\pm^{14}_{14}$	1.00	26.2723	0.24	14.91	0.95
1es1553	0.31130 (#8)	113.79(90)	1740303	1677696	$1807\pm^{15}_{15}$	1.00	28.3241	0.24	14.92	0.45
1es1553	0.37868 (#9)	119.25(98)	1809416	1817188	$1834\pm^{17}_{17}$	1.00	29.7795	0.44	15.16	-0.04
1es1553	0.39497 (#10)	90.13(98)	1751580	1813451	$1810\pm^{18}_{18}$	1.00	30.1314	0.31	15.02	0.02
3c249	0.24676 (#11)	78.14(93)	2639	2524	$282\pm^{141}_{104}$	1.00	26.9300	5.33E+11	16.40	0.03
3c249	0.30788 (#12)	81.25(88)	2639	2535	$697\pm^{234}_{175}$	1.00	28.2502	5.00E+19	16.46	0.35
3c249	0.30809 (#13)	81.15(88)	2639	2535	$701\pm^{236}_{177}$	1.00	28.2547	5.00E+19	16.46	0.47
3c249	0.31364 (#14)	78.36(88)	2639	2538	$758\pm^{250}_{193}$	1.00	28.3746	5.00E+19	16.46	1.72
3c273	0.00337 (#15)	–	–	–	–	–	21.6728	–	–	–
3c273	0.00533 (#16)	–	–	–	–	–	21.7151	–	–	–
3c273	0.00764 (#17)	–	–	–	–	–	21.7650	–	–	–
3c273	0.02947 (#18*)	61.61(38)	995937	nan	$4600\pm^{1762}_{886}$	0.84	22.2366	0.21	14.86	-0.00
3c273	0.04898 (#19)	63.63(45)	936604	nan	$1268\pm^{345}_{291}$	3.02	22.6580	0.23	14.91	0.84
3c273	0.06655 (#20*)	153.93(46)	912160	nan	$1021\pm^{260}_{212}$	3.36	23.0375	0.17	14.79	10.40
3c273	0.09018 (#21*)	100.60(47)	996642	nan	$931\pm^{250}_{186}$	3.57	23.5479	0.76	15.35	78.29
3c273	0.12007 (#22)	53.39(62)	1024121	1027398	$1102\pm^{252}_{235}$	3.32	24.1935	0.16	14.75	2.79
3c273	0.14660 (#23)	91.01(79)	921050	1030884	$2069\pm^{402}_{386}$	2.37	24.7666	0.27	14.97	17.90
3c273	0.15784 (#24)	115.64(86)	931929	1033805	$1143\pm^{230}_{202}$	3.21	25.0093	0.15	14.73	1.10
h1821	0.02438 (#25)	–	–	–	–	–	22.1266	–	–	–
h1821	0.10817 (#26)	95.28(70)	31345	42458	$1133\pm^{91}_{88}$	1.00	23.9365	398.31	16.08	0.11
h1821	0.12133 (#27)	100.65(84)	29451	43368	$1293\pm^{89}_{87}$	1.00	24.2207	1.29E+03	16.12	1.69
h1821	0.12147 (#28)	100.41(84)	29451	43368	$1292\pm^{89}_{85}$	1.00	24.2238	1.32E+04	16.15	1.90
h1821	0.16992 (#29)	141.11(98)	32964	42688	$1380\pm^{94}_{90}$	1.00	25.2703	1.11	15.48	0.88
h1821	0.17043 (#30)	142.88(98)	32977	42408	$1382\pm^{93}_{90}$	1.00	25.2813	0.87	15.40	1.58

h1821	0.21326 (#31)	109.00(98)	31699	41854	$1642\pm^{109}_{108}$	1.00	26.2064	1.73E+07	16.29	2.96
h1821	0.22497 (#32)	122.07(98)	32383	43022	$1546\pm^{108}_{106}$	1.00	26.4594	2.43	15.70	0.03
h1821	0.22522 (#33)	122.01(98)	32383	43022	$1543\pm^{109}_{106}$	1.00	26.4648	1.88	15.63	0.10
h1821	0.22639 (#34)	119.71(98)	32358	43044	$1535\pm^{108}_{104}$	1.00	26.4900	1.04	15.45	0.95
h1821	0.24531 (#35)	119.80(98)	31065	44448	$1591\pm^{120}_{113}$	1.00	26.8987	9.68	15.89	0.06
h1821	0.26657 (#36)	111.36(98)	30604	44448	$1501\pm^{135}_{123}$	1.00	27.3579	1.18E+07	16.26	3.28
h1821	0.28800 (#37)	134.30(98)	30054	39392	$1661\pm^{136}_{133}$	1.00	27.8208	1.42E+05	16.21	1.58
h1821	0.29658 (#38)	134.83(98)	31075	39131	$1569\pm^{132}_{127}$	1.00	28.0061	0.61	15.28	6.80
h1821	0.29680 (#39)	135.23(98)	31075	39131	$1574\pm^{131}_{127}$	1.00	28.0109	0.57	15.25	6.28
h2356	0.11461 (#40)	85.19(77)	491451	516214	$1312\pm^{17}_{17}$	1.00	24.0756	0.60	15.28	1.54
h2356	0.16512 (#41)	111.39(97)	497056	504552	$1325\pm^{18}_{18}$	1.00	25.1666	0.48	15.19	0.06
he0056	0.16392 (#42)	96.42(92)	162630	161955	$479\pm^{20}_{19}$	1.00	25.1407	1.34	15.54	-0.00
he0056	0.16492 (#43)	99.30(92)	162629	161955	$478\pm^{20}_{19}$	1.00	25.1623	1.23	15.51	0.02
he0226	0.01746 (#44)	23.70(19)	31712	nan	$123\pm^{40}_{35}$	1.00	21.9771	3.27	15.75	0.85
he0226	0.02679 (#45)	39.57(27)	31712	nan	$114\pm^{31}_{27}$	1.00	22.1787	1.19E+04	16.15	0.51
he0226	0.04121 (#46)	45.84(33)	31712	nan	$158\pm^{38}_{27}$	1.00	22.4901	5.00E+19	16.41	0.70
he0226	0.04535 (#47)	43.77(36)	31712	nan	$177\pm^{31}_{29}$	1.00	22.5796	5.00E+19	16.46	3.25
he0226	0.04609 (#48)	44.36(37)	31712	nan	$176\pm^{42}_{29}$	1.00	22.5955	5.00E+19	16.46	3.70
he0226	0.06015 (#49)	53.36(41)	31712	nan	$149\pm^{30}_{27}$	1.00	22.8992	122.85	16.03	0.40
he0226	0.06083 (#50)	51.97(41)	31712	nan	$141\pm^{29}_{26}$	1.00	22.9139	2.12	15.67	1.36
he0226	0.07023 (#51)	37.36(40)	31713	nan	$187\pm^{31}_{30}$	1.00	23.1170	5.00E+19	16.41	0.11
he0226	0.08375 (#52)	44.35(43)	31713	nan	$188\pm^{31}_{29}$	1.00	23.4090	151.54	16.01	0.56
he0226	0.08901 (#53)	43.41(45)	31713	nan	$177\pm^{31}_{27}$	1.00	23.5226	5.10E+16	16.46	0.17
he0226	0.08938 (#54)	43.45(45)	31713	nan	$177\pm^{28}_{26}$	1.00	23.5306	5.00E+19	16.46	0.44
he0226	0.08950 (#55)	43.43(45)	31713	nan	$177\pm^{30}_{25}$	1.00	23.5332	5.00E+19	16.41	0.45
he0226	0.09220 (#56)	50.37(48)	31713	31705	$158\pm^{28}_{27}$	1.00	23.5915	1.51E+14	16.41	0.00
he0226	0.10668 (#57)	72.04(63)	31713	31705	$193\pm^{37}_{27}$	1.00	23.9043	5.00E+19	16.46	2.49
he0226	0.11514 (#58)	76.88(72)	31713	31705	$222\pm^{39}_{30}$	1.00	24.0870	5.00E+19	16.41	2.99
he0226	0.11680 (#59)	80.69(74)	31713	31705	$229\pm^{34}_{28}$	1.00	24.1229	5.00E+19	16.41	0.56
he0226	0.11733 (#60)	85.55(74)	31713	31705	$230\pm^{32}_{28}$	1.00	24.1343	5.00E+19	16.41	0.27
he0226	0.12589 (#61)	80.14(78)	31713	31705	$242\pm^{34}_{31}$	1.00	24.3192	30.29	15.97	0.16
he0226	0.13832 (#62)	83.89(87)	31710	31705	$263\pm^{36}_{33}$	1.00	24.5877	2.36	15.69	0.65
he0226	0.15175 (#63)	89.30(91)	31708	31705	$251\pm^{34}_{31}$	1.00	24.8778	5.58E+03	16.15	0.00
he0226	0.15549 (#64)	93.36(91)	31708	31705	$240\pm^{34}_{31}$	1.00	24.9586	2.86E+07	16.30	0.18
he0226	0.16237 (#65)	100.56(90)	31707	31705	$223\pm^{34}_{30}$	1.00	25.1072	1.57E+08	16.34	0.28
he0226	0.16339 (#66)	99.03(90)	31706	31705	$228\pm^{34}_{29}$	1.00	25.1292	5.00E+19	16.41	1.02
he0226	0.16971 (#67)	101.88(94)	31706	31705	$234\pm^{33}_{30}$	1.00	25.2657	31.62	15.98	0.13

he0226	0.18619 (#68)	124.06(95)	31706	31705	$245\pm^{33}_{30}$	1.00	25.6217	2.16	15.66	0.65
he0226	0.18811 (#69)	120.64(94)	31706	31704	$254\pm^{34}_{31}$	1.00	25.6632	2.23	15.68	0.71
he0226	0.18891 (#70)	118.10(94)	31706	31704	$247\pm^{33}_{31}$	1.00	25.6805	1.68	15.60	1.08
he0226	0.19374 (#71)	104.01(94)	31706	31704	$234\pm^{33}_{31}$	1.00	25.7848	0.97	15.45	5.57
he0226	0.19453 (#72)	106.55(94)	31706	31704	$233\pm^{33}_{31}$	1.00	25.8018	0.88	15.41	6.18
he0226	0.19860 (#73)	120.02(93)	31706	31704	$266\pm^{35}_{32}$	1.00	25.8898	4.25	15.80	0.39
he0226	0.20055 (#74)	120.40(93)	31706	31704	$280\pm^{35}_{33}$	1.00	25.9319	1.07E+05	16.22	0.23
he0226	0.20703 (#75)	112.17(93)	31706	31704	$314\pm^{36}_{34}$	1.00	26.0718	2.03E+15	16.42	1.31
he0226	0.22009 (#76)	120.76(87)	31706	31704	$255\pm^{37}_{34}$	1.00	26.3539	7.21	15.87	0.19
he0226	0.22099 (#77)	119.34(87)	31706	31704	$260\pm^{36}_{34}$	1.00	26.3734	1.49E+05	16.22	0.27
he0226	0.23009 (#78)	123.04(89)	31707	31704	$282\pm^{39}_{35}$	1.00	26.5699	1.15E+04	16.14	0.00
he0226	0.23964 (#79)	122.92(92)	31707	31704	$314\pm^{41}_{38}$	1.00	26.7762	1.07E+13	16.37	1.38
he0226	0.24522 (#80)	115.07(90)	31708	31704	$293\pm^{42}_{39}$	1.00	26.8968	800.78	16.09	0.00
he0226	0.25099 (#81)	119.85(90)	31708	31704	$270\pm^{40}_{37}$	1.00	27.0214	3.49	15.77	0.34
he0226	0.27155 (#82)	120.66(94)	31709	31704	$262\pm^{40}_{37}$	1.00	27.4655	2.90E+09	16.34	1.18
he0226	0.27956 (#83)	118.26(89)	31709	31704	$292\pm^{43}_{39}$	1.00	27.6385	5.00E+19	16.41	2.01
he0226	0.28041 (#84)	121.45(88)	31709	31704	$281\pm^{46}_{39}$	1.00	27.6569	5.00E+19	16.41	0.86
he0226	0.29134 (#85)	114.15(85)	31709	31707	$303\pm^{45}_{41}$	1.00	27.8929	377.22	16.04	0.04
he0226	0.29213 (#86)	114.62(85)	31709	31707	$318\pm^{47}_{42}$	1.00	27.9100	2.36E+06	16.23	0.06
he0226	0.30939 (#87)	100.48(87)	31709	31713	$363\pm^{48}_{46}$	1.00	28.2828	2.14E+05	16.22	0.00
he0226	0.31833 (#88)	104.18(83)	31709	31716	$375\pm^{58}_{51}$	1.00	28.4759	1.43E+11	16.36	0.06
he0226	0.33965 (#89)	125.18(89)	31713	31717	$336\pm^{56}_{52}$	1.00	28.9364	5.00E+19	16.46	2.50
he0226	0.34036 (#90)	130.69(90)	31713	31717	$335\pm^{56}_{52}$	1.00	28.9518	5.00E+19	16.46	1.44
he0226	0.35493 (#91)	120.67(92)	31716	31717	$281\pm^{58}_{52}$	1.00	29.2665	1.04	15.45	3.03
he0226	0.35528 (#92)	120.85(92)	31716	31717	$282\pm^{58}_{53}$	1.00	29.2740	1.19	15.51	2.77
he0226	0.37281 (#93)	111.76(99)	31717	31717	$352\pm^{79}_{56}$	1.00	29.6527	5.00E+19	16.46	2.58
he0226	0.38420 (#94)	114.74(94)	31717	31717	$360\pm^{63}_{58}$	1.00	29.8987	3.90E+09	16.31	0.03
he0226	0.38636 (#95)	107.14(90)	31717	31717	$355\pm^{72}_{57}$	1.00	29.9454	5.00E+19	16.41	0.74
he0226	0.39642 (#96)	117.89(86)	31717	31717	$283\pm^{60}_{53}$	1.00	30.1627	5.75	15.85	0.48
he0226	0.39692 (#97)	121.57(86)	31717	31717	$282\pm^{62}_{55}$	1.00	30.1735	9.22E+03	16.17	0.04
he0226	0.39890 (#98)	118.58(86)	31717	31717	$289\pm^{62}_{55}$	1.00	30.2162	1.57E+03	16.13	0.18
he0226	0.40034 (#99)	117.15(85)	31717	31717	$273\pm^{59}_{53}$	1.00	30.2473	1.26	15.52	2.43
he0226	0.40274 (#100)	121.91(83)	31717	31717	$307\pm^{63}_{57}$	1.00	30.2992	2.44E+06	16.23	0.03
he0226	0.49225 (#101)	130.27(93)	31722	31717	$423\pm^{80}_{73}$	1.00	32.2326	2.00	15.64	1.03
he0226	0.49254 (#102)	123.54(92)	31722	31717	$434\pm^{80}_{74}$	1.00	32.2389	2.39	15.68	0.77
he0226	0.49280 (#103)	123.59(92)	31722	31717	$435\pm^{81}_{74}$	1.00	32.2445	2.78	15.70	0.70
he0226	0.49309 (#104)	129.01(93)	31722	31717	$423\pm^{79}_{73}$	1.00	32.2507	2.86	15.73	0.71

i22456	0.09858 (#105)	68.71(60)	79883	72481	$656\pm^{39}_{37}$	1.00	23.7293	15.89	15.93	0.02
i22456	0.09895 (#106)	68.38(60)	79752	73453	$659\pm^{38}_{37}$	1.00	23.7373	14.53	15.90	0.01
i22456	0.09931 (#107)	68.39(60)	79752	73453	$657\pm^{37}_{37}$	1.00	23.7451	7.91	15.86	0.00
i22456	0.09959 (#108)	74.98(61)	79883	73453	$669\pm^{37}_{37}$	1.00	23.7511	4.44	15.81	0.00
i22456	0.09989 (#109)	68.68(61)	79752	74286	$651\pm^{38}_{37}$	1.00	23.7576	2.19	15.67	0.18
i22456	0.10034 (#110)	69.76(62)	79883	74286	$656\pm^{37}_{37}$	1.00	23.7673	1.77	15.61	0.30
i22456	0.10101 (#111)	73.32(62)	79121	75007	$657\pm^{38}_{37}$	1.00	23.7818	1.90	15.64	0.26
i22456	0.10146 (#112)	75.43(63)	77663	75007	$665\pm^{36}_{42}$	1.00	23.7915	3.02	15.74	0.02
mr2251	0.01070 (#113)	–	–	–	–	–	21.8311	–	–	–
mrk421	0.01009 (#114)	–	–	–	–	–	21.8179	–	–	–
mrk876	0.00311 (#115)	–	–	–	–	–	21.6672	–	–	–
mrk876	0.06248 (#116)	41.89(45)	2651	nan	$495\pm^{152}_{120}$	1.00	22.9496	5.00E+19	16.46	0.83
mrk876	0.08579 (#117)	36.44(46)	2765	nan	$357\pm^{118}_{97}$	1.00	23.4531	5.00E+19	16.46	1.63
mrk876	0.11488 (#118)	73.35(75)	2743	2633	$529\pm^{144}_{121}$	1.00	24.0814	5.00E+19	16.46	0.00
mrk876	0.11517 (#119)	75.24(76)	2746	2633	$567\pm^{149}_{126}$	1.00	24.0877	5.00E+19	16.41	0.05
mrk876	0.11588 (#120)	76.60(76)	2743	2636	$603\pm^{153}_{130}$	1.00	24.1030	5.00E+19	16.46	0.14
ngc7469	0.00962 (#121)	–	–	–	–	–	21.8078	–	–	–
ngc7469	0.00994 (#122)	–	–	–	–	–	21.8147	–	–	–
ngc7469	0.01153 (#123)	–	–	–	–	–	21.8490	–	–	–
p1103	0.13556 (#124)	87.53(87)	15673	15681	$3494\pm^{169}_{164}$	1.00	24.5281	1.00	15.45	0.47
p1103	0.13937 (#125)	91.46(88)	15673	15681	$3603\pm^{170}_{165}$	1.00	24.6104	9.42	15.89	0.98
p1103	0.14099 (#126)	96.68(88)	15673	15681	$3562\pm^{166}_{161}$	1.00	24.6454	1.08	15.47	0.24
p1103	0.14126 (#127)	97.21(89)	15673	15681	$3537\pm^{166}_{160}$	1.00	24.6512	0.95	15.43	0.62
p1103	0.17277 (#128)	83.97(94)	15671	15681	$3424\pm^{156}_{152}$	1.00	25.3318	0.99	15.45	0.61
pg0003	0.16521 (#129)	110.21(91)	13034	12941	$284\pm^{60}_{53}$	1.00	25.1685	5.36	15.83	0.44
pg0003	0.20907 (#130)	119.20(94)	13033	12875	$302\pm^{63}_{55}$	1.00	26.1159	207.54	16.10	0.18
pg0003	0.29021 (#131)	124.39(88)	13035	12849	$347\pm^{85}_{74}$	1.00	27.8685	2.33E+04	16.16	0.03
pg0003	0.30551 (#132*)	138.04(89)	13035	12885	$291\pm^{75}_{64}$	1.00	28.1990	1.74	15.61	1.53
pg0003	0.30569 (#133*)	137.89(89)	13035	12885	$292\pm^{74}_{64}$	1.00	28.2029	1.76	15.62	1.68
pg0003	0.34757 (#134)	105.38(90)	13039	12932	$231\pm^{86}_{68}$	1.00	29.1075	1.22	15.51	4.27
pg0003	0.34788 (#135)	105.00(90)	13039	12932	$229\pm^{84}_{68}$	1.00	29.1142	1.28	15.53	4.76
pg0003	0.36452 (#136)	126.87(94)	13041	12932	$361\pm^{143}_{107}$	1.00	29.4736	5.00E+19	16.41	2.32
pg0003	0.36508 (#137)	128.24(95)	13041	12932	$358\pm^{99}_{86}$	1.00	29.4857	5.00E+19	16.46	3.18
pg0003	0.36572 (#138)	128.74(97)	13041	12932	$356\pm^{99}_{85}$	1.00	29.4996	5.00E+19	16.46	3.55
pg0003	0.36621 (#139)	130.11(96)	13041	12932	$349\pm^{116}_{93}$	1.00	29.5101	5.00E+19	16.46	3.05
pg0003	0.37029 (#140)	139.10(98)	13041	12932	$313\pm^{91}_{78}$	1.00	29.5983	5.00E+19	16.46	0.44
pg0003	0.38608 (#141)	106.39(88)	13041	12920	$115\pm^{65}_{46}$	1.00	29.9393	0.83	15.39	13.26

pg0003	0.38639 (#142)	114.18(87)	13041	12920	$151\pm^{74}_{56}$	1.00	29.9460	1.17	15.51	8.98
pg0003	0.40138 (#143)	124.56(86)	13041	12886	$432\pm^{127}_{117}$	1.00	30.2698	5.00E+19	16.46	2.95
pg0003	0.42192 (#144)	120.23(94)	13041	12843	$378\pm^{116}_{97}$	1.00	30.7135	1.35E+06	16.25	0.26
pg0157	0.14621 (#145)	89.37(90)	3707	3516	$333\pm^{101}_{84}$	1.00	24.7581	5.00E+19	16.46	0.32
pg0804	0.00382 (#146)	–	–	–	–	–	21.6825	–	–	–
pg0804	0.01851 (#147)	16.80(23)	29128	nan	$945\pm^{97}_{92}$	1.00	21.9998	1.20	15.51	1.89
pg0804	0.10216 (#148)	79.20(62)	28053	28091	$1727\pm^{87}_{84}$	1.00	23.8067	1.96	15.64	0.11
pg0804	0.10230 (#149)	79.21(62)	28053	28091	$1728\pm^{87}_{84}$	1.00	23.8097	1.99	15.66	0.10
pg0832	0.10772 (#150)	80.67(64)	20655	20637	$76\pm^{24}_{21}$	1.00	23.9268	2.10	15.66	1.33
pg0832	0.13230 (#151)	108.67(84)	20655	20637	$61\pm^{24}_{19}$	1.00	24.4577	5.00E+19	16.46	0.01
pg0832	0.15276 (#152)	120.88(91)	20654	20637	$47\pm^{21}_{16}$	1.00	24.8996	5.00E+19	16.41	0.35
pg0832	0.23308 (#153)	129.97(95)	20655	20637	$82\pm^{28}_{23}$	1.00	26.6345	5.01E+03	16.12	0.58
pg0832	0.32567 (#154)	75.57(61)	20656	20645	$67\pm^{36}_{26}$	1.00	28.6345	5.00E+19	16.41	0.03
pg0953	0.01560 (#155)	28.56(26)	12792	nan	$420\pm^{81}_{73}$	1.00	21.9370	1.99	15.66	1.29
pg0953	0.05891 (#156)	62.59(44)	12792	nan	$452\pm^{68}_{62}$	1.00	22.8725	101.52	16.01	0.26
pg0953	0.06807 (#157)	48.31(41)	12792	nan	$546\pm^{89}_{74}$	1.00	23.0703	5.00E+19	16.46	3.12
pg0953	0.11827 (#158)	75.73(75)	12792	12309	$500\pm^{67}_{61}$	1.00	24.1546	45.85	16.00	0.02
pg0953	0.14236 (#159)	105.46(88)	12786	12309	$548\pm^{75}_{68}$	1.00	24.6750	0.77	15.36	5.66
pg0953	0.14263 (#160)	109.34(89)	12785	12309	$547\pm^{74}_{69}$	1.00	24.6808	0.70	15.33	5.97
pg0953	0.14307 (#161)	107.64(88)	12785	12309	$540\pm^{74}_{68}$	1.00	24.6903	0.69	15.32	6.36
pg0953	0.22967 (#162)	126.93(87)	12777	12309	$692\pm^{88}_{81}$	1.00	26.5609	1.09	15.48	2.87
pg0953	0.23251 (#163)	116.37(87)	12777	12309	$645\pm^{85}_{78}$	1.00	26.6222	0.91	15.42	4.37
pg0953	0.23351 (#164)	118.01(88)	12777	12309	$650\pm^{85}_{78}$	1.00	26.6438	1.15	15.50	2.94
pg1115	0.12285 (#165)	111.34(78)	17510	16953	$307\pm^{48}_{44}$	1.00	24.2536	5.00E+19	16.41	3.46
pg1115	0.12313 (#166)	110.77(77)	17510	16953	$298\pm^{64}_{43}$	1.00	24.2596	5.00E+19	16.46	1.57
pg1115	0.13104 (#167*)	126.82(83)	17517	16953	$303\pm^{52}_{47}$	1.00	24.4305	3.92E+05	16.21	0.14
pg1115	0.15456 (#168*)	137.20(89)	17538	16953	$351\pm^{52}_{48}$	1.00	24.9385	8.10	15.88	0.22
pg1115	0.15467 (#169*)	137.21(89)	17538	16953	$351\pm^{53}_{48}$	1.00	24.9409	7.30	15.88	0.21
pg1116	0.05900 (#170)	49.53(36)	281330	nan	$597\pm^{19}_{19}$	1.00	22.8744	10.62	15.93	2.02
pg1116	0.05927 (#171)	43.85(35)	280940	nan	$590\pm^{19}_{19}$	1.00	22.8802	13.33	15.91	1.62
pg1116	0.11895 (#172)	95.95(79)	285653	287248	$652\pm^{16}_{16}$	1.00	24.1693	0.62	15.28	0.50
pg1116	0.13852 (#173)	94.61(91)	277702	291047	$693\pm^{19}_{19}$	1.00	24.5920	2.05	15.65	2.43
pg1116	0.16539 (#174)	104.05(93)	289660	291047	$750\pm^{19}_{19}$	1.00	25.1724	1.55	15.58	1.66
pg1116	0.16554 (#175)	100.41(92)	289658	290943	$751\pm^{19}_{19}$	1.00	25.1757	1.69	15.61	2.12
pg1116	0.16610 (#176)	106.71(93)	289658	291047	$760\pm^{19}_{19}$	1.00	25.1878	2.23	15.67	3.04
pg1116	0.16686 (#177)	105.29(92)	291239	290943	$756\pm^{19}_{19}$	1.00	25.2042	2.43	15.70	3.07
pg1116	0.17343 (#178)	112.47(96)	296094	285607	$756\pm^{18}_{18}$	1.00	25.3461	1.29	15.52	0.98

pg1211	0.00711 (#179)	–	–	–	–	–	21.7536	–	–	–
pg1211	0.05117 (#180)	45.23(34)	736547	nan	$672\pm^{13}_{13}$	1.00	22.7053	1.89E+05	16.21	13.49
pg1211	0.06449 (#181)	–	–	–	–	–	22.9930	–	–	–
pg1211	0.06491 (#182)	–	–	–	–	–	23.0021	–	–	–
pg1216	0.12362 (#183)	106.86(78)	11245	11258	$185\pm^{46}_{40}$	1.00	24.2702	5.00E+19	16.41	4.18
pg1216	0.12389 (#184)	105.56(77)	11245	11258	$183\pm^{66}_{49}$	1.00	24.2760	5.00E+19	16.46	2.64
pg1216	0.12463 (#185)	107.31(78)	11245	11258	$187\pm^{46}_{40}$	1.00	24.2920	5.00E+19	16.46	2.41
pg1216	0.12485 (#186)	106.17(77)	11245	11258	$186\pm^{46}_{40}$	1.00	24.2968	5.00E+19	16.46	1.71
pg1216	0.13499 (#187)	116.72(86)	11248	11258	$192\pm^{50}_{43}$	1.00	24.5158	5.30E+12	16.36	0.06
pg1216	0.26768 (#188)	113.01(93)	11258	11258	$223\pm^{67}_{53}$	1.00	27.3819	5.00E+19	16.46	0.14
pg1216	0.28199 (#189)	112.68(89)	11258	11258	$237\pm^{66}_{56}$	1.00	27.6910	2.97	15.73	0.87
pg1216	0.28237 (#190)	112.03(88)	11258	11258	$245\pm^{68}_{57}$	1.00	27.6992	166.16	16.01	0.43
pg1259	0.00220 (#191)	–	–	–	–	–	21.6475	–	–	–
pg1259	0.00762 (#192)	–	–	–	–	–	21.7646	–	–	–
pg1259	0.02217 (#193)	31.57(30)	11484	nan	$172\pm^{52}_{46}$	1.00	22.0789	5.00E+19	16.46	0.12
pg1259	0.04606 (#194)	45.32(42)	11485	nan	$178\pm^{51}_{39}$	1.00	22.5949	5.00E+19	16.46	1.04
pg1259	0.04650 (#195)	43.77(42)	11485	nan	$188\pm^{53}_{41}$	1.00	22.6044	5.00E+19	16.46	1.02
pg1259	0.19576 (#196)	107.87(92)	11483	11479	$236\pm^{54}_{46}$	1.00	25.8284	13.59	15.92	0.42
pg1259	0.21940 (#197)	110.09(92)	11483	11479	$267\pm^{65}_{56}$	1.00	26.3390	1.56E+05	16.23	0.10
pg1259	0.21953 (#198)	110.10(92)	11483	11479	$267\pm^{65}_{56}$	1.00	26.3418	4.06E+06	16.24	0.09
pg1259	0.22313 (#199)	105.90(93)	11483	11479	$275\pm^{64}_{56}$	1.00	26.4196	3.12E+09	16.33	0.00
pg1259	0.23284 (#200)	120.10(95)	11483	11479	$235\pm^{60}_{51}$	1.00	26.6293	5.00E+19	16.46	1.29
pg1259	0.23956 (#201)	123.67(95)	11483	11479	$179\pm^{54}_{45}$	1.00	26.7745	1.17E+14	16.41	0.01
pg1259	0.25973 (#202)	111.65(93)	11483	11479	$126\pm^{49}_{39}$	1.00	27.2102	5.00E+19	16.46	0.83
pg1259	0.31979 (#203)	80.12(82)	11483	11480	$296\pm^{92}_{70}$	1.00	28.5075	5.00E+19	16.46	0.67
pg1259	0.32472 (#204)	90.97(82)	11484	11480	$337\pm^{109}_{77}$	1.00	28.6140	5.00E+19	16.46	2.56
pg1307	0.14187 (#205)	117.92(89)	9837	9504	$210\pm^{60}_{45}$	1.00	24.6644	5.00E+19	16.46	0.58
pg1307	0.14214 (#206)	117.74(88)	9837	9504	$211\pm^{60}_{46}$	1.00	24.6702	5.00E+19	16.46	0.69
pg1309	0.17586 (#207)	112.33(93)	27265	26163	$153\pm^{28}_{25}$	1.00	25.3986	5.00E+19	16.46	3.00
pg1309	0.17745 (#208)	117.17(95)	27265	26163	$150\pm^{36}_{25}$	1.00	25.4329	5.00E+19	16.41	1.76
pg1309	0.17866 (#209)	121.37(94)	27265	26163	$155\pm^{35}_{25}$	1.00	25.4591	5.00E+19	16.46	2.13
pg1309	0.17930 (#210)	120.67(95)	27265	26163	$156\pm^{33}_{26}$	1.00	25.4729	5.00E+19	16.46	1.89
pg1309	0.17979 (#211)	121.42(94)	27265	26163	$157\pm^{29}_{25}$	1.00	25.4835	5.00E+19	16.46	1.65
pg1309	0.18069 (#212)	121.63(94)	27265	26163	$147\pm^{27}_{25}$	1.00	25.5029	5.00E+19	16.46	0.54
pg1309	0.18117 (#213)	119.61(95)	27265	26163	$144\pm^{29}_{25}$	1.00	25.5133	5.00E+19	16.46	0.17
pg1309	0.18139 (#214)	116.87(93)	27265	26163	$141\pm^{28}_{24}$	1.00	25.5180	5.00E+19	16.41	0.10
pg1309	0.18145 (#215)	116.88(93)	27265	26163	$141\pm^{29}_{25}$	1.00	25.5193	5.00E+19	16.46	0.09

pg1309	0.18192 (#216)	114.96(94)	27265	26163	$145\pm^{29}_{25}$	1.00	25.5295	5.00E+19	16.46	0.06
pg1309	0.18698 (#217)	107.23(91)	27265	26163	$158\pm^{35}_{26}$	1.00	25.6388	5.00E+19	16.46	1.76
pg1444	0.22031 (#218)	113.67(93)	17674	17137	$183\pm^{40}_{35}$	1.00	26.3587	1.70	15.61	1.34
pg1444	0.22676 (#219)	127.72(94)	17674	17137	$179\pm^{40}_{35}$	1.00	26.4980	4.83E+12	16.39	0.03
pg1444	0.26690 (#220)	132.30(93)	17674	17137	$145\pm^{39}_{33}$	1.00	27.3650	1.11	15.48	3.41
pg1444	0.26728 (#221)	132.11(94)	17674	17137	$146\pm^{40}_{34}$	1.00	27.3732	1.16	15.50	3.67
pg1444	0.26738 (#222)	132.08(94)	17674	17137	$146\pm^{40}_{34}$	1.00	27.3754	1.01	15.44	3.70
pg1444	0.26747 (#223)	127.49(93)	17674	17137	$143\pm^{39}_{33}$	1.00	27.3774	0.97	15.43	4.74
pg1626	0.13075 (#224)	124.04(83)	69157	68865	$386\pm^{48}_{46}$	1.00	24.4242	0.76	15.35	4.32
phl1811	0.07344 (#225)	–	–	–	–	–	23.1863	–	–	–
phl1811	0.07768 (#226)	–	–	–	–	–	23.2779	–	–	–
phl1811	0.08131 (#227)	–	–	–	–	–	23.3563	–	–	–
phl1811	0.13239 (#228)	–	–	–	–	–	24.4596	–	–	–
phl1811	0.13282 (#229)	–	–	–	–	–	24.4689	–	–	–
phl1811	0.13318 (#230)	–	–	–	–	–	24.4767	–	–	–
phl1811	0.13545 (#231)	–	–	–	–	–	24.5257	–	–	–
phl1811	0.15752 (#232)	–	–	–	–	–	25.0024	–	–	–
phl1811	0.15786 (#233)	–	–	–	–	–	25.0098	–	–	–
phl1811	0.17652 (#234)	118.26(84)	79254	77556	$35\pm^{12}_{11}$	1.00	25.4128	5.00E+19	16.46	1.08
phl1811	0.19157 (#235*)	164.17(89)	79254	76738	$35\pm^{13}_{11}$	1.00	25.7379	5.00E+19	16.41	0.13
phl1811	0.19194 (#236*)	167.21(88)	79254	76682	$34\pm^{13}_{11}$	1.00	25.7459	5.00E+19	16.46	0.06
phl1811	0.19220 (#237*)	167.23(88)	79254	76682	$34\pm^{12}_{11}$	1.00	25.7515	5.00E+19	16.46	0.03
pks0312	0.20188 (#238)	93.47(64)	23858	22982	$161\pm^{40}_{35}$	1.00	25.9606	5.00E+19	16.41	1.94
pks0312	0.20275 (#239*)	99.01(66)	23858	22982	$154\pm^{39}_{33}$	1.00	25.9794	5.00E+19	16.41	1.41
pks0405	0.09192 (#240)	67.08(46)	137245	nan	$358\pm^{19}_{18}$	1.00	23.5855	1.98	15.64	0.13
pks0405	0.09647 (#241)	69.21(48)	135771	138649	$361\pm^{19}_{19}$	1.00	23.6838	1.15	15.49	0.98
pks0405	0.14808 (#242)	88.65(90)	136323	137234	$373\pm^{19}_{19}$	1.00	24.7985	1.54	15.59	0.23
pks0405	0.16566 (#243)	79.70(91)	137140	137234	$394\pm^{21}_{20}$	1.00	25.1783	156.92	16.03	1.67
pks0405	0.16606 (#244)	79.75(92)	136407	137234	$395\pm^{21}_{20}$	1.00	25.1869	116.44	16.04	1.78
pks0405	0.16659 (#245)	78.27(91)	137924	137234	$394\pm^{21}_{20}$	1.00	25.1983	386.26	16.04	2.01
pks0405	0.16688 (#246)	78.15(91)	137924	137234	$395\pm^{21}_{20}$	1.00	25.2046	136.55	16.07	2.16
pks0405	0.16712 (#247)	83.54(92)	137941	137234	$391\pm^{21}_{20}$	1.00	25.2098	324.91	16.07	2.15
pks0405	0.18257 (#248)	113.72(95)	137986	136490	$365\pm^{20}_{19}$	1.00	25.5435	1.46	15.57	0.17
pks0405	0.18289 (#249)	114.40(96)	138000	136490	$365\pm^{20}_{19}$	1.00	25.5504	1.75	15.61	0.05
pks0405	0.24052 (#250)	109.18(95)	137976	138647	$413\pm^{23}_{22}$	1.00	26.7952	527.04	16.06	1.03
pks0405	0.24094 (#251)	104.97(95)	137961	138647	$410\pm^{23}_{22}$	1.00	26.8043	769.41	16.09	1.15
pks0405	0.24547 (#252)	98.26(94)	136439	138647	$386\pm^{23}_{23}$	1.00	26.9022	1.12	15.49	0.69

pks0405	0.29762 (#253)	98.20(89)	135766	137130	$382\pm^{27}_{26}$	1.00	28.0286	2.36	15.69	0.02
pks0405	0.34188 (#254)	98.93(90)	136321	138714	$379\pm^{29}_{28}$	1.00	28.9846	1.62	15.60	0.90
pks0405	0.34225 (#255)	98.19(90)	136322	138714	$381\pm^{29}_{28}$	1.00	28.9926	1.36	15.54	1.22
pks0405	0.35092 (#256)	86.77(91)	136325	138714	$392\pm^{32}_{31}$	1.00	29.1799	9.75E+08	16.29	2.55
pks0405	0.36075 (#257)	90.38(93)	137923	138714	$385\pm^{33}_{32}$	1.00	29.3922	5.90E+08	16.29	2.11
pks0405	0.36151 (#258)	92.10(93)	137923	138714	$376\pm^{32}_{32}$	1.00	29.4086	7.14E+04	16.21	1.10
pks0405	0.36329 (#259)	96.83(94)	138708	138714	$363\pm^{32}_{31}$	1.00	29.4471	2.23	15.68	0.16
pks0405	0.40570 (#260)	120.73(84)	137132	133905	$452\pm^{35}_{34}$	1.00	30.3631	1.13E+06	16.24	0.79
pks0405	0.40890 (#261)	110.16(86)	137167	134014	$491\pm^{42}_{35}$	1.00	30.4322	5.00E+19	16.46	6.95
pks0405	0.49505 (#262)	112.27(94)	138729	137202	$536\pm^{45}_{43}$	1.00	32.2931	0.74	15.34	3.45
pks0405	0.49530 (#263)	108.35(92)	138729	137169	$528\pm^{45}_{43}$	1.00	32.2985	0.84	15.40	4.18
pks0405	0.55506 (#264)	104.58(82)	132269	134976	$444\pm^{57}_{54}$	1.00	33.5893	5.00E+19	16.41	2.35
pks2005	0.06490 (#265)	59.89(42)	53473	nan	$2202\pm^{73}_{71}$	1.00	23.0018	0.93	15.42	0.74
pks2155	0.05405 (#266)	–	–	–	–	–	22.7675	–	–	–
pks2155	0.05707 (#267)	20.80(28)	1697089	nan	$679\pm^{108}_{82}$	4.85	22.8327	0.12	14.64	5.24
q0045	0.11052 (#268)	–	–	–	–	–	23.9872	–	–	–
q0045	0.13521 (#269)	–	–	–	–	–	24.5205	–	–	–
q1230	0.09518 (#270)	63.84(48)	39335	39139	$112\pm^{23}_{20}$	1.00	23.6559	5.00E+19	16.46	0.60
q1230	0.10318 (#271)	59.80(44)	39335	39139	$93\pm^{26}_{23}$	1.00	23.8287	1.68	15.61	2.91
q1230	0.10445 (#272)	62.04(47)	39335	39139	$100\pm^{26}_{23}$	1.00	23.8561	2.27	15.69	1.45
q1230	0.10530 (#273)	62.81(47)	39335	39139	$106\pm^{27}_{24}$	1.00	23.8745	9.63E+03	16.12	0.34
q1230	0.10596 (#274)	63.04(47)	39335	39139	$111\pm^{27}_{24}$	1.00	23.8887	1.15E+08	16.35	0.01
q1230	0.10666 (#275)	63.05(47)	39335	39139	$113\pm^{26}_{24}$	1.00	23.9039	1.65E+16	16.45	0.00
q1230	0.10809 (#276)	59.85(45)	39335	39139	$103\pm^{26}_{23}$	1.00	23.9347	5.00E+19	16.43	0.06
q1230	0.10820 (#277)	62.54(45)	39335	39139	$103\pm^{26}_{23}$	1.00	23.9371	5.00E+19	16.43	0.08
q1230	0.10861 (#278)	59.64(45)	39335	39139	$105\pm^{26}_{23}$	1.00	23.9460	5.00E+19	16.46	0.10
q1230	0.10906 (#279)	61.31(47)	39335	39139	$101\pm^{26}_{23}$	1.00	23.9557	1.17E+16	16.45	0.20
q1230	0.10935 (#280)	61.34(47)	39335	39139	$102\pm^{26}_{23}$	1.00	23.9620	5.00E+19	16.46	0.16
q1230	0.10956 (#281)	61.25(46)	39335	39139	$107\pm^{27}_{24}$	1.00	23.9665	5.00E+19	16.41	0.07
q1230	0.11707 (#282)	70.22(56)	39335	39139	$120\pm^{31}_{23}$	1.00	24.1287	5.00E+19	16.46	1.38
q1230	0.11743 (#283)	71.60(58)	39335	39139	$121\pm^{30}_{24}$	1.00	24.1365	5.00E+19	16.44	1.25
q1230	0.11781 (#284)	71.89(58)	39335	39139	$120\pm^{26}_{23}$	1.00	24.1447	5.00E+19	16.46	0.91
rbs1892	0.15752 (#285)	86.45(91)	4935	4865	$220\pm^{84}_{67}$	1.00	25.0024	4.32	15.80	0.66
rbs1892	0.17133 (#286)	86.80(94)	4937	4865	$309\pm^{139}_{95}$	1.00	25.3007	5.00E+19	16.46	2.67
rbs1892	0.19874 (#287)	104.23(94)	4937	4849	$500\pm^{129}_{110}$	1.00	25.8928	6.72E+10	16.36	0.06
rbs542	0.10323 (#288)	86.68(64)	192553	181905	$1543\pm^{32}_{31}$	1.00	23.8298	1.01	15.46	0.16
rbs542	0.10379 (#289)	87.77(65)	192488	181905	$1551\pm^{32}_{32}$	1.00	23.8419	1.30	15.52	0.52

rxj0439	0.11547 (#290)	95.23(74)	148931	151265	$506\pm^{20}_{20}$	1.00	24.0942	1.86	15.63	-0.00
rxj0439	0.21833 (#291)	118.05(95)	147527	149811	$588\pm^{27}_{26}$	1.00	26.3159	10.59	15.92	1.26
rxj0439	0.24235 (#292)	94.71(94)	148524	152414	$592\pm^{28}_{27}$	1.00	26.8348	22.37	15.94	0.81
rxj0439	0.24258 (#293)	103.01(95)	147411	152414	$590\pm^{28}_{27}$	1.00	26.8397	15.08	15.95	0.92
rxj0439	0.24313 (#294)	94.82(94)	147411	152414	$592\pm^{28}_{27}$	1.00	26.8516	5.89	15.85	0.50
rxj0439	0.24387 (#295)	93.90(94)	147412	152414	$593\pm^{29}_{27}$	1.00	26.8676	2.17	15.66	0.04
s50716	0.23145 (#296)	93.47(94)	75297	76133	$887\pm^{42}_{41}$	1.00	26.5993	1.61	15.59	0.03
ton28	0.13746 (#297)	111.07(90)	83595	86028	$225\pm^{23}_{21}$	1.00	24.5691	1.75E+03	16.13	0.16
ton28	0.13773 (#298)	110.95(90)	83595	86028	$227\pm^{22}_{22}$	1.00	24.5750	1.91E+04	16.15	0.30
ton28	0.13781 (#299)	111.91(90)	83595	86028	$227\pm^{23}_{22}$	1.00	24.5767	3.51E+04	16.17	0.35
ton28	0.17251 (#300)	98.29(95)	86114	85104	$203\pm^{19}_{18}$	1.00	25.3262	0.91	15.42	2.67
ton28	0.21259 (#301)	116.22(89)	84885	83740	$193\pm^{24}_{22}$	1.00	26.1919	351.23	16.09	0.06
ton28	0.24292 (#302)	105.70(82)	83762	86136	$178\pm^{26}_{24}$	1.00	26.8471	1.43	15.56	1.35
ton28	0.24859 (#303*)	126.01(83)	83842	86136	$232\pm^{28}_{26}$	1.00	26.9695	2.48	15.69	0.31
ton28	0.27338 (#304)	112.36(81)	83758	86136	$267\pm^{32}_{30}$	1.00	27.5050	1.00	15.44	2.14
ton28	0.33021 (#305)	117.99(85)	83660	84983	$277\pm^{37}_{34}$	1.00	28.7325	85.98	16.00	0.08
tons180	0.02340 (#306)	40.94(32)	193565	nan	$1151\pm^{32}_{30}$	1.00	22.1054	1.89	15.64	0.73
tons180	0.04360 (#307)	48.00(45)	180786	nan	$1149\pm^{28}_{27}$	1.00	22.5418	1.23	15.50	0.10
tons180	0.04560 (#308)	39.89(45)	180786	nan	$1198\pm^{28}_{27}$	1.00	22.5850	2.39E+03	16.12	14.42

Table B.3: O VII measurements with *XMM-Newton* data, at the prior redshift from the H I lines from Table A.2.

Target line		cmin	RGS1		RGS2		power–law		line component			ΔC
Name	z	(d.o.f.)	avg exp (s)	%	avg exp (s)	%	norm.	index	λ (Å)	τ_0	$\log N(\mathrm{cm}^{-2})$	(d.o.f.)
1es1028	0.13714 (#1)	92.78(90)	143804	9	146370	7	$1121\pm^{32}_{32}$	1.00	24.5622	$-0.33\pm^{0.82}_{0.55}$	$nan\pm^{nan}_{nan}$	0.27
1es1028	0.20383 (#2)	114.22(94)	146421	9	145107	9	$1207\pm^{32}_{35}$	1.00	26.0027	$0.03\pm^{0.97}_{0.83}$	$14.01\pm^{1.43}_{nan}$	-0.01
1es1028	0.22121 (#3)	101.58(92)	144278	9	146704	9	$1198\pm^{35}_{35}$	1.00	26.3781	$-0.70\pm^{0.67}_{0.48}$	$nan\pm^{nan}_{nan}$	1.33
1es1553	0.03466 (#4)	38.25(27)	1791095	9	nan	nan	$747\pm^{397}_{326}$	1.97	22.3487	$-0.18\pm^{0.33}_{0.25}$	$nan\pm^{nan}_{nan}$	0.53
1es1553	0.04273 (#5)	30.79(21)	1784759	9	nan	nan	$489\pm^{628}_{294}$	2.72	22.5230	$0.51\pm^{0.64}_{0.44}$	$15.21\pm^{0.28}_{0.85}$	2.85
1es1553	0.06364 (#6*)	64.48(28)	1661330	9	nan	nan	$27\pm^{12}_{9}$	7.49	22.9746	$0.53\pm^{0.63}_{0.44}$	$15.22\pm^{0.27}_{0.73}$	1.84
1es1553	0.21869 (#7)	108.81(87)	1691684	7	1788288	8	$1010\pm^{415}_{304}$	1.74	26.3237	$-0.01\pm^{0.65}_{0.08}$	$nan\pm^{nan}_{nan}$	-0.07
3c249	0.13470 (#8)	67.71(86)	2642	7	2524	10	$336\pm^{146}_{105}$	1.00	24.5095	$9.67E+04\pm^{1.00E+20}_{9.68E+04}$	$16.21\pm^{0.25}_{nan}$	0.52
3c249	0.26664 (#9)	79.78(93)	2639	31	2524	59	$306\pm^{146}_{111}$	1.00	27.3594	$0.17\pm^{1.00E+20}_{30.17}$	$14.78\pm^{1.68}_{nan}$	-0.00
3c273	0.00758 (#10)	–	–	–	–	–	–	–	21.7637	–	–	–
3c273	0.06707 (#11*)	35.22(22)	897879	5	nan	nan	$4641\pm^{37}_{41}$	1.00	23.0487	$0.24\pm^{0.31}_{0.30}$	$14.91\pm^{0.32}_{nan}$	0.86
3c273	0.07359 (#12*)	45.49(29)	930374	5	nan	nan	$4656\pm^{32}_{34}$	1.00	23.1895	$-0.10\pm^{0.21}_{0.19}$	$nan\pm^{nan}_{nan}$	0.39
3c273	0.13960 (#13)	68.74(61)	892303	4	1027847	3	$5246\pm^{31}_{31}$	1.00	24.6154	$-0.39\pm^{0.12}_{0.11}$	$nan\pm^{nan}_{nan}$	12.82
h1821	0.00944 (#14)	–	–	–	–	–	–	–	21.8039	–	–	–
h1821	0.06779 (#15)	48.43(43)	28966	55	nan	nan	$1081\pm^{99}_{91}$	1.00	23.0643	$8.21E+04\pm^{1.00E+20}_{5.68E+04}$	$16.18\pm^{0.28}_{0.02}$	1.16
h1821	0.08483 (#16)	62.62(44)	31062	57	nan	nan	$1008\pm^{91}_{87}$	1.00	23.4323	$13.36\pm^{1.80E+08}_{14.39}$	$15.89\pm^{0.40}_{nan}$	0.54
h1821	0.12147 (#17)	96.56(82)	30593	48	43368	41	$1284\pm^{89}_{85}$	1.00	24.2238	$10.07\pm^{2.49E+04}_{9.53}$	$15.88\pm^{0.29}_{0.65}$	1.85
h1821	0.19817 (#18)	79.32(81)	32357	53	41356	43	$1363\pm^{112}_{109}$	1.00	25.8805	$-1.36\pm^{1.36}_{0.72}$	$nan\pm^{nan}_{nan}$	1.30
h1821	0.21321 (#19)	110.19(98)	31737	48	41863	43	$1644\pm^{133}_{107}$	1.00	26.2053	$18.57\pm^{4.34E+07}_{17.25}$	$15.96\pm^{0.34}_{0.44}$	2.38
h1821	0.24531 (#20)	119.80(98)	31065	49	44448	47	$1591\pm^{120}_{113}$	1.00	26.8987	$0.44\pm^{17.76}_{1.60}$	$15.15\pm^{0.78}_{nan}$	0.06
h2356	0.03830 (#21)	60.56(47)	466679	7	nan	nan	$1093\pm^{15}_{15}$	1.00	22.4273	$0.02\pm^{0.48}_{0.70}$	$13.78\pm^{1.43}_{nan}$	-0.02
h2356	0.07881 (#22)	44.92(38)	468683	8	nan	nan	$1173\pm^{21}_{20}$	1.00	23.3023	$-0.79\pm^{0.59}_{0.46}$	$nan\pm^{nan}_{nan}$	2.04
h2356	0.10467 (#23)	52.51(56)	471489	8	510756	5	$1280\pm^{22}_{21}$	1.00	23.8609	$0.71\pm^{1.17}_{0.68}$	$15.33\pm^{0.30}_{1.43}$	1.39
h2356	0.15613 (#24)	105.03(97)	482157	6	504552	6	$1323\pm^{19}_{19}$	1.00	24.9724	$0.62\pm^{0.66}_{0.49}$	$15.29\pm^{0.24}_{0.62}$	2.10
he0226	0.14274 (#25)	83.16(89)	31710	21	31705	24	$257\pm^{34}_{31}$	1.00	24.6832	$-1.95\pm^{2.49}_{0.98}$	$nan\pm^{nan}_{nan}$	0.97
he0226	0.39890 (#26)	85.66(67)	31717	39	31717	70	$409\pm^{80}_{73}$	1.00	30.2162	$0.54\pm^{7.93E+07}_{30.54}$	$15.23\pm^{1.08}_{nan}$	0.01
he0226	0.41024 (#27)	81.69(56)	31717	38	31717	67	$421\pm^{91}_{82}$	1.00	30.4612	$0.21\pm^{4.66E+08}_{2.98}$	$14.87\pm^{1.42}_{nan}$	0.00
i22456	0.00443 (#28)	–	–	–	–	–	–	–	21.6957	–	–	–
i22456	0.09941 (#29)	74.98(61)	79883	51	73453	44	$671\pm^{38}_{37}$	1.00	23.7473	$0.18\pm^{15.96}_{1.63}$	$14.80\pm^{1.12}_{nan}$	0.00
mr2251	0.01068 (#30)	–	–	–	–	–	–	–	21.8307	–	–	–
mr2251	0.01449 (#31)	37.36(27)	446548	6	nan	nan	$2964\pm^{3361}_{1081}$	0.01	21.9130	$-0.65\pm^{0.43}_{0.34}$	$nan\pm^{nan}_{nan}$	2.50
mr2251	0.06131 (#32)	32.34(25)	452767	7	nan	nan	$117\pm^{170}_{69}$	5.55	22.9243	$2.49\pm^{13.28}_{1.77}$	$15.71\pm^{0.19}_{0.36}$	4.17
mr2251	0.06190 (#33)	29.54(24)	452283	7	nan	nan	$59\pm^{91}_{37}$	6.67	22.9370	$6.43\pm^{162.24}_{4.90}$	$15.86\pm^{0.16}_{0.29}$	5.95

mr2251	0.06276 (#34)	30.33(22)	451202	7	nan	nan	$57\pm^{104}_{37}$	6.71	22.9556	$3.48\pm^{9.04}_{2.61}$	$15.76\pm^{0.17}_{0.36}$	4.37
mr2251	0.06327 (#35*)	31.04(20)	449939	7	nan	nan	$30\pm^{81}_{20}$	7.77	22.9666	$1.82\pm^{4.06}_{1.51}$	$15.62\pm^{0.23}_{0.60}$	2.99
mr2251	0.06381 (#36*)	33.43(22)	451202	7	nan	nan	$148\pm^{162}_{116}$	5.14	22.9783	$0.01\pm^{0.93}_{0.65}$	$13.43\pm^{2.00}_{nan}$	-0.00
mrk478	0.06166 (#37)	61.33(42)	192118	15	nan	nan	$253\pm^{786}_{195}$	2.48	22.9319	$-0.49\pm^{5.63}_{1.27}$	$nan\pm^{nan}_{nan}$	0.07
mrk478	0.06578 (#38)	54.57(42)	192119	15	nan	nan	$606\pm^{1058}_{523}$	1.09	23.0208	$44.37\pm^{1.45E+06}_{45.85}$	$15.99\pm^{0.22}_{nan}$	3.82
mrk478	0.07213 (#39)	54.93(42)	192121	15	nan	nan	$640\pm^{1985}_{489}$	1.00	23.1580	$0.48\pm^{4.43}_{1.30}$	$15.19\pm^{0.63}_{nan}$	0.10
mrk876	0.01159 (#40)	–	–	–	–	–	–	–	21.8503	–	–	–
mrk876	0.05598 (#41)	44.97(46)	2714	12	nan	nan	$477\pm^{142}_{112}$	1.00	22.8092	$9.00E+03\pm^{1.00E+20}_{9.03E+03}$	$16.20\pm^{0.26}_{nan}$	0.21
mrk876	0.08709 (#42)	37.14(46)	2802	11	nan	nan	$345\pm^{146}_{103}$	1.00	23.4811	$2.64E+09\pm^{1.00E+20}_{2.64E+09}$	$16.35\pm^{0.11}_{inf}$	1.36
mrk876	0.08858 (#43)	37.69(46)	2802	10	nan	nan	$378\pm^{139}_{105}$	1.00	23.5133	$3.17E+12\pm^{1.00E+20}_{3.17E+12}$	$16.41\pm^{0.05}_{inf}$	1.70
mrk876	0.08917 (#44)	37.84(47)	2802	10	996	nan	$377\pm^{134}_{98}$	1.00	23.5261	$1.28E+13\pm^{1.00E+20}_{1.28E+13}$	$16.41\pm^{0.05}_{inf}$	1.65
mrk876	0.11487 (#45)	73.35(75)	2743	19	2633	28	$529\pm^{144}_{121}$	1.00	24.0812	$0.22\pm^{1.00E+20}_{30.22}$	$14.87\pm^{1.59}_{nan}$	0.00
ngc7469	0.00981 (#46)	–	–	–	–	–	–	–	21.8119	–	–	–
pg0003	0.08299 (#47)	59.05(43)	13037	19	nan	nan	$234\pm^{52}_{46}$	1.00	23.3926	$-3.31\pm^{3.02E+06}_{1.67}$	$nan\pm^{nan}_{nan}$	0.47
pg0003	0.17139 (#48)	111.61(94)	13033	24	12941	16	$332\pm^{65}_{54}$	1.00	25.3020	$14.29\pm^{1.08E+15}_{44.29}$	$15.93\pm^{0.50}_{nan}$	0.31
pg0003	0.22541 (#49)	114.13(94)	13034	39	12838	28	$231\pm^{58}_{50}$	1.00	26.4689	$0.46\pm^{3.20E+09}_{30.46}$	$15.17\pm^{1.17}_{nan}$	0.00
pg0003	0.38633 (#50)	104.20(85)	13041	125	12919	49	$115\pm^{65}_{47}$	1.00	29.9447	$-5.97\pm^{1.21}_{1.08}$	$nan\pm^{nan}_{nan}$	12.63
pg0003	0.42051 (#51)	114.71(91)	13041	92	12843	45	$362\pm^{115}_{95}$	1.00	30.6830	$-1.35\pm^{9.66E+09}_{2.59}$	$nan\pm^{nan}_{nan}$	0.06
pg0804	0.05015 (#52)	46.31(37)	27851	8	nan	nan	$1439\pm^{93}_{87}$	1.00	22.6832	$3.75E+05\pm^{1.00E+20}_{3.75E+05}$	$16.25\pm^{0.16}_{nan}$	7.42
pg0804	0.05576 (#53)	53.92(41)	28550	8	nan	nan	$1333\pm^{83}_{80}$	1.00	22.8044	$2.94\pm^{6.29E+04}_{32.94}$	$15.74\pm^{0.45}_{nan}$	0.29
pg0804	0.36379 (#54)	127.43(96)	29665	20	30901	12	$2024\pm^{141}_{134}$	1.00	29.4579	$-0.91\pm^{1.96}_{0.95}$	$nan\pm^{nan}_{nan}$	0.42
pg0832	0.01753 (#55)	–	–	–	–	–	–	–	21.9786	–	–	–
pg0832	0.02793 (#56)	52.15(36)	20654	133	nan	nan	$26\pm^{18}_{14}$	1.00	22.2033	$-6.69\pm^{1.61}_{1.73}$	$nan\pm^{nan}_{nan}$	9.82
pg0832	0.08748 (#57)	53.03(45)	20655	77	nan	nan	$71\pm^{25}_{19}$	1.00	23.4896	$1.15E+13\pm^{1.00E+20}_{1.15E+13}$	$16.41\pm^{0.05}_{inf}$	1.13
pg0832	0.10171 (#58)	73.57(56)	20655	68	20637	75	$84\pm^{30}_{22}$	1.00	23.7969	$3.93E+04\pm^{1.00E+20}_{3.94E+04}$	$16.21\pm^{0.25}_{nan}$	0.91
pg0832	0.18391 (#59)	60.33(41)	20654	143	20637	67	$70\pm^{54}_{32}$	1.00	25.5725	$1.66E+06\pm^{1.00E+20}_{1.66E+06}$	$16.28\pm^{0.12}_{nan}$	1.25
pg0832	0.27503 (#60)	124.41(86)	20656	150	20637	94	$58\pm^{29}_{21}$	1.00	27.5406	$-0.97\pm^{1.00E+20}_{29.03}$	$nan\pm^{nan}_{nan}$	0.01
pg0832	0.27694 (#61)	119.21(86)	20656	135	20637	95	$60\pm^{28}_{22}$	1.00	27.5819	$2.50\pm^{1.00E+20}_{32.50}$	$15.70\pm^{0.76}_{nan}$	0.02
pg0832	0.32572 (#62*)	136.80(85)	20656	238	20645	93	$51\pm^{28}_{20}$	1.00	28.6356	$-2.54\pm^{1.08E+05}_{2.21}$	$nan\pm^{nan}_{nan}$	0.31
pg0838	0.06583 (#63)	1.34(41)	1609	inf	nan	nan	$0\pm^{36}_{-0}$	1.00	23.0219	$2.00\pm^{1.00E+20}_{32.00}$	$15.64\pm^{0.82}_{nan}$	0.00
pg0838	0.08628 (#64)	16.24(44)	1609	90	nan	nan	$130\pm^{124}_{72}$	1.00	23.4636	$1.51E+04\pm^{1.00E+20}_{1.51E+04}$	$16.21\pm^{0.26}_{nan}$	0.17
pg0838	0.12676 (#65)	32.38(79)	1609	198	1519	38	$75\pm^{109}_{75}$	1.00	24.3380	$8.43E+12\pm^{1.00E+20}_{8.43E+12}$	$16.41\pm^{0.05}_{inf}$	0.75
pg0953	0.16319 (#66)	129.94(91)	12778	16	12309	8	$593\pm^{77}_{71}$	1.00	25.1249	$1.31\pm^{5.35E+03}_{2.85}$	$15.53\pm^{0.67}_{nan}$	0.09
pg0953	0.19221 (#67)	122.56(92)	12777	11	12309	10	$612\pm^{78}_{71}$	1.00	25.7517	$-0.51\pm^{475.06}_{1.65}$	$nan\pm^{nan}_{nan}$	0.03
pg1048	0.00642 (#68)	–	–	–	–	–	–	–	21.7387	–	–	–
pg1048	0.02414 (#69)	32.85(32)	18864	38	nan	nan	$156\pm^{38}_{33}$	1.00	22.1214	$61.26\pm^{1.00E+20}_{91.26}$	$16.02\pm^{0.38}_{nan}$	0.12
pg1115	0.09511 (#70)	47.02(50)	17510	31	16953	21	$325\pm^{54}_{46}$	1.00	23.6544	$7.12\pm^{1.00E+20}_{37.12}$	$15.85\pm^{0.56}_{nan}$	0.20

pg1115	0.12059 (#71)	98.56(73)	17510	33	16953	13	$310\pm^{48}_{44}$	1.00	24.2047	$1.36E+03\pm^{1.00E+20}_{1.39E+03}$	$16.12\pm^{0.34}_{nan}$	2.50
pg1115	0.12741 (#72)	107.59(76)	17513	30	16953	11	$311\pm^{51}_{47}$	1.00	24.3521	$0.00\pm^{8.23E+03}_{1.93}$	$13.12\pm^{3.04}_{nan}$	0.00
pg1116	0.04114 (#73)	41.06(39)	284047	15	nan	nan	$540\pm^{17}_{17}$	1.00	22.4886	$-0.84\pm^{0.90}_{0.61}$	$nan\pm^{nan}_{nan}$	1.16
pg1116	0.06251 (#74)	40.85(30)	283934	17	nan	nan	$549\pm^{22}_{21}$	1.00	22.9502	$1.33\pm^{140.93}_{2.32}$	$15.54\pm^{0.51}_{nan}$	0.23
pg1116	0.08382 (#75)	46.62(32)	284638	17	nan	nan	$588\pm^{22}_{18}$	1.00	23.4105	$2.02E+07\pm^{1.00E+20}_{1.99E+07}$	$16.29\pm^{0.17}_{0.08}$	8.15
pg1116	0.09210 (#76)	51.16(38)	292136	17	222826	11	$576\pm^{20}_{19}$	1.00	23.5894	$0.28\pm^{2.14}_{1.00}$	$14.98\pm^{0.72}_{nan}$	0.07
pg1116	0.09281 (#77)	50.89(38)	292136	17	222826	10	$579\pm^{19}_{19}$	1.00	23.6047	$0.59\pm^{2.86}_{1.14}$	$15.26\pm^{0.50}_{nan}$	0.25
pg1116	0.13373 (#78)	89.85(89)	277711	16	284726	12	$680\pm^{19}_{19}$	1.00	24.4886	$3.28\pm^{6.08}_{2.17}$	$15.75\pm^{0.16}_{0.28}$	5.37
pg1116	0.13851 (#79)	94.60(91)	277702	15	291047	12	$693\pm^{19}_{19}$	1.00	24.5918	$1.55\pm^{2.89}_{1.21}$	$15.58\pm^{0.23}_{0.53}$	2.45
pg1211	0.02586 (#80)	33.66(32)	769591	13	nan	nan	$575\pm^{12}_{12}$	1.00	22.1586	$-0.39\pm^{1.04}_{0.68}$	$nan\pm^{nan}_{nan}$	0.25
pg1211	0.05443 (#81)	49.81(35)	745965	14	nan	nan	$634\pm^{12}_{12}$	1.00	22.7757	$0.25\pm^{1.61}_{0.89}$	$14.94\pm^{0.70}_{nan}$	0.06
pg1216	0.00842 (#82)	–	–	–	–	–	–	–	21.7819	–	–	–
pg1216	0.07969 (#83)	53.17(43)	11245	40	nan	nan	$185\pm^{50}_{39}$	1.00	23.3213	$583.85\pm^{1.00E+20}_{613.85}$	$16.11\pm^{0.30}_{nan}$	0.44
pg1216	0.12372 (#84)	107.60(78)	11245	36	11258	15	$182\pm^{51}_{48}$	1.00	24.2724	$4.72E+06\pm^{1.00E+20}_{4.72E+06}$	$16.28\pm^{0.12}_{nan}$	3.27
pg1216	0.12473 (#85)	107.90(78)	11245	36	11258	15	$186\pm^{59}_{40}$	1.00	24.2942	$1.11E+04\pm^{1.00E+20}_{1.12E+04}$	$16.21\pm^{0.26}_{nan}$	1.76
pg1216	0.17950 (#86)	106.70(95)	11257	23	11258	31	$243\pm^{51}_{45}$	1.00	25.4772	$3.13E+09\pm^{1.00E+20}_{3.13E+09}$	$16.35\pm^{0.11}_{inf}$	2.17
pg1216	0.20014 (#87)	86.38(92)	11257	29	11258	46	$179\pm^{53}_{39}$	1.00	25.9230	$9.58E+05\pm^{1.00E+20}_{9.58E+05}$	$16.28\pm^{0.13}_{nan}$	1.23
pg1216	0.21258 (#88)	84.99(93)	11257	19	11258	27	$191\pm^{48}_{41}$	1.00	26.1917	$679.96\pm^{1.00E+20}_{709.96}$	$16.11\pm^{0.35}_{nan}$	0.49
pg1216	0.28204 (#89)	112.71(89)	11258	41	11258	68	$237\pm^{66}_{56}$	1.00	27.6921	$-2.70\pm^{5.32}_{1.34}$	$nan\pm^{nan}_{nan}$	0.83
pg1229	0.05018 (#90)	55.71(43)	24016	20	nan	nan	$521\pm^{63}_{49}$	1.00	22.6839	$2.38E+06\pm^{1.00E+20}_{2.38E+06}$	$16.28\pm^{0.12}_{nan}$	3.04
pg1259	0.05563 (#91)	50.01(43)	11485	47	nan	nan	$165\pm^{50}_{38}$	1.00	22.8016	$3.07E+09\pm^{1.00E+20}_{3.07E+09}$	$16.35\pm^{0.11}_{inf}$	0.63
pg1259	0.15136 (#92)	99.16(90)	11483	47	11479	39	$130\pm^{43}_{35}$	1.00	24.8694	$6.07\pm^{6.78E+16}_{36.07}$	$15.84\pm^{0.62}_{nan}$	0.08
pg1259	0.16647 (#93)	105.90(92)	11483	34	11479	49	$145\pm^{43}_{36}$	1.00	25.1958	$-2.40\pm^{9.65}_{1.49}$	$nan\pm^{nan}_{nan}$	0.61
pg1259	0.17893 (#94)	108.49(96)	11483	38	11479	42	$180\pm^{52}_{40}$	1.00	25.4649	$3.20E+04\pm^{1.00E+20}_{3.20E+04}$	$16.21\pm^{0.25}_{nan}$	0.92
pg1259	0.22376 (#95)	105.77(93)	11483	32	11479	49	$277\pm^{65}_{56}$	1.00	26.4332	$0.49\pm^{5.50E+12}_{30.49}$	$15.20\pm^{1.20}_{nan}$	0.01
pg1259	0.24126 (#96)	121.27(95)	11483	71	11479	62	$149\pm^{49}_{40}$	1.00	26.8112	$-2.43\pm^{2.39E+03}_{1.39}$	$nan\pm^{nan}_{nan}$	0.44
pg1259	0.31974 (#97)	80.23(82)	11483	42	11480	55	$293\pm^{92}_{69}$	1.00	28.5064	$819.38\pm^{1.00E+20}_{849.38}$	$16.11\pm^{0.30}_{nan}$	0.53
pg1259	0.36212 (#98)	114.78(79)	11487	85	11480	57	$291\pm^{96}_{78}$	1.00	29.4218	$5.74E+09\pm^{1.00E+20}_{5.74E+09}$	$16.35\pm^{0.11}_{inf}$	1.38
pg1259	0.38254 (#99)	134.54(94)	11487	66	11480	43	$351\pm^{94}_{79}$	1.00	29.8629	$-1.02\pm^{2.79E+05}_{2.46}$	$nan\pm^{nan}_{nan}$	0.04
pg1259	0.38266 (#100)	134.54(94)	11487	66	11480	43	$351\pm^{93}_{79}$	1.00	29.8655	$-0.93\pm^{5.36E+06}_{2.11}$	$nan\pm^{nan}_{nan}$	0.04
pg1307	0.08345 (#101)	53.56(43)	9827	33	nan	nan	$196\pm^{53}_{46}$	1.00	23.4025	$-4.57\pm^{1.90}_{1.20}$	$nan\pm^{nan}_{nan}$	2.97
pg1309	0.03861 (#102)	52.72(41)	27263	80	nan	nan	$74\pm^{24}_{17}$	1.00	22.4340	$5.94E+06\pm^{1.00E+20}_{5.94E+06}$	$16.28\pm^{0.18}_{nan}$	0.98
pg1309	0.17740 (#103)	116.75(95)	27265	32	26163	73	$153\pm^{33}_{25}$	1.00	25.4318	$7.33E+12\pm^{1.00E+20}_{7.33E+12}$	$16.41\pm^{0.05}_{inf}$	2.31
pg1309	0.17852 (#104)	121.37(94)	27265	33	26163	75	$155\pm^{35}_{26}$	1.00	25.4560	$9.71E+08\pm^{1.00E+20}_{9.71E+08}$	$16.35\pm^{0.11}_{inf}$	2.13
pg1309	0.17918 (#105)	120.71(95)	27265	33	26163	75	$154\pm^{28}_{26}$	1.00	25.4703	$2.60E+06\pm^{1.00E+20}_{2.60E+06}$	$16.28\pm^{0.12}_{nan}$	1.80
pg1309	0.18143 (#106)	116.88(93)	27265	33	26163	75	$141\pm^{28}_{25}$	1.00	25.5189	$7.45\pm^{1.00E+20}_{37.45}$	$15.86\pm^{0.60}_{nan}$	0.09

pg1444	0.22031 (#107)	113.67(93)	17674	27	17137	35	$183\pm^{40}_{35}$	1.00	26.3587	$-2.51\pm^{2.34}_{1.07}$	$nan\pm^{nan}_{nan}$	1.34
pg1626	0.06137 (#108)	–	–	–	–	–	–	–	22.9256	–	–	–
phl1811	0.05143 (#109)	–	–	–	–	–	–	–	22.7109	–	–	–
phl1811	0.05813 (#110)	–	–	–	–	–	–	–	22.8556	–	–	–
phl1811	0.08085 (#111)	–	–	–	–	–	–	–	23.3464	–	–	–
phl1811	0.08163 (#112)	–	–	–	–	–	–	–	23.3632	–	–	–
phl1811	0.12003 (#113)	77.84(58)	74729	91	79201	70	$33\pm^{15}_{14}$	1.00	24.1926	$6.97E+07\pm^{1.00E+20}_{6.97E+07}$	$16.33\pm^{0.13}_{-0.13}$	1.01
phl1811	0.15787 (#114)	–	–	–	–	–	–	–	25.0100	–	–	–
pks0312	0.11454 (#115)	64.38(70)	23887	39	22982	29	$266\pm^{37}_{35}$	1.00	24.0741	$4.42E+04\pm^{1.00E+20}_{4.42E+04}$	$16.21\pm^{0.25}_{nan}$	2.67
pks0405	0.02510 (#116)	41.67(34)	137701	23	nan	nan	$304\pm^{19}_{17}$	1.00	22.1422	$-0.00\pm^{67.52}_{1.38}$	$nan\pm^{nan}_{nan}$	-0.00
pks0405	0.05902 (#117)	53.75(40)	134613	23	nan	nan	$316\pm^{20}_{19}$	1.00	22.8748	$-1.86\pm^{1.00}_{0.63}$	$nan\pm^{nan}_{nan}$	2.69
pks0405	0.09719 (#118)	64.86(45)	135771	21	nan	nan	$354\pm^{19}_{19}$	1.00	23.6993	$-1.55\pm^{1.30}_{0.83}$	$nan\pm^{nan}_{nan}$	1.60
pks0405	0.10152 (#119)	65.13(49)	134959	21	138649	18	$355\pm^{19}_{19}$	1.00	23.7928	$-2.00\pm^{0.89}_{0.64}$	$nan\pm^{nan}_{nan}$	3.98
pks0405	0.10298 (#120)	68.35(50)	134879	21	138649	16	$368\pm^{20}_{20}$	1.00	23.8244	$-1.08\pm^{1.74}_{0.83}$	$nan\pm^{nan}_{nan}$	0.70
pks0405	0.19456 (#121)	116.94(93)	137986	20	134948	21	$405\pm^{21}_{21}$	1.00	25.8025	$18.91\pm^{3.63E+04}_{18.08}$	$15.92\pm^{0.25}_{0.52}$	1.98
pks0405	0.21976 (#122)	126.59(92)	137232	19	135759	24	$408\pm^{22}_{22}$	1.00	26.3468	$-1.02\pm^{1.30}_{0.80}$	$nan\pm^{nan}_{nan}$	0.87
pks0405	0.24564 (#123)	98.79(93)	136439	23	138647	30	$383\pm^{23}_{23}$	1.00	26.9058	$-1.04\pm^{1.25}_{0.70}$	$nan\pm^{nan}_{nan}$	0.95
pks0405	0.29748 (#124)	98.21(89)	135766	33	137130	34	$382\pm^{27}_{25}$	1.00	28.0256	$-0.20\pm^{3.89}_{1.16}$	$nan\pm^{nan}_{nan}$	0.01
pks0405	0.31016 (#125)	96.82(90)	137275	34	137114	39	$378\pm^{26}_{25}$	1.00	28.2995	$-2.30\pm^{0.65}_{0.47}$	$nan\pm^{nan}_{nan}$	6.68
pks0405	0.32502 (#126)	92.49(84)	135467	36	137166	41	$414\pm^{31}_{30}$	1.00	28.6204	$3.81\pm^{1.66E+03}_{4.17}$	$15.78\pm^{0.36}_{nan}$	0.79
pks0405	0.49508 (#127)	112.25(94)	138729	51	137202	58	$536\pm^{45}_{43}$	1.00	32.2937	$-2.11\pm^{0.90}_{0.58}$	$nan\pm^{nan}_{nan}$	3.47
pks0558	0.10472 (#128)	82.71(58)	705422	22	787021	25	$2580\pm^{30}_{21}$	1.00	23.8620	$0.07\pm^{0.62}_{0.22}$	$14.41\pm^{0.91}_{nan}$	0.22
pks2155	0.05708 (#129)	42.12(39)	1687774	3	nan	nan	$641\pm^{88}_{82}$	4.94	22.8329	$-0.29\pm^{0.12}_{0.11}$	$nan\pm^{nan}_{nan}$	6.22
pks2155	0.06236 (#130)	–	–	–	–	–	–	–	22.9470	–	–	–
pks2155	0.10586 (#131)	60.97(48)	1694875	3	1691927	3	$1743\pm^{77}_{762}$	3.33	23.8866	$-0.02\pm^{0.35}_{0.10}$	$nan\pm^{nan}_{nan}$	-0.23
q0045	0.05590 (#132)	48.77(38)	13827	153	nan	nan	$59\pm^{32}_{22}$	1.00	22.8074	$81.83\pm^{1.00E+20}_{111.83}$	$16.01\pm^{0.45}_{nan}$	0.14
q0045	0.06377 (#133)	–	–	–	–	–	–	–	22.9774	–	–	–
q1230	0.08344 (#134)	49.74(34)	39335	66	nan	nan	$83\pm^{24}_{21}$	1.00	23.4023	$-3.52\pm^{5.75}_{1.49}$	$nan\pm^{nan}_{nan}$	0.96
q1230	0.08540 (#135)	49.18(36)	39335	61	nan	nan	$99\pm^{24}_{23}$	1.00	23.4446	$33.06\pm^{1.00E+20}_{63.06}$	$15.99\pm^{0.47}_{nan}$	0.11
q1230	0.09444 (#136)	57.34(47)	39335	61	39139	97	$98\pm^{26}_{19}$	1.00	23.6399	$4.50E+04\pm^{1.00E+20}_{4.50E+04}$	$16.21\pm^{0.26}_{nan}$	1.01
q1230	0.10000 (#137)	69.52(51)	39335	69	39139	87	$67\pm^{22}_{19}$	1.00	23.7600	$-4.12\pm^{1.28}_{0.90}$	$nan\pm^{nan}_{nan}$	4.46
q1230	0.10525 (#138)	71.15(53)	39335	67	39139	75	$95\pm^{23}_{20}$	1.00	23.8734	$214.72\pm^{1.00E+20}_{244.72}$	$16.09\pm^{0.32}_{nan}$	0.19
q1230	0.10549 (#139)	74.01(55)	39335	67	39139	80	$93\pm^{22}_{20}$	1.00	23.8786	$1.38E+03\pm^{1.00E+20}_{1.41E+03}$	$16.12\pm^{0.34}_{nan}$	0.15
q1230	0.10566 (#140)	74.03(55)	39335	67	39139	80	$93\pm^{23}_{20}$	1.00	23.8823	$74.47\pm^{1.00E+20}_{104.47}$	$16.02\pm^{0.44}_{nan}$	0.12
q1230	0.10612 (#141)	75.39(55)	39335	67	39139	80	$90\pm^{22}_{20}$	1.00	23.8922	$4.67\pm^{1.00E+20}_{34.67}$	$15.79\pm^{0.62}_{nan}$	0.03
q1230	0.10639 (#142)	76.90(57)	39335	68	39139	75	$89\pm^{23}_{20}$	1.00	23.8980	$1.30\pm^{1.00E+20}_{31.30}$	$15.52\pm^{0.94}_{nan}$	0.01
q1230	0.10660 (#143)	76.91(57)	39335	68	39139	75	$89\pm^{22}_{20}$	1.00	23.9026	$0.41\pm^{1.00E+20}_{30.41}$	$15.12\pm^{1.29}_{nan}$	0.00

q1230	0.10853 (#144)	76.74(55)	39335	73	39139	71	$74\pm^{22}_{19}$	1.00	23.9442	$-2.92\pm^{2.29E+03}_{1.34}$	$nan\pm^{nan}_{nan}$	0.57
q1230	0.10940 (#145)	74.41(56)	39335	72	39139	71	$72\pm^{22}_{19}$	1.00	23.9630	$-3.09\pm^{21.88}_{1.26}$	$nan\pm^{nan}_{nan}$	0.77
q1230	0.12103 (#146)	95.35(67)	39335	75	39139	80	$87\pm^{26}_{20}$	1.00	24.2142	$1.63E+03\pm^{1.00E+20}_{1.66E+03}$	$16.12\pm^{0.32}_{nan}$	0.52
rbs1892	0.15567 (#147)	94.13(91)	4935	48	4865	18	$242\pm^{87}_{69}$	1.00	24.9625	$-2.82\pm^{4.80}_{1.52}$	$nan\pm^{nan}_{nan}$	0.82
rbs1892	0.15633 (#148)	86.99(91)	4935	52	4865	20	$214\pm^{82}_{65}$	1.00	24.9767	$-2.83\pm^{2.62}_{1.07}$	$nan\pm^{nan}_{nan}$	1.32
rbs1892	0.16343 (#149)	79.53(90)	4936	61	4865	21	$181\pm^{82}_{63}$	1.00	25.1301	$2.74E+05\pm^{1.00E+20}_{2.74E+05}$	$16.26\pm^{0.15}_{nan}$	0.91
rbs1892	0.17001 (#150)	90.53(95)	4937	50	4865	26	$293\pm^{132}_{93}$	1.00	25.2722	$1.99E+04\pm^{1.00E+20}_{1.99E+04}$	$16.21\pm^{0.26}_{nan}$	1.63
rbs1892	0.17155 (#151)	87.14(94)	4937	48	4865	27	$306\pm^{140}_{98}$	1.00	25.3055	$2.95E+06\pm^{1.00E+20}_{2.95E+06}$	$16.28\pm^{0.12}_{nan}$	2.29
rbs1892	0.17185 (#152)	86.42(95)	4937	48	4865	27	$313\pm^{126}_{95}$	1.00	25.3120	$6.31E+12\pm^{1.00E+20}_{6.31E+12}$	$16.41\pm^{0.05}_{inf}$	2.91
rbs542	0.04455 (#153)	57.17(47)	190972	9	nan	nan	$1168\pm^{28}_{29}$	1.00	22.5623	$-0.04\pm^{1.10}_{0.77}$	$nan\pm^{nan}_{nan}$	0.01
rbs542	0.04992 (#154)	55.96(47)	193118	10	nan	nan	$1213\pm^{28}_{28}$	1.00	22.6783	$3.30\pm^{12.51}_{2.52}$	$15.75\pm^{0.19}_{0.39}$	3.36
rxj0439	0.00550 (#155)	–	–	–	–	–	–	–	21.7188	–	–	–
rxj0439	0.17680 (#156)	120.22(96)	151878	14	151926	16	$592\pm^{24}_{24}$	1.00	25.4189	$1.65\pm^{7.84}_{1.84}$	$15.59\pm^{0.32}_{nan}$	0.88
s50716	0.00989 (#157)	–	–	–	–	–	–	–	21.8136	–	–	–
s50716	0.01766 (#158)	25.23(27)	76296	14	nan	nan	$651\pm^{42}_{41}$	1.00	21.9815	$1.72\pm^{69.52}_{2.48}$	$15.61\pm^{0.41}_{nan}$	0.41
s50716	0.08834 (#159)	48.91(39)	77059	12	nan	nan	$813\pm^{36}_{37}$	1.00	23.5081	$4.84E+04\pm^{5.27E+07}_{4.84E+04}$	$16.21\pm^{0.08}_{nan}$	7.95
s50716	0.14936 (#160)	100.74(92)	76556	10	76514	10	$894\pm^{39}_{38}$	1.00	24.8262	$-0.74\pm^{1.12}_{0.72}$	$nan\pm^{nan}_{nan}$	0.64
ton28	0.03357 (#161)	53.66(39)	81822	38	nan	nan	$137\pm^{18}_{17}$	1.00	22.3251	$-1.47\pm^{40.45}_{1.65}$	$nan\pm^{nan}_{nan}$	0.25
tons180	0.04304 (#162)	45.92(46)	181158	8	nan	nan	$1136\pm^{27}_{28}$	1.00	22.5297	$-0.34\pm^{0.92}_{0.66}$	$nan\pm^{nan}_{nan}$	0.24
tons210	0.06763 (#163)	48.59(41)	6728	10	nan	nan	$664\pm^{122}_{97}$	1.00	23.0608	$3.88E+06\pm^{1.00E+20}_{3.89E+06}$	$16.26\pm^{0.20}_{nan}$	0.73
tons210	0.08558 (#164)	51.90(45)	6728	8	nan	nan	$706\pm^{112}_{102}$	1.00	23.4485	$-2.10\pm^{4.91}_{1.34}$	$nan\pm^{nan}_{nan}$	0.63

Table B.4: O VII upper limit measurements with *XMM-Newton* data, at the prior redshift from the H I lines from Table A.2.

Target line		cmin	RGS1	RGS2	power–law		line component			ΔC
Name	z	(d.o.f.)	avg exp (s)	avg exp (s)	norm.	index	λ (Å)	τ_0	$\log N + (\mathrm{cm}^{-2})$	(d.o.f.)
1es1028	0.13714 (#1)	92.78(90)	143804	146370	$1121\pm^{32}_{32}$	1.00	24.5622	0.68	15.31	0.27
1es1028	0.20383 (#2)	114.22(94)	146421	145107	$1207\pm^{32}_{35}$	1.00	26.0027	0.90	15.41	-0.01
1es1028	0.22121 (#3)	101.58(92)	144278	146704	$1198\pm^{35}_{35}$	1.00	26.3781	0.58	15.26	1.33
1es1553	0.03466 (#4)	38.25(27)	1791095	nan	$747\pm^{397}_{326}$	1.97	22.3487	0.29	14.99	0.53
1es1553	0.04273 (#5)	30.79(21)	1784759	nan	$489\pm^{628}_{294}$	2.72	22.5230	0.54	15.23	2.85
1es1553	0.06364 (#6*)	64.48(28)	1661330	nan	$27\pm^{12}_{9}$	7.49	22.9746	0.53	15.23	1.84
1es1553	0.21869 (#7)	108.81(87)	1691684	1788288	$1010\pm^{415}_{304}$	1.74	26.3237	0.36	15.08	-0.07
3c249	0.13470 (#8)	67.71(86)	2642	2524	$336\pm^{146}_{105}$	1.00	24.5095	5.00E+19	16.46	0.52
3c249	0.26664 (#9)	79.78(93)	2639	2524	$306\pm^{146}_{111}$	1.00	27.3594	5.00E+19	16.46	-0.00
3c273	0.00758 (#10)	–	–	–	–	–	21.7637	–	–	–
3c273	0.06707 (#11*)	35.22(22)	897879	nan	$4641\pm^{37}_{41}$	1.00	23.0487	0.30	15.01	0.86
3c273	0.07359 (#12*)	45.49(29)	930374	nan	$4656\pm^{32}_{34}$	1.00	23.1895	0.20	14.84	0.39
3c273	0.13960 (#13)	68.74(61)	892303	1027847	$5246\pm^{31}_{31}$	1.00	24.6154	0.12	14.62	12.82
h1821	0.00944 (#14)	–	–	–	–	–	21.8039	–	–	–
h1821	0.06779 (#15)	48.43(43)	28966	nan	$1081\pm^{99}_{91}$	1.00	23.0643	5.00E+19	16.46	1.16
h1821	0.08483 (#16)	62.62(44)	31062	nan	$1008\pm^{91}_{87}$	1.00	23.4323	9.01E+07	16.29	0.54
h1821	0.12147 (#17)	96.56(82)	30593	43368	$1284\pm^{89}_{85}$	1.00	24.2238	1.24E+04	16.15	1.85
h1821	0.19817 (#18)	79.32(81)	32357	41356	$1363\pm^{112}_{109}$	1.00	25.8805	1.04	15.46	1.30
h1821	0.21321 (#19)	110.19(98)	31737	41863	$1644\pm^{133}_{107}$	1.00	26.2053	2.17E+07	16.29	2.38
h1821	0.24531 (#20)	119.80(98)	31065	44448	$1591\pm^{120}_{113}$	1.00	26.8987	9.68	15.89	0.06
h2356	0.03830 (#21)	60.56(47)	466679	nan	$1093\pm^{15}_{15}$	1.00	22.4273	0.59	15.27	-0.02
h2356	0.07881 (#22)	44.92(38)	468683	nan	$1173\pm^{21}_{20}$	1.00	23.3023	0.52	15.23	2.04
h2356	0.10467 (#23)	52.51(56)	471489	510756	$1280\pm^{22}_{21}$	1.00	23.8609	0.93	15.42	1.39
h2356	0.15613 (#24)	105.03(97)	482157	504552	$1323\pm^{19}_{19}$	1.00	24.9724	0.57	15.26	2.10
he0226	0.14274 (#25)	83.16(89)	31710	31705	$257\pm^{34}_{31}$	1.00	24.6832	1.74	15.61	0.97
he0226	0.39890 (#26)	85.66(67)	31717	31717	$409\pm^{80}_{73}$	1.00	30.2162	3.96E+07	16.30	0.01
he0226	0.41024 (#27)	81.69(56)	31717	31717	$421\pm^{91}_{82}$	1.00	30.4612	2.33E+08	16.29	0.00
i22456	0.00443 (#28)	–	–	–	–	–	21.6957	–	–	–
i22456	0.09941 (#29)	74.98(61)	79883	73453	$671\pm^{38}_{37}$	1.00	23.7473	8.80	15.88	0.00
mr2251	0.01068 (#30)	–	–	–	–	–	21.8307	–	–	–
mr2251	0.01449 (#31)	37.36(27)	446548	nan	$2964\pm^{3361}_{1081}$	0.01	21.9130	0.39	15.10	2.50
mr2251	0.06131 (#32)	32.34(25)	452767	nan	$117\pm^{170}_{69}$	5.55	22.9243	7.53	15.85	4.17

mr2251	0.06190 (#33)	29.54(24)	452283	nan	$59\pm^{91}_{37}$	6.67	22.9370	83.57	16.01	5.95
mr2251	0.06276 (#34)	30.33(22)	451202	nan	$57\pm^{104}_{37}$	6.71	22.9556	5.82	15.85	4.37
mr2251	0.06327 (#35*)	31.04(20)	449939	nan	$30\pm^{81}_{20}$	7.77	22.9666	2.78	15.72	2.99
mr2251	0.06381 (#36*)	33.43(22)	451202	nan	$148\pm^{162}_{116}$	5.14	22.9783	0.79	15.37	-0.00
mrk478	0.06166 (#37)	61.33(42)	192118	nan	$253\pm^{786}_{195}$	2.48	22.9319	3.45	15.77	0.07
mrk478	0.06578 (#38)	54.57(42)	192119	nan	$606\pm^{1058}_{523}$	1.09	23.0208	7.26E+05	16.21	3.82
mrk478	0.07213 (#39)	54.93(42)	192121	nan	$640\pm^{1985}_{489}$	1.00	23.1580	2.87	15.73	0.10
mrk876	0.01159 (#40)	–	–	–	–	–	21.8503	–	–	–
mrk876	0.05598 (#41)	44.97(46)	2714	nan	$477\pm^{142}_{112}$	1.00	22.8092	5.00E+19	16.46	0.21
mrk876	0.08709 (#42)	37.14(46)	2802	nan	$345\pm^{146}_{103}$	1.00	23.4811	5.00E+19	16.46	1.36
mrk876	0.08858 (#43)	37.69(46)	2802	nan	$378\pm^{139}_{105}$	1.00	23.5133	5.00E+19	16.46	1.70
mrk876	0.08917 (#44)	37.84(47)	2802	996	$377\pm^{134}_{98}$	1.00	23.5261	5.00E+19	16.46	1.65
mrk876	0.11487 (#45)	73.35(75)	2743	2633	$529\pm^{144}_{121}$	1.00	24.0812	5.00E+19	16.46	0.00
ngc7469	0.00981 (#46)	–	–	–	–	–	21.8119	–	–	–
pg0003	0.08299 (#47)	59.05(43)	13037	nan	$234\pm^{52}_{46}$	1.00	23.3926	1.51E+06	16.25	0.47
pg0003	0.17139 (#48)	111.61(94)	13033	12941	$332\pm^{65}_{54}$	1.00	25.3020	5.41E+14	16.42	0.31
pg0003	0.22541 (#49)	114.13(94)	13034	12838	$231\pm^{58}_{50}$	1.00	26.4689	1.60E+09	16.33	0.00
pg0003	0.38633 (#50)	104.20(85)	13041	12919	$115\pm^{65}_{47}$	1.00	29.9447	1.14	15.50	12.63
pg0003	0.42051 (#51)	114.71(91)	13041	12843	$362\pm^{115}_{95}$	1.00	30.6830	4.83E+09	16.31	0.06
pg0804	0.05015 (#52)	46.31(37)	27851	nan	$1439\pm^{93}_{87}$	1.00	22.6832	5.00E+19	16.41	7.42
pg0804	0.05576 (#53)	53.92(41)	28550	nan	$1333\pm^{83}_{80}$	1.00	22.8044	3.15E+04	16.15	0.29
pg0804	0.36379 (#54)	127.43(96)	29665	30901	$2024\pm^{141}_{134}$	1.00	29.4579	1.46	15.57	0.42
pg0832	0.01753 (#55)	–	–	–	–	–	21.9786	–	–	–
pg0832	0.02793 (#56)	52.15(36)	20654	nan	$26\pm^{18}_{14}$	1.00	22.2033	1.67	15.61	9.82
pg0832	0.08748 (#57)	53.03(45)	20655	nan	$71\pm^{25}_{19}$	1.00	23.4896	5.00E+19	16.46	1.13
pg0832	0.10171 (#58)	73.57(56)	20655	20637	$84\pm^{30}_{22}$	1.00	23.7969	5.00E+19	16.46	0.91
pg0832	0.18391 (#59)	60.33(41)	20654	20637	$70\pm^{54}_{32}$	1.00	25.5725	5.00E+19	16.41	1.25
pg0832	0.27503 (#60)	124.41(86)	20656	20637	$58\pm^{29}_{21}$	1.00	27.5406	5.00E+19	16.46	0.01
pg0832	0.27694 (#61)	119.21(86)	20656	20637	$60\pm^{28}_{22}$	1.00	27.5819	5.00E+19	16.46	0.02
pg0832	0.32572 (#62*)	136.80(85)	20656	20645	$51\pm^{28}_{20}$	1.00	28.6356	5.40E+04	16.18	0.31
pg0838	0.06583 (#63)	1.34(41)	1609	nan	$0\pm^{36}_{-0}$	1.00	23.0219	5.00E+19	16.46	0.00
pg0838	0.08628 (#64)	16.24(44)	1609	nan	$130\pm^{124}_{72}$	1.00	23.4636	5.00E+19	16.46	0.17
pg0838	0.12676 (#65)	32.38(79)	1609	1519	$75\pm^{109}_{75}$	1.00	24.3380	5.00E+19	16.46	0.75
pg0953	0.16319 (#66)	129.94(91)	12778	12309	$593\pm^{77}_{71}$	1.00	25.1249	2.68E+03	16.17	0.09
pg0953	0.19221 (#67)	122.56(92)	12777	12309	$612\pm^{78}_{71}$	1.00	25.7517	238.36	16.02	0.03
pg1048	0.00642 (#68)	–	–	–	–	–	21.7387	–	–	–
pg1048	0.02414 (#69)	32.85(32)	18864	nan	$156\pm^{38}_{33}$	1.00	22.1214	5.00E+19	16.41	0.12

pg1115	0.09511 (#70)	47.02(50)	17510	16953	$325\pm^{54}_{46}$	1.00	23.6544	5.00E+19	16.41	0.20
pg1115	0.12059 (#71)	98.56(73)	17510	16953	$310\pm^{48}_{44}$	1.00	24.2047	5.00E+19	16.46	2.50
pg1115	0.12741 (#72)	107.59(76)	17513	16953	$311\pm^{51}_{47}$	1.00	24.3521	4.12E+03	16.14	0.00
pg1116	0.04114 (#73)	41.06(39)	284047	nan	$540\pm^{17}_{17}$	1.00	22.4886	0.75	15.35	1.16
pg1116	0.06251 (#74)	40.85(30)	283934	nan	$549\pm^{22}_{21}$	1.00	22.9502	71.62	16.02	0.23
pg1116	0.08382 (#75)	46.62(32)	284638	nan	$588\pm^{22}_{18}$	1.00	23.4105	5.00E+19	16.46	8.15
pg1116	0.09210 (#76)	51.16(38)	292136	222826	$576\pm^{20}_{19}$	1.00	23.5894	1.57	15.59	0.07
pg1116	0.09281 (#77)	50.89(38)	292136	222826	$579\pm^{19}_{19}$	1.00	23.6047	2.00	15.65	0.25
pg1116	0.13373 (#78)	89.85(89)	277711	284726	$680\pm^{19}_{19}$	1.00	24.4886	4.13	15.79	5.37
pg1116	0.13851 (#79)	94.60(91)	277702	291047	$693\pm^{19}_{19}$	1.00	24.5918	2.05	15.65	2.45
pg1211	0.02586 (#80)	33.66(32)	769591	nan	$575\pm^{12}_{12}$	1.00	22.1586	0.86	15.41	0.25
pg1211	0.05443 (#81)	49.81(35)	745965	nan	$634\pm^{12}_{12}$	1.00	22.7757	1.25	15.53	0.06
pg1216	0.00842 (#82)	–	–	–	–	–	21.7819	–	–	–
pg1216	0.07969 (#83)	53.17(43)	11245	nan	$185\pm^{50}_{39}$	1.00	23.3213	5.00E+19	16.41	0.44
pg1216	0.12372 (#84)	107.60(78)	11245	11258	$182\pm^{51}_{48}$	1.00	24.2724	5.00E+19	16.41	3.27
pg1216	0.12473 (#85)	107.90(78)	11245	11258	$186\pm^{59}_{40}$	1.00	24.2942	5.00E+19	16.46	1.76
pg1216	0.17950 (#86)	106.70(95)	11257	11258	$243\pm^{51}_{45}$	1.00	25.4772	5.00E+19	16.46	2.17
pg1216	0.20014 (#87)	86.38(92)	11257	11258	$179\pm^{53}_{39}$	1.00	25.9230	5.00E+19	16.41	1.23
pg1216	0.21258 (#88)	84.99(93)	11257	11258	$191\pm^{48}_{41}$	1.00	26.1917	5.00E+19	16.46	0.49
pg1216	0.28204 (#89)	112.71(89)	11258	11258	$237\pm^{66}_{56}$	1.00	27.6921	3.33	15.76	0.83
pg1229	0.05018 (#90)	55.71(43)	24016	nan	$521\pm^{63}_{49}$	1.00	22.6839	5.00E+19	16.41	3.04
pg1259	0.05563 (#91)	50.01(43)	11485	nan	$165\pm^{50}_{38}$	1.00	22.8016	5.00E+19	16.46	0.63
pg1259	0.15136 (#92)	99.16(90)	11483	11479	$130\pm^{43}_{35}$	1.00	24.8694	3.39E+16	16.46	0.08
pg1259	0.16647 (#93)	105.90(92)	11483	11479	$145\pm^{43}_{36}$	1.00	25.1958	5.57	15.83	0.61
pg1259	0.17893 (#94)	108.49(96)	11483	11479	$180\pm^{52}_{40}$	1.00	25.4649	5.00E+19	16.46	0.92
pg1259	0.22376 (#95)	105.77(93)	11483	11479	$277\pm^{65}_{56}$	1.00	26.4332	2.75E+12	16.39	0.01
pg1259	0.24126 (#96)	121.27(95)	11483	11479	$149\pm^{49}_{40}$	1.00	26.8112	1.20E+03	16.12	0.44
pg1259	0.31974 (#97)	80.23(82)	11483	11480	$293\pm^{92}_{69}$	1.00	28.5064	5.00E+19	16.41	0.53
pg1259	0.36212 (#98)	114.78(79)	11487	11480	$291\pm^{96}_{78}$	1.00	29.4218	5.00E+19	16.46	1.38
pg1259	0.38254 (#99)	134.54(94)	11487	11480	$351\pm^{94}_{79}$	1.00	29.8629	1.40E+05	16.23	0.04
pg1259	0.38266 (#100)	134.54(94)	11487	11480	$351\pm^{93}_{79}$	1.00	29.8655	2.68E+06	16.24	0.04
pg1307	0.08345 (#101)	53.56(43)	9827	nan	$196\pm^{53}_{46}$	1.00	23.4025	1.55	15.59	2.97
pg1309	0.03861 (#102)	52.72(41)	27263	nan	$74\pm^{24}_{17}$	1.00	22.4340	5.00E+19	16.46	0.98
pg1309	0.17740 (#103)	116.75(95)	27265	26163	$153\pm^{33}_{25}$	1.00	25.4318	5.00E+19	16.46	2.31
pg1309	0.17852 (#104)	121.37(94)	27265	26163	$155\pm^{35}_{26}$	1.00	25.4560	5.00E+19	16.46	2.13
pg1309	0.17918 (#105)	120.71(95)	27265	26163	$154\pm^{28}_{26}$	1.00	25.4703	5.00E+19	16.41	1.80
pg1309	0.18143 (#106)	116.88(93)	27265	26163	$141\pm^{28}_{25}$	1.00	25.5189	5.00E+19	16.46	0.09

pg1444	0.22031 (#107)	113.67(93)	17674	17137	$183\pm^{40}_{35}$	1.00	26.3587	1.70	15.61	1.34
pg1626	0.06137 (#108)	–	–	–	–	–	22.9256	–	–	–
phl1811	0.05143 (#109)	–	–	–	–	–	22.7109	–	–	–
phl1811	0.05813 (#110)	–	–	–	–	–	22.8556	–	–	–
phl1811	0.08085 (#111)	–	–	–	–	–	23.3464	–	–	–
phl1811	0.08163 (#112)	–	–	–	–	–	23.3632	–	–	–
phl1811	0.12003 (#113)	77.84(58)	74729	79201	$33\pm^{15}_{14}$	1.00	24.1926	5.00E+19	16.46	1.01
phl1811	0.15787 (#114)	–	–	–	–	–	25.0100	–	–	–
pks0312	0.11454 (#115)	64.38(70)	23887	22982	$266\pm^{37}_{35}$	1.00	24.0741	5.00E+19	16.46	2.67
pks0405	0.02510 (#116)	41.67(34)	137701	nan	$304\pm^{19}_{17}$	1.00	22.1422	34.45	15.98	-0.00
pks0405	0.05902 (#117)	53.75(40)	134613	nan	$316\pm^{20}_{19}$	1.00	22.8748	0.81	15.38	2.69
pks0405	0.09719 (#118)	64.86(45)	135771	nan	$354\pm^{19}_{19}$	1.00	23.6993	1.07	15.48	1.60
pks0405	0.10152 (#119)	65.13(49)	134959	138649	$355\pm^{19}_{19}$	1.00	23.7928	0.77	15.36	3.98
pks0405	0.10298 (#120)	68.35(50)	134879	138649	$368\pm^{20}_{20}$	1.00	23.8244	1.29	15.52	0.70
pks0405	0.19456 (#121)	116.94(93)	137986	134948	$405\pm^{21}_{21}$	1.00	25.8025	1.82E+04	16.14	1.98
pks0405	0.21976 (#122)	126.59(92)	137232	135759	$408\pm^{22}_{22}$	1.00	26.3468	1.05	15.47	0.87
pks0405	0.24564 (#123)	98.79(93)	136439	138647	$383\pm^{23}_{23}$	1.00	26.9058	0.97	15.43	0.95
pks0405	0.29748 (#124)	98.21(89)	135766	137130	$382\pm^{27}_{25}$	1.00	28.0256	2.53	15.71	0.01
pks0405	0.31016 (#125)	96.82(90)	137275	137114	$378\pm^{26}_{25}$	1.00	28.2995	0.56	15.24	6.68
pks0405	0.32502 (#126)	92.49(84)	135467	137166	$414\pm^{31}_{30}$	1.00	28.6204	832.36	16.10	0.79
pks0405	0.49508 (#127)	112.25(94)	138729	137202	$536\pm^{45}_{43}$	1.00	32.2937	0.74	15.34	3.47
pks0558	0.10472 (#128)	82.71(58)	705422	787021	$2580\pm^{30}_{21}$	1.00	23.8620	0.42	15.14	0.22
pks2155	0.05708 (#129)	42.12(39)	1687774	nan	$641\pm^{88}_{82}$	4.94	22.8329	0.12	14.62	6.22
pks2155	0.06236 (#130)	–	–	–	–	–	22.9470	–	–	–
pks2155	0.10586 (#131)	60.97(48)	1694875	1691927	$1743\pm^{77}_{762}$	3.33	23.8866	0.22	14.89	-0.23
q0045	0.05590 (#132)	48.77(38)	13827	nan	$59\pm^{32}_{22}$	1.00	22.8074	5.00E+19	16.46	0.14
q0045	0.06377 (#133)	–	–	–	–	–	22.9774	–	–	–
q1230	0.08344 (#134)	49.74(34)	39335	nan	$83\pm^{24}_{21}$	1.00	23.4023	3.62	15.77	0.96
q1230	0.08540 (#135)	49.18(36)	39335	nan	$99\pm^{24}_{23}$	1.00	23.4446	5.00E+19	16.46	0.11
q1230	0.09444 (#136)	57.34(47)	39335	39139	$98\pm^{26}_{19}$	1.00	23.6399	5.00E+19	16.46	1.01
q1230	0.10000 (#137)	69.52(51)	39335	39139	$67\pm^{22}_{19}$	1.00	23.7600	1.09	15.47	4.46
q1230	0.10525 (#138)	71.15(53)	39335	39139	$95\pm^{23}_{20}$	1.00	23.8734	5.00E+19	16.41	0.19
q1230	0.10549 (#139)	74.01(55)	39335	39139	$93\pm^{22}_{20}$	1.00	23.8786	5.00E+19	16.46	0.15
q1230	0.10566 (#140)	74.03(55)	39335	39139	$93\pm^{23}_{20}$	1.00	23.8823	5.00E+19	16.46	0.12
q1230	0.10612 (#141)	75.39(55)	39335	39139	$90\pm^{22}_{20}$	1.00	23.8922	5.00E+19	16.41	0.03
q1230	0.10639 (#142)	76.90(57)	39335	39139	$89\pm^{23}_{20}$	1.00	23.8980	5.00E+19	16.46	0.01
q1230	0.10660 (#143)	76.91(57)	39335	39139	$89\pm^{22}_{20}$	1.00	23.9026	5.00E+19	16.41	0.00

q1230	0.10853 (#144)	76.74(55)	39335	39139	$74\pm^{22}_{19}$	1.00	23.9442	1.15E+03	16.11	0.57
q1230	0.10940 (#145)	74.41(56)	39335	39139	$72\pm^{22}_{19}$	1.00	23.9630	11.57	15.93	0.77
q1230	0.12103 (#146)	95.35(67)	39335	39139	$87\pm^{26}_{20}$	1.00	24.2142	5.00E+19	16.43	0.52
rbs1892	0.15567 (#147)	94.13(91)	4935	4865	$242\pm^{87}_{69}$	1.00	24.9625	3.16	15.75	0.82
rbs1892	0.15633 (#148)	86.99(91)	4935	4865	$214\pm^{82}_{65}$	1.00	24.9767	1.85	15.62	1.32
rbs1892	0.16343 (#149)	79.53(90)	4936	4865	$181\pm^{82}_{63}$	1.00	25.1301	5.00E+19	16.41	0.91
rbs1892	0.17001 (#150)	90.53(95)	4937	4865	$293\pm^{132}_{93}$	1.00	25.2722	5.00E+19	16.46	1.63
rbs1892	0.17155 (#151)	87.14(94)	4937	4865	$306\pm^{140}_{98}$	1.00	25.3055	5.00E+19	16.41	2.29
rbs1892	0.17185 (#152)	86.42(95)	4937	4865	$313\pm^{126}_{95}$	1.00	25.3120	5.00E+19	16.46	2.91
rbs542	0.04455 (#153)	57.17(47)	190972	nan	$1168\pm^{28}_{29}$	1.00	22.5623	0.93	15.42	0.01
rbs542	0.04992 (#154)	55.96(47)	193118	nan	$1213\pm^{28}_{28}$	1.00	22.6783	7.51	15.88	3.36
rxj0439	0.00550 (#155)	–	–	–	–	–	21.7188	–	–	–
rxj0439	0.17680 (#156)	120.22(96)	151878	151926	$592\pm^{24}_{24}$	1.00	25.4189	4.84	15.82	0.88
s50716	0.00989 (#157)	–	–	–	–	–	21.8136	–	–	–
s50716	0.01766 (#158)	25.23(27)	76296	nan	$651\pm^{42}_{41}$	1.00	21.9815	36.00	15.98	0.41
s50716	0.08834 (#159)	48.91(39)	77059	nan	$813\pm^{36}_{37}$	1.00	23.5081	2.64E+07	16.29	7.95
s50716	0.14936 (#160)	100.74(92)	76556	76514	$894\pm^{39}_{38}$	1.00	24.8262	0.92	15.43	0.64
ton28	0.03357 (#161)	53.66(39)	81822	nan	$137\pm^{18}_{17}$	1.00	22.3251	21.05	15.92	0.25
tons180	0.04304 (#162)	45.92(46)	181158	nan	$1136\pm^{27}_{28}$	1.00	22.5297	0.79	15.37	0.24
tons210	0.06763 (#163)	48.59(41)	6728	nan	$664\pm^{122}_{97}$	1.00	23.0608	5.00E+19	16.46	0.73
tons210	0.08558 (#164)	51.90(45)	6728	nan	$706\pm^{112}_{102}$	1.00	23.4485	3.12	15.75	0.63

Table B.5: O VIII measurements with *XMM-Newton* data, at the prior redshift from the O VI lines from Table A.1.

Target line		cmin	RGS1		RGS2		power–law		line component			ΔC
Name	z	(d.o.f.)	avg exp (s)	%	avg exp (s)	%	norm.	index	λ (Å)	τ_0	$\log N(\mathrm{cm}^{-2})$	(d.o.f.)
1es1028	0.12314 (#1)	33.31(31)	146792	8	nan	nan	$963\pm^{40}_{26}$	1.00	21.2947	$0.02\pm^{3.99}_{0.61}$	$14.13\pm^{2.00}_{nan}$	0.01
1es1028	0.13706 (#2)	–	–	–	–	–	–	–	21.5587	–	–	–
1es1028	0.33735 (#3)	92.62(96)	147900	8	144798	8	$1196\pm^{31}_{31}$	1.00	25.3562	$5.01\pm^{15.34}_{3.36}$	$16.16\pm^{0.15}_{0.24}$	6.58
1es1553	0.18759 (#4)	29.26(27)	1729540	9	nan	nan	$540\pm^{318}_{194}$	2.55	22.5167	$0.37\pm^{0.44}_{0.33}$	$15.43\pm^{0.29}_{0.90}$	1.81
1es1553	0.18775 (#5)	28.91(27)	1729540	9	nan	nan	$550\pm^{295}_{211}$	2.52	22.5197	$0.39\pm^{0.49}_{0.31}$	$15.45\pm^{0.29}_{0.62}$	2.20
1es1553	0.18984 (#6)	25.62(27)	1729542	9	nan	nan	$406\pm^{219}_{140}$	3.05	22.5594	$0.98\pm^{0.60}_{0.48}$	$15.77\pm^{0.14}_{0.23}$	8.20
1es1553	0.21631 (#7)	33.20(25)	1723969	9	nan	nan	$60\pm^{36}_{21}$	6.19	23.0612	$-0.08\pm^{0.43}_{0.30}$	$nan\pm^{nan}_{nan}$	0.03
1es1553	0.31130 (#8)	113.12(91)	1744157	7	1748313	7	$2268\pm^{757}_{440}$	0.67	24.8622	$1.01\pm^{0.37}_{0.33}$	$15.80\pm^{0.10}_{0.14}$	17.08
1es1553	0.37868 (#9)	113.07(88)	1784762	7	1713272	8	$1213\pm^{467}_{336}$	1.52	26.1398	$1.03\pm^{0.44}_{0.35}$	$15.79\pm^{0.11}_{0.14}$	15.34
1es1553	0.39497 (#10)	118.64(92)	1704141	7	1756581	9	$481\pm^{192}_{138}$	2.74	26.4486	$-0.20\pm^{0.19}_{0.18}$	$nan\pm^{nan}_{nan}$	1.31
3c249	0.24676 (#11)	41.19(50)	2644	37	2524	inf	$373\pm^{135}_{107}$	1.00	23.6386	$43.49\pm^{1.00E+20}_{73.49}$	$16.33\pm^{0.47}_{nan}$	0.10
3c249	0.30788 (#12)	70.28(91)	2641	15	2524	8	$269\pm^{119}_{90}$	1.00	24.7974	$-1.35\pm^{1.00E+20}_{2.77}$	$nan\pm^{nan}_{nan}$	0.05
3c249	0.30809 (#13)	70.31(91)	2641	15	2524	8	$271\pm^{119}_{91}$	1.00	24.8014	$-0.85\pm^{3.10E+14}_{29.15}$	$nan\pm^{nan}_{nan}$	0.02
3c249	0.31364 (#14)	73.37(90)	2640	17	2524	5	$377\pm^{139}_{111}$	1.00	24.9066	$4.71E+06\pm^{1.00E+20}_{4.71E+06}$	$16.62\pm^{0.18}_{nan}$	1.07
3c273	0.00337 (#15)	122.62(82)	1002935	3	1016589	3	$2162\pm^{179}_{168}$	2.23	19.0239	$-0.01\pm^{0.61}_{0.03}$	$nan\pm^{nan}_{nan}$	-0.27
3c273	0.00533 (#16)	121.19(82)	1000681	3	1016019	4	$2034\pm^{174}_{166}$	2.37	19.0611	$0.05\pm^{0.10}_{0.17}$	$14.58\pm^{0.47}_{nan}$	-0.06
3c273	0.00764 (#17)	119.15(82)	1000362	3	1015449	4	$1895\pm^{175}_{164}$	2.53	19.1049	$0.13\pm^{0.11}_{0.17}$	$14.99\pm^{0.26}_{nan}$	0.70
3c273	0.02947 (#18)	124.26(90)	979671	3	1010400	4	$2182\pm^{194}_{180}$	2.22	19.5188	$-0.00\pm^{0.16}_{0.14}$	$nan\pm^{nan}_{nan}$	0.00
3c273	0.04898 (#19)	97.81(72)	981682	3	1017674	4	$2995\pm^{379}_{339}$	1.54	19.8887	$-0.02\pm^{0.09}_{0.25}$	$nan\pm^{nan}_{nan}$	0.19
3c273	0.06655 (#20)	70.47(59)	1020346	4	1015505	4	$3584\pm^{502}_{559}$	1.18	20.2218	$-0.09\pm^{0.43}_{0.08}$	$nan\pm^{nan}_{nan}$	-0.58
3c273	0.09018 (#21)	39.08(47)	949280	4	nan	nan	$2360\pm^{380}_{338}$	2.03	20.6698	$0.15\pm^{0.31}_{0.14}$	$15.05\pm^{0.45}_{1.84}$	1.16
3c273	0.12007 (#22)	29.12(34)	930918	4	nan	nan	$2926\pm^{1141}_{776}$	1.62	21.2365	$0.01\pm^{0.13}_{0.30}$	$13.82\pm^{1.21}_{nan}$	-0.04
3c273	0.14660 (#23)	–	–	–	–	–	–	–	21.7395	–	–	–
3c273	0.15784 (#24)	34.61(25)	1047179	4	nan	nan	$2310\pm^{773}_{593}$	2.01	21.9526	$-0.53\pm^{0.17}_{0.15}$	$nan\pm^{nan}_{nan}$	12.16
h1821	0.02438 (#25)	127.18(98)	30082	34	44303	33	$1073\pm^{56}_{55}$	1.00	19.4222	$-0.48\pm^{1.75}_{0.82}$	$nan\pm^{nan}_{nan}$	0.18
h1821	0.10817 (#26)	50.54(39)	33073	43	nan	nan	$1206\pm^{79}_{77}$	1.00	21.0109	$-0.66\pm^{4.98}_{1.17}$	$nan\pm^{nan}_{nan}$	0.13
h1821	0.12133 (#27)	38.85(28)	33486	46	nan	nan	$1220\pm^{99}_{97}$	1.00	21.2604	$0.79\pm^{330,83}_{2.13}$	$15.70\pm^{0.69}_{nan}$	0.08
h1821	0.12147 (#28)	38.90(28)	33486	46	nan	nan	$1214\pm^{99}_{97}$	1.00	21.2631	$0.30\pm^{64.44}_{1.91}$	$15.34\pm^{1.02}_{nan}$	0.01
h1821	0.16992 (#29)	47.55(34)	32399	54	nan	nan	$970\pm^{94}_{91}$	1.00	22.1817	$0.21\pm^{8.43E+06}_{2.24}$	$15.20\pm^{1.38}_{nan}$	0.00
h1821	0.17043 (#30)	47.37(34)	32399	54	nan	nan	$986\pm^{100}_{91}$	1.00	22.1914	$4.63\pm^{6.81E+13}_{6.06}$	$16.15\pm^{0.61}_{nan}$	0.23
h1821	0.21326 (#31)	58.03(45)	29109	56	nan	nan	$975\pm^{94}_{92}$	1.00	23.0034	$-1.61\pm^{3.48}_{1.02}$	$nan\pm^{nan}_{nan}$	0.60
h1821	0.22497 (#32)	67.04(48)	29437	57	nan	nan	$945\pm^{94}_{91}$	1.00	23.2254	$-2.05\pm^{1.41}_{0.76}$	$nan\pm^{nan}_{nan}$	1.95
h1821	0.22522 (#33)	66.78(47)	29837	57	nan	nan	$962\pm^{94}_{90}$	1.00	23.2302	$-2.04\pm^{1.72}_{0.93}$	$nan\pm^{nan}_{nan}$	1.57

h1821	0.22639 (#34)	68.85(47)	29881	57	nan	nan	$947\pm^{93}_{89}$	1.00	23.2524	$-1.72\pm^{1.87}_{0.84}$	$nan\pm^{nan}_{nan}$	1.14
h1821	0.24531 (#35)	72.51(51)	31382	55	32028	39	$1052\pm^{92}_{86}$	1.00	23.6111	$3.97\pm^{6.56E+07}_{5.11}$	$16.12\pm^{0.54}_{nan}$	0.31
h1821	0.26657 (#36)	79.55(72)	31337	54	42756	42	$1040\pm^{83}_{81}$	1.00	24.0142	$-1.77\pm^{1.37}_{0.81}$	$nan\pm^{nan}_{nan}$	1.71
h1821	0.28800 (#37)	114.20(93)	27766	49	42046	40	$1294\pm^{95}_{91}$	1.00	24.4205	$2.11\pm^{97.57}_{2.56}$	$16.00\pm^{0.38}_{nan}$	0.65
h1821	0.29658 (#38)	111.33(97)	27950	49	42972	39	$1276\pm^{93}_{91}$	1.00	24.5832	$-1.34\pm^{1.14}_{0.71}$	$nan\pm^{nan}_{nan}$	1.58
h1821	0.29680 (#39)	112.27(97)	27836	49	43008	39	$1282\pm^{94}_{91}$	1.00	24.5873	$-1.12\pm^{1.32}_{0.75}$	$nan\pm^{nan}_{nan}$	1.00
h2356	0.11461 (#40)	57.52(40)	476224	7	nan	nan	$1072\pm^{17}_{14}$	1.00	21.1330	$0.01\pm^{2.12}_{0.23}$	$13.79\pm^{2.21}_{nan}$	0.03
h2356	0.16512 (#41)	37.80(32)	505443	7	nan	nan	$1093\pm^{17}_{20}$	1.00	22.0907	$-0.03\pm^{0.61}_{0.63}$	$nan\pm^{nan}_{nan}$	0.02
he0056	0.16392 (#42)	27.81(24)	160091	16	nan	nan	$356\pm^{24}_{22}$	1.00	22.0679	$31.45\pm^{5.71E+04}_{29.99}$	$16.31\pm^{0.23}_{0.40}$	2.53
he0056	0.16492 (#43)	28.43(24)	160091	16	nan	nan	$353\pm^{25}_{21}$	1.00	22.0869	$8.08\pm^{1.06E+04}_{7.85}$	$16.21\pm^{0.29}_{0.96}$	1.64
he0226	0.01746 (#44)	124.17(84)	31711	17	31707	30	$157\pm^{20}_{19}$	1.00	19.2910	$-1.87\pm^{2.58}_{1.13}$	$nan\pm^{nan}_{nan}$	0.93
he0226	0.02679 (#45)	131.34(93)	31711	20	31707	31	$154\pm^{20}_{18}$	1.00	19.4679	$-0.27\pm^{579.74}_{1.88}$	$nan\pm^{nan}_{nan}$	0.01
he0226	0.04121 (#46)	120.74(81)	31711	19	31707	33	$166\pm^{22}_{20}$	1.00	19.7413	$-1.70\pm^{4.07}_{1.34}$	$nan\pm^{nan}_{nan}$	0.53
he0226	0.04535 (#47)	113.12(77)	31711	22	31707	32	$161\pm^{22}_{20}$	1.00	19.8198	$-1.30\pm^{8.63}_{1.26}$	$nan\pm^{nan}_{nan}$	0.29
he0226	0.04609 (#48)	112.96(76)	31711	24	31707	32	$164\pm^{22}_{20}$	1.00	19.8339	$-0.63\pm^{109.55}_{1.94}$	$nan\pm^{nan}_{nan}$	0.04
he0226	0.06015 (#49)	84.08(65)	31711	30	31707	36	$121\pm^{22}_{20}$	1.00	20.1004	$-4.04\pm^{0.97}_{0.76}$	$nan\pm^{nan}_{nan}$	8.15
he0226	0.06083 (#50)	83.15(64)	31711	29	31707	36	$129\pm^{22}_{20}$	1.00	20.1133	$-3.38\pm^{1.02}_{0.73}$	$nan\pm^{nan}_{nan}$	5.31
he0226	0.07023 (#51)	66.31(54)	31711	29	31707	36	$170\pm^{24}_{23}$	1.00	20.2916	$0.37\pm^{1.57E+08}_{2.69}$	$15.42\pm^{1.24}_{nan}$	0.01
he0226	0.08375 (#52)	52.16(42)	31711	25	nan	nan	$196\pm^{28}_{23}$	1.00	20.5479	$4.04E+08\pm^{1.00E+20}_{4.04E+08}$	$16.65\pm^{0.14}_{-0.14}$	2.53
he0226	0.08901 (#53)	47.97(42)	31711	24	nan	nan	$183\pm^{25}_{23}$	1.00	20.6476	$-2.40\pm^{2.42}_{1.09}$	$nan\pm^{nan}_{nan}$	1.23
he0226	0.08938 (#54)	47.78(42)	31711	24	nan	nan	$182\pm^{25}_{23}$	1.00	20.6546	$-2.67\pm^{2.28}_{1.19}$	$nan\pm^{nan}_{nan}$	1.47
he0226	0.08950 (#55)	46.05(43)	31711	23	nan	nan	$182\pm^{25}_{23}$	1.00	20.6569	$-2.57\pm^{2.05}_{1.02}$	$nan\pm^{nan}_{nan}$	1.57
he0226	0.09220 (#56)	46.95(42)	31711	24	nan	nan	$186\pm^{25}_{23}$	1.00	20.7081	$-2.29\pm^{3.14}_{1.16}$	$nan\pm^{nan}_{nan}$	0.92
he0226	0.10668 (#57)	50.29(43)	31711	18	nan	nan	$175\pm^{26}_{24}$	1.00	20.9827	$-2.67\pm^{1.60}_{0.85}$	$nan\pm^{nan}_{nan}$	2.23
he0226	0.11514 (#58)	39.66(36)	31711	15	nan	nan	$203\pm^{30}_{27}$	1.00	21.1431	$3.88\pm^{5.21E+09}_{33.88}$	$16.12\pm^{0.54}_{nan}$	0.15
he0226	0.11680 (#59)	37.43(34)	31711	15	nan	nan	$207\pm^{37}_{25}$	1.00	21.1745	$5.70E+04\pm^{1.00E+20}_{5.70E+04}$	$16.54\pm^{0.25}_{nan}$	1.76
he0226	0.11733 (#60)	36.95(34)	31711	15	nan	nan	$202\pm^{39}_{25}$	1.00	21.1846	$2.48E+04\pm^{1.00E+20}_{2.48E+04}$	$16.54\pm^{0.26}_{nan}$	2.01
he0226	0.12589 (#61)	35.52(30)	31712	15	nan	nan	$206\pm^{36}_{27}$	1.00	21.3469	$1.54E+06\pm^{1.00E+20}_{1.54E+06}$	$16.62\pm^{0.12}_{nan}$	2.12
he0226	0.13832 (#62)	–	–	–	–	–	–	–	21.5825	–	–	–
he0226	0.15175 (#63)	–	–	–	–	–	–	–	21.8372	–	–	–
he0226	0.15549 (#64)	–	–	–	–	–	–	–	21.9081	–	–	–
he0226	0.16237 (#65)	33.50(25)	31712	27	nan	nan	$113\pm^{37}_{33}$	1.00	22.0385	$-5.22\pm^{1.12}_{1.03}$	$nan\pm^{nan}_{nan}$	15.81
he0226	0.16339 (#66)	33.20(26)	31712	28	nan	nan	$113\pm^{36}_{32}$	1.00	22.0579	$-5.22\pm^{1.07}_{0.98}$	$nan\pm^{nan}_{nan}$	16.22
he0226	0.16971 (#67)	40.73(28)	31712	36	nan	nan	$140\pm^{34}_{30}$	1.00	22.1777	$-2.91\pm^{9.88E+04}_{2.04}$	$nan\pm^{nan}_{nan}$	0.43
he0226	0.18619 (#68)	50.47(36)	31712	33	nan	nan	$175\pm^{30}_{27}$	1.00	22.4902	$2.41E+05\pm^{1.00E+20}_{2.41E+05}$	$16.59\pm^{0.15}_{nan}$	1.41
he0226	0.18811 (#69)	48.87(35)	31712	26	nan	nan	$219\pm^{37}_{30}$	1.00	22.5266	$5.13E+06\pm^{1.00E+20}_{5.13E+06}$	$16.62\pm^{0.12}_{nan}$	1.73
he0226	0.18891 (#70)	57.62(39)	31712	31	nan	nan	$196\pm^{30}_{28}$	1.00	22.5417	$2.30E+08\pm^{1.00E+20}_{2.30E+08}$	$16.69\pm^{0.11}_{-0.11}$	2.21

he0226	0.19374 (#71)	46.89(38)	31712	38	nan	nan	$168\pm^{30}_{28}$	1.00	22.6333	$5.60E+07\pm^{1.00E+20}_{5.60E+07}$	$16.66\pm^{0.14}_{-0.14}$	2.44
he0226	0.19453 (#72)	48.32(38)	31712	40	nan	nan	$157\pm^{34}_{26}$	1.00	22.6483	$609.96\pm^{1.00E+20}_{639.96}$	$16.45\pm^{0.30}_{nan}$	0.67
he0226	0.19860 (#73)	51.59(40)	31712	38	nan	nan	$161\pm^{31}_{28}$	1.00	22.7255	$0.09\pm^{1.14E+13}_{30.09}$	$14.85\pm^{1.87}_{nan}$	0.00
he0226	0.20055 (#74)	50.95(40)	31712	38	nan	nan	$166\pm^{29}_{27}$	1.00	22.7624	$4.03E+03\pm^{1.00E+20}_{4.06E+03}$	$16.52\pm^{0.27}_{nan}$	0.43
he0226	0.20703 (#75)	53.97(42)	31712	43	nan	nan	$158\pm^{30}_{27}$	1.00	22.8853	$-0.72\pm^{5.88E+08}_{2.56}$	$nan\pm^{nan}_{nan}$	0.01
he0226	0.22009 (#76)	36.18(41)	31713	38	nan	nan	$188\pm^{33}_{30}$	1.00	23.1329	$0.49\pm^{9.51E+12}_{30.49}$	$15.53\pm^{1.19}_{nan}$	0.00
he0226	0.22099 (#77)	39.39(41)	31713	36	nan	nan	$197\pm^{33}_{30}$	1.00	23.1500	$-0.73\pm^{2.25E+07}_{2.06}$	$nan\pm^{nan}_{nan}$	0.03
he0226	0.23009 (#78)	42.36(43)	31713	38	nan	nan	$209\pm^{33}_{28}$	1.00	23.3225	$5.39E+06\pm^{1.00E+20}_{5.39E+06}$	$16.62\pm^{0.18}_{nan}$	1.39
he0226	0.23964 (#79)	46.29(45)	31713	43	nan	nan	$171\pm^{30}_{27}$	1.00	23.5036	$-0.54\pm^{1.07E+08}_{2.36}$	$nan\pm^{nan}_{nan}$	0.01
he0226	0.24522 (#80)	46.47(48)	31713	44	31705	26	$152\pm^{29}_{27}$	1.00	23.6094	$-2.46\pm^{14.39}_{1.37}$	$nan\pm^{nan}_{nan}$	0.65
he0226	0.25099 (#81)	54.13(54)	31713	42	31705	21	$163\pm^{30}_{27}$	1.00	23.7188	$-0.31\pm^{8.20E+05}_{2.71}$	$nan\pm^{nan}_{nan}$	0.00
he0226	0.27155 (#82)	78.85(73)	31713	31	31705	21	$224\pm^{30}_{28}$	1.00	24.1086	$2.38E+03\pm^{1.00E+20}_{2.41E+03}$	$16.48\pm^{0.31}_{nan}$	1.20
he0226	0.27956 (#83)	79.52(77)	31713	30	31705	21	$224\pm^{32}_{29}$	1.00	24.2605	$-1.80\pm^{4.37}_{1.28}$	$nan\pm^{nan}_{nan}$	0.59
he0226	0.28041 (#84)	78.68(77)	31713	30	31705	20	$234\pm^{33}_{30}$	1.00	24.2766	$-1.37\pm^{16.51}_{1.34}$	$nan\pm^{nan}_{nan}$	0.27
he0226	0.29134 (#85)	83.52(84)	31711	25	31705	20	$238\pm^{35}_{32}$	1.00	24.4838	$-1.98\pm^{2.51}_{1.19}$	$nan\pm^{nan}_{nan}$	1.00
he0226	0.29213 (#86)	86.12(85)	31711	24	31705	21	$240\pm^{35}_{32}$	1.00	24.4988	$-1.84\pm^{2.32}_{0.97}$	$nan\pm^{nan}_{nan}$	1.02
he0226	0.30939 (#87)	97.61(90)	31709	22	31705	26	$246\pm^{33}_{30}$	1.00	24.8260	$5.29\pm^{1.90E+06}_{35.29}$	$16.16\pm^{0.46}_{nan}$	0.27
he0226	0.31833 (#88)	99.31(91)	31708	25	31705	27	$223\pm^{33}_{30}$	1.00	24.9955	$15.13\pm^{8.43E+09}_{45.13}$	$16.30\pm^{0.37}_{nan}$	0.49
he0226	0.33965 (#89)	102.15(94)	31706	18	31705	30	$273\pm^{39}_{31}$	1.00	25.3998	$68.61\pm^{2.31E+15}_{98.61}$	$16.34\pm^{0.44}_{nan}$	0.91
he0226	0.34036 (#90)	108.55(94)	31706	19	31705	28	$273\pm^{40}_{31}$	1.00	25.4132	$5.55E+03\pm^{1.00E+20}_{5.58E+03}$	$16.48\pm^{0.32}_{nan}$	1.70
he0226	0.35493 (#91)	115.28(93)	31706	22	31704	20	$247\pm^{33}_{30}$	1.00	25.6895	$-2.19\pm^{1.86}_{0.91}$	$nan\pm^{nan}_{nan}$	1.51
he0226	0.35528 (#92)	116.14(94)	31706	22	31704	20	$242\pm^{33}_{30}$	1.00	25.6961	$-2.30\pm^{1.48}_{0.79}$	$nan\pm^{nan}_{nan}$	2.04
he0226	0.37281 (#93)	117.30(93)	31706	19	31704	25	$305\pm^{42}_{33}$	1.00	26.0285	$84.87\pm^{1.84E+13}_{114.87}$	$16.34\pm^{0.39}_{nan}$	0.86
he0226	0.38420 (#94)	128.19(92)	31706	23	31704	27	$295\pm^{38}_{36}$	1.00	26.2444	$3.95E+05\pm^{1.00E+20}_{3.95E+05}$	$16.58\pm^{0.16}_{nan}$	2.16
he0226	0.38636 (#95)	130.09(92)	31706	21	31704	29	$281\pm^{36}_{34}$	1.00	26.2854	$3.47\pm^{1.45E+07}_{33.47}$	$16.10\pm^{0.52}_{nan}$	0.22
he0226	0.39642 (#96)	139.43(93)	31706	26	31704	30	$262\pm^{37}_{34}$	1.00	26.4761	$-1.35\pm^{5.03}_{1.41}$	$nan\pm^{nan}_{nan}$	0.35
he0226	0.39692 (#97*)	137.43(91)	31706	26	31704	30	$261\pm^{37}_{34}$	1.00	26.4856	$-1.58\pm^{3.70}_{1.34}$	$nan\pm^{nan}_{nan}$	0.52
he0226	0.39890 (#98)	135.24(93)	31707	25	31704	31	$270\pm^{38}_{35}$	1.00	26.5231	$-1.60\pm^{3.57}_{1.31}$	$nan\pm^{nan}_{nan}$	0.54
he0226	0.40034 (#99)	134.81(92)	31707	24	31704	30	$276\pm^{38}_{35}$	1.00	26.5504	$-0.65\pm^{63.36}_{1.81}$	$nan\pm^{nan}_{nan}$	0.05
he0226	0.40274 (#100)	137.73(93)	31707	23	31704	32	$295\pm^{39}_{36}$	1.00	26.5960	$6.17\pm^{7.88E+08}_{36.17}$	$16.17\pm^{0.45}_{nan}$	0.26
he0226	0.49225 (#101)	110.65(88)	31709	28	31712	47	$363\pm^{50}_{46}$	1.00	28.2931	$0.19\pm^{1.35E+05}_{2.56}$	$15.16\pm^{1.41}_{nan}$	0.00
he0226	0.49254 (#102)	110.33(88)	31709	28	31712	49	$359\pm^{49}_{46}$	1.00	28.2986	$-0.68\pm^{874.00}_{1.68}$	$nan\pm^{nan}_{nan}$	0.04
he0226	0.49280 (#103)	110.26(88)	31709	28	31712	49	$357\pm^{50}_{46}$	1.00	28.3035	$-1.08\pm^{54.49}_{1.75}$	$nan\pm^{nan}_{nan}$	0.12
he0226	0.49309 (#104)	109.11(87)	31709	29	31713	49	$348\pm^{49}_{46}$	1.00	28.3090	$-1.32\pm^{10.14}_{1.32}$	$nan\pm^{nan}_{nan}$	0.27
i22456	0.09858 (#105)	56.99(44)	79900	60	nan	nan	$498\pm^{28}_{27}$	1.00	20.8291	$2.67E+06\pm^{1.00E+20}_{1.34E+06}$	$16.62\pm^{0.12}_{0.00}$	4.29
i22456	0.09895 (#106)	60.07(44)	79900	60	nan	nan	$499\pm^{44}_{27}$	1.00	20.8361	$3.99E+04\pm^{1.00E+20}_{3.99E+04}$	$16.52\pm^{0.28}_{nan}$	3.98
i22456	0.09931 (#107)	59.72(44)	79900	60	nan	nan	$501\pm^{44}_{27}$	1.00	20.8429	$2.38E+04\pm^{1.00E+20}_{1.19E+04}$	$16.54\pm^{0.26}_{0.00}$	4.43

i22456	0.09959 (#108)	54.85(44)	79898	60	nan	nan	$498\pm^{28}_{27}$	1.00	20.8482	$1.73E+06\pm^{1.00E+20}_{1.63E+06}$	$16.62\pm^{0.12}_{0.07}$	4.62
i22456	0.09989 (#109)	55.11(44)	79898	60	nan	nan	$496\pm^{38}_{27}$	1.00	20.8539	$2.00E+04\pm^{1.00E+20}_{2.00E+04}$	$16.54\pm^{0.24}_{nan}$	4.24
i22456	0.10034 (#110)	55.73(44)	79898	60	nan	nan	$500\pm^{28}_{27}$	1.00	20.8624	$2.24E+04\pm^{1.00E+20}_{2.24E+04}$	$16.54\pm^{0.26}_{nan}$	4.33
i22456	0.10101 (#111)	55.60(44)	79897	60	nan	nan	$495\pm^{38}_{27}$	1.00	20.8751	$716.19\pm^{1.00E+20}_{606.50}$	$16.45\pm^{0.30}_{0.05}$	3.43
i22456	0.10146 (#112)	55.42(44)	79897	60	nan	nan	$499\pm^{28}_{28}$	1.00	20.8837	$6.78E+04\pm^{3.72E+11}_{6.07E+04}$	$16.55\pm^{0.18}_{0.07}$	3.55
mr2251	0.01070 (#113)	126.25(97)	415723	5	451165	5	$1562\pm^{16}_{16}$	1.00	19.1629	$-0.66\pm^{0.21}_{0.19}$	$nan\pm^{nan}_{nan}$	9.49
mrk421	0.01009 (#114*)	95.39(57)	1385032	10	1437210	10	$27095\pm^{56}_{49}$	1.00	19.1513	$0.09\pm^{0.11}_{0.02}$	$14.87\pm^{0.32}_{0.11}$	9.73
mrk876	0.00311 (#115)	98.25(96)	2693	31	2600	9	$283\pm^{87}_{69}$	1.00	19.0190	$5.15E+04\pm^{1.00E+20}_{5.16E+04}$	$16.54\pm^{0.21}_{nan}$	0.38
mrk876	0.06248 (#116)	59.48(66)	2754	16	2708	21	$362\pm^{110}_{83}$	1.00	20.1446	$3.78E+09\pm^{1.00E+20}_{3.78E+09}$	$16.69\pm^{0.07}_{inf}$	1.48
mrk876	0.08579 (#117)	44.05(43)	2804	10	nan	nan	$444\pm^{126}_{109}$	1.00	20.5866	$-3.42\pm^{2.47}_{1.14}$	$nan\pm^{nan}_{nan}$	1.79
mrk876	0.11488 (#118)	52.10(37)	2790	15	nan	nan	$714\pm^{157}_{165}$	1.00	21.1381	$1.66E+09\pm^{1.00E+20}_{1.66E+09}$	$16.69\pm^{0.11}_{inf}$	3.07
mrk876	0.11517 (#119)	52.51(37)	2790	15	nan	nan	$706\pm^{235}_{159}$	1.00	21.1436	$1.69E+06\pm^{1.00E+20}_{1.69E+06}$	$16.62\pm^{0.12}_{nan}$	2.62
mrk876	0.11588 (#120)	50.65(36)	2788	16	nan	nan	$705\pm^{157}_{137}$	1.00	21.1571	$7.43E+08\pm^{1.00E+20}_{7.43E+08}$	$16.69\pm^{0.11}_{inf}$	2.97
ngc7469	0.00962 (#121)	84.33(74)	631131	4	664074	4	$1941\pm^{17}_{17}$	1.00	19.1424	$2.35\pm^{0.90}_{0.64}$	$16.03\pm^{0.06}_{0.08}$	45.84
ngc7469	0.00994 (#122)	94.79(74)	630829	4	663435	4	$1942\pm^{17}_{17}$	1.00	19.1485	$2.92\pm^{1.08}_{0.81}$	$16.07\pm^{0.06}_{0.07}$	53.76
ngc7469	0.01153 (#123)	85.80(74)	622605	4	665535	4	$1939\pm^{17}_{17}$	1.00	19.1786	$3.35\pm^{1.86}_{1.00}$	$16.10\pm^{0.06}_{0.07}$	53.36
p1103	0.13556 (#124)	–	–	–	–	–	–	–	21.5302	–	–	–
p1103	0.13937 (#125)	–	–	–	–	–	–	–	21.6025	–	–	–
p1103	0.14099 (#126)	–	–	–	–	–	–	–	21.6332	–	–	–
p1103	0.14126 (#127)	–	–	–	–	–	–	–	21.6383	–	–	–
p1103	0.17277 (#128)	44.35(37)	15674	4	nan	nan	$2927\pm^{142}_{138}$	1.00	22.2357	$3.46E+04\pm^{7.18E+11}_{3.47E+04}$	$16.54\pm^{0.15}_{nan}$	6.11
pg0003	0.16521 (#129)	39.30(31)	13036	24	nan	nan	$287\pm^{72}_{63}$	1.00	22.0924	$-3.48\pm^{1.86}_{1.12}$	$nan\pm^{nan}_{nan}$	2.77
pg0003	0.20907 (#130)	38.93(42)	13036	22	nan	nan	$282\pm^{58}_{51}$	1.00	22.9240	$4.32E+05\pm^{1.00E+20}_{4.32E+05}$	$16.61\pm^{0.13}_{nan}$	0.89
pg0003	0.29021 (#131)	98.06(84)	13036	43	12941	11	$230\pm^{57}_{49}$	1.00	24.4624	$-2.91\pm^{1.47}_{0.87}$	$nan\pm^{nan}_{nan}$	2.68
pg0003	0.30551 (#132)	110.03(89)	13035	41	12941	9	$297\pm^{62}_{55}$	1.00	24.7525	$1.49E+05\pm^{1.00E+20}_{1.49E+05}$	$16.56\pm^{0.24}_{nan}$	1.06
pg0003	0.30569 (#133)	111.09(89)	13035	43	12941	9	$297\pm^{71}_{55}$	1.00	24.7559	$8.96E+04\pm^{1.00E+20}_{8.96E+04}$	$16.54\pm^{0.26}_{nan}$	1.07
pg0003	0.34757 (#134)	112.83(95)	13033	24	12938	19	$306\pm^{63}_{54}$	1.00	25.5499	$2.65\pm^{2.29E+13}_{32.65}$	$16.04\pm^{0.69}_{nan}$	0.09
pg0003	0.34788 (#135)	112.95(95)	13033	24	12938	20	$297\pm^{60}_{53}$	1.00	25.5558	$1.11\pm^{2.80E+09}_{31.11}$	$15.82\pm^{0.86}_{nan}$	0.03
pg0003	0.36452 (#136)	111.56(93)	13033	20	12904	26	$311\pm^{62}_{55}$	1.00	25.8713	$2.13\pm^{9.82E+12}_{32.13}$	$15.99\pm^{0.72}_{nan}$	0.04
pg0003	0.36508 (#137)	109.85(94)	13033	18	12903	28	$308\pm^{63}_{55}$	1.00	25.8819	$-0.48\pm^{3.01E+07}_{2.43}$	$nan\pm^{nan}_{nan}$	0.01
pg0003	0.36572 (#138)	108.78(93)	13033	16	12902	29	$322\pm^{64}_{56}$	1.00	25.8941	$-0.80\pm^{5.19E+05}_{2.38}$	$nan\pm^{nan}_{nan}$	0.03
pg0003	0.36621 (#139)	111.21(94)	13033	18	12901	27	$311\pm^{62}_{55}$	1.00	25.9033	$-1.12\pm^{5.70E+04}_{2.04}$	$nan\pm^{nan}_{nan}$	0.08
pg0003	0.37029 (#140)	111.68(94)	13033	20	12891	30	$338\pm^{67}_{60}$	1.00	25.9807	$8.09E+03\pm^{1.00E+20}_{8.12E+03}$	$16.50\pm^{0.30}_{nan}$	0.59
pg0003	0.38608 (#141)	106.87(92)	13033	32	12857	29	$250\pm^{69}_{51}$	1.00	26.2801	$3.31E+09\pm^{1.00E+20}_{3.31E+09}$	$16.69\pm^{0.11}_{inf}$	1.56
pg0003	0.38639 (#142)	106.91(93)	13033	33	12857	29	$237\pm^{59}_{49}$	1.00	26.2860	$4.16E+07\pm^{1.00E+20}_{4.16E+07}$	$16.64\pm^{0.16}_{-0.16}$	1.19
pg0003	0.40138 (#143)	126.94(94)	13034	33	12830	29	$339\pm^{76}_{60}$	1.00	26.5702	$6.72E+06\pm^{1.00E+20}_{6.72E+06}$	$16.62\pm^{0.18}_{nan}$	1.59

pg0003	0.42192 (#144)	130.53(94)	13034	47	12830	24	$305\pm^{79}_{64}$	1.00	26.9596	$11.39\pm^{1.48E+14}_{41.39}$	$16.26\pm^{0.50}_{nan}$	0.25
pg0157	0.14621 (#145)	–	–	–	–	–	–	–	21.7321	–	–	–
pg0804	0.00382 (#146)	96.91(99)	28317	7	30000	5	$1025\pm^{49}_{47}$	1.00	19.0324	$-1.17\pm^{1.08}_{0.70}$	$nan\pm^{nan}_{nan}$	1.42
pg0804	0.01851 (#147)	98.66(99)	27987	6	30600	5	$1068\pm^{52}_{50}$	1.00	19.3109	$1.16\pm^{7.95}_{1.65}$	$15.83\pm^{0.41}_{nan}$	0.46
pg0804	0.10216 (#148)	59.36(43)	28660	8	nan	nan	$1091\pm^{61}_{59}$	1.00	20.8970	$-0.30\pm^{9.75}_{1.42}$	$nan\pm^{nan}_{nan}$	0.02
pg0804	0.10230 (#149)	59.37(43)	28660	8	nan	nan	$1094\pm^{61}_{59}$	1.00	20.8996	$-0.11\pm^{11.49}_{1.46}$	$nan\pm^{nan}_{nan}$	0.00
pg0832	0.10772 (#150)	51.86(42)	20653	61	nan	nan	$49\pm^{17}_{14}$	1.00	21.0024	$1.39E+03\pm^{1.00E+20}_{1.42E+03}$	$16.46\pm^{0.34}_{nan}$	0.18
pg0832	0.13230 (#151)	33.25(28)	20654	53	nan	nan	$37\pm^{21}_{16}$	1.00	21.4684	$-3.53\pm^{2.47E+04}_{2.19}$	$nan\pm^{nan}_{nan}$	0.59
pg0832	0.15276 (#152)	–	–	–	–	–	–	–	21.8563	–	–	–
pg0832	0.23308 (#153)	50.44(43)	20655	85	nan	nan	$60\pm^{24}_{18}$	1.00	23.3792	$4.51E+09\pm^{1.00E+20}_{4.51E+09}$	$16.69\pm^{0.11}_{inf}$	0.38
pg0832	0.32567 (#154)	127.93(90)	20654	142	20637	171	$49\pm^{24}_{16}$	1.00	25.1347	$3.10E+04\pm^{1.00E+20}_{3.10E+04}$	$16.54\pm^{0.26}_{nan}$	0.65
pg0953	0.01560 (#155)	111.24(90)	12824	14	12310	13	$312\pm^{42}_{39}$	1.00	19.2558	$-1.55\pm^{2.98}_{1.04}$	$nan\pm^{nan}_{nan}$	0.65
pg0953	0.05891 (#156)	84.64(66)	12824	17	12310	22	$428\pm^{49}_{46}$	1.00	20.0769	$1.25E+03\pm^{1.37E+15}_{1.28E+03}$	$16.46\pm^{0.33}_{nan}$	0.71
pg0953	0.06807 (#157)	69.63(58)	12824	16	12310	21	$398\pm^{52}_{49}$	1.00	20.2506	$-2.42\pm^{2.69}_{1.17}$	$nan\pm^{nan}_{nan}$	1.18
pg0953	0.11827 (#158)	36.08(32)	12794	14	nan	nan	$444\pm^{71}_{65}$	1.00	21.2024	$-0.76\pm^{1.16E+04}_{1.97}$	$nan\pm^{nan}_{nan}$	0.04
pg0953	0.14236 (#159)	–	–	–	–	–	–	–	21.6591	–	–	–
pg0953	0.14263 (#160)	–	–	–	–	–	–	–	21.6643	–	–	–
pg0953	0.14307 (#161)	–	–	–	–	–	–	–	21.6726	–	–	–
pg0953	0.22967 (#162)	53.43(43)	12792	15	nan	nan	$475\pm^{71}_{65}$	1.00	23.3145	$-2.40\pm^{2.85}_{1.12}$	$nan\pm^{nan}_{nan}$	1.08
pg0953	0.23251 (#163)	49.94(43)	12792	14	nan	nan	$472\pm^{70}_{65}$	1.00	23.3684	$-3.04\pm^{27.69}_{1.60}$	$nan\pm^{nan}_{nan}$	0.68
pg0953	0.23351 (#164)	51.78(43)	12792	14	nan	nan	$480\pm^{72}_{67}$	1.00	23.3873	$-3.48\pm^{15.11}_{1.45}$	$nan\pm^{nan}_{nan}$	0.88
pg1115	0.12285 (#165)	41.88(32)	17510	23	nan	nan	$304\pm^{54}_{42}$	1.00	21.2892	$1.29E+07\pm^{1.00E+20}_{1.29E+07}$	$16.62\pm^{0.18}_{nan}$	1.56
pg1115	0.12313 (#166)	41.92(32)	17510	23	nan	nan	$300\pm^{57}_{41}$	1.00	21.2945	$4.11E+04\pm^{1.00E+20}_{4.11E+04}$	$16.54\pm^{0.25}_{nan}$	1.44
pg1115	0.13104 (#167*)	46.21(29)	17510	24	nan	nan	$319\pm^{61}_{46}$	1.00	21.4445	$3.29E+04\pm^{1.00E+20}_{3.29E+04}$	$16.54\pm^{0.25}_{nan}$	1.03
pg1115	0.15456 (#168)	–	–	–	–	–	–	–	21.8905	–	–	–
pg1115	0.15467 (#169)	–	–	–	–	–	–	–	21.8925	–	–	–
pg1116	0.05900 (#170)	85.18(69)	285035	13	294383	10	$469\pm^{12}_{12}$	1.00	20.0786	$-0.09\pm^{1.50}_{0.76}$	$nan\pm^{nan}_{nan}$	0.00
pg1116	0.05927 (#171)	85.16(69)	285035	13	294383	10	$470\pm^{12}_{12}$	1.00	20.0838	$0.09\pm^{1.80}_{0.80}$	$14.83\pm^{1.14}_{nan}$	0.03
pg1116	0.11895 (#172)	37.22(33)	285607	13	nan	nan	$509\pm^{16}_{16}$	1.00	21.2153	$0.65\pm^{2.98}_{1.16}$	$15.64\pm^{0.47}_{nan}$	0.31
pg1116	0.13852 (#173)	–	–	–	–	–	–	–	21.5863	–	–	–
pg1116	0.16539 (#174)	36.23(32)	288889	14	nan	nan	$549\pm^{18}_{18}$	1.00	22.0958	$0.72\pm^{3.01}_{1.18}$	$15.68\pm^{0.44}_{nan}$	0.38
pg1116	0.16554 (#175)	36.14(32)	288889	14	nan	nan	$549\pm^{19}_{18}$	1.00	22.0986	$0.84\pm^{3.58}_{1.23}$	$15.72\pm^{0.42}_{nan}$	0.48
pg1116	0.16610 (#176)	37.64(33)	289091	14	nan	nan	$548\pm^{18}_{18}$	1.00	22.1093	$1.26\pm^{4.92}_{1.50}$	$15.85\pm^{0.34}_{nan}$	0.80
pg1116	0.16686 (#177)	39.71(33)	289091	14	nan	nan	$545\pm^{18}_{17}$	1.00	22.1237	$1.18\pm^{5.60}_{1.46}$	$15.84\pm^{0.35}_{nan}$	0.73
pg1116	0.17343 (#178)	50.92(38)	289065	14	nan	nan	$531\pm^{16}_{16}$	1.00	22.2482	$-0.67\pm^{1.06}_{0.66}$	$nan\pm^{nan}_{nan}$	0.61
pg1211	0.00711 (#179)	130.66(97)	709355	11	767876	10	$488\pm^{7}_{7}$	1.00	19.0948	$0.42\pm^{0.61}_{0.46}$	$15.48\pm^{0.32}_{nan}$	1.02
pg1211	0.05117 (#180)	79.82(69)	726954	10	778637	10	$541\pm^{8}_{8}$	1.00	19.9302	$0.38\pm^{0.68}_{0.47}$	$15.44\pm^{0.36}_{nan}$	0.82

pg1211	0.06449 (#181)	80.33(55)	776352	11	776215	10	$557\pm^{9}_{9}$	1.00	20.1827	$-0.57\pm^{0.51}_{0.40}$	$nan\pm^{nan}_{nan}$	1.52
pg1211	0.06491 (#182)	77.87(55)	776352	11	776215	10	$560\pm^{9}_{9}$	1.00	20.1907	$-0.50\pm^{0.52}_{0.40}$	$nan\pm^{nan}_{nan}$	1.19
pg1216	0.12362 (#183)	42.81(30)	11245	26	nan	nan	$225\pm^{51}_{44}$	1.00	21.3038	$1.85E+09\pm^{1.00E+20}_{1.85E+09}$	$16.69\pm^{0.11}_{inf}$	1.17
pg1216	0.12389 (#184)	42.84(30)	11245	26	nan	nan	$222\pm^{50}_{44}$	1.00	21.3090	$2.64E+06\pm^{1.00E+20}_{2.64E+06}$	$16.62\pm^{0.12}_{nan}$	1.09
pg1216	0.12463 (#185)	43.15(30)	11245	26	nan	nan	$218\pm^{58}_{44}$	1.00	21.3230	$4.36E+03\pm^{1.00E+20}_{4.39E+03}$	$16.52\pm^{0.28}_{nan}$	0.72
pg1216	0.12485 (#186)	43.34(30)	11245	26	nan	nan	$216\pm^{58}_{43}$	1.00	21.3272	$203.43\pm^{1.00E+20}_{233.43}$	$16.43\pm^{0.32}_{nan}$	0.50
pg1216	0.13499 (#187)	–	–	–	–	–	–	–	21.5194	–	–	–
pg1216	0.26768 (#188)	88.48(70)	11245	33	11258	21	$157\pm^{56}_{41}$	1.00	24.0352	$1.14E+09\pm^{1.00E+20}_{1.14E+09}$	$16.69\pm^{0.11}_{inf}$	3.23
pg1216	0.28199 (#189)	109.24(79)	11245	36	11258	14	$184\pm^{46}_{39}$	1.00	24.3065	$80.21\pm^{1.00E+20}_{110.21}$	$16.37\pm^{0.43}_{nan}$	0.71
pg1216	0.28237 (#190)	109.62(79)	11245	36	11258	14	$184\pm^{46}_{39}$	1.00	24.3137	$41.22\pm^{1.00E+20}_{71.22}$	$16.33\pm^{0.47}_{nan}$	0.31
pg1259	0.00220 (#191)	124.99(93)	11480	60	11480	42	$106\pm^{26}_{24}$	1.00	19.0017	$809.18\pm^{1.00E+20}_{839.18}$	$16.45\pm^{0.35}_{nan}$	0.30
pg1259	0.00762 (#192)	122.32(92)	11480	63	11480	38	$112\pm^{30}_{24}$	1.00	19.1045	$6.51E+05\pm^{1.00E+20}_{6.51E+05}$	$16.62\pm^{0.13}_{nan}$	1.94
pg1259	0.02217 (#193)	129.87(93)	11480	52	11480	42	$99\pm^{27}_{23}$	1.00	19.3803	$-1.76\pm^{196.56}_{1.80}$	$nan\pm^{nan}_{nan}$	0.24
pg1259	0.04606 (#194)	94.97(77)	11479	35	11480	53	$122\pm^{32}_{26}$	1.00	19.8333	$663.51\pm^{1.00E+20}_{693.51}$	$16.45\pm^{0.30}_{nan}$	0.40
pg1259	0.04650 (#195)	92.99(76)	11479	33	11480	52	$123\pm^{30}_{26}$	1.00	19.8416	$933.16\pm^{1.00E+20}_{963.16}$	$16.45\pm^{0.34}_{nan}$	0.84
pg1259	0.19576 (#196)	53.02(43)	11485	37	nan	nan	$196\pm^{49}_{42}$	1.00	22.6716	$-0.32\pm^{1.00E+20}_{29.68}$	$nan\pm^{nan}_{nan}$	0.00
pg1259	0.21940 (#197)	47.70(41)	11485	46	nan	nan	$141\pm^{49}_{41}$	1.00	23.1198	$-5.05\pm^{1.34}_{1.05}$	$nan\pm^{nan}_{nan}$	6.35
pg1259	0.21953 (#198)	47.70(41)	11485	46	nan	nan	$141\pm^{48}_{41}$	1.00	23.1223	$-4.44\pm^{1.10}_{0.87}$	$nan\pm^{nan}_{nan}$	6.32
pg1259	0.22313 (#199)	51.02(41)	11485	51	nan	nan	$179\pm^{48}_{41}$	1.00	23.1905	$813.26\pm^{1.00E+20}_{843.26}$	$16.45\pm^{0.35}_{nan}$	0.27
pg1259	0.23284 (#200)	57.87(43)	11485	35	nan	nan	$221\pm^{53}_{47}$	1.00	23.3746	$-2.24\pm^{1.00E+20}_{27.76}$	$nan\pm^{nan}_{nan}$	0.06
pg1259	0.23956 (#201)	64.61(45)	11485	40	nan	nan	$204\pm^{49}_{45}$	1.00	23.5021	$33.63\pm^{1.00E+20}_{63.63}$	$16.32\pm^{0.47}_{nan}$	0.07
pg1259	0.25973 (#202)	74.33(62)	11485	44	11479	43	$204\pm^{59}_{41}$	1.00	23.8845	$1.57E+06\pm^{1.00E+20}_{1.57E+06}$	$16.62\pm^{0.13}_{nan}$	1.08
pg1259	0.31979 (#203)	106.65(91)	11483	41	11479	44	$148\pm^{44}_{36}$	1.00	25.0232	$0.35\pm^{1.00E+20}_{30.35}$	$15.41\pm^{1.39}_{nan}$	0.00
pg1259	0.32472 (#204)	104.67(91)	11483	40	11479	44	$156\pm^{49}_{38}$	1.00	25.1167	$8.44E+08\pm^{1.00E+20}_{8.44E+08}$	$16.69\pm^{0.11}_{inf}$	1.52
pg1307	0.14187 (#205)	–	–	–	–	–	–	–	21.6499	–	–	–
pg1307	0.14214 (#206)	–	–	–	–	–	–	–	21.6550	–	–	–
pg1309	0.17586 (#207)	38.46(33)	27263	75	nan	nan	$69\pm^{22}_{21}$	1.00	22.2943	$-0.02\pm^{1.00E+20}_{29.98}$	$nan\pm^{nan}_{nan}$	0.00
pg1309	0.17745 (#208)	38.48(35)	27263	74	nan	nan	$68\pm^{23}_{19}$	1.00	22.3245	$-1.02\pm^{1.00E+20}_{28.98}$	$nan\pm^{nan}_{nan}$	0.01
pg1309	0.17866 (#209)	39.78(36)	27263	76	nan	nan	$66\pm^{22}_{19}$	1.00	22.3474	$1.78\pm^{1.00E+20}_{31.78}$	$15.95\pm^{0.85}_{nan}$	0.01
pg1309	0.17930 (#210)	40.20(37)	27263	76	nan	nan	$66\pm^{22}_{19}$	1.00	22.3595	$7.63\pm^{1.00E+20}_{37.63}$	$16.21\pm^{0.59}_{nan}$	0.03
pg1309	0.17979 (#211)	40.62(37)	27263	76	nan	nan	$65\pm^{21}_{18}$	1.00	22.3688	$7.28\pm^{1.00E+20}_{37.28}$	$16.20\pm^{0.60}_{nan}$	0.03
pg1309	0.18069 (#212)	43.43(38)	27263	72	nan	nan	$74\pm^{22}_{19}$	1.00	22.3859	$1.91E+03\pm^{1.00E+20}_{1.94E+03}$	$16.48\pm^{0.32}_{nan}$	0.18
pg1309	0.18117 (#213)	43.39(38)	27263	72	nan	nan	$74\pm^{23}_{19}$	1.00	22.3950	$2.24E+03\pm^{1.00E+20}_{2.27E+03}$	$16.49\pm^{0.31}_{nan}$	0.23
pg1309	0.18139 (#214)	44.59(39)	27263	70	nan	nan	$79\pm^{21}_{18}$	1.00	22.3992	$2.25E+05\pm^{1.00E+20}_{2.25E+05}$	$16.59\pm^{0.16}_{nan}$	0.42
pg1309	0.18145 (#215)	44.58(39)	27263	70	nan	nan	$78\pm^{24}_{18}$	1.00	22.4003	$1.24E+05\pm^{1.00E+20}_{1.24E+05}$	$16.55\pm^{0.24}_{nan}$	0.42
pg1309	0.18192 (#216)	43.04(39)	27263	70	nan	nan	$78\pm^{25}_{18}$	1.00	22.4092	$1.58E+05\pm^{1.00E+20}_{1.58E+05}$	$16.56\pm^{0.24}_{nan}$	0.58
pg1309	0.18698 (#217)	43.52(37)	27263	77	nan	nan	$79\pm^{24}_{19}$	1.00	22.5051	$2.31E+04\pm^{1.00E+20}_{2.31E+04}$	$16.54\pm^{0.26}_{nan}$	0.52

pg1444	0.22031 (#218)	50.77(40)	17630	43	nan	nan	$104\pm^{38}_{33}$	1.00	23.1371	$-6.35\pm^{1.09}_{1.04}$	$nan\pm^{nan}_{nan}$	17.52
pg1444	0.22676 (#219)	57.73(42)	17630	44	nan	nan	$197\pm^{39}_{35}$	1.00	23.2594	$5.11E+04\pm^{1.00E+20}_{5.12E+04}$	$16.54\pm^{0.25}_{nan}$	0.81
pg1444	0.26690 (#220)	91.99(69)	17630	54	17137	37	$162\pm^{36}_{32}$	1.00	24.0204	$2.17\pm^{2.40E+16}_{32.17}$	$16.01\pm^{0.78}_{nan}$	0.06
pg1444	0.26728 (#221)	94.03(70)	17630	52	17137	37	$166\pm^{36}_{32}$	1.00	24.0276	$3.60\pm^{9.89E+14}_{33.60}$	$16.11\pm^{0.69}_{nan}$	0.09
pg1444	0.26738 (#222)	94.02(70)	17630	52	17137	37	$166\pm^{36}_{32}$	1.00	24.0295	$4.30\pm^{2.79E+16}_{34.30}$	$16.14\pm^{0.66}_{nan}$	0.10
pg1444	0.26747 (#223)	94.01(70)	17630	52	17137	37	$166\pm^{36}_{32}$	1.00	24.0312	$4.80\pm^{1.00E+20}_{34.80}$	$16.15\pm^{0.60}_{nan}$	0.11
pg1626	0.13075 (#224)	28.51(25)	69285	70	nan	nan	$214\pm^{44}_{42}$	1.00	21.4390	$-3.65\pm^{1.35}_{0.97}$	$nan\pm^{nan}_{nan}$	4.65
phl1811	0.07344 (#225)	64.36(45)	77298	71	78895	116	$51\pm^{0}_{0}$	1.00	20.3524	$9.66E+06\pm^{1.00}_{1.00}$	$16.62\pm^{0.00}_{-0.00}$	1.51
phl1811	0.07768 (#226)	59.44(40)	78263	67	78895	188	$51\pm^{12}_{11}$	1.00	20.4328	$71.63\pm^{1.00E+20}_{101.63}$	$16.37\pm^{0.37}_{nan}$	0.08
phl1811	0.08131 (#227)	49.10(33)	78178	68	nan	nan	$56\pm^{14}_{11}$	1.00	20.5016	$1.19E+09\pm^{1.00E+20}_{1.19E+09}$	$16.69\pm^{0.11}_{inf}$	1.80
phl1811	0.13239 (#228)	–	–	–	–	–	–	–	21.4701	–	–	–
phl1811	0.13282 (#229)	–	–	–	–	–	–	–	21.4783	–	–	–
phl1811	0.13318 (#230)	–	–	–	–	–	–	–	21.4851	–	–	–
phl1811	0.13545 (#231)	–	–	–	–	–	–	–	21.5281	–	–	–
phl1811	0.15752 (#232)	–	–	–	–	–	–	–	21.9466	–	–	–
phl1811	0.15786 (#233)	–	–	–	–	–	–	–	21.9530	–	–	–
phl1811	0.17652 (#234)	–	–	–	–	–	–	–	22.3068	–	–	–
phl1811	0.19157 (#235)	–	–	–	–	–	–	–	22.5922	–	–	–
phl1811	0.19194 (#236)	–	–	–	–	–	–	–	22.5992	–	–	–
phl1811	0.19220 (#237)	–	–	–	–	–	–	–	22.6041	–	–	–
pks0312	0.20188 (#238)	58.64(41)	23887	48	nan	nan	$194\pm^{38}_{35}$	1.00	22.7876	$-0.88\pm^{6.61E+16}_{29.12}$	$nan\pm^{nan}_{nan}$	0.01
pks0312	0.20275 (#239)	59.87(41)	23887	49	nan	nan	$181\pm^{37}_{34}$	1.00	22.8041	$-2.34\pm^{3.89E+10}_{2.36}$	$nan\pm^{nan}_{nan}$	0.14
pks0405	0.09192 (#240)	40.76(43)	137149	20	nan	nan	$285\pm^{15}_{14}$	1.00	20.7028	$-1.82\pm^{0.98}_{0.66}$	$nan\pm^{nan}_{nan}$	2.85
pks0405	0.09647 (#241)	44.12(43)	137149	20	nan	nan	$305\pm^{17}_{20}$	1.00	20.7891	$0.09\pm^{3.40E+14}_{3.47}$	$14.83\pm^{1.96}_{nan}$	-0.00
pks0405	0.14808 (#242)	–	–	–	–	–	–	–	21.7676	–	–	–
pks0405	0.16566 (#243)	34.33(32)	137647	22	nan	nan	$322\pm^{21}_{20}$	1.00	22.1009	$6.62\pm^{1.04E+04}_{6.85}$	$16.19\pm^{0.31}_{nan}$	1.05
pks0405	0.16606 (#244)	35.08(32)	137647	22	nan	nan	$320\pm^{20}_{20}$	1.00	22.1085	$8.30\pm^{3.94E+03}_{8.43}$	$16.24\pm^{0.29}_{nan}$	1.17
pks0405	0.16659 (#245)	37.18(33)	137675	22	nan	nan	$317\pm^{20}_{20}$	1.00	22.1185	$7.71\pm^{5.09E+03}_{7.93}$	$16.22\pm^{0.29}_{nan}$	0.98
pks0405	0.16688 (#246)	37.31(33)	137675	22	nan	nan	$316\pm^{19}_{19}$	1.00	22.1240	$5.33\pm^{9.17E+03}_{5.83}$	$16.17\pm^{0.33}_{nan}$	0.80
pks0405	0.16712 (#247)	37.91(33)	137675	22	nan	nan	$313\pm^{21}_{19}$	1.00	22.1286	$3.07\pm^{1.50E+03}_{3.80}$	$16.08\pm^{0.38}_{nan}$	0.51
pks0405	0.18257 (#248)	59.45(44)	136430	23	nan	nan	$304\pm^{18}_{17}$	1.00	22.4215	$-1.68\pm^{1.03}_{0.62}$	$nan\pm^{nan}_{nan}$	2.41
pks0405	0.18289 (#249)	63.38(44)	136430	23	nan	nan	$307\pm^{18}_{17}$	1.00	22.4276	$-1.49\pm^{1.39}_{0.83}$	$nan\pm^{nan}_{nan}$	1.39
pks0405	0.24052 (#250)	57.03(46)	137245	22	nan	nan	$367\pm^{20}_{19}$	1.00	23.5203	$8.95\pm^{8.33E+03}_{8.77}$	$16.24\pm^{0.29}_{1.11}$	1.43
pks0405	0.24094 (#251)	61.56(45)	137216	21	nan	nan	$377\pm^{21}_{19}$	1.00	23.5282	$13.92\pm^{4.89E+06}_{13.26}$	$16.29\pm^{0.28}_{0.65}$	1.85
pks0405	0.24547 (#252)	66.61(47)	136481	21	138649	28	$361\pm^{19}_{18}$	1.00	23.6141	$-0.97\pm^{1.84}_{0.90}$	$nan\pm^{nan}_{nan}$	0.52
pks0405	0.29762 (#253)	85.15(89)	133010	20	137234	19	$392\pm^{21}_{21}$	1.00	24.6029	$16.09\pm^{266.81}_{15.18}$	$16.24\pm^{0.20}_{0.48}$	2.58
pks0405	0.34188 (#254)	114.95(95)	137986	22	137234	21	$365\pm^{19}_{19}$	1.00	25.4420	$-0.18\pm^{2.58}_{1.09}$	$nan\pm^{nan}_{nan}$	0.02

pks0405	0.34225 (#255)	120.66(97)	138000	22	137943	21	$367\pm^{19}_{19}$	1.00	25.4491	$-0.30\pm^{2.31}_{0.98}$	$nan\pm^{nan}_{nan}$	0.05
pks0405	0.35092 (#256)	113.60(95)	138000	22	136470	22	$368\pm^{20}_{19}$	1.00	25.6134	$-0.58\pm^{1.90}_{0.85}$	$nan\pm^{nan}_{nan}$	0.23
pks0405	0.36075 (#257)	117.15(93)	137986	20	134948	21	$404\pm^{21}_{20}$	1.00	25.7998	$6.47\pm^{3.81E+03}_{6.09}$	$16.20\pm^{0.30}_{0.76}$	1.70
pks0405	0.36151 (#258)	115.63(94)	138000	20	134948	21	$404\pm^{20}_{20}$	1.00	25.8142	$54.17\pm^{5.50E+05}_{51.50}$	$16.34\pm^{0.23}_{0.29}$	3.70
pks0405	0.36329 (#259)	110.13(94)	138000	20	134948	21	$408\pm^{22}_{20}$	1.00	25.8480	$2.92E+04\pm^{4.34E+09}_{2.88E+04}$	$16.50\pm^{0.16}_{0.06}$	8.04
pks0405	0.40570 (#260)	109.37(95)	137975	19	138647	28	$415\pm^{23}_{21}$	1.00	26.6521	$0.37\pm^{20.34}_{1.50}$	$15.43\pm^{0.83}_{nan}$	0.05
pks0405	0.40890 (#261)	111.06(95)	137975	20	138647	29	$432\pm^{24}_{23}$	1.00	26.7127	$9.18\pm^{1.07E+03}_{8.55}$	$16.24\pm^{0.21}_{0.62}$	2.02
pks0405	0.49505 (#262)	96.58(89)	136537	33	137118	41	$387\pm^{26}_{25}$	1.00	28.3461	$-1.97\pm^{0.74}_{0.52}$	$nan\pm^{nan}_{nan}$	4.59
pks0405	0.49530 (#263)	97.66(89)	136537	33	137118	41	$389\pm^{27}_{26}$	1.00	28.3509	$-1.86\pm^{0.92}_{0.64}$	$nan\pm^{nan}_{nan}$	3.23
pks0405	0.55506 (#264)	98.30(94)	138708	47	138714	45	$363\pm^{31}_{30}$	1.00	29.4839	$-0.91\pm^{2.72}_{1.13}$	$nan\pm^{nan}_{nan}$	0.30
pks2005	0.06490 (#265)	60.15(62)	54472	6	54641	7	$1896\pm^{53}_{53}$	1.00	20.1905	$-1.05\pm^{0.79}_{0.54}$	$nan\pm^{nan}_{nan}$	1.94
pks2155	0.05405 (#266)	83.01(59)	1701313	3	1685268	3	$4444\pm^{444}_{409}$	1.55	19.9848	$0.00\pm^{0.13}_{0.11}$	$13.43\pm^{1.59}_{nan}$	0.01
pks2155	0.05707 (#267)	76.79(59)	1701521	3	1685268	3	$4316\pm^{448}_{438}$	1.62	20.0420	$0.25\pm^{0.26}_{0.08}$	$15.27\pm^{0.28}_{0.14}$	7.35
q0045	0.11052 (#268)	–	–	–	–	–	–	–	21.0555	–	–	–
q0045	0.13521 (#269)	–	–	–	–	–	–	–	21.5236	–	–	–
q1230	0.09518 (#270)	44.14(33)	39329	61	nan	nan	$48\pm^{19}_{18}$	1.00	20.7646	$-5.80\pm^{1.00E+20}_{2.21}$	$nan\pm^{nan}_{nan}$	1.10
q1230	0.10318 (#271)	48.14(34)	39330	67	nan	nan	$56\pm^{17}_{15}$	1.00	20.9163	$-2.54\pm^{76.95}_{1.48}$	$nan\pm^{nan}_{nan}$	0.59
q1230	0.10445 (#272)	48.96(34)	39330	69	nan	nan	$66\pm^{18}_{14}$	1.00	20.9404	$510.19\pm^{1.00E+20}_{540.19}$	$16.45\pm^{0.30}_{nan}$	0.28
q1230	0.10530 (#273)	49.30(34)	39331	72	nan	nan	$68\pm^{17}_{15}$	1.00	20.9565	$1.86E+07\pm^{1.00E+20}_{1.86E+07}$	$16.62\pm^{0.17}_{nan}$	0.84
q1230	0.10596 (#274)	46.27(33)	39331	70	nan	nan	$70\pm^{17}_{15}$	1.00	20.9690	$2.20E+06\pm^{1.00E+20}_{2.20E+06}$	$16.62\pm^{0.12}_{nan}$	1.07
q1230	0.10666 (#275)	46.39(34)	39331	72	nan	nan	$65\pm^{21}_{15}$	1.00	20.9823	$1.92E+04\pm^{1.00E+20}_{1.93E+04}$	$16.54\pm^{0.26}_{nan}$	0.96
q1230	0.10809 (#276)	45.09(33)	39331	83	nan	nan	$53\pm^{20}_{14}$	1.00	21.0094	$7.62E+08\pm^{1.00E+20}_{7.62E+08}$	$16.69\pm^{0.11}_{inf}$	1.29
q1230	0.10820 (#277)	45.09(33)	39331	83	nan	nan	$53\pm^{20}_{14}$	1.00	21.0115	$2.11E+09\pm^{1.00E+20}_{2.11E+09}$	$16.69\pm^{0.11}_{inf}$	1.29
q1230	0.10861 (#278)	48.14(33)	39331	85	nan	nan	$52\pm^{20}_{14}$	1.00	21.0192	$1.52E+04\pm^{1.00E+20}_{1.53E+04}$	$16.54\pm^{0.23}_{nan}$	1.02
q1230	0.10906 (#279)	44.60(32)	39332	82	nan	nan	$53\pm^{25}_{15}$	1.00	21.0278	$3.02E+04\pm^{1.00E+20}_{3.02E+04}$	$16.54\pm^{0.26}_{nan}$	1.08
q1230	0.10935 (#280)	44.06(32)	39332	82	nan	nan	$55\pm^{17}_{14}$	1.00	21.0333	$3.16E+11\pm^{1.00E+20}_{3.16E+11}$	$16.75\pm^{0.00}_{inf}$	1.71
q1230	0.10956 (#281)	43.57(32)	39332	82	nan	nan	$56\pm^{21}_{15}$	1.00	21.0373	$5.49E+08\pm^{1.00E+20}_{5.49E+08}$	$16.69\pm^{0.11}_{inf}$	1.56
q1230	0.11707 (#282)	39.83(27)	39333	64	nan	nan	$51\pm^{20}_{17}$	1.00	21.1796	$-5.35\pm^{1.11}_{1.02}$	$nan\pm^{nan}_{nan}$	13.29
q1230	0.11743 (#283)	34.85(25)	39333	60	nan	nan	$57\pm^{22}_{19}$	1.00	21.1865	$-4.41\pm^{0.92}_{0.82}$	$nan\pm^{nan}_{nan}$	11.53
q1230	0.11781 (#284)	35.43(25)	39333	60	nan	nan	$59\pm^{22}_{19}$	1.00	21.1937	$-4.31\pm^{0.95}_{0.82}$	$nan\pm^{nan}_{nan}$	10.59
rbs1892	0.15752 (#285)	–	–	–	–	–	–	–	21.9466	–	–	–
rbs1892	0.17133 (#286)	46.32(37)	4929	14	nan	nan	$312\pm^{101}_{76}$	1.00	22.2084	$2.84E+04\pm^{1.00E+20}_{2.85E+04}$	$16.54\pm^{0.25}_{nan}$	0.45
rbs1892	0.19874 (#287)	50.02(44)	4929	24	nan	nan	$332\pm^{100}_{76}$	1.00	22.7281	$65.39\pm^{1.00E+20}_{95.39}$	$16.35\pm^{0.45}_{nan}$	0.16
rbs542	0.10323 (#288)	48.13(48)	192804	9	nan	nan	$1054\pm^{22}_{22}$	1.00	20.9172	$-0.64\pm^{0.80}_{0.54}$	$nan\pm^{nan}_{nan}$	0.84
rbs542	0.10379 (#289)	48.09(47)	192375	9	nan	nan	$1053\pm^{22}_{22}$	1.00	20.9279	$-0.52\pm^{0.87}_{0.57}$	$nan\pm^{nan}_{nan}$	0.52
rxj0439	0.11547 (#290)	38.76(35)	151442	17	nan	nan	$337\pm^{18}_{18}$	1.00	21.1493	$-1.84\pm^{0.78}_{0.54}$	$nan\pm^{nan}_{nan}$	4.30
rxj0439	0.21833 (#291)	61.09(43)	145661	21	nan	nan	$419\pm^{22}_{22}$	1.00	23.0995	$-2.54\pm^{0.83}_{0.62}$	$nan\pm^{nan}_{nan}$	5.79

rxj0439	0.24235 (#292)	63.87(47)	151874	19	121198	15	$498\pm^{26}_{21}$	1.00	23.5550	$14.62\pm^{7.81E+03}_{13.54}$	$16.28\pm^{0.24}_{0.47}$	2.82
rxj0439	0.24258 (#293)	69.70(49)	151906	19	131963	21	$497\pm^{21}_{21}$	1.00	23.5593	$30.90\pm^{1.70E+04}_{29.84}$	$16.31\pm^{0.20}_{0.50}$	2.55
rxj0439	0.24313 (#294)	66.17(48)	151874	18	131963	22	$498\pm^{23}_{22}$	1.00	23.5697	$6.96\pm^{184.85}_{6.96}$	$16.18\pm^{0.25}_{2.79}$	1.44
rxj0439	0.24387 (#295)	71.95(50)	151906	18	137345	21	$497\pm^{22}_{21}$	1.00	23.5838	$1.28\pm^{13.88}_{1.95}$	$15.85\pm^{0.44}_{nan}$	0.33
s50716	0.23145 (#296)	57.72(42)	75697	12	nan	nan	$741\pm^{36}_{35}$	1.00	23.3483	$2.00\pm^{3.46E+04}_{3.48}$	$15.98\pm^{0.52}_{nan}$	0.15
ton28	0.13746 (#297)	–	–	–	–	–	–	–	21.5662	–	–	–
ton28	0.13773 (#298)	–	–	–	–	–	–	–	21.5714	–	–	–
ton28	0.13781 (#299)	–	–	–	–	–	–	–	21.5729	–	–	–
ton28	0.17251 (#300)	50.74(37)	81682	38	nan	nan	$131\pm^{18}_{17}$	1.00	22.2308	$-1.79\pm^{3.97}_{1.28}$	$nan\pm^{nan}_{nan}$	0.60
ton28	0.21259 (#301)	60.47(42)	81454	35	nan	nan	$188\pm^{20}_{19}$	1.00	22.9907	$0.13\pm^{3.65E+04}_{2.45}$	$15.01\pm^{1.52}_{nan}$	0.00
ton28	0.24292 (#302)	30.56(48)	85563	34	83705	38	$186\pm^{19}_{19}$	1.00	23.5658	$3.06\pm^{1.41E+07}_{33.06}$	$16.07\pm^{0.53}_{nan}$	0.18
ton28	0.24859 (#303)	52.11(52)	84503	35	85711	26	$180\pm^{20}_{19}$	1.00	23.6733	$-1.55\pm^{5.49}_{1.32}$	$nan\pm^{nan}_{nan}$	0.42
ton28	0.27338 (#304)	80.27(77)	85129	37	86614	30	$205\pm^{19}_{19}$	1.00	24.1433	$-1.67\pm^{2.16}_{1.04}$	$nan\pm^{nan}_{nan}$	0.97
ton28	0.33021 (#305)	107.71(94)	85874	26	86028	38	$199\pm^{20}_{19}$	1.00	25.2208	$-2.21\pm^{1.51}_{0.90}$	$nan\pm^{nan}_{nan}$	2.04
tons180	0.02340 (#306)	99.08(96)	177396	6	194071	7	$901\pm^{18}_{18}$	1.00	19.4037	$-0.01\pm^{0.89}_{0.46}$	$nan\pm^{nan}_{nan}$	-0.00
tons180	0.04360 (#307)	69.00(82)	187350	6	195496	7	$955\pm^{18}_{18}$	1.00	19.7867	$-0.03\pm^{0.88}_{0.48}$	$nan\pm^{nan}_{nan}$	-0.01
tons180	0.04560 (#308)	67.80(80)	187350	6	195974	7	$963\pm^{19}_{19}$	1.00	19.8246	$0.49\pm^{1.01}_{0.68}$	$15.54\pm^{0.38}_{nan}$	0.60

Table B.6: O VIII upper limit measurements with *XMM-Newton* data, at the prior redshift from the O VI lines from Table A.1.

Target line		cmin	RGS1	power–law		line component			ΔC	
Name	z	(d.o.f.)	avg exp (s)	norm.	index	λ (Å)	τ_0	$\log N + (\mathrm{cm}^{-2})$	(d.o.f.)	
1es1028	0.12314 (#1)	33.31(31)	146792	nan	$963\pm^{40}_{26}$	1.00	21.2947	2.30	16.01	0.01
1es1028	0.13706 (#2)	–	–	–	–	–	21.5587	–	–	–
1es1028	0.33735 (#3)	92.62(96)	147900	144798	$1196\pm^{31}_{31}$	1.00	25.3562	9.35	16.25	6.58
1es1553	0.18759 (#4)	29.26(27)	1729540	nan	$540\pm^{318}_{194}$	2.55	22.5167	0.39	15.45	1.81
1es1553	0.18775 (#5)	28.91(27)	1729540	nan	$550\pm^{295}_{211}$	2.52	22.5197	0.40	15.46	2.20
1es1553	0.18984 (#6)	25.62(27)	1729542	nan	$406\pm^{219}_{140}$	3.05	22.5594	0.54	15.56	8.20
1es1553	0.21631 (#7)	33.20(25)	1723969	nan	$60\pm^{36}_{21}$	6.19	23.0612	0.36	15.42	0.03
1es1553	0.31130 (#8)	113.12(91)	1744157	1748313	$2268\pm^{757}_{440}$	0.67	24.8622	0.35	15.41	17.08
1es1553	0.37868 (#9)	113.07(88)	1784762	1713272	$1213\pm^{467}_{336}$	1.52	26.1398	0.40	15.45	15.34
1es1553	0.39497 (#10)	118.64(92)	1704141	1756581	$481\pm^{192}_{138}$	2.74	26.4486	0.19	15.15	1.31
3c249	0.24676 (#11)	41.19(50)	2644	2524	$373\pm^{135}_{107}$	1.00	23.6386	5.00E+19	16.80	0.10
3c249	0.30788 (#12)	70.28(91)	2641	2524	$269\pm^{119}_{90}$	1.00	24.7974	5.00E+19	16.75	0.05
3c249	0.30809 (#13)	70.31(91)	2641	2524	$271\pm^{119}_{91}$	1.00	24.8014	1.55E+14	16.78	0.02
3c249	0.31364 (#14)	73.37(90)	2640	2524	$377\pm^{139}_{111}$	1.00	24.9066	5.00E+19	16.80	1.07
3c273	0.00337 (#15)	122.62(82)	1002935	1016589	$2162\pm^{179}_{168}$	2.23	19.0239	0.32	15.37	-0.27
3c273	0.00533 (#16)	121.19(82)	1000681	1016019	$2034\pm^{174}_{166}$	2.37	19.0611	0.14	15.02	-0.06
3c273	0.00764 (#17)	119.15(82)	1000362	1015449	$1895\pm^{175}_{164}$	2.53	19.1049	0.14	15.03	0.70
3c273	0.02947 (#18)	124.26(90)	979671	1010400	$2182\pm^{194}_{180}$	2.22	19.5188	0.15	15.06	0.00
3c273	0.04898 (#19)	97.81(72)	981682	1017674	$2995\pm^{379}_{339}$	1.54	19.8887	0.17	15.12	0.19
3c273	0.06655 (#20)	70.47(59)	1020346	1015505	$3584\pm^{502}_{559}$	1.18	20.2218	0.26	15.28	-0.58
3c273	0.09018 (#21)	39.08(47)	949280	nan	$2360\pm^{380}_{338}$	2.03	20.6698	0.22	15.23	1.16
3c273	0.12007 (#22)	29.12(34)	930918	nan	$2926\pm^{1141}_{776}$	1.62	21.2365	0.22	15.21	-0.04
3c273	0.14660 (#23)	–	–	–	–	–	21.7395	–	–	–
3c273	0.15784 (#24)	34.61(25)	1047179	nan	$2310\pm^{773}_{593}$	2.01	21.9526	0.16	15.08	12.16
h1821	0.02438 (#25)	127.18(98)	30082	44303	$1073\pm^{56}_{55}$	1.00	19.4222	1.28	15.85	0.18
h1821	0.10817 (#26)	50.54(39)	33073	nan	$1206\pm^{79}_{77}$	1.00	21.0109	3.07	16.07	0.13
h1821	0.12133 (#27)	38.85(28)	33486	nan	$1220\pm^{99}_{97}$	1.00	21.2604	166.48	16.36	0.08
h1821	0.12147 (#28)	38.90(28)	33486	nan	$1214\pm^{99}_{97}$	1.00	21.2631	33.18	16.30	0.01
h1821	0.16992 (#29)	47.55(34)	32399	nan	$970\pm^{94}_{91}$	1.00	22.1817	4.22E+06	16.56	0.00
h1821	0.17043 (#30)	47.37(34)	32399	nan	$986\pm^{100}_{91}$	1.00	22.1914	3.40E+13	16.74	0.23
h1821	0.21326 (#31)	58.03(45)	29109	nan	$975\pm^{94}_{92}$	1.00	23.0034	2.25	16.01	0.60
h1821	0.22497 (#32)	67.04(48)	29437	nan	$945\pm^{94}_{91}$	1.00	23.2254	1.09	15.81	1.95

h1821	0.22522 (#33)	66.78(47)	29837	nan	$962\pm^{94}_{90}$	1.00	23.2302	1.32	15.88	1.57
h1821	0.22639 (#34)	68.85(47)	29881	nan	$947\pm^{93}_{89}$	1.00	23.2524	1.36	15.87	1.14
h1821	0.24531 (#35)	72.51(51)	31382	32028	$1052\pm^{92}_{86}$	1.00	23.6111	3.28E+07	16.64	0.31
h1821	0.26657 (#36)	79.55(72)	31337	42756	$1040\pm^{83}_{81}$	1.00	24.0142	1.09	15.82	1.71
h1821	0.28800 (#37)	114.20(93)	27766	42046	$1294\pm^{95}_{91}$	1.00	24.4205	50.06	16.34	0.65
h1821	0.29658 (#38)	111.33(97)	27950	42972	$1276\pm^{93}_{91}$	1.00	24.5832	0.93	15.76	1.58
h1821	0.29680 (#39)	112.27(97)	27836	43008	$1282\pm^{94}_{91}$	1.00	24.5873	1.03	15.80	1.00
h2356	0.11461 (#40)	57.52(40)	476224	nan	$1072\pm^{17}_{14}$	1.00	21.1330	1.17	15.84	0.03
h2356	0.16512 (#41)	37.80(32)	505443	nan	$1093\pm^{17}_{20}$	1.00	22.0907	0.62	15.62	0.02
he0056	0.16392 (#42)	27.81(24)	160091	nan	$356\pm^{24}_{22}$	1.00	22.0679	2.86E+04	16.51	2.53
he0056	0.16492 (#43)	28.43(24)	160091	nan	$353\pm^{25}_{21}$	1.00	22.0869	5.33E+03	16.48	1.64
he0226	0.01746 (#44)	124.17(84)	31711	31707	$157\pm^{20}_{19}$	1.00	19.2910	1.85	15.97	0.93
he0226	0.02679 (#45)	131.34(93)	31711	31707	$154\pm^{20}_{18}$	1.00	19.4679	290.81	16.39	0.01
he0226	0.04121 (#46)	120.74(81)	31711	31707	$166\pm^{22}_{20}$	1.00	19.7413	2.71	16.06	0.53
he0226	0.04535 (#47)	113.12(77)	31711	31707	$161\pm^{22}_{20}$	1.00	19.8198	4.95	16.16	0.29
he0226	0.04609 (#48)	112.96(76)	31711	31707	$164\pm^{22}_{20}$	1.00	19.8339	55.75	16.35	0.04
he0226	0.06015 (#49)	84.08(65)	31711	31707	$121\pm^{22}_{20}$	1.00	20.1004	0.87	15.74	8.15
he0226	0.06083 (#50)	83.15(64)	31711	31707	$129\pm^{22}_{20}$	1.00	20.1133	0.88	15.73	5.31
he0226	0.07023 (#51)	66.31(54)	31711	31707	$170\pm^{24}_{23}$	1.00	20.2916	7.86E+07	16.65	0.01
he0226	0.08375 (#52)	52.16(42)	31711	nan	$196\pm^{28}_{23}$	1.00	20.5479	5.00E+19	16.80	2.53
he0226	0.08901 (#53)	47.97(42)	31711	nan	$183\pm^{25}_{23}$	1.00	20.6476	1.76	15.95	1.23
he0226	0.08938 (#54)	47.78(42)	31711	nan	$182\pm^{25}_{23}$	1.00	20.6546	1.73	15.96	1.47
he0226	0.08950 (#55)	46.05(43)	31711	nan	$182\pm^{25}_{23}$	1.00	20.6569	1.54	15.92	1.57
he0226	0.09220 (#56)	46.95(42)	31711	nan	$186\pm^{25}_{23}$	1.00	20.7081	2.15	16.00	0.92
he0226	0.10668 (#57)	50.29(43)	31711	nan	$175\pm^{26}_{24}$	1.00	20.9827	1.23	15.84	2.23
he0226	0.11514 (#58)	39.66(36)	31711	nan	$203\pm^{30}_{27}$	1.00	21.1431	2.60E+09	16.64	0.15
he0226	0.11680 (#59)	37.43(34)	31711	nan	$207\pm^{37}_{25}$	1.00	21.1745	5.00E+19	16.80	1.76
he0226	0.11733 (#60)	36.95(34)	31711	nan	$202\pm^{39}_{25}$	1.00	21.1846	5.00E+19	16.80	2.01
he0226	0.12589 (#61)	35.52(30)	31712	nan	$206\pm^{36}_{27}$	1.00	21.3469	5.00E+19	16.75	2.12
he0226	0.13832 (#62)	–	–	–	–	–	21.5825	–	–	–
he0226	0.15175 (#63)	–	–	–	–	–	21.8372	–	–	–
he0226	0.15549 (#64)	–	–	–	–	–	21.9081	–	–	–
he0226	0.16237 (#65)	33.50(25)	31712	nan	$113\pm^{37}_{33}$	1.00	22.0385	1.08	15.82	15.81
he0226	0.16339 (#66)	33.20(26)	31712	nan	$113\pm^{36}_{32}$	1.00	22.0579	1.02	15.80	16.22
he0226	0.16971 (#67)	40.73(28)	31712	nan	$140\pm^{34}_{30}$	1.00	22.1777	4.94E+04	16.52	0.43
he0226	0.18619 (#68)	50.47(36)	31712	nan	$175\pm^{30}_{27}$	1.00	22.4902	5.00E+19	16.75	1.41
he0226	0.18811 (#69)	48.87(35)	31712	nan	$219\pm^{37}_{30}$	1.00	22.5266	5.00E+19	16.75	1.73

he0226	0.18891 (#70)	57.62(39)	31712	nan	$196\pm^{30}_{28}$	1.00	22.5417	5.00E+19	16.80	2.21
he0226	0.19374 (#71)	46.89(38)	31712	nan	$168\pm^{30}_{28}$	1.00	22.6333	5.00E+19	16.80	2.44
he0226	0.19453 (#72)	48.32(38)	31712	nan	$157\pm^{34}_{26}$	1.00	22.6483	5.00E+19	16.75	0.67
he0226	0.19860 (#73)	51.59(40)	31712	nan	$161\pm^{31}_{28}$	1.00	22.7255	5.69E+12	16.70	0.00
he0226	0.20055 (#74)	50.95(40)	31712	nan	$166\pm^{29}_{27}$	1.00	22.7624	5.00E+19	16.80	0.43
he0226	0.20703 (#75)	53.97(42)	31712	nan	$158\pm^{30}_{27}$	1.00	22.8853	2.94E+08	16.64	0.01
he0226	0.22009 (#76)	36.18(41)	31713	nan	$188\pm^{33}_{30}$	1.00	23.1329	4.75E+12	16.71	0.00
he0226	0.22099 (#77)	39.39(41)	31713	nan	$197\pm^{33}_{30}$	1.00	23.1500	1.13E+07	16.60	0.03
he0226	0.23009 (#78)	42.36(43)	31713	nan	$209\pm^{33}_{28}$	1.00	23.3225	5.00E+19	16.80	1.39
he0226	0.23964 (#79)	46.29(45)	31713	nan	$171\pm^{30}_{27}$	1.00	23.5036	5.37E+07	16.62	0.01
he0226	0.24522 (#80)	46.47(48)	31713	31705	$152\pm^{29}_{27}$	1.00	23.6094	7.88	16.21	0.65
he0226	0.25099 (#81)	54.13(54)	31713	31705	$163\pm^{30}_{27}$	1.00	23.7188	4.10E+05	16.60	0.00
he0226	0.27155 (#82)	78.85(73)	31713	31705	$224\pm^{30}_{28}$	1.00	24.1086	5.00E+19	16.80	1.20
he0226	0.27956 (#83)	79.52(77)	31713	31705	$224\pm^{32}_{29}$	1.00	24.2605	2.83	16.07	0.59
he0226	0.28041 (#84)	78.68(77)	31713	31705	$234\pm^{33}_{30}$	1.00	24.2766	8.93	16.24	0.27
he0226	0.29134 (#85)	83.52(84)	31711	31705	$238\pm^{35}_{32}$	1.00	24.4838	1.85	15.97	1.00
he0226	0.29213 (#86)	86.12(85)	31711	31705	$240\pm^{35}_{32}$	1.00	24.4988	1.65	15.93	1.02
he0226	0.30939 (#87)	97.61(90)	31709	31705	$246\pm^{33}_{30}$	1.00	24.8260	9.52E+05	16.61	0.27
he0226	0.31833 (#88)	99.31(91)	31708	31705	$223\pm^{33}_{30}$	1.00	24.9955	4.21E+09	16.67	0.49
he0226	0.33965 (#89)	102.15(94)	31706	31705	$273\pm^{39}_{31}$	1.00	25.3998	1.16E+15	16.77	0.91
he0226	0.34036 (#90)	108.55(94)	31706	31705	$273\pm^{40}_{31}$	1.00	25.4132	5.00E+19	16.80	1.70
he0226	0.35493 (#91)	115.28(93)	31706	31704	$247\pm^{33}_{30}$	1.00	25.6895	1.39	15.88	1.51
he0226	0.35528 (#92)	116.14(94)	31706	31704	$242\pm^{33}_{30}$	1.00	25.6961	1.14	15.82	2.04
he0226	0.37281 (#93)	117.30(93)	31706	31704	$305\pm^{42}_{33}$	1.00	26.0285	9.19E+12	16.71	0.86
he0226	0.38420 (#94)	128.19(92)	31706	31704	$295\pm^{38}_{36}$	1.00	26.2444	5.00E+19	16.75	2.16
he0226	0.38636 (#95)	130.09(92)	31706	31704	$281\pm^{36}_{34}$	1.00	26.2854	7.27E+06	16.62	0.22
he0226	0.39642 (#96)	139.43(93)	31706	31704	$262\pm^{37}_{34}$	1.00	26.4761	3.22	16.09	0.35
he0226	0.39692 (#97*)	137.43(91)	31706	31704	$261\pm^{37}_{34}$	1.00	26.4856	2.52	16.05	0.52
he0226	0.39890 (#98)	135.24(93)	31707	31704	$270\pm^{38}_{35}$	1.00	26.5231	2.44	16.04	0.54
he0226	0.40034 (#99)	134.81(92)	31707	31704	$276\pm^{38}_{35}$	1.00	26.5504	32.58	16.30	0.05
he0226	0.40274 (#100)	137.73(93)	31707	31704	$295\pm^{39}_{36}$	1.00	26.5960	3.94E+08	16.62	0.26
he0226	0.49225 (#101)	110.65(88)	31709	31712	$363\pm^{50}_{46}$	1.00	28.2931	6.76E+04	16.53	0.00
he0226	0.49254 (#102)	110.33(88)	31709	31712	$359\pm^{49}_{46}$	1.00	28.2986	437.84	16.39	0.04
he0226	0.49280 (#103)	110.26(88)	31709	31712	$357\pm^{50}_{46}$	1.00	28.3035	28.12	16.29	0.12
he0226	0.49309 (#104)	109.11(87)	31709	31713	$348\pm^{49}_{46}$	1.00	28.3090	5.73	16.18	0.27
i22456	0.09858 (#105)	56.99(44)	79900	nan	$498\pm^{28}_{27}$	1.00	20.8291	5.00E+19	16.75	4.29
i22456	0.09895 (#106)	60.07(44)	79900	nan	$499\pm^{44}_{27}$	1.00	20.8361	5.00E+19	16.80	3.98

i22456	0.09931 (#107)	59.72(44)	79900	nan	$501\pm^{44}_{27}$	1.00	20.8429	5.00E+19	16.80	4.43
i22456	0.09959 (#108)	54.85(44)	79898	nan	$498\pm^{28}_{27}$	1.00	20.8482	5.00E+19	16.75	4.62
i22456	0.09989 (#109)	55.11(44)	79898	nan	$496\pm^{38}_{27}$	1.00	20.8539	5.00E+19	16.78	4.24
i22456	0.10034 (#110)	55.73(44)	79898	nan	$500\pm^{28}_{27}$	1.00	20.8624	5.00E+19	16.80	4.33
i22456	0.10101 (#111)	55.60(44)	79897	nan	$495\pm^{38}_{27}$	1.00	20.8751	5.00E+19	16.75	3.43
i22456	0.10146 (#112)	55.42(44)	79897	nan	$499\pm^{28}_{28}$	1.00	20.8837	1.86E+11	16.71	3.55
mr2251	0.01070 (#113)	126.25(97)	415723	451165	$1562\pm^{16}_{16}$	1.00	19.1629	0.20	15.19	9.49
mrk421	0.01009 (#114*)	95.39(57)	1385032	1437210	$27095\pm^{56}_{49}$	1.00	19.1513	0.06	14.70	9.73
mrk876	0.00311 (#115)	98.25(96)	2693	2600	$283\pm^{87}_{69}$	1.00	19.0190	5.00E+19	16.76	0.38
mrk876	0.06248 (#116)	59.48(66)	2754	2708	$362\pm^{110}_{83}$	1.00	20.1446	5.00E+19	16.76	1.48
mrk876	0.08579 (#117)	44.05(43)	2804	nan	$444\pm^{126}_{109}$	1.00	20.5866	1.80	15.95	1.79
mrk876	0.11488 (#118)	52.10(37)	2790	nan	$714\pm^{157}_{165}$	1.00	21.1381	5.00E+19	16.80	3.07
mrk876	0.11517 (#119)	52.51(37)	2790	nan	$706\pm^{235}_{159}$	1.00	21.1436	5.00E+19	16.75	2.62
mrk876	0.11588 (#120)	50.65(36)	2788	nan	$705\pm^{157}_{137}$	1.00	21.1571	5.00E+19	16.80	2.97
ngc7469	0.00962 (#121)	84.33(74)	631131	664074	$1941\pm^{17}_{17}$	1.00	19.1424	0.77	15.70	45.84
ngc7469	0.00994 (#122)	94.79(74)	630829	663435	$1942\pm^{17}_{17}$	1.00	19.1485	0.95	15.77	53.76
ngc7469	0.01153 (#123)	85.80(74)	622605	665535	$1939\pm^{17}_{17}$	1.00	19.1786	1.43	15.90	53.36
p1103	0.13556 (#124)	–	–	–	–	–	21.5302	–	–	–
p1103	0.13937 (#125)	–	–	–	–	–	21.6025	–	–	–
p1103	0.14099 (#126)	–	–	–	–	–	21.6332	–	–	–
p1103	0.14126 (#127)	–	–	–	–	–	21.6383	–	–	–
p1103	0.17277 (#128)	44.35(37)	15674	nan	$2927\pm^{142}_{138}$	1.00	22.2357	3.59E+11	16.69	6.11
pg0003	0.16521 (#129)	39.30(31)	13036	nan	$287\pm^{72}_{63}$	1.00	22.0924	1.49	15.91	2.77
pg0003	0.20907 (#130)	38.93(42)	13036	nan	$282\pm^{58}_{51}$	1.00	22.9240	5.00E+19	16.75	0.89
pg0003	0.29021 (#131)	98.06(84)	13036	12941	$230\pm^{57}_{49}$	1.00	24.4624	1.17	15.83	2.68
pg0003	0.30551 (#132)	110.03(89)	13035	12941	$297\pm^{62}_{55}$	1.00	24.7525	5.00E+19	16.80	1.06
pg0003	0.30569 (#133)	111.09(89)	13035	12941	$297\pm^{71}_{55}$	1.00	24.7559	5.00E+19	16.80	1.07
pg0003	0.34757 (#134)	112.83(95)	13033	12938	$306\pm^{63}_{54}$	1.00	25.5499	1.15E+13	16.72	0.09
pg0003	0.34788 (#135)	112.95(95)	13033	12938	$297\pm^{60}_{53}$	1.00	25.5558	1.40E+09	16.67	0.03
pg0003	0.36452 (#136)	111.56(93)	13033	12904	$311\pm^{62}_{55}$	1.00	25.8713	4.91E+12	16.70	0.04
pg0003	0.36508 (#137)	109.85(94)	13033	12903	$308\pm^{63}_{55}$	1.00	25.8819	1.50E+07	16.61	0.01
pg0003	0.36572 (#138)	108.78(93)	13033	12902	$322\pm^{64}_{56}$	1.00	25.8941	2.59E+05	16.58	0.03
pg0003	0.36621 (#139)	111.21(94)	13033	12901	$311\pm^{62}_{55}$	1.00	25.9033	2.85E+04	16.50	0.08
pg0003	0.37029 (#140)	111.68(94)	13033	12891	$338\pm^{67}_{60}$	1.00	25.9807	5.00E+19	16.80	0.59
pg0003	0.38608 (#141)	106.87(92)	13033	12857	$250\pm^{69}_{51}$	1.00	26.2801	5.00E+19	16.80	1.56
pg0003	0.38639 (#142)	106.91(93)	13033	12857	$237\pm^{59}_{49}$	1.00	26.2860	5.00E+19	16.80	1.19
pg0003	0.40138 (#143)	126.94(94)	13034	12830	$339\pm^{76}_{60}$	1.00	26.5702	5.00E+19	16.80	1.59

pg0003	0.42192 (#144)	130.53(94)	13034	12830	$305\pm^{79}_{64}$	1.00	26.9596	7.39E+13	16.75	0.25
pg0157	0.14621 (#145)	–	–	–	–	–	21.7321	–	–	–
pg0804	0.00382 (#146)	96.91(99)	28317	30000	$1025\pm^{49}_{47}$	1.00	19.0324	0.89	15.75	1.42
pg0804	0.01851 (#147)	98.66(99)	27987	30600	$1068\pm^{52}_{50}$	1.00	19.3109	4.80	16.15	0.46
pg0804	0.10216 (#148)	59.36(43)	28660	nan	$1091\pm^{61}_{59}$	1.00	20.8970	5.58	16.17	0.02
pg0804	0.10230 (#149)	59.37(43)	28660	nan	$1094\pm^{61}_{59}$	1.00	20.8996	6.47	16.20	0.00
pg0832	0.10772 (#150)	51.86(42)	20653	nan	$49\pm^{17}_{14}$	1.00	21.0024	5.00E+19	16.80	0.18
pg0832	0.13230 (#151)	33.25(28)	20654	nan	$37\pm^{21}_{16}$	1.00	21.4684	1.24E+04	16.49	0.59
pg0832	0.15276 (#152)	–	–	–	–	–	21.8563	–	–	–
pg0832	0.23308 (#153)	50.44(43)	20655	nan	$60\pm^{24}_{18}$	1.00	23.3792	5.00E+19	16.80	0.38
pg0832	0.32567 (#154)	127.93(90)	20654	20637	$49\pm^{24}_{16}$	1.00	25.1347	5.00E+19	16.80	0.65
pg0953	0.01560 (#155)	111.24(90)	12824	12310	$312\pm^{42}_{39}$	1.00	19.2558	2.01	15.98	0.65
pg0953	0.05891 (#156)	84.64(66)	12824	12310	$428\pm^{49}_{46}$	1.00	20.0769	6.83E+14	16.78	0.71
pg0953	0.06807 (#157)	69.63(58)	12824	12310	$398\pm^{52}_{49}$	1.00	20.2506	1.93	15.98	1.18
pg0953	0.11827 (#158)	36.08(32)	12794	nan	$444\pm^{71}_{65}$	1.00	21.2024	5.82E+03	16.51	0.04
pg0953	0.14236 (#159)	–	–	–	–	–	21.6591	–	–	–
pg0953	0.14263 (#160)	–	–	–	–	–	21.6643	–	–	–
pg0953	0.14307 (#161)	–	–	–	–	–	21.6726	–	–	–
pg0953	0.22967 (#162)	53.43(43)	12792	nan	$475\pm^{71}_{65}$	1.00	23.3145	1.98	15.98	1.08
pg0953	0.23251 (#163)	49.94(43)	12792	nan	$472\pm^{70}_{65}$	1.00	23.3684	14.65	16.24	0.68
pg0953	0.23351 (#164)	51.78(43)	12792	nan	$480\pm^{72}_{67}$	1.00	23.3873	8.28	16.21	0.88
pg1115	0.12285 (#165)	41.88(32)	17510	nan	$304\pm^{54}_{42}$	1.00	21.2892	5.00E+19	16.80	1.56
pg1115	0.12313 (#166)	41.92(32)	17510	nan	$300\pm^{57}_{41}$	1.00	21.2945	5.00E+19	16.80	1.44
pg1115	0.13104 (#167*)	46.21(29)	17510	nan	$319\pm^{61}_{46}$	1.00	21.4445	5.00E+19	16.80	1.03
pg1115	0.15456 (#168)	–	–	–	–	–	21.8905	–	–	–
pg1115	0.15467 (#169)	–	–	–	–	–	21.8925	–	–	–
pg1116	0.05900 (#170)	85.18(69)	285035	294383	$469\pm^{12}_{12}$	1.00	20.0786	1.13	15.82	0.00
pg1116	0.05927 (#171)	85.16(69)	285035	294383	$470\pm^{12}_{12}$	1.00	20.0838	1.30	15.87	0.03
pg1116	0.11895 (#172)	37.22(33)	285607	nan	$509\pm^{16}_{16}$	1.00	21.2153	2.07	15.99	0.31
pg1116	0.13852 (#173)	–	–	–	–	–	21.5863	–	–	–
pg1116	0.16539 (#174)	36.23(32)	288889	nan	$549\pm^{18}_{18}$	1.00	22.0958	2.10	16.00	0.38
pg1116	0.16554 (#175)	36.14(32)	288889	nan	$549\pm^{19}_{18}$	1.00	22.0986	2.40	16.02	0.48
pg1116	0.16610 (#176)	37.64(33)	289091	nan	$548\pm^{18}_{18}$	1.00	22.1093	3.21	16.08	0.80
pg1116	0.16686 (#177)	39.71(33)	289091	nan	$545\pm^{18}_{17}$	1.00	22.1237	3.53	16.11	0.73
pg1116	0.17343 (#178)	50.92(38)	289065	nan	$531\pm^{16}_{16}$	1.00	22.2482	0.86	15.73	0.61
pg1211	0.00711 (#179)	130.66(97)	709355	767876	$488\pm^{7}_{7}$	1.00	19.0948	0.54	15.57	1.02
pg1211	0.05117 (#180)	79.82(69)	726954	778637	$541\pm^{8}_{8}$	1.00	19.9302	0.57	15.59	0.82

pg1211	0.06449 (#181)	80.33(55)	776352	776215	$557\pm^{9}_{9}$	1.00	20.1827	0.46	15.51	1.52
pg1211	0.06491 (#182)	77.87(55)	776352	776215	$560\pm^{9}_{9}$	1.00	20.1907	0.46	15.51	1.19
pg1216	0.12362 (#183)	42.81(30)	11245	nan	$225\pm^{51}_{44}$	1.00	21.3038	5.00E+19	16.80	1.17
pg1216	0.12389 (#184)	42.84(30)	11245	nan	$222\pm^{50}_{44}$	1.00	21.3090	5.00E+19	16.75	1.09
pg1216	0.12463 (#185)	43.15(30)	11245	nan	$218\pm^{58}_{44}$	1.00	21.3230	5.00E+19	16.80	0.72
pg1216	0.12485 (#186)	43.34(30)	11245	nan	$216\pm^{58}_{43}$	1.00	21.3272	5.00E+19	16.75	0.50
pg1216	0.13499 (#187)	–	–	–	–	–	21.5194	–	–	–
pg1216	0.26768 (#188)	88.48(70)	11245	11258	$157\pm^{56}_{41}$	1.00	24.0352	5.00E+19	16.80	3.23
pg1216	0.28199 (#189)	109.24(79)	11245	11258	$184\pm^{46}_{39}$	1.00	24.3065	5.00E+19	16.80	0.71
pg1216	0.28237 (#190)	109.62(79)	11245	11258	$184\pm^{46}_{39}$	1.00	24.3137	5.00E+19	16.80	0.31
pg1259	0.00220 (#191)	124.99(93)	11480	11480	$106\pm^{26}_{24}$	1.00	19.0017	5.00E+19	16.80	0.30
pg1259	0.00762 (#192)	122.32(92)	11480	11480	$112\pm^{30}_{24}$	1.00	19.1045	5.00E+19	16.75	1.94
pg1259	0.02217 (#193)	129.87(93)	11480	11480	$99\pm^{27}_{23}$	1.00	19.3803	99.18	16.39	0.24
pg1259	0.04606 (#194)	94.97(77)	11479	11480	$122\pm^{32}_{26}$	1.00	19.8333	5.00E+19	16.75	0.40
pg1259	0.04650 (#195)	92.99(76)	11479	11480	$123\pm^{30}_{26}$	1.00	19.8416	5.00E+19	16.79	0.84
pg1259	0.19576 (#196)	53.02(43)	11485	nan	$196\pm^{49}_{42}$	1.00	22.6716	5.00E+19	16.80	0.00
pg1259	0.21940 (#197)	47.70(41)	11485	nan	$141\pm^{49}_{41}$	1.00	23.1198	1.19	15.85	6.35
pg1259	0.21953 (#198)	47.70(41)	11485	nan	$141\pm^{48}_{41}$	1.00	23.1223	0.99	15.77	6.32
pg1259	0.22313 (#199)	51.02(41)	11485	nan	$179\pm^{48}_{41}$	1.00	23.1905	5.00E+19	16.80	0.27
pg1259	0.23284 (#200)	57.87(43)	11485	nan	$221\pm^{53}_{47}$	1.00	23.3746	5.00E+19	16.80	0.06
pg1259	0.23956 (#201)	64.61(45)	11485	nan	$204\pm^{49}_{45}$	1.00	23.5021	5.00E+19	16.80	0.07
pg1259	0.25973 (#202)	74.33(62)	11485	11479	$204\pm^{59}_{41}$	1.00	23.8845	5.00E+19	16.75	1.08
pg1259	0.31979 (#203)	106.65(91)	11483	11479	$148\pm^{44}_{36}$	1.00	25.0232	5.00E+19	16.80	0.00
pg1259	0.32472 (#204)	104.67(91)	11483	11479	$156\pm^{49}_{38}$	1.00	25.1167	5.00E+19	16.80	1.52
pg1307	0.14187 (#205)	–	–	–	–	–	21.6499	–	–	–
pg1307	0.14214 (#206)	–	–	–	–	–	21.6550	–	–	–
pg1309	0.17586 (#207)	38.46(33)	27263	nan	$69\pm^{22}_{21}$	1.00	22.2943	5.00E+19	16.80	0.00
pg1309	0.17745 (#208)	38.48(35)	27263	nan	$68\pm^{23}_{19}$	1.00	22.3245	5.00E+19	16.75	0.01
pg1309	0.17866 (#209)	39.78(36)	27263	nan	$66\pm^{22}_{19}$	1.00	22.3474	5.00E+19	16.80	0.01
pg1309	0.17930 (#210)	40.20(37)	27263	nan	$66\pm^{22}_{19}$	1.00	22.3595	5.00E+19	16.80	0.03
pg1309	0.17979 (#211)	40.62(37)	27263	nan	$65\pm^{21}_{18}$	1.00	22.3688	5.00E+19	16.80	0.03
pg1309	0.18069 (#212)	43.43(38)	27263	nan	$74\pm^{22}_{19}$	1.00	22.3859	5.00E+19	16.80	0.18
pg1309	0.18117 (#213)	43.39(38)	27263	nan	$74\pm^{23}_{19}$	1.00	22.3950	5.00E+19	16.80	0.23
pg1309	0.18139 (#214)	44.59(39)	27263	nan	$79\pm^{21}_{18}$	1.00	22.3992	5.00E+19	16.75	0.42
pg1309	0.18145 (#215)	44.58(39)	27263	nan	$78\pm^{24}_{18}$	1.00	22.4003	5.00E+19	16.80	0.42
pg1309	0.18192 (#216)	43.04(39)	27263	nan	$78\pm^{25}_{18}$	1.00	22.4092	5.00E+19	16.80	0.58
pg1309	0.18698 (#217)	43.52(37)	27263	nan	$79\pm^{24}_{19}$	1.00	22.5051	5.00E+19	16.80	0.52

pg1444	0.22031 (#218)	50.77(40)	17630	nan	$104\pm^{38}_{33}$	1.00	23.1371	1.07	15.81	17.52
pg1444	0.22676 (#219)	57.73(42)	17630	nan	$197\pm^{39}_{35}$	1.00	23.2594	5.00E+19	16.80	0.81
pg1444	0.26690 (#220)	91.99(69)	17630	17137	$162\pm^{36}_{32}$	1.00	24.0204	1.20E+16	16.78	0.06
pg1444	0.26728 (#221)	94.03(70)	17630	17137	$166\pm^{36}_{32}$	1.00	24.0276	4.95E+14	16.79	0.09
pg1444	0.26738 (#222)	94.02(70)	17630	17137	$166\pm^{36}_{32}$	1.00	24.0295	1.40E+16	16.79	0.10
pg1444	0.26747 (#223)	94.01(70)	17630	17137	$166\pm^{36}_{32}$	1.00	24.0312	5.00E+19	16.75	0.11
pg1626	0.13075 (#224)	28.51(25)	69285	nan	$214\pm^{44}_{42}$	1.00	21.4390	1.16	15.84	4.65
phl1811	0.07344 (#225)	64.36(45)	77298	78895	$51\pm^{0}_{0}$	1.00	20.3524	1.00	15.79	1.51
phl1811	0.07768 (#226)	59.44(40)	78263	78895	$51\pm^{12}_{11}$	1.00	20.4328	5.00E+19	16.75	0.08
phl1811	0.08131 (#227)	49.10(33)	78178	nan	$56\pm^{14}_{11}$	1.00	20.5016	5.00E+19	16.80	1.80
phl1811	0.13239 (#228)	–	–	–	–	–	21.4701	–	–	–
phl1811	0.13282 (#229)	–	–	–	–	–	21.4783	–	–	–
phl1811	0.13318 (#230)	–	–	–	–	–	21.4851	–	–	–
phl1811	0.13545 (#231)	–	–	–	–	–	21.5281	–	–	–
phl1811	0.15752 (#232)	–	–	–	–	–	21.9466	–	–	–
phl1811	0.15786 (#233)	–	–	–	–	–	21.9530	–	–	–
phl1811	0.17652 (#234)	–	–	–	–	–	22.3068	–	–	–
phl1811	0.19157 (#235)	–	–	–	–	–	22.5922	–	–	–
phl1811	0.19194 (#236)	–	–	–	–	–	22.5992	–	–	–
phl1811	0.19220 (#237)	–	–	–	–	–	22.6041	–	–	–
pks0312	0.20188 (#238)	58.64(41)	23887	nan	$194\pm^{38}_{35}$	1.00	22.7876	3.31E+16	16.79	0.01
pks0312	0.20275 (#239)	59.87(41)	23887	nan	$181\pm^{37}_{34}$	1.00	22.8041	1.94E+10	16.70	0.14
pks0405	0.09192 (#240)	40.76(43)	137149	nan	$285\pm^{15}_{14}$	1.00	20.7028	0.82	15.72	2.85
pks0405	0.09647 (#241)	44.12(43)	137149	nan	$305\pm^{17}_{20}$	1.00	20.7891	1.70E+14	16.78	-0.00
pks0405	0.14808 (#242)	–	–	–	–	–	21.7676	–	–	–
pks0405	0.16566 (#243)	34.33(32)	137647	nan	$322\pm^{21}_{20}$	1.00	22.1009	5.20E+03	16.48	1.05
pks0405	0.16606 (#244)	35.08(32)	137647	nan	$320\pm^{20}_{20}$	1.00	22.1085	1.97E+03	16.49	1.17
pks0405	0.16659 (#245)	37.18(33)	137675	nan	$317\pm^{20}_{20}$	1.00	22.1185	2.55E+03	16.49	0.98
pks0405	0.16688 (#246)	37.31(33)	137675	nan	$316\pm^{19}_{19}$	1.00	22.1240	4.59E+03	16.48	0.80
pks0405	0.16712 (#247)	37.91(33)	137675	nan	$313\pm^{21}_{19}$	1.00	22.1286	752.48	16.44	0.51
pks0405	0.18257 (#248)	59.45(44)	136430	nan	$304\pm^{18}_{17}$	1.00	22.4215	0.82	15.71	2.41
pks0405	0.18289 (#249)	63.38(44)	136430	nan	$307\pm^{18}_{17}$	1.00	22.4276	1.11	15.82	1.39
pks0405	0.24052 (#250)	57.03(46)	137245	nan	$367\pm^{20}_{19}$	1.00	23.5203	4.17E+03	16.52	1.43
pks0405	0.24094 (#251)	61.56(45)	137216	nan	$377\pm^{21}_{19}$	1.00	23.5282	2.45E+06	16.56	1.85
pks0405	0.24547 (#252)	66.61(47)	136481	138649	$361\pm^{19}_{18}$	1.00	23.6141	1.37	15.88	0.52
pks0405	0.29762 (#253)	85.15(89)	133010	137234	$392\pm^{21}_{21}$	1.00	24.6029	141.00	16.42	2.58
pks0405	0.34188 (#254)	114.95(95)	137986	137234	$365\pm^{19}_{19}$	1.00	25.4420	1.83	15.97	0.02

pks0405	0.34225 (#255)	120.66(97)	138000	137943	$367\pm^{19}_{19}$	1.00	25.4491	1.64	15.93	0.05
pks0405	0.35092 (#256)	113.60(95)	138000	136470	$368\pm^{20}_{19}$	1.00	25.6134	1.37	15.87	0.23
pks0405	0.36075 (#257)	117.15(93)	137986	134948	$404\pm^{21}_{20}$	1.00	25.7998	1.91E+03	16.47	1.70
pks0405	0.36151 (#258)	115.63(94)	138000	134948	$404\pm^{20}_{20}$	1.00	25.8142	2.75E+05	16.56	3.70
pks0405	0.36329 (#259)	110.13(94)	138000	134948	$408\pm^{22}_{20}$	1.00	25.8480	2.17E+09	16.65	8.04
pks0405	0.40570 (#260)	109.37(95)	137975	138647	$415\pm^{23}_{21}$	1.00	26.6521	10.92	16.21	0.05
pks0405	0.40890 (#261)	111.06(95)	137975	138647	$432\pm^{24}_{23}$	1.00	26.7127	537.25	16.41	2.02
pks0405	0.49505 (#262)	96.58(89)	136537	137118	$387\pm^{26}_{25}$	1.00	28.3461	0.63	15.63	4.59
pks0405	0.49530 (#263)	97.66(89)	136537	137118	$389\pm^{27}_{26}$	1.00	28.3509	0.78	15.70	3.23
pks0405	0.55506 (#264)	98.30(94)	138708	138714	$363\pm^{31}_{30}$	1.00	29.4839	1.93	15.98	0.30
pks2005	0.06490 (#265)	60.15(62)	54472	54641	$1896\pm^{53}_{53}$	1.00	20.1905	0.66	15.64	1.94
pks2155	0.05405 (#266)	83.01(59)	1701313	1685268	$4444\pm^{444}_{409}$	1.55	19.9848	0.12	14.97	0.01
pks2155	0.05707 (#267)	76.79(59)	1701521	1685268	$4316\pm^{448}_{438}$	1.62	20.0420	0.17	15.11	7.35
q0045	0.11052 (#268)	–	–	–	–	–	21.0555	–	–	–
q0045	0.13521 (#269)	–	–	–	–	–	21.5236	–	–	–
q1230	0.09518 (#270)	44.14(33)	39329	nan	$48\pm^{19}_{18}$	1.00	20.7646	5.00E+19	16.75	1.10
q1230	0.10318 (#271)	48.14(34)	39330	nan	$56\pm^{17}_{15}$	1.00	20.9163	39.22	16.33	0.59
q1230	0.10445 (#272)	48.96(34)	39330	nan	$66\pm^{18}_{14}$	1.00	20.9404	5.00E+19	16.75	0.28
q1230	0.10530 (#273)	49.30(34)	39331	nan	$68\pm^{17}_{15}$	1.00	20.9565	5.00E+19	16.80	0.84
q1230	0.10596 (#274)	46.27(33)	39331	nan	$70\pm^{17}_{15}$	1.00	20.9690	5.00E+19	16.75	1.07
q1230	0.10666 (#275)	46.39(34)	39331	nan	$65\pm^{21}_{15}$	1.00	20.9823	5.00E+19	16.80	0.96
q1230	0.10809 (#276)	45.09(33)	39331	nan	$53\pm^{20}_{14}$	1.00	21.0094	5.00E+19	16.80	1.29
q1230	0.10820 (#277)	45.09(33)	39331	nan	$53\pm^{20}_{14}$	1.00	21.0115	5.00E+19	16.80	1.29
q1230	0.10861 (#278)	48.14(33)	39331	nan	$52\pm^{20}_{14}$	1.00	21.0192	5.00E+19	16.77	1.02
q1230	0.10906 (#279)	44.60(32)	39332	nan	$53\pm^{25}_{15}$	1.00	21.0278	5.00E+19	16.80	1.08
q1230	0.10935 (#280)	44.06(32)	39332	nan	$55\pm^{17}_{14}$	1.00	21.0333	5.00E+19	16.75	1.71
q1230	0.10956 (#281)	43.57(32)	39332	nan	$56\pm^{21}_{15}$	1.00	21.0373	5.00E+19	16.80	1.56
q1230	0.11707 (#282)	39.83(27)	39333	nan	$51\pm^{20}_{17}$	1.00	21.1796	1.06	15.81	13.29
q1230	0.11743 (#283)	34.85(25)	39333	nan	$57\pm^{22}_{19}$	1.00	21.1865	0.87	15.73	11.53
q1230	0.11781 (#284)	35.43(25)	39333	nan	$59\pm^{22}_{19}$	1.00	21.1937	0.88	15.74	10.59
rbs1892	0.15752 (#285)	–	–	–	–	–	21.9466	–	–	–
rbs1892	0.17133 (#286)	46.32(37)	4929	nan	$312\pm^{101}_{76}$	1.00	22.2084	5.00E+19	16.80	0.45
rbs1892	0.19874 (#287)	50.02(44)	4929	nan	$332\pm^{100}_{76}$	1.00	22.7281	5.00E+19	16.80	0.16
rbs542	0.10323 (#288)	48.13(48)	192804	nan	$1054\pm^{22}_{22}$	1.00	20.9172	0.67	15.64	0.84
rbs542	0.10379 (#289)	48.09(47)	192375	nan	$1053\pm^{22}_{22}$	1.00	20.9279	0.72	15.67	0.52
rxj0439	0.11547 (#290)	38.76(35)	151442	nan	$337\pm^{18}_{18}$	1.00	21.1493	0.66	15.64	4.30
rxj0439	0.21833 (#291)	61.09(43)	145661	nan	$419\pm^{22}_{22}$	1.00	23.0995	0.73	15.68	5.79

rxj0439	0.24235 (#292)	63.87(47)	151874	121198	$498\pm^{26}_{21}$	1.00	23.5550	3.91E+03	16.50	2.82
rxj0439	0.24258 (#293)	69.70(49)	151906	131963	$497\pm^{21}_{21}$	1.00	23.5593	8.51E+03	16.48	2.55
rxj0439	0.24313 (#294)	66.17(48)	151874	131963	$498\pm^{23}_{22}$	1.00	23.5697	95.90	16.40	1.44
rxj0439	0.24387 (#295)	71.95(50)	151906	137345	$497\pm^{22}_{21}$	1.00	23.5838	7.92	16.23	0.33
s50716	0.23145 (#296)	57.72(42)	75697	nan	$741\pm^{36}_{35}$	1.00	23.3483	1.73E+04	16.48	0.15
ton28	0.13746 (#297)	–	–	–	–	–	21.5662	–	–	–
ton28	0.13773 (#298)	–	–	–	–	–	21.5714	–	–	–
ton28	0.13781 (#299)	–	–	–	–	–	21.5729	–	–	–
ton28	0.17251 (#300)	50.74(37)	81682	nan	$131\pm^{18}_{17}$	1.00	22.2308	2.63	16.05	0.60
ton28	0.21259 (#301)	60.47(42)	81454	nan	$188\pm^{20}_{19}$	1.00	22.9907	1.82E+04	16.50	0.00
ton28	0.24292 (#302)	30.56(48)	85563	83705	$186\pm^{19}_{19}$	1.00	23.5658	7.04E+06	16.58	0.18
ton28	0.24859 (#303)	52.11(52)	84503	85711	$180\pm^{20}_{19}$	1.00	23.6733	3.40	16.10	0.42
ton28	0.27338 (#304)	80.27(77)	85129	86614	$205\pm^{19}_{19}$	1.00	24.1433	1.60	15.93	0.97
ton28	0.33021 (#305)	107.71(94)	85874	86028	$199\pm^{20}_{19}$	1.00	25.2208	1.21	15.85	2.04
tons180	0.02340 (#306)	99.08(96)	177396	194071	$901\pm^{18}_{18}$	1.00	19.4037	0.68	15.65	-0.00
tons180	0.04360 (#307)	69.00(82)	187350	195496	$955\pm^{18}_{18}$	1.00	19.7867	0.68	15.66	-0.01
tons180	0.04560 (#308)	67.80(80)	187350	195974	$963\pm^{19}_{19}$	1.00	19.8246	0.84	15.74	0.60

Table B.7: O VIII measurements with *XMM-Newton* data, at the prior redshift from the H I lines from Table A.2.

Target line		cmin	RGS1		RGS2		power–law		line component			ΔC
Name	z	(d.o.f.)	avg exp (s)	%	avg exp (s)	%	norm.	index	λ (Å)	τ_0	$\log N(\mathrm{cm}^{-2})$	(d.o.f.)
1es1028	0.13714 (#1)	–	–	–	–	–	–	–	21.5602	–	–	–
1es1028	0.20383 (#2)	62.35(44)	146640	9	nan	nan	$1006\pm^{29}_{29}$	1.00	22.8246	$0.05\pm^{2.21}_{0.94}$	$14.58\pm^{1.44}_{nan}$	0.01
1es1028	0.22121 (#3)	57.62(42)	144940	9	nan	nan	$1031\pm^{32}_{31}$	1.00	23.1541	$-1.47\pm^{0.70}_{0.53}$	$nan\pm^{nan}_{nan}$	3.89
1es1553	0.03466 (#4)	90.75(81)	1722815	7	1780022	7	$752\pm^{116}_{96}$	2.09	19.6172	$-0.03\pm^{0.65}_{0.06}$	$nan\pm^{nan}_{nan}$	-0.41
1es1553	0.04273 (#5)	89.06(72)	1720386	8	1774803	7	$776\pm^{127}_{108}$	2.01	19.7702	$0.08\pm^{0.18}_{0.21}$	$14.82\pm^{0.47}_{nan}$	0.14
1es1553	0.06364 (#6)	46.18(56)	1785421	8	1740261	7	$1161\pm^{253}_{220}$	1.18	20.1666	$0.07\pm^{0.22}_{0.32}$	$14.72\pm^{0.61}_{nan}$	-0.04
1es1553	0.21869 (#7)	36.89(28)	1666450	9	nan	nan	$36\pm^{20}_{13}$	7.01	23.1064	$-0.43\pm^{0.30}_{0.26}$	$nan\pm^{nan}_{nan}$	2.52
3c249	0.13470 (#8)	–	–	–	–	–	–	–	21.5139	–	–	–
3c249	0.26664 (#9)	53.79(69)	2644	23	2524	18	$320\pm^{120}_{95}$	1.00	24.0155	$1.16E+13\pm^{1.00E+20}_{1.16E+13}$	$16.75\pm^{0.05}_{inf}$	1.35
3c273	0.00758 (#10)	83.67(67)	1048814	3	1012144	3	$3696\pm^{17}_{17}$	1.00	19.1037	$0.04\pm^{0.42}_{0.05}$	$14.45\pm^{1.06}_{nan}$	0.77
3c273	0.06707 (#11)	77.60(60)	1015660	4	1019511	4	$3919\pm^{16}_{16}$	1.00	20.2316	$-0.04\pm^{0.44}_{0.08}$	$nan\pm^{nan}_{nan}$	-0.35
3c273	0.07359 (#12)	63.12(54)	922775	4	1018570	4	$3920\pm^{17}_{16}$	1.00	20.3553	$-0.03\pm^{0.41}_{0.09}$	$nan\pm^{nan}_{nan}$	-0.21
3c273	0.13960 (#13)	–	–	–	–	–	–	–	21.6068	–	–	–
h1821	0.00944 (#14)	120.55(98)	30556	35	43312	33	$1002\pm^{55}_{53}$	1.00	19.1390	$-0.92\pm^{1.21}_{0.70}$	$nan\pm^{nan}_{nan}$	0.86
h1821	0.06779 (#15)	81.53(61)	31940	36	43282	34	$1055\pm^{61}_{60}$	1.00	20.2453	$-0.65\pm^{3.61}_{1.09}$	$nan\pm^{nan}_{nan}$	0.15
h1821	0.08483 (#16)	49.50(43)	30565	41	nan	nan	$1106\pm^{71}_{68}$	1.00	20.5684	$-1.02\pm^{2.54}_{0.94}$	$nan\pm^{nan}_{nan}$	0.43
h1821	0.12147 (#17)	44.27(31)	30928	49	nan	nan	$1128\pm^{97}_{95}$	1.00	21.2631	$-0.74\pm^{6.44}_{1.40}$	$nan\pm^{nan}_{nan}$	0.14
h1821	0.19817 (#18)	63.03(48)	30824	55	nan	nan	$974\pm^{88}_{85}$	1.00	22.7173	$-2.05\pm^{2.15}_{0.88}$	$nan\pm^{nan}_{nan}$	1.17
h1821	0.21321 (#19)	58.22(45)	29048	55	nan	nan	$1010\pm^{95}_{92}$	1.00	23.0025	$-1.40\pm^{5.08}_{1.10}$	$nan\pm^{nan}_{nan}$	0.40
h1821	0.24531 (#20)	69.92(50)	31312	54	36214	40	$1107\pm^{101}_{88}$	1.00	23.6111	$9.21\pm^{7.55E+13}_{10.06}$	$16.24\pm^{0.52}_{nan}$	0.61
h2356	0.03830 (#21)	97.28(88)	479869	6	503477	6	$1019\pm^{12}_{13}$	1.00	19.6862	$0.40\pm^{0.47}_{0.45}$	$15.47\pm^{0.28}_{nan}$	1.03
h2356	0.07881 (#22)	54.41(41)	506719	6	263751	5	$1072\pm^{15}_{15}$	1.00	20.4542	$-0.54\pm^{0.45}_{0.35}$	$nan\pm^{nan}_{nan}$	1.77
h2356	0.10467 (#23)	43.81(39)	507154	6	nan	nan	$1072\pm^{16}_{15}$	1.00	20.9445	$-0.74\pm^{0.38}_{0.31}$	$nan\pm^{nan}_{nan}$	3.88
h2356	0.15613 (#24)	37.69(29)	503603	7	nan	nan	$1088\pm^{19}_{18}$	1.00	21.9202	$0.05\pm^{0.64}_{0.62}$	$14.56\pm^{1.10}_{nan}$	-0.01
he0226	0.14274 (#25)	–	–	–	–	–	–	–	21.6664	–	–	–
he0226	0.39890 (#26)	130.12(94)	31707	25	31704	28	$265\pm^{37}_{34}$	1.00	26.5231	$-1.60\pm^{3.61}_{1.31}$	$nan\pm^{nan}_{nan}$	0.53
he0226	0.41024 (#27)	136.42(96)	31707	25	31704	32	$274\pm^{38}_{35}$	1.00	26.7382	$-1.81\pm^{2.41}_{0.97}$	$nan\pm^{nan}_{nan}$	0.89
i22456	0.00443 (#28)	130.08(99)	76706	53	81909	47	$381\pm^{22}_{21}$	1.00	19.0440	$-2.01\pm^{0.61}_{0.44}$	$nan\pm^{nan}_{nan}$	6.46
i22456	0.09941 (#29)	59.72(44)	79900	60	nan	nan	$501\pm^{38}_{27}$	1.00	20.8448	$3.13E+04\pm^{1.00E+20}_{3.13E+04}$	$16.54\pm^{0.26}_{nan}$	4.43
mr2251	0.01068 (#30)	121.16(93)	414226	5	451165	5	$1243\pm^{275}_{224}$	1.52	19.1625	$-0.67\pm^{0.22}_{0.20}$	$nan\pm^{nan}_{nan}$	9.71
mr2251	0.01449 (#31)	122.62(90)	428129	5	462131	5	$1173\pm^{252}_{199}$	1.69	19.2347	$0.07\pm^{0.39}_{0.25}$	$14.74\pm^{0.78}_{nan}$	0.13
mr2251	0.06131 (#32)	68.20(47)	466085	5	461291	5	$2234\pm^{1198}_{730}$	0.41	20.1224	$1.29\pm^{1.11}_{0.72}$	$15.86\pm^{0.16}_{0.28}$	5.66
mr2251	0.06190 (#33)	62.95(47)	466085	5	461291	5	$2211\pm^{1157}_{717}$	0.45	20.1336	$3.43\pm^{2.87}_{1.58}$	$16.10\pm^{0.10}_{0.14}$	16.53

mr2251	0.06276 (#34)	50.87(49)	466106	5	461162	4	$2612\pm^{1875}_{645}$	0.13	20.1499	$24.01\pm^{44.38}_{15.19}$	$16.30\pm^{0.05}_{0.08}$	38.86
mr2251	0.06327 (#35)	44.88(49)	466112	5	461008	4	$2740\pm^{1569}_{769}$	0.03	20.1596	$30.33\pm^{110.01}_{19.55}$	$16.32\pm^{0.04}_{0.07}$	45.67
mr2251	0.06381 (#36)	45.72(49)	466112	5	461008	4	$2376\pm^{1389}_{647}$	0.33	20.1698	$19.77\pm^{318.94}_{11.43}$	$16.31\pm^{0.07}_{0.07}$	45.47
mrk478	0.06166 (#37)	76.63(64)	202266	13	202111	12	$465\pm^{14}_{14}$	1.00	20.1291	$-0.09\pm^{1.95}_{0.94}$	$nan\pm^{nan}_{nan}$	0.00
mrk478	0.06578 (#38)	70.27(61)	204255	14	201677	12	$472\pm^{14}_{15}$	1.00	20.2072	$0.13\pm^{2.23}_{1.06}$	$15.00\pm^{1.02}_{nan}$	-0.00
mrk478	0.07213 (#39)	54.18(51)	200098	13	200301	12	$492\pm^{16}_{15}$	1.00	20.3276	$3.42\pm^{129.59}_{3.09}$	$16.09\pm^{0.25}_{0.71}$	1.94
mrk876	0.01159 (#40)	84.83(96)	2656	58	2600	11	$174\pm^{70}_{54}$	1.00	19.1797	$8.15E+07\pm^{1.00E+20}_{8.15E+07}$	$16.62\pm^{0.12}_{-0.12}$	0.81
mrk876	0.05598 (#41)	59.57(72)	2736	34	2708	18	$227\pm^{89}_{64}$	1.00	20.0214	$4.30E+04\pm^{1.00E+20}_{4.30E+04}$	$16.54\pm^{0.25}_{nan}$	0.48
mrk876	0.08709 (#42)	42.06(43)	2804	10	nan	nan	$414\pm^{119}_{103}$	1.00	20.6112	$-4.18\pm^{1.43}_{1.00}$	$nan\pm^{nan}_{nan}$	4.24
mrk876	0.08858 (#43)	42.31(44)	2805	10	nan	nan	$419\pm^{123}_{105}$	1.00	20.6395	$-4.01\pm^{1.48}_{0.99}$	$nan\pm^{nan}_{nan}$	3.77
mrk876	0.08917 (#44)	42.90(43)	2804	10	nan	nan	$427\pm^{125}_{107}$	1.00	20.6507	$-3.76\pm^{1.65}_{1.00}$	$nan\pm^{nan}_{nan}$	2.96
mrk876	0.11487 (#45)	52.10(37)	2790	15	nan	nan	$714\pm^{237}_{160}$	1.00	21.1379	$5.33E+09\pm^{1.00E+20}_{5.33E+09}$	$16.69\pm^{0.11}_{inf}$	3.07
ngc7469	0.00981 (#46)	85.67(65)	629599	4	665412	4	$1934\pm^{17}_{17}$	1.00	19.1460	$2.83\pm^{1.01}_{0.77}$	$16.06\pm^{0.06}_{0.07}$	51.59
pg0003	0.08299 (#47)	56.55(41)	13036	36	nan	nan	$169\pm^{41}_{36}$	1.00	20.5335	$-2.19\pm^{8.22E+03}_{1.87}$	$nan\pm^{nan}_{nan}$	0.31
pg0003	0.17139 (#48)	45.45(37)	13036	24	nan	nan	$315\pm^{63}_{56}$	1.00	22.2096	$-0.59\pm^{1.00E+20}_{2.38}$	$nan\pm^{nan}_{nan}$	0.01
pg0003	0.22541 (#49)	47.36(42)	13037	29	nan	nan	$145\pm^{50}_{43}$	1.00	23.2338	$-4.47\pm^{1.05}_{0.87}$	$nan\pm^{nan}_{nan}$	8.09
pg0003	0.38633 (#50)	107.06(92)	13033	32	12857	29	$248\pm^{69}_{50}$	1.00	26.2848	$1.54E+07\pm^{1.00E+20}_{1.54E+07}$	$16.62\pm^{0.17}_{nan}$	1.31
pg0003	0.42051 (#51)	129.11(93)	13034	47	12830	27	$327\pm^{75}_{64}$	1.00	26.9329	$1.24E+04\pm^{1.00E+20}_{1.24E+04}$	$16.54\pm^{0.26}_{nan}$	0.73
pg0804	0.05015 (#52)	80.99(78)	28468	6	30600	4	$1084\pm^{53}_{49}$	1.00	19.9108	$-0.03\pm^{3.38}_{1.16}$	$nan\pm^{nan}_{nan}$	0.00
pg0804	0.05576 (#53)	70.57(71)	28779	6	30600	5	$1101\pm^{55}_{53}$	1.00	20.0172	$10.40\pm^{1.46E+04}_{40.40}$	$16.22\pm^{0.26}_{nan}$	1.53
pg0804	0.36379 (#54)	131.95(97)	30110	7	29227	6	$1657\pm^{86}_{84}$	1.00	25.8575	$-1.38\pm^{1.07}_{0.72}$	$nan\pm^{nan}_{nan}$	1.74
pg0832	0.01753 (#55)	–	–	–	–	–	–	–	19.2924	–	–	–
pg0832	0.02793 (#56)	–	–	–	–	–	–	–	19.4896	–	–	–
pg0832	0.08748 (#57)	59.08(42)	20650	99	nan	nan	$41\pm^{16}_{12}$	1.00	20.6186	$2.35E+06\pm^{1.00E+20}_{2.35E+06}$	$16.62\pm^{0.12}_{nan}$	0.57
pg0832	0.10171 (#58)	53.76(42)	20652	78	nan	nan	$29\pm^{15}_{12}$	1.00	20.8884	$-4.03\pm^{2.72}_{1.45}$	$nan\pm^{nan}_{nan}$	1.81
pg0832	0.18391 (#59)	40.73(29)	20654	138	nan	nan	$36\pm^{22}_{16}$	1.00	22.4469	$-4.07\pm^{3.66}_{1.66}$	$nan\pm^{nan}_{nan}$	1.60
pg0832	0.27503 (#60)	100.19(76)	20655	80	20637	113	$76\pm^{24}_{20}$	1.00	24.1746	$-1.15\pm^{6.74E+13}_{28.85}$	$nan\pm^{nan}_{nan}$	0.04
pg0832	0.27694 (#61)	100.69(77)	20655	94	20637	103	$63\pm^{23}_{18}$	1.00	24.2108	$1.32\pm^{1.00E+20}_{31.32}$	$15.86\pm^{0.91}_{nan}$	0.01
pg0832	0.32572 (#62)	–	–	–	–	–	–	–	25.1357	–	–	–
pg0838	0.06583 (#63)	34.64(61)	1623	24	1514	75	$244\pm^{130}_{88}$	1.00	20.2081	$5.03E+04\pm^{1.00E+20}_{5.03E+04}$	$16.54\pm^{0.25}_{nan}$	0.40
pg0838	0.08628 (#64)	23.30(42)	1619	54	nan	nan	$186\pm^{121}_{78}$	1.00	20.5959	$9.17E+08\pm^{1.00E+20}_{9.17E+08}$	$16.69\pm^{0.11}_{inf}$	0.39
pg0838	0.12676 (#65)	8.14(29)	1609	72	nan	nan	$73\pm^{103}_{73}$	1.00	21.3634	$5.09E+12\pm^{1.00E+20}_{5.09E+12}$	$16.75\pm^{0.05}_{inf}$	0.20
pg0953	0.16319 (#66)	32.74(29)	12792	13	nan	nan	$419\pm^{81}_{73}$	1.00	22.0541	$-2.49\pm^{2.50}_{1.06}$	$nan\pm^{nan}_{nan}$	1.46
pg0953	0.19221 (#67)	49.32(42)	12792	21	nan	nan	$417\pm^{66}_{61}$	1.00	22.6043	$-1.21\pm^{227.99}_{1.61}$	$nan\pm^{nan}_{nan}$	0.15
pg1048	0.00642 (#68)	130.68(89)	18905	22	18341	40	$165\pm^{26}_{24}$	1.00	19.0817	$-0.28\pm^{9.29E+03}_{2.10}$	$nan\pm^{nan}_{nan}$	0.00
pg1048	0.02414 (#69)	121.85(91)	18905	22	18341	48	$157\pm^{26}_{23}$	1.00	19.4177	$-0.98\pm^{185.56}_{1.83}$	$nan\pm^{nan}_{nan}$	0.09
pg1115	0.09511 (#70)	54.44(43)	17542	15	nan	nan	$312\pm^{40}_{40}$	1.00	20.7633	$889.83\pm^{1.00E+20}_{919.83}$	$16.45\pm^{0.35}_{nan}$	0.07

pg1115	0.12059 (#71)	43.07(32)	17510	23	nan	nan	$290\pm^{49}_{45}$	1.00	21.2464	$5.39\pm^{1.65E+11}_{35.39}$	$16.16\pm^{0.57}_{nan}$	0.14
pg1115	0.12741 (#72)	42.59(29)	17510	25	nan	nan	$274\pm^{50}_{45}$	1.00	21.3757	$-1.39\pm^{135.48}_{1.81}$	$nan\pm^{nan}_{nan}$	0.18
pg1116	0.04114 (#73)	87.87(85)	280360	13	294383	11	$456\pm^{11}_{11}$	1.00	19.7400	$2.58\pm^{6.98}_{1.74}$	$16.05\pm^{0.17}_{0.32}$	4.54
pg1116	0.06251 (#74)	79.62(66)	285035	13	294383	10	$480\pm^{13}_{12}$	1.00	20.1452	$4.15\pm^{51.81}_{3.31}$	$16.13\pm^{0.21}_{0.40}$	3.41
pg1116	0.08382 (#75)	44.01(43)	287898	13	nan	nan	$470\pm^{13}_{13}$	1.00	20.5492	$-1.19\pm^{0.61}_{0.44}$	$nan\pm^{nan}_{nan}$	3.46
pg1116	0.09210 (#76)	46.83(43)	287898	12	nan	nan	$499\pm^{13}_{13}$	1.00	20.7062	$0.53\pm^{2.55}_{1.08}$	$15.56\pm^{0.52}_{nan}$	0.19
pg1116	0.09281 (#77)	49.13(44)	288074	12	nan	nan	$497\pm^{13}_{13}$	1.00	20.7197	$0.46\pm^{2.50}_{1.13}$	$15.51\pm^{0.57}_{nan}$	0.12
pg1116	0.13373 (#78)	34.69(29)	296156	14	nan	nan	$516\pm^{16}_{17}$	1.00	21.4955	$12.96\pm^{138.59}_{12.14}$	$16.23\pm^{0.18}_{0.51}$	2.54
pg1116	0.13851 (#79)	–	–	–	–	–	–	–	21.5861	–	–	–
pg1211	0.02586 (#80)	108.44(86)	736771	11	780487	11	$490\pm^{7}_{7}$	1.00	19.4503	$-0.44\pm^{0.38}_{0.31}$	$nan\pm^{nan}_{nan}$	1.62
pg1211	0.05443 (#81)	83.50(61)	752151	10	777295	10	$566\pm^{8}_{8}$	1.00	19.9920	$-0.58\pm^{0.39}_{0.32}$	$nan\pm^{nan}_{nan}$	2.55
pg1216	0.00842 (#82)	112.05(92)	11245	43	11250	41	$100\pm^{26}_{22}$	1.00	19.1196	$-1.91\pm^{18.19}_{1.36}$	$nan\pm^{nan}_{nan}$	0.42
pg1216	0.07969 (#83)	61.07(43)	11245	40	11250	0	$134\pm^{37}_{32}$	1.00	20.4709	$-4.17\pm^{2.47}_{1.40}$	$nan\pm^{nan}_{nan}$	2.23
pg1216	0.12372 (#84*)	47.41(31)	11245	31	nan	nan	$212\pm^{52}_{42}$	1.00	21.3057	$2.13E+04\pm^{1.00E+20}_{2.14E+04}$	$16.54\pm^{0.26}_{nan}$	0.88
pg1216	0.12473 (#85*)	47.65(31)	11245	31	nan	nan	$211\pm^{55}_{41}$	1.00	21.3249	$3.48E+04\pm^{1.00E+20}_{3.48E+04}$	$16.54\pm^{0.25}_{nan}$	0.63
pg1216	0.17950 (#86)	55.47(38)	11245	30	nan	nan	$190\pm^{49}_{41}$	1.00	22.3633	$0.54\pm^{1.00E+20}_{30.54}$	$15.57\pm^{1.22}_{nan}$	0.00
pg1216	0.20014 (#87)	56.76(42)	11245	69	nan	nan	$145\pm^{40}_{33}$	1.00	22.7547	$5.57E+07\pm^{1.00E+20}_{5.57E+07}$	$16.65\pm^{0.15}_{-0.15}$	0.44
pg1216	0.21258 (#88)	45.73(40)	11245	53	nan	nan	$138\pm^{43}_{36}$	1.00	22.9905	$-4.11\pm^{2.19}_{1.29}$	$nan\pm^{nan}_{nan}$	2.17
pg1216	0.28204 (#89)	109.28(79)	11245	36	11258	14	$185\pm^{46}_{40}$	1.00	24.3075	$107.15\pm^{1.00E+20}_{137.15}$	$16.40\pm^{0.34}_{nan}$	0.67
pg1229	0.05018 (#90)	102.73(72)	24011	21	24007	19	$394\pm^{38}_{36}$	1.00	19.9114	$1.82\pm^{2.89E+03}_{31.82}$	$15.95\pm^{0.55}_{nan}$	0.17
pg1259	0.05563 (#91)	91.28(69)	11479	52	11480	59	$114\pm^{32}_{25}$	1.00	20.0147	$3.04E+04\pm^{1.00E+20}_{3.04E+04}$	$16.54\pm^{0.25}_{nan}$	0.34
pg1259	0.15136 (#92)	–	–	–	–	–	–	–	21.8298	–	–	–
pg1259	0.16647 (#93)	32.56(32)	11484	33	nan	nan	$155\pm^{50}_{42}$	1.00	22.1163	$-1.42\pm^{1.26E+14}_{2.24}$	$nan\pm^{nan}_{nan}$	0.07
pg1259	0.17893 (#94)	39.84(42)	11484	36	nan	nan	$163\pm^{42}_{36}$	1.00	22.3525	$1.52E+06\pm^{1.00E+20}_{1.52E+06}$	$16.62\pm^{0.12}_{nan}$	1.00
pg1259	0.22376 (#95)	58.87(41)	11485	46	nan	nan	$216\pm^{63}_{46}$	1.00	23.2025	$1.97E+06\pm^{1.00E+20}_{1.97E+06}$	$16.62\pm^{0.13}_{nan}$	1.05
pg1259	0.24126 (#96)	61.99(46)	11485	40	11479	nan	$194\pm^{48}_{41}$	1.00	23.5343	$-0.93\pm^{1.00E+20}_{2.70}$	$nan\pm^{nan}_{nan}$	0.03
pg1259	0.31974 (#97)	106.65(91)	11483	41	11479	44	$148\pm^{44}_{36}$	1.00	25.0223	$0.54\pm^{1.00E+20}_{30.54}$	$15.57\pm^{1.23}_{nan}$	0.00
pg1259	0.36212 (#98)	107.88(92)	11483	28	11479	32	$236\pm^{54}_{47}$	1.00	25.8258	$-1.97\pm^{19.74}_{1.34}$	$nan\pm^{nan}_{nan}$	0.41
pg1259	0.38254 (#99)	106.89(91)	11483	29	11479	40	$273\pm^{64}_{55}$	1.00	26.2130	$-0.95\pm^{1.28E+07}_{2.00}$	$nan\pm^{nan}_{nan}$	0.04
pg1259	0.38266 (#100)	106.88(91)	11483	29	11479	40	$272\pm^{64}_{55}$	1.00	26.2152	$-1.00\pm^{2.39E+06}_{2.09}$	$nan\pm^{nan}_{nan}$	0.05
pg1307	0.08345 (#101)	49.47(43)	9851	11	nan	nan	$199\pm^{44}_{39}$	1.00	20.5422	$-2.82\pm^{4.13}_{1.36}$	$nan\pm^{nan}_{nan}$	0.96
pg1309	0.03861 (#102)	113.84(79)	27332	89	26079	77	$46\pm^{15}_{11}$	1.00	19.6920	$1.21E+09\pm^{1.00E+20}_{1.21E+09}$	$16.69\pm^{0.10}_{inf}$	1.82
pg1309	0.17740 (#103)	47.95(38)	27263	86	nan	nan	$59\pm^{20}_{17}$	1.00	22.3235	$-2.14\pm^{1.00E+20}_{2.48}$	$nan\pm^{nan}_{nan}$	0.12
pg1309	0.17852 (#104)	48.79(39)	27263	88	nan	nan	$59\pm^{20}_{17}$	1.00	22.3447	$-1.22\pm^{1.00E+20}_{28.78}$	$nan\pm^{nan}_{nan}$	0.02
pg1309	0.17918 (#105)	49.59(40)	27263	88	nan	nan	$58\pm^{20}_{17}$	1.00	22.3573	$-0.51\pm^{1.00E+20}_{29.49}$	$nan\pm^{nan}_{nan}$	0.00
pg1309	0.18143 (#106)	54.59(42)	27263	81	nan	nan	$70\pm^{21}_{17}$	1.00	22.3999	$95.88\pm^{1.00E+20}_{125.88}$	$16.38\pm^{0.41}_{nan}$	0.18
pg1444	0.22031 (#107)	50.77(40)	17630	43	nan	nan	$104\pm^{38}_{33}$	1.00	23.1371	$-6.35\pm^{1.09}_{1.04}$	$nan\pm^{nan}_{nan}$	17.52

pg1626	0.06137 (#108)	77.10(65)	69300	62	67705	52	$197\pm^{24}_{24}$	1.00	20.1236	$-1.17\pm^{389.37}_{1.45}$	$nan\pm^{nan}_{nan}$	0.16
phl1811	0.05143 (#109*)	129.49(67)	75753	86	78895	104	$29\pm^{9}_{8}$	1.00	19.9351	$-1.81\pm^{4.24E+04}_{2.05}$	$nan\pm^{nan}_{nan}$	0.22
phl1811	0.05813 (#110*)	121.07(62)	77392	85	78895	100	$28\pm^{9}_{8}$	1.00	20.0621	$-1.31\pm^{1.00E+20}_{28.69}$	$nan\pm^{nan}_{nan}$	0.03
phl1811	0.08085 (#111)	54.95(37)	78263	74	78895	inf	$47\pm^{11}_{10}$	1.00	20.4929	$2.01E+04\pm^{1.00E+20}_{2.01E+04}$	$16.54\pm^{0.26}_{nan}$	1.02
phl1811	0.08163 (#112)	53.36(36)	78263	74	nan	nan	$49\pm^{11}_{10}$	1.00	20.5077	$2.85E+06\pm^{1.00E+20}_{2.85E+06}$	$16.62\pm^{0.12}_{nan}$	1.08
phl1811	0.12003 (#113)	–	–	–	–	–	–	–	21.2358	–	–	–
phl1811	0.15787 (#114)	–	–	–	–	–	–	–	21.9532	–	–	–
pks0312	0.11454 (#115)	27.80(20)	23881	37	nan	nan	$218\pm^{42}_{38}$	1.00	21.1317	$1.37E+03\pm^{1.00E+20}_{1.40E+03}$	$16.46\pm^{0.34}_{nan}$	0.86
pks0405	0.02510 (#116)	113.13(93)	134903	16	138652	19	$261\pm^{13}_{12}$	1.00	19.4359	$4.17\pm^{126.34}_{3.84}$	$16.13\pm^{0.25}_{0.75}$	1.85
pks0405	0.05902 (#117)	69.58(67)	137242	19	138652	17	$263\pm^{13}_{13}$	1.00	20.0790	$3.25\pm^{1.29E+03}_{3.79}$	$16.09\pm^{0.37}_{nan}$	0.63
pks0405	0.09719 (#118)	43.14(43)	137149	20	nan	nan	$305\pm^{16}_{14}$	1.00	20.8027	$-0.02\pm^{1.00E+20}_{3.62}$	$nan\pm^{nan}_{nan}$	0.00
pks0405	0.10152 (#119)	47.15(43)	137149	20	nan	nan	$319\pm^{15}_{15}$	1.00	20.8848	$4.58\pm^{9.06E+03}_{4.97}$	$16.14\pm^{0.32}_{nan}$	0.83
pks0405	0.10298 (#120)	43.50(43)	137148	20	nan	nan	$317\pm^{16}_{15}$	1.00	20.9125	$0.36\pm^{22.57}_{1.61}$	$15.42\pm^{0.85}_{nan}$	0.03
pks0405	0.19456 (#121)	47.40(42)	134792	23	nan	nan	$344\pm^{29}_{18}$	1.00	22.6489	$6.59E+06\pm^{1.00E+20}_{6.26E+06}$	$16.62\pm^{0.12}_{0.04}$	13.44
pks0405	0.21976 (#122)	58.71(41)	133933	25	nan	nan	$335\pm^{20}_{20}$	1.00	23.1266	$-0.95\pm^{3.38}_{1.22}$	$nan\pm^{nan}_{nan}$	0.26
pks0405	0.24564 (#123)	62.85(45)	136481	20	nan	nan	$365\pm^{19}_{19}$	1.00	23.6173	$-0.87\pm^{2.01}_{0.97}$	$nan\pm^{nan}_{nan}$	0.39
pks0405	0.29748 (#124)	79.55(87)	133010	20	137174	19	$392\pm^{22}_{21}$	1.00	24.6002	$9.55\pm^{895.66}_{8.54}$	$16.24\pm^{0.20}_{0.46}$	2.68
pks0405	0.31016 (#125)	83.17(91)	137132	19	137234	21	$382\pm^{20}_{19}$	1.00	24.8406	$-0.75\pm^{1.39}_{0.76}$	$nan\pm^{nan}_{nan}$	0.48
pks0405	0.32502 (#126)	81.66(91)	137139	18	137234	22	$390\pm^{21}_{20}$	1.00	25.1224	$1.21\pm^{16.95}_{1.74}$	$15.85\pm^{0.43}_{nan}$	0.45
pks0405	0.49508 (#127)	96.67(89)	136537	33	137118	41	$387\pm^{26}_{25}$	1.00	28.3467	$-2.00\pm^{0.78}_{0.54}$	$nan\pm^{nan}_{nan}$	4.48
pks0558	0.10472 (#128)	56.06(47)	718011	24	nan	nan	$1867\pm^{16}_{16}$	1.00	20.9455	$-0.74\pm^{0.23}_{0.21}$	$nan\pm^{nan}_{nan}$	9.26
pks2155	0.05708 (#129)	58.70(51)	1703911	3	1685268	3	$4654\pm^{438}_{514}$	1.45	20.0422	$-0.03\pm^{0.78}_{0.02}$	$nan\pm^{nan}_{nan}$	-1.12
pks2155	0.06236 (#130)	47.13(42)	1703863	3	1685268	3	$3901\pm^{490}_{417}$	1.82	20.1423	$0.14\pm^{0.14}_{0.13}$	$15.04\pm^{0.28}_{1.00}$	1.63
pks2155	0.10586 (#131)	53.78(37)	1701058	3	nan	nan	$3620\pm^{354}_{403}$	2.02	20.9671	$0.02\pm^{0.09}_{0.16}$	$14.11\pm^{0.80}_{nan}$	-0.07
q0045	0.05590 (#132)	–	–	–	–	–	–	–	20.0199	–	–	–
q0045	0.06377 (#133)	–	–	–	–	–	–	–	20.1691	–	–	–
q1230	0.08344 (#134)	47.77(33)	39327	59	nan	nan	$68\pm^{18}_{17}$	1.00	20.5420	$2.51\pm^{2.29E+15}_{32.51}$	$16.04\pm^{0.72}_{nan}$	0.03
q1230	0.08540 (#135)	48.90(35)	39327	60	nan	nan	$64\pm^{15}_{13}$	1.00	20.5792	$0.00\pm^{9.25E+16}_{30.00}$	$12.67\pm^{4.12}_{nan}$	0.00
q1230	0.09444 (#136)	42.77(29)	39328	56	nan	nan	$64\pm^{19}_{18}$	1.00	20.7506	$-2.79\pm^{1.00E+20}_{27.21}$	$nan\pm^{nan}_{nan}$	0.09
q1230	0.10000 (#137)	42.86(29)	39328	60	nan	nan	$55\pm^{18}_{15}$	1.00	20.8560	$-3.67\pm^{2.82}_{1.31}$	$nan\pm^{nan}_{nan}$	1.71
q1230	0.10525 (#138)	43.32(30)	39329	65	nan	nan	$73\pm^{21}_{16}$	1.00	20.9555	$2.12E+04\pm^{1.00E+20}_{2.13E+04}$	$16.54\pm^{0.26}_{nan}$	0.78
q1230	0.10549 (#139)	43.13(30)	39329	65	nan	nan	$74\pm^{22}_{16}$	1.00	20.9601	$2.02E+06\pm^{1.00E+20}_{2.02E+06}$	$16.62\pm^{0.12}_{nan}$	0.99
q1230	0.10566 (#140)	43.20(30)	39329	65	nan	nan	$73\pm^{22}_{16}$	1.00	20.9633	$3.03E+04\pm^{1.00E+20}_{3.04E+04}$	$16.54\pm^{0.26}_{nan}$	0.90
q1230	0.10612 (#141)	39.76(29)	39330	63	nan	nan	$77\pm^{23}_{16}$	1.00	20.9720	$1.38E+09\pm^{1.00E+20}_{1.38E+09}$	$16.69\pm^{0.11}_{inf}$	1.52
q1230	0.10639 (#142)	40.21(30)	39330	65	nan	nan	$72\pm^{23}_{17}$	1.00	20.9772	$2.30E+06\pm^{1.00E+20}_{2.30E+06}$	$16.62\pm^{0.12}_{nan}$	1.23
q1230	0.10660 (#143)	39.93(30)	39330	65	nan	nan	$73\pm^{23}_{16}$	1.00	20.9811	$1.95E+09\pm^{1.00E+20}_{1.95E+09}$	$16.69\pm^{0.11}_{inf}$	1.54
q1230	0.10853 (#144)	39.15(27)	39331	86	nan	nan	$50\pm^{20}_{15}$	1.00	21.0177	$2.90E+09\pm^{1.00E+20}_{2.90E+09}$	$16.69\pm^{0.08}_{inf}$	1.22

q1230	0.10940 (#145)	39.98(27)	39331	96	nan	nan	$49\pm^{17}_{14}$	1.00	21.0342	$1.31E+12\pm^{1.00E+20}_{1.31E+12}$	$16.75\pm^{0.00}_{inf}$	1.53
q1230	0.12103 (#146)	–	–	–	–	–	–	–	21.2547	–	–	–
rbs1892	0.15567 (#147)	–	–	–	–	–	–	–	21.9115	–	–	–
rbs1892	0.15633 (#148)	–	–	–	–	–	–	–	21.9240	–	–	–
rbs1892	0.16343 (#149)	33.64(29)	4929	10	nan	nan	$164\pm^{103}_{79}$	1.00	22.0586	$-6.14\pm^{1.50}_{1.44}$	$nan\pm^{nan}_{nan}$	11.71
rbs1892	0.17001 (#150)	45.15(35)	4929	14	nan	nan	$243\pm^{126}_{104}$	1.00	22.1834	$-4.41\pm^{1.56E+08}_{1.80}$	$nan\pm^{nan}_{nan}$	1.30
rbs1892	0.17155 (#151)	46.20(37)	4929	14	nan	nan	$316\pm^{102}_{77}$	1.00	22.2126	$4.74E+06\pm^{1.00E+20}_{4.74E+06}$	$16.62\pm^{0.18}_{nan}$	0.59
rbs1892	0.17185 (#152)	46.34(37)	4929	14	nan	nan	$311\pm^{104}_{75}$	1.00	22.2183	$2.09E+04\pm^{1.00E+20}_{2.09E+04}$	$16.54\pm^{0.26}_{nan}$	0.56
rbs542	0.04455 (#153)	100.05(84)	197378	8	212046	8	$956\pm^{19}_{19}$	1.00	19.8047	$-0.25\pm^{0.65}_{0.47}$	$nan\pm^{nan}_{nan}$	0.23
rbs542	0.04992 (#154)	97.00(77)	197040	8	212046	8	$962\pm^{18}_{18}$	1.00	19.9065	$-0.04\pm^{0.97}_{0.50}$	$nan\pm^{nan}_{nan}$	-0.01
rxj0439	0.00550 (#155)	111.59(94)	146061	18	150968	15	$276\pm^{12}_{12}$	1.00	19.0643	$2.72\pm^{19.78}_{2.59}$	$16.05\pm^{0.26}_{1.04}$	1.50
rxj0439	0.17680 (#156)	56.53(41)	146765	20	nan	nan	$365\pm^{22}_{19}$	1.00	22.3121	$14.37\pm^{8.72E+03}_{13.75}$	$16.25\pm^{0.28}_{0.64}$	1.68
s50716	0.00989 (#157)	106.78(94)	74106	11	75858	11	$613\pm^{25}_{24}$	1.00	19.1475	$1.40\pm^{6.33}_{1.62}$	$15.88\pm^{0.34}_{nan}$	0.82
s50716	0.01766 (#158)	104.96(94)	74441	11	76625	10	$604\pm^{25}_{24}$	1.00	19.2948	$-0.48\pm^{1.26}_{0.72}$	$nan\pm^{nan}_{nan}$	0.28
s50716	0.08834 (#159)	40.33(43)	77052	11	nan	nan	$620\pm^{28}_{27}$	1.00	20.6349	$-1.52\pm^{1.01}_{0.68}$	$nan\pm^{nan}_{nan}$	2.22
s50716	0.14936 (#160)	–	–	–	–	–	–	–	21.7919	–	–	–
ton28	0.03357 (#161)	104.99(91)	83993	29	86174	29	$124\pm^{12}_{11}$	1.00	19.5965	$-1.25\pm^{2.69}_{1.03}$	$nan\pm^{nan}_{nan}$	0.52
tons180	0.04304 (#162)	73.60(82)	187350	6	195496	7	$956\pm^{19}_{19}$	1.00	19.7760	$-0.08\pm^{0.71}_{0.52}$	$nan\pm^{nan}_{nan}$	0.03
tons210	0.06763 (#163)	71.27(58)	6723	15	6719	6	$382\pm^{71}_{64}$	1.00	20.2423	$-2.67\pm^{3.16}_{1.20}$	$nan\pm^{nan}_{nan}$	1.12
tons210	0.08558 (#164)	52.71(42)	6725	18	nan	nan	$460\pm^{80}_{73}$	1.00	20.5826	$-1.42\pm^{2.97E+04}_{1.84}$	$nan\pm^{nan}_{nan}$	0.14

Table B.8: O VIII upper limit measurements with *XMM-Newton* data, at the prior redshift from the H I lines from Table A.2.

Target line		cmin	RGS1	RGS2	power–law		line component			ΔC
Name	z	(d.o.f.)	avg exp (s)	avg exp (s)	norm.	index	λ (Å)	τ_0	$\log N + (\mathrm{cm}^{-2})$	(d.o.f.)
1es1028	0.13714 (#1)	–	–	–	–	–	21.5602	–	–	–
1es1028	0.20383 (#2)	62.35(44)	146640	nan	$1006\pm^{29}_{29}$	1.00	22.8246	1.57	15.92	0.01
1es1028	0.22121 (#3)	57.62(42)	144940	nan	$1031\pm^{32}_{31}$	1.00	23.1541	0.62	15.62	3.89
1es1553	0.03466 (#4)	90.75(81)	1722815	1780022	$752\pm^{116}_{96}$	2.09	19.6172	0.35	15.41	-0.41
1es1553	0.04273 (#5)	89.06(72)	1720386	1774803	$776\pm^{127}_{108}$	2.01	19.7702	0.19	15.17	0.14
1es1553	0.06364 (#6)	46.18(56)	1785421	1740261	$1161\pm^{253}_{220}$	1.18	20.1666	0.27	15.31	-0.04
1es1553	0.21869 (#7)	36.89(28)	1666450	nan	$36\pm^{20}_{13}$	7.01	23.1064	0.28	15.32	2.52
3c249	0.13470 (#8)	–	–	–	–	–	21.5139	–	–	–
3c249	0.26664 (#9)	53.79(69)	2644	2524	$320\pm^{120}_{95}$	1.00	24.0155	5.00E+19	16.80	1.35
3c273	0.00758 (#10)	83.67(67)	1048814	1012144	$3696\pm^{17}_{17}$	1.00	19.1037	0.23	15.24	0.77
3c273	0.06707 (#11)	77.60(60)	1015660	1019511	$3919\pm^{16}_{16}$	1.00	20.2316	0.26	15.29	-0.35
3c273	0.07359 (#12)	63.12(54)	922775	1018570	$3920\pm^{17}_{16}$	1.00	20.3553	0.25	15.27	-0.21
3c273	0.13960 (#13)	–	–	–	–	–	21.6068	–	–	–
h1821	0.00944 (#14)	120.55(98)	30556	43312	$1002\pm^{55}_{53}$	1.00	19.1390	0.95	15.77	0.86
h1821	0.06779 (#15)	81.53(61)	31940	43282	$1055\pm^{61}_{60}$	1.00	20.2453	2.35	16.02	0.15
h1821	0.08483 (#16)	49.50(43)	30565	nan	$1106\pm^{71}_{68}$	1.00	20.5684	1.74	15.93	0.43
h1821	0.12147 (#17)	44.27(31)	30928	nan	$1128\pm^{97}_{95}$	1.00	21.2631	3.92	16.12	0.14
h1821	0.19817 (#18)	63.03(48)	30824	nan	$974\pm^{88}_{85}$	1.00	22.7173	1.51	15.90	1.17
h1821	0.21321 (#19)	58.22(45)	29048	nan	$1010\pm^{95}_{92}$	1.00	23.0025	3.09	16.07	0.40
h1821	0.24531 (#20)	69.92(50)	31312	36214	$1107\pm^{101}_{88}$	1.00	23.6111	3.78E+13	16.75	0.61
h2356	0.03830 (#21)	97.28(88)	479869	503477	$1019\pm^{12}_{13}$	1.00	19.6862	0.46	15.52	1.03
h2356	0.07881 (#22)	54.41(41)	506719	263751	$1072\pm^{15}_{15}$	1.00	20.4542	0.40	15.46	1.77
h2356	0.10467 (#23)	43.81(39)	507154	nan	$1072\pm^{16}_{15}$	1.00	20.9445	0.35	15.40	3.88
h2356	0.15613 (#24)	37.69(29)	503603	nan	$1088\pm^{19}_{18}$	1.00	21.9202	0.63	15.63	-0.01
he0226	0.14274 (#25)	–	–	–	–	–	21.6664	–	–	–
he0226	0.39890 (#26)	130.12(94)	31707	31704	$265\pm^{37}_{34}$	1.00	26.5231	2.46	16.04	0.53
he0226	0.41024 (#27)	136.42(96)	31707	31704	$274\pm^{38}_{35}$	1.00	26.7382	1.69	15.94	0.89
i22456	0.00443 (#28)	130.08(99)	76706	81909	$381\pm^{22}_{21}$	1.00	19.0440	0.53	15.56	6.46
i22456	0.09941 (#29)	59.72(44)	79900	nan	$501\pm^{38}_{27}$	1.00	20.8448	5.00E+19	16.80	4.43
mr2251	0.01068 (#30)	121.16(93)	414226	451165	$1243\pm^{275}_{224}$	1.52	19.1625	0.21	15.19	9.71
mr2251	0.01449 (#31)	122.62(90)	428129	462131	$1173\pm^{252}_{199}$	1.69	19.2347	0.32	15.38	0.13
mr2251	0.06131 (#32)	68.20(47)	466085	461291	$2234\pm^{1198}_{730}$	0.41	20.1224	0.92	15.76	5.66

mr2251	0.06190 (#33)	62.95(47)	466085	461291	$2211\pm^{1157}_{717}$	0.45	20.1336	2.23	16.00	16.53
mr2251	0.06276 (#34)	50.87(49)	466106	461162	$2612\pm^{1875}_{645}$	0.13	20.1499	29.78	16.31	38.86
mr2251	0.06327 (#35)	44.88(49)	466112	461008	$2740\pm^{1569}_{769}$	0.03	20.1596	64.78	16.34	45.67
mr2251	0.06381 (#36)	45.72(49)	466112	461008	$2376\pm^{1389}_{647}$	0.33	20.1698	165.19	16.35	45.47
mrk478	0.06166 (#37)	76.63(64)	202266	202111	$465\pm^{14}_{14}$	1.00	20.1291	1.45	15.91	0.00
mrk478	0.06578 (#38)	70.27(61)	204255	201677	$472\pm^{14}_{15}$	1.00	20.2072	1.65	15.93	-0.00
mrk478	0.07213 (#39)	54.18(51)	200098	200301	$492\pm^{16}_{15}$	1.00	20.3276	66.34	16.33	1.94
mrk876	0.01159 (#40)	84.83(96)	2656	2600	$174\pm^{70}_{54}$	1.00	19.1797	5.00E+19	16.75	0.81
mrk876	0.05598 (#41)	59.57(72)	2736	2708	$227\pm^{89}_{64}$	1.00	20.0214	5.00E+19	16.80	0.48
mrk876	0.08709 (#42)	42.06(43)	2804	nan	$414\pm^{119}_{103}$	1.00	20.6112	1.22	15.85	4.24
mrk876	0.08858 (#43)	42.31(44)	2805	nan	$419\pm^{123}_{105}$	1.00	20.6395	1.23	15.85	3.77
mrk876	0.08917 (#44)	42.90(43)	2804	nan	$427\pm^{125}_{107}$	1.00	20.6507	1.32	15.86	2.96
mrk876	0.11487 (#45)	52.10(37)	2790	nan	$714\pm^{237}_{160}$	1.00	21.1379	5.00E+19	16.80	3.07
ngc7469	0.00981 (#46)	85.67(65)	629599	665412	$1934\pm^{17}_{17}$	1.00	19.1460	0.89	15.74	51.59
pg0003	0.08299 (#47)	56.55(41)	13036	nan	$169\pm^{41}_{36}$	1.00	20.5335	4.11E+03	16.46	0.31
pg0003	0.17139 (#48)	45.45(37)	13036	nan	$315\pm^{63}_{56}$	1.00	22.2096	5.00E+19	16.80	0.01
pg0003	0.22541 (#49)	47.36(42)	13037	nan	$145\pm^{50}_{43}$	1.00	23.2338	0.96	15.76	8.09
pg0003	0.38633 (#50)	107.06(92)	13033	12857	$248\pm^{69}_{50}$	1.00	26.2848	5.00E+19	16.80	1.31
pg0003	0.42051 (#51)	129.11(93)	13034	12830	$327\pm^{75}_{64}$	1.00	26.9329	5.00E+19	16.80	0.73
pg0804	0.05015 (#52)	80.99(78)	28468	30600	$1084\pm^{53}_{49}$	1.00	19.9108	2.27	16.01	0.00
pg0804	0.05576 (#53)	70.57(71)	28779	30600	$1101\pm^{55}_{53}$	1.00	20.0172	7.34E+03	16.46	1.53
pg0804	0.36379 (#54)	131.95(97)	30110	29227	$1657\pm^{86}_{84}$	1.00	25.8575	0.90	15.76	1.74
pg0832	0.01753 (#55)	–	–	–	–	–	19.2924	–	–	–
pg0832	0.02793 (#56)	–	–	–	–	–	19.4896	–	–	–
pg0832	0.08748 (#57)	59.08(42)	20650	nan	$41\pm^{16}_{12}$	1.00	20.6186	5.00E+19	16.75	0.57
pg0832	0.10171 (#58)	53.76(42)	20652	nan	$29\pm^{15}_{12}$	1.00	20.8884	2.08	15.99	1.81
pg0832	0.18391 (#59)	40.73(29)	20654	nan	$36\pm^{22}_{16}$	1.00	22.4469	2.66	16.05	1.60
pg0832	0.27503 (#60)	100.19(76)	20655	20637	$76\pm^{24}_{20}$	1.00	24.1746	3.37E+13	16.74	0.04
pg0832	0.27694 (#61)	100.69(77)	20655	20637	$63\pm^{23}_{18}$	1.00	24.2108	5.00E+19	16.77	0.01
pg0832	0.32572 (#62)	–	–	–	–	–	25.1357	–	–	–
pg0838	0.06583 (#63)	34.64(61)	1623	1514	$244\pm^{130}_{88}$	1.00	20.2081	5.00E+19	16.80	0.40
pg0838	0.08628 (#64)	23.30(42)	1619	nan	$186\pm^{121}_{78}$	1.00	20.5959	5.00E+19	16.80	0.39
pg0838	0.12676 (#65)	8.14(29)	1609	nan	$73\pm^{103}_{73}$	1.00	21.3634	5.00E+19	16.80	0.20
pg0953	0.16319 (#66)	32.74(29)	12792	nan	$419\pm^{81}_{73}$	1.00	22.0541	1.78	15.95	1.46
pg0953	0.19221 (#67)	49.32(42)	12792	nan	$417\pm^{66}_{61}$	1.00	22.6043	114.80	16.36	0.15
pg1048	0.00642 (#68)	130.68(89)	18905	18341	$165\pm^{26}_{24}$	1.00	19.0817	4.65E+03	16.53	0.00
pg1048	0.02414 (#69)	121.85(91)	18905	18341	$157\pm^{26}_{23}$	1.00	19.4177	93.69	16.39	0.09

pg1115	0.09511 (#70)	54.44(43)	17542	nan	$312\pm^{40}_{40}$	1.00	20.7633	5.00E+19	16.80	0.07
pg1115	0.12059 (#71)	43.07(32)	17510	nan	$290\pm^{49}_{45}$	1.00	21.2464	8.25E+10	16.71	0.14
pg1115	0.12741 (#72)	42.59(29)	17510	nan	$274\pm^{50}_{45}$	1.00	21.3757	68.65	16.37	0.18
pg1116	0.04114 (#73)	87.87(85)	280360	294383	$456\pm^{11}_{11}$	1.00	19.7400	4.36	16.14	4.54
pg1116	0.06251 (#74)	79.62(66)	285035	294383	$480\pm^{13}_{12}$	1.00	20.1452	27.56	16.31	3.41
pg1116	0.08382 (#75)	44.01(43)	287898	nan	$470\pm^{13}_{13}$	1.00	20.5492	0.53	15.56	3.46
pg1116	0.09210 (#76)	46.83(43)	287898	nan	$499\pm^{13}_{13}$	1.00	20.7062	1.82	15.95	0.19
pg1116	0.09281 (#77)	49.13(44)	288074	nan	$497\pm^{13}_{13}$	1.00	20.7197	1.82	15.97	0.12
pg1116	0.13373 (#78)	34.69(29)	296156	nan	$516\pm^{16}_{17}$	1.00	21.4955	75.36	16.37	2.54
pg1116	0.13851 (#79)	–	–	–	–	–	21.5861	–	–	–
pg1211	0.02586 (#80)	108.44(86)	736771	780487	$490\pm^{7}_{7}$	1.00	19.4503	0.35	15.40	1.62
pg1211	0.05443 (#81)	83.50(61)	752151	777295	$566\pm^{8}_{8}$	1.00	19.9920	0.36	15.42	2.55
pg1216	0.00842 (#82)	112.05(92)	11245	11250	$100\pm^{26}_{22}$	1.00	19.1196	9.78	16.25	0.42
pg1216	0.07969 (#83)	61.07(43)	11245	11250	$134\pm^{37}_{32}$	1.00	20.4709	1.93	15.98	2.23
pg1216	0.12372 (#84*)	47.41(31)	11245	nan	$212\pm^{52}_{42}$	1.00	21.3057	5.00E+19	16.80	0.88
pg1216	0.12473 (#85*)	47.65(31)	11245	nan	$211\pm^{55}_{41}$	1.00	21.3249	5.00E+19	16.80	0.63
pg1216	0.17950 (#86)	55.47(38)	11245	nan	$190\pm^{49}_{41}$	1.00	22.3633	5.00E+19	16.80	0.00
pg1216	0.20014 (#87)	56.76(42)	11245	nan	$145\pm^{40}_{33}$	1.00	22.7547	5.00E+19	16.80	0.44
pg1216	0.21258 (#88)	45.73(40)	11245	nan	$138\pm^{43}_{36}$	1.00	22.9905	1.74	15.95	2.17
pg1216	0.28204 (#89)	109.28(79)	11245	11258	$185\pm^{46}_{40}$	1.00	24.3075	5.00E+19	16.75	0.67
pg1229	0.05018 (#90)	102.73(72)	24011	24007	$394\pm^{38}_{36}$	1.00	19.9114	1.46E+03	16.47	0.17
pg1259	0.05563 (#91)	91.28(69)	11479	11480	$114\pm^{32}_{25}$	1.00	20.0147	5.00E+19	16.80	0.34
pg1259	0.15136 (#92)	–	–	–	–	–	21.8298	–	–	–
pg1259	0.16647 (#93)	32.56(32)	11484	nan	$155\pm^{50}_{42}$	1.00	22.1163	6.28E+13	16.76	0.07
pg1259	0.17893 (#94)	39.84(42)	11484	nan	$163\pm^{42}_{36}$	1.00	22.3525	5.00E+19	16.75	1.00
pg1259	0.22376 (#95)	58.87(41)	11485	nan	$216\pm^{63}_{46}$	1.00	23.2025	5.00E+19	16.75	1.05
pg1259	0.24126 (#96)	61.99(46)	11485	11479	$194\pm^{48}_{41}$	1.00	23.5343	5.00E+19	16.75	0.03
pg1259	0.31974 (#97)	106.65(91)	11483	11479	$148\pm^{44}_{36}$	1.00	25.0223	5.00E+19	16.80	0.00
pg1259	0.36212 (#98)	107.88(92)	11483	11479	$236\pm^{54}_{47}$	1.00	25.8258	10.54	16.26	0.41
pg1259	0.38254 (#99)	106.89(91)	11483	11479	$273\pm^{64}_{55}$	1.00	26.2130	6.38E+06	16.58	0.04
pg1259	0.38266 (#100)	106.88(91)	11483	11479	$272\pm^{64}_{55}$	1.00	26.2152	1.20E+06	16.57	0.05
pg1307	0.08345 (#101)	49.47(43)	9851	nan	$199\pm^{44}_{39}$	1.00	20.5422	2.75	16.06	0.96
pg1309	0.03861 (#102)	113.84(79)	27332	26079	$46\pm^{15}_{11}$	1.00	19.6920	5.00E+19	16.79	1.82
pg1309	0.17740 (#103)	47.95(38)	27263	nan	$59\pm^{20}_{17}$	1.00	22.3235	5.00E+19	16.75	0.12
pg1309	0.17852 (#104)	48.79(39)	27263	nan	$59\pm^{20}_{17}$	1.00	22.3447	5.00E+19	16.80	0.02
pg1309	0.17918 (#105)	49.59(40)	27263	nan	$58\pm^{20}_{17}$	1.00	22.3573	5.00E+19	16.80	0.00
pg1309	0.18143 (#106)	54.59(42)	27263	nan	$70\pm^{21}_{17}$	1.00	22.3999	5.00E+19	16.80	0.18

pg1444	0.22031 (#107)	50.77(40)	17630	nan	$104\pm^{38}_{33}$	1.00	23.1371	1.07	15.81	17.52
pg1626	0.06137 (#108)	77.10(65)	69300	67705	$197\pm^{24}_{24}$	1.00	20.1236	195.41	16.35	0.16
phl1811	0.05143 (#109*)	129.49(67)	75753	78895	$29\pm^{9}_{8}$	1.00	19.9351	2.12E+04	16.48	0.22
phl1811	0.05813 (#110*)	121.07(62)	77392	78895	$28\pm^{9}_{8}$	1.00	20.0621	5.00E+19	16.80	0.03
phl1811	0.08085 (#111)	54.95(37)	78263	78895	$47\pm^{11}_{10}$	1.00	20.4929	5.00E+19	16.80	1.02
phl1811	0.08163 (#112)	53.36(36)	78263	nan	$49\pm^{11}_{10}$	1.00	20.5077	5.00E+19	16.75	1.08
phl1811	0.12003 (#113)	–	–	–	–	–	21.2358	–	–	–
phl1811	0.15787 (#114)	–	–	–	–	–	21.9532	–	–	–
pks0312	0.11454 (#115)	27.80(20)	23881	nan	$218\pm^{42}_{38}$	1.00	21.1317	5.00E+19	16.80	0.86
pks0405	0.02510 (#116)	113.13(93)	134903	138652	$261\pm^{13}_{12}$	1.00	19.4359	65.09	16.33	1.85
pks0405	0.05902 (#117)	69.58(67)	137242	138652	$263\pm^{13}_{13}$	1.00	20.0790	645.42	16.41	0.63
pks0405	0.09719 (#118)	43.14(43)	137149	nan	$305\pm^{16}_{14}$	1.00	20.8027	5.00E+19	16.75	0.00
pks0405	0.10152 (#119)	47.15(43)	137149	nan	$319\pm^{15}_{15}$	1.00	20.8848	4.53E+03	16.45	0.83
pks0405	0.10298 (#120)	43.50(43)	137148	nan	$317\pm^{16}_{15}$	1.00	20.9125	12.09	16.22	0.03
pks0405	0.19456 (#121)	47.40(42)	134792	nan	$344\pm^{29}_{18}$	1.00	22.6489	5.00E+19	16.75	13.44
pks0405	0.21976 (#122)	58.71(41)	133933	nan	$335\pm^{20}_{20}$	1.00	23.1266	2.30	16.02	0.26
pks0405	0.24564 (#123)	62.85(45)	136481	nan	$365\pm^{19}_{19}$	1.00	23.6173	1.49	15.91	0.39
pks0405	0.29748 (#124)	79.55(87)	133010	137174	$392\pm^{22}_{21}$	1.00	24.6002	452.10	16.40	2.68
pks0405	0.31016 (#125)	83.17(91)	137132	137234	$382\pm^{20}_{19}$	1.00	24.8406	1.08	15.81	0.48
pks0405	0.32502 (#126)	81.66(91)	137139	137234	$390\pm^{21}_{20}$	1.00	25.1224	9.34	16.22	0.45
pks0405	0.49508 (#127)	96.67(89)	136537	137118	$387\pm^{26}_{25}$	1.00	28.3467	0.66	15.64	4.48
pks0558	0.10472 (#128)	56.06(47)	718011	nan	$1867\pm^{16}_{16}$	1.00	20.9455	0.22	15.21	9.26
pks2155	0.05708 (#129)	58.70(51)	1703911	1685268	$4654\pm^{438}_{514}$	1.45	20.0422	0.40	15.46	-1.12
pks2155	0.06236 (#130)	47.13(42)	1703863	1685268	$3901\pm^{490}_{417}$	1.82	20.1423	0.13	15.01	1.63
pks2155	0.10586 (#131)	53.78(37)	1701058	nan	$3620\pm^{354}_{403}$	2.02	20.9671	0.13	14.99	-0.07
q0045	0.05590 (#132)	–	–	–	–	–	20.0199	–	–	–
q0045	0.06377 (#133)	–	–	–	–	–	20.1691	–	–	–
q1230	0.08344 (#134)	47.77(33)	39327	nan	$68\pm^{18}_{17}$	1.00	20.5420	1.15E+15	16.74	0.03
q1230	0.08540 (#135)	48.90(35)	39327	nan	$64\pm^{15}_{13}$	1.00	20.5792	4.63E+16	16.80	0.00
q1230	0.09444 (#136)	42.77(29)	39328	nan	$64\pm^{19}_{18}$	1.00	20.7506	5.00E+19	16.80	0.09
q1230	0.10000 (#137)	42.86(29)	39328	nan	$55\pm^{18}_{15}$	1.00	20.8560	2.06	16.00	1.71
q1230	0.10525 (#138)	43.32(30)	39329	nan	$73\pm^{21}_{16}$	1.00	20.9555	5.00E+19	16.80	0.78
q1230	0.10549 (#139)	43.13(30)	39329	nan	$74\pm^{22}_{16}$	1.00	20.9601	5.00E+19	16.75	0.99
q1230	0.10566 (#140)	43.20(30)	39329	nan	$73\pm^{22}_{16}$	1.00	20.9633	5.00E+19	16.80	0.90
q1230	0.10612 (#141)	39.76(29)	39330	nan	$77\pm^{23}_{16}$	1.00	20.9720	5.00E+19	16.80	1.52
q1230	0.10639 (#142)	40.21(30)	39330	nan	$72\pm^{23}_{17}$	1.00	20.9772	5.00E+19	16.75	1.23
q1230	0.10660 (#143)	39.93(30)	39330	nan	$73\pm^{23}_{16}$	1.00	20.9811	5.00E+19	16.80	1.54

q1230	0.10853 (#144)	39.15(27)	39331	nan	$50\pm^{20}_{15}$	1.00	21.0177	5.00E+19	16.77	1.22
q1230	0.10940 (#145)	39.98(27)	39331	nan	$49\pm^{17}_{14}$	1.00	21.0342	5.00E+19	16.75	1.53
q1230	0.12103 (#146)	–	–	–	–	–	21.2547	–	–	–
rbs1892	0.15567 (#147)	–	–	–	–	–	21.9115	–	–	–
rbs1892	0.15633 (#148)	–	–	–	–	–	21.9240	–	–	–
rbs1892	0.16343 (#149)	33.64(29)	4929	nan	$164\pm^{103}_{79}$	1.00	22.0586	1.47	15.91	11.71
rbs1892	0.17001 (#150)	45.15(35)	4929	nan	$243\pm^{126}_{104}$	1.00	22.1834	7.82E+07	16.64	1.30
rbs1892	0.17155 (#151)	46.20(37)	4929	nan	$316\pm^{102}_{77}$	1.00	22.2126	5.00E+19	16.80	0.59
rbs1892	0.17185 (#152)	46.34(37)	4929	nan	$311\pm^{104}_{75}$	1.00	22.2183	5.00E+19	16.80	0.56
rbs542	0.04455 (#153)	100.05(84)	197378	212046	$956\pm^{19}_{19}$	1.00	19.8047	0.56	15.59	0.23
rbs542	0.04992 (#154)	97.00(77)	197040	212046	$962\pm^{18}_{18}$	1.00	19.9065	0.74	15.69	-0.01
rxj0439	0.00550 (#155)	111.59(94)	146061	150968	$276\pm^{12}_{12}$	1.00	19.0643	11.19	16.27	1.50
rxj0439	0.17680 (#156)	56.53(41)	146765	nan	$365\pm^{22}_{19}$	1.00	22.3121	4.37E+03	16.51	1.68
s50716	0.00989 (#157)	106.78(94)	74106	75858	$613\pm^{25}_{24}$	1.00	19.1475	3.97	16.12	0.82
s50716	0.01766 (#158)	104.96(94)	74441	76625	$604\pm^{25}_{24}$	1.00	19.2948	0.99	15.78	0.28
s50716	0.08834 (#159)	40.33(43)	77052	nan	$620\pm^{28}_{27}$	1.00	20.6349	0.84	15.73	2.22
s50716	0.14936 (#160)	–	–	–	–	–	21.7919	–	–	–
ton28	0.03357 (#161)	104.99(91)	83993	86174	$124\pm^{12}_{11}$	1.00	19.5965	1.86	15.97	0.52
tons180	0.04304 (#162)	73.60(82)	187350	195496	$956\pm^{19}_{19}$	1.00	19.7760	0.62	15.62	0.03
tons210	0.06763 (#163)	71.27(58)	6723	6719	$382\pm^{71}_{64}$	1.00	20.2423	2.18	16.00	1.12
tons210	0.08558 (#164)	52.71(42)	6725	nan	$460\pm^{80}_{73}$	1.00	20.5826	1.49E+04	16.49	0.14

Appendix C. Analysis Tables, *Chandra*

Table C.1: O VII measurements with *Chandra* data, at the prior redshift from the O VI lines from Table A.1.

Target line		cmin	RGS1		power–law		line component			ΔC
Name	z	(d.o.f.)	avg exp (s)	% $\frac{B}{D+B}$	norm.	index	λ (Å)	τ_0	log N(cm^{-2})	(d.o.f.)
1es1028	0.12314 (#1)	32.34(39)	148933	24	$1757\pm^{63}_{62}$	1	24.2598	$-0.56\pm^{0.97}_{0.68}$	$nan\pm^{nan}_{nan}$	0.44
1es1028	0.13706 (#2)	35.52(39)	148933	24	$1830\pm^{64}_{63}$	1	24.5605	$1.29\pm^{3.09}_{1.34}$	$15.56\pm^{0.30}_{nan}$	0.99
1es1028	0.33735 (#3)	37.26(39)	148933	25	$2138\pm^{81}_{79}$	1	28.8868	$-0.66\pm^{0.98}_{0.74}$	$nan\pm^{nan}_{nan}$	0.56
1es1553	0.18759 (#4)	44.14(38)	495645	22	$3135\pm^{48}_{48}$	1	25.6519	$0.34\pm^{0.57}_{0.46}$	$15.06\pm^{0.37}_{nan}$	0.58
1es1553	0.18775 (#5)	44.13(38)	495645	22	$3135\pm^{48}_{48}$	1	25.6554	$0.35\pm^{0.62}_{0.47}$	$15.07\pm^{0.37}_{nan}$	0.58
1es1553	0.18984 (#6)	42.53(38)	495645	22	$3106\pm^{48}_{48}$	1	25.7005	$-0.38\pm^{0.40}_{0.36}$	$nan\pm^{nan}_{nan}$	1.00
1es1553	0.21631 (#7)	51.98(38)	495645	23	$3137\pm^{49}_{49}$	1	26.2723	$0.29\pm^{0.58}_{0.46}$	$15.00\pm^{0.42}_{nan}$	0.42
1es1553	0.31130 (#8)	36.35(38)	495645	25	$3202\pm^{53}_{54}$	1	28.3241	$-0.04\pm^{0.53}_{0.44}$	$nan\pm^{nan}_{nan}$	0.01
1es1553	0.37868 (#9)	48.60(38)	495645	28	$3322\pm^{62}_{61}$	1	29.7795	$-0.69\pm^{0.39}_{0.33}$	$nan\pm^{nan}_{nan}$	2.89
1es1553	0.39497 (#10)	39.90(38)	495645	28	$3374\pm^{65}_{64}$	1	30.1314	$-0.48\pm^{0.47}_{0.37}$	$nan\pm^{nan}_{nan}$	1.16
h1821	0.02438 (#11)	44.15(32)	470152	2	$888\pm^{22}_{21}$	1	22.1266	$0.33\pm^{0.73}_{0.58}$	$15.05\pm^{0.44}_{nan}$	0.32
h1821	0.10817 (#12)	50.75(39)	470152	1	$1103\pm^{21}_{21}$	1	23.9365	$-1.08\pm^{0.34}_{0.31}$	$nan\pm^{nan}_{nan}$	8.78
h1821	0.12133 (#13)	46.33(38)	470152	1	$1202\pm^{22}_{22}$	1	24.2207	$0.22\pm^{0.59}_{0.46}$	$14.89\pm^{0.49}_{nan}$	0.22
h1821	0.12147 (#14)	46.13(38)	470152	1	$1203\pm^{22}_{22}$	1	24.2238	$0.32\pm^{0.57}_{0.49}$	$15.04\pm^{0.39}_{nan}$	0.44
h1821	0.16992 (#15)	37.35(38)	470152	1	$1107\pm^{23}_{23}$	1	25.2703	$-0.07\pm^{0.57}_{0.45}$	$nan\pm^{nan}_{nan}$	0.02
h1821	0.17043 (#16)	37.01(38)	470152	1	$1104\pm^{23}_{23}$	1	25.2813	$-0.29\pm^{0.50}_{0.40}$	$nan\pm^{nan}_{nan}$	0.39
h1821	0.21326 (#17)	33.42(38)	470152	2	$1090\pm^{25}_{25}$	1	26.2064	$-0.81\pm^{0.40}_{0.33}$	$nan\pm^{nan}_{nan}$	3.65
h1821	0.22497 (#18)	31.24(39)	470152	2	$1097\pm^{26}_{25}$	1	26.4594	$0.54\pm^{0.84}_{0.63}$	$15.24\pm^{0.32}_{nan}$	0.74
h1821	0.22522 (#19)	31.59(39)	470152	2	$1095\pm^{26}_{25}$	1	26.4648	$0.37\pm^{0.78}_{0.60}$	$15.10\pm^{0.42}_{nan}$	0.37
h1821	0.22639 (#20)	32.44(39)	470152	2	$1098\pm^{26}_{25}$	1	26.4900	$0.28\pm^{0.73}_{0.57}$	$14.99\pm^{0.48}_{nan}$	0.23
h1821	0.24531 (#21)	28.82(38)	470152	2	$1103\pm^{27}_{27}$	1	26.8987	$1.09\pm^{1.14}_{0.81}$	$15.51\pm^{0.22}_{0.52}$	2.16
h1821	0.26657 (#22)	39.22(39)	470152	2	$1157\pm^{29}_{29}$	1	27.3579	$-0.17\pm^{0.65}_{0.50}$	$nan\pm^{nan}_{nan}$	0.09
h1821	0.28800 (#23)	48.59(33)	470152	1	$1265\pm^{37}_{37}$	1	27.8208	$-0.77\pm^{0.52}_{0.42}$	$nan\pm^{nan}_{nan}$	2.16
h1821	0.29658 (#24)	45.10(33)	470152	2	$1326\pm^{41}_{40}$	1	28.0061	$-1.47\pm^{0.70}_{0.51}$	$nan\pm^{nan}_{nan}$	3.22
h1821	0.29680 (#25)	45.72(34)	470152	2	$1338\pm^{42}_{41}$	1	28.0109	$-1.81\pm^{0.92}_{0.68}$	$nan\pm^{nan}_{nan}$	2.92
h2356	0.11461 (#26)	26.64(38)	586697	29	$2314\pm^{37}_{37}$	1	24.0756	$1.22\pm^{0.88}_{0.64}$	$15.55\pm^{0.16}_{0.27}$	4.89
h2356	0.16512 (#27)	34.18(39)	586697	29	$2408\pm^{39}_{39}$	1	25.1666	$1.14\pm^{1.03}_{0.70}$	$15.49\pm^{0.18}_{0.33}$	3.76
mr2251	0.01070 (#28)	33.00(30)	78434	15	$3031\pm^{114}_{110}$	1	21.8311	$0.03\pm^{1.37}_{0.76}$	$13.99\pm^{1.55}_{nan}$	0.00
pg1116	0.05900 (#29)	33.16(38)	355485	54	$756\pm^{36}_{36}$	1	22.8744	$-1.74\pm^{0.82}_{0.64}$	$nan\pm^{nan}_{nan}$	3.69
pg1116	0.05927 (#30)	32.42(38)	355485	54	$755\pm^{36}_{35}$	1	22.8802	$-1.62\pm^{0.62}_{0.46}$	$nan\pm^{nan}_{nan}$	4.50
pg1116	0.11895 (#31)	40.85(38)	355485	51	$878\pm^{38}_{37}$	1	24.1693	$11.94\pm^{6.77E+03}_{9.95}$	$15.94\pm^{0.18}_{0.31}$	4.27
pg1116	0.13852 (#32)	41.11(33)	355485	50	$886\pm^{42}_{41}$	1	24.5920	$-1.72\pm^{0.53}_{0.42}$	$nan\pm^{nan}_{nan}$	6.79
pg1116	0.16539 (#33)	28.52(32)	355485	50	$949\pm^{44}_{43}$	1	25.1724	$0.32\pm^{2.20}_{1.10}$	$15.03\pm^{0.70}_{nan}$	0.06

pg1116	0.16554 (#34)	28.43(32)	355485	50	$952\pm^{44}_{43}$	1	25.1757	$0.51\pm^{2.08}_{1.17}$	$15.23\pm^{0.53}_{nan}$	0.16
pg1116	0.16610 (#35)	30.58(33)	355485	50	$948\pm^{44}_{43}$	1	25.1878	$0.99\pm^{2.90}_{1.35}$	$15.47\pm^{0.37}_{nan}$	0.51
pg1116	0.16686 (#36)	30.77(32)	355485	50	$944\pm^{44}_{43}$	1	25.2042	$1.23\pm^{5.36}_{1.51}$	$15.52\pm^{0.36}_{nan}$	0.64
pg1116	0.17343 (#37)	30.83(36)	355485	50	$941\pm^{41}_{41}$	1	25.3461	$-0.67\pm^{1.12}_{0.71}$	$nan\pm^{nan}_{nan}$	0.50
pg1211	0.00711 (#38)	28.35(30)	133595	1	$1244\pm^{60}_{58}$	1	21.7536	$0.27\pm^{1.59}_{0.95}$	$14.97\pm^{0.67}_{nan}$	0.07
pg1211	0.05117 (#39)	48.13(38)	133595	1	$1465\pm^{67}_{65}$	1	22.7053	$0.99\pm^{3.42}_{1.33}$	$15.44\pm^{0.36}_{nan}$	0.50
pg1211	0.06449 (#40)	49.38(39)	133595	1	$1592\pm^{67}_{65}$	1	22.9930	$-0.20\pm^{1.65}_{0.88}$	$nan\pm^{nan}_{nan}$	0.03
pg1211	0.06491 (#41)	51.45(38)	133595	1	$1586\pm^{67}_{65}$	1	23.0021	$-0.05\pm^{1.64}_{1.03}$	$nan\pm^{nan}_{nan}$	0.00
pks0405	0.09192 (#42)	36.05(39)	376096	69	$494\pm^{35}_{35}$	1	23.5855	$0.49\pm^{6.13}_{1.64}$	$15.21\pm^{0.69}_{nan}$	0.06
pks0405	0.09647 (#43)	44.38(39)	376096	68	$538\pm^{35}_{35}$	1	23.6838	$24.63\pm^{4.19E+06}_{21.48}$	$16.00\pm^{0.30}_{0.24}$	3.85
pks0405	0.14808 (#44)	51.46(38)	376096	68	$537\pm^{38}_{37}$	1	24.7985	$-1.29\pm^{1.53}_{0.95}$	$nan\pm^{nan}_{nan}$	0.86
pks0405	0.16566 (#45)	45.81(38)	376096	68	$569\pm^{40}_{37}$	1	25.1783	$1.30E+05\pm^{1.00E+20}_{6.50E+04}$	$16.24\pm^{0.24}_{0.00}$	7.23
pks0405	0.16606 (#46)	53.91(39)	376096	68	$577\pm^{38}_{37}$	1	25.1869	$1.87E+03\pm^{1.00E+20}_{1.64E+03}$	$16.22\pm^{0.20}_{0.17}$	6.26
pks0405	0.16659 (#47)	47.68(38)	376096	68	$566\pm^{39}_{38}$	1	25.1983	$5.16E+03\pm^{1.00E+20}_{5.04E+03}$	$16.22\pm^{0.19}_{0.19}$	5.02
pks0405	0.16688 (#48)	47.52(38)	376096	68	$569\pm^{39}_{38}$	1	25.2046	$1.42E+06\pm^{1.00E+20}_{1.38E+06}$	$16.30\pm^{0.18}_{0.10}$	5.35
pks0405	0.16712 (#49)	49.50(39)	376096	69	$549\pm^{38}_{38}$	1	25.2098	$1.50E+04\pm^{1.00E+20}_{1.42E+04}$	$16.23\pm^{0.26}_{0.10}$	4.34
pks0405	0.18257 (#50)	42.98(38)	376096	69	$543\pm^{38}_{38}$	1	25.5435	$4.90\pm^{1.21E+04}_{5.02}$	$15.81\pm^{0.32}_{nan}$	0.95
pks0405	0.18289 (#51)	42.87(38)	376096	69	$545\pm^{39}_{38}$	1	25.5504	$4.75\pm^{516.69}_{4.79}$	$15.88\pm^{0.24}_{nan}$	1.09
pks0405	0.24052 (#52)	44.44(38)	376096	68	$610\pm^{42}_{41}$	1	26.7952	$-0.84\pm^{1.97}_{0.90}$	$nan\pm^{nan}_{nan}$	0.36
pks0405	0.24094 (#53)	44.76(38)	376096	68	$618\pm^{40}_{41}$	1	26.8043	$-0.00\pm^{4.81}_{1.21}$	$nan\pm^{nan}_{nan}$	-0.00
pks0405	0.24547 (#54)	44.46(38)	376096	68	$595\pm^{42}_{41}$	1	26.9022	$-1.24\pm^{1.52}_{0.92}$	$nan\pm^{nan}_{nan}$	0.81
pks0405	0.29762 (#55)	35.29(38)	376096	69	$613\pm^{44}_{44}$	1	28.0286	$-0.78\pm^{2.21}_{1.02}$	$nan\pm^{nan}_{nan}$	0.26
pks0405	0.34188 (#56)	38.18(39)	376096	73	$566\pm^{48}_{46}$	1	28.9846	$44.15\pm^{4.03E+06}_{41.46}$	$16.01\pm^{0.26}_{0.27}$	2.12
pks0405	0.34225 (#57)	38.30(39)	376096	73	$567\pm^{47}_{46}$	1	28.9926	$24.34\pm^{3.79E+05}_{23.38}$	$16.03\pm^{0.25}_{0.60}$	2.00
pks0405	0.35092 (#58)	32.95(38)	376096	71	$622\pm^{48}_{48}$	1	29.1799	$37.67\pm^{4.43E+06}_{36.03}$	$16.07\pm^{0.27}_{0.47}$	2.62
pks0405	0.36075 (#59)	38.91(39)	376096	74	$537\pm^{49}_{48}$	1	29.3922	$-1.01\pm^{2.61}_{1.02}$	$nan\pm^{nan}_{nan}$	0.34
pks0405	0.36151 (#60)	37.68(39)	376096	74	$542\pm^{49}_{48}$	1	29.4086	$-0.85\pm^{3.28}_{1.10}$	$nan\pm^{nan}_{nan}$	0.21
pks0405	0.36329 (#61)	33.65(38)	376096	74	$517\pm^{49}_{48}$	1	29.4471	$-2.22\pm^{1.09}_{0.73}$	$nan\pm^{nan}_{nan}$	2.88
pks0405	0.40570 (#62)	52.38(39)	376096	76	$564\pm^{55}_{54}$	1	30.3631	$2.21\pm^{2.29E+03}_{3.42}$	$15.73\pm^{0.50}_{nan}$	0.26
pks0405	0.40890 (#63)	47.45(39)	376096	77	$529\pm^{56}_{54}$	1	30.4322	$-0.06\pm^{58.07}_{1.62}$	$nan\pm^{nan}_{nan}$	-0.00
pks0405	0.49505 (#64)	37.44(39)	376096	77	$501\pm^{56}_{55}$	1	32.2931	$-1.91\pm^{1.38}_{0.76}$	$nan\pm^{nan}_{nan}$	1.61
pks0405	0.49530 (#65)	37.74(38)	376096	78	$490\pm^{56}_{55}$	1	32.2985	$-2.23\pm^{1.72}_{1.03}$	$nan\pm^{nan}_{nan}$	1.56
pks0405	0.55506 (#66)	35.55(39)	376096	75	$662\pm^{62}_{60}$	1	33.5893	$1.34E+03\pm^{1.00E+20}_{1.29E+03}$	$16.16\pm^{0.25}_{0.18}$	3.09
pks2005	0.06490 (#67)	35.79(38)	282191	1	$1954\pm^{63}_{62}$	1	23.0018	$-0.67\pm^{0.89}_{0.68}$	$nan\pm^{nan}_{nan}$	0.65
tons180	0.02340 (#68)	36.68(34)	76753	2	$1801\pm^{112}_{107}$	1	22.1054	$-0.76\pm^{1.51}_{0.85}$	$nan\pm^{nan}_{nan}$	0.38
tons180	0.04360 (#69)	28.48(39)	76753	2	$1826\pm^{117}_{112}$	1	22.5418	$-0.90\pm^{1.15}_{0.75}$	$nan\pm^{nan}_{nan}$	0.77
tons180	0.04560 (#70)	25.72(39)	76753	3	$1796\pm^{118}_{113}$	1	22.5850	$-1.39\pm^{0.95}_{0.71}$	$nan\pm^{nan}_{nan}$	2.08

3c273	0.00337 (#71)	–	–	–	–	–	21.6728	–	–	–
3c273	0.00533 (#72)	34.47(31)	69608	8	$5635\pm^{153}_{150}$	1	21.7151	$-0.95\pm^{0.54}_{0.44}$	$nan\pm^{nan}_{nan}$	2.87
3c273	0.00764 (#73)	31.25(31)	69608	8	$5772\pm^{159}_{155}$	1	21.7650	$0.02\pm^{0.83}_{0.61}$	$13.86\pm^{1.56}_{nan}$	0.00
3c273	0.02947 (#74)	32.45(39)	69608	8	$5842\pm^{144}_{141}$	1	22.2366	$0.77\pm^{1.10}_{0.78}$	$15.38\pm^{0.29}_{nan}$	1.06
3c273	0.04898 (#75)	44.84(39)	69608	8	$6048\pm^{150}_{147}$	1	22.6580	$-0.66\pm^{0.56}_{0.43}$	$nan\pm^{nan}_{nan}$	1.48
3c273	0.06655 (#76)	50.06(39)	69608	9	$6143\pm^{154}_{152}$	1	23.0375	$-1.09\pm^{0.54}_{0.47}$	$nan\pm^{nan}_{nan}$	3.80
3c273	0.09018 (#77)	44.86(38)	69608	8	$6487\pm^{155}_{153}$	1	23.5479	$1.79\pm^{1.92}_{1.09}$	$15.65\pm^{0.17}_{0.31}$	3.91
3c273	0.12007 (#78)	35.19(38)	69608	7	$7164\pm^{163}_{163}$	1	24.1935	$0.07\pm^{0.81}_{0.59}$	$14.39\pm^{1.01}_{nan}$	0.01
3c273	0.14660 (#79)	47.68(39)	69608	7	$7544\pm^{172}_{169}$	1	24.7666	$-0.45\pm^{0.60}_{0.46}$	$nan\pm^{nan}_{nan}$	0.68
3c273	0.15784 (#80)	40.68(39)	69608	7	$7512\pm^{172}_{170}$	1	25.0093	$0.46\pm^{0.99}_{0.70}$	$15.18\pm^{0.40}_{nan}$	0.42
mrk421	0.01009 (#81)	26.88(21)	638847	1	$73974\pm^{239}_{230}$	1	21.8179	$-0.18\pm^{0.06}_{0.06}$	$nan\pm^{nan}_{nan}$	9.92
pks2155	0.05405 (#82)	20.69(25)	319334	5	$16258\pm^{147}_{139}$	1	22.7675	$0.32\pm^{0.28}_{0.21}$	$15.03\pm^{0.24}_{0.46}$	2.54
pks2155	0.05707 (#83)	17.03(22)	319334	5	$16350\pm^{156}_{151}$	1	22.8327	$0.29\pm^{0.26}_{0.22}$	$14.99\pm^{0.25}_{0.62}$	2.00

Table C.2: O VII upper limit measurements with *Chandra* data, at the prior redshift from the O VI lines from Table A.1.

Target line		cmin	RGS1	power–law		line component			ΔC
Name	z	(d.o.f.)	avg exp (s)	norm.	index	λ (Å)	τ_0	$\log N + (\mathrm{cm}^{-2})$	(d.o.f.)
1es1028	0.12314 (#1)	32.34(39)	148933	$1757\pm^{63}_{62}$	1	24.2598	0.83	15.40	0.44
1es1028	0.13706 (#2)	35.52(39)	148933	$1830\pm^{64}_{63}$	1	24.5605	2.22	15.71	0.99
1es1028	0.33735 (#3)	37.26(39)	148933	$2138\pm^{81}_{79}$	1	28.8868	0.86	15.43	0.56
1es1553	0.18759 (#4)	44.14(38)	495645	$3135\pm^{48}_{48}$	1	25.6519	0.51	15.23	0.58
1es1553	0.18775 (#5)	44.13(38)	495645	$3135\pm^{48}_{48}$	1	25.6554	0.55	15.24	0.58
1es1553	0.18984 (#6)	42.53(38)	495645	$3106\pm^{48}_{48}$	1	25.7005	0.38	15.11	1.00
1es1553	0.21631 (#7)	51.98(38)	495645	$3137\pm^{49}_{49}$	1	26.2723	0.52	15.23	0.42
1es1553	0.31130 (#8)	36.35(38)	495645	$3202\pm^{53}_{54}$	1	28.3241	0.48	15.21	0.01
1es1553	0.37868 (#9)	48.60(38)	495645	$3322\pm^{62}_{61}$	1	29.7795	0.36	15.08	2.89
1es1553	0.39497 (#10)	39.90(38)	495645	$3374\pm^{65}_{64}$	1	30.1314	0.42	15.13	1.16
h1821	0.02438 (#11)	44.15(32)	470152	$888\pm^{22}_{21}$	1	22.1266	0.66	15.32	0.32
h1821	0.10817 (#12)	50.75(39)	470152	$1103\pm^{21}_{21}$	1	23.9365	0.33	15.05	8.78
h1821	0.12133 (#13)	46.33(38)	470152	$1202\pm^{22}_{22}$	1	24.2207	0.53	15.23	0.22
h1821	0.12147 (#14)	46.13(38)	470152	$1203\pm^{22}_{22}$	1	24.2238	0.53	15.24	0.44
h1821	0.16992 (#15)	37.35(38)	470152	$1107\pm^{23}_{23}$	1	25.2703	0.51	15.21	0.02
h1821	0.17043 (#16)	37.01(38)	470152	$1104\pm^{23}_{23}$	1	25.2813	0.45	15.16	0.39
h1821	0.21326 (#17)	33.42(38)	470152	$1090\pm^{25}_{25}$	1	26.2064	0.36	15.08	3.65
h1821	0.22497 (#18)	31.24(39)	470152	$1097\pm^{26}_{25}$	1	26.4594	0.74	15.36	0.74
h1821	0.22522 (#19)	31.59(39)	470152	$1095\pm^{26}_{25}$	1	26.4648	0.69	15.34	0.37
h1821	0.22639 (#20)	32.44(39)	470152	$1098\pm^{26}_{25}$	1	26.4900	0.65	15.32	0.23
h1821	0.24531 (#21)	28.82(38)	470152	$1103\pm^{27}_{27}$	1	26.8987	0.97	15.47	2.16
h1821	0.26657 (#22)	39.22(39)	470152	$1157\pm^{29}_{29}$	1	27.3579	0.57	15.26	0.09
h1821	0.28800 (#23)	48.59(33)	470152	$1265\pm^{37}_{37}$	1	27.8208	0.47	15.18	2.16
h1821	0.29658 (#24)	45.10(33)	470152	$1326\pm^{41}_{40}$	1	28.0061	0.60	15.27	3.22
h1821	0.29680 (#25)	45.72(34)	470152	$1338\pm^{42}_{41}$	1	28.0109	0.80	15.40	2.92

h2356	0.11461 (#26)	26.64(38)	586697	$2314\pm^{37}_{37}$	1	24.0756	0.76	15.38	4.89
h2356	0.16512 (#27)	34.18(39)	586697	$2408\pm^{39}_{39}$	1	25.1666	0.87	15.40	3.76
mr2251	0.01070 (#28)	33.00(30)	78434	$3031\pm^{114}_{110}$	1	21.8311	1.07	15.46	0.00
pg1116	0.05900 (#29)	33.16(38)	355485	$756\pm^{36}_{36}$	1	22.8744	0.73	15.37	3.69
pg1116	0.05927 (#30)	32.42(38)	355485	$755\pm^{36}_{35}$	1	22.8802	0.54	15.23	4.50
pg1116	0.11895 (#31)	40.85(38)	355485	$878\pm^{38}_{37}$	1	24.1693	3.39E+03	16.12	4.27
pg1116	0.13852 (#32)	41.11(33)	355485	$886\pm^{42}_{41}$	1	24.5920	0.47	15.18	6.79
pg1116	0.16539 (#33)	28.52(32)	355485	$949\pm^{44}_{43}$	1	25.1724	1.65	15.62	0.06
pg1116	0.16554 (#34)	28.43(32)	355485	$952\pm^{44}_{43}$	1	25.1757	1.63	15.64	0.16
pg1116	0.16610 (#35)	30.58(33)	355485	$948\pm^{44}_{43}$	1	25.1878	2.12	15.71	0.51
pg1116	0.16686 (#36)	30.77(32)	355485	$944\pm^{44}_{43}$	1	25.2042	3.44	15.77	0.64
pg1116	0.17343 (#37)	30.83(36)	355485	$941\pm^{41}_{41}$	1	25.3461	0.91	15.42	0.50
pg1211	0.00711 (#38)	28.35(30)	133595	$1244\pm^{60}_{58}$	1	21.7536	1.27	15.53	0.07
pg1211	0.05117 (#39)	48.13(38)	133595	$1465\pm^{67}_{65}$	1	22.7053	2.38	15.68	0.50
pg1211	0.06449 (#40)	49.38(39)	133595	$1592\pm^{67}_{65}$	1	22.9930	1.27	15.52	0.03
pg1211	0.06491 (#41)	51.45(38)	133595	$1586\pm^{67}_{65}$	1	23.0021	1.33	15.56	0.00
pks0405	0.09192 (#42)	36.05(39)	376096	$494\pm^{35}_{35}$	1	23.5855	3.89	15.83	0.06
pks0405	0.09647 (#43)	44.38(39)	376096	$538\pm^{35}_{35}$	1	23.6838	2.09E+06	16.28	3.85
pks0405	0.14808 (#44)	51.46(38)	376096	$537\pm^{38}_{37}$	1	24.7985	1.24	15.55	0.86
pks0405	0.16566 (#45)	45.81(38)	376096	$569\pm^{40}_{37}$	1	25.1783	5.00E+19	16.48	7.23
pks0405	0.16606 (#46)	53.91(39)	376096	$577\pm^{38}_{37}$	1	25.1869	5.00E+19	16.42	6.26
pks0405	0.16659 (#47)	47.68(38)	376096	$566\pm^{39}_{38}$	1	25.1983	5.00E+19	16.42	5.02
pks0405	0.16688 (#48)	47.52(38)	376096	$569\pm^{39}_{38}$	1	25.2046	5.00E+19	16.48	5.35
pks0405	0.16712 (#49)	49.50(39)	376096	$549\pm^{38}_{38}$	1	25.2098	5.00E+19	16.48	4.34
pks0405	0.18257 (#50)	42.98(38)	376096	$543\pm^{38}_{38}$	1	25.5435	6.03E+03	16.12	0.95
pks0405	0.18289 (#51)	42.87(38)	376096	$545\pm^{39}_{38}$	1	25.5504	260.74	16.06	1.09
pks0405	0.24052 (#52)	44.44(38)	376096	$610\pm^{42}_{41}$	1	26.7952	1.43	15.56	0.36
pks0405	0.24094 (#53)	44.76(38)	376096	$618\pm^{40}_{41}$	1	26.8043	3.01	15.74	-0.00
pks0405	0.24547 (#54)	44.46(38)	376096	$595\pm^{42}_{41}$	1	26.9022	1.22	15.54	0.81

pks0405	0.29762 (#55)	35.29(38)	376096	$613\pm^{44}_{44}$	1	28.0286	1.62	15.60	0.26
pks0405	0.34188 (#56)	38.18(39)	376096	$566\pm^{48}_{46}$	1	28.9846	2.02E+06	16.26	2.12
pks0405	0.34225 (#57)	38.30(39)	376096	$567\pm^{47}_{46}$	1	28.9926	1.89E+05	16.26	2.00
pks0405	0.35092 (#58)	32.95(38)	376096	$622\pm^{48}_{48}$	1	29.1799	2.21E+06	16.33	2.62
pks0405	0.36075 (#59)	38.91(39)	376096	$537\pm^{49}_{48}$	1	29.3922	1.82	15.62	0.34
pks0405	0.36151 (#60)	37.68(39)	376096	$542\pm^{49}_{48}$	1	29.4086	2.19	15.67	0.21
pks0405	0.36329 (#61)	33.65(38)	376096	$517\pm^{49}_{48}$	1	29.4471	0.91	15.43	2.88
pks0405	0.40570 (#62)	52.38(39)	376096	$564\pm^{55}_{54}$	1	30.3631	1.15E+03	16.19	0.26
pks0405	0.40890 (#63)	47.45(39)	376096	$529\pm^{56}_{54}$	1	30.4322	29.84	16.06	-0.00
pks0405	0.49505 (#64)	37.44(39)	376096	$501\pm^{56}_{55}$	1	32.2931	1.07	15.46	1.61
pks0405	0.49530 (#65)	37.74(38)	376096	$490\pm^{56}_{55}$	1	32.2985	1.37	15.58	1.56
pks0405	0.55506 (#66)	35.55(39)	376096	$662\pm^{62}_{60}$	1	33.5893	5.00E+19	16.42	3.09
pks2005	0.06490 (#67)	35.79(38)	282191	$1954\pm^{63}_{62}$	1	23.0018	0.78	15.39	0.65
tons180	0.02340 (#68)	36.68(34)	76753	$1801\pm^{112}_{107}$	1	22.1054	1.18	15.49	0.38
tons180	0.04360 (#69)	28.48(39)	76753	$1826\pm^{117}_{112}$	1	22.5418	0.95	15.43	0.77
tons180	0.04560 (#70)	25.72(39)	76753	$1796\pm^{118}_{113}$	1	22.5850	0.83	15.40	2.08
3c273	0.00337 (#71)	–	–	–	–	21.6728	–	–	–
3c273	0.00533 (#72)	34.47(31)	69608	$5635\pm^{153}_{150}$	1	21.7151	0.49	15.21	2.87
3c273	0.00764 (#73)	31.25(31)	69608	$5772\pm^{159}_{155}$	1	21.7650	0.72	15.35	0.00
3c273	0.02947 (#74)	32.45(39)	69608	$5842\pm^{144}_{141}$	1	22.2366	0.94	15.46	1.06
3c273	0.04898 (#75)	44.84(39)	69608	$6048\pm^{150}_{147}$	1	22.6580	0.50	15.20	1.48
3c273	0.06655 (#76)	50.06(39)	69608	$6143\pm^{154}_{152}$	1	23.0375	0.51	15.23	3.80
3c273	0.09018 (#77)	44.86(38)	69608	$6487\pm^{155}_{153}$	1	23.5479	1.51	15.60	3.91
3c273	0.12007 (#78)	35.19(38)	69608	$7164\pm^{163}_{163}$	1	24.1935	0.70	15.32	0.01
3c273	0.14660 (#79)	47.68(39)	69608	$7544\pm^{172}_{169}$	1	24.7666	0.53	15.23	0.68
3c273	0.15784 (#80)	40.68(39)	69608	$7512\pm^{172}_{170}$	1	25.0093	0.84	15.40	0.42
mrk421	0.01009 (#81)	26.88(21)	638847	$73974\pm^{239}_{230}$	1	21.8179	0.06	14.34	9.92
pks2155	0.05405 (#82)	20.69(25)	319334	$16258\pm^{147}_{139}$	1	22.7675	0.25	14.93	2.54
pks2155	0.05707 (#83)	17.03(22)	319334	$16350\pm^{156}_{151}$	1	22.8327	0.24	14.92	2.00

Table C.3: O VII measurements with *Chandra* data, at the prior redshift from the H I lines from Table A.2.

Target line		cmin	RGS1		power–law		line component			ΔC
Name	z	(d.o.f.)	avg exp (s)	% $\frac{B}{D+B}$	norm.	index	λ (Å)	τ_0	log N(cm^{-2})	(d.o.f.)
1es1028	0.13714 (#1)	35.38(39)	148933	24	$1831\pm^{64}_{63}$	1	24.5622	$1.34\pm^{2.73}_{1.32}$	$15.58\pm^{0.28}_{1.74}$	1.14
1es1028	0.20383 (#2)	38.65(38)	148933	24	$1963\pm^{69}_{68}$	1	26.0027	$1.18\pm^{2.92}_{1.29}$	$15.52\pm^{0.31}_{nan}$	0.87
1es1028	0.22121 (#3)	35.87(38)	148933	23	$2058\pm^{71}_{70}$	1	26.3781	$0.80\pm^{2.27}_{1.13}$	$15.39\pm^{0.38}_{nan}$	0.48
1es1553	0.03466 (#4)	38.20(38)	495645	25	$2408\pm^{40}_{39}$	1	22.3487	$-0.03\pm^{0.50}_{0.43}$	$nan\pm^{nan}_{nan}$	0.00
1es1553	0.04273 (#5)	54.53(38)	495645	25	$2461\pm^{41}_{41}$	1	22.5230	$0.31\pm^{0.61}_{0.49}$	$15.03\pm^{0.41}_{nan}$	0.42
1es1553	0.06364 (#6)	48.63(38)	495645	24	$2557\pm^{43}_{42}$	1	22.9746	$-1.05\pm^{0.36}_{0.32}$	$nan\pm^{nan}_{nan}$	7.56
1es1553	0.21869 (#7)	44.59(38)	495645	23	$3121\pm^{49}_{48}$	1	26.3237	$-0.47\pm^{0.39}_{0.35}$	$nan\pm^{nan}_{nan}$	1.52
3c273	0.00758 (#8)	31.25(31)	69608	8	$5771\pm^{159}_{155}$	1	21.7637	$0.01\pm^{0.82}_{0.62}$	$13.58\pm^{1.83}_{nan}$	0.00
3c273	0.06707 (#9)	47.38(38)	69608	9	$6182\pm^{155}_{152}$	1	23.0487	$-0.98\pm^{0.55}_{0.47}$	$nan\pm^{nan}_{nan}$	3.03
3c273	0.07359 (#10)	46.82(39)	69608	8	$6324\pm^{156}_{154}$	1	23.1895	$2.44\pm^{3.08}_{1.40}$	$15.74\pm^{0.15}_{0.25}$	5.26
3c273	0.13960 (#11)	35.63(39)	69608	7	$7537\pm^{171}_{168}$	1	24.6154	$0.62\pm^{1.06}_{0.73}$	$15.29\pm^{0.33}_{nan}$	0.77
h1821	0.00944 (#12)	21.13(18)	470152	2	$900\pm^{29}_{28}$	1	21.8039	$-0.36\pm^{0.52}_{0.42}$	$nan\pm^{nan}_{nan}$	0.63
h1821	0.06779 (#13)	35.37(36)	470152	2	$970\pm^{23}_{22}$	1	23.0643	$-0.12\pm^{0.68}_{0.56}$	$nan\pm^{nan}_{nan}$	0.04
h1821	0.08483 (#14)	41.18(32)	470152	2	$1048\pm^{24}_{23}$	1	23.4323	$-0.01\pm^{0.53}_{0.42}$	$nan\pm^{nan}_{nan}$	0.00
h1821	0.12147 (#15)	46.13(38)	470152	1	$1203\pm^{22}_{22}$	1	24.2238	$0.32\pm^{0.57}_{0.49}$	$15.04\pm^{0.39}_{nan}$	0.44
h1821	0.19817 (#16)	30.74(38)	470152	2	$1134\pm^{25}_{25}$	1	25.8805	$2.58\pm^{2.94}_{1.42}$	$15.70\pm^{0.13}_{0.21}$	6.87
h1821	0.21321 (#17)	33.49(38)	470152	2	$1090\pm^{25}_{25}$	1	26.2053	$-0.81\pm^{0.40}_{0.34}$	$nan\pm^{nan}_{nan}$	3.57
h1821	0.24531 (#18)	28.82(38)	470152	2	$1103\pm^{27}_{27}$	1	26.8987	$1.09\pm^{1.14}_{0.81}$	$15.51\pm^{0.22}_{0.52}$	2.16
h2356	0.03830 (#19)	36.54(38)	586697	29	$2132\pm^{35}_{35}$	1	22.4273	$-0.09\pm^{0.48}_{0.42}$	$nan\pm^{nan}_{nan}$	0.06
h2356	0.07881 (#20)	54.01(38)	586697	30	$2125\pm^{35}_{35}$	1	23.3023	$-0.02\pm^{0.44}_{0.48}$	$nan\pm^{nan}_{nan}$	0.01
h2356	0.10467 (#21)	36.31(39)	586697	29	$2213\pm^{37}_{36}$	1	23.8609	$-0.54\pm^{0.41}_{0.35}$	$nan\pm^{nan}_{nan}$	1.85
h2356	0.15613 (#22)	33.28(38)	586697	29	$2378\pm^{39}_{39}$	1	24.9724	$-0.08\pm^{0.50}_{0.41}$	$nan\pm^{nan}_{nan}$	0.03
mr2251	0.01068 (#23)	33.00(30)	78434	15	$3031\pm^{114}_{110}$	1	21.8307	$0.05\pm^{1.37}_{0.78}$	$14.25\pm^{1.29}_{nan}$	0.00
mr2251	0.01449 (#24)	29.99(31)	78434	15	$3080\pm^{115}_{112}$	1	21.9130	$-0.44\pm^{0.93}_{0.71}$	$nan\pm^{nan}_{nan}$	0.30
mr2251	0.06131 (#25)	45.89(38)	78434	16	$3079\pm^{107}_{105}$	1	22.9243	$-0.40\pm^{1.04}_{0.77}$	$nan\pm^{nan}_{nan}$	0.20
mr2251	0.06190 (#26)	47.80(39)	78434	16	$3092\pm^{108}_{106}$	1	22.9370	$0.36\pm^{1.54}_{1.00}$	$15.09\pm^{0.59}_{nan}$	0.11
mr2251	0.06276 (#27)	43.10(38)	78434	17	$3142\pm^{109}_{106}$	1	22.9556	$4.57\pm^{12.54}_{3.52}$	$15.80\pm^{0.19}_{0.34}$	3.42
mr2251	0.06327 (#28)	50.52(39)	78434	16	$3223\pm^{118}_{110}$	1	22.9666	$14.07\pm^{1.71E+03}_{11.29}$	$15.96\pm^{0.16}_{0.23}$	6.82
mr2251	0.06381 (#29)	48.05(38)	78434	16	$3234\pm^{109}_{107}$	1	22.9783	$16.70\pm^{89.76}_{13.12}$	$15.97\pm^{0.11}_{0.18}$	7.99
mrk478	0.06166 (#30)	28.21(39)	80466	23	$1423\pm^{75}_{73}$	1	22.9319	$-1.81\pm^{0.63}_{0.48}$	$nan\pm^{nan}_{nan}$	5.15
mrk478	0.06578 (#31)	39.37(38)	80466	23	$1469\pm^{76}_{74}$	1	23.0208	$-1.02\pm^{1.08}_{0.70}$	$nan\pm^{nan}_{nan}$	1.01
mrk478	0.07213 (#32)	37.11(39)	80466	22	$1556\pm^{77}_{75}$	1	23.1580	$11.51\pm^{56.54}_{9.70}$	$15.94\pm^{0.15}_{0.32}$	3.39
pg1116	0.04114 (#33)	35.29(39)	355485	53	$772\pm^{36}_{35}$	1	22.4886	$-0.16\pm^{1.61}_{0.98}$	$nan\pm^{nan}_{nan}$	0.02

pg1116	0.06251 (#34)	38.29(38)	355485	54	$760\pm^{36}_{36}$	1	22.9502	$-0.65\pm^{1.45}_{0.94}$	$nan\pm^{nan}_{nan}$	0.30
pg1116	0.08382 (#35)	35.87(39)	355485	54	$756\pm^{36}_{35}$	1	23.4105	$1.23\pm^{4.23}_{1.53}$	$15.54\pm^{0.34}_{nan}$	0.61
pg1116	0.09210 (#36)	43.67(38)	355485	54	$772\pm^{36}_{36}$	1	23.5894	$3.27\pm^{159.72}_{2.74}$	$15.80\pm^{0.26}_{0.57}$	2.02
pg1116	0.09281 (#37)	35.22(37)	355485	54	$759\pm^{37}_{36}$	1	23.6047	$4.29\pm^{26.23}_{3.78}$	$15.80\pm^{0.24}_{0.59}$	1.92
pg1116	0.13373 (#38)	41.71(34)	355485	49	$1001\pm^{43}_{41}$	1	24.4886	$20.93\pm^{519.78}_{18.48}$	$15.96\pm^{0.17}_{0.21}$	6.99
pg1116	0.13851 (#39)	47.35(34)	355485	49	$947\pm^{42}_{41}$	1	24.5918	$-1.45\pm^{0.60}_{0.46}$	$nan\pm^{nan}_{nan}$	4.33
pg1211	0.02586 (#40)	27.92(37)	133595	1	$1286\pm^{58}_{56}$	1	22.1586	$-1.38\pm^{0.66}_{0.51}$	$nan\pm^{nan}_{nan}$	3.58
pg1211	0.05443 (#41)	46.97(38)	133595	1	$1522\pm^{67}_{66}$	1	22.7757	$2.08\pm^{7.09}_{1.80}$	$15.71\pm^{0.23}_{0.72}$	1.60
pks0405	0.02510 (#42)	29.08(36)	376096	68	$481\pm^{35}_{34}$	1	22.1422	$-0.35\pm^{3.48}_{1.14}$	$nan\pm^{nan}_{nan}$	0.04
pks0405	0.05902 (#43)	38.62(38)	376096	68	$512\pm^{36}_{35}$	1	22.8748	$-1.07\pm^{1.88}_{1.11}$	$nan\pm^{nan}_{nan}$	0.47
pks0405	0.09719 (#44)	40.81(38)	376096	67	$550\pm^{36}_{36}$	1	23.6993	$3.12E+03\pm^{2.80E+08}_{3.10E+03}$	$16.23\pm^{0.09}_{0.28}$	6.32
pks0405	0.10152 (#45)	37.76(39)	376096	68	$505\pm^{36}_{35}$	1	23.7928	$-1.12\pm^{1.48}_{0.79}$	$nan\pm^{nan}_{nan}$	0.76
pks0405	0.10298 (#46)	38.10(38)	376096	68	$505\pm^{36}_{35}$	1	23.8244	$-1.31\pm^{1.57}_{0.99}$	$nan\pm^{nan}_{nan}$	0.84
pks0405	0.19456 (#47)	25.03(38)	376096	69	$528\pm^{39}_{38}$	1	25.8025	$-1.54\pm^{1.28}_{0.82}$	$nan\pm^{nan}_{nan}$	1.43
pks0405	0.21976 (#48)	38.16(38)	376096	70	$555\pm^{41}_{40}$	1	26.3468	$0.83\pm^{29.27}_{1.99}$	$15.39\pm^{0.61}_{nan}$	0.10
pks0405	0.24564 (#49)	44.65(38)	376096	68	$596\pm^{42}_{41}$	1	26.9058	$-1.04\pm^{1.62}_{0.81}$	$nan\pm^{nan}_{nan}$	0.61
pks0405	0.29748 (#50)	35.20(38)	376096	69	$612\pm^{45}_{44}$	1	28.0256	$-0.97\pm^{2.04}_{1.15}$	$nan\pm^{nan}_{nan}$	0.36
pks0405	0.31016 (#51)	42.41(38)	376096	72	$565\pm^{45}_{44}$	1	28.2995	$1.34\pm^{340.45}_{2.33}$	$15.58\pm^{0.50}_{nan}$	0.24
pks0405	0.32502 (#52)	32.33(38)	376096	74	$548\pm^{50}_{44}$	1	28.6204	$237.19\pm^{4.49E+10}_{217.51}$	$16.12\pm^{0.23}_{0.11}$	3.20
pks0405	0.49508 (#53)	37.52(38)	376096	78	$489\pm^{56}_{55}$	1	32.2937	$-1.99\pm^{1.32}_{0.74}$	$nan\pm^{nan}_{nan}$	1.80
pks2155	0.05708 (#54)	13.67(23)	319334	4	$16704\pm^{152}_{151}$	1	22.8329	$0.50\pm^{0.28}_{0.25}$	$15.20\pm^{0.16}_{0.27}$	5.40
pks2155	0.06236 (#55)	30.32(25)	319334	5	$16439\pm^{143}_{142}$	1	22.9470	$-0.38\pm^{0.19}_{0.17}$	$nan\pm^{nan}_{nan}$	4.35
pks2155	0.10586 (#56)	38.15(34)	319334	4	$18205\pm^{129}_{129}$	1	23.8866	$-0.12\pm^{0.19}_{0.18}$	$nan\pm^{nan}_{nan}$	0.52
tons180	0.04304 (#57)	28.54(38)	76753	2	$1841\pm^{117}_{112}$	1	22.5297	$-0.54\pm^{1.43}_{0.84}$	$nan\pm^{nan}_{nan}$	0.24

Table C.4: O VII upper limit measurements with *Chandra* data, at the prior redshift from the H I lines from Table A.2.

Target line		cmin	RGS1	power–law		line component			ΔC
Name	z	(d.o.f.)	avg exp (s)	norm.	index	λ (Å)	τ_0	$\log N + (\mathrm{cm}^{-2})$	(d.o.f.)
1es1028	0.13714 (#1)	35.38(39)	148933	$1831\pm^{64}_{63}$	1	24.5622	2.02	15.70	1.14
1es1028	0.20383 (#2)	38.65(38)	148933	$1963\pm^{69}_{68}$	1	26.0027	2.11	15.69	0.87
1es1028	0.22121 (#3)	35.87(38)	148933	$2058\pm^{71}_{70}$	1	26.3781	1.70	15.62	0.48
1es1553	0.03466 (#4)	38.20(38)	495645	$2408\pm^{40}_{39}$	1	22.3487	0.47	15.19	0.00
1es1553	0.04273 (#5)	54.53(38)	495645	$2461\pm^{41}_{41}$	1	22.5230	0.55	15.25	0.42
1es1553	0.06364 (#6)	48.63(38)	495645	$2557\pm^{43}_{42}$	1	22.9746	0.34	15.07	7.56
1es1553	0.21869 (#7)	44.59(38)	495645	$3121\pm^{49}_{48}$	1	26.3237	0.37	15.10	1.52
3c273	0.00758 (#8)	31.25(31)	69608	$5771\pm^{159}_{155}$	1	21.7637	0.72	15.36	0.00
3c273	0.06707 (#9)	47.38(38)	69608	$6182\pm^{155}_{152}$	1	23.0487	0.51	15.23	3.03
3c273	0.07359 (#10)	46.82(39)	69608	$6324\pm^{156}_{154}$	1	23.1895	2.24	15.72	5.26
3c273	0.13960 (#11)	35.63(39)	69608	$7537\pm^{171}_{168}$	1	24.6154	0.89	15.43	0.77
h1821	0.00944 (#12)	21.13(18)	470152	$900\pm^{29}_{28}$	1	21.8039	0.47	15.18	0.63
h1821	0.06779 (#13)	35.37(36)	470152	$970\pm^{23}_{22}$	1	23.0643	0.62	15.30	0.04
h1821	0.08483 (#14)	41.18(32)	470152	$1048\pm^{24}_{23}$	1	23.4323	0.48	15.18	0.00
h1821	0.12147 (#15)	46.13(38)	470152	$1203\pm^{22}_{22}$	1	24.2238	0.53	15.24	0.44
h1821	0.19817 (#16)	30.74(38)	470152	$1134\pm^{25}_{25}$	1	25.8805	2.18	15.66	6.87
h1821	0.21321 (#17)	33.49(38)	470152	$1090\pm^{25}_{25}$	1	26.2053	0.37	15.09	3.57
h1821	0.24531 (#18)	28.82(38)	470152	$1103\pm^{27}_{27}$	1	26.8987	0.97	15.47	2.16
h2356	0.03830 (#19)	36.54(38)	586697	$2132\pm^{35}_{35}$	1	22.4273	0.45	15.18	0.06
h2356	0.07881 (#20)	54.01(38)	586697	$2125\pm^{35}_{35}$	1	23.3023	0.46	15.19	0.01
h2356	0.10467 (#21)	36.31(39)	586697	$2213\pm^{37}_{36}$	1	23.8609	0.38	15.11	1.85
h2356	0.15613 (#22)	33.28(38)	586697	$2378\pm^{39}_{39}$	1	24.9724	0.45	15.18	0.03
mr2251	0.01068 (#23)	33.00(30)	78434	$3031\pm^{114}_{110}$	1	21.8307	1.08	15.47	0.00
mr2251	0.01449 (#24)	29.99(31)	78434	$3080\pm^{115}_{112}$	1	21.9130	0.82	15.41	0.30
mr2251	0.06131 (#25)	45.89(38)	78434	$3079\pm^{107}_{105}$	1	22.9243	0.90	15.44	0.20

mr2251	0.06190 (#26)	47.80(39)	78434	$3092\pm^{108}_{106}$	1	22.9370	1.27	15.56	0.11
mr2251	0.06276 (#27)	43.10(38)	78434	$3142\pm^{109}_{106}$	1	22.9556	8.03	15.89	3.42
mr2251	0.06327 (#28)	50.52(39)	78434	$3223\pm^{118}_{110}$	1	22.9666	861.22	16.12	6.82
mr2251	0.06381 (#29)	48.05(38)	78434	$3234\pm^{109}_{107}$	1	22.9783	51.44	16.03	7.99
mrk478	0.06166 (#30)	28.21(39)	80466	$1423\pm^{75}_{73}$	1	22.9319	0.55	15.24	5.15
mrk478	0.06578 (#31)	39.37(38)	80466	$1469\pm^{76}_{74}$	1	23.0208	0.89	15.41	1.01
mrk478	0.07213 (#32)	37.11(39)	80466	$1556\pm^{77}_{75}$	1	23.1580	33.12	16.05	3.39
pg1116	0.04114 (#33)	35.29(39)	355485	$772\pm^{36}_{35}$	1	22.4886	1.30	15.57	0.02
pg1116	0.06251 (#34)	38.29(38)	355485	$760\pm^{36}_{36}$	1	22.9502	1.20	15.54	0.30
pg1116	0.08382 (#35)	35.87(39)	355485	$756\pm^{36}_{35}$	1	23.4105	2.88	15.77	0.61
pg1116	0.09210 (#36)	43.67(38)	355485	$772\pm^{36}_{36}$	1	23.5894	81.23	16.01	2.02
pg1116	0.09281 (#37)	35.22(37)	355485	$759\pm^{37}_{36}$	1	23.6047	15.00	15.97	1.92
pg1116	0.13373 (#38)	41.71(34)	355485	$1001\pm^{43}_{41}$	1	24.4886	269.13	16.07	6.99
pg1116	0.13851 (#39)	47.35(34)	355485	$947\pm^{42}_{41}$	1	24.5918	0.53	15.23	4.33
pg1211	0.02586 (#40)	27.92(37)	133595	$1286\pm^{58}_{56}$	1	22.1586	0.59	15.27	3.58
pg1211	0.05443 (#41)	46.97(38)	133595	$1522\pm^{67}_{66}$	1	22.7757	4.45	15.87	1.60
pks0405	0.02510 (#42)	29.08(36)	376096	$481\pm^{35}_{34}$	1	22.1422	2.31	15.68	0.04
pks0405	0.05902 (#43)	38.62(38)	376096	$512\pm^{36}_{35}$	1	22.8748	1.49	15.61	0.47
pks0405	0.09719 (#44)	40.81(38)	376096	$550\pm^{36}_{36}$	1	23.6993	1.40E+08	16.30	6.32
pks0405	0.10152 (#45)	37.76(39)	376096	$505\pm^{36}_{35}$	1	23.7928	1.14	15.48	0.76
pks0405	0.10298 (#46)	38.10(38)	376096	$505\pm^{36}_{35}$	1	23.8244	1.28	15.56	0.84
pks0405	0.19456 (#47)	25.03(38)	376096	$528\pm^{39}_{38}$	1	25.8025	1.05	15.48	1.43
pks0405	0.21976 (#48)	38.16(38)	376096	$555\pm^{41}_{40}$	1	26.3468	15.63	15.97	0.10
pks0405	0.24564 (#49)	44.65(38)	376096	$596\pm^{42}_{41}$	1	26.9058	1.22	15.50	0.61
pks0405	0.29748 (#50)	35.20(38)	376096	$612\pm^{45}_{44}$	1	28.0256	1.59	15.63	0.36
pks0405	0.31016 (#51)	42.41(38)	376096	$565\pm^{45}_{44}$	1	28.2995	171.39	16.03	0.24
pks0405	0.32502 (#52)	32.33(38)	376096	$548\pm^{50}_{44}$	1	28.6204	2.24E+10	16.34	3.20
pks0405	0.49508 (#53)	37.52(38)	376096	$489\pm^{56}_{55}$	1	32.2937	1.03	15.45	1.80
pks2155	0.05708 (#54)	13.67(23)	319334	$16704\pm^{152}_{151}$	1	22.8329	0.26	14.96	5.40

pks2155	0.06236 (#55)	30.32(25)	319334	$16439\pm^{143}_{142}$	1	22.9470	0.18	14.80	4.35
pks2155	0.10586 (#56)	38.15(34)	319334	$18205\pm^{129}_{129}$	1	23.8866	0.18	14.81	0.52
tons180	0.04304 (#57)	28.54(38)	76753	$1841\pm^{117}_{112}$	1	22.5297	1.14	15.49	0.24

Table C.5: O VIII measurements with *Chandra* data, at the prior redshift from the O VI lines from Table A.1.

Target line		cmin	RGS1		power–law		line component			ΔC
Name	z	(d.o.f.)	avg exp (s)	% $\frac{B}{D+B}$	norm.	index	λ (Å)	τ_0	$\log N(\mathrm{cm}^{-2})$	(d.o.f.)
1es1028	0.12314 (#1)	35.82(30)	148933	23	$1585\pm^{62}_{61}$	1	21.2947	$-0.79\pm^{0.77}_{0.55}$	$nan\pm^{nan}_{nan}$	1.19
1es1028	0.13706 (#2)	–	–	–	–	–	21.5587	–	–	–
1es1028	0.33735 (#3)	34.59(38)	148933	24	$1851\pm^{66}_{65}$	1	25.3562	$-0.24\pm^{1.24}_{0.72}$	$nan\pm^{nan}_{nan}$	0.07
1es1553	0.18759 (#4)	43.76(33)	495645	25	$2462\pm^{44}_{44}$	1	22.5167	$0.23\pm^{0.63}_{0.47}$	$15.23\pm^{0.50}_{nan}$	0.23
1es1553	0.18775 (#5)	43.78(32)	495645	25	$2464\pm^{44}_{44}$	1	22.5197	$0.24\pm^{0.63}_{0.48}$	$15.25\pm^{0.48}_{nan}$	0.23
1es1553	0.18984 (#6)	40.55(33)	495645	25	$2490\pm^{43}_{43}$	1	22.5594	$0.20\pm^{1.23}_{0.76}$	$15.18\pm^{0.73}_{nan}$	0.06
1es1553	0.21631 (#7)	30.16(26)	495645	24	$2584\pm^{53}_{52}$	1	23.0612	$-0.45\pm^{0.44}_{0.38}$	$nan\pm^{nan}_{nan}$	1.20
1es1553	0.31130 (#8)	50.56(39)	495645	22	$2998\pm^{46}_{44}$	1	24.8622	$-0.05\pm^{0.58}_{0.33}$	$nan\pm^{nan}_{nan}$	-0.03
1es1553	0.37868 (#9)	48.06(39)	495645	23	$3124\pm^{49}_{48}$	1	26.1398	$-0.37\pm^{0.41}_{0.35}$	$nan\pm^{nan}_{nan}$	0.89
1es1553	0.39497 (#10)	41.84(38)	495645	23	$3095\pm^{49}_{49}$	1	26.4486	$-0.63\pm^{0.38}_{0.33}$	$nan\pm^{nan}_{nan}$	2.79
h1821	0.02438 (#11)	37.76(38)	470152	2	$858\pm^{15}_{14}$	1	19.4222	$0.63\pm^{0.63}_{0.50}$	$15.63\pm^{0.24}_{0.63}$	1.80
h1821	0.10817 (#12)	44.34(38)	470152	2	$854\pm^{17}_{17}$	1	21.0109	$-0.90\pm^{0.39}_{0.34}$	$nan\pm^{nan}_{nan}$	4.97
h1821	0.12133 (#13)	42.59(31)	470152	2	$879\pm^{20}_{20}$	1	21.2604	$-0.16\pm^{0.53}_{0.45}$	$nan\pm^{nan}_{nan}$	0.12
h1821	0.12147 (#14)	42.69(31)	470152	2	$880\pm^{20}_{20}$	1	21.2631	$-0.03\pm^{0.54}_{0.47}$	$nan\pm^{nan}_{nan}$	0.00
h1821	0.16992 (#15)	54.02(38)	470152	2	$895\pm^{20}_{20}$	1	22.1817	$0.27\pm^{0.78}_{0.56}$	$15.29\pm^{0.50}_{nan}$	0.20
h1821	0.17043 (#16)	53.61(38)	470152	2	$897\pm^{20}_{20}$	1	22.1914	$0.48\pm^{0.83}_{0.61}$	$15.53\pm^{0.34}_{nan}$	0.64
h1821	0.21326 (#17)	33.98(34)	470152	2	$944\pm^{23}_{23}$	1	23.0034	$-0.56\pm^{0.58}_{0.47}$	$nan\pm^{nan}_{nan}$	0.99
h1821	0.22497 (#18)	38.17(32)	470152	2	$997\pm^{24}_{24}$	1	23.2254	$-0.67\pm^{0.43}_{0.38}$	$nan\pm^{nan}_{nan}$	2.59
h1821	0.22522 (#19)	38.06(32)	470152	2	$997\pm^{24}_{24}$	1	23.2302	$-0.63\pm^{0.38}_{0.32}$	$nan\pm^{nan}_{nan}$	2.71
h1821	0.22639 (#20)	38.11(32)	470152	2	$1000\pm^{24}_{24}$	1	23.2524	$-0.54\pm^{0.42}_{0.36}$	$nan\pm^{nan}_{nan}$	1.78
h1821	0.24531 (#21)	38.80(33)	470152	1	$1114\pm^{23}_{23}$	1	23.6111	$0.73\pm^{0.69}_{0.56}$	$15.70\pm^{0.23}_{0.58}$	2.00
h1821	0.26657 (#22)	38.28(37)	470152	1	$1161\pm^{22}_{22}$	1	24.0142	$-0.26\pm^{0.46}_{0.40}$	$nan\pm^{nan}_{nan}$	0.36
h1821	0.28800 (#23)	41.01(38)	470152	1	$1232\pm^{23}_{23}$	1	24.4205	$0.65\pm^{0.75}_{0.55}$	$15.64\pm^{0.25}_{0.76}$	1.56
h1821	0.29658 (#24)	36.87(39)	470152	1	$1194\pm^{23}_{22}$	1	24.5832	$-1.05\pm^{0.30}_{0.26}$	$nan\pm^{nan}_{nan}$	9.64
h1821	0.29680 (#25)	37.18(39)	470152	1	$1194\pm^{23}_{23}$	1	24.5873	$-1.13\pm^{0.35}_{0.32}$	$nan\pm^{nan}_{nan}$	9.31
h2356	0.11461 (#26)	31.02(33)	586697	28	$2121\pm^{36}_{35}$	1	21.1330	$0.09\pm^{0.55}_{0.42}$	$14.82\pm^{0.80}_{nan}$	0.04
h2356	0.16512 (#27)	28.36(34)	586697	29	$2145\pm^{37}_{37}$	1	22.0907	$0.16\pm^{0.58}_{0.45}$	$15.10\pm^{0.60}_{nan}$	0.13
mr2251	0.01070 (#28)	31.58(39)	78434	12	$2572\pm^{71}_{70}$	1	19.1629	$1.15\pm^{1.55}_{0.99}$	$15.86\pm^{0.25}_{0.76}$	1.61
pg1116	0.05900 (#29)	33.05(38)	355485	54	$617\pm^{29}_{28}$	1	20.0786	$0.41\pm^{3.40}_{1.22}$	$15.47\pm^{0.67}_{nan}$	0.08
pg1116	0.05927 (#30)	31.93(39)	355485	54	$629\pm^{29}_{28}$	1	20.0838	$0.46\pm^{3.09}_{1.21}$	$15.51\pm^{0.61}_{nan}$	0.11
pg1116	0.11895 (#31)	26.57(31)	355485	55	$654\pm^{34}_{35}$	1	21.2153	$0.06\pm^{2.25}_{1.09}$	$14.71\pm^{1.34}_{nan}$	0.00
pg1116	0.13852 (#32)	–	–	–	–	–	21.5863	–	–	–
pg1116	0.16539 (#33)	31.16(34)	355485	52	$773\pm^{36}_{35}$	1	22.0958	$-0.80\pm^{1.05}_{0.66}$	$nan\pm^{nan}_{nan}$	0.73

pg1116	0.16554 (#34)	31.18(34)	355485	52	$774\pm^{36}_{36}$	1	22.0986	$-0.83\pm^{1.08}_{0.77}$	$nan\pm^{nan}_{nan}$	0.72
pg1116	0.16610 (#35)	31.39(35)	355485	52	$775\pm^{36}_{35}$	1	22.1093	$-0.68\pm^{1.15}_{0.73}$	$nan\pm^{nan}_{nan}$	0.49
pg1116	0.16686 (#36)	31.82(35)	355485	52	$782\pm^{36}_{35}$	1	22.1237	$-0.09\pm^{1.64}_{1.00}$	$nan\pm^{nan}_{nan}$	0.01
pg1116	0.17343 (#37)	35.93(38)	355485	53	$762\pm^{34}_{34}$	1	22.2482	$-0.25\pm^{1.49}_{0.93}$	$nan\pm^{nan}_{nan}$	0.05
pg1211	0.00711 (#38)	42.02(38)	133595	1	$998\pm^{34}_{33}$	1	19.0948	$0.63\pm^{1.71}_{0.91}$	$15.62\pm^{0.39}_{nan}$	0.44
pg1211	0.05117 (#39)	30.00(38)	133595	1	$1107\pm^{40}_{39}$	1	19.9302	$-0.28\pm^{0.99}_{0.65}$	$nan\pm^{nan}_{nan}$	0.12
pg1211	0.06449 (#40)	33.49(39)	133595	1	$1148\pm^{42}_{41}$	1	20.1827	$-0.36\pm^{0.92}_{0.63}$	$nan\pm^{nan}_{nan}$	0.21
pg1211	0.06491 (#41)	33.15(39)	133595	1	$1145\pm^{42}_{41}$	1	20.1907	$-0.58\pm^{0.83}_{0.62}$	$nan\pm^{nan}_{nan}$	0.58
pks0405	0.09192 (#42)	40.79(38)	376096	68	$455\pm^{31}_{30}$	1	20.7028	$0.68\pm^{15.16}_{1.73}$	$15.66\pm^{0.63}_{nan}$	0.10
pks0405	0.09647 (#43)	39.78(39)	376096	68	$467\pm^{30}_{30}$	1	20.7891	$3.79\pm^{2.39E+03}_{3.59}$	$16.17\pm^{0.36}_{0.98}$	1.33
pks0405	0.14808 (#44)	25.19(31)	376096	69	$472\pm^{37}_{37}$	1	21.7676	$3.60\pm^{41.40}_{4.08}$	$16.10\pm^{0.32}_{nan}$	0.66
pks0405	0.16566 (#45)	27.87(34)	376096	68	$471\pm^{35}_{34}$	1	22.1009	$-1.37\pm^{1.55}_{0.99}$	$nan\pm^{nan}_{nan}$	0.92
pks0405	0.16606 (#46)	28.23(35)	376096	68	$474\pm^{35}_{34}$	1	22.1085	$-1.06\pm^{1.74}_{0.89}$	$nan\pm^{nan}_{nan}$	0.57
pks0405	0.16659 (#47)	28.80(35)	376096	68	$479\pm^{34}_{34}$	1	22.1185	$-0.71\pm^{2.38}_{0.96}$	$nan\pm^{nan}_{nan}$	0.23
pks0405	0.16688 (#48)	28.85(35)	376096	68	$480\pm^{35}_{35}$	1	22.1240	$-0.65\pm^{2.34}_{1.23}$	$nan\pm^{nan}_{nan}$	0.16
pks0405	0.16712 (#49)	28.91(35)	376096	68	$481\pm^{35}_{34}$	1	22.1286	$-0.53\pm^{2.71}_{1.10}$	$nan\pm^{nan}_{nan}$	0.10
pks0405	0.18257 (#50)	32.17(38)	376096	68	$522\pm^{34}_{34}$	1	22.4215	$22.05\pm^{1.84E+06}_{20.83}$	$16.33\pm^{0.28}_{0.47}$	2.54
pks0405	0.18289 (#51)	31.77(38)	376096	68	$525\pm^{35}_{34}$	1	22.4276	$202.85\pm^{1.38E+07}_{200.07}$	$16.43\pm^{0.20}_{0.34}$	3.03
pks0405	0.24052 (#52)	33.13(38)	376096	68	$525\pm^{36}_{35}$	1	23.5203	$37.40\pm^{1.39E+06}_{34.36}$	$16.40\pm^{0.25}_{0.32}$	3.46
pks0405	0.24094 (#53)	32.74(38)	376096	68	$527\pm^{36}_{35}$	1	23.5282	$318.70\pm^{1.41E+07}_{310.60}$	$16.45\pm^{0.21}_{0.20}$	3.93
pks0405	0.24547 (#54)	39.22(39)	376096	69	$487\pm^{36}_{35}$	1	23.6141	$-0.83\pm^{2.07}_{1.10}$	$nan\pm^{nan}_{nan}$	0.28
pks0405	0.29762 (#55)	42.66(38)	376096	66	$595\pm^{38}_{38}$	1	24.6029	$1.38\pm^{34.30}_{2.09}$	$15.90\pm^{0.44}_{nan}$	0.32
pks0405	0.34188 (#56)	40.28(39)	376096	68	$552\pm^{39}_{38}$	1	25.4420	$2.15\pm^{36.43}_{2.78}$	$16.00\pm^{0.39}_{nan}$	0.45
pks0405	0.34225 (#57)	41.57(38)	376096	68	$540\pm^{38}_{38}$	1	25.4491	$1.27\pm^{157.44}_{2.16}$	$15.90\pm^{0.47}_{nan}$	0.26
pks0405	0.35092 (#58)	43.57(39)	376096	70	$504\pm^{38}_{38}$	1	25.6134	$-1.24\pm^{1.65}_{0.91}$	$nan\pm^{nan}_{nan}$	0.75
pks0405	0.36075 (#59)	24.67(38)	376096	69	$526\pm^{39}_{38}$	1	25.7998	$-1.81\pm^{1.29}_{0.90}$	$nan\pm^{nan}_{nan}$	1.84
pks0405	0.36151 (#60)	25.83(39)	376096	68	$534\pm^{39}_{38}$	1	25.8142	$-1.10\pm^{1.80}_{1.03}$	$nan\pm^{nan}_{nan}$	0.53
pks0405	0.36329 (#61)	31.24(38)	376096	69	$545\pm^{39}_{38}$	1	25.8480	$-0.25\pm^{3.44}_{1.34}$	$nan\pm^{nan}_{nan}$	0.02
pks0405	0.40570 (#62)	41.81(38)	376096	68	$614\pm^{42}_{41}$	1	26.6521	$1.10\pm^{85.63}_{1.96}$	$15.84\pm^{0.52}_{nan}$	0.23
pks0405	0.40890 (#63)	39.69(39)	376096	68	$624\pm^{45}_{40}$	1	26.7127	$26.09\pm^{3.07E+07}_{23.51}$	$16.29\pm^{0.30}_{0.19}$	2.91
pks0405	0.49505 (#64)	40.12(38)	376096	71	$570\pm^{45}_{44}$	1	28.3461	$-1.06\pm^{2.05}_{0.96}$	$nan\pm^{nan}_{nan}$	0.47
pks0405	0.49530 (#65)	40.23(38)	376096	71	$571\pm^{45}_{44}$	1	28.3509	$-1.00\pm^{2.23}_{1.19}$	$nan\pm^{nan}_{nan}$	0.34
pks0405	0.55506 (#66)	33.01(39)	376096	74	$545\pm^{50}_{49}$	1	29.4839	$-0.77\pm^{4.84}_{1.25}$	$nan\pm^{nan}_{nan}$	0.14
pks2005	0.06490 (#67)	35.04(39)	282191	1	$1757\pm^{42}_{41}$	1	20.1905	$-0.44\pm^{0.55}_{0.45}$	$nan\pm^{nan}_{nan}$	0.71
tons180	0.02340 (#68)	38.98(38)	76753	1	$1528\pm^{42}_{41}$	1	19.4037	$-0.36\pm^{0.66}_{0.52}$	$nan\pm^{nan}_{nan}$	0.36
tons180	0.04360 (#69)	26.47(39)	76753	1	$1554\pm^{44}_{43}$	1	19.7867	$-0.81\pm^{0.59}_{0.51}$	$nan\pm^{nan}_{nan}$	1.91
tons180	0.04560 (#70)	28.12(38)	76753	1	$1572\pm^{44}_{44}$	1	19.8246	$-0.06\pm^{0.81}_{0.64}$	$nan\pm^{nan}_{nan}$	0.01

3c273	0.00337 (#71)	46.56(38)	69608	6	$5095\pm^{100}_{98}$	1	19.0239	$1.31\pm^{1.06}_{0.75}$	$15.91\pm^{0.17}_{0.30}$	4.12
3c273	0.00533 (#72)	48.67(39)	69608	6	$5091\pm^{100}_{99}$	1	19.0611	$1.27\pm^{1.07}_{0.75}$	$15.89\pm^{0.18}_{0.32}$	3.85
3c273	0.00764 (#73)	49.34(38)	69608	6	$5102\pm^{102}_{100}$	1	19.1049	$1.21\pm^{1.39}_{0.83}$	$15.84\pm^{0.20}_{0.41}$	2.91
3c273	0.02947 (#74)	26.95(24)	69608	7	$5335\pm^{146}_{144}$	1	19.5188	$-0.28\pm^{0.64}_{0.47}$	$nan\pm^{nan}_{nan}$	0.27
3c273	0.04898 (#75)	40.99(39)	69608	7	$5480\pm^{125}_{122}$	1	19.8887	$-1.55\pm^{0.39}_{0.34}$	$nan\pm^{nan}_{nan}$	12.07
3c273	0.06655 (#76)	44.57(38)	69608	8	$5539\pm^{132}_{124}$	1	20.2218	$-0.04\pm^{0.84}_{0.53}$	$nan\pm^{nan}_{nan}$	-0.01
3c273	0.09018 (#77)	29.87(38)	69608	8	$5748\pm^{134}_{131}$	1	20.6698	$3.34\pm^{4.82}_{2.01}$	$16.09\pm^{0.14}_{0.22}$	6.58
3c273	0.12007 (#78)	34.40(31)	69608	7	$5957\pm^{156}_{154}$	1	21.2365	$1.69\pm^{1.76}_{1.05}$	$15.98\pm^{0.18}_{0.33}$	3.75
3c273	0.14660 (#79)	31.78(31)	69608	8	$5708\pm^{157}_{153}$	1	21.7395	$-0.36\pm^{0.69}_{0.55}$	$nan\pm^{nan}_{nan}$	0.34
3c273	0.15784 (#80)	26.34(30)	69608	8	$5883\pm^{161}_{158}$	1	21.9526	$1.60\pm^{1.95}_{1.09}$	$15.95\pm^{0.19}_{0.40}$	3.00
mrk421	0.01009 (#81)	28.92(9)	638847	1	$1273\pm^{5}_{5}$	1	19.1513	$0.09\pm^{0.08}_{0.05}$	$14.84\pm^{0.26}_{0.36}$	3.66
pks2155	0.05405 (#82)	50.63(39)	319334	4	$13905\pm^{93}_{91}$	1	19.9848	$0.15\pm^{0.22}_{0.19}$	$15.08\pm^{0.36}_{nan}$	0.73
pks2155	0.05707 (#83)	42.86(39)	319334	4	$13877\pm^{90}_{91}$	1	20.0420	$0.07\pm^{0.20}_{0.20}$	$14.75\pm^{0.55}_{nan}$	0.10

Table C.6: O VIII upper limit measurements with *Chandra* data, at the prior redshift from the O VI lines from Table A.1.

Target line		cmin	RGS1	power–law		line component			ΔC
Name	z	(d.o.f.)	avg exp (s)	norm.	index	λ (Å)	τ_0	$\log N + (\mathrm{cm}^{-2})$	(d.o.f.)
1es1028	0.12314 (#1)	35.82(30)	148933	$1585\pm^{62}_{61}$	1	21.2947	0.66	15.64	1.19
1es1028	0.13706 (#2)	–	–	–	–	21.5587	–	–	–
1es1028	0.33735 (#3)	34.59(38)	148933	$1851\pm^{66}_{65}$	1	25.3562	0.98	15.77	0.07
1es1553	0.18759 (#4)	43.76(33)	495645	$2462\pm^{44}_{44}$	1	22.5167	0.55	15.58	0.23
1es1553	0.18775 (#5)	43.78(32)	495645	$2464\pm^{44}_{44}$	1	22.5197	0.56	15.58	0.23
1es1553	0.18984 (#6)	40.55(33)	495645	$2490\pm^{43}_{43}$	1	22.5594	0.99	15.80	0.06
1es1553	0.21631 (#7)	30.16(26)	495645	$2584\pm^{53}_{52}$	1	23.0612	0.41	15.48	1.20
1es1553	0.31130 (#8)	50.56(39)	495645	$2998\pm^{46}_{44}$	1	24.8622	0.45	15.52	-0.03
1es1553	0.37868 (#9)	48.06(39)	495645	$3124\pm^{49}_{48}$	1	26.1398	0.38	15.45	0.89
1es1553	0.39497 (#10)	41.84(38)	495645	$3095\pm^{49}_{49}$	1	26.4486	0.35	15.42	2.79
h1821	0.02438 (#11)	37.76(38)	470152	$858\pm^{15}_{14}$	1	19.4222	0.56	15.59	1.80
h1821	0.10817 (#12)	44.34(38)	470152	$854\pm^{17}_{17}$	1	21.0109	0.37	15.43	4.97
h1821	0.12133 (#13)	42.59(31)	470152	$879\pm^{20}_{20}$	1	21.2604	0.49	15.55	0.12
h1821	0.12147 (#14)	42.69(31)	470152	$880\pm^{20}_{20}$	1	21.2631	0.51	15.56	0.00
h1821	0.16992 (#15)	54.02(38)	470152	$895\pm^{20}_{20}$	1	22.1817	0.67	15.65	0.20
h1821	0.17043 (#16)	53.61(38)	470152	$897\pm^{20}_{20}$	1	22.1914	0.72	15.68	0.64
h1821	0.21326 (#17)	33.98(34)	470152	$944\pm^{23}_{23}$	1	23.0034	0.52	15.57	0.99
h1821	0.22497 (#18)	38.17(32)	470152	$997\pm^{24}_{24}$	1	23.2254	0.40	15.47	2.59
h1821	0.22522 (#19)	38.06(32)	470152	$997\pm^{24}_{24}$	1	23.2302	0.35	15.41	2.71
h1821	0.22639 (#20)	38.11(32)	470152	$1000\pm^{24}_{24}$	1	23.2524	0.39	15.46	1.78
h1821	0.24531 (#21)	38.80(33)	470152	$1114\pm^{23}_{23}$	1	23.6111	0.63	15.64	2.00
h1821	0.26657 (#22)	38.28(37)	470152	$1161\pm^{22}_{22}$	1	24.0142	0.43	15.49	0.36
h1821	0.28800 (#23)	41.01(38)	470152	$1232\pm^{23}_{23}$	1	24.4205	0.65	15.64	1.56
h1821	0.29658 (#24)	36.87(39)	470152	$1194\pm^{23}_{22}$	1	24.5832	0.28	15.32	9.64
h1821	0.29680 (#25)	37.18(39)	470152	$1194\pm^{23}_{23}$	1	24.5873	0.33	15.40	9.31

h2356	0.11461 (#26)	31.02(33)	586697	$2121\pm^{36}_{35}$	1	21.1330	0.48	15.53	0.04
h2356	0.16512 (#27)	28.36(34)	586697	$2145\pm^{37}_{37}$	1	22.0907	0.52	15.56	0.13
mr2251	0.01070 (#28)	31.58(39)	78434	$2572\pm^{71}_{70}$	1	19.1629	1.27	15.90	1.61
pg1116	0.05900 (#29)	33.05(38)	355485	$617\pm^{29}_{28}$	1	20.0786	2.31	16.03	0.08
pg1116	0.05927 (#30)	31.93(39)	355485	$629\pm^{29}_{28}$	1	20.0838	2.15	16.01	0.11
pg1116	0.11895 (#31)	26.57(31)	355485	$654\pm^{34}_{35}$	1	21.2153	1.67	15.96	0.00
pg1116	0.13852 (#32)	–	–	–	–	21.5863	–	–	–
pg1116	0.16539 (#33)	31.16(34)	355485	$773\pm^{36}_{35}$	1	22.0958	0.86	15.74	0.73
pg1116	0.16554 (#34)	31.18(34)	355485	$774\pm^{36}_{36}$	1	22.0986	0.93	15.79	0.72
pg1116	0.16610 (#35)	31.39(35)	355485	$775\pm^{36}_{35}$	1	22.1093	0.94	15.78	0.49
pg1116	0.16686 (#36)	31.82(35)	355485	$782\pm^{36}_{35}$	1	22.1237	1.32	15.91	0.01
pg1116	0.17343 (#37)	35.93(38)	355485	$762\pm^{34}_{34}$	1	22.2482	1.21	15.87	0.05
pg1211	0.00711 (#38)	42.02(38)	133595	$998\pm^{34}_{33}$	1	19.0948	1.31	15.86	0.44
pg1211	0.05117 (#39)	30.00(38)	133595	$1107\pm^{40}_{39}$	1	19.9302	0.82	15.72	0.12
pg1211	0.06449 (#40)	33.49(39)	133595	$1148\pm^{42}_{41}$	1	20.1827	0.78	15.70	0.21
pg1211	0.06491 (#41)	33.15(39)	133595	$1145\pm^{42}_{41}$	1	20.1907	0.72	15.68	0.58
pks0405	0.09192 (#42)	40.79(38)	376096	$455\pm^{31}_{30}$	1	20.7028	8.45	16.26	0.10
pks0405	0.09647 (#43)	39.78(39)	376096	$467\pm^{30}_{30}$	1	20.7891	1.20E+03	16.50	1.33
pks0405	0.14808 (#44)	25.19(31)	376096	$472\pm^{37}_{37}$	1	21.7676	22.74	16.36	0.66
pks0405	0.16566 (#45)	27.87(34)	376096	$471\pm^{35}_{34}$	1	22.1009	1.27	15.90	0.92
pks0405	0.16606 (#46)	28.23(35)	376096	$474\pm^{35}_{34}$	1	22.1085	1.31	15.87	0.57
pks0405	0.16659 (#47)	28.80(35)	376096	$479\pm^{34}_{34}$	1	22.1185	1.67	15.93	0.23
pks0405	0.16688 (#48)	28.85(35)	376096	$480\pm^{35}_{35}$	1	22.1240	1.79	16.00	0.16
pks0405	0.16712 (#49)	28.91(35)	376096	$481\pm^{35}_{34}$	1	22.1286	1.90	15.98	0.10
pks0405	0.18257 (#50)	32.17(38)	376096	$522\pm^{34}_{34}$	1	22.4215	9.18E+05	16.59	2.54
pks0405	0.18289 (#51)	31.77(38)	376096	$525\pm^{35}_{34}$	1	22.4276	6.92E+06	16.61	3.03
pks0405	0.24052 (#52)	33.13(38)	376096	$525\pm^{36}_{35}$	1	23.5203	6.97E+05	16.62	3.46
pks0405	0.24094 (#53)	32.74(38)	376096	$527\pm^{36}_{35}$	1	23.5282	7.03E+06	16.64	3.93
pks0405	0.24547 (#54)	39.22(39)	376096	$487\pm^{36}_{35}$	1	23.6141	1.59	15.96	0.28

pks0405	0.29762 (#55)	42.66(38)	376096	$595\pm^{38}_{38}$	1	24.6029	18.19	16.31	0.32
pks0405	0.34188 (#56)	40.28(39)	376096	$552\pm^{39}_{38}$	1	25.4420	19.60	16.34	0.45
pks0405	0.34225 (#57)	41.57(38)	376096	$540\pm^{38}_{38}$	1	25.4491	79.80	16.33	0.26
pks0405	0.35092 (#58)	43.57(39)	376096	$504\pm^{38}_{38}$	1	25.6134	1.28	15.87	0.75
pks0405	0.36075 (#59)	24.67(38)	376096	$526\pm^{39}_{38}$	1	25.7998	1.10	15.85	1.84
pks0405	0.36151 (#60)	25.83(39)	376096	$534\pm^{39}_{38}$	1	25.8142	1.42	15.92	0.53
pks0405	0.36329 (#61)	31.24(38)	376096	$545\pm^{39}_{38}$	1	25.8480	2.39	16.07	0.02
pks0405	0.40570 (#62)	41.81(38)	376096	$614\pm^{42}_{41}$	1	26.6521	43.80	16.33	0.23
pks0405	0.40890 (#63)	39.69(39)	376096	$624\pm^{45}_{40}$	1	26.7127	1.54E+07	16.58	2.91
pks0405	0.49505 (#64)	40.12(38)	376096	$570\pm^{45}_{44}$	1	28.3461	1.50	15.92	0.47
pks0405	0.49530 (#65)	40.23(38)	376096	$571\pm^{45}_{44}$	1	28.3509	1.71	15.99	0.34
pks0405	0.55506 (#66)	33.01(39)	376096	$545\pm^{50}_{49}$	1	29.4839	3.04	16.09	0.14
pks2005	0.06490 (#67)	35.04(39)	282191	$1757\pm^{42}_{41}$	1	20.1905	0.50	15.55	0.71
tons180	0.02340 (#68)	38.98(38)	76753	$1528\pm^{42}_{41}$	1	19.4037	0.59	15.61	0.36
tons180	0.04360 (#69)	26.47(39)	76753	$1554\pm^{44}_{43}$	1	19.7867	0.55	15.59	1.91
tons180	0.04560 (#70)	28.12(38)	76753	$1572\pm^{44}_{44}$	1	19.8246	0.73	15.70	0.01
3c273	0.00337 (#71)	46.56(38)	69608	$5095\pm^{100}_{98}$	1	19.0239	0.91	15.78	4.12
3c273	0.00533 (#72)	48.67(39)	69608	$5091\pm^{100}_{99}$	1	19.0611	0.91	15.78	3.85
3c273	0.00764 (#73)	49.34(38)	69608	$5102\pm^{102}_{100}$	1	19.1049	1.11	15.82	2.91
3c273	0.02947 (#74)	26.95(24)	69608	$5335\pm^{146}_{144}$	1	19.5188	0.55	15.58	0.27
3c273	0.04898 (#75)	40.99(39)	69608	$5480\pm^{125}_{122}$	1	19.8887	0.37	15.43	12.07
3c273	0.06655 (#76)	44.57(38)	69608	$5539\pm^{132}_{124}$	1	20.2218	0.68	15.66	-0.01
3c273	0.09018 (#77)	29.87(38)	69608	$5748\pm^{134}_{131}$	1	20.6698	3.41	16.09	6.58
3c273	0.12007 (#78)	34.40(31)	69608	$5957\pm^{156}_{154}$	1	21.2365	1.40	15.93	3.75
3c273	0.14660 (#79)	31.78(31)	69608	$5708\pm^{157}_{153}$	1	21.7395	0.62	15.63	0.34
3c273	0.15784 (#80)	26.34(30)	69608	$5883\pm^{161}_{158}$	1	21.9526	1.52	15.94	3.00
mrk421	0.01009 (#81)	28.92(9)	638847	$1273\pm^{5}_{5}$	1	19.1513	0.06	14.70	3.66
pks2155	0.05405 (#82)	50.63(39)	319334	$13905\pm^{93}_{91}$	1	19.9848	0.21	15.20	0.73
pks2155	0.05707 (#83)	42.86(39)	319334	$13877\pm^{90}_{91}$	1	20.0420	0.20	15.18	0.10

Table C.7: O VIII measurements with *Chandra* data, at the prior redshift from the H I lines from Table A.2.

Target line		cmin	RGS1		power–law		line component			ΔC
Name	z	(d.o.f.)	avg exp (s)	% $\frac{B}{D+B}$	norm.	index	λ (Å)	τ_0	$\log N(\mathrm{cm}^{-2})$	(d.o.f.)
1es1028	0.20383 (#2)	24.47(38)	148933	25	$1653\pm^{61}_{59}$	1	22.8246	$-1.22\pm^{0.69}_{0.52}$	$nan\pm^{nan}_{nan}$	2.76
1es1028	0.22121 (#3)	26.80(38)	148933	25	$1757\pm^{63}_{61}$	1	23.1541	$3.82\pm^{13.01}_{2.75}$	$16.13\pm^{0.19}_{0.32}$	3.68
1es1553	0.03466 (#4)	51.93(39)	495645	21	$2174\pm^{31}_{31}$	1	19.6172	$0.21\pm^{0.53}_{0.42}$	$15.19\pm^{0.49}_{nan}$	0.23
1es1553	0.04273 (#5)	42.22(38)	495645	22	$2213\pm^{32}_{32}$	1	19.7702	$0.00\pm^{0.58}_{0.35}$	$13.57\pm^{2.03}_{nan}$	0.00
1es1553	0.06364 (#6)	42.31(39)	495645	23	$2255\pm^{35}_{35}$	1	20.1666	$0.86\pm^{0.85}_{0.59}$	$15.74\pm^{0.21}_{0.44}$	2.66
1es1553	0.21869 (#7)	36.69(30)	495645	24	$2585\pm^{49}_{48}$	1	23.1064	$-0.35\pm^{0.43}_{0.35}$	$nan\pm^{nan}_{nan}$	0.78
3c273	0.00758 (#8)	49.20(38)	69608	6	$5103\pm^{101}_{99}$	1	19.1037	$1.21\pm^{1.27}_{0.81}$	$15.85\pm^{0.19}_{0.39}$	3.07
3c273	0.06707 (#9)	46.91(39)	69608	8	$5560\pm^{124}_{134}$	1	20.2316	$0.02\pm^{0.67}_{0.65}$	$14.14\pm^{1.51}_{nan}$	-0.01
3c273	0.07359 (#10)	43.29(38)	69608	8	$5652\pm^{130}_{128}$	1	20.3553	$1.00\pm^{1.61}_{0.87}$	$15.78\pm^{0.25}_{0.79}$	1.54
3c273	0.13960 (#11)	–	–	–	–	–	21.6068	–	–	–
h1821	0.00944 (#12)	38.66(39)	470152	2	$824\pm^{14}_{14}$	1	19.1390	$-0.32\pm^{0.39}_{0.35}$	$nan\pm^{nan}_{nan}$	0.75
h1821	0.06779 (#13)	39.35(38)	470152	2	$852\pm^{16}_{15}$	1	20.2453	$2.02\pm^{1.67}_{0.98}$	$15.98\pm^{0.13}_{0.19}$	7.79
h1821	0.08483 (#14)	44.68(39)	470152	2	$843\pm^{16}_{16}$	1	20.5684	$-0.26\pm^{0.45}_{0.37}$	$nan\pm^{nan}_{nan}$	0.39
h1821	0.12147 (#15)	42.69(31)	470152	2	$880\pm^{20}_{20}$	1	21.2631	$-0.03\pm^{0.54}_{0.47}$	$nan\pm^{nan}_{nan}$	0.00
h1821	0.19817 (#16)	49.67(39)	470152	2	$931\pm^{22}_{22}$	1	22.7173	$1.16\pm^{1.47}_{0.86}$	$15.83\pm^{0.21}_{0.49}$	2.27
h1821	0.21321 (#17)	35.27(35)	470152	2	$948\pm^{23}_{23}$	1	23.0025	$-0.55\pm^{0.60}_{0.48}$	$nan\pm^{nan}_{nan}$	0.93
h1821	0.24531 (#18)	32.59(30)	470152	1	$1130\pm^{25}_{24}$	1	23.6111	$0.85\pm^{0.73}_{0.58}$	$15.76\pm^{0.20}_{0.44}$	2.67
h2356	0.03830 (#19)	39.37(39)	586697	25	$2067\pm^{29}_{29}$	1	19.6862	$-0.53\pm^{0.35}_{0.31}$	$nan\pm^{nan}_{nan}$	2.38
h2356	0.07881 (#20)	40.55(38)	586697	27	$2087\pm^{32}_{32}$	1	20.4542	$-0.51\pm^{0.35}_{0.30}$	$nan\pm^{nan}_{nan}$	2.15
h2356	0.10467 (#21)	41.21(38)	586697	28	$2108\pm^{31}_{31}$	1	20.9445	$0.01\pm^{0.52}_{0.38}$	$13.73\pm^{1.83}_{nan}$	0.00
h2356	0.15613 (#22)	28.52(30)	586697	28	$2138\pm^{39}_{39}$	1	21.9202	$-0.08\pm^{0.48}_{0.40}$	$nan\pm^{nan}_{nan}$	0.05
mr2251	0.01068 (#23)	31.54(39)	78434	12	$2573\pm^{72}_{70}$	1	19.1625	$1.17\pm^{1.54}_{0.99}$	$15.87\pm^{0.24}_{0.73}$	1.66
mr2251	0.01449 (#24)	25.42(39)	78434	12	$2473\pm^{71}_{70}$	1	19.2347	$-1.12\pm^{0.54}_{0.44}$	$nan\pm^{nan}_{nan}$	3.77
mr2251	0.06131 (#25)	43.48(38)	78434	15	$2702\pm^{88}_{86}$	1	20.1224	$3.21\pm^{12.08}_{2.17}$	$16.12\pm^{0.17}_{0.31}$	3.98
mr2251	0.06190 (#26)	43.84(39)	78434	15	$2700\pm^{88}_{86}$	1	20.1336	$3.41\pm^{9.45}_{2.46}$	$16.11\pm^{0.18}_{0.34}$	3.61
mr2251	0.06276 (#27)	43.50(38)	78434	15	$2697\pm^{88}_{86}$	1	20.1499	$2.98\pm^{54.62}_{1.92}$	$16.13\pm^{0.17}_{0.30}$	4.11
mr2251	0.06327 (#28)	43.55(39)	78434	15	$2707\pm^{88}_{87}$	1	20.1596	$5.13\pm^{32.32}_{3.54}$	$16.20\pm^{0.14}_{0.25}$	5.17
mr2251	0.06381 (#29)	41.59(38)	78434	15	$2714\pm^{89}_{87}$	1	20.1698	$7.99\pm^{14.98}_{5.86}$	$16.22\pm^{0.14}_{0.23}$	5.94
mrk478	0.06166 (#30)	37.08(38)	80466	20	$1284\pm^{61}_{60}$	1	20.1291	$-1.60\pm^{0.68}_{0.51}$	$nan\pm^{nan}_{nan}$	4.08
mrk478	0.06578 (#31)	38.24(39)	80466	20	$1328\pm^{63}_{61}$	1	20.2072	$0.96\pm^{5.56}_{1.48}$	$15.77\pm^{0.43}_{nan}$	0.35
mrk478	0.07213 (#32)	34.86(38)	80466	20	$1330\pm^{62}_{60}$	1	20.3276	$21.99\pm^{1.46E+03}_{18.85}$	$16.30\pm^{0.16}_{0.19}$	4.58
pg1116	0.04114 (#33)	38.61(39)	355485	52	$635\pm^{27}_{27}$	1	19.7400	$0.85\pm^{3.32}_{1.35}$	$15.75\pm^{0.43}_{nan}$	0.34
pg1116	0.06251 (#34)	31.45(38)	355485	54	$631\pm^{29}_{28}$	1	20.1452	$-0.69\pm^{1.20}_{0.71}$	$nan\pm^{nan}_{nan}$	0.48

pg1116	0.08382 (#35)	36.50(38)	355485	55	$618\pm^{30}_{29}$	1	20.5492	$-0.65\pm^{1.33}_{0.89}$	$nan\pm^{nan}_{nan}$	0.34
pg1116	0.09210 (#36)	33.90(38)	355485	55	$632\pm^{30}_{30}$	1	20.7062	$1.27\pm^{7.97}_{1.66}$	$15.85\pm^{0.39}_{nan}$	0.50
pg1116	0.09281 (#37)	33.80(38)	355485	55	$633\pm^{30}_{30}$	1	20.7197	$1.43\pm^{8.70}_{1.75}$	$15.89\pm^{0.37}_{nan}$	0.61
pg1116	0.13373 (#38)	21.48(30)	355485	52	$757\pm^{36}_{36}$	1	21.4955	$0.31\pm^{4.31}_{1.24}$	$15.35\pm^{0.80}_{nan}$	0.04
pg1116	0.13851 (#39)	–	–	–	–	–	21.5861	–	–	–
pg1211	0.02586 (#40)	33.54(38)	133595	1	$1070\pm^{37}_{36}$	1	19.4503	$1.44\pm^{2.02}_{1.18}$	$15.94\pm^{0.23}_{0.65}$	1.73
pg1211	0.05443 (#41)	30.17(39)	133595	1	$1124\pm^{41}_{40}$	1	19.9920	$-0.98\pm^{0.63}_{0.48}$	$nan\pm^{nan}_{nan}$	2.25
pks0405	0.02510 (#42)	32.93(39)	376096	63	$432\pm^{24}_{23}$	1	19.4359	$0.83\pm^{5.37}_{1.61}$	$15.75\pm^{0.49}_{nan}$	0.21
pks0405	0.05902 (#43)	31.53(38)	376096	68	$431\pm^{29}_{28}$	1	20.0790	$1.75\pm^{35.93}_{2.44}$	$15.96\pm^{0.42}_{nan}$	0.37
pks0405	0.09719 (#44)	37.54(38)	376096	68	$470\pm^{30}_{30}$	1	20.8027	$719.82\pm^{8.55E+03}_{727.42}$	$16.45\pm^{0.10}_{nan}$	3.80
pks0405	0.10152 (#45)	39.29(39)	376096	67	$462\pm^{31}_{30}$	1	20.8848	$-0.97\pm^{1.70}_{0.93}$	$nan\pm^{nan}_{nan}$	0.49
pks0405	0.10298 (#46)	33.14(39)	376096	67	$466\pm^{31}_{30}$	1	20.9125	$1.46\pm^{175.16}_{2.15}$	$15.94\pm^{0.42}_{nan}$	0.38
pks0405	0.19456 (#47)	32.55(38)	376096	68	$514\pm^{35}_{35}$	1	22.6489	$-0.83\pm^{1.97}_{1.11}$	$nan\pm^{nan}_{nan}$	0.30
pks0405	0.21976 (#48)	37.95(38)	376096	68	$537\pm^{36}_{36}$	1	23.1266	$1.69\pm^{199.14}_{2.35}$	$15.98\pm^{0.42}_{nan}$	0.41
pks0405	0.24564 (#49)	39.21(39)	376096	69	$487\pm^{35}_{35}$	1	23.6173	$-0.78\pm^{2.16}_{0.93}$	$nan\pm^{nan}_{nan}$	0.29
pks0405	0.29748 (#50)	42.61(38)	376096	66	$595\pm^{38}_{37}$	1	24.6002	$1.31\pm^{153.91}_{1.98}$	$15.91\pm^{0.44}_{nan}$	0.37
pks0405	0.31016 (#51)	50.26(39)	376096	68	$547\pm^{37}_{37}$	1	24.8406	$3.28\pm^{6.44E+03}_{3.32}$	$16.12\pm^{0.40}_{nan}$	1.07
pks0405	0.32502 (#52)	53.39(38)	376096	68	$543\pm^{39}_{37}$	1	25.1224	$-0.25\pm^{6.77}_{1.30}$	$nan\pm^{nan}_{nan}$	0.01
pks0405	0.49508 (#53)	40.12(38)	376096	71	$570\pm^{45}_{44}$	1	28.3467	$-1.07\pm^{2.07}_{0.99}$	$nan\pm^{nan}_{nan}$	0.46
pks2155	0.05708 (#54)	42.87(39)	319334	4	$13878\pm^{90}_{95}$	1	20.0422	$0.08\pm^{0.18}_{0.21}$	$14.81\pm^{0.49}_{nan}$	0.09
pks2155	0.06236 (#55)	43.07(39)	319334	4	$13944\pm^{92}_{93}$	1	20.1423	$-0.07\pm^{0.19}_{0.18}$	$nan\pm^{nan}_{nan}$	0.14
pks2155	0.10586 (#56)	36.85(39)	319334	4	$14826\pm^{95}_{94}$	1	20.9671	$-0.01\pm^{0.31}_{0.12}$	$nan\pm^{nan}_{nan}$	-0.04
tons180	0.04304 (#57)	24.70(38)	76753	1	$1560\pm^{44}_{43}$	1	19.7760	$-0.78\pm^{0.60}_{0.51}$	$nan\pm^{nan}_{nan}$	1.75

Table C.8: O VIII upper limit measurements with *Chandra* data, at the prior redshift from the H I lines from Table A.2.

Target line		cmin	RGS1	power–law		line component			ΔC
Name	z	(d.o.f.)	avg exp (s)	norm.	index	λ (Å)	τ_0	$\log N + (\mathrm{cm}^{-2})$	(d.o.f.)
1es1028	0.13714 (#1)	–	–	–	–	21.5602	–	–	–
1es1028	0.20383 (#2)	24.47(38)	148933	$1653\pm^{61}_{59}$	1	22.8246	0.61	15.63	2.76
1es1028	0.22121 (#3)	26.80(38)	148933	$1757\pm^{63}_{61}$	1	23.1541	7.88	16.23	3.68
1es1553	0.03466 (#4)	51.93(39)	495645	$2174\pm^{31}_{31}$	1	19.6172	0.48	15.52	0.23
1es1553	0.04273 (#5)	42.22(38)	495645	$2213\pm^{32}_{32}$	1	19.7702	0.46	15.51	0.00
1es1553	0.06364 (#6)	42.31(39)	495645	$2255\pm^{35}_{35}$	1	20.1666	0.72	15.68	2.66
1es1553	0.21869 (#7)	36.69(30)	495645	$2585\pm^{49}_{48}$	1	23.1064	0.39	15.44	0.78
3c273	0.00758 (#8)	49.20(38)	69608	$5103\pm^{101}_{99}$	1	19.1037	1.04	15.81	3.07
3c273	0.06707 (#9)	46.91(39)	69608	$5560\pm^{124}_{134}$	1	20.2316	0.66	15.64	-0.01
3c273	0.07359 (#10)	43.29(38)	69608	$5652\pm^{130}_{128}$	1	20.3553	1.24	15.85	1.54
3c273	0.13960 (#11)	–	–	–	–	21.6068	–	–	–
h1821	0.00944 (#12)	38.66(39)	470152	$824\pm^{14}_{14}$	1	19.1390	0.37	15.44	0.75
h1821	0.06779 (#13)	39.35(38)	470152	$852\pm^{16}_{15}$	1	20.2453	1.33	15.87	7.79
h1821	0.08483 (#14)	44.68(39)	470152	$843\pm^{16}_{16}$	1	20.5684	0.41	15.46	0.39
h1821	0.12147 (#15)	42.69(31)	470152	$880\pm^{20}_{20}$	1	21.2631	0.51	15.56	0.00
h1821	0.19817 (#16)	49.67(39)	470152	$931\pm^{22}_{22}$	1	22.7173	1.17	15.83	2.27
h1821	0.21321 (#17)	35.27(35)	470152	$948\pm^{23}_{23}$	1	23.0025	0.54	15.58	0.93
h1821	0.24531 (#18)	32.59(30)	470152	$1130\pm^{25}_{24}$	1	23.6111	0.65	15.66	2.67
h2356	0.03830 (#19)	39.37(39)	586697	$2067\pm^{29}_{29}$	1	19.6862	0.33	15.39	2.38
h2356	0.07881 (#20)	40.55(38)	586697	$2087\pm^{32}_{32}$	1	20.4542	0.33	15.38	2.15
h2356	0.10467 (#21)	41.21(38)	586697	$2108\pm^{31}_{31}$	1	20.9445	0.45	15.50	0.00
h2356	0.15613 (#22)	28.52(30)	586697	$2138\pm^{39}_{39}$	1	21.9202	0.44	15.49	0.05
mr2251	0.01068 (#23)	31.54(39)	78434	$2573\pm^{72}_{70}$	1	19.1625	1.27	15.90	1.66
mr2251	0.01449 (#24)	25.42(39)	78434	$2473\pm^{71}_{70}$	1	19.2347	0.49	15.54	3.77
mr2251	0.06131 (#25)	43.48(38)	78434	$2702\pm^{88}_{86}$	1	20.1224	7.12	16.24	3.98

mr2251	0.06190 (#26)	43.84(39)	78434	$2700\pm^{88}_{86}$	1	20.1336	5.95	16.20	3.61
mr2251	0.06276 (#27)	43.50(38)	78434	$2697\pm^{88}_{86}$	1	20.1499	28.27	16.29	4.11
mr2251	0.06327 (#28)	43.55(39)	78434	$2707\pm^{88}_{87}$	1	20.1596	17.93	16.31	5.17
mr2251	0.06381 (#29)	41.59(38)	78434	$2714\pm^{89}_{87}$	1	20.1698	10.42	16.26	5.94
mrk478	0.06166 (#30)	37.08(38)	80466	$1284\pm^{61}_{60}$	1	20.1291	0.59	15.61	4.08
mrk478	0.06578 (#31)	38.24(39)	80466	$1328\pm^{63}_{61}$	1	20.2072	3.52	16.10	0.35
mrk478	0.07213 (#32)	34.86(38)	80466	$1330\pm^{62}_{60}$	1	20.3276	740.13	16.42	4.58
pg1116	0.04114 (#33)	38.61(39)	355485	$635\pm^{27}_{27}$	1	19.7400	2.34	16.05	0.34
pg1116	0.06251 (#34)	31.45(38)	355485	$631\pm^{29}_{28}$	1	20.1452	0.95	15.77	0.48
pg1116	0.08382 (#35)	36.50(38)	355485	$618\pm^{30}_{29}$	1	20.5492	1.11	15.85	0.34
pg1116	0.09210 (#36)	33.90(38)	355485	$632\pm^{30}_{30}$	1	20.7062	4.82	16.14	0.50
pg1116	0.09281 (#37)	33.80(38)	355485	$633\pm^{30}_{30}$	1	20.7197	5.23	16.16	0.61
pg1116	0.13373 (#38)	21.48(30)	355485	$757\pm^{36}_{36}$	1	21.4955	2.78	16.06	0.04
pg1116	0.13851 (#39)	–	–	–	–	21.5861	–	–	–
pg1211	0.02586 (#40)	33.54(38)	133595	$1070\pm^{37}_{36}$	1	19.4503	1.60	15.97	1.73
pg1211	0.05443 (#41)	30.17(39)	133595	$1124\pm^{41}_{40}$	1	19.9920	0.56	15.58	2.25
pks0405	0.02510 (#42)	32.93(39)	376096	$432\pm^{24}_{23}$	1	19.4359	3.49	16.15	0.21
pks0405	0.05902 (#43)	31.53(38)	376096	$431\pm^{29}_{28}$	1	20.0790	19.18	16.33	0.37
pks0405	0.09719 (#44)	37.54(38)	376096	$470\pm^{30}_{30}$	1	20.8027	4.64E+03	16.52	3.80
pks0405	0.10152 (#45)	39.29(39)	376096	$462\pm^{31}_{30}$	1	20.8848	1.32	15.89	0.49
pks0405	0.10298 (#46)	33.14(39)	376096	$466\pm^{31}_{30}$	1	20.9125	88.66	16.32	0.38
pks0405	0.19456 (#47)	32.55(38)	376096	$514\pm^{35}_{35}$	1	22.6489	1.54	15.96	0.30
pks0405	0.21976 (#48)	37.95(38)	376096	$537\pm^{36}_{36}$	1	23.1266	100.75	16.35	0.41
pks0405	0.24564 (#49)	39.21(39)	376096	$487\pm^{35}_{35}$	1	23.6173	1.55	15.91	0.29
pks0405	0.29748 (#50)	42.61(38)	376096	$595\pm^{38}_{37}$	1	24.6002	77.94	16.32	0.37
pks0405	0.31016 (#51)	50.26(39)	376096	$547\pm^{37}_{37}$	1	24.8406	3.22E+03	16.49	1.07
pks0405	0.32502 (#52)	53.39(38)	376096	$543\pm^{39}_{37}$	1	25.1224	4.04	16.17	0.01
pks0405	0.49508 (#53)	40.12(38)	376096	$570\pm^{45}_{44}$	1	28.3467	1.53	15.93	0.46
pks2155	0.05708 (#54)	42.87(39)	319334	$13878\pm^{90}_{95}$	1	20.0422	0.20	15.18	0.09

pks2155	0.06236 (#55)	43.07(39)	319334	$13944\pm^{92}_{93}$	1	20.1423	0.18	15.15	0.14
pks2155	0.10586 (#56)	36.85(39)	319334	$14826\pm^{95}_{94}$	1	20.9671	0.22	15.21	-0.04
tons180	0.04304 (#57)	24.70(38)	76753	$1560\pm^{44}_{43}$	1	19.7760	0.55	15.60	1.75